EVOLUTION OF REPRODUCTIVE ORGANS IN LAND PLANTS

EDITED BY: Xin Wang, Zhong-Jian Liu, Borja Cascales-Miñana and José Bienvenido Diez

PUBLISHED IN: Frontiers in Plant Science

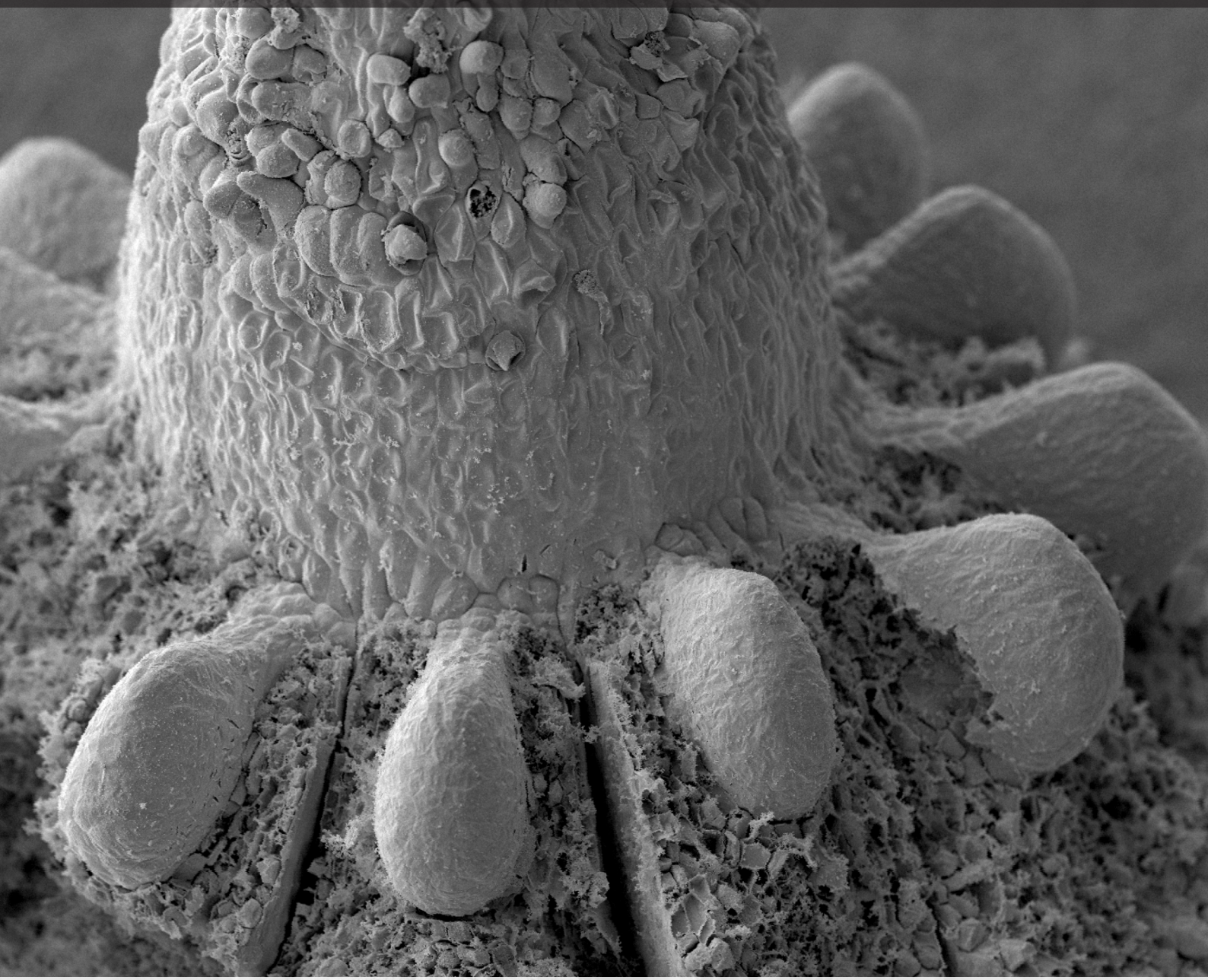

frontiers Research Topics

ISSN 1664-8714
ISBN 978-2-88945-440-2
DOI 10.3389/978-2-88945-440-2

About Frontiers

Frontiers is more than just an open-access publisher of scholarly articles: it is a pioneering approach to the world of academia, radically improving the way scholarly research is managed. The grand vision of Frontiers is a world where all people have an equal opportunity to seek, share and generate knowledge. Frontiers provides immediate and permanent online open access to all its publications, but this alone is not enough to realize our grand goals.

Frontiers Journal Series

The Frontiers Journal Series is a multi-tier and interdisciplinary set of open-access, online journals, promising a paradigm shift from the current review, selection and dissemination processes in academic publishing. All Frontiers journals are driven by researchers for researchers; therefore, they constitute a service to the scholarly community. At the same time, the Frontiers Journal Series operates on a revolutionary invention, the tiered publishing system, initially addressing specific communities of scholars, and gradually climbing up to broader public understanding, thus serving the interests of the lay society, too.

Dedication to Quality

Each Frontiers article is a landmark of the highest quality, thanks to genuinely collaborative interactions between authors and review editors, who include some of the world's best academicians. Research must be certified by peers before entering a stream of knowledge that may eventually reach the public - and shape society; therefore, Frontiers only applies the most rigorous and unbiased reviews.
Frontiers revolutionizes research publishing by freely delivering the most outstanding research, evaluated with no bias from both the academic and social point of view.
By applying the most advanced information technologies, Frontiers is catapulting scholarly publishing into a new generation.

What are Frontiers Research Topics?

Frontiers Research Topics are very popular trademarks of the Frontiers Journals Series: they are collections of at least ten articles, all centered on a particular subject. With their unique mix of varied contributions from Original Research to Review Articles, Frontiers Research Topics unify the most influential researchers, the latest key findings and historical advances in a hot research area! Find out more on how to host your own Frontiers Research Topic or contribute to one as an author by contacting the Frontiers Editorial Office: **researchtopics@frontiersin.org**

EVOLUTION OF REPRODUCTIVE ORGANS IN LAND PLANTS

Topic Editors:
Xin Wang, Nanjing Institute of Geology and Palaeontology, CAS, China
Zhong-Jian Liu, National Orchid Conservation Center of China, China
Borja Cascales-Miñana, Evo-Eco-Paleo, UMR 8198-CNRS, University of Lille, France
José Bienvenido Diez, University of Vigo, Spain

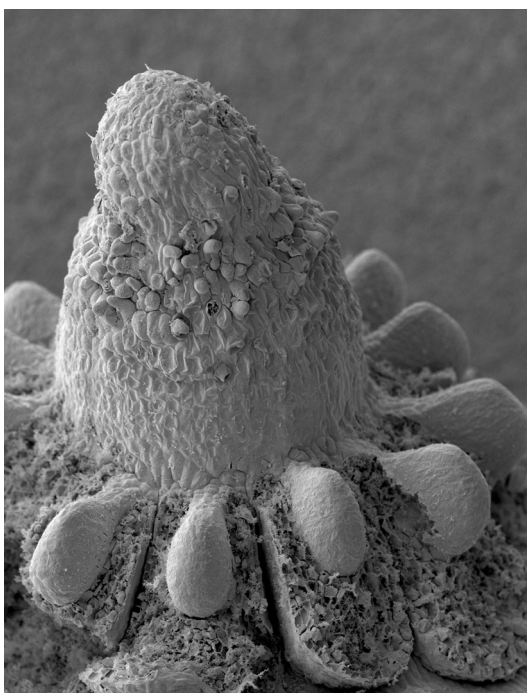

A dissected gynoecium of a basal angiosperm showing ovules attached to the floral axis.
Image: Xin Zhang (makexyz@163.com).

The great diversity of land plants (especially angiosperms) is mainly reflected in the diversity of various reproductive organs of plants. However, despite long time intensive investigations, there are still uncertainties and sometimes misunderstandings over the nature and evolution of reproductive organs in land plants. With the new advances made in various fields of botany (especially at molecular level), there is increasing light shed on some aspects of flowers

(reproductive organs of angiosperms). In this ebook, we collect 15 papers reporting new understanding on plant reproductive organs. These works range from morphology and anatomy to molecular regulatory networks underlying traditional observations. We understand this single book cannot reach our goal, but we do hope that this book can contribute to or initiate some efforts leading to the final solution of some problems concerning the homology and evolution of reproductive organs in plants.

Citation: Wang, X., Liu, Z-J., Cascales-Miñana, B., Diez, J. B., eds. (2018). Evolution of Reproductive Organs in Land Plants. Lausanne: Frontiers Media. doi: 10.3389/978-2-88945-440-2

Table of Contents

frontiers in Plant Science

EDITORIAL
published: 31 January 2018
doi: 10.3389/fpls.2018.00054

Editorial: Evolution of Reproductive Organs in Land Plants

Xin Wang[1], Zhong-Jian Liu[2], Borja Cascales-Miñana[3] and José B. Diez[4]*

[1] CAS Key Laboratory of Economic Stratigraphy and Palaeogeography, Nanjing Institute of Geology and Paleontology (CAS), Nanjing, China, [2] Orchid Conservation & Research Center, Shenzhen, China, [3] Evo-Eco-Paleo, UMR 8198-Centre National de la Recherche Scientifique, University of Lille, Villeneuve d'Ascq, France, [4] Department of Geosciences, University of Vigo, Vigo, Spain

Keywords: reproductive organs, morphology, anatomy, genes, evolution, flowers, hydridization, MADS-box

Editorial on the Research Topic

Evolution of Reproductive Organs in Land Plants

The evolution of plant life has left its footprints in various ways, either as fossils, as morphology and/or anatomy, or as genes embodied in cells of living organisms. Extant plants are the consequence of over-400-million-years of evolution that are reflected in the innovations of reproductive organs throughout their evolutionary history, such as the occurrence of seeds, ovaries, flowers, inflorescences, and their functions. Thus, understanding different plant reproductive organs and their innovations is essential for the correct interpretation of plant evolution and their phylogenetic relationships. This eBook aims to shed light on the evolution of reproductive organs through papers documenting variations of reproductive organs at different levels, ranging from molecular to morphological, in hopes of triggering further investigations in this field. Below, we highlight the progresses covered in this thematic special volume.

Scientific observation is an active process in which an observer recognizes objects that fall within pre-existing concepts. Considering this framework, it is assumed that (1) perspective decides the outcome of observations and that (2) a new perspective could create the foundation for a new observation. In light of new concepts of sexual reproduction and "Plant Morphogenesis 123," Bai organized the major morphological traits into five categories, and viewed a plant as a colony of integrated plant developmental units that are each produced via one life cycle. This function-based perspective allows us to view plants in a new way.

Embryogenesis and seed formation are key events in the history of plants. Three papers in this eBook address these issues from different perspectives. To elucidate the seed maturation program, Han et al. surveyed the evolution of the LAFL [L: *LEAFY COTYLEDON1* (*LEC1*) and *LEC1-LIKE* (*L1L*), belonging to *NF-YB* gene family; A: *ABSCISIC ACID INSENSITIVE3* (*ABI3*); F: *FUSCA3* (*FUS3*); L: *LEC2* (*LEAFY COTYLEDON2*). The latter three genes belong to B3-AFL gene family related to embryo development] gene network, which is thought to orchestrate the accumulation of storage compounds and acquisition of desiccation tolerance in seed maturation, among various major plant lineages. Their result indicates that the origin of the embryo-development-related AFL gene family dates back to a common ancestor of the bryophytes and vascular plants. LAFL genes are likely related to spore and seed maturation, and the varying expression patterns of LAFL genes across the major vascular plant lineages may shed new light on the diversifying history of seed plants. Meanwhile, Li et al. and Fang et al. performed related studies using *Adiantum capillus-veneris* from different perspectives. Li et al. characterized the expression patterns of six embryogenesis-associated genes during the somatic embryogenesis of *A. capillus-veneris*. Some of these gene families diversified rapidly in embryophytes, suggesting a rapid evolution of embryogenesis-associated genes in the tracheophyte development. Fang et al. examined the

OPEN ACCESS

Edited by:
Elena M. Kramer, Harvard University, United States

Reviewed by:
Annette Becker, Justus Liebig Universität Gießen, Germany

****Correspondence:***
Xin Wang
xinwang@nigpas.ac.cn

Specialty section:
This article was submitted to Plant Evolution and Development, a section of the journal Frontiers in Plant Science

Received: *08 December 2017*
Accepted: *10 January 2018*
Published: *31 January 2018*

Citation:
Wang X, Liu Z-J, Cascales-Miñana B and Diez JB (2018) Editorial: Evolution of Reproductive Organs in Land Plants. Front. Plant Sci. 9:54. doi: 10.3389/fpls.2018.00054

expression pattern of AcLEC1 in *A. capillus-veneris*, and linked sugar treatments with induction of AcLEC1 expression and accumulation of storage products (two characteristic features of seed maturation). Thus, inductive expression of LEC1 homologs during embryogenesis appears to be a key innovation for the origin of seeds.

For long time, the nature and origin of the placenta and carpel (especially in the Centrosperms) has been perplexing, so a rational interpretation is badly needed. Guo et al. conducted a detailed anatomical observation of the vascular bundles within the pistils of *Dianthus chinensis*, and propose a novel interpretation for the nature and origin of these carpels. The vascular bundles are amphicribral in the placenta and collateral in the ovary wall. In light of the discoveries of modern molecular biology, in which development of the placenta and ovary wall have been found to be controlled by separate gene combinations, Guo et al. favors the composite nature of carpels suggested by the Unifying Theory.

The fantastic movement of petals during floral expansion attracts much attention from the general public. Liu et al. studied thermogenic *Magnolia denudata* to explore the biological roles of petal movements. They found that the floral chamber formed by petal movements could facilitate development of the male gametophyte and seed set, and that pollination could accelerate the closure of the inner petals. These findings elucidate the biological roles of petal movements.

Differentiation of flowers within the same inflorescence is an interesting evo-devo phenomenon. Sterile and fertile flowers play important roles in pollinator attraction and sexual reproduction. Lu et al. investigated this regulatory mechanism using *Viburnum macrocephalum* f. *keteleeri*. They developed a *de novo*-assembled floral reference transcriptome, and compared the expression patterns of fertile and sterile flowers at different developmental stages. Combined with morphological and cytological differences between fertile and sterile flowers, they identified many genes and transcription factors potentially involved in regulating the differentiation and development of fertile and sterile flowers within the same inflorescence. This research sheds new light on genes regulating the differentiation of flowers of angiosperms.

Tapetum development is important for the successful reproduction of plants. Previous studies indicated that a "CTCC" sequence within DYT1 (a core regulatory gene of anther development) promoter was indispensable for correct DYT1 expression. Zhou et al. employed site mutation assays to identify the function roles of these nucleotides. They found that the "T" and final "C" of "CTCC" were essential for the temporal and spatial specificity of DYT1 expression. The substitution of two flanking nucleotides of "CTCC" hardly affected the normal promoter function, suggesting that the "CTCC" sequence is a canonical *cis*-element.

Hybridization accompanied by polyploidization and apomixis is a driving force of evolution and speciation in many plants. *Cotoneaster* (Rosaceae), which includes about 150 species, is a good example to study the evolutionary process of hybridization associated with polyploidy and apomixis. Li et al. investigated all the *Cotoneaster* taxa distributed in a small region of Malipo, Yunnan, China. Their study provided convincing evidence for natural hybridization between *Cotoneaster dielsianus* and *Cotoneaster glaucophyllus*. They revealed that all the hybrid individuals were derivatives of one initial F1 via apomixis, and *C. glaucophyllus* served as maternal parent at the initial hybridizing event. Anthropological disturbance appears to have facilitated the hybridization between *C. dielsianus* and *C. glaucophyllus*.

Both compatible and incompatible pollen-stigma interactions are of interest in botany. Zhang et al. applied RNA-seq technology in a comprehensive time-course experiment to explore gene expression during compatible/incompatible pollen-stigma interactions in *Brassica napus*. In contrast to the moderate changes in gene expression both in compatible pollination (PC) and incompatible pollination (PI) within 10 min, drastic changes showed up by 30 min (especially in PI). Stage specific DEGs (Differentially Expressed Genes) were identified. The most highly expressed genes were identified and annotated, and the top 10 highly expressed genes and 37 activated metabolic pathways were revealed. The incompatible response had more complicated signal transduction networks. Niu et al. identified two orchid species displaying gametophytic self-incompatibility (GSI) and investigated their molecular mechanisms by comparative genomics approaches. They analyzed the female determinants of RNase-based GSI in both monocots and eudicots, and identified a novel SI mechanism in orchids.

MADS-box genes are important for floral organ morphogenesis. Two papers in this eBook studied these genes to address the evolution of flowers. Chen et al. analyzed the genomes and large-scale transcriptomes in all the orders of gymnosperms and basal angiosperms. They identified gymnosperm orthologs of 11 genes and characterized a novel subfamily, GMADS, within gymnosperms. ABCE prototype genes have relatively conserved gene number in gymnosperms, but expanded in angiosperms, whereas SVP, SOC1, and GMADS had demonstrated a reversed pattern, namely, expanded in gymnosperms but conserved in angiosperms. The evolutionary history of all MIKC^c gene clades apparently reflects the history of seed plants (including gymnosperms and angiosperms). The duplication and expression transition of ABCE model MIKC^c genes in the ancestor of angiosperms may have triggered the occurrence of the first flower, providing new insights on the origin of the flowers. Cheng et al. performed a whole-genome survey and identified 34 MADS-box genes in the bamboo species *Phyllostachys edulis*. Their detailed analysis of gene structure and motifs, phylogenetic classification, comparison of gene divergence, and duplication indicated that the ABCDE model is quite conservative throughout monocots and eudicots, and that PheMADS15 might be a regulator of flowering transition in *P. edulis*.

The interaction between the stigma and its insect pollinators is important for successful pollination. Jin et al. studied *Mazus miquelii* (Phrymaceae) with a bilobed stigma to characterize this interaction. They found that larger pollinators transferred more pollen grains to the stigma, causing a rapid stigmatic response and a higher percentage of permanent closures. The permanent closure of a stigma was determined by the size of stigmatic pollen

load. The stigma behavior in *M. miquelii* is likely a mechanism of pollinator selection to maximize pollination success.

The Diptera (true flies) are among the most important flower-visiting insects, and they were abundant in the Mesozoic. Zhang and Wang reviewed the fossil record and early evolution of some Mesozoic lower brachyceran flies together with new records in Burmese amber. The fossil records revealed that some flower-visiting groups diversified in the mid-Cretaceous. The evolution of brachyceran groups appears coupled with that of angiosperms.

It is apparent that the limited number of papers in this eBook cannot tell all the stories of evolution of reproductive organs in plants. We are sure future research will enhance our understanding of this topic.

AUTHOR CONTRIBUTIONS

All authors listed have made a substantial, direct and intellectual contribution to the work, and approved it for publication.

FUNDING

This research was supported by National Natural Science Foundation of China (41688103, 91514302, 41572046) awarded to XW; and State Forestry Administration of China (No. 2005-122), Science and Technology Project of Guangdong (No. 2011B060400011), and Special Funds for Environmental Projects of Shenzhen (No. 2013-02) awarded to Z-JL.

Conflict of Interest Statement: The authors declare that the research was conducted in the absence of any commercial or financial relationships that could be construed as a potential conflict of interest.

frontiers in Plant Science

HYPOTHESIS AND THEORY
published: 15 March 2017
doi: 10.3389/fpls.2017.00345

Reconsideration of Plant Morphological Traits: From a Structure-Based Perspective to a Function-Based Evolutionary Perspective

*Shu-Nong Bai**

State Key Laboratory of Protein and Plant Gene Research, College of Life Science, Quantitative Biology Center, Peking University, Beijing, China

This opinion article proposes a novel alignment of traits in plant morphogenesis from a function-based evolutionary perspective. As a member species of the ecosystem on Earth, we human beings view our neighbor organisms from our own sensing system. We tend to distinguish forms and structures (i.e., "morphological traits") mainly through vision. Traditionally, a plant was considered to be consisted of three parts, i.e., the shoot, the leaves, and the root. Based on such a "structure-based perspective," evolutionary analyses or comparisons across species were made on particular parts or their derived structures. So far no conceptual framework has been established to incorporate the morphological traits of all three land plant phyta, i.e., bryophyta, pteridophyta and spermatophyta, for evolutionary developmental analysis. Using the tenets of the recently proposed concept of sexual reproduction cycle, the major morphological traits of land plants can be aligned into five categories from a function-based evolutionary perspective. From this perspective, and the resulting alignment, a new conceptual framework emerges, called "Plant Morphogenesis 123." This framework views a plant as a colony of integrated plant developmental units that are each produced via one life cycle. This view provided an alternative perspective for evolutionary developmental investigation in plants.

Keywords: morphological traits, function-based evolutionary perspective, sexual reproduction cycle, plant developmental unit, plant morphogenesis 123

OPEN ACCESS

Edited by:
Xin Wang,
Nanjing Institute of Geology and Paleontology (CAS), China

Reviewed by:
Dazhong Dave Zhao,
University of Wisconsin-Milwaukee, USA
Meng-Xiang Sun,
Wuhan University, China

***Correspondence:**
Shu-Nong Bai
shunongb@pku.edu.cn

Specialty section:
This article was submitted to Plant Evolution and Development, a section of the journal Frontiers in Plant Science

Received: *13 January 2017*
Accepted: *27 February 2017*
Published: *15 March 2017*

Citation:
Bai S-N (2017) Reconsideration of Plant Morphological Traits: From a Structure-Based Perspective to a Function-Based Evolutionary Perspective. Front. Plant Sci. 8:345. doi: 10.3389/fpls.2017.00345

INTRODUCTION

According to the Oxford Dictionary, a "trait" is defined as "a distinguishing quality or characteristic, typically one belonging to a person" and more specifically, a "genetically determined characteristic." Biologists know that characteristics ranging from a single base pair of nucleic acid to the overall shape of an organism can be determined genetically. Therefore, traits are meaningful only when considered in a specific context. Here, I will discuss traits in terms of morphology and consider morphological traits from a function-based evolutionary perspective.

Where and how present-day organisms were originated in the biological world are long-lasting, fundamental questions. While Darwin's theory of evolution established a conceptual framework, the survival of fittest under natural selection, for answering such questions, the detailed mechanisms remain elusive. For many years, the ancestral relationships or family lineages among

species, i.e., phylogeny, were mainly determined based on the similarity of morphological traits. During the past decades, one of the most impressive advances in biology was the discovery, based on mutant analyses, that many complicated morphological traits are determined by a single or a few proteins encoded by genes inherited in a Mendelian manner and that some such genes are conserved across species. This discovery prompted scientists to explore whether innovations in morphological traits during evolution were associated with a gain or loss of the genes determining these traits. Such analyses launched the field of "evolutionary developmental biology," abbreviated as "Evo-Devo" (Gilbert et al., 1996; Goodman and Coughlin, 2000; Raff, 2000; Gilbert, 2003).

Evo-Devo studies initially focused on comparisons of animal genes. It has long been known that most animal individuals develop from a single cell (zygote) and that their morphological traits emerge or form primarily through embryogenesis. This common morphogenetic pattern, centering mainly on embryogenesis, establishes a framework for comparing morphological traits among different species.

Investigations of plants, like those of animals, began with observations of their appearance, or "surface" according to Gifford and Foster (1989). Traditionally, a plant was considered to be consisted of three parts, i.e., the shoot, the leaves, and the root (Strasburger et al., 1976). Based on such a "structure-based perspective," evolutionary analyses or comparisons across species were made on particular parts or their derived structures. However, morphogenetic patterns in plants are fundamentally different from those of animals. One of the most prominent differences is that no visible process equivalent to animal embryogenesis has been observed in the plant kingdom (Waddington, 1966). Some authors have defined plant embryogenesis as encompassing the period from zygote to seed formation (Goldberg et al., 1994). If this definition is valid, mosses and ferns do not undergo "embryogenesis," since these plants do not produce seeds. The concept of "alternation of generations" was proposed by Hofmeister in the 1850s (Kaplan and Cooke, 1996). This concept, i.e., that all the land plants have both sporophyte (diploid) and gametophyte (haploid), has been used as a framework for comparing morphological traits among diverse species. In recent years, much effort has been devoted to explore evolutionary innovations focusing on the particular parts or their derived structures across phyla (reviewed by Harrison, 2017). However, most of these studies have involved comparing closely related angiosperm species (Irish and Benfey, 2004; Preston et al., 2011; Della Pina et al., 2014). This situation aroused an enthusiastic discussion at a recent NPH symposium about whether there are unique themes that define plant Evo-Devo (Liao et al., 2016).

It is perfectly legitimate to choose any morphological trait, such as the number or color of spots on a petal or the formation of root hairs, as a target for exploring the underlying regulatory mechanism and its origin in closely related species (Martins et al., 2016) or even across phyla (Menand et al., 2007). These efforts underscore the well-established principle that new traits emerge from interactions between genetic variation and environmental selection, with some details differing among studies. However, core questions in evolutionary theory related to plants remain, such as how photoautotrophic organisms diverged from a common ancestor, and what key evolutionary innovations resulted in the divergence of the major lineages.

Advances in DNA sequencing technology make it no longer difficult to obtain genome information for a species of interest, nor to find differences among genomes used for comparison. The problem is how to determine what these sequence differences truly mean. Two questions need to be answered: whether the differences in DNA sequences are responsible for particular traits, and whether the traits in the species being compared are evolutionarily related. It is relatively easy to determine the causal relationship between a single DNA sequence and the targeted trait through modern genetic analysis. However, similarity of DNA sequences may not necessarily indicate evolutionary relationships of traits of interest, as protein complexes, metabolic processes, and regulatory networks (in short, cellular functions) are highly complex and approximately 10 times more proteins than genes have been annotated. From this perspective, elaborating evolutionary innovations or relationships between traits is beyond the scope of DNA sequence analysis.

Traditionally, morphology deals with the study of the form and structure of an organism. Recent Evo-Devo studies have explored the relationships between morphological traits and the (possibly) corresponding genes from an evolutionary perspective. However, a fundamental element has largely been neglected in plant Evo-Devo studies, the role of photoautotrophism. If we are asked to identify the most basic difference between plants and animals, the best answer is likely their manner of energy acquisition: plants are photoautotrophic and animals are heterotrophic. Considering the essential roles of the efficiency of energy acquisition and environmental adaptation in the evolutionary selection of morphological traits, if we analyze morphological traits from a function-based evolutionary perspective rather than structure-based perspective, derived from the tradition of morphology, could we uncover a new scenario?

UNDERLYING PRINCIPLES FOR INVESTIGATIONS BASED ON A FUNCTION-BASED EVOLUTIONARY PERSPECTIVE

Based on the current literature, morphological traits can be grouped in roughly three classes: one includes morphological traits investigated due to personal interest, such as sepal color or spots on petals; another comprises those with application significance, such as crop productivity and quality; and the third includes those with evolutionary importance, such as vascular tissues, seeds and flowers, associated with particular taxonomic groups. These ways of grouping and comparisons of morphological traits are all derived from the traditional structure-based perspective. To align morphological traits from a function-based evolutionary perspective, some background information is needed.

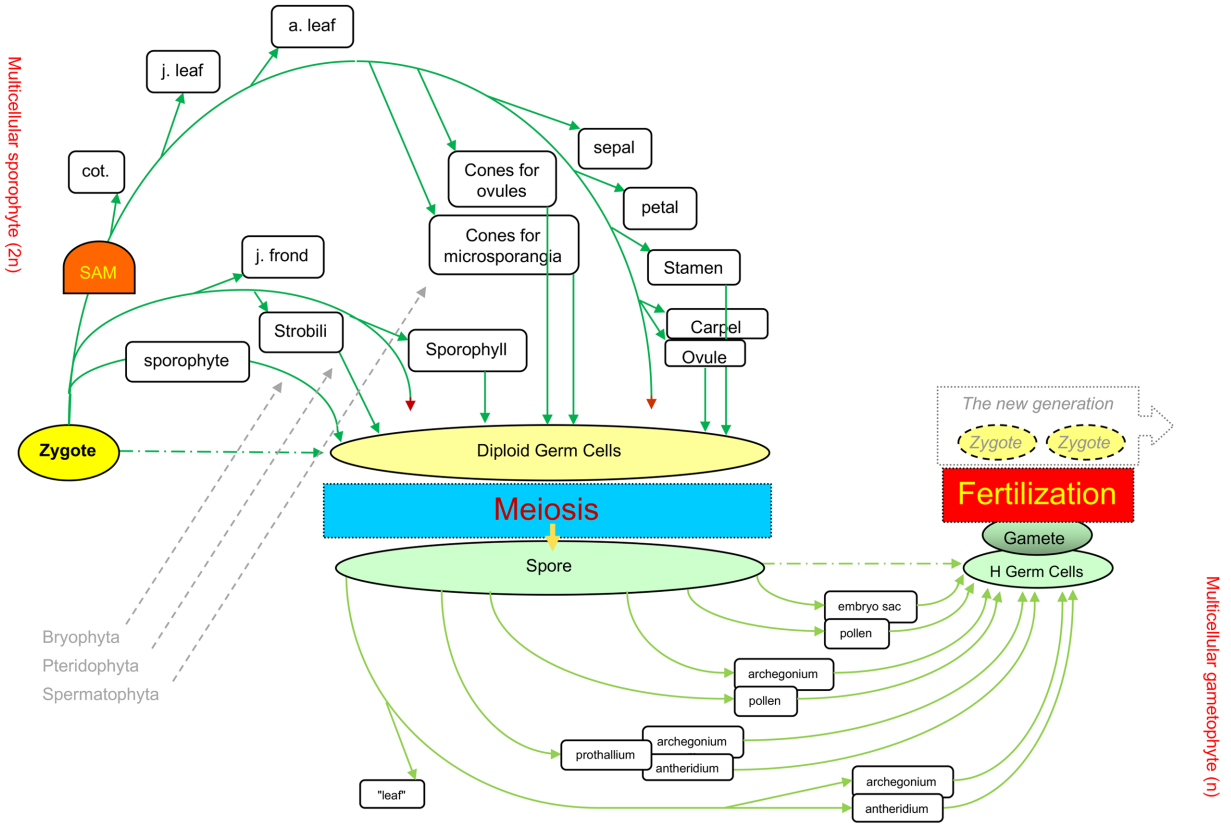

FIGURE 1 | Different levels of elaboration around the core processes in the life cycles of the three plant phyla. The sexual reproduction cycle (Bai, 2015a) from one zygote to the next generation's zygotes through meiosis and fertilization is the backbone of the lifecycle for all three land plant groups, Bryophyta, Pteridophyta, and Spermatophyta. Green arrows show the differentiation of various organ types in diploid phase, and light green for organs in haploid phase. Dark red arrowheads indicate unlimited tip growth activity. cot., cotyledons; j. leaf, juvenile leaf (e.g., rosette leaves in *Arabidopsis*); a. leaf, adult leaf (e.g., cauline leaves in *Arabidopsis*). This figure was revised from Figure 1.9 in Bai and Xu (2013).

The current mainstream concept of plant developmental programs (the underlying mechanism for morphogenesis) states that plants have an indeterminate developmental program (Goldberg, 1988). However, when all land plants are considered, their life cycles include clear starting and ending points, i.e., zygotes and gametes, respectively. Between these two points, another unique cell turns from diploid to haploid, i.e., the meiotic cell (which arises from the diploid germ cell, DGC), leading to meiosis and spore formation (Bai, 1999, 2015a; Bai and Xu, 2013; Zhao et al., 2017; **Figure 1**).

The core process of the eukaryotes life cycle comprises three unique or core cells (zygotes, meiotic cells, and gametes), which serve as reference points, and three events that occur at the unicellular level, i.e., meiosis, fertilization, and heterogametogenesis (Bai, 1999). Such a core process was recently described as an ancestral process originating from unicellular eukaryotes, and designated as the sexual reproduction cycle (SRC) (Bai and Xu, 2013; Bai, 2015a). The SRC represents a modified cell cycle that functions as the ultimate mechanism that helps eukaryotes adapt to unpredictable environmental changes and serves as a backbone upon which multicellular organisms are derived via the interpolation of multicellular structures into the two (diploid and haploid) intervals of the life cycle (Bai, 2015a; **Figure 1**).

Possibly owing to their different manners of energy acquisition, i.e., photoautotrophism for plants and heterotrophism for animals and fungi, three different patterns of interpolation of multicellular structures have evolved in animals, fungi, and plants (**Figure 2**). The formation of multicellular structures in the animal and fungal kingdoms is interpolated once into the first (diploid) and second (haploid) intervals of the SRC respectively. By contrast, the formation of multicellular structures in the plant kingdom is interpolated twice: into both intervals of the SRC. The different patterns of interpolation in multicellular structure formation in animals versus plants results in two different developmental programs (Bai, 2015b, 2016; **Figure 3**). Animals develop via the "dichotomous mode," meaning that cells derived from the zygote soon diverge into two lineages: one that differentiates into the germline, functioning as a carrier of the SRC, and one that differentiates into the soma, functioning in energy acquisition and environmental responses. The early stages of soma differentiation, together with germline development, can be considered to represent embryogenesis. By contrast, plants develop via the "double-ring mode," meaning

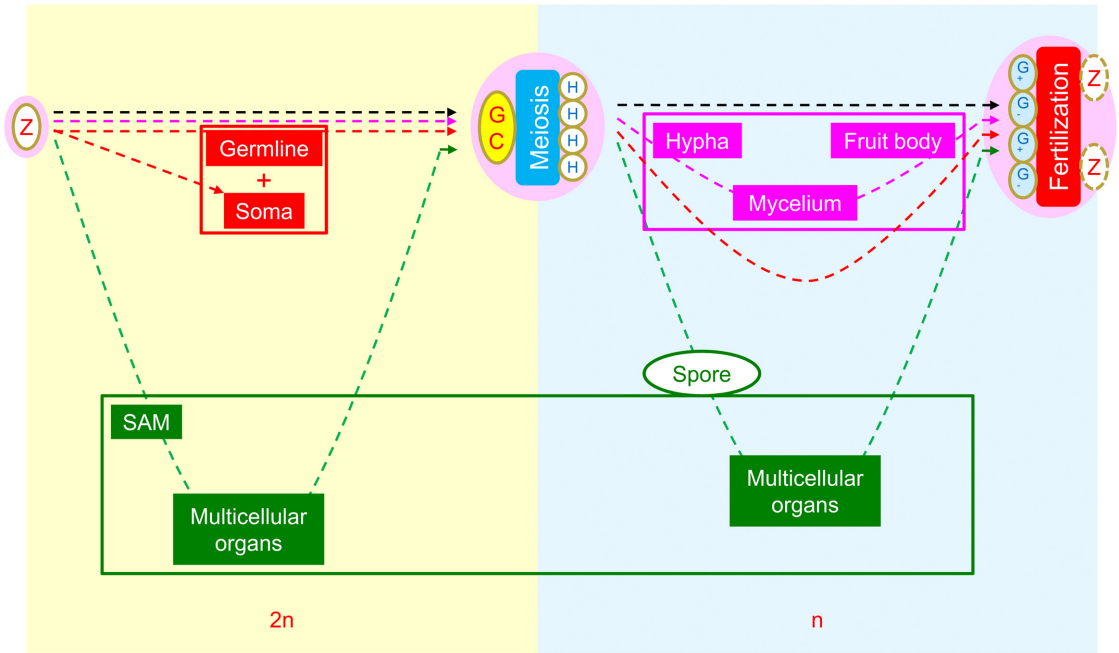

FIGURE 2 | Comparison of morphogenetic strategies of animals, fungi, and plants within the framework of the SRC. Yellow background indicates the diploid phase and blue background indicates the haploid phase. In the intervals between zygote and diploid germ cells, the interpolation of multicellular structures occurs in animals (red) and plants (green), whereas none are present in fungi (pink). In the intervals between meiotically produced cells and gametogenic cells, the interpolation of multicellular structures occurs in fungi and plants but not in animals. Reprinted from Bai (2015a).

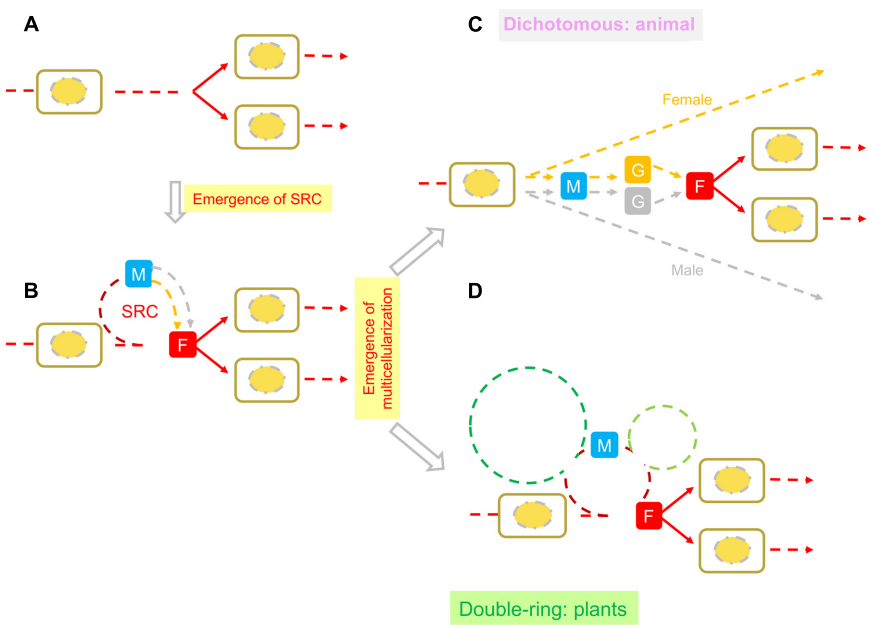

FIGURE 3 | Comparison of SRC-derived developmental modes in animals and plants. (A) Represents a cell cycle, i.e., one diploid cell becomes two cells through mitosis; **(B)** Represents the SRC (sexual reproduction cycle, Bai, 2015a). Two arrows (orange and gray) between M (meiosis) and F (fertilization) represent heterogametogenesis. **(C)** Represents the "dichotomous mode" for animal development. Orange and gray lines represent female and male soma and germlines, respectively, and orange and gray Gs represent female and male gametogenesis, respectively. **(D)** Represents the "double-ring mode" of plant development. On the SRC backbone, the green dashed ring on the left represents diploid multicellular structures composed of various types of organs; the light green ring on the right represents haploid multicellular structures composed of various types of organs. This figure was modified from Figure 16 in Bai (2016).

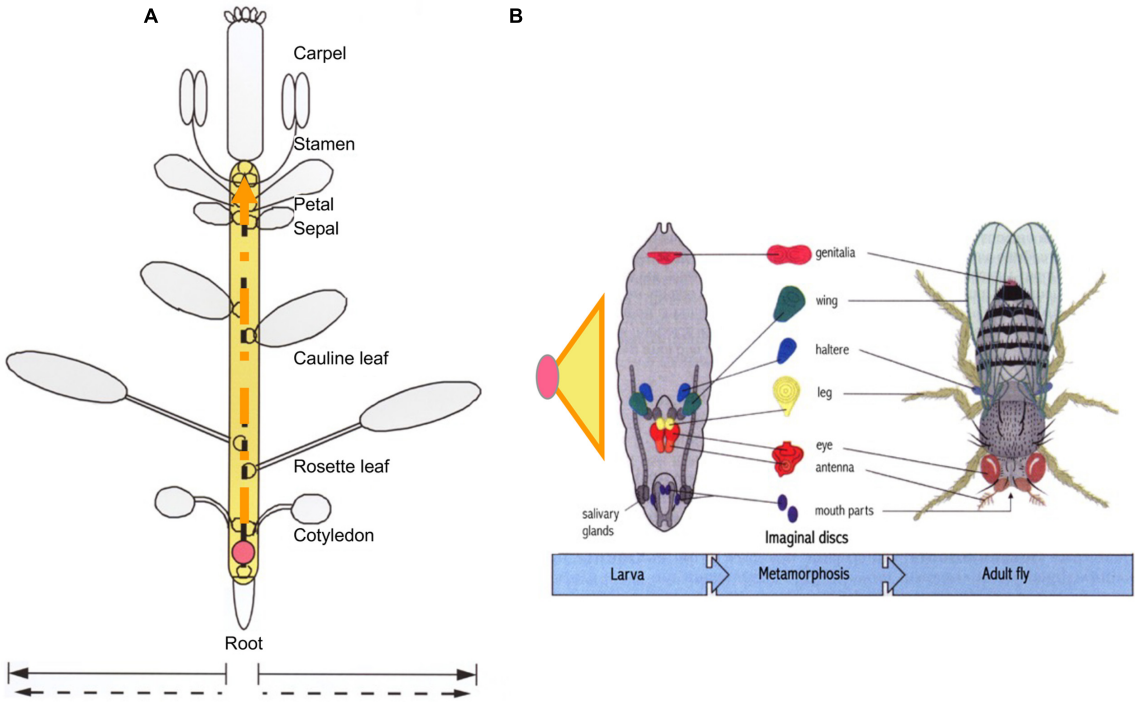

FIGURE 4 | Comparison of developmental units in plants and animals required for life-cycle completion. While plant growth tip generated from a zygote (pink circle) can produce numerous lateral organs and branches, only seven organ types in *Arabidopsis* are present in a complete the life cycle **(A)**. The half circles along the dashed orange arrow represent organ primordia. By comparison, the basic structure required for *Drosophila* to complete its life cycle is the embryo, elaborated from a zygote to larva. Embryogenesis is represented by an orange-lined yellow triangle **(B)**. Unlike animal individuals, which contain limited types and numbers of organs in a determined pattern, the functionally equivalent structure in plants is the imaginal unit shown in **(A)**, referred to as a "developmental unit," rather than the whole plant. According to this perspective, the structural equivalent of an animal embryo would be the process represented as the yellow area in **(A)**. Orange dashed lines in the yellow region indicate that the process is relatively open but ultimately limited. **(B)** Was modified from Figures 2–6 in Wolpert et al. (2007) edited Principles of Development. This figure was modified from Figure 6 in Bai (1999).

that all cells derived from the zygote differentiate into somatic structures required for photoautotrophy. In response to external and internal stress, along with increased photosynthetic tissue area, some cells are induced to differentiate into DGCs to help the plant prepare to adapt to these stresses through autonomous genetic variations generated via meiosis. This process represents the first ring, from zygote to DGCs via the formation of sporophytes with sequentially formed organ types (e.g., in *Arabidopsis*: cotyledons, rosette and cauline leaves, sepals, petals, stamens, and carpels). After meiosis, multicellular structure formation is interpolated into the second interval of the SRC, from spores into haploid germ cells (HGCs, which differentiate into gametes), and the second ring (gametophyte) is formed.

Based on the above view, if embryogenesis (consisting of soma and germline development, i.e., dichotomous development) is the core process shared by all animal species during morphogenesis, then double ring development can be considered the core process shared by all plant species during their morphogenesis. Taking *Arabidopsis* as an example, the multicellular structures carrying out the core process in the first (diploid) ring can be thought of as a combination of limited types (not numbers) of organs derived from the growth tip (**Figure 4**). Such a combination has been designated as a "plant developmental unit (PDU)" (Bai, 1999; Bai and Xu, 2013). The early development of these organs (i.e., the primordia) is therefore functionally equivalent to animal embryogenesis, and was designated as a "virtual embryo" by Da-Ming Zhang (Institute of Botany, Chinese Academy of Sciences), in contrast to the physical animal embryo (a "visual embryo"; Bai, 2016).

From this perspective, it becomes clears that we can use the "SRC-derived double ring" as a frame of reference to align morphological traits for Evo-Devo analysis. As morphological traits are regarded as evolutionary consequences of adaptation to improve energy acquisition (photosynthesis), environmental responses (particularly for SRC completion), and growth in extreme environments, I refer to this view of trait description and classification as a "function-based evolutionary perspective."

ALIGNMENT OF TRAITS FROM A FUNCTION-BASED EVOLUTIONARY PERSPECTIVE

Traditionally, plant morphology refers to investigations of "hidden aspects of form, structure, and reproduction that

constitute the bases for the interpretation of similarities and differences among plants" (Gifford and Foster, 1989). Although more sophisticated tools, including microscopy, genetics, and molecular biological tools, have progressively been developed and applied to these types of investigations, all of the targeted phenomena, i.e., morphological traits, are initially described based on forms or "surface perspectives" observed by the human eye and interpreted through the faculty of reasoning. It is therefore understandable that observers after the 18th century treated plants as individuals (like animal individuals) comprising three major parts: the shoot, the leaves, and the root (Strasburger et al., 1976). Morphological traits were compared among the structures of "individuals" of various species, primarily following the principles of homology and analogy, referred here as a structure-based perspective. However, the founding fathers of modern botany, such as Grew and Malpighi in the 17th century, treated a plant as a colony, in which each bud is treated as an individual that completes a life cycle (review in Arber, 1950). Although this insightful concept has been marginalized by the mainstream community of modern plant morphologists, it was utilized by a few scholars such as Waddington (1966), who wrote that "a branch... gives rise to a whole new cycle of growth and development." The concept of a SRC-derived double ring mode of plant development (as described above, with branches representing partial units, as they generally produce organ types that had not yet formed from where the buds had initiated) echoes and is reviving this classic concept (Bai, 1999, 2015a,b, 2016; Bai and Xu, 2013). In the remainder of this article, I will attempt to align morphological traits from a function-based evolutionary perspective.

First, morphological traits must be classified into unicellular and multicellular traits. As mentioned above, SRC first evolved in unicellular eukaryotes. All differentiation processes and interactions completed and exhibited at the unicellular level could be classified as morphological traits at the unicellular level. Included in this class are cell shape, size, and structure; cell division and fusion; and modified cell cycle, i.e., the SRC (consisting of three core cell types and the three core events mentioned above). However, due to space constraints, these traits will not be discussed here.

The other class of morphological traits includes those exhibited at the multicellular level. These traits can be further classified into five categories: (1) those associated with the formation of multicellular structures facilitating photosynthesis and therefore representing outgrowth of a larger structure from the unicellular SRC; (2) those exhibiting diversified differentiation of multicellular structures upon exposure to internal and external stresses, such that structures become smaller and finally return to the unicellularity of the SRC; (3) those derived to ensure heterogametogenesis (sex differentiation); (4) those facilitating the completion of the SRC and the life cycle (sex behavior); and (5) those derived for adaptation to extreme or particular environmental stresses.

Morphological Traits Facilitating Photosynthesis

Table 1 shows an alignment of morphological traits that facilitate photosynthesis from the function-based evolutionary perspective. In this category, the key function is facilitating photosynthesis. The multicellular structures required for this function can form in both diploid (sporophytes) and haploid (gametophytes) in all three land-plant phyla, i.e., bryophytes (mainly gametophytes), pteridophytes (both sporophytes and gametophytes), and spermatophytes (mainly sporophytes). The differentiation of multicellular structures can be further grouped into three subcategories: (1) basic structures for maximizing photosynthetic surface area (facilitating energy acquisition), e.g., linear or columnar structures (filaments/twigs/stems), foliage structures (leaves), and branches; (2) multicellularized growth tips; and (3) structures for optimizing photosynthesis, such as stomata.

From this perspective, it is clear that the morphological traits considered in traditional morphology, such as shoots, leaves, and roots, are derived from combinations of the elements listed in **Table 1**. It also elucidates why the Lindenmayer's L-system, elaborated by Prusinkiewicz, which treats plant morphogenesis as an "axil tree" following "rewriting" rules, is so powerful for simulating plant morphology and morphogenetic processes (Prusinkiewicz and Lindenmayer, 1990[1]). Such astonishing success implies that there must be simple principles underlying plant morphogenesis, in contrast to the traditional belief that the rules for plant morphogenesis are species-specific and difficult to define. Furthermore, from this perspective, it is clear that, as suggested by the L-system, plant morphogenesis is carried out by the repeated use of similar principles or rules to generate similar structures with modifications, resulting in endless branching. This concept explains the insight the founding fathers proposed: that each bud as an individual to complete its life cycle. The next challenge is to identify the molecular mechanisms underlying these "simple principles."

Morphological Traits Associated with Decrease of Multicellularity upon Exposure to Stress

As mentioned above, SRC was proposed to represent the ultimate mechanism that allows plants adapt to unpredictable environmental changes (Bai, 2015a). This mechanism facilitates adaptation by autonomously increasing genetic variations through meiosis and transmitting the best adaptations to the next generation through fertilization. Since plants are photoautotrophic organisms, they acquire energy through photosynthesis: the larger the surface area available for photosynthesis, the better. However, the larger the photosynthetic surface, the larger its interface with the environment, increasing the requirement for the plant to cope with unpredicted environmental changes and for internal mechanical support for this large surface. This internal mechanical support, as far as we know, comes from

[1]http://algorithmicbotany.org

TABLE 1 | Alignment of morphological traits facilitating photosynthesis from a function-based evolutionary perspective.

	Subcategories	Underlying factors				Morphology observed		Reference
Form of multicellular structures for photosynthesis, away from unicellularity in the SRC	Axial growth for increase of photosynthetic surface area	Linear growth	Region	Speed		The combination of growth region and speed results in diversified patterns in axial structures, which serve as basic elements for more complicated structures such as stems, leaves, and roots (a particularly stem-like structure)		Ligrone et al., 2012; Raven and Edwards, 2001; Prusinkiewicz and Lindenmayer, 1990
			Tip	Quick, slow, and stopped				
			Middle					
			Base					
		Branching	Single plane	Asymmetric		Alternate branching of stems		Gifford and Foster, 1989
				Combination of symmetric and asymmetric	Non-webbed	Opposite branching of stems		Tsukaya, 2014; Scagel, 1984
					Webbed	Foliage structures (leaves) in all three phyla (bryophytes, pteridophytes, and spermatophytes)		
			Multiple planes			Other forms of branching, e.g., spiral		
	Multicellularized growth tip	Randomly arranged				Gymnosperm SAM		Gifford and Foster, 1989
		Layered arranged				Angiosperm SAM		
	Optimizing photosynthesis	CO_2: opening to air				Stomatal complex		Han and Torii, 2016
		H_2O		Absorption		Root hairs and rhizoids		Jones and Dolan, 2012
				Transportation		Vascular bundles	Xylem	Lucas et al., 2013
							Phloem	
							Cambium	
		Light: phototropism				Particular cell type or differential growth		Briggs, 2014

the cell wall. In turn, cell walls generate internal mechanic stress. This factor, along with the increase in photosynthetic surface area, increases internal/external stresses and affect the morphogenetic process to (in time) bring about new morphological traits.

Table 2 shows an alignment of morphological traits associated with the decrease of multicellularity back toward unicellularity in the SRC upon stress, from a function-based evolutionary perspective. The first type of change in this category is a reduction in photosynthetic surface area. Such changes are induced by the increased stress that occurs along with the increased photosynthetic surface area. Regardless of whether the direct causes of this stress are internal, external, or a combination of these, the resulting changes should be sequential and gradual. Using *Arabidopsis* as an example, sequential changes in organ type are observed, from rosette leaves to cauline leaves to sepals, petals, stamens, and carpels (**Figure 4**). Even among rosette leaves, there are obvious sequential changes in leaf shape and size (Poethig, 1997). In addition, at higher latitudes, day-length and temperature exhibit seasonal changes, imposing additional environmental stress on plants. Traditionally, these changes were separately investigated as phase changes for sequential changes in rosette leaf shape and size (Poethig, 1990), flowering for changes from rosettes to bolting (Bernier et al., 1981; Koornneef et al., 1991), and floral organ identity determination for sequential changes in the four floral organ types (Coen and Meyerowitz, 1991). Such a separation was pragmatically sound in the last century. Therefore, these changes have received tremendous amounts of attention, and great progress has been made in understanding the underlying genetic mechanisms. However, a continuity of organ-type changes has been also noted (Bernier et al., 1981; Lord et al., 1994). Such continuity has been supported at the molecular level, as miR156 play roles in both heterophylly and flowering (reviewed by Poethig, 2013). From the perspective of the SRC, the continuity viewpoint might represent a better description of this process than the traditional ones described above, and it is possible to integrate all of the data generated separately into this new paradigm (Bai, 2016; **Figures 1**, **3**, **4**).

The second type of morphological traits in the decrease of multicellularity category involves the transition from somatic cells to germ cells. These changes essentially occur at the unicellular level and will not be discussed here in detail. However, since all of these changes occur in cell clusters in either diploid or haploid multicellular structures, they are considered here to represent a single subcategory.

The third type of morphological trait in this category involves those I collectively refer to as "-ium" formations: the sporangium, antheridium, and archegonium (for convenience, not exactly taken from their Latin or Greek suffixes). In unicellular eukaryotes, somatic cells are directly induced to undergo meiosis or heterogametogenesis. In multicellular eukaryotes, such transitions/differentiation occur in specific multicellular structures and receive support in nutritional supply and protection against environmental stresses. Therefore, the structures utilized to support and protect cells committed to undergoing meiosis and heterogametogenesis, i.e., the protective "-ium" structures, understandably exhibit new morphological traits consistent with their functions.

The induction of germ cells and reproductive organs after a period vegetative growth is a widely accepted concept in plant biology. However, how such a sequential process evolved is a matter of controversy. A recent finding triggered the idea of the SRC-derived double ring mode to describe plant development: in rice stamens during development, the MADS protein OsMADS58 (annotated as a C-class protein required for stamen and carpel identity determination) binds photosynthetic genes, inhibits their expression, and participates in establishing the hypoxia niche (Chen et al., 2015). This finding, together with the finding that hypoxia triggers meiotic fate determination in maize (Kelliher and Walbot, 2012), suggests that in the first interval of the SRC (from zygote to meiotic cell formation), photosynthesis and DGC induction are mutually exclusive. Sequential changes in organ types may ultimately be determined by the balance of two opposing driving forces: photosynthesis and stress responses.

Morphological Traits Associated with Sex Differentiation

Sexual reproduction cycle, a mechanism that eukaryotes ultimately use to adapt to environmental changes, comprises three core events: meiosis, fertilization, and heterogametogenesis (Bai and Xu, 2013; Bai, 2015a). The key functions of heterogametogenesis can be thought of as harnessing genetic variations and simultaneously enhancing heterogeneity by labeling meiotically produced haploid cells (Bai, 2015a). From this point of view, so-called "sex differentiation" refers not to the germ line/cells themselves (as they are already progenitor cells for heterogametogenesis) but rather to mechanisms occurring in the soma of multicellular eukaryotes to ensure heterogametogenesis. Such mechanisms fulfill two basic functions: (1) setting divergence points, which determine the differentiation of somatic organs into male or female organs (e.g., antheridia and archegonia in plants and testis and ovaries in animals) and (2) niche establishment, which helps support and protect germ cell differentiation.

In animals, only one set of multicellular structures is interpolated into the first interval (diploid) of the SRC. In the dichotomous mode strategy (**Figures 2**, **3**), cell lineages for germ cells and soma diverge during early embryogenesis. Heterogametogenesis is carried out by the germline after it migrates into the gonads and is determined by the sexual identity of the gonad. Therefore, sex differentiation can be viewed as a mechanism occurring in diploid soma that centers on gonad differentiation.

In plants, by contrast, multicellular structures are interpolated into both intervals of the SRC (**Figure 2**). Therefore, two transitions from somatic cells to germ cells (DGC and HGC) occur in two multicellular structures, sporophytes and gametophytes respectively. The first transition, which occurs in sporophytes, results in the production of meiotic cells, whereas the second transition, which occurs in gametophytes, results in gamete cell production. If we accept the above definition of sex

TABLE 2 | Alignment of morphological traits associated with the decrease of multicellularity back toward unicellularity in the SRC upon stress from a function-based evolutionary perspective.

	Subcategories	Underlying factors				Morphology observed	Reference
Back to unicellularity in the SRC	Reduction in photosynthetic surface area	Response to internal signals	Physical (mechanic pressure)	Turgor		Size and shapes	Buchanan et al., 2000
				Cell wall			
				Gravity			
			Chemical	e.g., Sugar, miRNA			
		Response to seasonal signals	Photoperiod	Diploid		Sequential changes in organ types (including heterophylly, flowering and floral organ formation in angiosperms) in response to respectively or in combination upon exposure to signals	Buchanan et al., 2000; Hohe et al., 2002
			Temperature				
				Haploid		Mainly observed for induction of germ cell/ "-ium" differentiation, not reduction in photosynthetic surface area, probably due to lack of observation	
			Others				
	Induction of germ cells from somatic cells	DGC	Homospory			Bryophytes and some of pteridophytes	Cove, 2005
			Heterospory	Micro-		Some of pteridophytes and spermatophytes	Gifford and Foster, 1989
				Mega-			
		HGC	Isogamete			Non-existent in land plants	Scagel, 1984
			Anisogamete	Small	Mobile	Sperm cells in bryophytes and pteridophytes	
					Non-M	Sperm cells in spermatophytes	
				Large		Eggs	
	"-ium" formation: supportive and protective	Diploid: sporangium	Homo	Terminal at axis		Singular or clustered in bryophytes, *Psilotum*, etc.	Scagel, 1984
					Distributed in foliage	Clustered in diverse patterns in ferns	Tanahashi et al., 2005;
			Hetero	Micro-	1-D (dimension)	Singular at terminus, e.g., *Selaginella*	Schulz et al., 2010;
					2-D	Clustered on foliage structures, basal angiosperm stamens	Li et al., 2013
					3-D	Clustered, e.g., eudicot and monocot stamens	
				Mega-	Spore-dispersal	Lycophytes	
					Spore-retained	Ovules in spermatophytes with various modifications	
		Haploid	Antheridium		Elaborated	Bryophytes and pteridophytes	
					Reduced	Spermatophytes	
			Archegonium		Elaborated	Bryophytes and pteridophytes	
					Reduced	Gymnosperms	
						Angiosperms	

differentiation as mechanisms occurring in the soma to ensure heterogametogenesis, only the differentiation of antheridia and archegonia in gametophytes of bryophytes and pteridophytes, the second interval of the SRC, satisfy both functions that ensure heterogametogenesis (**Table 3**).

Stamens and ovules in angiosperms are essentially elaborated heterosporangia. The differentiation of these organs occurs during the first interval of the SRC, between zygote and DGC formation, which ensures the successful transition from somatic cells to DGC for meiosis, not heterogametogenesis. Using our definition, such a differentiation process should not be referred to as sex differentiation, as it does not directly lead to heterogametogenesis. However, as the gametophytes of spermatophytes, especially in angiosperms, have a severely reduced cell number, there are no enough cells for antheridia and archegonia differentiation, one of the two functions involved in sex differentiation, i.e., divergence point setting was canalized to be carried out by heterosporogenesis in spermatophytes. Since heterosporogenesis does not directly lead to heterogametogenesis but did fulfil one of the two functions in sex differentiation, it is reasonable to refer to it as "pseudo-sex-differentiation." By contrast, the differentiation of antheridia and archegonia can be considered "real sex differentiation."

In additional to the presence of two germ cells in plants, DGC and HGC, the relationship between germ line/cells and the somatic tissues/organs supporting and protecting the germ line/cells also differ between animals and plants. In animals, as described above, germline and somatic organ formation initiate separately from a spatiotemporal perspective. By contrast, initiation of germ cells and the somatic cells/tissues surrounding them for support and protection during both the diploid and haploid phases in plants are concurrent spatiotemporally. These differences complicate comparisons of sex differentiation in animals versus plants, even though both types of organisms are derived from the SRC. This is an interesting issue that should be further explored.

Morphological Traits Associated with Sexual Behaviors

In unicellular eukaryotes, gametes are mobilized in water to facilitate their meeting. In multicellular eukaryotes, gametes differentiate in various protective structures, especially female gametes, i.e., eggs. On the other hand, the key advantage of the SRC is that it autonomously increases genetic variation to help the organism adapt to unpredictable environmental changes. Thus, maintaining proper heterogeneity through heterogametogenesis is an essential property of the SRC (Bai, 2015a). To satisfy both the needs for gametes to meet and to maintain heterogeneity, multicellular eukaryotes must evolve mechanisms to facilitate outcrossing, ensuring proper functioning of the SRC.

Most animal individuals are dioecious and have evolved mechanisms that force individuals to actively search for mating partners to complete their SRC. Such mechanisms are generally referred to as "sexual behavior," including courtship for intersexual individuals and mating competition for intrasexual individuals. By contrast, plants are sessile and cannot move like animals to help complete the SRC. However, specific multicellular structures have evolved to help fulfill these functions. Morphological traits associated with these functions can therefore be referred to as "sexual behavior" in comparison with that of animals.

Table 4 lists major morphological traits associated with these process. To facilitate the meeting of gametes, two functions are required: spore dispersal and gamete delivery. Endothecia in sporangia have evolved to facilitate the dispersal of spores, including homospores in bryophytes and pteridophytes and microspores in spermatophytes. For gamete delivery, while sperm cells are mainly delivered simply via water during gametophyte development in bryophytes and pteridophytes, very complicated multicellular structures have evolved for sperm delivery in spermatophytes. For example, the pollen tube has evolved as a carrier of sperm, with astonishingly complicated behaviors. Other prominent morphological traits include the structures in angiosperm sporophytes, including the stigmas of carpels for pollen collection and petals and associated structures to attract pollinators. The latter exhibit tremendous, fascinating variations that have evolved during interactions with pollinators. Three mechanisms are used to maintain heterogeneity or to promote outcrossing, i.e., self-incompatibility, the production of morphological differences in reproduction organs, and unisexual flower production. While self-incompatibility mainly results

TABLE 3 | Alignment of morphological traits associated with sex differentiation from a function-based evolutionary perspective.

	Subcategories	Underlying factors	Morphology observed	Reference
Sex differentiation	Real	Heterogametogenesis	An event in SRC and differentiation at the unicellular level	Bai, 2015a
		Structures ensure HG in gametophytes	Hermaphroditic gametophytes: antheridium and archegonium differentiate in the same gametophyte	This paper
		Precocious divergence of An/Ar differentiation prior to initiation of An/Ar during gametophyte development	Dioecious gametophytes: antheridia and archegonia differentiate in separate gametophytes	
	Pseudo	Heterosporangia, as a sporophyte structures, function in setting divergence point for heterogametogenesis	Micro- and mega-sporangia in Lycophytes	This paper
			Microsporophyll/stamens and ovules in spermatophytes	Gifford and Foster, 1989

TABLE 4 | Alignment of morphological traits associated with sexual behaviors from a function-based evolutionary perspective.

	Subcategories	Underlying factors					Morphology observed	Reference
Sexual behavior	Facilitation of gamete meeting	Diploidy	Environmental interactions	Protection of sporangia, for both groups in spermatophytes			Ovulifeous scales and carpels	Gifford and Foster, 1989
				Platform for pollen-collection, only for angiosperms			Stigma in carpels	Scagel, 1984
			Spore-dispersal	In sporangia of homosporous, heterosporous in non-seeds plants and of microsporophyll and stamen in spermatophytes			Endothecium	
			Sophisticated structures facilitating gamete meeting	Attraction of pollinators, petals and sepals	Visual	Colors, shapes	Colored spots, etc.	
					Olfactory	Volatile materials		
					Taste	Secreted components	Nectary	
				Interaction of M/F partners		Sperms/egg		
						Pollen tube/female parts		
						Pollen/stigma		
		Haploidy		Sperm mobility in bryophytes, pteridophytes and a few gymnosperms				Gifford and Foster, 1989
				Sperm delivery: pollen tubes (derived from filament structures in moss)		Attraction		Higashiyama and Takeuchi, 2015
						Guidance		
						Burst and check		
	Promotion of outcrossing	Self-incompatibility		Diploidy		Sporophytic		Bai and Xu, 2013
						Gametophytic		
				Haploidy				
		Morphological difference		Sporophytes (stamen/ovule)		Spatial	Distyly	Scagel, 1984
						Temporal	Dichogamy	
				Gametophytes		Dioecy		
		Unisexual flowers (USF)		Flowers	Environmentally induced	Internal, e.g., hormonal		Bai and Xu, 2013
						External, e.g., light/temperature/...		
					Genetically fixed	Specific genes		
						Specific loci	Autosome	
							Heterochromosomes	
					Pseudo-unisexual flower		Male sterility	
				Colonies	Mixed USF in a single colony		Monoecious	
					Separated USF in two colonies		Dioecious	

from invisible genetic mechanisms, the other two mechanisms are mainly associated with the specification of morphological characteristics.

Morphological Traits Associated with Particular Stress Responses

Some traits have evolved to help plants cope with particular environmental stresses. These traits include those for adaptation to life on land, such as cutin formation (to prevent rapid water evaporation) and archegonia or embryo sacs plus ovules (to protect eggs and zygotes, an important seed trait). Since plants are sessile organisms, one unique way that plants ensure effective energy usage is to maximize the utilization of synthesized materials while minimizing exposure to environmental stress. Some traits appear to be associated with the latter functions, such as senescence, programmed cell death, and abscission of dead organs. The third subcategory is morphological changes to help the plant adapt to specific or extreme environmental conditions, such as the development of enlarged shoot tips or roots for assimilate storage. The morphological traits associated with these functions are listed in **Table 5**.

Some morphological changes that occur in plants upon exposure to biotic stress are not discussed here for two reasons: (1) biotic stress responses are highly complicated and are difficult to summarize concisely, and (2) morphological responses induced by pathogen infection appear to result from a combination of regulatory mechanisms that were originally utilized for abiotic environmental stress or internal stress responses (Zhu et al., 2005; Chen et al., 2007; Wang et al., 2007; Campos et al., 2016; Jin et al., 2016; also see reviews of Huot et al., 2014; Chaiwanon et al., 2016), although particular signaling systems have evolved for pathogen recognition, and a huge variety of secondary metabolic pathways have evolved for plant–pathogen interactions.

FUNCTION-BASED MORPHOLOGY: PLANT MORPHOGENESIS 123

Almost all morphological traits mentioned in botanical textbooks and the literature are listed in **Tables 1**–**5** but have been aligned in an unconventional manner. It might take some time to become accustomed to the logic and principles underlying such a new alignment. However, based on the "function-based evolutionary perspective," it is clear that the morphological traits described to date, regardless of species, can be aligned to the "double-ring" process derived from the SRC. As mentioned above, such an alignment of morphological traits demonstrates that the double-ring process can indeed be treated as a frame of reference equivalent to animal embryogenesis, as it functions as a core process shared by all plant species. To further integrate the concepts of the SRC, the double-ring mode, and morphological traits, I propose a new conceptual framework to better understand the process of plant morphogenesis: Plant Morphogenesis 123. This conceptual framework describes plant morphogenesis on three levels:

Level one is ONE starting point: the SRC. All plants are multicellular eukaryotes, with morphogenesis derived from the SRC, a modified cell cycle representing the ultimate mechanism for environmental adaptation. This concept explains why all plants possess core cells (zygote, meiotic cells, and gametes) and

TABLE 5 | Alignment of morphological traits associated with particular stress responses from a function-based evolutionary perspective.

	Subcategories	Underlying factors		Morphology observed	Reference
Adaptation to environmental stresses	Land habitat	Efficient water usage		Cutin	Scagel, 1984
		Trichome and fibers			Smith et al., 2010
		Protection of SRC core cells	Zygote and embryo	Archegonia in non-seed plants and ovules (seeds) in seed plants	
			Spore	Spore walls and pollenin	
			Egg and embryo sac	Endosperm (derived from double fertilization in angiosperms)	
	Energy saving	Senescence		Color change, structural degradation, abscission, etc.	
		Cell death			
		Abscission			
	Extreme conditions	Storage organs		Tubers	
				Tuberous roots	
				Storage stems	
		Other abnormal organs		Thorns	
				Tendrils	
				Abnormal leaves to capture insects	

undergo core unicellular events (meiosis, heterogametogenesis, and fertilization). This concept also explains the relationship between multicellular structures and the unicellular SRC: interpolation of multicellular structures into the two intervals between the three core cells (**Figures 1**, **2**).

Level two consists of TWO themes. One theme is the method of building of multicellular structures. Since the L-system is a successful way to describe plant morphogenesis (Prusinkiewicz and Lindenmayer, 1990; Prusinkiewicz and Runions, 2012), there must be corresponding molecular mechanisms underlying this process. The other theme is the regulation or driving forces of changes in morphological structure. As discussed above, most morphological changes (represented by the morphology of lateral organs that initiate from growth tips) are ultimately driven by two forces: photoautotrophy and stress responses.

Level three is the most complicated, representing THREE sequential steps in morphogenesis during the completion of the plant life cycle. The first step is photoautotrophism driving an increase in surface area for photosynthesis and away from the unicellularity of the SRC. The second step is the increased external and internal stress that accompanies the increase in the surface area available for photosynthesis. The third step involves this increase in stress driving a reduction in the surface area available for photosynthesis and compelling the morphogenesis back toward the unicellularity of the SRC.

Through Plant Morphogenesis 123, the life cycle is completed, a PDU forms, and numerous PDUs are integrated into the colony that we refer to as a plant.

Using Plant Morphogenesis 123 as a frame of reference, it becomes obvious that some fundamental issues in plant morphogenesis have not yet been properly addressed. One issue is that little is known about the generally applied molecular mechanisms underlying so-called "axial growth" proposed by Prusinkiewicz and Lindenmayer (1990) (**Table 1**), although such a model has been successfully used for computer simulation of plant morphogenesis and is supported by some molecular data (Prusinkiewicz et al., 2007, 2009; Bayer et al., 2009; Bilsborough et al., 2011; O'Connor et al., 2014; Yoshida et al., 2014; Zadnikova et al., 2016). Since this mechanism is so fundamental for the formation of multicellular structures, many more investigations of this topic are expected.

Another issue is the multicellularization of growth tips. Much effort has been devoted to genetic analysis of the organization of the shoot apical meristem in angiosperms (Barton, 2010; Pautler et al., 2013; Tanaka et al., 2013; Tameshige et al., 2015). However, single or double cells function quite well as growth tips to generate lateral organs in both bryophytes and pteridophytes. How do the growth tips become multicellularized in spermatophytes? While multicellularization is clearly an important evolutionary innovation, little is known about this process, although some efforts have been made to this end (review see Plackett et al., 2015).

Finally, from a more traditional viewpoint, morphogenesis in angiosperms can be divided into two phases, vegetative and reproductive, with flowering representing a transition point. However, according to Plant Morphogenesis 123, all organ types interpolated into the interval between zygotes and meiotic cells, such as in angiosperms, are sequentially generated, with modifications driven by two forces: photoautotrophism and stress responses. Flowering involves only part of this series; photoperiodic responses and vernalization are the main additional mechanisms used by plants growing at higher latitudes to adapt to seasonal changes in the environment. Using this new conceptual framework, I am optimistic that the ultimate regulatory mechanisms underlying morphological changes during the entire (not partial) process will be discovered.

CONCLUSION

There is a common saying that "seeing is believing." This is true in some circumstances. However, our human-centered viewpoint has brought about an inappropriate frame of reference for interpreting plant morphogenesis, i.e., viewing a plant as an individual equivalent to an individual animal. Although tremendous progress has been made in describing and interpreting plant morphogenesis and in deciphering its underlying molecular mechanisms, some fundamental questions remain. Among these are whether a determinate program underlies plant development, whether there is a common process equivalent to animal embryogenesis shared by diverse plant species following the divergence of photoautotrophic organisms from a common ancestor, and what are the key evolutionary innovations underlying the divergence of the major lineages.

Looking back through the history of the study of plant morphology, it is clear that such questions have originated from human-centered observations and interpretations of this process. Therefore, without changing the historical perspective of plant morphology, the puzzle cannot be solved. By echoing and reviving the classic way of observing and interpreting plant morphology proposed by the founding fathers of modern botany, i.e., to view a plant as a colony of developmental units (Waddington, 1966; Bai, 1999), I developed Plant Morphogenesis 123 as a new conceptual framework for plant morphogenesis. Using this framework, morphological traits are aligned following the SRC-derived double ring mode. From this function-based evolutionary perspective, we can better identify the evolutionary significance of any morphological trait in plants. In turn, it becomes easier to identify which morphological traits are important for understanding key evolutionary innovations.

This conceptual framework is undoubtedly unfamiliar to most readers as it, and indeed the concept of the SRC, is so new. According to Gifford and Foster (1989), plant morphology studies have gone from the "casual inspection on surface aspects of plants" to "systematic inspection of hidden aspects of form, structure, and reproduction that constitute the basis for the interpretation of similarities and differences among plants." From this perspective, the exploration of

nature is similar to assembling a jigsaw puzzle: one can carefully examine the picture on the box, diligently collect and examine the pieces, and properly assemble the pieces together according to the picture. In exploring nature, data must be collected diligently and assembled carefully and properly as well. The only difference is that there is no one fixed "picture" used as a reference for data assembly. Therefore, it is not surprising that when a conceptual framework no longer provides a solid basis for assembling or integrating new data, a change in the conceptual framework or paradigm shift should be considered. Using a new conceptual framework, available data can be realigned to obtain a better "picture." More importantly, if the paradigm shift is appropriate, new opportunities for exploration will emerge.

AUTHOR CONTRIBUTIONS

The author confirms being the sole contributor of this work and approved it for publication.

FUNDING

This work was supported by grants from Ministry of Science and Technology of the People's Republic of China (2013CB126901).

ACKNOWLEDGMENTS

I would like to thank Prof. Xin Wang of Nanjing Institute of Geology and Paleontology, Chinese Academy of Sciences, for his invitation to contribute to *Frontiers* for the special issue on the topic "Evolution of Reproductive Organs in Land Plants." I also thank Prof. Guang-Yuan Rao of Peking University, Prof. Mitsuyasu Hasebe of the National Institute for Basic Biology, Japan and Prof. Jill Harrison of Bristol University, UK for their comments and suggestions on the manuscript and Prof. Yi Li and his postdoc, Dr. Lian Jin, for their helpful discussions on the molecular mechanisms underlying the effects of pathogens on plant morphogenetic traits.

REFERENCES

Arber, A. R. (1950). *The Natural Philosophy of Plant Form*. Cambridge: Cambridge University Press.

Bai, S. N. (1999). "Phenomena, interpretation of the phenomena, and the developmental unit in plants," in *Advances in Plant Sciences (in Chinese)*, ed. C. Li (Beijing: Higher Education Press).

Bai, S. N. (2015a). The concept of the sexual reproduction cycle and its evolutionary significance. *Front. Plant Sci.* 6:11. doi: 10.3389/fpls.2015.00011

Bai, S. N. (2015b). Plant developmental program: sexual reproduction cycle derived "double ring." *Sci. Sin. Vitae* 45, 811–819.

Bai, S. N. (2016). Make a new cloth for a grown body: from plant developmental unit to plant developmental program. *Annu. Rev. New Biol.* 2015, 73–116.

Bai, S. N., and Xu, Z. H. (2013). Unisexual cucumber flowers, sex and sex differentiation. *Int. Rev. Cell Mol. Biol.* 304, 1–55. doi: 10.1016/B978-0-12-407696-9.00001-4

Barton, M. K. (2010). Twenty years on: the inner workings of the shoot apical meristem, a developmental dynamo. *Dev. Biol.* 341, 95–113. doi: 10.1016/j.ydbio.2009.11.029

Bayer, E. M., Smith, R. S., Mandel, T., Nakayama, N., Sauer, M., Prusinkiewicz, P., et al. (2009). Integration of transport-based models for phyllotaxis and midvein formation. *Genes Dev.* 23, 373–384. doi: 10.1101/gad.497009

Bernier, G., Kinet, J.-M., and Sachs, R. M. (1981). *The Physiology of Flowering*. Boca Raton, FL: CRC Press.

Bilsborough, G. D., Runions, A., Barkoulas, M., Jenkins, H. W., Hasson, A., Galinha, C., et al. (2011). Model for the regulation of *Arabidopsis thaliana* leaf margin development. *Proc. Natl. Acad. Sci. U.S.A.* 108, 3424–3429. doi: 10.1073/pnas.1015162108

Briggs, W. R. (2014). Phototropism: some history, some puzzles, and a look ahead. *Plant Physiol.* 164, 13–23. doi: 10.1104/pp.113.230573

Buchanan, B. B., Gruissem, W., and Jones, R. L. (2000). *Biochemistry and Molecular Biology of Plants*. Rockville, MD: ASPP.

Campos, M. L., Yoshida, Y., Major, I. T., de Oliveira Ferreira, D., Weraduwage, S. M., Froehlich, J. E., et al. (2016). Rewiring of jasmonate and phytochrome B signalling uncouples plant growth-defense tradeoffs. *Nat. Commun.* 7:12570. doi: 10.1038/ncomms12570

Chaiwanon, J., Wang, W., Zhu, J. Y., Oh, E., and Wang, Z. Y. (2016). Information integration and communication in plant growth regulation. *Cell* 164, 1257–1268. doi: 10.1016/j.cell.2016.01.044

Chen, R., Shen, L. P., Wang, D. H., Wang, F. G., Zeng, H. Y., Chen, Z. S., et al. (2015). A gene expression profiling of early rice stamen development that reveals inhibition of photosynthetic genes by OsMADS58. *Mol. Plant* 8, 1069–1089. doi: 10.1016/j.molp.2015.02.004

Chen, Z., Agnew, J. L., Cohen, J. D., He, P., Shan, L., Sheen, J., et al. (2007). *Pseudomonas syringae* type III effector AvrRpt2 alters *Arabidopsis thaliana* auxin physiology. *Proc. Natl. Acad. Sci. U.S.A.* 104, 20131–20136. doi: 10.1073/pnas.0704901104

Coen, E. S., and Meyerowitz, E. M. (1991). The war of the whorls: genetic interactions controlling flower development. *Nature* 353, 31–37. doi: 10.1038/353031a0

Cove, D. (2005). The moss *Physcomitrella patens*. *Annu. Rev. Genet.* 39, 339–358. doi: 10.1146/annurev.genet.39.073003.110214

Della Pina, S., Souer, E., and Koes, R. (2014). Arguments in the evo-devo debate: say it with flowers! *J. Exp. Bot.* 65, 2231–2242. doi: 10.1093/jxb/eru111

Gifford, E. M., and Foster, A. S. (1989). *Morphology and Evolution of Vascular Plants*. New York, NY: W.H. Freeman and Co.

Gilbert, S. F. (2003). Opening Darwin's black box: teaching evolution through developmental genetics. *Nat. Rev. Genet.* 4, 735–741. doi: 10.1038/nrg1159

Gilbert, S. F., Opitz, J. M., and Raff, R. A. (1996). Resynthesizing evolutionary and developmental biology. *Dev. Biol.* 173, 357–372. doi: 10.1006/dbio.1996.0032

Goldberg, R. B. (1988). Plants: novel developmental processes. *Science* 240, 1460–1467. doi: 10.1126/science.3287622

Goldberg, R. B., de Paiva, G., and Yadegari, R. (1994). Plant embryogenesis: zygote to seed. *Science* 266, 605–614. doi: 10.1126/science.266.5185.605

Goodman, C. S., and Coughlin, B. C. (2000). Introduction. The evolution of evo-devo biology. *Proc. Natl. Acad. Sci. U.S.A.* 97, 4424–4425. doi: 10.1073/pnas.97.9.4424

Han, S. K., and Torii, K. U. (2016). Lineage-specific stem cells, signals and asymmetries during stomatal development. *Development* 143, 1259–1270. doi: 10.1242/dev.127712

Harrison, C. J. (2017). Development and genetics in the evolution of land plant body plans. *Philos. Trans. R. Soc. Lond. B Biol. Sci.* 372:20150490. doi: 10.1098/rstb.2015.0490

Higashiyama, T., and Takeuchi, H. (2015). The mechanism and key molecules involved in pollen tube guidance. *Annu. Rev. Plant Biol.* 66, 393–413. doi: 10.1146/annurev-arplant-043014-115635

Hohe, A., Rensing, S. A., Mildner, M., Lang, D., and Reski, R. (2002). Day length and temperature strongly influence sexual reproduction and expression of a novel MADDS-box gene in the moss *Physcomitrella patens*. *Plant Biol.* 4, 595–602. doi: 10.1055/s-2002-35440

Huot, B., Yao, J., Montgomery, B. L., and He, S. Y. (2014). Growth-defense tradeoffs in plants: a balancing act to optimize fitness. *Mol. Plant* 7, 1267–1287. doi: 10.1093/mp/ssu049

Irish, V. F., and Benfey, P. N. (2004). Beyond *Arabidopsis*. Translational biology meets evolutionary developmental biology. *Plant Physiol.* 135, 611–614. doi: 10.1104/pp.104.041632

Jin, L., Qin, Q., Wang, Y., Pu, Y., Liu, L., Wen, X., et al. (2016). Rice dwarf virus P2 protein hijacks auxin signaling by directly targeting the rice OsIAA10 protein, enhancing viral infection and disease development. *PLoS Pathog.* 12:e1005847. doi: 10.1371/journal.ppat.1005847

Jones, V. A. S., and Dolan, L. (2012). The evolution of root hairs and rhizoids. *Ann. Bot.* 110, 205–212. doi: 10.1093/aob/mcs136

Kaplan, D. R., and Cooke, T. J. (1996). The genius of Wilhelm Hofmeister: the origin of causal-analytical research in plant development. *Am. J. Bot.* 83, 1647–1660. doi: 10.2307/2445841

Kelliher, T., and Walbot, V. (2012). Hypoxia triggers meiotic fate acquisition in maize. *Science* 337, 345–348. doi: 10.1126/science.1220080

Koornneef, M., Hanhart, C. J., and van der Veen, J. H. (1991). A genetic and physiological analysis of late flowering mutants in *Arabidopsis thaliana*. *Mol. Gen. Genet.* 229, 57–66. doi: 10.1007/BF00264213

Li, X., Fang, Y.-H., Yang, J., Bai, S.-N., and Rao, G.-Y. (2013). Overview of the morphology, anatomy, and ontogeny of *Adiantum capillus-veneris*: an experimental system to study the development of ferns. *J. Syst. Evol.* 51, 499–510. doi: 10.1111/jse.12034

Liao, I. T., Shan, H., Xu, G., and Zhang, R. (2016). Bridging evolution and development in plants. *New Phytol.* 212, 827–830. doi: 10.1111/nph.14294

Ligrone, R., Duckett, J. G., and Renzaglia, K. S. (2012). The origin of the sporophyte shoot in land plants: a bryological perspective. *Ann. Bot.* 110, 935–941. doi: 10.1093/aob/mcs176

Lord, E. M., Crone, W., and Hill, J. P. (1994). Timing of events during flower organogenesis: *Arabidopsis* as a model system. *Curr. Top. Dev. Biol.* 29, 325–356. doi: 10.1016/S0070-2153(08)60554-2

Lucas, W. J., Groover, A., Lichtenberger, R., Furuta, K., Yadav, S. R., Helariutta, Y., et al. (2013). The plant vascular system: evolution, development and functions. *J. Integr. Plant Biol.* 55, 294–388. doi: 10.1111/jipb.12041

Martins, T. R., Jiang, P., and Rausher, M. D. (2016). How petals change their spots: cis-regulatory re-wiring in *Clarkia* (Onagraceae). *New Phytol.* doi: 10.1111/nph.14163 [Epub ahead of print].

Menand, B., Yi, K., Jouannic, S., Hoffmann, L., Ryan, E., Linstead, P., et al. (2007). An ancient mechanism controls the development of cells with a rooting function in land plants. *Science* 316, 1477–1480. doi: 10.1126/science.1142618

O'Connor, D. L., Runions, A., Sluis, A., Bragg, J., Vogel, J. P., Prusinkiewicz, P., et al. (2014). A division in PIN-mediated auxin patterning during organ initiation in grasses. *PLoS Comput. Biol.* 10:e1003447. doi: 10.1371/journal.pcbi.1003447

Pautler, M., Tanaka, W., Hirano, H. Y., and Jackson, D. (2013). Grass meristems I: shoot apical meristem maintenance, axillary meristem determinacy and the floral transition. *Plant Cell Physiol.* 54, 302–312. doi: 10.1093/pcp/pct025

Plackett, A. R., Di Stilio, V. S., and Langdale, J. A. (2015). Ferns: the missing link in shoot evolution and development. *Front. Plant Sci.* 6:972. doi: 10.3389/fpls.2015.00972

Poethig, R. S. (1990). Phase change and the regulation of shoot morphogenesis in plants. *Science* 250, 923–930. doi: 10.1126/science.250.4983.923

Poethig, R. S. (1997). Leaf morphogenesis in flowering plants. *Plant Cell* 9, 1077–1087. doi: 10.1105/tpc.9.7.1077

Poethig, R. S. (2013). Vegetative phase change and shoot maturation in plants. *Curr. Top. Dev. Biol.* 105, 125–152. doi: 10.1016/B978-0-12-396968-2.00005-1

Preston, J. C., Hileman, L. C., and Cubas, P. (2011). Reduce, reuse, and recycle: developmental evolution of trait diversification. *Am. J. Bot.* 98, 397–403. doi: 10.3732/ajb.1000279

Prusinkiewicz, P., Crawford, S., Smith, R. S., Ljung, K., Bennett, T., Ongaro, V., et al. (2009). Control of bud activation by an auxin transport switch. *Proc. Natl. Acad. Sci. U.S.A.* 106, 17431–17436. doi: 10.1073/pnas.0906696106

Prusinkiewicz, P., Erasmus, Y., Lane, B., Harder, L. D., and Coen, E. (2007). Evolution and development of inflorescence architectures. *Science* 316, 1452–1456. doi: 10.1126/science.1140429

Prusinkiewicz, P., and Lindenmayer, A. (1990). *The Algorithmic Beauty of Plants*. New York, NY: Springer-Verlag. doi: 10.1007/978-1-4613-8476-2

Prusinkiewicz, P., and Runions, A. (2012). Computational models of plant development and form. *New Phytol.* 193, 549–569. doi: 10.1111/j.1469-8137.2011.04009.x

Raff, R. A. (2000). Evo-devo: the evolution of a new discipline. *Nat. Rev. Genet.* 1, 74–79. doi: 10.1038/35049594

Raven, J. A., and Edwards, D. (2001). Roots: evolutionary origins and biogeochemical significance. *J. Exp. Bot.* 52, 381–401. doi: 10.1093/jexbot/52.suppl_1.381

Scagel, R. E. (1984). *Plants, An Evolutionary Survey*. Belmont, CA: Wadsworth Pub Co.

Schulz, C., Little, D. P., Stevenson, D. W., Bauer, D., Moloney, C., and Stützel, T. (2010). An overview of the morphology, anatomy, and life cycle of a new model species: the lycophyte *Selaginella apoda* (L.) Spring. *Int. J. Plant Sci.* 171, 693–712. doi: 10.1086/654902

Smith, A. M., Coupland, G., Dolan, L., Harberd, N., Jones, J., Martin, C., et al. (2010). *Plant Biology*. New York, NY: Garland Science.

Strasburger, E., Denffer, D. V., Bell, P. R., and Coombe, D. (1976). *Strasburger's Textbook of Botany*. New York, NY: Longman.

Tameshige, T., Hirakawa, Y., Torii, K. U., and Uchida, N. (2015). Cell walls as a stage for intercellular communication regulating shoot meristem development. *Front. Plant Sci.* 6:324. doi: 10.3389/fpls.2015.00324

Tanahashi, T., Sumikawa, N., Kato, M., and Hasebe, M. (2005). Diversification of gene function: homologs of the floral regulator FLO/LFY control the first zygotic cell division in the moss *Physcomitrella patens*. *Development* 132, 1727–1736. doi: 10.1242/dev.01709

Tanaka, W., Pautler, M., Jackson, D., and Hirano, H. Y. (2013). Grass meristems II: inflorescence architecture, flower development and meristem fate. *Plant Cell Physiol.* 54, 313–324. doi: 10.1093/pcp/pct016

Tsukaya, H. (2014). Comparative leaf development in angiosperms. *Curr. Opin. Plant Biol.* 17, 103–109. doi: 10.1016/j.pbi.2013.11.012

Waddington, C. H. (1966). *Principles of Development and Differentiation*. New York, NY: Macmillan.

Wang, D., Pajerowska-Mukhtar, K., Culler, A. H., and Dong, X. (2007). Salicylic acid inhibits pathogen growth in plants through repression of the auxin signaling pathway. *Curr. Biol.* 17, 1784–1790. doi: 10.1016/j.cub.2007.09.025

Wolpert, L., Jessel, T., Lawrence, P., Meyerowitz, E., Robertson, E., and Smith, J. (2007). *Principles of Development*. Oxford: Oxford University Press.

Yoshida, S., Barbier de Reuille, P., Lane, B., Bassel, G. W., Prusinkiewicz, P., Smith, R. S., et al. (2014). Genetic control of plant development by overriding a geometric division rule. *Dev. Cell* 29, 75–87. doi: 10.1016/j.devcel.2014.02.002

Zadnikova, P., Wabnik, K., Abuzeineh, A., Gallemi, M., Van Der Straeten, D., Smith, R. S., et al. (2016). A model of differential growth-guided apical hook formation in plants. *Plant Cell* 28, 2464–2477. doi: 10.1105/tpc.15.00569

Zhao, F., Zheng, Y. F., Zeng, T., Sun, R., Yang, J. Y., Li, Y., et al. (2017). Phosphorylation of SPOROCYTELESS/NOZZLE by MPK3/6 is required for Arabidopsis anther development. *Plant Physiol.* doi: 10.1104/pp.16.01765 [Epub ahead of print].

Zhu, S., Gao, F., Cao, X., Chen, M., Ye, G., Wei, C., et al. (2005). The rice dwarf virus P2 protein interacts with ent-kaurene oxidases in vivo, leading to reduced biosynthesis of gibberellins and rice dwarf symptoms. *Plant Physiol.* 139, 1935–1945. doi: 10.1104/pp.105.072306

Conflict of Interest Statement: The author declares that the research was conducted in the absence of any commercial or financial relationships that could be construed as a potential conflict of interest.

frontiers in Plant Science

ORIGINAL RESEARCH
published: 03 May 2017
doi: 10.3389/fpls.2017.00656

Analysis of MADS-Box Gene Family Reveals Conservation in Floral Organ ABCDE Model of Moso Bamboo (*Phyllostachys edulis*)

*Zhanchao Cheng†, Wei Ge†, Long Li†, Dan Hou, Yanjun Ma, Jun Liu, Qingsong Bai, Xueping Li, Shaohua Mu and Jian Gao**

Key Laboratory of Bamboo and Rattan Science and Technology of the State Forestry Administration, International Centre for Bamboo and Rattan, Beijing, China

Mini chromosome maintenance 1, agamous, deficiens, and serum response factor (MADS)-box genes are transcription factors which play fundamental roles in flower development and regulation of floral organ identity. However, till date, identification and functions of MADS-box genes remain largely unclear in *Phyllostachys edulis*. In view of this, we performed a whole-genome survey and identified 34 MADS-box genes in *P. edulis*, and based on phylogeny, they were classified as MIKC^C, MIKC*, Mα, and Mβ. The detailed analysis about gene structure and motifs, phylogenetic classification, comparison of gene divergence and duplication are provided. Interestingly, expression patterns for most genes were found similar to those of *Arabidopsis* and rice, indicating that the well-established ABCDE model can be applied to *P. edulis*. Moreover, we overexpressed *PheMADS15*, an *AP1*-like gene, in *Arabidopsis*, and found that the transgenic plants have early flowering phenotype, suggesting that *PheMADS15* might be a regulator of flowering transition in *P. edulis*. Taken together, this study provides not only insightful comprehension but also useful information for understanding the functions of MADS-box genes in *P. edulis*.

Keywords: *Phyllostachys edulis*, MADS-box, floral organ, ABCDE model, *PheMADS15*

OPEN ACCESS

Edited by:
Borja Cascales-Miñana, University of Liège, Belgium

Reviewed by:
Chengcai Chu, Institute of Genetics and Developmental Biology (CAS), China
Veronica Gregis, Università degli Studi di Milano, Italy

****Correspondence:***
Jian Gao
gaojianicbr@163.com

† These authors have contributed equally to this work.

Specialty section:
This article was submitted to Plant Evolution and Development, a section of the journal Frontiers in Plant Science

Received: *13 January 2017*
Accepted: *10 April 2017*
Published: *03 May 2017*

Citation:
Cheng Z, Ge W, Li L, Hou D, Ma Y, Liu J, Bai Q, Li X, Mu S and Gao J (2017) Analysis of MADS-Box Gene Family Reveals Conservation in Floral Organ ABCDE Model of Moso Bamboo (Phyllostachys edulis). Front. Plant Sci. 8:656. doi: 10.3389/fpls.2017.00656

INTRODUCTION

Phyllostachys edulis is one of the most important non-timber forest products in the world. They flower at the end of very long vegetative growth phases, often followed by the death of large areas of *P. edulis*. They show a cyclic recurrence of flowering, the intervals of which are basically definite varying from a few years to 120 years or longer. In this case, studying the mechanism of *P. edulis* flowering time is very challenging, and it is quite difficult to determine the key regulatory genes involved in floral formation and transition in *P. edulis*.

The mini chromosome maintenance 1, agamous, deficiens, and serum response factor (MADS)-box family members, identified originally as floral homeotic genes, are important transcription factors for plant development (Purugganan, 1997; Theissen et al., 2000; Jack, 2001; Nam et al., 2003; Pařenicová et al., 2003). In plants, the type I comprises M-type genes and type II group includes most well-known MIKC-type genes (Arora et al., 2007), named after the four basic components of the MADS (M) domain: the Intervening (I) domain, the Keratin (K) domain, and the C-terminal (C) domain (Kramer et al., 1998). MIKC-type genes have been further divided into two subgroups, MIKC^C- and MIKC*-types, due to different exon/intron structures (Henschel et al., 2002; Kofuji et al., 2003). Type I MADS-box genes have been categorized into Mα, Mβ, Mγ, and Mδ

clades based on the phylogenetic relationships of conserved MADS-box domain (Pařenicová et al., 2003). In most plants, type I genes experience a higher number of births and deaths than type II genes, due to more frequent segmental gene duplications and weaker purifying selection (Nam et al., 2004).

The genetic ABCDE model of floral organ development can be applied to dicot plants, mainly in *Arabidopsis*, snapdragon and petunia (Coen and Meyerowitz, 1991; Angenent and Colombo, 1996; Theißen and Saedler, 2001). Generally, A and B class genes together are required for petal development, B and C class genes cooperate to control stamen development. A and C class genes are, respectively, involved in sepal and carpel development. D class genes function in ovule development, while E class proteins are expressed in all four whorls of floral organs by forming MADS-box protein complexes with proteins of other classes (Pelaz et al., 2000; Favaro et al., 2003; Pinyopich et al., 2003). In *Arabidopsis*, *APETALA1* (*AP1*) and *APETALA2* (*AP2*) belong to the A-function genes; B-function genes include *APETALA3* (*AP3*), *PISTILLATA* (*PI*); the C-function gene is *AGAMOUS* (*AG*); *SEPALLATA1*, *2*, *3* and *4* (*SEP1*, *2*, *3*, *4*/*AGL2*, *4*, *9*, *3*) form the E-function genes (Yanofsky et al., 1990; Jack et al., 1992; Mandel et al., 1992; Goto and Meyerowitz, 1994; Jofuku et al., 1994; Huang et al., 1995; Savidge et al., 1995; Mandel and Yanofsky, 1998; Pelaz et al., 2000; Ditta et al., 2004).

Poaceae family is generally known for monocot crops such as rice (*Oryza sativa*), maize (*Zea mays*), wheat (*Triticum* spp.) and barley (*Hordeum vulgare*) (Grass Phylogeny Working Group et al., 2001). However, Bambusoideae is quite distinct from other members of Poaceae and is known for its unique floral organization and morphology (Grass Phylogeny Working Group et al., 2001; Rudall et al., 2005; Whipple et al., 2007). In rice and bamboo, each grass spikelet is the structural unit of grass flowers, which consists of a number of florets. In addition, the floret contains four whorls, such as lemma and palea (whorl 1), two lodicules (whorl 2), six stamens (whorl 3), and gynoecium (whorl 4) (Nagasawa et al., 2003). Like eudicots, MADS-box genes in rice and maize are divided into ABCDE gene classes. (Ambrose et al., 2000; Nagasawa et al., 2003; Kater et al., 2006; Yamaguchi et al., 2006; Preston and Kellogg, 2007; Yao et al., 2008; Cui et al., 2010; Li et al., 2011). Few of the MADS-box genes are functionally characterized in different plants. For instance, three *AP1*/*FUL*-like genes (*OsMADS14*, *OsMADS15,* and *OsMADS18*) coordinately act in the shoot apical meristem in rice (Kobayashi et al., 2012). Maize *Silky1* and rice *SPW1* or Os*MADS16*, orthologs of the *Arabidopsis AP3*, cause homeotic transformations of stamens to carpels and lodicules to lemma- or palea-like structures (Ambrose et al., 2000; Nagasawa et al., 2003; Whipple et al., 2004). Rice *OsMADS3*, belonging to the *AG* homolog gene, is, respectively, involved in stamen, ovule and late anther development (Kramer et al., 2004; Yamaguchi et al., 2006; Hu et al., 2011; Li et al., 2011). In rice, *OsMADS13* and *OsMADS21*, two D class genes, are involved in ovule identity specification and floral meristem termination (Dreni et al., 2007; Li et al., 2011). Simultaneous four rice *SEP*-like genes, *LHS1*, *OsMADS5*, *OsMADS7,* and *OsMADS8*, play a key role in all floral organs development (Cui et al., 2010). However, for bamboo, especially *P. edulis*, fewer genes were reported to play roles in specifying flower development, their genetic interactions remained to be answered (Tian et al., 2005, 2006; Li et al., 2009; Shih et al., 2014). Therefore, it is necessary to systematically study MADS-box genes related to flower development in bamboo.

In *Arabidopsis*, class A genes are represented by *AP1* (Mandel et al., 1992) and *AP2* (Jofuku et al., 1994). *AP1* and *LEAFY* (*LFY*) are floral meristem-identity genes that confer identity on developing floral primordia (Weigel et al., 1992). The *LFY*, *AP1*, *CAULFLOWER* (*CAL*) and *AP2* genes appear to mutually reinforce each other, leading to a sharp transition from vegetative to reproductive development (Ferrándiz et al., 2000). In addition, *AP1*, *AGAMOUS LIKE24* (*AGL24*) and *SHORT VEGETATIVE PHASE* (*SVP*) act redundantly to control the identity of the floral meristem and to repress expression of class B, C, and E genes in *Arabidopsis* (Gregis et al., 2009). Genetic evidence suggests that *SUPPRESSOR OF CONSTANS 1* (*SOC1*) and *FLOWERING LOCUS T* (*FT*) function are closely associated with the activation of *AP1* (Teper-Bamnolker and Samach, 2005; Lee and Lee, 2010). Some results strongly show that not only *SOC1*, but also *AP1* can activate *LFY* (Liljegren et al., 1999; Lee and Lee, 2010). *TERMINAL FLOWER 1* (*TFL1*) is involved in the maintenance of the inflorescence meristem by preventing the expression of floral meristem identity genes such as *AP1* and *LFY* in the shoot apical meristem, which in turn is negatively regulated by *LFY* (Irish and Sussex, 1990; Schultz and Haughn, 1991; Weigel et al., 1992; Bowman et al., 1993). Moreover, *TFL1* function is compromised by constitutive *AP1* activity (Liljegren et al., 1999).

Extensive duplications in Poaceae resulted in the expansion and diversification of gene families. Duplications of MADS-box genes have contributed to understanding of the origin and evolution of developmental mechanisms in plant (Alvarez-Buylla et al., 2000a; Shan et al., 2009). Variance in gene family sizes occurred in a number of families in bamboo. *P. edulis* underwent a whole-genome duplication (WGD) event, which resulted in 5,370 gene losses (28% of the total genes in the collinear regions) in comparison to rice (Peng et al., 2013). In addition, some genes displayed expression subfunctionalization; for example, the genes in flowering promotion pathways (the photoperiod, gibberellin, ambient-temperature pathways) and floral pathway integrator (FPI) genes (Ehrenreich et al., 2009; Fornara et al., 2010) were not highly expressed in bamboo floral tissues. Low expression of FPI genes, which are involved in floral meristem identity, could signify that the flowering promotion pathways in bamboo may be different.

In this study, we performed a comprehensive identification and phylogenetic analysis of the MADS-box gene family in *P. edulis*. A total of 34 MADS-box genes were identified and subjected to phylogenetic, gene structure, and domain analyses. We also studied the expression patterns of *P. edulis* MADS-box genes under normal and abiotic stress conditions. Furthermore, expression profiles and anatomical expression were generated to screen candidate genes involved in flower development and the floral transition. The function of one of these genes, *PheMADS15*, an *AP1*-like gene, was also characterized in transgenic *Arabidopsis*. This work provides useful information on the function of this important family of transcription

factors in *P. edulis*, and with both a genome sequence and a transcriptome, future systematic studies can evaluate structure-function relationships.

MATERIALS AND METHODS

Database Searches for the Identification of MADS-Box Family Members in *P. edulis*

MADS-box protein sequences of *Arabidopsis* and *O. sativa* have been obtained from TAIR (The *Arabidopsis* Information Resource[1]) and Rice Genome Annotation Project[2], respectively. *P. edulis* MADS-box protein sequences were collected from Bamboo Genome Database[3] and the accession numbers are shown in Supplementary Table S1.

The MADS-box domains were predicted through Hidden Markov Model (HMM) and redundant sequences were removed using the protein alignments with ClustalX 1.83 (Thompson et al., 1997). Information of ID accession numbers, ORF length, amino acids number, molecular weight, and isoelectric point of each protein is provided in Supplementary Table S1. For all MADS-box genes, ExPASY[4] was employed to find the molecular weight and PI of each protein, as they were not available in the Bamboo Genome Database.

Phylogenetic Analysis

Multiple sequence alignments of MADS-box full-length proteins were performed using ClustalX 1.83[5] (Thompson et al., 1997). The un-rooted neighbor-joining method (Saitou and Nei, 1987) was used to construct the phylogenetic tree in MEGA 6.0[6] (Tamura et al., 2013) software with 1000 bootstrap replicates.

Conserved Motif and Gene Structure Analysis

Multiple EM for Motif Elicitation (MEME) version 4.9.1[7] (Bailey and Elkan, 1995) was used to identify conserved motifs in candidate sequences with following parameters: number of repetitions = any, maximum number of motifs = 20, minimum width ≥ 6, and maximum width ≤ 200.

The MADS-box full-length cDNA sequences and the corresponding genomic DNA were collected from Bamboo Genome Database[8]. The Gene Structure Display Server (GSDS[9]) (Guo et al., 2007) was employed to identify information on intron/exon structure of the MADS-box genes.

[1]http://www.arabidopsis.org/

[2]http://rice.plantbiology.msu.edu/

[3]http://202.127.18.221/bamboo/down.php

[4]http://web.expasy.org/compute_pi/

[5]http://www.clustal.org/

[6]http://www.megasoftware.net/mega.html

[7]http://alternate.meme-suite.org/tools/meme

[8]http://www.bamboogdb.com/

[9]http://gsds.cbi.pku.edu.cn/

Calculation of K_a/K_s Values and Divergence Times Estimation

Alignment of nucleotide sequences of *P. edulis* MADS-box gene pairs were aligned with ClustalX 1.83, respectively. The DNAsp5 software was used to calculate the synonymous substitution (K_s) and non-synonymous substitution (K_a) rates. K_a/K_s values were used to estimate the two types of substitutions events. The K_s value was calculated for each of the MADS-box gene pairs and then used to calculate the divergence time of the duplication event ($T = K_s/2\lambda$) using the formula: $T = K_s/2\lambda$ (Lynch and Conery, 2000), with the divergence rate $\lambda = 6.5 \times 10^{-9}$ (Peng et al., 2013).

Plant Material

Arabidopsis plants were grown under long daylight exposure (16 h light/8 h dark) in light growth incubator maintained at 23°C with 40 to 50% humidity, and an irradiance of approximately 118 μmol m^{-2} s^{-1}.

The flower buds and flower of *P. edulis* at different flowering developmental stages were collected in Dajing County, Guilin (E 110°17′-110°47′; N 25°04′-25°48′) in Guangxi Zhuang Autonomous Region from April to August, 2012. Flower development was distinguished by four phases: the floral bud formation stage, the inflorescence growing stage, the bloom stage, the embryo formation stage (Gao et al., 2014).

Expression Profile Analysis

Reads per kilobase of exon model per million mapped reads (RPKM) values of flowering tissues at floral organ development and shoot growth were imported into Cluster 3.0 (de Hoon et al., 2004) for windows and Java TreeView (Saldanha, 2004) to generate the heat maps. RPKM values were shown in Supplementary Table S4.

Quantitative Real-Time PCR (QPCR)

Total RNA was extracted using the Trizol reagent (Invitrogen, USA). The quality and purified RNA was initially assessed on an agarose gel and NanoDrop 8000 spectrophotometer (NanoDrop, Thermo Scientific, Germany), and then the integrity of RNA samples was further evaluated using an Agilent 2100 Bioanalyzer (Agilent Technologies, USA). For qPCR, Primer 3 Input (version 4.0) was used to design the specific primers according to the MADS-box gene sequences. Detailed descriptions were provided in Supplementary Table S5. Data acquisition and analyses were performed by the Roche Light Cycler software.

Subcellular Localization and Transcriptional Activation

The subcellular localization of PheMADS15 was performed by transfecting GFP-tagged PheMADS15 into rice stem and sheath protoplasts (Zhang et al., 2011). The full-length cDNA of *PheMADS15* was fused in frame with the GFP cDNA and ligated between the CaMV 35S promoter and the nopaline synthase terminator. The fluorescence signals in transfected protoplasts were examined using a confocal laser scanning microscope (Leica Microsystems).

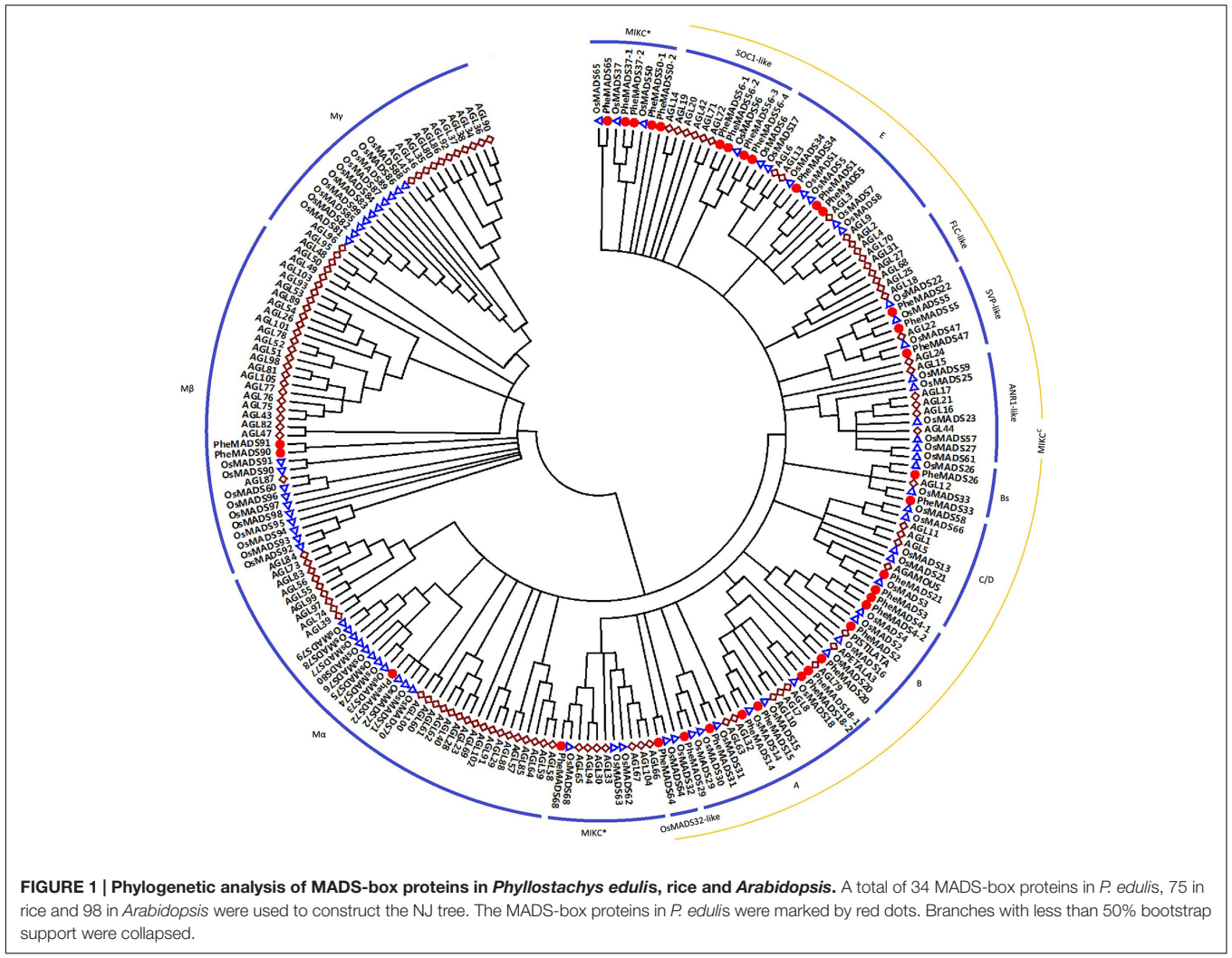

FIGURE 1 | Phylogenetic analysis of MADS-box proteins in *Phyllostachys edulis*, rice and *Arabidopsis*. A total of 34 MADS-box proteins in *P. edulis*, 75 in rice and 98 in *Arabidopsis* were used to construct the NJ tree. The MADS-box proteins in *P. edulis* were marked by red dots. Branches with less than 50% bootstrap support were collapsed.

The transcriptional activation activity of PheMADS15 was tested by transforming the pGBKT7 construct containing a fusion of PheMADS15 and the GAL4 DNA-binding domain into the yeast strain PJ69-4a. The yeast strain contains the *His-3* and *LacZ* reporter genes. The transformed yeast cells were grown on synthetic defined plates with or without *His* and assayed for β-galactosidase activity.

In Situ Hybridization

RNA hybridization and immunological detection of the hybridized probes were performed based on the protocol described previously (de Almeida Engler et al., 2001). The specific probes of *PheMADS15*, *PheMADS4-1*, *PheMADS3*, *PheMADS21*, and *PheMADS5* were designed and synthesized by GENEWIZ (Supplementary Table S6). Images were obtained using the Olympus Nikon E600 microscope.

Overexpression

The 35S:PheMADS15 sequence was amplified using specific primers (forward, 5′-GGTACCATGGGGCGCGGGAAG GTG-3′; reverse, 5′-CCCAAGCTTTCATGAAGGACGAGGA AGAGTCTG-3′) by RT-PCR with 2 μl cDNA from leaves of *P. edulis*. The product was initially cloned into pGEM-T Easy vector and then 35S:pCAMBIA2300 vector. The 35S:PheMADS15 construct was introduced into wild-type *Arabidopsis* plants (Columbia-0) through *Agrobacterium*-mediated transformation (Feldmann and Marks, 1987).

RESULTS

Identification and Phylogenetic Analysis of *P. edulis* MADS-Box Genes

A total of 34 non-redundant MADS-box genes were identified in the *P. edulis* genome using rice MADS-box domain sequences as queries. To determine the evolutionary relationship of these genes in *P. edulis* and other species, we constructed a Neighbor-Joining phylogenetic tree of MADS-box proteins from *P. edulis*, rice and *Arabidopsis*. According to the previously reports in rice and *Arabidopsis*, the proteins can be classified into five functional groups (Pařenicová et al., 2003; Arora et al., 2007).

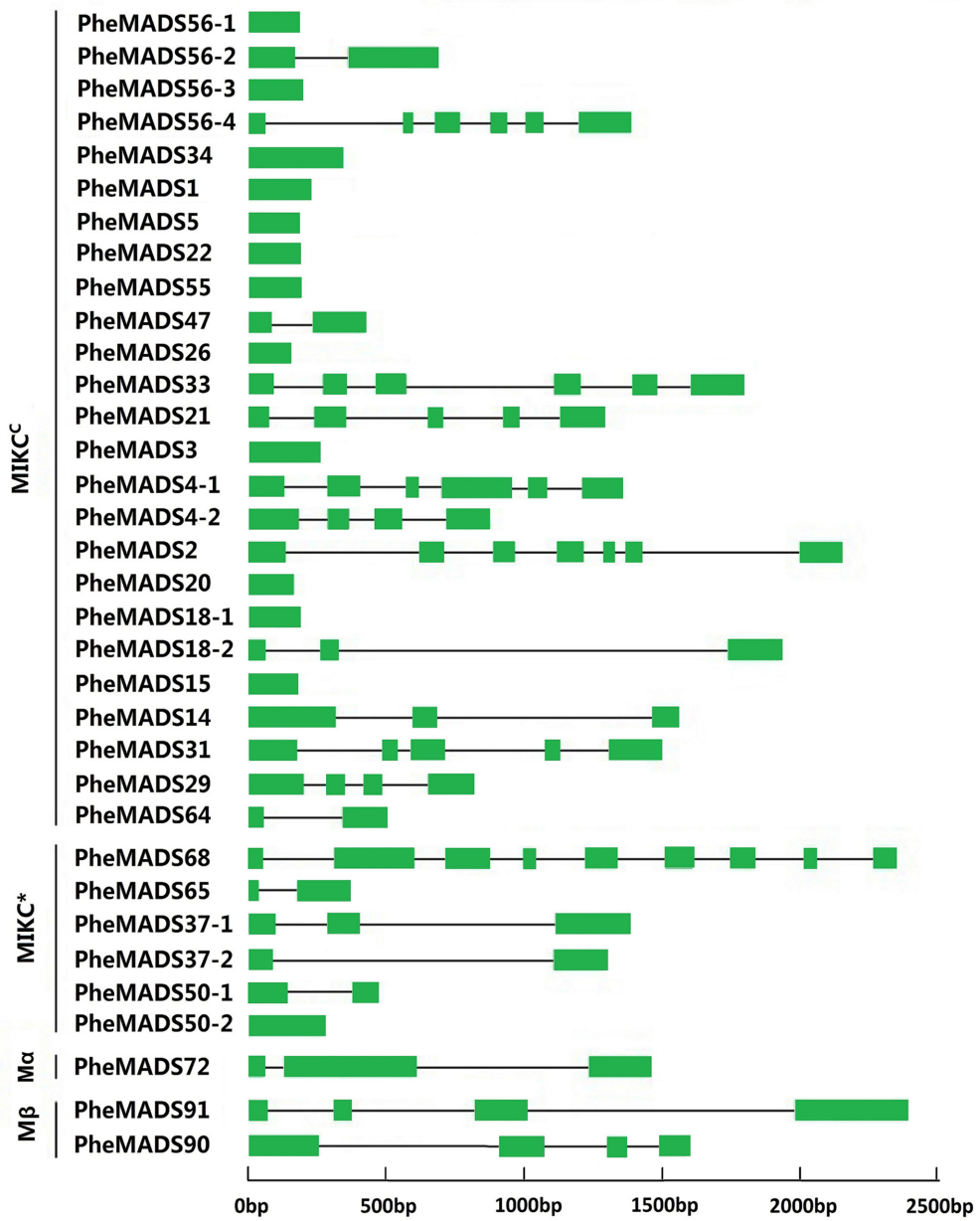

FIGURE 2 | Phylogenetic relationship and gene structure analysis of MADS-box genes in *P. edulis*. Un-rooted neighbor-joining tree was constructed from the alignment of full-length amino acid sequences using the MEGA5 package. Branches with less than 50% bootstrap values were collapsed. Lengths of exons and introns of each MADS-box gene were displayed proportionally. The green solid boxes represent exons; black lines represent introns.

Of the 34 identified *P. edulis* MADS-box genes, 31 grouped into the type II clade subdividing into 25 MIKC^C-type genes and six MIKC*-type genes (**Figure 1**). MIKC^C-type genes were further divided into nine classic clades: *SOC1*-like (four genes), E (three genes), *SVP*-like (three genes), Bs (two genes), C/D (two genes), B (four genes), A (six genes), and *OsMADS32*-like (one gene). In this study, genes belonging to *FLC*-clade were absent in *P. edulis* and rice, which may be specific to *Arabidopsis*. Interestingly, *PheMADS64* was grouped with *OsMADS32*-like which is a novel monocot MADS-box gene (Sang et al., 2012). However, in contrast to previous research, the *OsMADS64* was found to cluster with *OsMADS32* to form a *OsMADS32*-like group instead of the MIKC* group (Arora et al., 2007). In the case of type I genes, including Mα and Mβ, *PheMADS90* and *PheMADS91* were identified as Mβ and *PheMADS72* grouped with Mα, but nothing grouped with the Mγ clade. Mγ, *FLC*-like and *ANR1*-like MADS-box genes were absent from *P. edulis*, indicating that these genes might have been lost after the

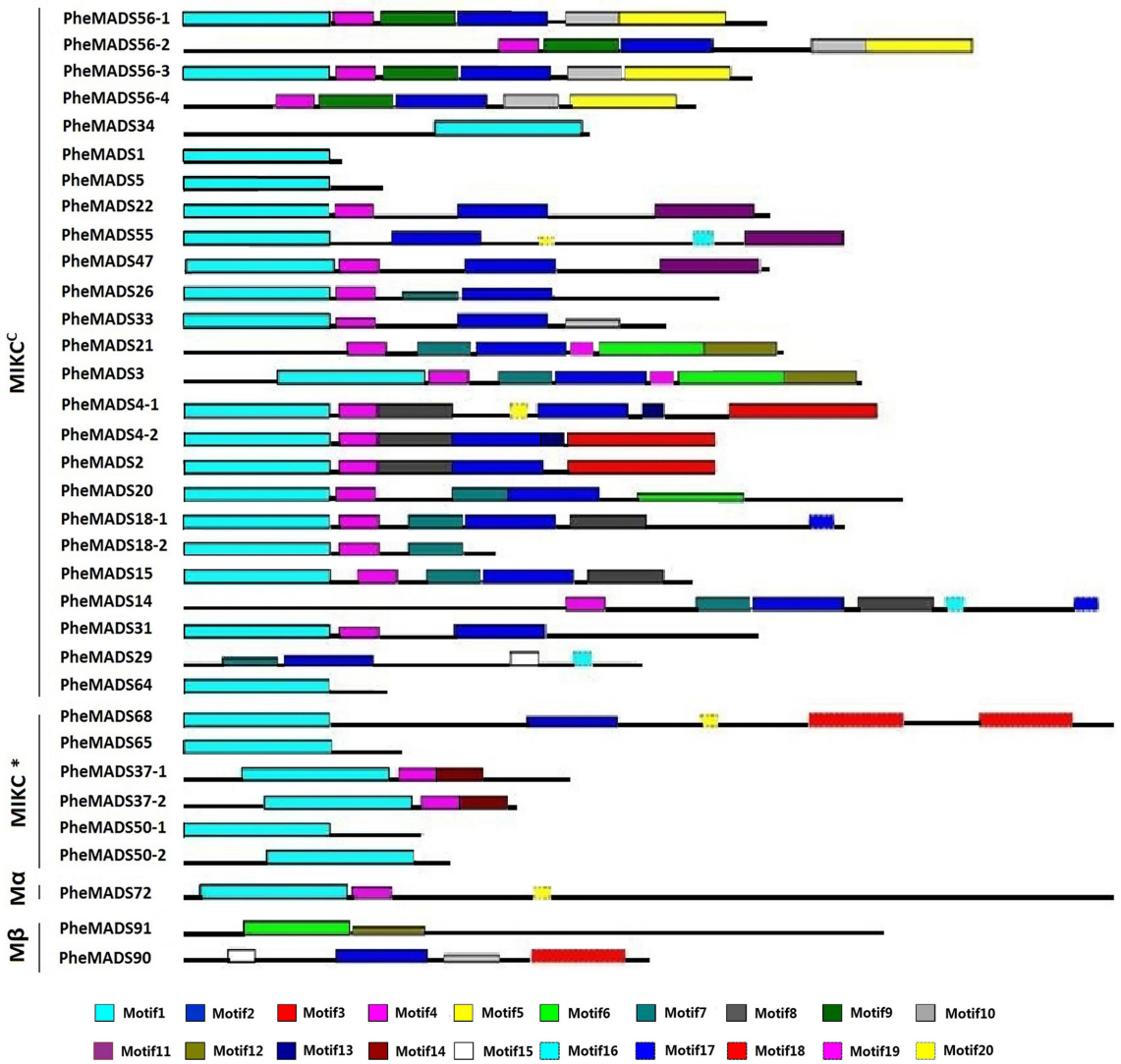

FIGURE 3 | Distribution of conserved motifs in *P. edulis* MADS-box proteins identified using MEME search tool. Schematic representation of motifs identified in *P. edulis* MADS-box proteins using MEME motif search tool for each group given separately. Each motif is represented by a number in colored box. Length of box does not correspond to length of motif. Order of the motifs corresponds to position of motifs in individual protein sequence. For detail of motifs refer to Supplementary Material.

divergence of monocots and dicots. In addition, a phylogenetic tree with bootstrap values was constructed to identify putative orthologs in *Arabidopsis*, rice and *P. edulis* using the complete protein sequences (Supplementary Table S1).

Gene Structure and Conserved Motif Distribution Analysis

To better understand the structural diversity of *P. edulis* MADS-box genes, intron/exon arrangements and conserved motifs were compared with phylogenetics. The MEME motif search tool and GSDS were employed to identify conserved motifs and gene structures in MADS-box genes. Intron/exon arrangements in *P. edulis* MADS-box genes were different among MIKC^C and MIKC* genes (**Figure 2**), similar to reports in *Arabidopsis* and rice. Nearly half of MIKC^C genes lacked introns, but only one MIKC* gene lacked an intron (*PheMADS50-2*). The number of introns in remaining MADS-box genes ranged from 1 to 8. The length of MADS-box proteins varied from 62 to 376 amino acids (Supplementary Table S1).

The MEME program was used to analyze conserved motifs in MADS-box proteins followed by SMART annotation, resulting in the identification of 20 conserved motifs (**Figure 3** and Supplementary Table S3). In all 34 *P. edulis* MADS-box proteins, excluding Mγ, most of MIKC^C and MIKC* groups had motif 1-type MADS domain. Motifs 2, 8, 9, and 10 were localized in the K domain. Motif 4 was also conserved across many of the MADS-box proteins, excluding Mβ, which was found in the I

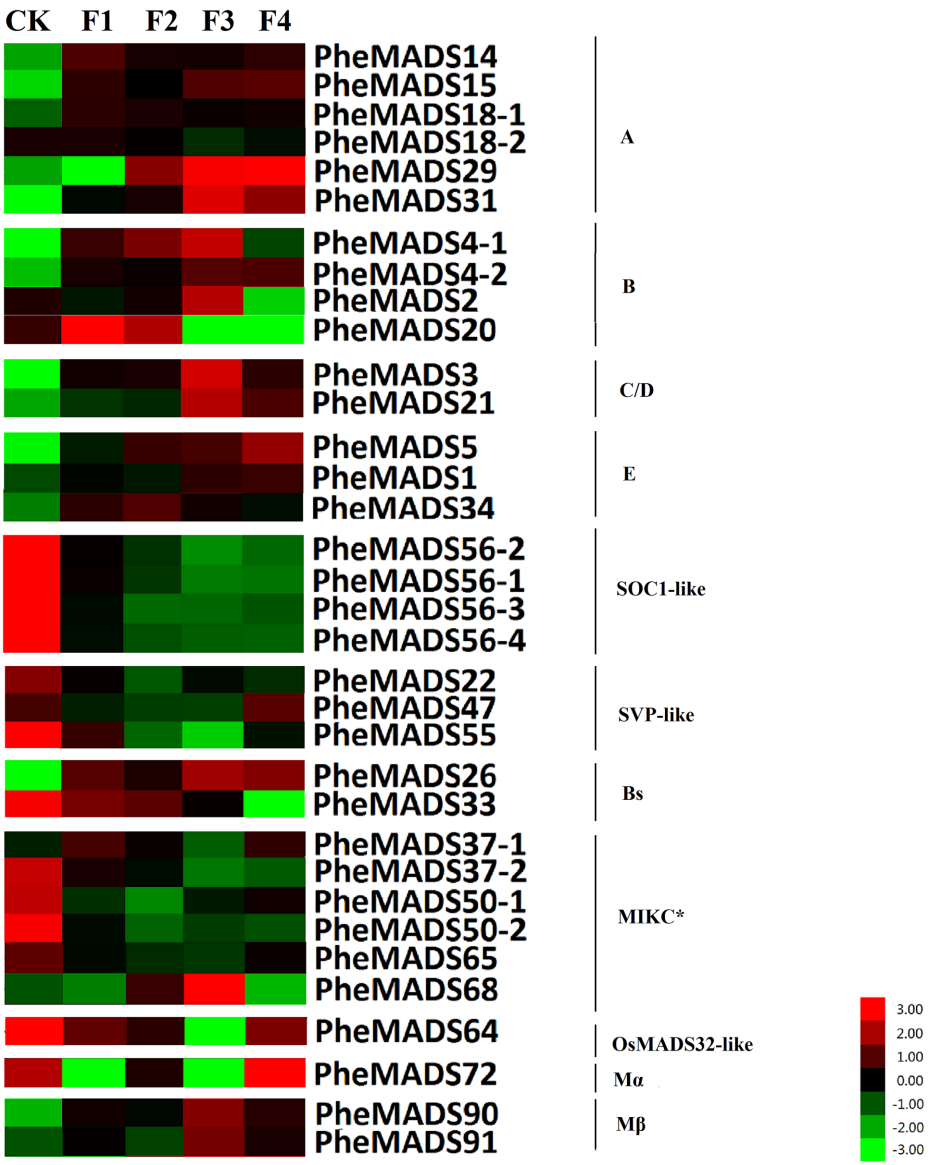

FIGURE 4 | Expression Analysis of MADS-box genes in *P. edulis*. Hierarchical cluster display of expression profile for 34 MADS-box genes showing different expression levels in during floral organ development (CK, F1, F2, F3, and F4). Color bar at the base represents RPKM expression values, thereby green color representing low level expression, black shows medium level expression and red signifies high level expression.

domain. Most of the unconserved motifs (3, 5–7, 11–20) were located in C-terminus, which is typically the most diverse region in MADS-box proteins (Kramer et al., 1998). The sequences and lengths of all the motifs were given in Supplementary Table S3.

The Analysis of Expression Patterns of PheMADS-Box Genes during Floral Organ Development

MADS-box gene expression was tested at five broad categories in flowers described by Gao et al. (2014). The expression profiles were expanded by including transcriptomes from the Transcriptome Sequencing Bamboo Genome Database, including: leaves from non-flowering (CK) and four flowering developmental stages (F) of *P. edulis* (Supplementary Table S4). MADS-box genes were classified into 11 groups based on phylogenetic analysis during flowering developmental stages (**Figure 4**). The expression levels of the A and B class PheMADS genes were high in F1 and F2 and decreased through floral maturity. In contrast, the expressions of C, D, and E class PheMADS genes were reduced at the floral bud formation stage, increased at the third flowering developmental stage and embryo formation stage. Besides, *PheMADS26* (Bs-class), *PheMADS68* (MIKC*-type) and *PheMADS72* (Mβ-class) were expressed predominantly at the floral formation stage.

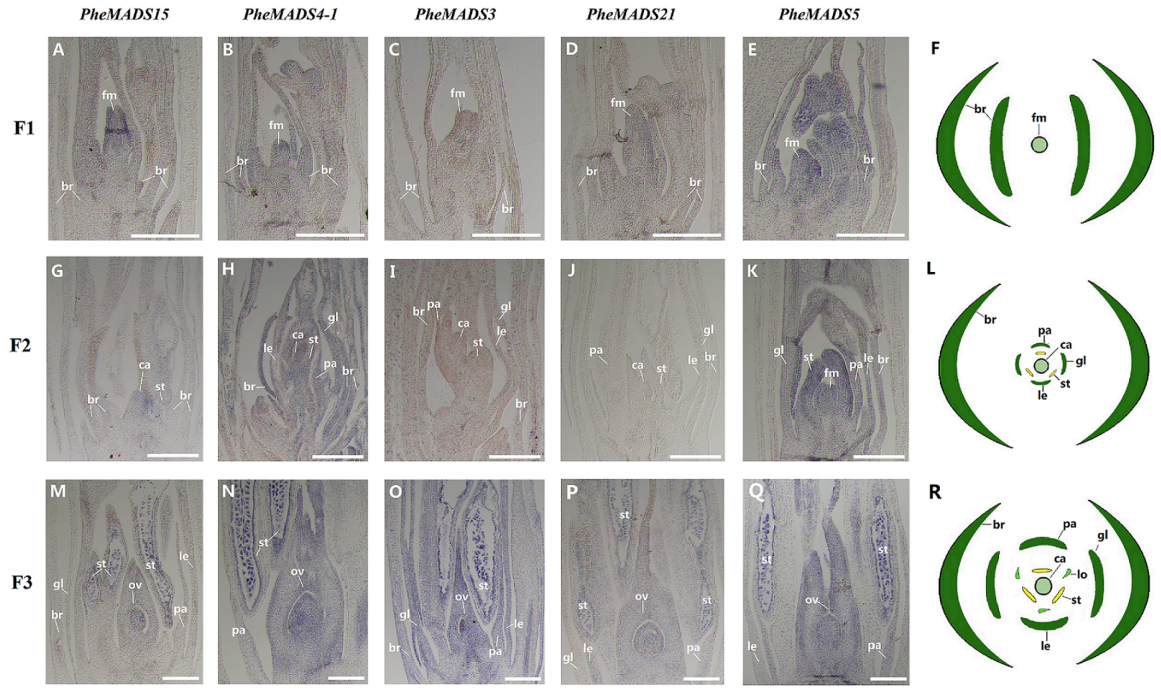

FIGURE 5 | *In situ* analysis of *PheMADS15*, *PheMADS4-1*, *PheMADS3*, *PheMADS21,* and *PheMADS5*. F1: The floral bud formation stage. F2: The inflorescence growing stage. F3: The flowers with both pistils and stamens emerging from glumes at bloom stage. A-S: *In situ* localization of *PheMADS15* **(A,G,M)**, *PheMADS4-1* **(B,H,N)**, *PheMADS3* **(C,I,O)**, *PheMADS21* **(D,J,P)** and *PheMADS5* **(E,K,Q)** transcripts from F1 to F3; floral diagrams of F1 **(F)**, F2 **(L)**, and F3 **(R)**. fm, floral meristem; br, bract; gl, glume; le, lemma; pa, palea; st, stamen; ca, capel; ov, ovule. Bars = 100 μm.

From the outer to the inner whorl within the floral organ, the *P. edulis* flower consisted of four concentric whorls comprising lemma (whorl 1), palea (whorl 1), three lodicules (whorl 2), three stamens (whorl 3) and in the center, pistil (whorl 4) in which the ovule develops (**Figures 5F,L,R** and Supplementary Figure S3). These organs together formed a floret. Our results indicated that A-class genes, *PheMADS14*, *PheMADS15,* and *PheMADS18-1* were expressed throughout, and higher at the floral bud formation stage, while *PheMADS29* and *PheMADS30* were preferentially expressed from F2 to F4 (**Figure 4**). Based on *in situ* hybridization analysis, *PheMADS15* was expressed in the early spikelet meristem, the primordia of flower organs, and the reproductive organs (**Figures 5A,G,M**). Based on the phylogenetic tree analysis, the C and D class contain *PheMADS3* and *PheMADS21* (**Figure 1**). *PheMADS3* and *PheMADS21* were mainly expressed in stamen and pistils formation stage (**Figure 4**). In addition, the *in situ* hybridization data showed that *PheMADS3* and *PheMADS21* mRNA were highly expressed in the stamen and developing embryo (**Figures 5C,D,I,J,O,P**). These data were consistent with those of *PheMADS3* and *PheMADS21* from RNA-seq. The E class genes in the *SEP* lineage in *P. edulis* were *PheMADS1*, *PheMADS5,* and *PheMADS34*. *PheMADS1* and *PheMADS5* were highly expressed in the third flowering developmental stage and embryo formation stage (**Figure 4**). The spatial and temporal expression patterns *PheMADS5* were detected from the early floral bud to the maturely floral organ by *in situ* hybridization in *P. edulis* (**Figures 5E,K,Q**). However, *PheMADS34* was expressed predominantly at the floral bud formation stage and declined during floral development. In addition, the functionally characterized MADS-box genes of rice and *Arabidopsis* are listed in Supplementary Table S2 which provided support toward ABCDE model. Sense controls for five MADS-box genes are in **Figure 6**.

On the contrary, the expression of the remaining genes of *PheMADSs* was lower than that of ABCDE PheMADS genes in *P. edulis* floral development. However, *PheMADS26* (Bs-class), *PheMADS68* (MIKC*-type) and *PheMADS72* (Mβ-class) were expressed predominantly at the floral formation stage (**Figure 4**). Perhaps these genes might be also involved in the development of flower organs.

To confirm that *PheMADS* genes from RNA-seq are expressed, eight genes were selected for validation by qPCR (**Figure 7**). The expression of two *PheMADS* genes (*PheMADS3* and *15*) were up-regulated in floral tissues 10-fold more than non-flowering leaves. However, the expression of *PheMADS56-1* decreased significantly during flower development. According to the qPCR results, the expression patterns for all eight genes from qPCR were similar to that obtained from the Illumina analysis, thus strengthening the reliability of the RNA-seq data.

Duplication and Functional Divergence of MADS-Box Gene Pairs in *P. edulis*

A significant role for gene duplication in the proliferation and evolution of biological complexity of MADS-box genes has been postulated in many divergent plant species (Alvarez-Buylla et al.,

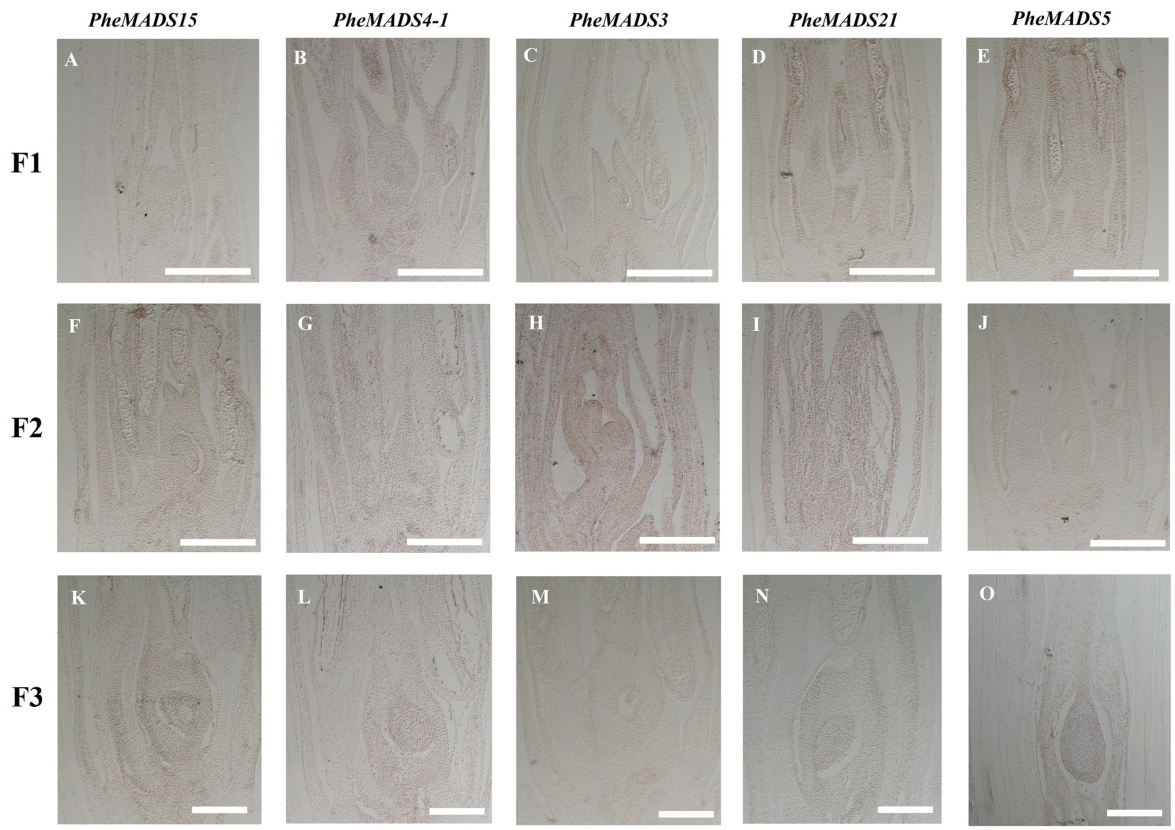

FIGURE 6 | Sense controls of *PheMADS15*, *PheMADS4-1*, *PheMADS3*, *PheMADS21,* and *PheMADS5*. F1: The floral bud formation stage. F2: The inflorescence growing stage. F3: The flowers with both pistils and stamens emerging from glumes at bloom stage. **(A–O)** Sense controls for *PheMADS15* **(A,F,K)**, *PheMADS4-1* **(B,G,L)**, *PheMADS3* **(C,H,M)**, *PheMADS21* **(D,I,N),** and *PheMADS5* **(E,J,O)** transcripts from F1 to F3. Bars = 100 μm.

2000b; Shan et al., 2009). Most duplicated genes diverge to compartmentalize function (sub-functionalization) or gain novel function (neo-functionalization), and can increase biological complexity (Lynch and Conery, 2000; Ohno, 2013). A rate of 6.5×10^{-9} substitution per synonymous site per year was used to calculate the divergence time between 13 pairs of closely related MADS-box genes in a phylogenetic tree (Gaut et al., 1996). The divergence for most PheMADS-box gene pairs is around 10 to 30 MYA (Million Years Ago) (**Table 1**), which is a similar time fram as the *P. edulis* WGD event (Peng et al., 2013), which occurred later than *Brachypodium* at ∼70 MYA (Wei et al., 2014). In contrast, six gene pairs (*PheMADS50-1/50-2*, *1/5*, *14/15*, *64/65*, *90/91,* and *26/33*) diverged 31 to 119 MYA, which does not correlate with the *P. edulis* WGD.

A K_a/K_s ratio less than 1 is indicative of purifying selection and a ratio greater than 1 is indicative of diversifying selection. With pairwise comparisons we found that for all 13 PheMADS-box gene pairs evolved under purifying selection (**Table 1**). Interestingly, further analyses indicated that some closely related gene pairs had different expression patterns and subtle functional divergence. Most notably, for MIKC*-type, *PheMADS37-1* expressed predominantly during floral development, whereas *PheMADS37-2* expression was detectable in leaves from non-flowering plants. These results indicated that PheMADS-box genes diverged in function whilst also undergoing strong purifying selection.

Identification and Sequence Analysis of the *PheMADS15* Gene

To elucidate the role of *PheMADS15* in flower formation in *P. edulis*, we identified the *PheMADS15* cDNA encoding a highly conserved MADS domain. *PheMADS15* appeared to be a full-length cDNA of 630 bp encoding a protein of 209 amino acids residues (Supplementary Figure S2).

While green fluorescent protein (GFP) alone exhibited a dispersed cytoplasmic distribution, GFP tagged *PheMADS15* was indeed located in the nucleus, in accordance with its function as a transcription factor (**Figure 8A**). In addition, we fused PheMADS15 with the GAL4 DNA-binding domain (GAL4DB) and tested its ability in a yeast reporter construct. PheMADS15 was able to activate the expression of the *His-3* and β-*Gal* reporter gene (**Figure 8B**). *PheMADS15* was highly expressed in early blooming stages (**Figure 5A**), closely followed by later blooming stages, but just above detection in leaf samples. These results indicated that *PheMADS15* might play an important role in flower formation at an early stage, as a transcription factor.

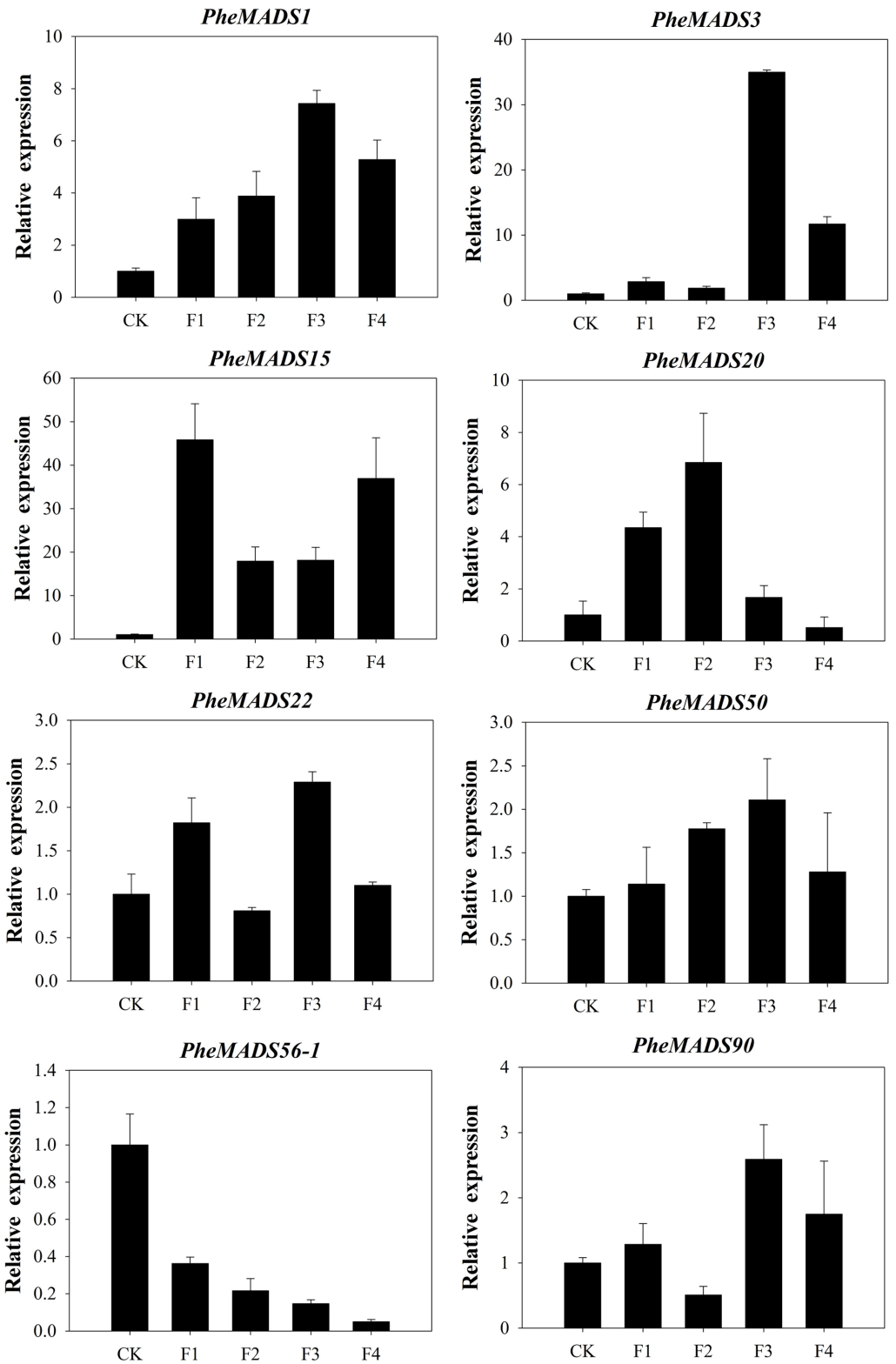

FIGURE 7 | The expression profiles of eight selected genes from flowering tissues in different flower developmental stages and leaves of non-flowering plants (CK). The transcript levels were normalized to that of TIP41 (Fan et al., 2013), and the level of each gene in the control was set at 1.0. Error bars represented the SD for three independent experiments.

TABLE 1 | Estimated divergence period of MADS-box gene pairs in *Phyllostachys edulis*.

Gene pairs			K_s	K_a	K_a/K_s	MYA
PheMADS37-1	vs.	PheMADS37-2	0.1375	0.0499	0.3629	10.58
PheMADS4-1	vs.	PheMADS4-2	0.143	0.0176	0.1230	11
PheMADS56-3	vs.	PheMADS56-4	0.2129	0.1504	0.7064	16.38
PheMADS3	vs.	PheMADS21	0.2468	0.192	0.7779	18.98
PheMADS18-1	vs.	PheMADS18-2	0.2528	0.0839	0.3319	19.45
PheMADS56-1	vs.	PheMADS56-2	0.2794	0.2123	0.7598	21.49
PheMADS22	vs.	PheMADS55	0.3963	0.2558	0.6455	30.48
PheMADS50-1	vs.	PheMADS50-2	0.4059	0.1858	0.4578	31.22
PheMADS1	vs.	PheMADS5	0.4651	0.0442	0.0950	35.78
PheMADS14	vs.	PheMADS15	0.4727	0.2265	0.4792	36.36
PheMADS64	vs.	PheMADS65	0.5772	0.3373	0.5844	44.4
PheMADS90	vs.	PheMADS91	1.1226	0.9097	0.8104	86.35
PheMADS26	vs.	PheMADS33	1.5552	0.4713	0.3030	119.63

K_s, synonymous substitution rate; K_a, non-synonymous substitution rate; MYA, million years ago.

Overexpression of *PheMADS15* in *Arabidopsis* Plants (Wild-Type) Promotes Flowering Time

To further investigate the role of *PheMADS15* in the transcriptional regulation of flowering time, *PheMADS15* was overexpressed in *Arabidopsis* (WT). At least 54 transgenic plants expressing *PheMADS15* were generated and examined for their morphology in the T_1 generation (Supplementary Figure S1). The overexpressed plants showed an early flowering phenotype (**Figures 9A,B**). We further investigated the expression of *SOC1*, *LFY,* and *TFL1* in the T_3 generation to ascertain the downstream effects of this construct (**Figure 9C**). *SOC1* and *LFY* had a dramatic expression increases, while *TFL1* expression was rather low in compared to wild type (**Figure 9C**), which was a similar phenomenon exhibited by overexpression of *Arabidopsis AP1* (Liljegren et al., 1999).

DISCUSSION

The Slow Birth and Death Rate for MADS-Box Genes of *P. edulis*

The MADS-box gene family in plants has expanded though gene duplication events owing to multiple whole genome duplication events in many plants (Gaut, 2002; Paterson et al., 2004; Yu et al., 2005). Most of the Type II MADS-box genes that mainly control flower development were generally associated with some whole genome duplication events (Causier et al., 2005). On the contrary, the duplications inducing more Type I MADS-box genes can be attributed to smaller scale local duplication events (Nam et al., 2004). We found that *P. edulis* had a comparable number of MADS-box genes in type II group, but significantly fewer of Mα and Mβ genes than rice and *Arabidopsis*, indicating that *P. edulis* genome experienced tandem duplications (Vogel et al., 1992; Guo et al., 2004). Six pairs (*PheMADS37-1/37-2*, *PheMADS4-1/4-2*, *PheMADS56-3/56-4*, *PheMADS3/21*, *PheMADS18-1/18-2,* and *PheMADS56-1/56-2*) in *P. edulis* had very consistent divergence times, suggesting that these gene pairs followed the WGD event of *P. edulis*. However, for Mβ, *PheMADS90/91* divergence was estimated at about 86 MYA and represented a anciently duplicated gene pair, indicating a smaller scale local duplication event. Thus, for *P. edulis*, fewer duplication events led to a slower birth and death rate after bamboo diverged from other grasses (Peng et al., 2013).

ABCDE Genes Have Important Functional Conservation and Diversification among *P. edulis*, Rice and *Arabidopsis*

MADS-box genes have been found to evolve through neofunctionalization or subfunctionalization after gene duplication events (Irish and Litt, 2005). Moreover, we found that homologous MADS-box genes had different expression profiles, which offered some evidence about functional divergence occurring after the divergence of *P. edulis*, rice and *Arabidopsis* (Vogel et al., 1992).

In *Arabidopsis*, *AP1* played an important role in the determination of the identity of sepals and petals and furthermore specifies floral meristem identity (Kater et al., 2006). The *AP1* homolog *OsMADS14* was highly expressed in inflorescence and caryopses through transcript analysis (Pelucchi et al., 2002). Besides, *OsMADS15* and *OsMADS18* were activated in the meristem at phase transition in rice (Kobayashi et al., 2012). In *Bambusa edulis*, as the A class gene, *BeMADS14* was expressed throughout, but higher in the lemma and pistil, *BeMADS15* was detected in the lemma and palea (Shih et al., 2014). Based on RNA-seq analysis, *PheMADS14* showed a similar expression pattern, but very low expression in floral organs differentiation stage (**Figure 4**). Meanwhile *PheMADS15* mRNA obviously accumulated in the meristem at phase transition by *in situ* hybridization. These data showed that *PheMADS15* was involved in flower bud differentiation. The expression pattern of *PheMADS18-1* and *PheMADS18-2* which were detected in flower bud formation, was different from *OsMADS18* with high expression in leaves following germination (Fornara et al., 2004). In *P. edulis*, *PheMADS29* and *PheMADS31* were mainly expressed in mature organs and developing caryopses. These data were consistent with that of *OsMADS29*, which was expressed in seed development of rice (Yang et al., 2012). Our results showed that five *AP1*-like genes were uniformly expressed in *P. edulis* floral organs. This similar expression pattern in floral organs was also shown for *AP1*-like genes in *Arabidopsis* (Mandel et al., 1992) and rice (Arora et al., 2007).

In *Arabidopsis*, *AP3* and *PI*, two class B floral organ identity genes, belonged to the *DEF*-like and *GLO*-like gene groups, respectively (Jack et al., 1992; Goto and Meyerowitz, 1994). Rice *in situ* hybridization data showed that two *PI* homologs, *OsMADS2* and *OsMADS4* played important roles in lodicule and stamen development (Yao et al., 2008). Whether of *PI* or *AP3* lineage, the mRNA of B class genes (*PheMADS2*, *PheMADS4-1* and *PheMADS4-2*) showed a similar expression pattern: mainly

in stamen development (F3) (**Figure 4**). Rice *OsMADS16*/*SPW1* and maize *SILKY1* (*SL*) mRNA were detected mainly in the lodicules and stamen primordia during floral development, but not in developing carpels (Ambrose et al., 2000; Nagasawa et al., 2003). In wheat, the expression of *TaAP3* was obviously accumulated in mature female organs, but the function of *TaAP3* was unknown (Paollacci et al., 2007). To further explore the spatial and temporal expression pattern of B class genes, a stronger expression of *PheMADS4-1* was observed in stamen by *in situ* hybridization (**Figures 5B,H,N**). For *B. edulis*, *BeMADS2*, the *PI*/*GLO*-like gene, also displayed similar expression patterns with *PheMADS4-1*, was highly expressed in anthers (Shih et al., 2014). This result correlated with that of *PI* and *AP3*. However, only *PheMADS20* was strongly expressed in the spikelet primordia before lemma and palea initiation (F1) (**Figure 4**).

In *Arabidopsis*, *AG* was a typical class C gene (Yanofsky et al., 1990). As proposed by the ABC model, the *AG* gene was essential to specify stamen and carpel identity and floral determinacy. In rice, analysis of *osmads3 osmads58* double mutant revealed the fact that *OsMADS3* and *OsMADS58* were involved in reproductive organ identity and accumulation of lodicules in the whorl 3 and whorl 4 (Dreni et al., 2011). Besides, in wheat, *TaAG-1* and *TaAG-2* transcripts were highly expressed in the stamens and pistils (Paollacci et al., 2007). *PheMADS3*, was also detected in stamens, carpels and ovule primordial by *in situ* hybridization (**Figure 5O**). *PheMADS21* was also part of the *AG*-lineage and mainly expressed in anthers and pistils, with especially high levels in anthers by *in situ* hybridization (**Figure 5P**). In *Arabidopsis*, the class D gene, *STK*, was exclusively expressed in ovules (Pinyopich et al., 2003). In rice, two class D

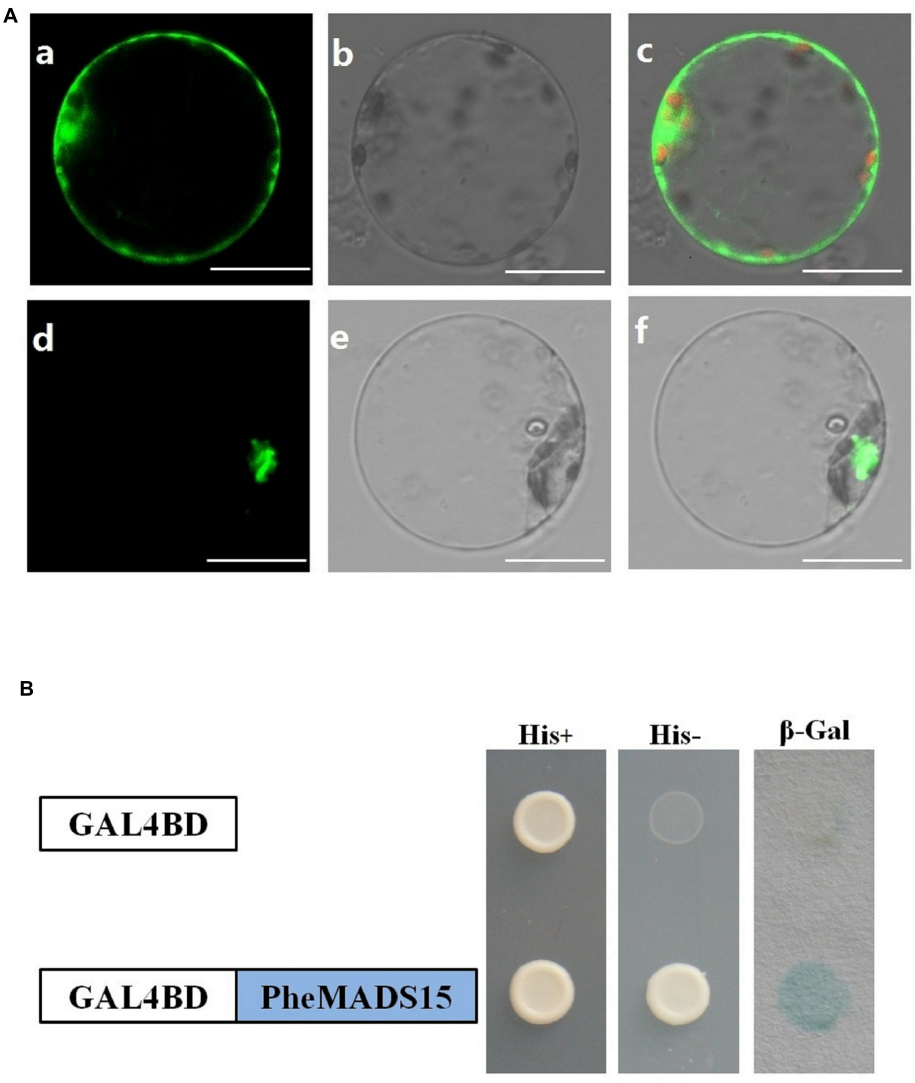

FIGURE 8 | Subcellular localization and transcriptional activation analysis of PheMADS15. (A) (a–c), rice protoplasts expressing 35S-GFP, (d–f), rice protoplasts expressing PheMADS15-GFP. Bar = 10 μm. **(B)** Transcriptional activation analysis of full-length PheMADS15 fused with the GAL4 DNA binding domain in yeast showing its ability to activate the expression of the *His-3* and β-Gal reporter genes.

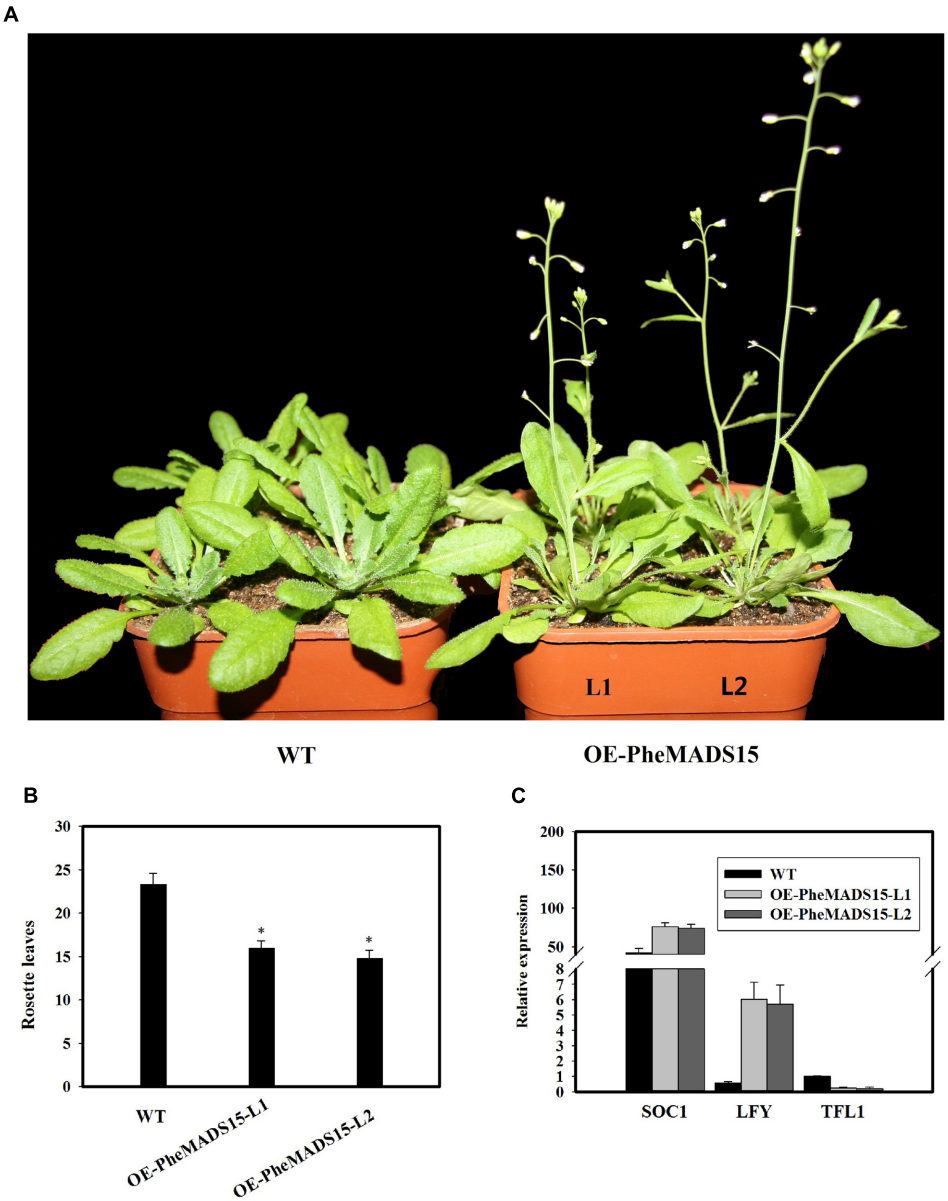

FIGURE 9 | Analysis of an early flowering phenotype by overexpression of *PheMADS15* in *Arabidopsis*. (A) The flowering phenotype of wild-type (WT), OEPheMADS15-L1 and OEPheMADS15-L2 grown for 4 weeks at 23°C under long-day conditions. **(B)** Flowering time scored as the number of rosette leaves at flowering of wild-type and transgenic plants at 23°C under long-day conditions. **(C)** Transcript levels of *SOC1*, *LFY,* and *TFL1* in wild-type and transgenic plants (L1 and L2) were evaluated by qPCR. *Arabidopsis* β-tubulin expression was used as a control. Total RNA from 5-week-old whole- *Arabidopsis* tissues, including leaves and shoot apex, were used for *PheMADS15*, *SOC1*, *LFY,* and *TFL1* examination. Error bars indicate standard deviations. Asterisks indicate a statistically significant difference between wild-type and transgenic plants ($P < 0.05$ by student's *t*-test).

genes have been identified, namely *OsMADS13* (Lopez-Dee et al., 1999) and *OsMADS21* (Lee et al., 2003) based on phylogenetic reconstruction. The expression pattern of *OsMADS13* which was specifically expressed in the ovule was very similar to maize *ZAG2* and *Arabidopsis STK* (Schmidt et al., 1993; Lopez-Dee et al., 1999; Dreni et al., 2007). Moreover, the expression region of *OsMADS21* which was highly expressed in the inner cell layers of the ovary and in the ovule integuments, overlapped with that of *OsMADS13* (Dreni et al., 2007). The expression pattern of *PheMADS21* was slightly different from the *Arabidopsis* ortholog *STK* and the rice ortholog *OsMADS21*. Thus, much deeper investigations are needed to further substantiate the classification and functioning of *PheMADS3* and *PheMADS21*.

In *Arabidopsis*, the E class genes, such as *Arabidopsis SEP* genes were involved in the specification of sepal, petal, stamen, carpel, and ovule identity and interact with the class A, B,

C, and D genes to form higher order MADS-box protein complexes (Honma and Goto, 2001; Pelaz et al., 2001; Favaro et al., 2003). In *P. edulis*, three E class genes, such as *PheMADS1*, *PheMADS5,* and *PheMADS34* belonged to the *SEP* lineage. On *in situ* hybridization analysis, *PheMADS5* was highly expressed throughout the floral meristem and subsequently detected in palea, lemma, and anthers in the mature flower (**Figures 5E,K,Q**). In rice, *OsMADS5*, a *SEP*-like gene, caused homeotic transformation of all floral organs except the lemma into leaf-like organs (Cui et al., 2010). The expression of *PheMADS34* which was high in flower bud formation, was similar to *OsMADS34.* However, *OsMADS34* played a key role in lemma/palea, lodicules, stamens, and carpel (Gao et al., 2010). These findings show many significant differences can be observed between rice and moso bamboo. Future functional studies will have to explore biological function of these *PheMADS* genes.

Overexpression of *PheMADS15* Promotes Flowering Time

In rice, *OsMADS14* and *OsMADS15* were previously identified as flowering regulators (Kim et al., 2007; Lu et al., 2012). Here, we report the identification and characterization of a MADS-box gene from *P. edulis*, *PheMADS15*, which through ectopic overexpression triggered earlier flowering time in *Arabidopsis*. *PheMADS15*, an *AP1*-like gene, is highly expressed during flower bud morphological differentiation (**Figure 5A**) and it is located in the nucleus (**Figure 8B**). *LFY* and *AP1* which were expressed in the converted floral meristems primarily control *Arabidopsis* flower meristems (Shannon and Meeks-Wagner, 1991; Weigel et al., 1992; Ferrándiz et al., 2000). In this study, early flowering time was also observed in *35S*: *PheMADS15* transgenic *Arabidopsis*. Meanwhile, the expression level of *LFY* and *SOC1* was up-regulated in *35S*:*PheMADS15* transgenic *Arabidopsis* compared with wild type *Arabidopsis*. *SOC1* promoted floral transitions and is considered as one of the core regulators of flowering in *Arabidopsis* (Moon et al., 2003; Liu et al., 2008; Lee and Lee, 2010; Dorca-Fornell et al., 2011). *AP1* is another positive regulator of *LFY* and is highly expressed in converted floral meristems (Liljegren et al., 1999). In addition, *OsMADS14*, *OsMADS15,* and *OsMADS18*, three *AP1/FUL*-like genes, were involved in the regulation of flowering time (Kobayashi et al., 2012). This leads us to suspect that *PheMADS15* promotes flowering time by regulating *LFY* and *SOC1* directly or indirectly. This is consistent with the previous reports about some *AP1*-like genes (Weigel et al., 1992), suggesting that *PheMADS15* is a functional ortholog of *Arabidopsis AP1*. Further research on the transcriptional regulatory network mediated by PheMADSs will increase knowledge surrounding the transcriptional regulation of flowering time in *P. edulis*.

AUTHOR CONTRIBUTIONS

ZC, WG, and LL performed all the experiments, data analysis and wrote the paper. XL and SM analyzed data. DH, YM, JL, and QB revised the manuscript. JG designed and supervised experiments.

FUNDING

This work was supported by National High Technology Research and Development Program of China "Moso Bamboo Functional Genomics Research" (Grant No.2013AA102607-4), the National Natural Science Foundation of China (31570673) and Fundamental Research Funds of ICBR [grant No.1632015009].

ACKNOWLEDGMENTS

The authors thank CC (Institute of Genetics and Developmental Biology, Chinese Academy of Sciences, Beijing, China) for providing rice protoplast transformation technology platform and Prof. Xiaoting Qi (Capital Normal University, Beijing, China) for providing the yeast strain PJ69-4a.

SUPPLEMENTARY MATERIAL

The Supplementary Material for this article can be found online at: http://journal.frontiersin.org/article/10.3389/fpls.2017.00656/full#supplementary-material

REFERENCES

Alvarez-Buylla, E. R., Liljegren, S. J., Pelaz, S., Gold, S. E., Burgeff, C., Ditta, G. S., et al. (2000a). MADS-box gene evolution beyond flowers: expression in pollen, endosperm, guard cells, roots and trichomes. *Plant J.* 24, 457–466.

Alvarez-Buylla, E. R., Pelaz, S., Liljegren, S. J., Gold, S. E., Burgeff, C., Ditta, G. S., et al. (2000b). An ancestral MADS-box gene duplication occurred before the divergence of plants and animals. *Proc. Natl. Acad. Sci. U.S.A.* 97, 5328–5333.

Ambrose, B. A., Lerner, D. R., Ciceri, P., Padilla, C. M., Yanofsky, M. F., and Schmidt, R. J. (2000). Molecular and genetic analyses of the *Silky1* gene reveal conservation in floral organ specification between eudicots and monocots. *Mol. Cell* 5, 569–579. doi: 10.1016/S1097-2765(00)80450-5

Angenent, G. C., and Colombo, L. (1996). Molecular control of ovule development. *Trends Plant Sci.* 1, 228–232. doi: 10.1016/S1360-1385(96)86900-0

Arora, R., Agarwal, P., Ray, S., Singh, A. K., Singh, V. P., Tyagi, A. K., et al. (2007). MADS-box gene family in rice: genome-wide identification, organization and expression profiling during reproductive development and stress. *BMC Genomics* 8:242. doi: 10.1186/1471-2164-8-242

Bailey, T. L., and Elkan, C. (1995). "The value of prior knowledge in discovering motifs with MEME," in *Proceedings of the Third International Conference on Intelligent Systems for Molecular Biology*, Vol. 3, Menlo Park, CA, 21–29.

Bowman, J. L., Alvarez, J., Weigel, D., Meyerowitz, E. M., and Smyth, D. R. (1993). Control of flower development in *Arabidopsis thaliana* by *APETALA1* and interacting genes. *Development* 119, 721–721.

Causier, B., Castillo, R., Zhou, J., Ingram, R., Xue, Y., Schwarz-Sommer, Z., et al. (2005). Evolution in action: following function in duplicated floral homeotic genes. *Curr. Biol.* 15, 1508–1512. doi: 10.1016/j.cub.2005.07.063

Coen, E. S., and Meyerowitz, E. M. (1991). The war of the whorls: genetic interactions controlling flower development. *Nature* 353, 31–37. doi: 10.1038/353031a0

Cui, R., Han, J., Zhao, S., Su, K., Wu, F., Du, X., et al. (2010). Functional conservation and diversification of class E floral homeotic genes in rice (*Oryza sativa*). *Plant J.* 61, 767–781. doi: 10.1111/j.1365-313X.2009.04101.x

de Almeida Engler, J., De Groodt, R., Van Montagu, M., and Engler, G. (2001). *In situ* hybridization to mRNA of *Arabidopsis* tissue sections. *Methods* 23, 325–334. doi: 10.1006/meth.2000.1144

de Hoon, M. J., Imoto, S., Nolan, J., and Miyano, S. (2004). Open source clustering software. *Bioinformatics* 20, 1453–1454. doi: 10.1093/bioinformatics/bth078

Ditta, G., Pinyopich, A., and Robles, P. (2004). The *SEP4* gene of *Arabidopsis thaliana* functions in floral organ and meristem identity. *Curr. Biol.* 14, 1935–1940. doi: 10.1016/j.cub.2004.10.028

Dorca-Fornell, C., Gregis, V., Grandi, V., Coupland, G., Colombo, L., and Kater, M. M. (2011). The *Arabidopsis SOC1*-like genes *AGL42, AGL71* and *AGL72* promote flowering in the shoot apical and axillary meristems. *Plant J.* 67, 1006–1017. doi: 10.1111/j.1365-313X.2011.04653.x

Dreni, L., Jacchia, S., Fornara, F., Fornari, M., Ouwerkerk, P. B., An, G., et al. (2007). The D-lineage MADS-box gene *OsMADS13* controls ovule identity in rice. *Plant J.* 52, 690–699. doi: 10.1111/j.1365-313X.2007.03272.x

Dreni, L., Pilatone, A., Yun, D., Erreni, S., Pajoro, A., Caporali, E., et al. (2011). Functional analysis of all *AGAMOUS* subfamily members in rice reveals their roles in reproductive organ identity determination and meristem determinacy. *Plant Cell* 23, 2850–2863. doi: 10.1105/tpc.111.087007

Ehrenreich, I. M., Hanzawa, Y., Chou, L., Roe, J. L., Kover, P. X., and Purugganan, M. D. (2009). Candidate gene association mapping of *Arabidopsis* flowering time. *Genetics* 183, 325–335. doi: 10.1534/genetics.109.105189

Fan, C., Ma, J., Guo, Q., Li, X., Wang, H., and Lu, M. (2013). Selection of reference genes for quantitative real-time PCR in bamboo (*Phyllostachys edulis*). *PLoS ONE* 8:e56573. doi: 10.1371/journal.pone.0056573

Favaro, R., Pinyopich, A., Battaglia, R., Kooiker, M., Borghi, L., Ditta, G., et al. (2003). MADS-box protein complexes control carpel and ovule development in *Arabidopsis*. *Plant Cell* 15, 2603–2611. doi: 10.1105/tpc.015123

Feldmann, K. A., and Marks, M. D. (1987). Agrobacterium-mediated transformation of germinating seeds of *Arabidopsis thaliana*: a non-tissue culture approach. *Mol. Genet. Genomics* 208, 1–9. doi: 10.1007/BF00330414

Ferrándiz, C., Gu, Q., Martienssen, R., and Yanofsky, M. F. (2000). Redundant regulation of meristem identity and plant architecture by *FRUITFULL*, *APETALA1* and *CAULIFLOWER*. *Development* 127, 725–734.

Fornara, F., de Montaigu, A., and Coupland, G. (2010). SnapShot: control of flowering in *Arabidopsis*. *Cell* 141, 550. doi: 10.1016/j.cell.2010.04.024

Fornara, F., Paøenicová, L., Falasca, G., Pelucchi, N., Masiero, S., Ciannamea, S., et al. (2004). Functional characterization of *OsMADS18*, a member of the *AP1/SQUA* subfamily of MADS-box genes. *Plant Physiol.* 135, 2207–2219. doi: 10.1104/pp.104.045039

Gao, J., Zhang, Y., Zhang, C., Qi, F., Li, X., Mu, S., et al. (2014). Characterization of the floral Transcriptome of moso bamboo (*Phyllostachys edulis*). at Different flowering developmental stages by transcriptome sequencing and RNA-Seq analysis. *PLoS ONE* 9:e98910. doi: 10.1371/journal.pone.0098910

Gao, X., Liang, W., Yin, C., Ji, S., Wang, H., Su, X., et al. (2010). The *SEPALLATA*-like gene *OsMADS34* is required for rice inflorescence and spikelet development. *Plant Physiol.* 153, 728–740. doi: 10.1104/pp.110.156711

Gaut, B. S. (2002). Evolutionary dynamics of grass genomes. *New Phytol.* 154, 15–28. doi: 10.1046/j.1469-8137.2002.00352.x

Gaut, B. S., Morton, B. R., McCaig, B. C., and Clegg, M. T. (1996). Substitution rate comparisons between grasses and palms: synonymous rate differences at the nuclear gene *Adh* parallel rate differences at the plastid gene *rbcL*. *Proc. Natl. Acad. Sci. U.S.A.* 93, 10274–10279. doi: 10.1073/pnas.93.19.10274

Goto, K., and Meyerowitz, E. M. (1994). Function and regulation of the *Arabidopsis* floral homeotic gene *PISTILLATA*. *Gene. Dev.* 8, 1548–1560. doi: 10.1101/gad.8.13.1548

Grass Phylogeny Working Group, Barker, N. P., Clark, L. G., Davis, J. I, Duvall, M. R., Guala, G. F., et al. (2001). Phylogeny and subfamilial classification of the grasses (Poaceae). *Ann. Mo. Bot. Gard.* 88, 373–457. doi: 10.2307/3298585

Gregis, V., Sessa, A., Dorca-Fornell, C., and Kater, M. M. (2009). The *Arabidopsis* floral meristem identity genes *AP1*, *AGL24* and *SVP* directly repress class B and C floral homeotic genes. *Plant J.* 60, 626–637. doi: 10.1111/j.1365-313X.2009.03985.x

Guo, A. Y., Zhu, Q. H., Chen, X., and Luo, J. C. (2007). GSDS: a gene structure display server. *Yi Chuan* 29, 1023–1026. doi: 10.1360/yc-007-1023

Guo, X. Y., Xu, G. H., Zhang, Y., Hu, W. M., and Fan, L. J. (2004). Small-scale duplications play a significant role in rice genome evolution. *Rice Sci.* 12, 173–178.

Henschel, K., Kofuji, R., Hasebe, M., Saedler, H., Munster, T., and Theissen, G. (2002). Two ancient classes of MIKC-type MADS-box genes are present in the Moss *Physcomitrella patens*. *Mol. Biol. Evol.* 19, 801–814. doi: 10.1093/oxfordjournals.molbev.a004137

Honma, T., and Goto, K. (2001). Complexes of MADS-box proteins are sufficient to convert leaves into floral organs. *Nature* 409, 525–529. doi: 10.1038/35054083

Hu, L. F., Liang, W. Q., Yin, C. S., Cui, X., Zong, J., Wang, X., et al. (2011). Rice MADS3 regulates ROS homeostasis during late anther development. *Plant Cell* 23, 515–533. doi: 10.1105/tpc.110.074369

Huang, H., Tudor, M., and Weiss, C. A. (1995). The *Arabidopsis* MADS-box gene *AGL3* is widely expressed and encodes a sequence-specific DNA-binding protein. *Plant. Mol. Biol.* 28, 549–567. doi: 10.1007/BF00020401

Irish, V. F., and Litt, A. (2005). Flower development and evolution: gene duplication, diversification and redeployment. *Curr. Opin. Genet. Dev.* 15, 454–460. doi: 10.1016/j.gde.2005.06.001

Irish, V. F., and Sussex, I. M. (1990). Function of the apetala-1 gene during *Arabidopsis* floral development. *Plant Cell* 2, 741–753. doi: 10.1105/tpc.2.8.741

Jack, T. (2001). Plant development going MADS. *Plant Mol. Biol.* 46, 515–520. doi: 10.1023/A:1010689126632

Jack, T., Brockman, L. L., and Meyerowitz, E. M. (1992). The homeotic gene *APETALA3* of *Arabidopsis thaliana* encodes a MADS-box and is expressed in petals and stamens. *Cell* 68, 683–697. doi: 10.1016/0092-8674(92)90144-2

Jofuku, K. D., Den Boer, B., Van Montagu, M., and Okamuro, J. K. (1994). Control of *Arabidopsis* flower and seed development by the homeotic gene *APETALA2*. *Plant Cell* 6, 1211–1225. doi: 10.1105/tpc.6.9.1211

Kater, M. M., Dreni, L., and Colombo, L. (2006). Functional conservation of MADS-box factors controlling floral organ identity in rice and *Arabidopsis*. *J. Exp. Bot.* 57, 3433–3444. doi: 10.1093/jxb/erl097

Kim, S. L., Lee, S., Kim, H. J., Nam, H. G., and An, G. (2007). *OsMADS51* is a short-day flowering promoter that functions upstream of *Ehd1*, *OsMADS14*, and *Hd3a*. *Plant Physiol.* 145, 1484–1494. doi: 10.1104/pp.107.103291

Kobayashi, K., Yasuno, N., and Sato, Y. (2012). Inflorescence meristem identity in rice is specified by overlapping functions of three *AP1/FUL*-like MADS-box genes and *PAP2*, a *SEPALLATA* MADS-box gene. *Plant Cell* 24, 1848–1859. doi: 10.1105/tpc.112.097105

Kofuji, R., Sumikawa, N., Yamasaki, M., Kondo, K., Ueda, K., Ito, M., et al. (2003). Evolution and divergence of the MADS-box gene family based on genome-wide expression analyses. *Mol. Biol. Evol.* 20, 1963–1977. doi: 10.1093/molbev/msg216

Kramer, E. M., Dorit, R. L., and Irish, V. F. (1998). Molecular evolution of genes controlling petal and stamen development: duplication and divergence within the *APETALA3* and *PISTILLATA* MADS-box gene lineages. *Genetics* 149, 765–783.

Kramer, E. M., Jaramillo, M. A., and Di Stilio, V. S. (2004). Patterns of gene duplication and functional evolution during the diversification of the *AGAMOUS* subfamily of MADS-box genes in angiosperms. *Genetics* 166, 1011–1023. doi: 10.1534/genetics.166.2.1011

Lee, J., and Lee, I. (2010). Regulation and function of *SOC1*, a flowering pathway integrator. *J. Exp. Bot.* 61, 2247–2254. doi: 10.1093/jxb/erq098

Lee, S., Jeon, J. S., An, K., Moon, Y. H., Lee, S., Chung, Y. Y., et al. (2003). Alteration of floral organ identity in rice through ectopic expression of *OsMADS16*. *Planta* 217, 904–911. doi: 10.1007/s00425-003-1066-8

Li, D., Yang, C., Li, X., Gan, Q., Zhao, X., and Zhu, L. (2009). Functional characterization of rice *OsDof12*. *Planta* 229, 1159–1169. doi: 10.1007/s00425-009-0893-7

Li, H., Liang, W., Hu, Y., Zhu, L., Yin, C., Xu, J., et al. (2011). Rice *MADS6* interacts with the floral homeotic genes *SUPERWOMAN1*, *MADS3*, *MADS58*, *MADS13* and *DROOPING LEAF* in specifying floral organ identities and meristem fate. *Plant Cell* 23, 2536–2552. doi: 10.1105/tpc.111.087262

Liljegren, S. J., Gustafson Brown, C., Pinyopich, A., Ditta, G. S., and Yanofsky, M. F. (1999). Interactions among *APETALA1*, *LEAFY* and *TERMINAL FLOWER1* specify meristem fate. *Plant Cell* 11, 1007–1018. doi: 10.1105/tpc.11.6.1007

Liu, C., Chen, H., Er, H. L., Soo, H. M., Kumar, P. P., Han, J. H., et al. (2008). Direct interaction of *AGL24* and *SOC1* integrates flowering signals in *Arabidopsis*. *Development* 135, 1481–1491. doi: 10.1242/dev.020255

Lopez-Dee, Z. P., Wittich, P., Enrico, P. M., Rigola, D., Del Buono, I., Gorla, M. S., et al. (1999). *OsMADS13*, a novel rice MADS-box gene expressed during ovule development. *Dev. Genet.* 25, 237–244. doi: 10.1002/(SICI)1520-6408(1999)25:3<237::AID-DVG6>3.0.CO;2-L

Lu, S. J., Wei, H., Wang, Y., Wang, H. M., Yang, R. F., Zhang, X. B., et al. (2012). Overexpression of a transcription factor *OsMADS15* modifies plant architecture and flowering time in rice (*Oryza sativa* L.). *Plant Mol. Biol. Rep.* 30, 1461–1469. doi: 10.1007/s11105-012-0468-9

Lynch, M., and Conery, J. S. (2000). The evolutionary fate and consequences of duplicate genes. *Science* 290, 1151–1155. doi: 10.1126/science.290.5494.1151

Mandel, M. A., Gustafson Brown, C., Savidge, B., and Yanofsky, M. F. (1992). Molecular characterization of the *Arabidopsis* floral homeotic gene *APETALA1*. *Nature* 360, 273–277. doi: 10.1038/360273a0

Mandel, M. A., and Yanofsky, M. F. (1998). The *Arabidopsis AGL 9* MADS-box gene is expressed in young flower primordia. *Sex. Plant Reprod.* 11, 22–28. doi: 10.1007/s004970050116

Moon, J., Suh, S. S., Lee, H., Choi, K. R., Hong, C. B., Paek, N. C., et al. (2003). The *SOC1* MADS-box gene integrates vernalization and gibberellin signals for flowering in *Arabidopsis*. *Plant J.* 35, 613–623. doi: 10.1046/j.1365-313X.2003.01833.x

Nagasawa, N., Miyoshi, M., Sano, Y., Satoh, H., Hirano, H., Sakai, H., et al. (2003). *SUPERWOMAN1* and *DROOPING LEAF* genes control floral organ identity in rice. *Development* 130, 705–718. doi: 10.1242/dev.00294

Nam, J., dePamphilis, C. W., Ma, H., and Nei, M. (2003). Antiquity and evolution of the MADS-box gene family controlling flower development in plants. *Mol. Biol. Evol.* 20, 1435–1447. doi: 10.1093/molbev/msg152

Nam, J., Kim, J., Lee, S., An, G., Ma, H., and Nei, M. (2004). Type I MADS-box genes have experienced faster birth-and-death evolution than type II MADS-box genes in angiosperms. *Proc. Natl. Acad. Sci. U.S.A.* 101, 1910–1915. doi: 10.1073/pnas.0308430100

Ohno, S. (2013). *Evolution by Gene Duplication*. Berlin: Springer Science and Business Media.

Paollacci, A. R., Tanzarella, O. A., Porceddu, E., Varotto, S., and Ciaffi, M. (2007). Molecular and phylogenetic analysis of MADS-box genes of MIKC type and chromosome location of *SEP*-like genes in wheat (*Triticum aestivum* L.). *Mol. Genet. Genomics* 278, 689–708. doi: 10.1007/s00438-007-0285-2

Pařenicová, L., de Folter, S., Kieffer, M., Horner, D. S., Favalli, C., Busscher, J., et al. (2003). Molecular and phylogenetic analyses of the complete MADS-box transcription factor family in *Arabidopsis* new openings to the MADS world. *Plant Cell* 15, 1538–1551. doi: 10.1105/tpc.011544

Paterson, A., Bowers, J., and Chapman, B. (2004). Ancient polyploidization predating divergence of the cereals, and its consequences for comparative genomics. *Proc. Natl. Acad. Sci. U.S.A.* 101, 9903–9908. doi: 10.1073/pnas.0307901101

Pelaz, S., Ditta, G. S., Baumann, E., Wisman, E., and Yanofsky, M. F. (2000). B and C floral organ identity functions require *SEPALLATA* MADS-box genes. *Nature* 405, 200–203. doi: 10.1038/35012103

Pelaz, S., Tapia-López, R., Alvarez-Buylla, E. R., and Yanofsky, M. F. (2001). Conversion of leaves into petals in *Arabidopsis*. *Curr. Biol.* 11, 182–184. doi: 10.1016/S0960-9822(01)00024-0

Pelucchi, N., Fornara, F., Favalli, C., Masiero, S., Lago, C., Pè, E. M., et al. (2002). Comparative analysis of rice MADS-box genes expressed during flower development. *Sex. Plant Reprod.* 15, 113–122. doi: 10.1007/s00497-002-0151-7

Peng, Z., Lu, Y., Li, L., Zhao, Q., Feng, Q., Gao, Z., et al. (2013). The draft genome of the fast-growing non-timber forest species moso bamboo (*Phyllostachys heterocycla*). *Nat. Genet.* 45, 456–461. doi: 10.1038/ng.2569

Pinyopich, A., Ditta, G. S., Savidge, B., Liljegren, S. J., Baumann, E., Wisman, E., et al. (2003). Assessing the redundancy of MADS-box genes during carpel and ovule development. *Nature* 424, 85–88. doi: 10.1038/nature01741

Preston, J. C., and Kellogg, E. A. (2007). Conservation and divergence of *APETALA1/FRUITFULL*-like gene function in grasses: evidence from gene expression analyses. *Plant J.* 52, 69–81. doi: 10.1111/j.1365-313X.2007.03209.x

Purugganan, M. D. (1997). The MADS-box floral homeotic gene lineages predate the origin of seed plants: phylogenetic and molecular clock estimates. *J. Mol. Evol.* 45, 392–396. doi: 10.1007/PL00006244

Rudall, P. J., Stuppy, W., Cunniff, J., Kellogg, E. A., and Briggs, B. G. (2005). Evolution of reproductive structures in grasses (Poaceae) inferred by sister-group comparison with their putative closest living relatives, Ecdeiocoleaceae. *Am. J. Bot.* 92, 1432–1443. doi: 10.3732/ajb.92.9.1432

Saitou, N., and Nei, M. (1987). The neighbor-joining method: a new method for reconstructing phylogenetic trees. *Mol. Biol. Evol.* 4, 406–425.

Saldanha, A. J. (2004). Java Treeview-extensible visualization of microarray data. *Bioinformatics* 20, 3246–3248. doi: 10.1093/bioinformatics/bth349

Sang, X., Li, Y., and Luo, Z. (2012). *CHIMERIC FLORAL ORGANS1*, encoding a monocot-specific MADS-box protein, regulates floral organ identity in rice. *Plant Physiol.* 160, 788–807. doi: 10.1104/pp.112.200980

Savidge, B., Rounsley, S. D., and Yanofsky, M. F. (1995). Temporal relationship between the transcription of two *Arabidopsis* MADS-box genes and the floral organ identity genes. *Plant Cell* 7, 721–733. doi: 10.1105/tpc.7.6.721

Schmidt, R. J., Veit, B., Mandel, M. A., Mena, M., Hake, S., and Yanofsky, M. F. (1993). Identification and molecular characterization of *ZAG1*, the maize homolog of the *Arabidopsis* floral homeotic gene *AGAMOUS*. *Plant Cell* 5, 729–737. doi: 10.1105/tpc.5.7.729

Schultz, E. A., and Haughn, G. W. (1991). *LEAFY*, a homeotic gene that regulates inflorescence development in *Arabidopsis*. *Plant Cell* 3, 771–781. doi: 10.1105/tpc.3.8.771

Shan, H., Zahn, L., Guindon, S., Wall, P. K., Kong, H., Ma, H., et al. (2009). Evolution of plant MADS-box transcription factors: evidence for shifts in selection associated with early angiosperm diversification and concerted gene duplications. *Mol. Biol. Evol.* 26, 2229–2244. doi: 10.1093/molbev/msp129

Shannon, S., and Meeks-Wagner, D. R. (1991). A mutation in the *Arabidopsis TFL1* gene affects inflorescence meristem development. *Plant Cell* 3, 877–892. doi: 10.1105/tpc.3.9.877

Shih, M. C., Chou, M. L., Yue, J. J., Hsu, C. T., Chang, W. J., Ko, S. S., et al. (2014). *BeMADS1* is a key to delivery MADSs into nucleus in reproductive tissues-De novo characterization of *Bambusa edulis* transcriptome and study of MADS genes in bamboo floral development. *BMC Plant Biol.* 14:179. doi: 10.1186/1471-2229-14-179

Tamura, K., Stecher, G., Peterson, D., Filipski, A., and Kumar, S. (2013). MEGA6: molecular evolutionary genetics analysis version 6.0. *Mol. Biol. Evol.* 30, 2725–2729. doi: 10.1093/molbev/mst197

Teper-Bamnolker, P., and Samach, A. (2005). The flowering integrator FT regulates *SEPALLATA3* and *FRUITFULL* accumulation in *Arabidopsis* leaves. *Plant Cell* 17, 2661–2675. doi: 10.1105/tpc.105.035766

Theissen, G., Becker, A., Di Rosa, A., Kanno, A., Kim, J. T., Munster, T., et al. (2000). A short history of MADS-box genes in plants. *Plant Mol. Biol.* 42, 115–149. doi: 10.1023/A:1006332105728

Theißen, G., and Saedler, H. (2001). Plant biology: floral quartets. *Nature* 409, 469–471. doi: 10.1038/35054172

Thompson, J. D., Gibson, T. J., Plewniak, F., Jeanmougin, F., and Higgins, D. G. (1997). The CLUSTAL_X windows interface: flexible strategies for multiple sequence alignment aided by quality analysis tools. *Nucleic Acids Res.* 25, 4876–4882. doi: 10.1093/nar/25.24.4876

Tian, B., Chen, Y., Li, D., and Yan, Y. (2006). Cloning and characterization of a bamboo Leafy Hull Sterile1 homologous gene: full length research paper. *Mitochondr. DNA* 17, 143–151.

Tian, B., Chen, Y., Yan, Y., and Li, D. (2005). Isolation and ectopic expression of a bamboo MADS-box gene. *Chin. Sci. Bull.* 50, 217–224. doi: 10.1007/BF02897530

Vogel, J. P., Garvin, D. F., and Mockler, T. C. (1992). *LEAFY* controls floral meristem identity in *Arabidopsis*. *Cell* 69, 843–859. doi: 10.1016/0092-8674(92)90295-N

Wei, B., Zhang, R.-Z., Guo, J.-J., Liu, D.-M., Li, A.-L., Fan, R.-C., et al. (2014). Genome-wide analysis of the MADS-box gene family in *Brachypodium distachyon*. *PLoS ONE* 9:e84781. doi: 10.1371/journal.pone.0084781

Weigel, D., Alvarez, J., Smyth, D. R., Yanofsky, M. F., and Meyerowitz, E. M. (1992). *LEAFY* controls floral meristem identity in Arabidopsis. *Cell* 69, 843–859. doi: 10.1016/0092-8674(92)90295-N

Whipple, C. J., Ciceri, P., and Padilla, C. M. (2004). Conservation of B-class floral homeotic gene function between maize and *Arabidopsis*. *Development* 2004, 6083–6091. doi: 10.1242/dev.01523

Whipple, C. J., Zanis, M. J., Kellogg, E. A., and Schmidt, R. J. (2007). Conservation of B class gene expression in the second whorl of a basal grass and outgroups links the origin of lodicules and petals. *Proc. Natl. Acad. Sci. U.S.A.* 104, 1081–1086. doi: 10.1073/pnas.0606434104

Yamaguchi, T., Lee, D. Y., Miyao, A., Hirochika, H., An, G. H., and Hirano, H.-Y. (2006). Functional diversification of the two C-class MADS box genes *OsMADS3* and *OsMADS58* in *Oryza sativa*. *Plant Cell* 18, 15–28. doi: 10.1105/tpc.105.037200

Yang, X., Wu, F., Lin, X., Du, X., Chong, K., Gramzow, L., et al. (2012). Live and let die - the B_{sister} MADS-box gene *OsMADS29* controls the degeneration of cells in maternal tissues during seed development of rice (*Oryza sativa*). *PLoS ONE* 7:e51435. doi: 10.1371/journal.pone.0051435

Yanofsky, M. F., Ma, H., Bowman, J. L., Drews, G. N., Feldmann, K. A., and Meyerowitz, E. M. (1990). The protein encoded by the *Arabidopsis* homeotic gene *agamous* resembles transcription factors. *Nature* 346, 35–39. doi: 10.1038/346035a0

Yao, S.-G., Ohmori, S., Kimizu, M., and Yoshida, H. (2008). Unequal genetic redundancy of rice *PISTILLATA* orthologs, *OsMADS2* and *OsMADS4*, in lodicule and stamen development. *Plant Cell Physiol.* 49, 853–857. doi: 10.1093/pcp/pcn050

Yu, J., Wang, J., Lin, W., Li, S., Li, H., Zhou, J., et al. (2005). The genomes of *Oryza sativa*: a history of duplications. *PLoS Biol.* 3:e38. doi: 10.1371/journal.pbio.0030038

Zhang, Y., Su, J., Duan, S., Ao, Y., Dai, J., Liu, J., et al. (2011). A highly efficient rice green tissue protoplast system for transient gene expression and studying light/chloroplast-related processes. *Plant Methods* 7:30. doi: 10.1186/1746-4811-7-30

Conflict of Interest Statement: The authors declare that the research was conducted in the absence of any commercial or financial relationships that could be construed as a potential conflict of interest.

frontiers in Plant Science

ORIGINAL RESEARCH
published: 30 May 2017
doi: 10.3389/fpls.2017.00895

Evolutionary Analysis of MIKC^C-Type MADS-Box Genes in Gymnosperms and Angiosperms

*Fei Chen, Xingtan Zhang, Xing Liu and Liangsheng Zhang**

Center for Genomics and Biotechnology, Key Laboratory of Ministry of Education for Genetics, Breeding and Multiple Utilization of Crops, Fujian Provincial Key Laboratory of Haixia Applied Plant Systems Biology, Fujian Agriculture and Forestry University, Fuzhou, China

MIKC^C-type MADS-box genes encode transcription factors that control floral organ morphogenesis and flowering time in flowering plants. Here, in order to determine when the subfamilies of MIKC^C originated and their early evolutionary trajectory, we sampled and analyzed the genomes and large-scale transcriptomes representing all the orders of gymnosperms and basal angiosperms. Through phylogenetic inference, the MIKC^C-type MADS-box genes were subdivided into 14 monophyletic clades. Among them, the gymnosperm orthologs of *AGL6, SEP*, *AP1*, *GMADS*, *SOC1*, *AGL32*, *AP3*/*PI*, *SVP*, *AGL15*, *ANR1*, and *AG* were identified. We identified and characterized the origin of a novel subfamily *GMADS* within gymnosperms but lost orthologs in monocots and Brassicaceae. ABCE model prototype genes were relatively conserved in terms of gene number in gymnosperms, but expanded in angiosperms, whereas *SVP*, *SOC1*, and *GMADS* had dramatic expansions in gymnosperms but conserved in angiosperms. Our results provided the most detailed evolutionary history of all MIKC^C gene clades in gymnosperms and angiosperms. We proposed that although the near complete set of MIKC^C genes had evolved in gymnosperms, the duplication and expressional transition of ABCE model MIKC^C genes in the ancestor of angiosperms triggered the first flower.

Keywords: MADS-box genes, ABCE model, gymnosperms, basal angiosperms, molecular evolution, flowering

OPEN ACCESS

Edited by:
Xin Wang,
Nanjing Institute of Geology and Paleontology (CAS), China

Reviewed by:
Wen-Chieh Tsai,
National Cheng Kung University, China
Simon Scofield,
Cardiff University, United Kingdom
Yang Liu,
University of Connecticut, United States

****Correspondence:***
Liangsheng Zhang
fafuzhang@163.com

Specialty section:
This article was submitted to Plant Evolution and Development, a section of the journal Frontiers in Plant Science

Received: *27 January 2017*
Accepted: *12 May 2017*
Published: *30 May 2017*

Citation:
Chen F, Zhang X, Liu X and Zhang L (2017) Evolutionary Analysis of MIKC^C-Type MADS-Box Genes in Gymnosperms and Angiosperms. Front. Plant Sci. 8:895. doi: 10.3389/fpls.2017.00895

INTRODUCTION

MADS-box genes encode a family of transcription factors (TFs) that have fundamental roles in controlling the development in plants, animals, and fungi (Becker et al., 2000). Phylogenetic analysis of eukaryotic MADS-box genes identified the following two super clades: type I and type II genes. Type I TFs only contain one MADS domain, whereas type II TFs harbor an additional K-box at the C-terminal. MIKC^c and MIKC* together constitute the type II MADS-box genes in plants (Becker and Theißen, 2003). The split of MIKC^c and MIKC* genes happened in the ancestor of all land plants (Gramzow and Theissen, 2010). MIKC^c genes are concisely studied in expression patterns or mutant phenotypes and best known for their functions (Becker and Theißen, 2003), especially in flowering plants that work as floral organ identity genes. These floral organ identity MIKC^c-type MADS-box genes have been subdivided into the following four classes: A, B, C, and E genes that provide five different homeotic functions, with A specifying sepals, A+B+E for petals, B+C+E for stamens, C+E for carpels, and D (sister of C genes) for ovules (Angenent and Colombo, 1991; Weigel and Meyerowitz, 1994).

A phylogenomic study of 17 plants, including eudicots, monocots, spike moss (*Selaginella moellendorffii*), and *Physcomitrella patens* identified 1,295 MADS-box genes, and classified MIKC^c

genes into the following 14 clades: *StMADS11*, *AGL17*, *AGL12*, *TM3*, *FLC*, *AGL6*, *AGL2*, *SQUA*, *AG*, *TM8*, *OsMADS32*, *DEF*/*GLO*, *GGM13*, *AGL15* (Gramzow and Theißen, 2013). An early study covering gymnosperms, *Gnetum* sp., and *Cycas* sp., revealed that *AG*, *AGL6*, *AGL12*, *DEF+GLO*, *GGM13*, *STMADS11,* and *TM3-like* genes very likely existed in the ancestor of angiosperms and gymnosperms (Becker and Theißen, 2003). A comprehensive analysis of three conifer genomes suggests 11–14 type II MADS genes in the most recent common ancestor of seed plants (Gramzow et al., 2014). Another study covering 27 flowering plants traced back to 11 seed plant specific MIKC^c clades (Gramzow and Theißen, 2015). However, the confidence and resolution on the early evolution of MIKC^c genes will be largely restricted and lead to conflict results without a comprehensive analysis of all orders of gymnosperms and basal angiosperms.

The gymnosperms, including conifers, cycads, ginkgo, and gnetophytes, belong to the seed bearing plants that do not produce flowers. Gymnosperm seeds are borne on the scales of cones such as with pine and spruce trees, rather than angiosperm seeds, which are encased in a fruit. Decoding the molecular genetics and evolution of reproductive organ formation is essential, however, gymnosperms usually have very large genomes, thereby hindered the deciphering gymnosperm genomes. Up to date (November 30, 2016), only the genomes of *Picea abies* (Nystedt et al., 2013) and *Ginkgo biloba* (Guan et al., 2016) have been reported in gymnosperms. In *P. abies*, among 278 putative MADS-box genes, only 41 genes were expressed (Nystedt et al., 2013).

Flowering plants are involved in our daily lives including energy, material, food, and culture. In taxonomy, which plant, the amborella or water lily is the most basal angiosperm remains as a great abominable mystery. Thereby the sampling without a water lily genome would probably lead to wrong result when studying the MIKC^c genes in these basal angiosperms and even in implicating the number of clades in the ancestor of seed plants. Actually, basal angiosperms constitute about 175 species from the following three orders: Amborellales, Nymphaeales, and Austrobaileyales (Zeng et al., 2014), in which only the genome sequence of *Amborella trichopoda* was released. Thirty-six *Amborella* MIKC^c MADS-box genes were identified and classified into main clades such as *AP1*, *AGL6*, *AGL2*, *AGL9*, *AP3*, *PI*, *AG*, *STK* (Project, 2013), underscoring the importance of *Amborella* for understanding the evolution of MADS-box genes.

In this study, we relied on the recently released genomes and large-scale of transcriptomes of both gymnosperms and angiosperms (sampling from all orders of gymnosperms and basal angiosperms) to characterize and analyze the MIKC^c MADS-box genes. We identified the complete set of MIKC^c MADS-box genes from gymnosperms and basal angiosperms. The expression of ginkgo MIKC^c MADS-box genes in reproductive organs was also studied. We report the MIKC^c MADS-box genes from samples of each order of seed plants, laying the foundation for functional analysis of the early evolution of flower formation and gymnosperm reproductive organ formation.

MATERIALS AND METHODS

Data Retrieval

The genome and transcriptome data of *G. biloba* were downloaded from the ginkgo genome sequencing project (gigadb.org/dataset/100209). The available genome of *Pinus taeda* (Neale et al., 2014) was downloaded from congenie.org. *Pinus sylvestris*'s genome was downloaded from dendrome.ucdavis.edu/treegenes. We also performed blast search against the 6,337 proteins from Cycadales species and 1,924 proteins from Gnetales species from NCBI's protein database[1]. The water lily *Nymphaea colorata* genome was recently sequenced by our own sequenced genome project and could be found from our database www.angiosperms.org (unpublished). The genome of *Amborella* was downloaded from www.amborella.org. All the other MADS-box genes from transcriptome sequences were downloaded from OneKP project (Matasci et al., 2014). All four orders of gymnosperms (Pinales, Ginkgoales, Cycadales, Gnetales) and all three orders of basal angiosperms Nymphaeales, Amborellales, Austrobaileyales were covered in this study. The sampled species with abbreviations were listed in **Table 1**.

Identification of MADS-Box Genes

For those genome sequences, MADS-box genes were predicted using HMMER software (Finn et al., 2011) with the seeds built based on an alignment of reliable MADS genes from all groups of MADS-domain proteins from the representative species *Arabidopsis thaliana*, *Oryza sativa*, and *P. abies*. For the transcriptome sequences in OneKP database[2], redundant sequences were already removed. MADS-box genes were predicted using BLASTP tool (Altschul et al., 1990) using the functional annotated *Arabidopsis* orthologs as the seeds against the OneKP database.

Sequence Alignment and Phylogenetic Analysis

Multiple sequences were aligned using the accurate alignment software MAFFT (Katoh and Standley, 2013) with default parameters. For the large alignment, the fast and accurate near maximum-likelihood phylogenetic trees were constructed using FastTree software using the JTT+CAT model (Price et al., 2009). In the phylogenetic tree, supporting values below 50 were generally regarded unreliable and hided.

RESULTS

Major Clades of MIKC^c MADS-Box Genes in Gymnosperms

Based on the survey of three gymnosperm (*P. taeda, P. sylvestris, G. biloba*) and eight angiosperm (*Vitis vinifera, A. thaliana, Populus trichocarpa, Ananas comosus, O. sativa, Sorghum*

[1]https://www.ncbi.nlm.nih.gov

[2]http://db.cngb.org/blast4onekp/blast

TABLE 1 | Samples used in this study and the number of MIKC^c genes found in each plant.

Clade	Order	Family	Species	Gene symbol	MIKC^c
	Amborellales	Amborellaceae	*Amborella trichopoda*	URDJ	7
	Amborellales	Amborellaceae	*Amborella trichopoda**	scaffold	15
	Nymphaeales	Nymphaeaceae	*Nymphaea colorata**	Nym	13
	Nymphaeales	Nymphaeaceae	*Nymphaea* sp.	PZRT	3
	Nymphaeales	Nymphaeaceae	*Nuphar advena*	WTKZ	2
	Austrobaileyales	Austrobaileyaceae	*Austrobaileya scandens*	FZJL	10
	Austrobaileyales	Schisanclraceae	*Kadsura heterodita*	NWMY	3
Angiosperms	Austrobaileyales	Schisanclraceae	*Illicium parviflorum*	ROAP	5
	Austrobaileyales	Schisanclraceae	*Illicium floridanum*	VZCI	9
	Ceratophyllales	Ceratophyllaceae	*Ceratophyllum demersum*	NPND	4
	Vitales	Vitaceae	*Vitis vinifera**	VIT	31
	Brassicales	Brassicaceae	*Arabidopsis thaliana**	At	37
	Malpighiales	Salicaceae	*Populus trichocarpa**	Potri	56
	Poales	Bromeliaceae	*Ananas comosus**	Aco	25
	Poales	Poaceae	*Oryza sativa**	Loc OS	32
	Poales	Poaceae	*Sorghum bicolor**	Sorbic	30
	Cycadales	Zamiaceae	*Encephalartos barteri*	GNQG	3
	Cycadales	Stangeriaceae	*Stangeria eriopus*	KAWQ	4
	Cycadales	Zamiaceae	*Dioon edule*	WLIC	2
	Cycadales	Cycadaceae	*Cycas micholitzii*	XZUY	4
	Ginkgoales	Ginkgoaceae	*Ginkgo biloba*	SGTW	10
	Gnetales	Gnetaceae	*Gnetum montanum*	GTHK	6
	Gnetales	Welwitschiaceae	*Welwitschia mirabilis*	TOXE	3
	Gnetales	Ephedraceae	*Ephedra sinica*	VDAO	2
	Pinales	Pinaceae	*Pines taeda**	PITA	12
	Pinales	Pinaceae	*Pines sylvestris**	MA	5
	Ginkgoales	Ginkgoaceae	*Ginkgo biloba**	Gb	11
	Pinales	Podocarpaceae	*Falcatifolinm taxoides*	ROWR	11
	Pinales	Cupressaceae	*Chamaecyparis lawsoniana*	AIGO	11
	Pinales	Pinaceae	*Pseudolarix amabilis*	AQFM	11
	Pinales	Pinaceae	*Nothotsuga longibracteata*	AREG	7
	Pinales	Cupressaceae	*Widdringtonia cedarbergensis* AUDE		8
	Pinales	Pinaceae	*Picea engelmannii*	AWQB	9
	Pinales	Podocarpaceae	*Microstrobos fitzgeraldii*	BBDD	2
	Pinales	Taxaceae	*Austrotaxus spicata*	BTTS	6
	Pinales	Cupressaceae	*Platycladus orientalis*	BUWV	9
	Pinales	Podocarpaceae	*Manoao colensoi*	CDFR	7
	Pinales	Cupressaceae	*Tetraclinis* sp.	CGDN	6
	Pinales	Pinaceae	*Pinus radiata*	DZQM	9
	Pinales	Taxaceae	*Torreya taxifolia*	EFMS	10
	Pinales	Podocarpaceae	*Prumnopitys andina*	EGLZ	10
	Pinales	Cupressaceae	*Pilgerodendron uviferum*	ETCJ	10
	Pinales	Cupressaceae	*Taxodium distichum*	FHST	12
	Pinales	Podocarpaceae	*Dacrycarpus compactus*	FMWZ	8
	Pinales	Cupressaceae	*Calocedrus decurrens*	FRPM	10
	Pinales	Pinaceae	*Tsuga heterophylla*	GAMH	8
	Pinales	Pinaceae	*Cedrus libani*	GGEA	11
	Pinales	Cupressaceae	*Diselma archeri*	GKCZ	10
	Pinales	Taxaceae	*Torreya nucifera*	HQOM	11
	Pinales	Cephalotaxaceae	*Amentotaxns argotaenia*	IAJW	4
	Pinales	Cupressaceae	*Callitris gracilis*	IFLI	4
	Pinales	Pinaceae	*Pinus parviflora*	IIOL	19

(Continued)

TABLE 1 | Continued

Clade	Order	Family	Species	Gene symbol	MIKC^c
Gymnosperms	Pinales	Pinaceae	*Pseudotsuga wilsoniana*	IOVS	11
	Pinales	Podocarpaceae	*Dacrydium balansae*	IZGN	10
	Pinales	Pinaceae	*Pinus ponderosa*	JBND	9
	Pinales	Cupressaceae	*Neocallitropsis pancheri*	JDQB	7
	Pinales	Podocarpaceae	*Phyllocladus hypophyllus*	JRNA	10
	Pinales	Pinaceae	*Keteleeria evelyniana*	JUWL	12
	Pinales	Podocarpaceae	*Parasitaxus usla*	JZVE	9
	Pinales	Podocarpaceae	*Sundacarpus amarus*	KLGF	8
	Pinales	Pinaceae	*Pines jeffreyi*	MFTM	9
	Pinales	Podocarpaceae	*Microcachrys tetragona*	MHGD	8
	Pinales	Araucariaceae	*Agathis robusla*	MIXZ	4
	Pinales	Pinaceae	*Cathaya argyrophylla*	NPRL	13
	Pinales	Cupressaceae	*Metasequoia glyptostroboides* NRXL		16
	Pinales	Cupressaceae	*Cunninghamia lanceolata*	OUOI	11
	Pinales	Cupressaceae	*Papuacedrus papuana*	OVIJ	9
	Pinales	Podocarpaceae	*Halocarpus bidwillii*	OWFC	12
	Pinales	Podocarpaceae	*Falcatifolium taxoides*	PLYX	5
	Pinales	Podocarpaceae	*Saxegothaea conspicua*	QCGM	6
	Pinales	Cupressaceae	*Sequoiadendron giganteum*	QFAE	4
	Pinales	Podocarpaceae	*Falcatifolium taxoides*	QHBI	3
	Pinales	Cupressaceae	*Cupressus dupreziana*	QNGJ	8
	Pinales	Cupressaceae	*Taiwania cryptomerioides*	QSNJ	9
	Pinales	Cupressaceae	*Callitris macleayana*	RMMV	6
	Pinales	Araucariaceae	*Wollemia nobilis*	RSCE	8
	Pinales	Podocarpaceae	*Podocarpus coriaceus*	SCEB	8
	Pinales	Cupressaceae	*Fokienia hodginsii*	UEVI	10
	Pinales	Podocarpaceae	*Nageia nagi*	UUJS	5
	Pinales	Podocarpaceae	*Retrophyllum minus*	VGSX	10
	Pinales	Pinaceae	*Abies lasiocarpa*	VSRH	8
	Pinales	Pinaceae	*Larix speciosa*	WVWN	9
	Pinales	Taxaceae	*Taxus baccata*	WWSS	4
	Pinales	Cupressaceae	*Athrotaxis cupressoides*	XIRK	8
	Pinales	Podocarpaceae	*Podocarpus rubens*	XLGK	7
	Pinales	Cupressaceae	*Juniperus scopulorum*	XMGP	5
	Pinales	Cupressaceae	*Microbiota decussata*	XQSG	15
	Pinales	Sciaclopityaceae	*Sciadopitys verticillata*	YFZK	4
	Pinales	Taxaceae	*Pseudotaxus chienii*	YLPM	10
	Pinales	Cupressaceae	*Austrocedrus chilensis*	YYPE	13

**Indicates this species has the available genome sequence.*

bicolor, A. trichopoda, N. colorata) genomes, the following 14 major clades of MIKC^c MADS-box genes were characterized: *SEP*, *AGL6*, *AP1*, *FLC*, *GMADS*, *SOC1*, *AGL32*, *AP3*/*PI*, *SVP*, *AGL15*, *ANR1*, *AG*, *AGL12*, *MADS32* (**Figure 1**). However, gymnosperm genes were distributed into the following six clades: *AGL6*, *GMADS*, *AGL32*, *SVP*, *AGL15*, *AG*. This is partly because only 12, 5, 11 MIKC^c MADS-box genes found in *P. taeda*, *P. sylvestris*, *G. biloba*, respectively (**Table 1**). These 28 MIKC^c MADS-box gymnosperm genes might be useful in studying the early evolution of MIKC^c MADS-box genes, however, their limited number may not have a full coverage, and may lead to incomplete evolutionary reconstruction.

Refinement of Clade Classification Using Large-Scale Transcriptome Data

Due to the limited genomic sequences of gymnosperms and basal angiosperms, the transcriptome data of often-neglected species covering gymnosperms and basal angiosperms was employed (**Table 1**) to reveal the evolutionary details. These include 8 basal angiosperms covering all three orders and 71 gymnosperms from all the orders of gymnosperms. We identified 623 MIKC^c MADS-box genes from the basal angiosperm and gymnosperm transcriptomes. In the gymnosperm transcriptomes alone 580 MIKC^c MADS-box genes were identified, which was 20-fold more than those from three gymnosperm genomes.

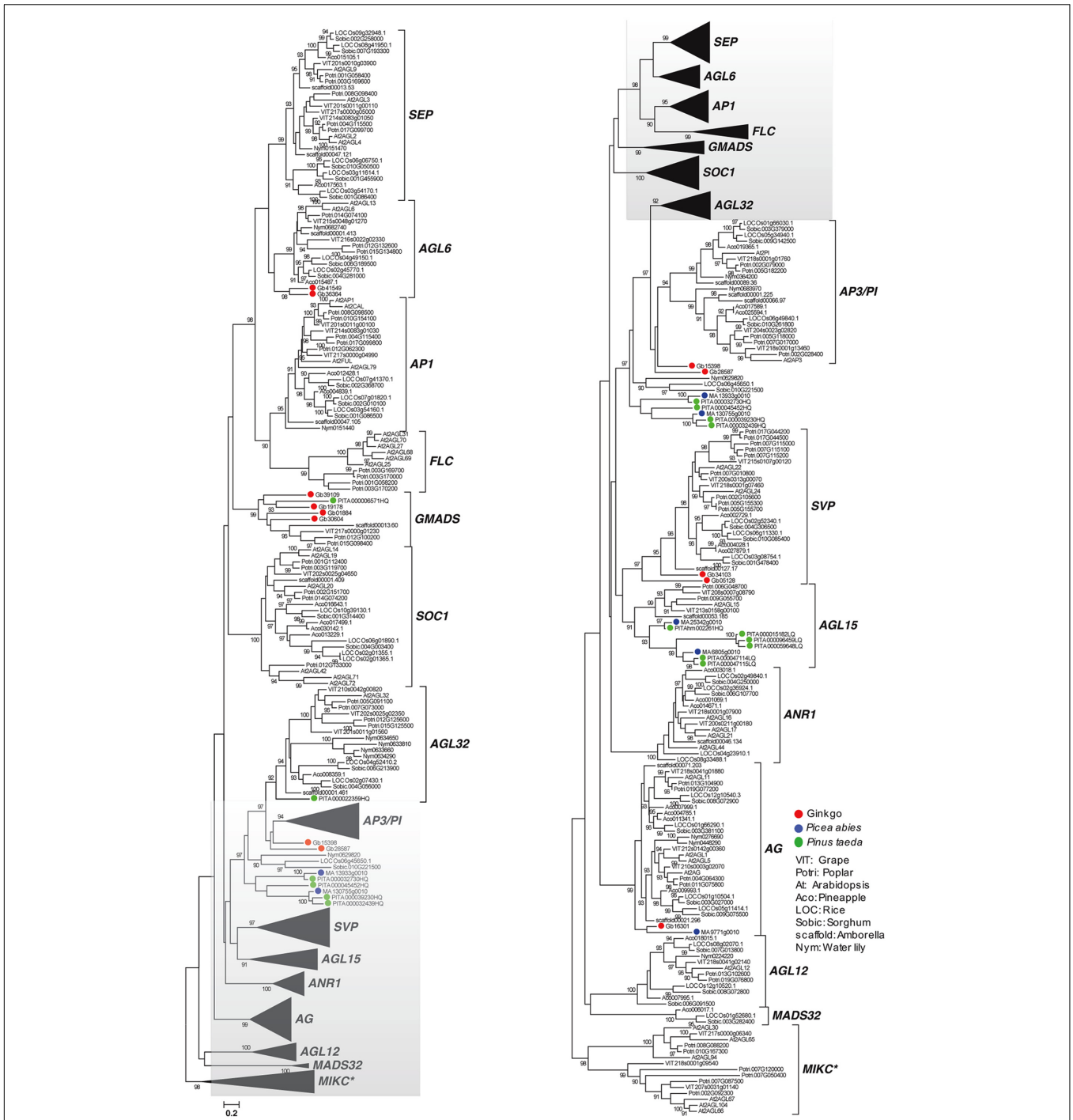

FIGURE 1 | Genome-wide analysis of MIKC^c MADS-box genes using gymnosperm, basal angiosperm, and crown angiosperm genomes. Sequences from gymnosperms were labeled = with the following colors: red for ginkgo, green for *Pinus taeda*, and blue for *Picea abies*.

Relying on more gymnosperm and angiosperm sequences, the details of the characterized clades were revealed. The 13rd clade MADS32 with sequences from both basal angiosperm *Amborella* and three monocots was also detected. No *Arabidopsis* genes were found in the monophyly (**Figure 2**). Due to the limited information, we proposed to name this clade of genes as *MADS32* based on the name of a rice ortholog *OsMADS32*. So taken together, the following 14 MIKC^c clades were characterized from basal angiosperms and gymnosperms: *SVP*, *MADS32*, *AP3*/*PI*, *AGL32*, *AGL15*, *AG*, *ANR1*, *AGL12*, *SOC1*, *GMADS*, *FLC*, *AP1*/*FUL*, *AGL6*, and *SEP* (**Figure 2**).

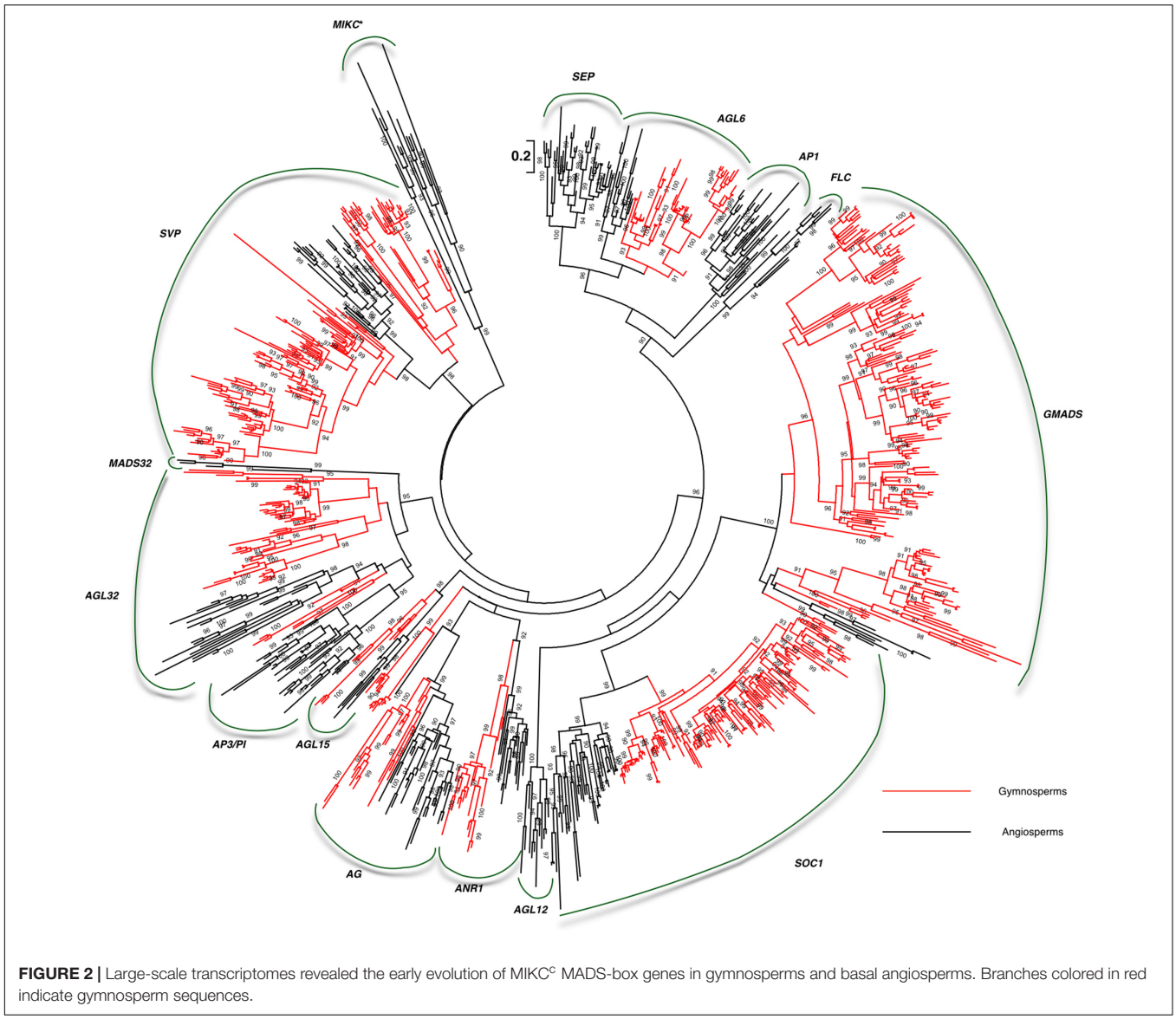

FIGURE 2 | Large-scale transcriptomes revealed the early evolution of MIKC^c MADS-box genes in gymnosperms and basal angiosperms. Branches colored in red indicate gymnosperm sequences.

Since different researchers preferred their own nomenclature standards in classifying the MIKC^c MADS-box genes, which often leads to confusion for the public or beginners. We listed the current representative classifications in **Table 2**. Currently, we have identified all the reported clades and refined several clades based on more representative sequences from all orders of gymnosperms and angiosperms.

Evolution of A-, B-, C-, E-Function Genes

A-function *AP1*/*FUL* genes were only found in angiosperms. In the basal angiosperm stage, *AP1*/*FUL* genes retained a single copy in both sequenced *Amborella* and *Nymphaea* genomes showing the conserved evolution trajectory (**Figure 3**). However in monocots, two groups were found in the near-basal monocot pineapple (*Ananas comosus*) and they diverged into three groups in the crown monocots rice and sorghum. In the eudicots, three groups were clearly identified from basal plant grape to crown plant *Arabidopsis*, leading to the origin of divergence of *AP1* and *FUL* genes.

SEP and *AGL6* formed a very close sister group (**Figure 3**). *SEP* clade consisted only angiosperm genes, whereas *AGL6* was made-up of one group of angiosperm genes, and two groups of gymnosperm genes and suggests *SEP* and *AGL6* diverged within the ancestor of seed plants. Moreover, because basal gymnosperm (ginkgo) genes were found in both groups of *AGL6*, which suggests a duplication event occurred in the ancestor of gymnosperm and contributed the two groups. In the *AGL6* clade, only one group of angiosperm genes was found, whereas three groups of angiosperm genes were found in the *SEP* clade because of the sampling from basal angiosperms to crown angiosperms. Two groups of *SEP* genes contained genes from basal angiosperms, monocots and eudicots, but the third group of *SEP* only contained monocot genes.

TABLE 2 | Classifications of MIKC^c from several reports.

Shan et al., 2009; Xue et al., 2010	Gramzow et al., 2014	Heijmans et al., 2012	Our report
AP1			*AP1*
SEP		*SQUA, SEP*	*SEP*
AGL6		*AGL6*	*AGL6*
FLC	*AGL2/AGL6/SQUA/FLC*	*FLC*	*FLC*
AGL12	*AGL12*	*AGL12*	*AGL12*
AG	*AGAMOUS*	*AG, FBP11*	*AG*
S0C1	*TM3*	*TM3*	*SOC1*
SVP	*StMADS11*	*STMADS11*	*SVP*
ANR1	*AGL17*	*AGL17*	*ANR1*
AGL15	*AGL15, GpMADS4*	*AGL15*	*AGL15*
AP3/PI			*AP3/PI*
AGL32	*DEF/GLO/OsMADS32/GGNGGM13, GLO, DEF, TM6*		*AGL32, MADS32*
	TM8	*TM8*	*GMADS*
Sum = 12 clades	Sum = 10 clades	Sum = 16 clades	Sum = 14 clades

The representative reports (Shan et al., 2009; Xue et al., 2010; Heijmans et al., 2012; Gramzow et al., 2014) on the classifications and our proposed classification were also shown.

AP3 encodes a MADS-box protein that specifies petal and stamen identities, and *PI* encodes a MADS-box required for the specification of petal and stamen identities. The two groups, *AP3* and *PI,* each consisted of genes from both basal and crown angiosperms (**Figure 3**), suggesting that they diverged in the ancestor of angiosperms, which were most likely yielded by the angiosperm specific whole genome duplication (WGD).

AGL32 consisted of genes from both gymnosperms and angiosperms (**Figure 3**), suggesting it originated in the ancestor of seed plants. In gymnosperms, it radiated into three groups, which was not revealed analyzing the three genomes. In angiosperms, *AGL32* had two groups in the rosids.

C-function genes were the sister groups of *AG* in the angiosperms, but they had close orthologs in the gymnosperms (**Figure 3**). Although this C clade in basal gymnosperm preserved a single copy of the genes, they were duplicated in crown gymnosperms. For example, in species classified in the Pinales three copies were found in *Papuacedrus papuana* (with gene identity: OVIJ), two copies were identified in *Microbiota decussata* (XQSG) and *Platycladus orientalis* (BUWV).

Expansion of *SVP*, *SOC1*, and *GMADS* Genes in Gymnosperms

SVP, *SOC1*, and *GMADS* are generally not regarded as core genes involved in the floral organ formation, and only very limited information of these clades are available. However, the genes are essential for other aspects for flowering, such as the agents for flowering time control [*SVP* (Li et al., 2015); *SOC1* (Liu et al., 2016); (Gao et al., 2016)]. Therefore, we set-out to characterize their evolutionary trajectory.

SVP

SVP encodes a MADS-box TF acting as a central regulator of flowering time, and were found in both gymnosperms and angiosperms (**Figure 2**). In angiosperms, only one monophyletic group was evolved. Full coverage of data showed that *SVP* retained a single copy in basal angiosperms, however, they duplicated in tree groups of the Poaceae and three groups in rosid. In gymnosperms, two monophylic groups of *SVP*s were clustered. *SVP*s were subdivided into two groups in group I, and further divided into seven groups in group II. *SVP* expanded into more copies in gymnosperms than that in angiosperms. SVP genes were expressed in young shoot, young shoot, leaf, young leaf both in basal angiosperms and gymnosperms as detected in transcriptome sequencing.

SOC1

Although *SOC1* was not found in the three genomes of gymnosperms (**Figure 1**), 141 gymnosperm *SOC1* genes were recognized. Phylogenetic analysis showed that 10 groups were identified in the crown Pinales species. Unlike the dramatic expansion of *SOC1* in gymnosperms, basal-most angiosperms, Amborella, had only a single copy (**Figure 2**). However, basal angiosperms *Austrobaileya scandens* (FZJL) and *Illicium floridanum* (VZCI), *Illicium parviflorum* (ROAP) all had duplicated into two subgroups, which nested together, and had a complicated evolutionary history. In crown angiosperms, three subgroups of *SOC1* were found in eudicots and two subgroups identified in monocots.

GMADS

We found a highly supported monopyly with supporting values 99. In this monophyly, no *Arabidopsis* ortholog was detected, which possibly led to its neglect of characterization (**Figure 1**). This monophyly covers orthologs from gymnosperms, basal angiosperms, and eudicots, showing the consistency of its evolutionary history. Transcriptome data was then employed, which covered gymnosperms and basal angiosperms (**Table 1**), to reveal the evolutionary details. MIKC^c genes were found among the transcriptomes of 8 basal angiosperms and 71 gymnosperms (**Table 1**). We identified 188 members from the novel subfamily, making it the largest subfamily among all MADS-box gene

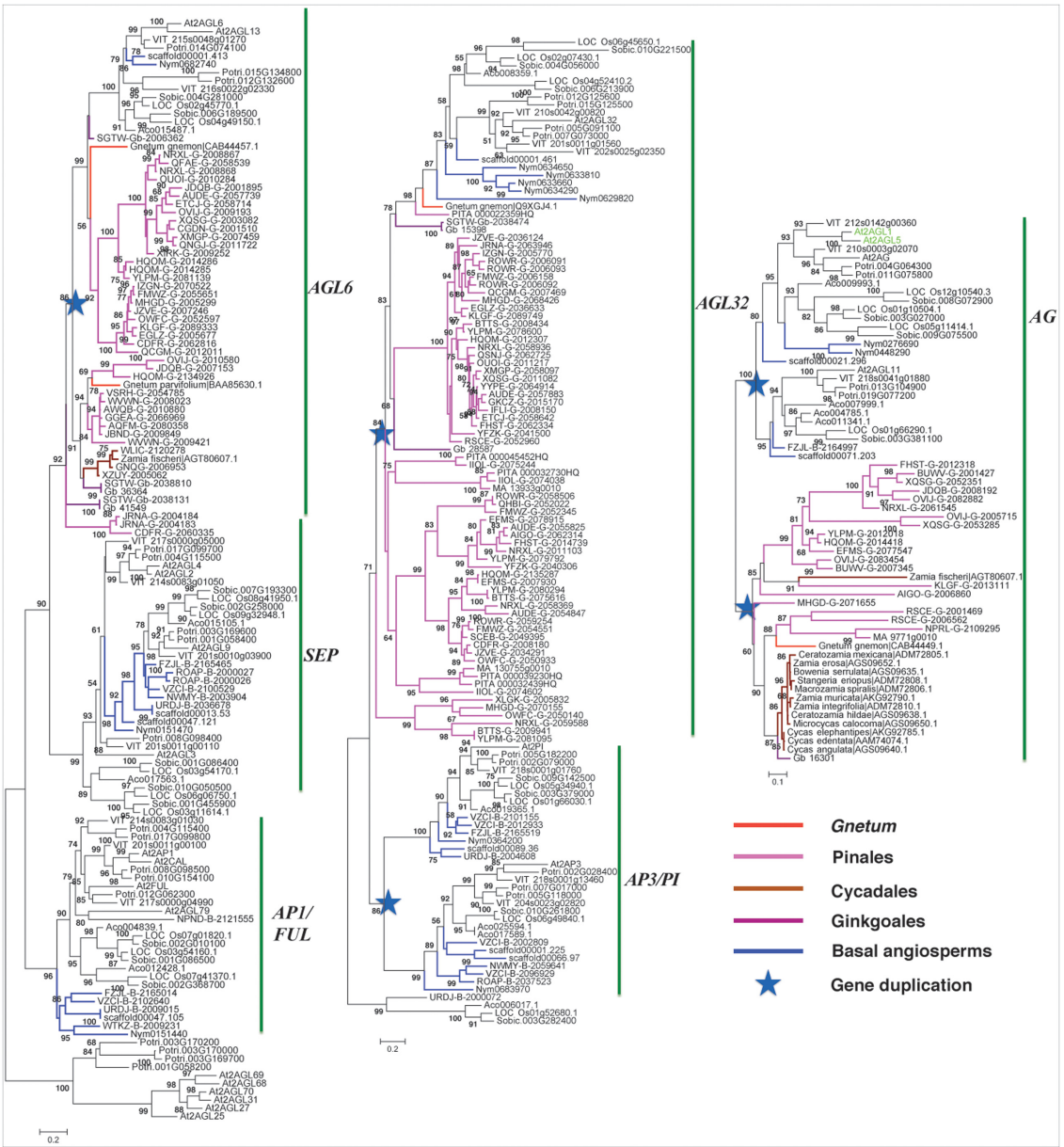

FIGURE 3 | Phylogeny of the ABCE model genes in gymnosperms and angiosperms. Branches colored in blue, purple, red, magenta, and coffee-color indicate basal angiosperm, ginkgo, Gnetales, Pinales, and Cycadales sequences, respectively. *Arabidopsis* sequences were colored in green. The star indicates the gene duplication event.

family (**Figure 2**). Besides, 10 subgroups were characterized in the crown gymnosperms. Because determining the phylogenetic relationship of this novel clade with other MADS-box genes was difficult and its lack of name, we proposed to name this clade of genes as *GMADS* for its significant expansion in gymnosperms.

Evolution Atlas of All MIKC^c Clades in Seed Plants

Among all the 14 clades, we found 8 clades *AGL6*, *GMADS*, *SOC1*, *ANR1*, *AG*, *AGL15*, *AGL32*, *SVP* cover multiple sequences from both gymnosperms and angiosperms (**Figure 4**), suggesting they originated at least in the most recent common ancestor of seed plants. The following seven clades SEP, FLC, AGL32, AP1, AGL12, AP3/PI, MADS32 were identified only in angiosperms. No clade was specific to gymnosperms (**Figure 4**).

Expressional Profiling of Ginkgo MIKC^c-Type MADS-Box Genes

The gingko genome encoded 11 MIKC^c-type MADS-box genes, which was distributed into the following five clades: *AGL6*,

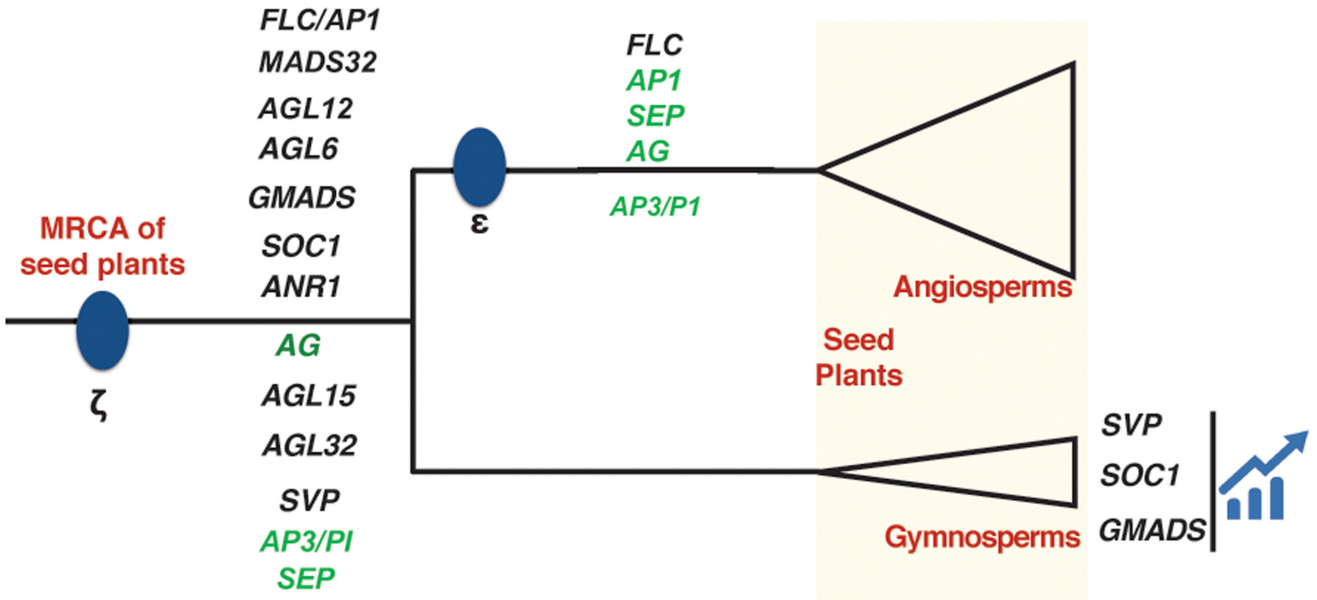

FIGURE 4 | Evolution of MIKC^c clades plotted on a phylogenetic tree of seed plants. Two whole genome duplication (WGD) events ζ and ε have been marked in blue dots. Three clades expanded significantly in gymnosperms were also presented. The ABCE genes were colored in green.

GMADS, *AP3/PI*, *SVP*, *AG*, and covered three major functional clades A/E, B, C. Because the genome has been recently sequenced (Guan et al., 2016), *G. biloba* serves as a good model for functional and comparative studies. The expression of these 11 genes was quantified using three transcriptomes covering reproductive (male and female) and vegetative (stem and leaf) organs, and all the 11 genes were well-quantified in the transcriptomes. *AG* (*Gb_16301*), *AGL6* (*Gb_41549*), *AP3/PI* (*Gb_28587*), *GMADS* (*Gb_01884* and *Gb_30604*) genes were specifically expressed in the reproductive organs with no expression detected in the vegetative organs stem and leaf (**Table 3**). The four *GMADS* genes were expressed significantly higher in reproductive organs than in vegetative organs. The two ginkgo *SVP* orthologs had divergent expression patterns. *Gb_05128* was expressed strongly in reproductive organs, whereas *Gb_34103* had strong expression in both reproductive and vegetative organs, which suggested their divergent functions.

DISCUSSION

The Gymnosperm and Angiosperm MIKC^c-Type MADS-Box Genes

Although the MIKC^c genes were detected in the crown gymnosperm *P. abies* and other three Pinales species (Gramzow et al., 2014), genes from a single gymnosperm order could not represent the ancestral state of gymnosperms made up of four orders. High resolution and systematic analysis of basal angiosperm and gymnosperm MIKC^c MADS-box genes is lacking due to the lack of omics data in previous studies. In this study, all the orders of

TABLE 3 | Expressional profile of 11 ginkgo MIKC^c genes.

MADS-box clade	Gene Id	Female reproductive organ	Male reproductive organ	Leaves and stems of seedlings
AG	*Gb 16301*	80.83	290.18	0
AGL6	*Gb 41549*	23	37.79	0
AGL6	*Gb 36364*	28.77	115.6	0.92
AP3/PI	*Gb 28587*	0	0.18	0
AP3/PI	*Gb 15398*	32.13	4.25	16.83
GMADS	*Gb 01884*	25.53	87.12	0
GMADS	*Gb 39109*	1.29	5.02	4
GMADS	*Gb 19178*	1.62	1.31	0.94
GMADS	*Gb 30604*	15.34	79.43	0
SVP	*Gb 05128*	19.41	46.73	0.99
SVP	*Gb 34103*	0.63	49.01	51.48

gymnosperms and basal angiosperms were sampled, to show the high resolution of early evolution of MIKC^c-type MADS-box genes. Our preliminary study using three gymnosperm genomes identified the presence of gymnosperm orthologs in clades *AGL6*, *GMADS*, *AGL32*, *AP3*/*PI*, *SVP*, *AGL15*, *AG*. In addition, large-scale transcriptome data revealed gymnosperm orthologs from *SEP-AGL6-AP1* group, *SOC1*, *ANR1*, *AGL12*. *OsMADS32* clade was reported to be monocot specific (Sang et al., 2012), however, our transcriptome analysis revealed an ortholog from *Amborella*, which was not found in *Amborella* genome, supporting the high resolution of our transcriptome sampling. The *GpMADS4-like* gene clade was thought to be gymnosperm specific (Gramzow et al., 2014), however, it is part of AGL15 in our classification with supporting value 98 in the tree, suggesting the accuracy of our phylogeny.

Gymnosperms often have very large genomes, however polyploidy, usually leading to rapid increase in genome size, is rare among in this group (Gramzow et al., 2014). Only 28 MIKC^c MADS-box genes were found in genome sequenced *P. taeda*, *P. sylvestris*, *G. biloba*, collectively. In contrast, 38 genes were found in *O. sativa* (Arora et al., 2007), 37 in *A. thaliana* (Becker and Theißen, 2003), and 38 in *Vitis vinifera* (Díaz-Riquelme et al., 2009), which are significantly standing out compared to those very large gymnosperm genomes. In basal angiosperms, 15 and 13 MIKC^c MADS-box genes were detected in *Amborella* and water lily *N. colorata*, respectively. All these lines of evidences suggest that WGD contribute greatly to its expansion in crown angiosperms.

Specifically, *SOC1, SVP, GMADS* clades expanded greatly in gymnosperms and no functional study has been reported in gymnosperms. *GMADS* might control specific and unknown roles in gymnosperm reproductive organ development based on their expressional analysis in this study. Limited expression in vegetative tissues such as leaf and stem of *GMADS* and *SVP* genes were also reported in this study and previous report (Gramzow et al., 2014). The *SOC1* genes (or *TM3-like*) were also reported to have expression in both vegetative and reproductive organs (Gramzow et al., 2014). Considering their vital roles in regulating flowering time in angiosperms, we propose that among their diverse roles that triggering the reproductive organ development by *GMADS* and *SVP* genes in gymnosperms be included. In summary, the near complete set of MIKC^c type MADS-box genes in gymnosperms suggests the genetic material was the progenitor of the first flower.

The ABCE Model Prototype Genes in Gymnosperms

After analyzing the ABC model genes in *P. abies*, A/G/E, B, C/D gene ancestors were present (Project, 2013), although only C-function gene was confirmed in the MRCA of seed plants reported. In basal angiosperms, *Eschscholzia californica*, *SEP* may have the same functions like *AP1* of A-function genes (Zahn et al., 2010). The A-class and E-class genes had two groups of orthologs in gymnosperms. So, we hypothesized that gymnosperm *AGL6* orthologs may have functions in reproductive organ formation. Our hypothesis is supported by expressional analysis of a ginkgo *AGL6* ortholog *Gb_36364*, which had very high expression in both male and female reproductive organs. We also hypothesized that the two diverged gymnosperm *AGL6* groups will have different functions, similar to the functional divergence of A-function and E-function genes, which needs future functional analysis.

For *AP3*/*PI* genes controlling the B-functions, and *AG* genes controlling the C- and D-functions, gymnosperm ancestors were traced back to as early as the emergence of ginkgo. No orthologs were identified in the Cycadales, another gymnosperm early branch. These genes were specifically expressed in reproductive organs and not detected in the transcriptome. A high quality genome from Cycadales species will be highly favored. In angiosperms, the heterodimerization of AP3 and PI proteins is necessary for B-function (Project, 2013). We have detected the gene duplication of AGL32 orthologs in gymnosperms, and the duplicates only form homodimers in *Gnetum* and *Picea* (Project, 2013) suggesting that the protein-protein interaction form is a crucial step in the origin of B-function, but not gene duplication for angiosperms.

CONCLUSION

In this report, we sampled and analyzed species from all the orders of gymnosperms and the less-visited basal angiosperms including both newly released genomes and high quality large-scale transcriptomes. The major MIKC^c-type MADS-box genes were characterized and we identified a new clade *GMADS*. The ABCE model prototype genes were relatively conserved in terms of gene number in gymnosperms, but expanded in angiosperms. In contrast, *SVP*, *SOC1*, and *GMADS* have dramatic expansion in gymnosperms, but retained conserved in angiosperms. The expression atlas of all MIKC^c genes in various organs from ginkgo was measured for the first time in this study. Our results provided strong evidence for the early evolution of MIKC^c MADS-box genes and high resolution evolution trajectory, which will largely enhance our understanding of this key transcription family and shed light on decoding its functional correlation to reproductive organ formation in gymnosperms and angiosperms. This study also illustrated the near complete set of MIKC^c genes in gymnosperms and suggest that genome duplication, together with expressional transition of MIKC^c genes in the ancestor of flowering plants are the major contribution to the first flower.

AUTHOR CONTRIBUTIONS

LZ designed the research. FC and LZ collected and analyzed the data. FC, XZ, XL, and LZ wrote, revised, and approved the manuscript.

ACKNOWLEDGMENTS

This work was supported by the National Natural Science Foundation of China (81502437), Fujian-Taiwan Joint Innovative Center for Germplasm Resources and Cultivation of Crop [Fujian 2011 Program (2015)75], and a start-up fund from Fujian Agriculture and Forestry University to LZ.

REFERENCES

Altschul, S. F., Gish, W., Miller, W., Myers, E. W., and Lipman, D. J. (1990). Basic local alignment search tool. *J. Mol. Biol.* 215, 403–410. doi: 10.1016/S0022-2836(05)80360-2

Angenent, G. C., and Colombo, L. (1991). Molecualr control of ovule developemnt. *Trends Plant Sci.* 47, 362–369.

Arora, R., Agarwal, P., Ray, S., Singh, A. K., Singh, V. P., Tyagi, A. K., et al. (2007). MADS-box gene family in rice: genome-wide identification, organization and expression profiling during reproductive development and stress. *BMC Genomics* 8:242. doi: 10.1186/1471-2164-8-242

Becker, A., and Theißen, G. (2003). The major clades of MADS-box genes and their role in the development and evolution of flowering plants. *Mol. Phylogenet. Evol.* 29, 464–489. doi: 10.1016/S1055-7903(03)00207-0

Becker, A., Winter, K. U., Meyer, B., Saedler, H., and Theißen, G. (2000). MADS-box gene diversity in seed plants 300 million years ago. *Mol. Bio. Evol.* 17, 1425–1434. doi: 10.1093/oxfordjournals.molbev.a026243

Díaz-Riquelme, J., Lijavetzky, D., Martínez-Zapater, J. M., and Carmona, M. J. (2009). Genome-wide analysis of MIKCC-type MADS box genes in grapevine. *Plant Physiol.* 149, 354–369. doi: 10.1104/pp.108.131052

Finn, R. D., Clements, J., and Eddy, S. R. (2011). HMMER web server: interactive sequence similarity searching. *Nucleic Acids Res.* 39, W29–W37. doi: 10.1093/nar/gkr367

Gao, X., Walworth, A. E., Mackie, C., and Song, G. (2016). Overexpression of blueberry *FLOWERING LOCUS T* is associated with changes in the expression of phytohormone-related genes in blueberry plants. *Hort. Res.* 3:16053. doi: 10.1038/hortres.2016.53

Gramzow, L., and Theissen, G. (2010). A hitchhiker's guide to the MADS world of plants. *Genome Biol.* 11:214. doi: 10.1186/gb-2010-11-6-214

Gramzow, L., and Theißen, G. (2013). Phylogenomics of MADS-box genes in plants — two opposing life styles in one gene family. *Biology* 2, 1150–1164. doi: 10.3390/biology2031150

Gramzow, L., and Theißen, G. (2015). Phylogenomics reveals surprising sets of essential and dispensable clades of MIKC^c-group MADS-box genes in flowering plants. *J. Exp. Zool. B Mol. Dev. Evol.* 324, 353–362. doi: 10.1002/jez.b.22598

Gramzow, L., Weilandt, L., and Theißen, G. (2014). MADS goes genomic in conifers: towards determining the ancestral set of MADS-box genes in seed plants. *Ann. Bot.* 114, 1407–1429. doi: 10.1093/aob/mcu066

Guan, R., Zhao, Y., Zhang, H., Fan, G., Liu, X., Zhou, W., et al. (2016). Draft genome of the living fossil *Ginkgo biloba*. *Gigascience* 5, 49. doi: 10.1186/s13742-016-0154-1PMID:27871309

Heijmans, K., Morel, P., and Vandenbussche, M. (2012). MADS-box genes and floral development: the dark side in *Posidonia oceanica* cadmium induces changes in DNA. *J. Exp. Bot.* 63, 5397–5404. doi: 10.1093/jxb/ers233

Katoh, K., and Standley, D. M. (2013). MAFFT multiple sequence alignment software version 7: improvements in performance and usability. *Mol. Biol. Evol.* 30, 772–780. doi: 10.1093/molbev/mst010

Li, C., Chen, C., Gao, L., Yang, S., Nguyen, V., Shi, X., et al. (2015). The *Arabidopsis* SWI2/SNF2 chromatin remodeler BRAHMA regulates polycomb function during vegetative development and directly activates the flowering repressor gene SVP. *PLoS Genet.* 11:e1004944. doi: 10.1371/journal.pgen.1004944

Liu, X.-R., Pan, T., Liang, W.-Q., Gao, L., Wang, X.-J., Li, H.-Q., et al. (2016). Overexpression of an orchid (*Dendrobium nobile*) *SOC1/TM3*-like ortholog, *DnAGL19*, in *Arabidopsis* regulates *HOS1-FT* expression. *Front. Plant Sci.* 7:99. doi: 10.3389/fpls.2016.00099

Matasci, N., Hung, L., Yan, Z., Carpenter, E. J., Wickett, N. J., Mirarab, S., et al. (2014). Data access for the 1,000 Plants (1KP) project. *Gigascience* 3:17. doi: 10.1186/2047-217X-3-17

Neale, D. B., Wegrzyn, J. L., Stevens, K. A., Zimin, A. V., Puiu, D., Crepeau, M. W., et al. (2014). Decoding the massive genome of loblolly pine using haploid DNA and novel assembly strategies. *Genome Biol.* 15:R59. doi: 10.1186/gb-2014-15-3-r59

Nystedt, B., Street, N. R., and Wetterbom, A. (2013). The Norway spruce genome sequence and conifer genome evolution. *Nature* 497, 579–584. doi: 10.1038/nature12211

Price, M. N., Dehal, P. S., and Arkin, A. P. (2009). FastTree: computing large minimum evolution trees with profiles instead of a distance matrix. *Mol. Biol. Evol.* 26, 1641–1650. doi: 10.1093/molbev/msp077

Project, A. G. (2013). The *Amborella* genome and the evolution of flowering plants. *Science* 342:1241089. doi: 10.1126/science.1241089

Sang, X., Li, Y., Luo, Z., Ren, D., Fang, L., Wang, N., et al. (2012). *CHIMERIC FLORAL ORGANS1*, encoding a monocot-specific MADS box protein, regulates floral organ identity in rice. *Plant Physiol.* 160, 788–807. doi: 10.1104/pp.112.200980

Shan, H., Zahn, L., Guindon, S., Wall, P. K., Kong, H., Ma, H., et al. (2009). Evolution of plant MADS box transcription factors: evidence for shifts in selection associated with early angiosperm diversification and concerted gene duplications. *Mol. Biol. Evol.* 26, 2229–2244. doi: 10.1093/molbev/msp129

Weigel, D., and Meyerowitz, E. M. (1994). The ABCs of floral homeotic genes. *Cell* 78, 203–209. doi: 10.1016/0092-8674(94)90291-7

Xue, H., Xu, G., Guo, C., Shan, H., and Kong, H. (2010). Comparative evolutionary analysis of MADS-box genes in *Arabidopsis thaliana* and *A. lyrata*. *Biodivers. Sci.* 18, 109–119. doi: 10.1111/j.1469-8137.2009.03164.x

Zahn, L. M., Ma, X., Altman, N. S., Zhang, Q., Wall, P. K., Tian, D., et al. (2010). Comparative transcriptomics among floral organs of the basal eudicot *Eschscholzia californica* as reference for floral evolutionary developmental studies. *Genome Biol.* 11:R101. doi: 10.1186/gb-2010-11-10-r101

Zeng, L., Zhang, Q., Sun, R., Kong, H., Zhang, N., and Ma, H. (2014). Resolution of deep angiosperm phylogeny using conserved nuclear genes and estimates of early divergence times. *Nat. Commun.* 5, 4956. doi: 10.1038/ncomms5956

Conflict of Interest Statement: The authors declare that the research was conducted in the absence of any commercial or financial relationships that could be construed as a potential conflict of interest.

frontiers in Plant Science

ORIGINAL RESEARCH
published: 04 April 2017
doi: 10.3389/fpls.2017.00439

Evolutionary Analysis of the *LAFL* Genes Involved in the Land Plant Seed Maturation Program

*Jing-Dan Han[1], Xia Li[2], Chen-Kun Jiang[1], Gane K.-S. Wong[3,4,5], Carl J. Rothfels[6] and Guang-Yuan Rao[1]**

[1] School of Life Sciences, Peking University, Beijing, China, [2] RDFZ XiShan School, Beijing, China, [3] Department of Biological Sciences, University of Alberta, Edmonton, AB, Canada, [4] Department of Medicine, University of Alberta, Edmonton, AB, Canada, [5] BGI-Shenzhen, Beishan Industrial Zone, Shenzhen, China, [6] University Herbarium and Department of Integrative Biology, University of California, Berkeley, CA, USA

Seeds are one of the most significant innovations in the land plant lineage, critical to the diversification and adaptation of plants to terrestrial environments. From perspective of seed evo-devo, the most crucial developmental stage in this innovation is seed maturation, which includes accumulation of storage reserves, acquisition of desiccation tolerance, and induction of dormancy. Based on previous studies of seed development in the model plant *Arabidopsis thaliana*, seed maturation is mainly controlled by the LAFL regulatory network, which includes *LEAFY COTYLEDON1* (*LEC1*) and *LEC1-LIKE* (*L1L*) of the *NF-YB* gene family, and *ABSCISIC ACID INSENSITIVE3* (*ABI3*), *FUSCA3* (*FUS3*), and *LEC2* (*LEAFY COTYLEDON2*) of the B3-*AFL* gene family. In the present study, molecular evolution of these *LAFL* genes was analyzed, using representative species from across the major plant lineages. Additionally, to elucidate the molecular mechanisms of the seed maturation program, co-expression pattern analyses of *LAFL* genes were conducted across vascular plants. The results show that the origin of *AFL* gene family dates back to a common ancestor of bryophytes and vascular plants, while *LEC1*-type genes are only found in vascular plants. *LAFL* genes of vascular plants likely specify their co-expression in two different developmental phrases, spore and seed maturation, respectively, and expression patterns vary slightly across the major vascular plants lineages. All the information presented in this study will provide insights into the origin and diversification of seed plants.

Keywords: seed maturation program, LAFL network, gene structure, expression analysis, phylogenetic analysis

OPEN ACCESS

Edited by:
Zhong-Jian Liu,
The Orchid Conservation & Research Center of Shenzhen, China

Reviewed by:
Pablo Daniel Jenik,
Franklin & Marshall College, USA
Marie Monniaux,
Max Planck Institute for Plant Breeding Research, Germany

****Correspondence:***
Guang-Yuan Rao
rao@pku.edu.cn

Specialty section:
This article was submitted to Plant Evolution and Development, a section of the journal Frontiers in Plant Science

Received: *19 January 2017*
Accepted: *14 March 2017*
Published: *04 April 2017*

Citation:
Han J-D, Li X, Jiang C-K, Wong GK-S, Rothfels CJ and Rao G-Y (2017) Evolutionary Analysis of the LAFL Genes Involved in the Land Plant Seed Maturation Program. Front. Plant Sci. 8:439. doi: 10.3389/fpls.2017.00439

INTRODUCTION

Seeds, as propagules and dispersal units, play very important roles in the adaptation of seed plants to terrestrial environments (Kenrick and Crane, 1997; Becker and Marin, 2009; Radoeva and Weijers, 2014). Seed development is an intricate process, which can be divided into two conceptually distinct phases: embryo morphogenesis and seed maturation (Goldberg et al., 1994; Harada, 1997; Gutierrez et al., 2007). Seed maturation, which includes all of the events occurring after cell division has ceased within the embryo (following Harada, 1997), can be considered as a developmental module that is added after embryogenesis. It is accomplished with the accumulation of nutrient reserves, the acquisition of desiccation tolerance, the desiccation of seeds,

the suppression of precocious germination, and the induction of dormancy (Goldberg et al., 1994; Harada, 1997); these features are each thought to be important in the adaptation of plants to variable and harsh terrestrial environments. Overall, it was considered that seed maturation is a more recently derived adaptation program of land plants (Harada, 1997; Santos-Mendoza et al., 2008).

According to previous studies, especially of Arabidopsis, the seed maturation program involves complex regulatory networks that regulates a large set of genes (Verdier et al., 2013; Righetti et al., 2015). The LAFL network is one of those regulatory networks, which includes *LEAFY COTYLEDON1* (*LEC1*) and *LEC1-LIKE* (*L1L*) of the *NF-YB* gene family, and *ABSCISIC ACID INSENSITIVE3* (*ABI3*), *FUSCA3* (*FUS3*), and *LEC2* (*LEAFY COTYLEDON2*) of the B3-*AFL* gene family (Suzuki et al., 1997; Luerßen et al., 1998; Santos-Mendoza et al., 2008; Suzuki and McCarty, 2008; Swaminathan et al., 2008; Xie et al., 2008; Jia et al., 2013; Kirkbride et al., 2013). On a basic level, this network was thought to orchestrate the accumulation of storage compounds and the acquisition of desiccation tolerance in seed maturation (Harada, 1997; Santos-Mendoza et al., 2008; Jia et al., 2013; Radoeva and Weijers, 2014). Meanwhile, the LAFL network also represses the expression of genes required for the transition from embryonic to vegetative developments, i.e., the suppression of precocious germination (Giraudat et al., 1992; Nambara et al., 1992; Stone et al., 2001).

Four conserved protein domains can be recognized in the B3-*AFL* gene family regulatory factors of *Arabidopsis thaliana*, designated A, B1, B2, and B3 (Giraudat et al., 1992; Suzuki et al., 1997). The A-domain is a functional acidic activation domain found at the N-terminal (McCarty et al., 1991). The B1-domain consists of about 30 amino acids (AAs) involved in the physical interaction with the bZIP transcription factor, such as *ABI5* (*ABSCISIC ACID INSENSITIVE5*; Nakamura et al., 2001). The B2-domain consists of about 15 AAs, which have been shown to be responsible for the ABA-dependent activation of ABA-regulated genes, through the ABA-response element (ABRE; Hill et al., 1996; Bies-Etheve et al., 1999; Ezcurra et al., 2000). The B3-domain, composed of about 100 AAs, has been shown to act as the DNA binding domain (Suzuki et al., 1997; Nag et al., 2005). For the *AFL* family genes, *ABI3* has all the recognized domains of this gene family (Giraudat et al., 1992; Suzuki et al., 1997). *FUS3* contains the A, B2, and B3 domains, but the A-domain in the C-terminal (Lu et al., 2010). *LEC2* has only the B2 and B3 domains. In the monocots, there are different names for *AFL* genes. For example, five *AFL* gene homologous were found in *Oryza sativa*, e.g., *OsVP1*, *OsLFL1*, and *OsIDEFs*. *OsVP1,* which contains A, B1, B2, and B3 domains, is homologous with Arabidopsis *AtABI3* (Hattori et al., 1994), and *OsLFL1* is homologous with Arabidopsis *AtFUS3* (Peng et al., 2008). Another three *OsIDEFs* are considered to be *AtLEC2* type genes, but the relationship among them remains unclear (Kobayashi et al., 2007; Sreenivasulu and Wobus, 2013).

In Arabidopsis, *AFL* genes are mainly expressed in embryo development, but at different developmental stages. *AtLEC2* is expressed at early stages of embryogenesis, while *AtABI3* and *AtFUS3* are highly expressed at late stages (Stone et al., 2001; Kroj et al., 2003; Gazzarrini et al., 2004; Tsuchiya et al., 2004; To et al., 2006; Santos-Mendoza et al., 2008; Fatihi et al., 2016). According to studies in other plants, the *AFL* family genes are generally expressed in reproductive organs. For instance, *OsLFL1* is expressed exclusively in spikes and young embryos (Peng et al., 2008). In *Zea mays*, *ZmaAFL* genes are preferentially expressed in pollen and caryopses (Grimault et al., 2015), and in *Chamaecyparis nootkatensis*, a gymnosperm species, its *CnABI3* was detected in the megagametophytes and mature dormant embryos (Zeng and Kermode, 2004).

LEC1-type (*LEC1* and *L1L*) genes are of the intron-less type of the *NF-YB* family, which are derived from the intron-rich ones, and their earliest occurrence appears to be in a common ancestor of vascular plants (Yang et al., 2005; Xie et al., 2008). *LEC1* and *L1L* genes are highly expressed in embryonic cells and extra-embryonic tissues during seed development (Lotan et al., 1998; Kwong et al., 2003). Expression and function analyses of *LEC1* homologs in other species indicate that *LEC1* is essential for seed maturation (Stephenson et al., 2007; Cao et al., 2011; Salvini et al., 2012; Tang et al., 2015). In seedless vascular plants (lycophytes and ferns), the expression of *LEC1* is restricted to reproductive structures. In *Selaginella moellendorffii* (a lycophyte), high expression of *SmoLEC1* was found in strobili, where megasporangia and microsporangia are located (Kirkbride et al., 2013). Additionally, the maximal expression of *AcaLEC1* was detected in mature sporangia of the fern *Adiantum capillus-veneris* (Fang et al., unpublished data).

Complex interactions between the *LAFL* genes were found in *Arabidopsis*. For instance, the expression of *LEC1* can activate *ABI3*, *FUS3*, and *LEC2*, whereas the ectopic expression of *LEC2* up-regulates *LEC1* activity in vegetative tissues (Kagaya et al., 2005b; Stone et al., 2007; Guo et al., 2013). The function of *LAFL* genes involves many aspects of seed maturation including seed storage protein (SSP), late-embryogenesis- abundant (LEA) proteins, hormone metabolism, and signaling pathways (Parcy et al., 1994; Nakamura et al., 2001; Kagaya et al., 2005a,b; Alonso et al., 2009; Yamamoto et al., 2009).

The LAFL network is crucial for seed maturation, and great efforts have been made to investigate the functions of this network genes in *Arabidopsis*, but little attention was paid to the evolution of the network as a whole. With the increased availability of genomic data and a refined understanding of the distribution of *LAFL* genes, this work is now feasible. To better understand the origin and evolution of *LAFL* genes, we performed phylogenetic analyses on an extensive dataset of *NF-YB* and *AFL* gene family sequences, focusing particularly on previously underrepresented groups, such as algae, bryophytes, monilophytes, and "early diverging" angiosperms. In addition, we analyzed expression patterns of the LAFL network using online databases and our newly generated qRT-PCR data from *S. moellendorffii* and *A. capillus-veneris* (representing lycophytes and monilophytes, respectively). With these data, coupled with aforementioned phylogenetic analyses and *cis*-element information, we elucidate the evolution of *LAFL* genes and their association with the seed maturation program.

MATERIALS AND METHODS

Gene Family Datasets

LAFL genes belong to two gene families: the *NF-YB* gene family and the *AFL* gene family, where the latter is a member of the B3 superfamily. To build our dataset of *AFL* genes, we first queried the Pfam database[1] for B3 superfamily genes from three chlorophytes (*Volvox carteri*, *Chlamydomonas reinhardtii*, and *Chlorella variabilis*), one moss (*Physcomitrella patens*), one lycophyte (*S. moellendorffii*), and six flowering plants (*Brachypodium sylvaticum*, *Oryza sativa*, *Zea mays*, *Populus trichocarpa*, *Glycine max,* and *A. thaliana*; Supplementary Table S1); this search resulted in 730 sequences. Then, for a better understanding of the evolution of the *AFL* gene family specifically, we BLASTed the coding sequences of Arabidopsis *ABI3*, *FUS3* and *LEC2* against four primary sources: Phytozome[2], ConGenIE[3], the *Klebsormidium flaccidum* Genome Project[4] (Hori et al., 2014), and the OneKP database[5]. These queries yielded 253 sequences spanning 68 species representing all major lineages of land plants. The retrieved sequences generally span the complete coding region, but some lack a few AAs at either end. The retrieved sequences range from 200 to 800 AAs in length (Supplementary Table S2).

To obtain sequences of the *NF-YB* gene family, we BLASTed Arabidopsis *LEC1* and *L1L* coding sequences against five primary sources: NCBI (National Center for Biotechnology Information[6]), Phytozome[2], ConGenIE[3], the *Klebsormidium flaccidum* Genome Project[4], and the OneKP project[5]. In total, 263 sequences spanning 29 species were collected, ranging from 100 to 300 AAs in length (Supplementary Table S3).

Sequence Alignment

All alignments were performed at AA level. For the phylogenetic analysis of the B3 superfamily, only the B3 domain was used for alignment. For the *NF-YB* and *AFL* gene families, full-length protein sequences were used. These sequences were aligned with the MAFFT webserver ([7]Katoh and Standley, 2013). Based on sequence characteristics, we selected an alignment strategy of FFT-NS-i (*NF-YB* gene family), FFT-NS-1(B3 superfamily), and E-INS-i (*AFL* gene family), respectively.

Phylogenetic Analysis

The final alignments were analyzed using Protest (Abascal et al., 2005) to choose the best-fitting AA model; the JTT + I + G substitution model was selected for all alignments according to the AIC and BIC selection criteria. Maximum likelihood (ML) phylogenetic analyses were performed with RaxML (Stamatakis et al., 2008) and evaluated by the bootstrap method using 1000 replicates. Trees were observed and edited for presentation using FigTree v1.4.2.[8] Based on phylogenetic reconstruction of the B3 superfamily (Supplementary Figure S1), we re-built a dataset with an ingroup sample of 253 *AFL* genes, and an outgroup of 11 B3 genes from four algal species for further phylogenetic analysis of *AFL* gene family (**Figures 1A**, **2A**, **Table 1**, and Supplementary Table S2). For bryophytes and vascular plants, further phylogenetic analyses were carried out, respectively (**Figures 1B**, **2B**). In addition, phylogeny reconstruction of the *NF-YB* family was performed using the data set containing 263 sequences of 29 species with whole genome sequences (Supplementary Figure S3). To explore the relationship of *LEC1*-type genes and *NF-YB* family genes in non-vascular plants, 65 sequences of 26 species were used for further phylogenetic analysis (**Table 1** and **Figure 4**).

Gene Structure and *Cis*-Elements Analysis

For the *AFL* family genes, we characterized their AA composition and the position of the B1, B2 and B3 domains, because these are known as identification criteria for *AFL* genes (McCarty et al., 1991; Giraudat et al., 1992; Suzuki et al., 1997; Nag et al., 2005; Lu et al., 2010). The AA composition of B1, B2, and B3 domains was analyzed by the WebLogo online (**Figures 2D**, **3D**[9]). We performed the intron-exon and position analyses of the *NF-YB* family genes by using their full-length DNA sequences (**Figure 4** and Supplementary Table S3).

To characterize *cis*-elements in the 5′ flanking region of *LAFL* genes, the 1.5 kb fragment containing promoter and 5′ UTR of six *AFL* genes and 40 *LEC1*-type genes were analyzed by PLACE ([10]this database is temporarily terminated now) and MatInspector (Genomatix Software Suite[11]) online (**Figures 3**, **4** and Supplementary Table S5). Promoter sequences of *A. capillus-veneris LEC1* were cloned through genome walking (primers in Supplementary Table S4).

Expression Analysis by qRT-PCR

To investigate the expression of *LAFL* genes in different vascular plants, the publicly available expression data as well as the expression data of *LEC1* homologs in *S. moellendorffii* and *A. capillus-veneris* (*SmoLEC1* expression data in Kirkbride et al., 2013, *AcaLEC1* unpublished expression data) were used to construct an expression heat map, where analyzed species include one monocot (rice), two eudicots (Arabidopsis and soybean), and one gymnosperm (*Picea abies*; Supplementary Figure S3). In addition, we chose *S. moellendorffii* and *A. capillus-veneris* as non-seed plant representatives using qRT-PCR to characterize *AFL* genes expression patterns at different developmental stages. With respect to sampling for these two species, *S. moellendorffii* roots, shoots, microphylls, strobili, and bulbils were collected in the field (Sichuan Province, voucher specimen was deposited in Peking University Herbarium, PEY). For

[1]https://pfam.xfam.org/family/PF02362#tabview=tab0

[2]https://phytozome.jgi.doe.gov/pz/portal.html

[3]congenie.org

[4]www.plantmorphogenesis.bio.titech.ac.jp/âlgae_genome_project/klebsormidium/index.html

[5]https://db.cngb.org/blast4onekp/

[6]www.ncbi.nlm.nih.gov

[7]http://mafft.cbrc.jp/alignment/server/

[8]http://tree.bio.ed.ac.uk/software/figtree/

[9]weblogo.berkeley.edu

[10]sogo.dna.affrc.go.jp/

[11]https://www.genomatix.de/solutions/genomatix-software-suite.html

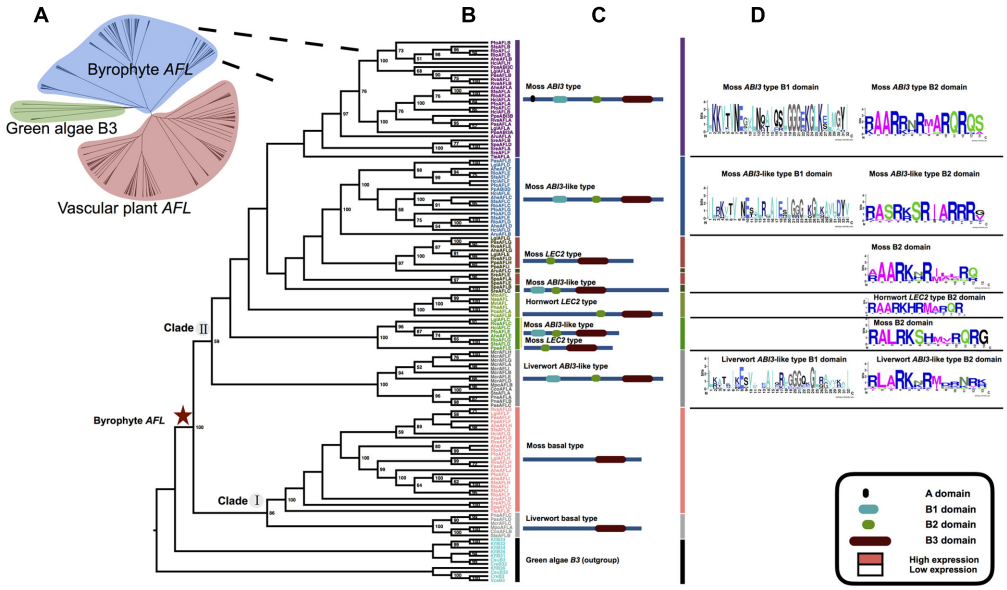

FIGURE 1 | Phylogenetic relationships of plant *AFL* gene family and the details of bryophyte. (A) ML unrooted tree of the plant *AFL* gene family comprising 264 sequences from 72 taxa (**Table 1**; for species names see Supplementary Table S2). **(B)** ML rooted tree of bryophyte *AFL* using green algae B3 sequences as outgroups (black). Numbers on the branches indicate bootstrap values calculated from 1,000 replicates. Only values higher than 50% are shown. **(C)** Domain structure of each clade and type, two clades divided into 10 types in total. **(D)** Amino acids (AAs) characteristic of the B1 and B2 domain. The sequence logo was generated using WebLogo (weblogo.berkeley.edu/).

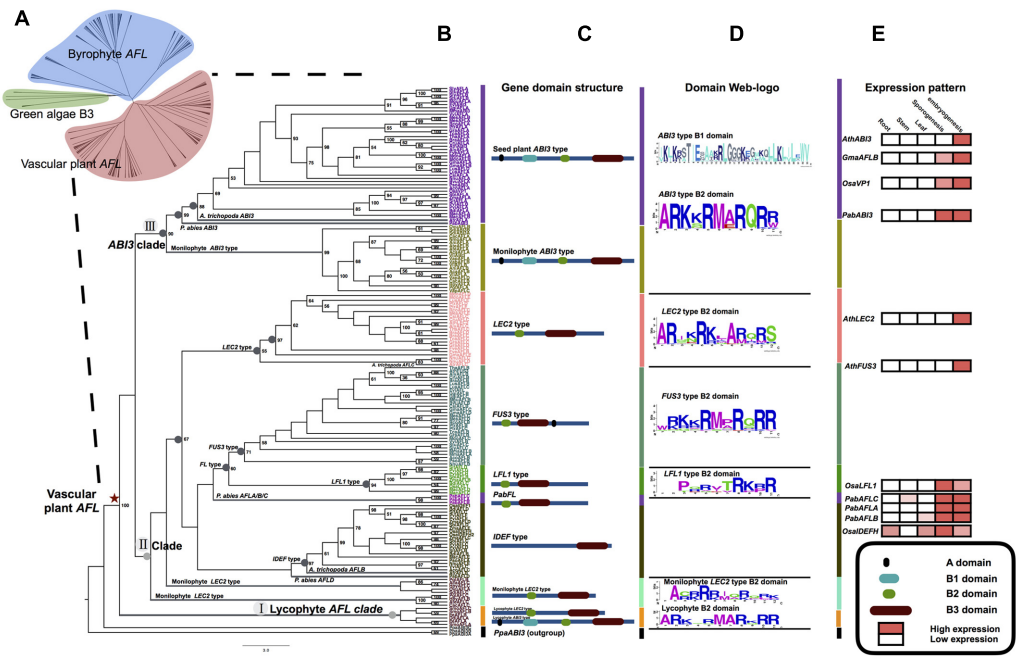

FIGURE 2 | Phylogenetic relationships of plant *AFL* gene family and the details of the part of vascular plant. (A) ML phylogenetic relationships of plant *AFL* gene family comprising 264 sequences from 72 taxa (**Table 1** for species names see Supplementary Table S2). **(B)** ML rooted tree of vascular plant *AFL* using *PpaABI3* sequences as outgroups (black). Numbers at the branches indicate bootstrap values calculated from 1,000 replicates. Only values higher than 50% are shown. **(C)** Domain structure of each clade and type, three clades divided into 10 types in total. **(D)** AAs characteristic of the B1 and B2 domain. The sequence logo was generated using WebLogo (weblogo.berkeley.edu/). **(E)** Expression pattern analysis of several *AFL* genes; expression levels are calculated using the database GENEVESTIGATOR, ConGenIE (Supplementary Figure S3), and data from previous studies (Zeng et al., 2003; Zhang and Xue, 2013).

TABLE 1 | Sampling in *LAFL* genes phylogenies.

			Classification	*AFL* species (sequences)		*LEC1*-type species (sequences)	
		Green algae	Chlorophyta	3 (5)	B3	2 (2)	NF-YB
			Charophyta	1 (6)	B3	1 (1)	NF-YB
Land plant (embryophytes)	Non-seed plant	Bryophyte	Moss	9 (66)	AFL	2 (10)	NF-YB
			Liverwort	4 (9)	AFL	1 (2)	NF-YB
			Hornwort	5 (6)	AFL	1 (1)	NF-YB
		Pteridophyte	Lycophyte	3 (6)	AFL	1 (5)	NF-YB
			Monilophyte	11 (30)	AFL	1 (5)	NF-YB
	Seed plant	Gymnosperm	Conifer	1 (5)	AFL	1 (2)	LEC1-type
		Angiosperm	Basal	1 (5)	AFL	2 (2)	LEC1-type
			Monocot	7 (35)	AFL	5 (10)	LEC1-type
			Eudicot	27 (91)	AFL	9 (25)	LEC1-type
			Total numbers	**72 (264)**		**26 (65)**	

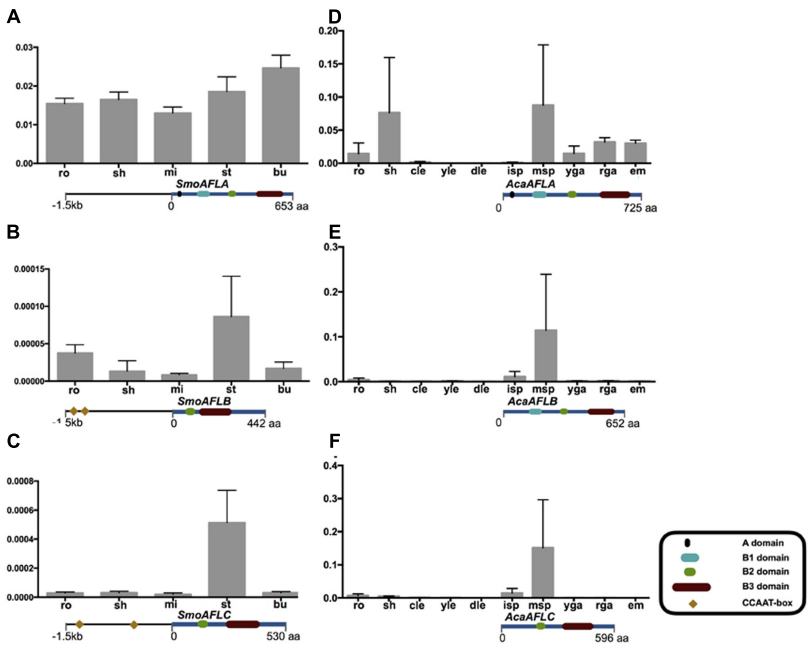

FIGURE 3 | *AFL* mRNA levels in various organs of non-seed plants examined by qRT-PCR. The CCAAT-box *cis*-elements of the promoter 1.5 kb region of three *SmoAFL* genes are highlighted in yellow blocks with an arranged number. *Selaginella moellendorffii* **(A–C)**, ro, roots; sh, shoots; mi, microphylls; st, strobili; bu, bulbils. *Adiantum capillus-veneris* **(D–F)**, ro, roots; sh, shoots; cle, curled leaves; yle, young leaves; dle, developed leaves; isp, immature sporangia; msp, mature sporangia; yga, young gametophytes; rga, reproductive gametophytes; em, embryos. The detail of each gene domain structure see Supplementary Figure S4.

A. capillus-veneris, samples were collected from plants cultivated in the greenhouse of Peking University (Voucher specimen was deposited in PEY). We chose roots, shoots, curled leaves, young leaves, fully developed leaves, immature sporangia, mature sporangia, immature gametophytes, reproductive gametophytes, and embryos as materials (Li et al., 2013). Total RNA of plant materials was isolated with Plant RNA Extraction Reagent (Invitrogen, USA) and purified with an RNeasy Mini kit according to the manufacturer's instructions (Qiagen, Germany). The RNA was then converted to cDNA by reverse transcription with FastQuant RT Kit (Tiangen, China). The qRT-PCR was performed on an Applied Biosystems 7500 Real-Time PCR System (ABI) using cDNA templates mixed with primers (Supplementary Table S4) and SYBR® Premix Ex Tax Mix (Takara, Japan). *SmoACTIN* and *AcaACTIN* were selected as the internal standard gene (primer sequences in Supplementary Table S4). Relative expression was calculated via delta-delta threshold method ($2^{-\Delta CT}$; Livak and Schmittgen, 2001). Results were summarized as means ± SE of three biological repeats.

RESULTS

Phylogenetic Analysis of *LAFL* Genes

The sequence retrieval and phylogenetic analysis of the B3 gene superfamily showed that no *AFL* sequences were found in

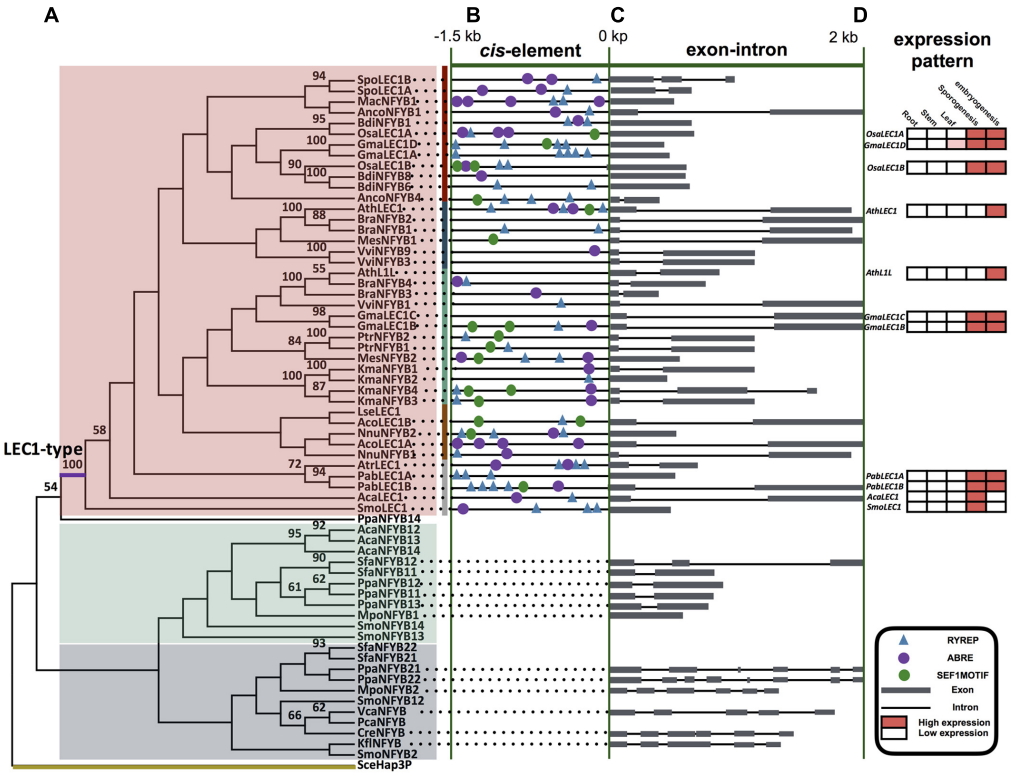

FIGURE 4 | *LEC1*-type and non *LEC1*-type genes of *NF-YB* gene family. (A) ML tree of plant *LEC1*-type and non *LEC1*-type genes comprising 66 sequences from 27 taxa (for species names see Supplementary Table S3). Numbers on the branches indicate bootstrap values calculated from 1,000 replicates. Only values higher than 50% are shown. Non-seed plant intron-rich clade, non-seed plant intron-less clade, and *LEC1*-type clade are color-coded with gray, green, and red, respectively. **(B)** The conserved *cis*-elements in the promoter 1.5 kb region of *LEC1*-type genes. Details are shown in Supplementary Table S5 with the number and sequence of motifs. **(C)** Exon-intron changes at several *LEC1*-type and non *LEC1*-type genes. Details are shown in Supplementary Table S5. **(D)** Expression pattern analysis of several *LEC1*-type genes; expression levels are calculated using the database GENEVESTIGATOR, ConGenIE (Supplementary Figure S3), and data from experimental studies (Kirkbride et al., 2013; Fang et al., unpublished data).

Chlorophytes and Charophytes (Supplementary Figure S1 and Table S1). The B3 domain of *AFL* genes is highly conserved in seed plants (Supplementary Table S2). According to phylogenetic analysis of *AFL* genes in land plants, the cluster of bryophytes and vascular plants can be recognized although they were not strongly supported in the tree (**Figures 1A**, **2A**).

Phylogenetic analysis of bryophyte *AFL* genes showed them to form two clades, clade I and clade II (**Figure 1B**). Clade I is composed of sequences from liverworts and mosses, while clade II has sequences from liverworts, mosses and hornworts. Mosses have many more *AFL* gene homologs than do liverworts or hornworts (**Figure 1B** and **Table 1**).

In the phylogenetic tree of vascular plant *AFL* genes, three major clades, clade I (lycophyte *AFL* clade), clade II, and clade III (*ABI3* clade) can be recognized (**Table 1** and **Figure 2B**). Clade I is composed of all lycophyte *AFL* genes including those of *LEC2* type and *ABI3* type (**Figure 2B**). All monilophyte *ABI3* genes cluster with seed-plant *ABI3* genes as a clade with strong support (clade III) (**Figure 2B**), while monilophyte *LEC2* type genes group with the remaining seed plant *LEC2* and *FUS3* genes in clade II (**Figure 2B**). These results indicated that lycophyte *AFL* clade represents an ancient lineage of *AFL* gene family, and monilophyte *AFL* genes are more closely with those of seed plants. In the clade II, we can find five gene types with strong support, i.e., *LEC2* type, *FUS3* type, *LFL1* type, *PabFL* type, and *IDEF* type, respectively (**Figures 2B,C**). In the genome of the gymnosperm *P. abies*, there were five *AFL* sequences, and three of them (*PabAFLA/B/C*) are associated with *FUS3* and *LFL1* types. In the "early diverging" angiosperm *Amborella trichopoda* genome (Albert et al., 2013), there were three *AFL* sequences, none of them of *FUS3* type. One *ABI3* gene was clustered in the seed plant *ABI3* type clade strong support, one was clustered with the *LEC2* type sequences and the other was clustered in the *IDEF* clade.

Phylogenetic analyses of the *NF-YB* family showed that *LEC1*-type genes formed a clade and were only present in vascular plants (**Figure 4** and Supplementary Figure S3, Table S3), in agreement with previous results (Xie et al., 2008). The number of *LEC1*-type genes in lycophytes, monilophytes, conifers, "early diverging" angiosperms, monocots, and eudicots averages 1.0, 1.0, 2.0, 1.0, 2.0, and 2.7 per species, respectively (**Table 1**). *AcaLEC1* of the fern *A. capillus-veneris* was cloned and identified by this study for first time.

Gene Structure Analysis of *LAFL* Genes

Domain structure analysis of bryophyte *AFL* genes showed that clade I genes only have one B3 domain in the C-terminal. This structure is similar to B3 genes in green algae. In clade II, *ABI3* type genes were easily recognized by the A domain, B1 (about 30 AA), B2 (about 14 AA) and B3 (about 100 AA) domain, while *ABI3*-like genes lack of the A domain. *LEC2* type genes had one unstable B2 domain in middle position and B3 domain in C-terminal. Notably, liverworts only had the clade I and *ABI3*-like *AFL* genes. We did not find *FUS3* type genes in bryophytes (**Figures 1C,D**), suggesting that *FUS3* may not arise. Domain structure analysis of vascular plant *AFL* genes showed that there were nine structure types in three clades with specific B2 domain AA characteristics (**Figure 2D**).

Our analyses of *NF-YB* gene sequences revealed that: (1) the *NF-YB* sequences restricted to algae are of the intron-rich type; (2) the liverwort *Marchantia polymorpha* contains both an intron-rich and an intron-less *NF-YB* gene; (3) six sequences occur in moss *Physcomitrella patens* including both intron-rich and intron-less ones; (4) *LEC1*-type genes, belonging to intron-less *NF-YB* genes, were only found in vascular plants. All those findings suggest that the intron-less type of *NF-YB* genes was derived from the intron-rich ones through gene duplication and intron loss in early land plants (**Figure 4C**, **Table 1**, and Supplementary Figure S3).

Cis-Element Prediction of *LAFL* Genes

According to comparative analysis of *cis*-elements in regulatory region of *AFL* gene pairs between the seed plant Arabidopsis and the non-seed plant *S. moellendorffii*, we found that there was CCAAT-box in *AthABI3*, *AthFUS3*, *AthLEC2*, *SmoAFLB,* and *SmoAFLC* (**Figure 4** and Supplementary Table S5). By *cis*-elements prediction in the promoter region of 40 *LEC1*-type genes, we found that (1) *LEC1* had more *cis*-elements than do *L1L* genes in seed plants; (2) there is not a significant difference in *cis*-element components in *LEC1* genes from seed and non-seed plants: almost all the *cis*-elements identified in Arabidopsis can be found in the *LEC1* promoter of *S. moellendorffii* and *A. capillus-veneris* (**Figure 4B** and Supplementary Table S5).

Expression Pattern Analyses of *LAFL* Genes

LAFL gene expression was restricted to seed development in Arabidopsis but occurs both in maturing seeds and inflorescences in other species, e.g., soybean, rice, and maize (**Figure 4D** and Supplementary Figure S4). For *LAFL* genes of *P. abies* (a gymnosperm), they were mainly expressed in leaves and cones. *SmoLEC1* and *AcaLEC1* were each only expressed in strobili and mature sporangia, and were not detected in tissues undergoing embryogenesis (**Figure 4D**).

The qRT-PCR results showed that the mRNA levels of *SmoAFLA* (lycophyte *ABI3* type) were nearly identical across organs (roots, shoots, microphylls, strobili, and bulbils) of *S. moellendorffii*. The levels of mRNA of *SmoAFLB* and *SmoAFLC* (lycophyte *LEC2* type) were higher in strobili than other organs. In *A. capillus-veneris* (a fern) the levels of mRNA of *AcaAFLA* (one monilophyte *ABI3* type) were higher in shoots and mature sporangia than other organs. The mRNA of *AcaAFLB* (another monilophyte *ABI3* type) and *AcaAFLC* (monilophyte *LEC2* type) were only detected in mature sporangia (**Figure 3** and Supplementary Figures S2, S4).

DISCUSSION

LAFL Network and Seed Maturation

Previous studies showed that many genes are involved in seed maturation (Goldberg et al., 1994; Harada, 1997; Radoeva and Weijers, 2014). Among them, the *AFL* family of B3 transcription factors (TFs) and the *LEC1*-type of *NF-YB* TFs, which together form LAFL regulatory network, are considered to play key roles in seed maturation. Although there were studies on the evolution of *LEC1*-type genes (Xie et al., 2008), *AFL* genes (Li et al., 2010; Carbonero et al., 2016), this study presents a comprehensive analysis of *LAFL* genes by integrating their phylogeny, gene structure, *cis*-elements and expression patterns together for a better understanding of the evolution of seed maturation programs during plant evolution.

Evolution and Function Differentiation of *AFL* Genes

According to our extensive phylogenic and gene structure analyses, *LEC2* type and *ABI3* type genes evolved in a common ancestor of bryophytes and vascular plants, and their gene structure is very conservative. However, *FUS3* type genes were only found in seed plants (**Figures 1**, **2**), suggesting that *FUS3* genes originate relatively late in the *AFL* family.

In embryophytes, *LEC2* type genes had one B2 domain in a middle position and a B3 domain in the C-terminal. In the seedless species *S. moellendorffii* (lycophyte) and *A. capillus-veneris* (fern), the expression pattern of *LEC2* type genes (*SmoAFLB*, *SmoAFLC*, and *AcaAFLC*) was restricted to shoots (*S. moellendorffii*) and maturing spores (both *S. moellendorffii* and *A. capillus-veneris*; **Figure 3**). In the "early diverging" angiosperm *Amborella trichopoda*, there were three *AFL* genes. One of them is of *ABI3* type, and the other two are *LEC2* type and *IDEF* type, respectively. Interestingly, *IDEF* type genes were identified only from monocots, and have only B3 domain in C-terminal (Kobayashi et al., 2007), which is different from LEC2 gene structure (**Figure 2C**). In rice, *OsaIDEF* transcripts are constitutively present in roots, leaves, inflorescences, and seeds. In eudicots, *LEC2* plays central roles in seed embryogenesis and morphogenesis (**Figure 2** and Supplementary Figure S4). All these data suggest that *LEC2* and *IDEF* type genes diverged very early, and *LEC2* type genes may be lost in monocots.

During the review of this manuscript, Carbonero et al. (2016) published their work on the AFL family. In agreement with our results, they suggest that the origin of the AFL family traces back to a common ancestor of bryophytes and vascular plants, and that this family has expanded in the angiosperms. However, due to different sampling regimes and sequence coverage, there are some different results between these two studies, especially relating to the evolution of *LEC2* genes. According to Carbonero

et al. (2016), seven *LEC2* genes were described from three monocots, *Oryza sativa*, *Brachypodium distachyon* and *Hordeum vulgare* (all grasses), but the relationship of those seven genes with other *AFL* homologs needs to be verified; differences in gene structure, phylogenetic position, and expression pattern suggests that these may not be *LEC2* genes.

Considering *ABI3* genes of land plants, there is a clear evolutionary trajectory according to our study. Phylogenetically, monilophyte *ABI3* genes are more closely related to those of seed plants, rather than to lycophyte *ABI3* types. In *P. abies* (gymnosperm) and *Amborella trichopoda* ("early diverging" angiosperm), there was only one *PabABI3* and *AtrABI3* sequence, respectively. This may be due to the lack of a lineage-specific whole genome duplication (WGD) in these species (Albert et al., 2013; Nystedt et al., 2013). Expression patterns of *SmoAFLA* (*S. moellendorffii,* one lycophyte *ABI3* type) are more similar to those of bryophyte *ABI3* type genes, which are only expressed in vegetative tissues (**Figure 3**; Khandelwal et al., 2010). The expression of *AcaAFLA* and *AcaAFLB* (*A. capillus-veneris*, two monilophyte *ABI3* type genes) are found in shoots and spore maturation, which are consistent with that of *PabABI3* (*P. abies*) (**Figures 2B,C,E**, **3**). This suggest the expression pattern of *ABI3* genes has slightly differentiated across major land plant lineages.

FUS3 type genes appear to have originated relatively late because they are restricted to the seed plant clade. Three *PabAFL* sequences (*PabAFLA, B, and C*) from the gymnosperm *P. abies* belong to *Pab-FL* (*FUS3* and *LFL*) type clade, which is associated with *FUS3* type and *LFL* type. These finding, coupled with expression patterns of *PabAFLA/B/C* genes suggest that the *Pab-FL* type may represent ancestral *FUS3/LFL* gene function. There is no *FUS3* type member in *Amborella trichopoda*, which suggests that *FUS3* type genes likely originated in a common ancestor of seed plants and were subsequently lost in *Amborella*. In eudicots and monocots, *FL* genes are divided to *FUS3* type and *LFL* type, respectively. *OsLFL1,* involved in the photoperiodic flowering of rice and expressed exclusively in spikes and young embryos, is functionally similar to *AthFUS3* in Arabidopsis (Peng et al., 2008; Tiedemann et al., 2008). The *FUS3* type (found only in eudicots) and the *LFL* type (restricted to monocots) are clustered together with strong bootstrap support, and they have similar domain structure and functions (**Figures 2B,C,E**, **3**).

Evolution of the *LEC1-Type* Genes

As members of the LAFL network, *LEC1*-type genes are CCAAT-binding factors (CBFs), which are present in all eukaryotes (Forsburg and Guarente, 1989; Mantovani, 1999; Matuoka and Chen, 2002; Siefers et al., 2009; Dolfini et al., 2012). There is no clear correlation between expression patterns and the classification of *NF-YB* family genes with an exception of the *LEC1*-type genes, which are considered seed-specific (Stephenson et al., 2007; Salvini et al., 2012). Arabidopsis *LEC1*-type genes (*AthLEC1* and *AthL1L*) have significant functions at late stages of embryogenesis (Lotan et al., 1998; Kwong et al., 2003). Our phylogenetic analyses of the *NF-YB* gene family support some findings of previous studies, e.g., only one intron-rich type of *NF-YB* genes occurs in chlorophytes, the intron-less genes are derived from the intron-rich ones, and *LEC1*-type genes are restricted to vascular plants (Xie et al., 2008; Cagliari et al., 2014; **Table 1** and **Figures 4A,C**).

In addition, there are some new findings, e.g., only one copy of the intron-rich type of *NF-YB* genes is found in the alga *Klebsormidium flaccidum*, which is considered to be one of the closest relatives of land plants (Hori et al., 2014). The liverwort *Marchantia polymorpha*, one of the earliest diverged land plants (Rövekamp et al., 2016), has two copies of *NF-YB* genes in its genome, one of which is intron-rich and the other intron-less. The six copies found in the moss *Physcomitrella patens*, have been proven to originate from duplication events (Yang et al., 2005; Rensing et al., 2008; Xie et al., 2008). In addition, our analyses demonstrate that there is only one copy of *LEC1*-type genes in the genome of *S. moellendorffii* (lycophyte), *A. capillus-veneris* (fern), *P. abies* (gymnosperm), and *Amborella trichopoda* ("early diverging" angiosperm). These data support that *LEC1* and *L1L* genes result from the duplication of *LEC1*-type genes likely occurring after the origin of extant angiosperms (**Table 1** and **Figures 4A,C**).

The *Cis*-Element Prediction and Co-expression of *LAFL* Genes

The LAFL network has been considered to play central roles in seed maturation, and *LAFL* genes regulate different facets of this developmental process by their interactions with up- and down-stream genes (Harada, 1997; Santos-Mendoza et al., 2008; Fatihi et al., 2016; González-Morales et al., 2016). The *cis*-element prediction shows that *LEC1* genes of seed plants and non-seed plants have similar *cis*-elements, suggesting the *LEC1*-type genes could be regulated by similar regulators (**Figure 4**). Among the *cis*-elements of *LEC1*, RYREPART and ABRE are thought to be very important for *LEC1* activity. The RYREPEAT is considered to be a RY-like element, and the binding site of the B3 domain (Braybrook et al., 2006; Mönke et al., 2012; Wang and Perry, 2013; Tang et al., 2015). The ABRE is functionally important in many ABA-regulated genes (Fan et al., 2015). Additionally, *LEC1*, as a subunit of the CCAAT-box binding factor (CBF), activates its downstream genes by the CCAAT-box element (Junker et al., 2012). According to the CCAAT-box element prediction of *AFL* genes in *S. moellendorffii*, there is a CCAAT-box element in the regulatory region of its *AFL* genes, e.g., *SmoAFLB* and *SmoAFLC* (**Figure 3**).

The findings presented in this study suggest that a partial LAFL network, consisting of *ABI3* and *LEC2* genes, arose in a common ancestor of land plants, and then became more complex with the occurrence of *FUS3* and *LEC1* genes. With evolution of vascular plants, *LAFL* network genes likely specify their co-expression in two different developmental processes, spore and seed maturation, respectively. The co-expression of *LAFL* genes in these two processes alone or simultaneously, which correspond to two reproductive structures, suggest that the biological process involved in spore maturation is similar to those of seed maturation.

AUTHOR CONTRIBUTIONS

J-DH analyzed data and drafted the manuscript. XL and C-KJ carried out the experiments. GW and CR provided some samples and analyzed sequences. G-YR designed the research.

FUNDING

This work was supported by the National Natural Science Foundation of China (NSFC, Grant no. 91231105).

ACKNOWLEDGMENT

We are grateful to Prof. Ji Yang of Fudan University for discussions, and two reviewers for their critical comments on the manuscript.

SUPPLEMENTARY MATERIAL

The Supplementary Material for this article can be found online at: http://journal.frontiersin.org/article/10.3389/fpls.2017.00439/full#supplementary-material

REFERENCES

Abascal, F., Zardoya, R., and Posada, D. (2005). ProtTest: selection of best-fit models of protein evolution. *Bioinformatics* 21, 2104–2105. doi: 10.1093/bioinformatics/bti263

Albert, V. A., Barbazuk, W. B., Der, J. P., Leebens-Mack, J., Ma, H., Palmer, J. D., et al. (2013). The *Amborella* genome and the evolution of flowering plants. *Science* 342:1241089. doi: 10.1126/science.1241089

Alonso, R., Oñate-Sánchez, L., Weltmeier, F., Ehlert, A., Diaz, I., Dietrich, K., et al. (2009). A pivotal role of the basic leucine zipper transcription factor bZIP53 in the regulation of *Arabidopsis* seed maturation gene expression based on heterodimerization and protein complex formation. *Plant Cell* 21, 1747–1761. doi: 10.1105/tpc.108.062968

Becker, B., and Marin, B. (2009). Streptophyte algae and the origin of embryophytes. *Ann. Bot.* 103, 999–1004. doi: 10.1093/aob/mcp044

Bies-Etheve, N., da Silva Conceicao, A., Koornneef, M., Léon-Kloosterziel, K., Valon, C., and Delseny, M. (1999). Importance of the B2 domain of the Arabidopsis ABI3 protein for Em and 2S albumin gene regulation. *Plant Mol. Biol.* 6, 1045–1054. doi: 10.1023/A:1006252512202

Braybrook, S. A., Stone, S. L., Park, S., Bui, A. Q., Le, B. H., Fischer, R. L., et al. (2006). Genes directly regulated by LEAFY COTYLEDON2 provide insight into the control of embryo maturation and somatic embryogenesis. *Proc. Natl. Acad. Sci. U.S.A.* 103, 3468–3473. doi: 10.1073/pnas.0511331103

Cagliari, A., Turchetto-Zolet, A. C., Korbes, A. P., dos Santos Maraschin, F., Margis, R., and Margis-Pinheiro, M. (2014). New insights on the evolution of Leafy cotyledon1 (LEC1) type genes in vascular plants. *Genomics* 103, 380–387. doi: 10.1016/j.ygeno.2014.03.005

Cao, S., Kumimoto, R. W., Siriwardana, C. L., Risinger, J. R., and Holt, B. F. III (2011). Identification and characterization of NF-Y transcription factor families in the monocot model plant *Brachypodium distachyon*. *PLoS ONE* 6:e21805. doi: 10.1371/journal.pone.0021805

Carbonero, P., Iglesias-Fernández, R., and Vicente-Carbajosa, J. (2016). The AFL subfamily of B3 transcription factors: evolution and function in angiosperm seeds. *J. Exp. Bot.* 4, 871–880. doi: 10.1093/jxb/erw458

Dolfini, D., Gatta, R., and Mantovani, R. (2012). NF-Y and the transcriptional activation of CCAAT promoters. *Crit. Rev. Biochem. Mol. Biol.* 47, 29–49. doi: 10.3109/10409238.2011.628970

Ezcurra, I., Wycliffe, P., Nehlin, L., Ellerström, M., and Rask, L. (2000). Transactivation of the *Brassica napus* napin promoter by ABI3 requires interaction of the conserved B2 and B3 domains of ABI3 with different *cis*-elements: B2 mediates activation through an ABRE, whereas B3 interacts with an RY/G-box. *Plant J.* 24, 57–66. doi: 10.1046/j.1365-313x.2000.00857.x

Fan, K., Shen, H., Bibi, N., Li, F., Yuan, S., Wang, M., et al. (2015). Molecular evolution and species-specific expansion of the NAP members in plants. *J. Integr. Plant Biol.* 57, 673–687. doi: 10.1111/jipb.12344

Fatihi, A., Boulard, C., Bouyer, D., Baud, S., Dubreucq, B., and Lepiniec, L. (2016). Deciphering and modifying LAFL transcriptional regulatory network in seed for improving yield and quality of storage compounds. *Plant Sci.* 250, 198–204. doi: 10.1016/j.plantsci.2016.06.013

Forsburg, S. L., and Guarente, L. (1989). Identification and characterization of HAP4: a third component of the CCAAT-bound HAP2/HAP3 heteromer. *Genes Dev.* 3, 1166–1178. doi: 10.1101/gad.3.8.1166

Gazzarrini, S., Tsuchiya, Y., Lumba, S., Okamoto, M., and McCourt, P. (2004). The transcription factor FUSCA3 controls developmental timing in Arabidopsis through the hormones gibberellin and abscisic acid. *Dev. Cell* 7, 373–385. doi: 10.1016/j.devcel.2004.06.017

Giraudat, J., Hauge, B. M., Valon, C., Smalle, J., Parcy, F., and Goodman, H. (1992). Isolation of the Arabidopsis ABI3 gene by positional cloning. *Plant Cell* 4, 1251–1261. doi: 10.1105/tpc.4.10.1251

Goldberg, R. B., de Paiva, P., and Yadegari, R. (1994). Plant embryogenesis: zygote to seed. *Science* 266, 605–614. doi: 10.1126/science.266.5185.605

González-Morales, S. I., Chávez-Montes, R. A., Hayano-Kanashiro, C., Alejo-Jacuinde, G., Rico-Cambron, T. Y., de Folter, S., et al. (2016). Regulatory network analysis reveals novel regulators of seed desiccation tolerance in *Arabidopsis thaliana*. *Proc. Natl. Acad. Sci. U.S.A.* 113, E5232–E5241. doi: 10.1073/pnas.1610985113

Grimault, A., Gendrot, G., Chaignon, S., Gilard, F., Tcherkezd, G., Thévenine, J., et al. (2015). Role of B3 domain transcription factors of the AFL family in maize kernel filling. *Plant Sci.* 236, 116–125. doi: 10.1016/j.plantsci.2015.03.021

Guo, X., Hou, X., Fang, J., Wei, P., Xu, B., Chen, M., et al. (2013). The rice GERMINATION DEFECTIVE 1, encoding a B3 domain transcriptional repressor, regulates seed germination and seedling development by integrating GA and carbohydrate metabolism. *Plant J.* 75, 403–416. doi: 10.1111/tpj.12209

Gutierrez, L., Wuytswinkel, O., Castelain, M., and Bellini, C. (2007). Combined networks regulating seed maturation. *Trends Plant Sci.* 12, 294–300. doi: 10.1016/j.tplants.2007.06.003

Harada, J. J. (1997). "Seed maturation and control of dormancy," in *Cellular and Molecular Biology of Plant Seed Development*, eds B. A. Larkins and I. K. Vasil (Gainesville, FL: University of Florida Press), 545–592. doi: 10.1007/978-94-015-8909-3_15

Hattori, T., Terada, T., and Hamasuna, S. T. (1994). Sequence and functional analysis of the rice gene homologous to maize *Vp1*. *Plant Mol. Biol.* 24, 805–810. doi: 10.1007/BF00029862

Hill, A., Nantel, A., Rock, C. D., and Quatrano, R. S. (1996). A conserved domain of the *viviparous*-1 gene product enhances the DNA binding activity of the bZIP protein EmBP-1 and other transcription factors. *J. Biol. Chem.* 271, 3366–3374. doi: 10.1074/jbc.271.7.3366

Hori, K., Maruyama, F., Fujisawa, T., Togashi, T., Yamamoto, N., Seo, M., et al. (2014). *Klebsormidium flaccidum* genome reveals primary factors for plant terrestrial adaptation. *Nat. Commun.* 5:3978. doi: 10.1038/ncomms4978

Jia, H., Suzuki, M., and McCarty, D. R. (2013). Regulation of the seed to seedling developmental phase transition by the LAFL and VAL transcription factor networks. *WIREs Dev. Biol.* 3, 135–145. doi: 10.1002/wdev.126

Junker, A., Mönke, G., Rutten, T., Keilwagen, J., Seifert, M., Thi, T. M., et al. (2012). Elongation-related functions of LEAFY COTYLEDON1 during the development of *Arabidopsis thaliana*. *Plant J.* 71, 427–442. doi: 10.1111/j.1365-313X.2012.04999.x

Kagaya, Y., Okuda, R., Ban, A., Toyoshima, R., Tsutsumida, K., Usui, H., et al. (2005a). Indirect ABA-dependent regulation of seed storage protein genes by FUSCA3 transcription factor in *Arabidopsis*. *Plant Cell Physiol.* 46, 300–311. doi: 10.1093/pcp/pci031

Kagaya, Y., Toyoshima, R., Okuda, R., Usui, H., Yamamoto, A., and Hattori, T. (2005b). LEAFY COTYLEDON1 controls seed storage protein genes through

its regulation of *FUSCA3* and *ABSCISIC ACID INSENSITIVE3*. *Plant Cell Physiol.* 46, 399–406. doi: 10.1093/pcp/pci048

Katoh, K., and Standley, D. M. (2013). MAFFT multiple sequence alignment software version 7: improvements in performance and usability. *Mol. Biol. Evol.* 30, 772–780. doi: 10.1093/molbev/mst010

Kenrick, P., and Crane, P. (1997). The origin and early evolution of plants on land. *Nature* 389, 33–39. doi: 10.1038/37918

Khandelwal, A., Cho, S. H., Marella, H., Sakata, Y., Perroud, P. F., Pan, A., et al. (2010). Role of ABA and ABI3 in desiccation tolerance. *Science* 327, 546–546. doi: 10.1126/science.1183672

Kirkbride, R. C., Fischer, R. L., and Harada, J. J. (2013). LEAFY COTYLEDON1, a key regulator of seed development, is expressed in vegetative and sexual propagules of *Selaginella moellendorffii*. *PLoS ONE* 8:e67971. doi: 10.1371/journal.pone.0067971

Kobayashi, T., Ogo, Y., Itai, R. N., Nakanishi, H., Takahashi, M., Mori, S., et al. (2007). The transcription factor IDEF1 regulates the response to and tolerance of iron deficiency in plants. *Proc. Natl. Acad. Sci. U.S.A.* 104, 19150–19155. doi: 10.1073/pnas.0707010104

Kroj, T., Savino, G., Valon, C., Giraudat, J., and Parcy, F. (2003). Regulation of storage protein gene expression in *Arabidopsis*. *Development* 130, 6065–6073. doi: 10.1242/dev.00814

Kwong, R. W., Bui, A. Q., Lee, H., Kwong, L. W., Fischer, R. L., Goldberg, R. B., et al. (2003). LEAFY COTYLEDON1-LIKE defines a class of regulators essential for embryo development. *Plant Cell* 15, 5–18. doi: 10.1105/tpc.006973

Li, X., Fang, Y. H., Yang, J., Bai, S. N., and Rao, G. Y. (2013). Overview of the morphology, anatomy and ontogeny of *Adiantum capillus-veneris*: an experimental system to study the development of ferns. *J. Syst. Evol.* 51, 499–510. doi: 10.1111/jse.12034

Li, Y., Jin, K., Zhu, Z., and Yang, J. (2010). Stepwise origin and functional diversification of the AFL subfamily B3 genes during land plant evolution. *J. Bioinform. Comput. Biol.* 8, 33–45. doi: 10.1142/S0219720010005129

Livak, K. J., and Schmittgen, T. D. (2001). Analysis of relative gene expression data using real-time quantitative PCR and the 2-ΔΔCT method. *Methods* 25, 402–408. doi: 10.1006/meth.2001.1262

Lotan, T., Ohto, M., Yee, K. M., West, M. A. L., Lo, R., Kwong, R. W., et al. (1998). *Arabidopsis* LEAFY COTYLEDON1 is sufficient to induce embryo development in vegetative cells. *Cell* 93, 1195–1205. doi: 10.1016/S0092-8674(00)81463-4

Lu, Q. S., Paz, J., Pathmanathan, A., Chiu, R. S., Tsai, A., and Gazzarrini, S. (2010). The C-terminal domain of FUSCA3 negatively regulates mRNA and protein levels, and mediates sensitivity to the hormones abscisic acid and gibberellic acid in Arabidopsis. *Plant J.* 64, 100–113. doi: 10.1111/j.1365-313X.2010.04307.x

Luerßen, H., Kirik, V., Herrmann, P., and Miséra, S. (1998). FUSCA3 encodes a protein with a conserved VP1/ABI3-like B3 domain which is of functional importance for the regulation of seed maturation in *Arabidopsis thaliana*. *Plant J.* 15, 755–764. doi: 10.1046/j.1365-313X.1998.00259.x

Mantovani, R. (1999). The molecular biology of the CCAAT-binding factor NF-Y. *Gene* 239, 15–27. doi: 10.1016/S0378-1119(99)00368-6

Matuoka, K., and Chen, K. Y. (2002). Transcriptional regulation of cellular ageing by the CCAAT box-binding factor CBF/NF-Y. *Ageing Res. Rev.* 1, 639–651. doi: 10.1016/S1568-1637(02)00026-0

McCarty, D. R., Hattori, T., Carson, C. B., Vasil, V., Lazar, M., and Vasil, I. K. (1991). The *Viviparous*-1 developmental gene of maize encodes a novel transcriptional activator. *Cell* 66, 895–905. doi: 10.1016/0092-8674(91)90436-3

Mönke, G., Seifert, M., Keilwagen, J., Mohr, M., Grosse, I., Hähnel, U., et al. (2012). Toward the identification and regulation of the *Arabidopsis thaliana* ABI3 regulon. *Nucleic Acids Res.* 40, 8240–8254. doi: 10.1093/nar/gks594

Nag, R., Maity, M. K., and DasGupta, M. (2005). Dual DNA binding property of *ABA insensitive* 3 like factors targeted to promoters responsive to ABA and auxin. *Plant Mol. Biol.* 59, 821–838. doi: 10.1007/s11103-005-1387-z

Nakamura, S., Lynch, T. J., and Finkelstein, R. R. (2001). Physical interactions between ABA response loci of *Arabidopsis*. *Plant J.* 26, 627–635. doi: 10.1046/j.1365-313x.2001.01069.x

Nambara, E., Naito, S., and McCourt, P. (1992). A mutant of *Arabidopsis* which is defective in seed development and storage protein accumulation is a new abi3 allele. *Plant J.* 2, 435–441. doi: 10.1111/j.1365-313X.1992.00435.x

Nystedt, B., Street, N. R., Wetterbom, A., Zuccolo, A., Lin, Y. C., Scofield, D. G., et al. (2013). The Norway spruce genome sequence and conifer genome evolution. *Nature* 497, 579–584. doi: 10.1038/nature12211

Parcy, F., Valon, C., Raynal, M., Gaubier-Comella, P., Delseny, M., and Giraudat, J. (1994). Regulation of gene expression programs during Arabidopsis seed development: roles of the ABI3 locus and of endogenous abscisic acid. *Plant Cell* 6, 1567–1582. doi: 10.1105/tpc.6.11.1567

Peng, L. T., Shia, Z. Y., Lia, L., Shen, G. Z., and Zhang, J. L. (2008). Overexpression of transcription factor OsLFL1 delays flowering time in *Oryza sativa*. *J. Plant Physiol.* 165, 876–885. doi: 10.1016/j.jplph.2007.07.010

Radoeva, T., and Weijers, D. (2014). A roadmap to embryo identity in plants. *Trends Plant Sci.* 19, 709–716. doi: 10.1016/j.tplants.2014.06.009

Rensing, S. A., Lang, D., Zimmer, A. D., Terry, A., Salamov, A., Shapiro, H., et al. (2008). The Physcomitrella genome reveals evolutionary insights into the conquest of land by plants. *Science* 319, 64–69. doi: 10.1126/science.1150646

Righetti, K., Vu, J., Pelletier, S., Vu, B., Glaab, E., Lalanne, D., et al. (2015). Inference of longevity-related genes from a robust coexpression network of seed maturation identifies regulators linking seed storability to biotic defense-related pathways. *Plant Cell* 27, 2692–2708. doi: 10.1105/tpc.15.00632

Rövekamp, M., Bowman, J. L., and Grossniklaus, U. (2016). Marchantia MpRKD regulates the gametophyte-sporophyte transition by keeping egg cells quiescent in the absence of fertilization. *Curr. Biol.* 26, 1–8. doi: 10.1016/j.cub.2016.05.028

Salvini, M., Sani, E., Fambrini, M., Pistelli, L., Pucciariello, C., and Pugliesi, C. (2012). Molecular analysis of a sunflower gene encoding an homologous of the B subunit of a CAAT binding factor. *Mol. Biol. Rep.* 39, 6449–6465. doi: 10.1007/s11033-012-1463-9

Santos-Mendoza, M., Dubreucq, B., Baud, S., Parcy, F., Caboche, M., and Lepiniec, L. (2008). Deciphering gene regulatory networks that control seed development and maturation in Arabidopsis. *Plant J.* 54, 608–620. doi: 10.1111/j.1365-313X.2008.03461.x

Siefers, N., Dang, K. K., Kumimoto, R. W., Bynum, W. E., Tayrose, G., and Holt, B. F. (2009). Tissue-specific expression patterns of Arabidopsis NF-Y transcription factors suggest potential for extensive combinatorial complexity. *Plant Physiol.* 149, 625–641. doi: 10.1104/pp.108.130591

Sreenivasulu, N., and Wobus, U. (2013). Seed-development programs: a systems biology-based comparison between dicots and monocots. *Annu. Rev. Plant Biol.* 64, 189–217. doi: 10.1146/annurev-arplant-050312-120215

Stamatakis, A., Hoover, P., and Rougemont, J. (2008). A rapid bootstrap algorithm for the RAxML web servers. *Syst. Biol.* 57, 758–771. doi: 10.1080/10635150802429642

Stephenson, T. J., McIntyre, C. L., Collet, C., and Xue, G. P. (2007). Genome-wide identification and expression analysis of the NF-Y family of transcription factors in *Triticum aestivum*. *Plant Mol. Biol.* 65, 77–92. doi: 10.1007/s11103-007-9200-9

Stone, S., Braybrook, S., Paula, S., Kwong, L., Meuser, J., Pelletier, J., et al. (2007). *Arabidopsis* LEAFY COTYLEDON2 induces maturation traits and auxin activity: implications for somatic embryogenesis. *Proc. Natl. Acad. Sci. U.S.A.* 105, 3151–3156. doi: 10.1073/pnas.0712364105

Stone, S. L., Kwong, L. W., Yee, K. M., Pelletier, J., Lepiniec, L., Fischer, R., et al. (2001). LEAFY COTYLEDON2 encodes a B3 domain transcription factor that induces embryo development. *Proc. Natl. Acad. Sci. U.S.A.* 98, 11806–11811. doi: 10.1073/pnas.201413498

Suzuki, M., Kao, C., and McCarty, D. (1997). The conserved B3 domain of VIVIPAROUS1 has a cooperative DNA binding activity. *Plant Cell* 9, 799–807. doi: 10.1105/tpc.9.5.799

Suzuki, M., and McCarty, D. R. (2008). Functional symmetry of the B3 network controlling seed development. *Curr. Opin. Plant Biol.* 11, 548–553. doi: 10.1016/j.pbi.2008.06.015

Swaminathan, K., Peterson, K., and Jack, T. (2008). The plant B3 superfamily. *Trends Plant Sci.* 12, 647–655. doi: 10.1016/j.tplants.2008.09.006

Tang, G., Xu, P., Liu, W., Liu, Z., and Shan, L. (2015). Cloning and characterization of 5' flanking regulatory sequences of AhLEC1B gene from *Arachis hypogaea* L. *PLoS ONE* 10:e0139213. doi: 10.1371/journal.pone.0139213

Tiedemann, J., Rutten, T., Mönke, G., Vorwieger, A., Rolletschek, H., Meissner, D., et al. (2008). Dissection of a complex seed phenotype: novel insights of FUSCA3 regulated developmental processes. *Dev. Biol.* 317, 1–12. doi: 10.1016/j.ydbio.2008.01.034

To, A., Valon, C., Savino, G., Guilleminot, J., Devic, M., Giraudat, J., et al. (2006). A network of local and redundant gene regulation governs *Arabidopsis* seed maturation. *Plant Cell* 18, 1642–1651. doi: 10.1105/tpc.105.039925

Tsuchiya, Y., Nambara, E., Naito, S., and McCourt, P. (2004). The FUS3 transcription factor functions through the epidermal regulator TTG1 during embryogenesis in *Arabidopsis*. *Plant J.* 37, 73–81. doi: 10.1046/j.1365-313X.2003.01939.x

Verdier, J., Torres-Jerez, I., Wang, M., Andriankaja, A., Allen, S., He, J., et al. (2013). Establishment of the lotus japonicus gene expression atlas (LjGEA) and its use to explore legume seed maturation. *Plant J.* 74, 351–362. doi: 10.1111/tpj.12119

Wang, F., and Perry, S. E. (2013). Identification of direct targets of FUSCA3, a key regulator of Arabidopsis seed development. *Plant Physiol.* 161, 1251–1264. doi: 10.1104/pp.112.212282

Xie, Z., Li, X., Glover, B. J., Bai, S. N., Rao, G. Y., Luo, J., et al. (2008). Duplication and functional diversification of HAP3 genes leading to the origin of the seed-developmental regulatory gene, LEAFY COTYLEDON1 (LEC1), in nonseed plant genomes. *Mol. Biol. Evol.* 25, 1581–1592. doi: 10.1093/molbev/msn105

Yamamoto, A., Kagaya, Y., Toyoshima, R., Kagaya, M., Takeda, S., and Hattori, T. (2009). Arabidopsis NF-YB subunits LEC1 and LEC1-LIKE activate transcription by interacting with seed-specific ABRE-binding factors. *Plant J.* 58, 843–856. doi: 10.1111/j.1365-313X.2009.03817.x

Yang, J., Xie, Z., and Glover, B. J. (2005). Asymmetric evolution of duplicate genes encoding the CCAAT-binding factor NF-Y in plant genomes. *New Phytol.* 165, 623–632. doi: 10.1111/j.1469-8137.2004.01260.x

Zeng, Y., and Kermode, A. R. (2004). A gymnosperm ABI3 gene functions in a severe abscisic acid-insensitive mutant of *Arabidopsis* (abi3-6) to restore the wild-type phenotype and demonstrates a strong synergistic effect with sugar in the inhibition of post-germinative growth. *Plant Mol. Biol.* 56, 731–746. doi: 10.1007/s11103-004-4952-y

Zeng, Y., Raimondi, N., and Kermode, A. R. (2003). Role of an ABI_3 homologue in dormancy maintenance of yellow-cedar seeds and in the activation of storage protein and Em gene promoters. *Plant Mol. Biol.* 51, 39–49. doi: 10.1023/A:1020762304937

Zhang, J.-J., and Xue, H.-W. (2013). *OsLEC1*/*OsHAP3E* participates in the determination of meristem identity in both vegetative and reproductive developments of rice. *J. Integr. Plant Biol.* 55, 232–249. doi: 10.1111/jipb.12025

Conflict of Interest Statement: The authors declare that the research was conducted in the absence of any commercial or financial relationships that could be construed as a potential conflict of interest.

frontiers in Plant Science

ORIGINAL RESEARCH
published: 27 April 2017
doi: 10.3389/fpls.2017.00658

Expression Analyses of Embryogenesis-Associated Genes during Somatic Embryogenesis of *Adiantum capillus-veneris* L. *In vitro*: New Insights into the Evolution of Reproductive Organs in Land Plants

Xia Li[1†], Jing-Dan Han[2†], Yu-Han Fang[2], Shu-Nong Bai[2] and Guang-Yuan Rao[2]*

[1] RDFZ XiShan School, Beijing, China, [2] School of Life Sciences, Peking University, Beijing, China

An efficient *in vitro* regeneration system *via* somatic embryogenesis (SE) was developed for a fern species *Adiantum capillus-veneris*. Adventitious shoots, green globular bodies (GGBs) and calli were obtained with the maximal induction rate on the Murashige and Skoog (MS) medium of low concentrations of 6-benzyladenine (BA) (0–1.0 mg/L), 2.0 mg/L BA without 2,4-dichlorophenoxyacetic acid (2,4-D), 0.5 mg/L 2,4-D and 0.5–1.0 mg/L 6-BA, respectively. Cyto-morphological and histological changes in the shoot development *via* calli and GGBs were examined. For a better understanding of these developmental events, expression patterns of six genes, *AcLBD16*, *AcAGL*, *AcBBM*, *AcWUS*, *AcRKD,* and *AcLEC1*, were characterized during SE. *AcBBM* and *AcLEC1* were ubiquitously expressed in direct SE (adventitious shoots and GGBs) the maximal expression of *AcBBM* in mature GGBs, and the high expression of *AcLEC1* in GGB initiation and adventitious shoots. During the indirect SE, *AcLBD16*, *AcLEC1*, *AcRKD,* and *AcWUS* were highly expressed in mature calli. Additionally, phylogenetic analyses showed that *AcWUS, AcBBM, AcLBD, AcAGL, AcRKD,* and their homologs of other green plants formed monophyletic clades, respectively. Some of these gene families, however, diversified rapidly with the occurrence of embryophytes, suggesting that embryogenesis-associated genes could experience a rapid evolution with the colonization of plants to terrestrial environments. Expression and phylogenetic analyses of those embryogenesis-associated genes by the aid of *in vitro* regeneration system of *A. capillus-veneris* provide new insights into the evolution of reproductive organs in land plants.

Keywords: *Adiantum capillus-veneris*, somatic embryogenesis, embryogenesis-associated genes, gene expression, phylogenetic analysis

OPEN ACCESS

Edited by:
Zhong-Jian Liu,
The Orchid Conservation and Research Center of Shenzhen, China

Reviewed by:
Hongzhi Kong,
Institute of Botany (CAS), China
Wen-Chieh Tsai,
National Cheng Kung University, Taiwan

***Correspondence:**
Guang-Yuan Rao
rao@pku.edu.cn

[†]These authors have contributed equally to this work.

Specialty section:
This article was submitted to Plant Evolution and Development, a section of the journal Frontiers in Plant Science

Received: *12 January 2017*
Accepted: *11 April 2017*
Published: *27 April 2017*

Citation:
Li X, Han J-D, Fang Y-H, Bai S-N and Rao G-Y (2017) Expression Analyses of Embryogenesis-Associated Genes during Somatic Embryogenesis of Adiantum capillus-veneris L. In vitro: New Insights into the Evolution of Reproductive Organs in Land Plants. Front. Plant Sci. 8:658. doi: 10.3389/fpls.2017.00658

INTRODUCTION

The occurrence of embryos was presumably one of the most significant innovations during plant evolution, which is crucial for plant reproduction (Kenrick and Crane, 1997; Becker and Marin, 2009; Pires and Dolan, 2012; Radoeva and Weijers, 2014). Obviously, embryogenesis is a defining feature of land plants, and establishes the basic body plan of sporophytes. In addition to zygote-derived embryogenesis, other modes of embryogenesis have been described, such as somatic embryogenesis (SE). SE is the biological process through which a whole individual is regenerated from somatic tissues via their dedifferentiation and redifferentiation (Fehér, 2015; Loyola-Vargas and Ochoa-Alejo, 2016). Not only is SE one of the most powerful tools in plant biotechnology, but it also becomes an efficient approach to study the mechanisms of the embryo development (Radoeva and Weijers, 2014; Fehér, 2015; Loyola-Vargas and Ochoa-Alejo, 2016).

SE can be divided into two types: one is the direct SE where the embryos are formed from the organized tissue without an intervening callus stage; another is the indirect SE where the embryo formation experiences a callus phase (Radoeva and Weijers, 2014). Genetic studies in the past decades have identified and cloned the genes and loci required for initiation and progression of zygotic embryogenesis (ZE) in Arabidopsis (Tzafrir et al., 2004; Radoeva and Weijers, 2014; Mikuła et al., 2015), but not in non-seed plants. According to previous studies, the similarity in the regulatory mechanisms that underlie SE and ZE has recently become evident at the molecular level (Tzafrir et al., 2004; Radoeva and Weijers, 2014; Loyola-Vargas and Ochoa-Alejo, 2016). Thus, the SE system can be used to investigate the progression and morphogenetic events during embryogenesis of early land plants, and also to examine the ZE regulatory mechanisms by analyzing the expression pattern of embryogenesis-associated genes during their SE. These data will provide insights into the evolution of reproductive organs in land plants.

Although the tissue culture of ferns has been studied for decades (Beck and Caponetti, 1983; Fernández et al., 1997; Bertrand et al., 1999; Fernández and Revilla, 2003; Liao and Wu, 2011; Mallón et al., 2011), only a few species, such as the tree fern *Cyathea delgadii*, was described concerning SE (Mikuła et al., 2015). As ferns are the closest living relatives of spermatophytes (Pryer et al., 2001), this group of plants has been useful subjects for evolutionary, morphological and developmental studies (Johnson and Renzaglia, 2009; Li et al., 2013; Vasco et al., 2013). In terms of SE, ferns have been apparently under-investigated compared to spermatophytes, and the molecular mechanism underlying the control of SE is poorly understood.

Recently, efforts have been made to describe SE at the molecular level in seed plants, and several groups of genes associated with this process have been revealed. PINs, Aux/IAAs, AUXIN RESPONSE FACTORS (ARFs) as well as LATERAL ORGAN BOUNDARIES DOMAIN (LBD) family have been shown to be involved in auxin generating somatic embryos (Jenik and Barton, 2005; Leyser, 2005). In addition, a series of transcription regulator genes are strongly implicated in this process. Among members of the APETALA2/ethylene-responsive factor (AP2/ERF) family, BABY BOOM (BBM) is a key transcription regulator that has been detected to involve the induction of SE (Boutilier et al., 2002). AGAMOUS like-15 (AGL15), a MADS-domain transcription factor, is involved in meristem development and also functions as a transcriptional activator during somatic embryo formation (Harding et al., 2003). WUSCHEL (WUS) and WUS-related homeobox domain (WOX), which are homeodomain containing transcription factors, regulate stem cell fate during embryo formation and have also been detected during SE (Zuo et al., 2002; Iwase et al., 2011). The RKD (RWP-RK domain-containing) proteins, such as RKD1, RKD2, and RKD4, are another class of transcription factors involved in early embryogenesis and female gametogenesis (Koszegi et al., 2011).

As a leptosporangiate fern, *Adiantum capillus-veneris* has become the subject of many cytological, developmental, physiological, and phylogenetic studies (Pryer et al., 2001; Wada, 2007; Xie et al., 2008; Li et al., 2013). Although there are several literatures on the direct SE of *A. capillus-veneris*, few of them have presented sufficient histological evidence to describe this process (Salomé et al., 1985; Amaki and Higuchi, 1991; Somer et al., 2010). In addition, the genes required to regulate callus and GGB induction and development are not well defined in *A. capillus-veneris*. It is also believed that expression analyses of the genes regulating SE can provide insights into this developmental process (Chugh and Khurana, 2002; Stasolla et al., 2004).

In the present work, we established a regeneration system *via* SE for *A. capillus-veneris* and three types of regeneration structure, i.e., shoots, GGBs and calli, were obtained. The main developmental events leading to the generation of shoots from calli and GGBs of *A. capillus-veneris* were examined by histological analyses. For a better understanding of the genes and regulatory mechanisms behind the fern SE, six homologous genes of Arabidopsis *LBD16, WUS*, *LEC1*, *RKD4*, *AGL15*, *BBM* were identified and cloned from *A. capillus-veneris*. Meanwhile, phylogenetic analyses of those genes of the main lineages of land plants including bryophytes, monilophytes, gymnosperms and angiosperms were conducted for their molecular evolution. In addition, the expression patterns of those genes were characterized during the crucial steps of the SE *via* GGBs and calli. All of the above analyses will shed insights into the evolution of reproductive organs in land plants.

MATERIALS AND METHODS

Plant Induction System

For the induction system, explants of circinate leaflets from the sporophytes of *A. capillus-veneris* cultivated in the greenhouse of Peking University (Beijing, China) were cultured on full strength Murashige and Skoog medium (MS) or ½ MS medium supplemented with different concentrations of 2,4-dichlorophenoxyacetic acid (2,4-D) and 6-benzyladenine (BA) as follows: 0/0, 0.5/0, 1.0/0, 1.5/0, 2.0/0; 0/0.5, 0.5/0.5, 1.0/0.5,

1.5/0.5, 2.0/0.5; 0/1.0, 0.5/1.0, 1.0/1.0, 1.5/1.0, 2.0/1.0; 0/1.5, 0.5/1.5, 1.0/1.5, 1.5/1.5, 2.0/1.5; 0/2.0, 0.5/2.0, 1.0/2.0, 1.0/2.0, 1.5/2.0, and 2.0/2.0 mg/L. All cultures were maintained at 25 ± 1°C under a 16/8 h (light/dark) cycle and then transferred into induction medium ∼30 days later for further observation and proliferation.

Somatic Embryogenesis Induction and Statistical Analysis

The shoots and green global bodies (GGBs) were generated from direct SE, whereas calli were produced by indirect SE according to the aforementioned SE's definition (**Table S1**). The GGBs continuously increased in size in the selected medium. When the size of GGBs was 8–10 mm in diameter, they were cut into 3–4 pieces (∼3 mm in diameter) and then transplanted into the same medium subculture. In parallel, primary calli from the best induction medium (>80%) were cut into the same small size (∼3 mm in diameter) and then transplanted into their original initiation medium.

GGBs were transferred to shoot induction medium containing 0.5 mg/L BA under aseptic conditions. Shoots were observed at ∼20 days. When most of the shoots had several leaves, they were transplanted into the PGR-free MS medium. For shoot induction from calli, MS and ½ MS medium with 0, 0.5, 1.0, 1.5, or 2.0 mg/L BA were chosen as the regeneration media. Calli were excised to ∼3 mm in diameter and subcultured in the regeneration medium, which was renewed every 20 days. After 3 months of subculture, the total number of shoots per callus was calculated.

To induce roots, multiple shoot clusters were cut into small pieces (∼5 mm in diameter) and then transferred to ½ MS medium supplemented with 0.5 mg/L naphthaleneacetic acid (NAA). After incubation for a total of 40 days, the well-developed plantlets were gently washed to remove agar and transferred from the culture flask to plastic pots containing vermiculite and nutrition soil [1:1 (v/v)].

The induction of shoots, GGBs and calli were repeated two times, with each replicate comprising 6–15 explants in a single Petri plate. The differentiation of shoots from calli involved 10 calli and three experimental replicates were conducted. All data were analyzed using one-way ANOVA followed by Duncan's multiple range test with significance level of $P < 0.05$ (IBM_ SPSS ver. 16).

Microscopic Preparation

For histological characterization, samples were fixed in formalin-alcohol-acetic acid (50% ethanol: formaldehyde: acetic acid, 91:5:4) for >24 h. The samples were dehydrated in an ethanol series and then an alcohol-acetone series (ethanol: acetone, 2:1, 1:1, 1:2, 0:1, and 0:1, changed every 30-min). For semithin sections, the tissues were then subjected to an acetone-Spurr's resin series (acetone: resin, 2:1, 1:1, 1:2, 0:1, 0:1, and 0:1) changed every 8 h. Finally, the samples were embedded in Spurr's resin. Sections (3 μm thick) were cut using a microtome (Leitz, 1512, Germany) and stained with 2% basic fuchsin. Images were observed and captured with a light microscope (Zeiss Axioskop 2 Plus, Germany) coupled with Axioplan software. For scanning electron microscopy (SEM), the samples were critical-point dried in CO_2 (HCP-2; Hitachi, Tokyo, Japan) for 6 h. The dried samples were mounted, sputter-coated with gold palladium (Hitachi E-1010), and viewed under a Hitachi S-4800 SEM at 10.0 kV.

Gene Cloning and Sequencing

Arabidopsis LBD16 (AT2G42430), AGL15 (AT5G13790), BBM (AT5G17430), WUSCHEL (AT2g17950), and RKD4 (AT5G53040) protein sequences were used as queries to find the homologs in the RNA-Seq database of *A. capillus-veneris* (Li et al., unpublished data). All the homologs, designated AcLBD16, AcAGL, AcBBM, AcWUS, and AcRKD were verified by sequencing coding DNA sequences using appropriate primers (**Table S2**). All these genes and their sequence were submitted to GenBank under accession number KP238200–KP238204.

Quantitative RT-PCR (qRT-PCR) Analysis

For qRT-PCR analysis, nine samples were used to identify the genes' expression patterns. Explant leaflets and eight different tissues at adventitious shoot, GGB and callus developmental stages were chosen: the initiation stage (14-day), mature stage (40-day), callus-embryo transition stage and GGB-/callus-derived shoots. Total RNA was isolated with Plant RNA Extraction Reagent (Invitrogen, USA) and purified with an RNeasy Mini kit according to the manufacturer's instructions (Qiagen, Germany). RNA was then converted to cDNA by reverse transcription with a FastQuant RT Kit (Tiangen, China). qRT-PCR was performed on an Applied Biosystems 7500 Real-Time PCR System (ABI) with the reaction mixture containing cDNA templates, primers (**Table S3**) and SYBR® Premix Ex Tax Mix (Takara, Japan). Transcript levels were normalized against the *A. capillus-veneris* actin gene (*AcACTIN*) transcript levels using appropriate primers (**Table S3**). Relative expression was calculated *via* the delta-delta threshold method ($2^{-\Delta\Delta C}$T) (Livak and Schmittgen, 2001). Results were expressed as means ± SE (standard error) of two biological repeats.

Phylogenetic Analysis

To gain insight into the evolutionary relationships of AcLBD16, AcAGL, AcBBM, AcWUS, and AcRKD with their counterparts in other plants, we performed the exhaustive phylogenetic analyses of LBD gene superfamily, and AP2, MADS-box, WOX, and RKD gene family. The homologous amino acid sequences of *A. thaliana*, *Oryza sativa*, *Amborella trichopoda*, *Picea abies*, *A. capillus-veneris*, *Selaginella moellendorffii*, *Physcomitrella patens*, *Marchantia polymorpha*, and algae were retrieved from databases Phytozome (http://phytozome.jgi.doe.gov/pz/portal.html), ConGenIE (http://congenie.org), and the *Klebsormidium flaccidum* genome project (http://www.plantmorphogenesis.bio.titech.ac.jp/~algae_genome_project/klebsormidium/index.html) (**Table S4**). The sequences were aligned using the online version of MAFFT (http://mafft.cbrc.jp/alignment/software/) (Katoh and Standley, 2013). The final alignments were analyzed using Protest (Abascal et al., 2005) to choose the best-fit models at amino acid level for molecular evolution. Maximum likelihood (ML) phylogenetic analyses were performed with RaxML and statistically evaluated by the bootstrap method using 1000

replicates (Stamatakis et al., 2008). Trees were edited using FigTree v1.4.2. (http://tree.bio.ed.ac.uk/software/figtree/).

RESULTS

Somatic Embryogenesis Induction System

Three induction systems of SE were produced by adventitious shoots, GGBs and calli when explants were cultured on the basal medium supplemented with different concentrations of 2,4-D and BA (**Figure 1**, **Table S1**). After ∼2 weeks' culture, differentiated shoots were first observed on PGR-free media (**Figures 1A,E**). When the concentration of BA was increased to 1.5 mg/L and 2.0 mg/L, few shoots but GGBs were produced (**Figures 1B,F**). Under low concentrations of 2,4-D, a primary callus was induced after 2 weeks of culture (**Figures 1C,G**), while in higher concentrations of 2,4-D, e.g., from 1.5 to 2.0 mg/L, fewer calli were induced and they had a soft texture, dispersing cells on the medium (**Figure 1D**). When GGBs or calli were moved to the medium free of 2,4-D and with a lower concentration of BA, shoots readily formed within 5 months of incubation (**Figure 1I**). Well-developed shoots were transferred onto the rooting medium comprising ½ MS basal medium supplemented with 0.5 mg/L NAA to promote root formation (**Figure 1J**). Subsequently, more than 10 roots were produced after approximately 4 weeks of culture (**Figure 1K**). By this stage, plantlets had developed from the explants. When transplanted into soil, ∼90% of the plantlets survived and produced spores 2 months later (**Figure 1L**).

Cyto-Morphological Evidence for Direct Somatic Embryogenesis

Adventitious shoots compacted with some trichomes had obvious shoot apices, leaves and roots (**Figures 1E**,**2A,B**). The globular dark-green GGBs appeared 2 weeks after the incubation of explants (**Figures 1B,F**,**2C**). Multiple meristematic zones were found inside the initial GGB tissue (**Figure 2D**). Thereafter, many hair-like adventitious shoots formed on the surface of GGBswhen they were moved to the 2, 4-D-free medium with lower BA (**Figures 2E–H**). By the means of qRT-PCR analysis, we examined the expression patterns of six selected genes during *A. capillus-veneris* direct SE. As our results showed, *AcLEC1* is functionally pleiotropic, and it was highly

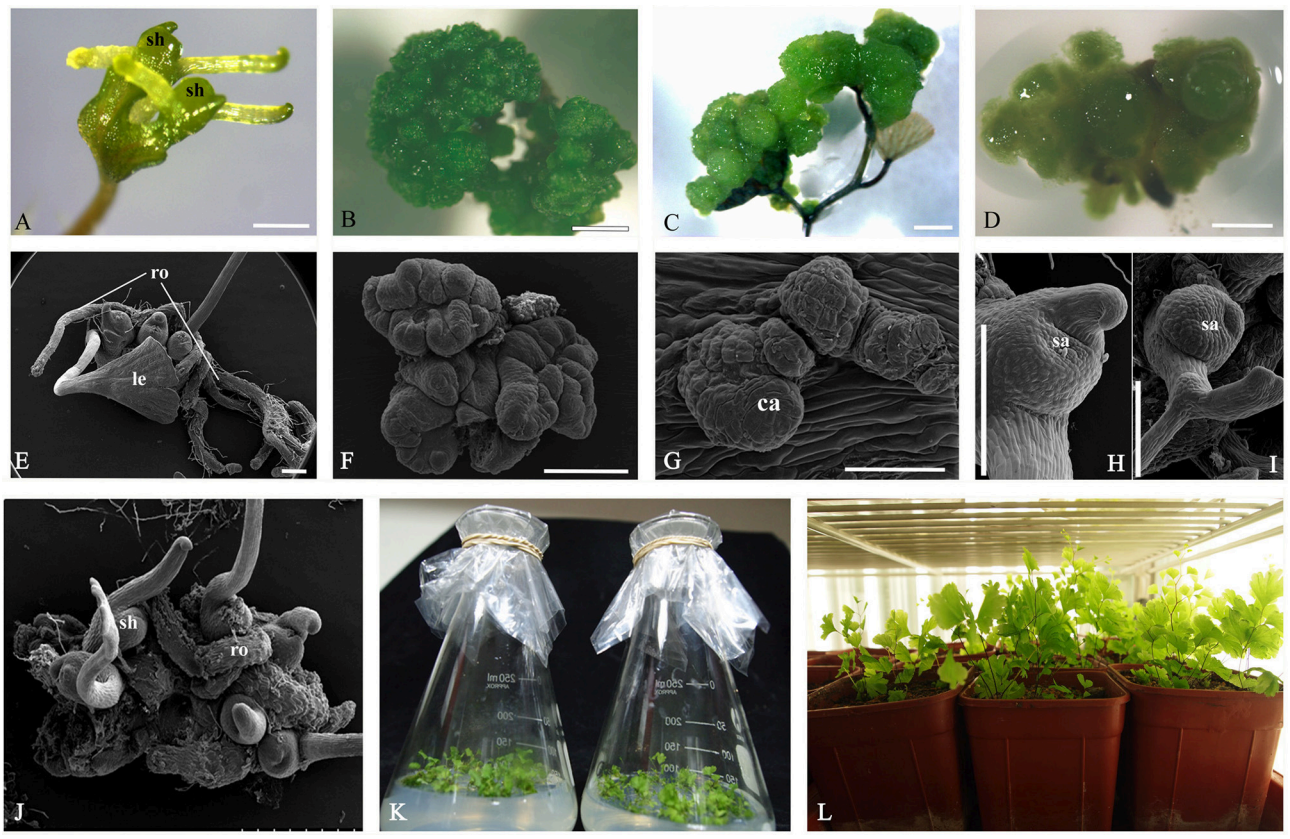

FIGURE 1 | Somatic embryogenesis induction system in *Adiantum capillus-veneris*. (A,E) Adventitious shoots formed on medium without PGR. **(B,E)** GGBs cultured on medium with 2.0 mg/L 6-BA. **(C,G)** Callus formed on medium with 0.5 mg/L 2, 4-D and 0.5 mg/L 6-BA. **(D)** Dispersed cells cultured on medium with 2.0 mg/L 2,4-D and 0.5 mg/L 6-BA. **(H)** Adventitious shoots derived from callus; **(I)** Shoots of sexual reproduction from archegonium. **(J)** Well-developed shoots. **(K)** Root formation of shoots on ½ MS medium with 0.5 mg/L NAA in flask; **(L)** Rooted plantlets transferred to pots for acclimatization. Ca, callus; sh, shoot; ro, root; le, leaf; sa, shoot apex. Bars = 500 μm.

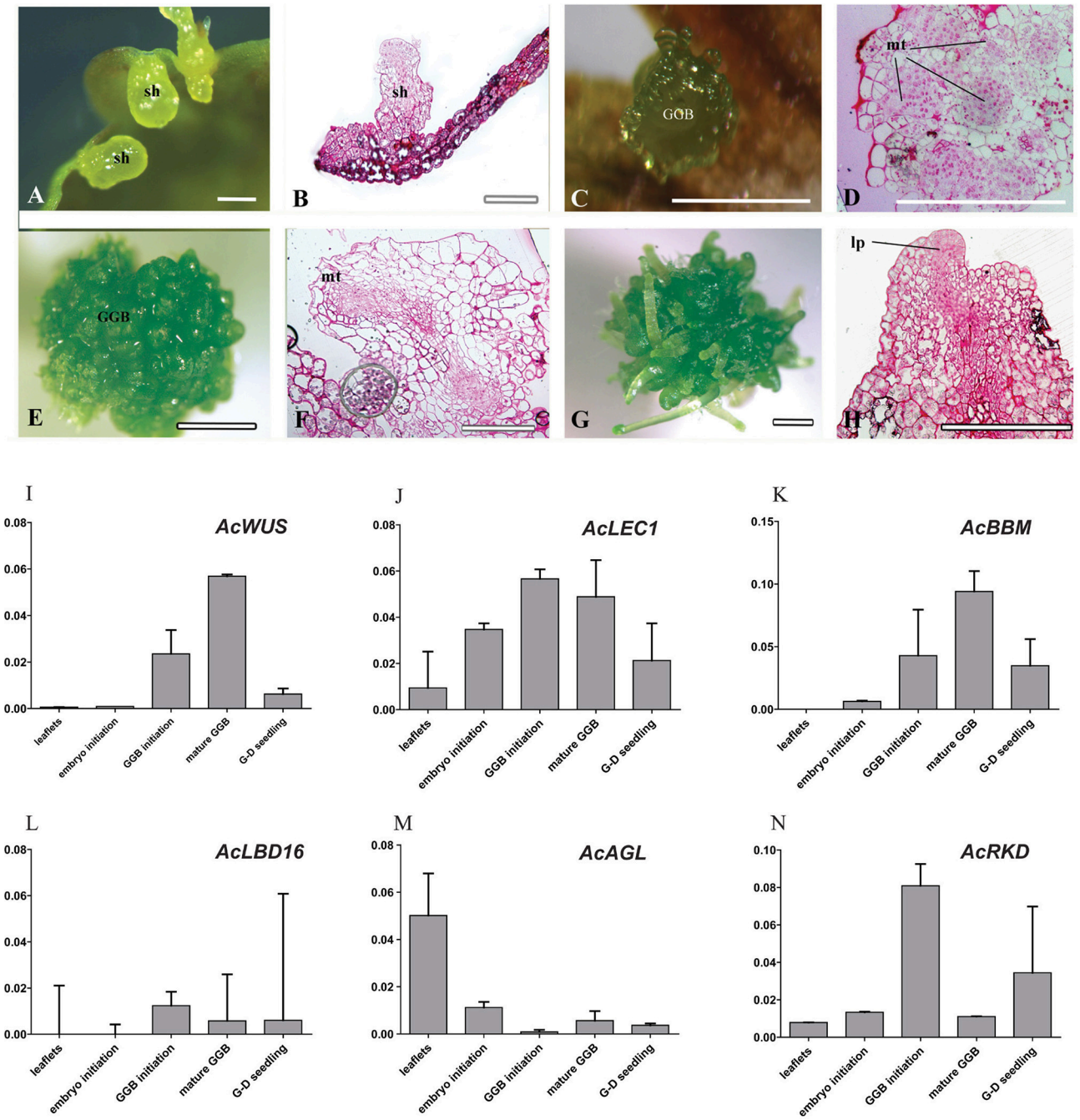

FIGURE 2 | Cyto-morphological and gene expression of adventitious shoots and GGBs. (A) Shoots formed on medium without PGR. **(B)** Histological section of initiated shoots (14-day). **(C)** Initiated GGBs (14-day). **(D)** Vertical section of initiated GGBs. **(E)** Mature GGBs (40-day). **(F)** Vertical section of mature GGBs (40-day). **(G)** GGB-derived shoots cultured on medium without PGR. **(H)** Vertical section of GGB-derived shoots. **(I–N)** Expression of *AcWUS, AcLEC1, AcBBM, AcLBD16, AcAGL, AcRKD* during shoots and GGBs-derived somatic embryogenesis. dcz, dividing cells zone; GGB, green globular body; lp, leaf primordium; mt, meristematic tissue. Bars = 500 μm.

expressed in the initiation phase of embryos and GGBs, and mature GGBs, respectively (**Figure 2J**). However, the expression decreased in GGB-derived seedlings as the shoots continued to regenerate (**Figure 2J**). *AcWUS* and *AcBBM* had similar expression patterns with expression peak in the mature GGBs and low point in embyro initiation (**Figures 2I,K**). *AcRKD* was only highly expressed at GGB initiation stage during the direct SE (**Figure 2N**). Comparing to the explant leaflets, expressions of *AcLBD16* and *AcAGL* were rarely detectable in shoot and GGB development phases (**Figures 2L,M**).

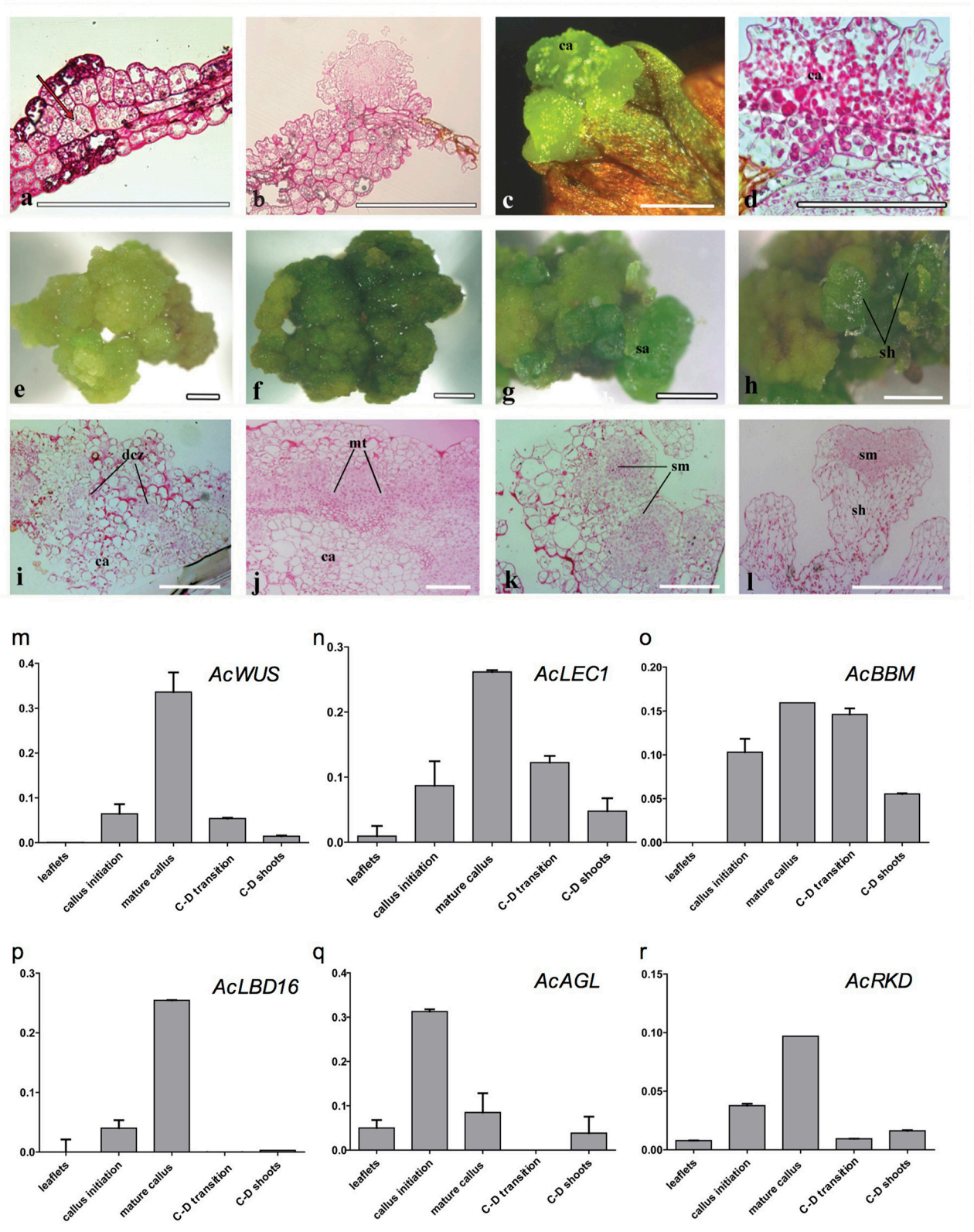

FIGURE 3 | Cyto-morphological and gene expression during callus-derived somatic embryogenesis. (a) The callus originated from the mesophyll cells. **(b)** Primary callus lump of the leaf. **(c)** Initiated callus (14-day) formed on medium with 0.5 mg/L 2,4-D and 0.5 mg/L 6-BA. **(d)** Vertical section of initiated callus. **(e)** Mature callus (40-day) on medium with 0.5 mg/L 2,4-D and 0.5 mg/L 6-BA. **(i)** Vertical section of mature callus. **(f–h)** Callus-embryo transition on medium with 0.5 mg/L

(Continued)

FIGURE 3 | Continued
BA. **(j–k)** Vertical section of callus showing meristemoids. **(l)** Vertical section showing shoot meristem. **(m–r)** Expression of *AcWUS, AcLEC1, AcBBM, AcLBD16, AcAGL, AcRKD* during callus-derived somatic embryogenesis. dcz, dividing cells zone; ca, callus; mt, meristematic tissue; sa, shoot apical; sh, shoot; sm, shoot meritem. Bars = 500 μm.

Callus Induction and Callus-Derived Shoot Organogenesis

Histological analysis revealed that the callus originated from the mesophyll cells, especially those closely connected to marginal veins of the pinnately lobes of explant leaflets (**Figure 3a**). The callus, an undifferentiated mass of friable light green tissue, lacked embryo-like structures or apical meristems (**Figures 3b–d**). The best production (>90%) of calli was found on media with 0.5 mg/L 2,4-D and 0.5–1.0 mg/L BA, where there was no significant difference in the callus productivity between hormone combinations in the two basal media (**Table S1**). When growing to ∼1 cm in diameter, calli were cut into small pieces (∼3 mm in diameter) and then transplanted into the same medium for subculture. Their cells divided actively and gave rise to fresh light green calli with multiple meristemoid zones after ∼1 month inoculation (**Figures 3e,i**). **Table S1** showed the effect of BA on shoot regeneration from calli. Among various PGRs tested, the highest frequency of shoot regeneration from calli (60–70%) and number of shoots per callus (4–5) were observed on either MS or ½ MS medium containing 0.5 mg/L BA (**Table 1**). After the first 40 days of culture, calli became compact and green (**Figure 3f**). At this time, meristemoids were produced inside rather than on the surface of the calli and shoot primordia formed (**Figure 3j**). After 3 months' culture, each callus produced several shoots (**Figures 3g–l**). During this indirect SE, expressions of *AcWUS*, *AcLEC1*, *AcLBD16* and *AcRKD* were clearly detected in callus development phases, with the maximum expression in mature calli (40-day calli), and then decreased (**Figures 3m,n,p,r**). *AcAGL* expressed during callus formation with higher expression levels at callus initiation (14-day calli) and in mature calli (40-day calli) (**Figure 3q**). Up-regulated expression of *AcBBM* was detected in the entire callus development and reached apeakat mature callus stage (**Figure 3o**). It was also highly expressed during the callus-embryo transition (C-D transition), but showed a low expression when shoots became visible (C-D shoots) (**Figure 3o**).

TABLE 1 | Callus-based shoot regeneration of *A. capillus-veneris*.

Treatment BA (mg/L)	Percentage of callus producing shoots (%)[1]		Average number of buds per callus[1]	
	MS	1/2 MS	MS	1/2 MS
0	$23.33^{abc} \pm 8.89$	$26.67^{abc} \pm 4.44$	$0.63^{A} \pm 0.11$	$0.70^{A} \pm 0.13$
0.5	$63.33^{e} \pm 8.89$	$76.67^{f} \pm 4.44$	$4.20^{E} \pm 0.38$	$5.00^{F} \pm 0.20$
1.0	$36.67^{cd} \pm 4.44$	$46.67^{d} \pm 4.44$	$3.33^{D} \pm 0.22$	$4.10^{E} \pm 0.13$
1.5	$30.00^{bc} \pm 0$	$33.33^{bcd} \pm 0.04$	$1.93^{C} \pm 0.22$	$2.07^{C} \pm 0.04$
2.0	$13.33^{a} \pm 4.44$	$20.00^{ab} \pm 6.67$	$0.30^{A} \pm 0.07$	$1.27^{B} \pm 0.11$

Data show mean ± SE of three replicates, each comprising 9–10 explants. Different letters in a column indicate significant differences at $P < 0.05$ according to Duncan's multiple range test.
[1] *The diameter of the calli was 8–10 mm.*

Identification and Phylogenetic Analysis of *AcWUS, AcBBM, AcLBD16, AcAGL, and AcRKD*

Phylogenetic analyses were performed to analyze evolution of *AcWUS, AcBBM, AcLBD16, AcAGL,* and *AcRKD* and their homologs in other green plants (**Figure 4**). The gene trees showed that these genes and their homologs of other green plants formed monophyletic clades, respectively (**Figure 4**). However, tree topologies were also found for these gene families, suggesting that they could experience different evolutionary trajectories during plant evolution.

The phylogenetic tree of *WOX* gene family showed that there were three clades, and the *AcWUS* was grouped with the *WUS* counterparts as a strong supported clade (**Figure 4D**). Within the *WUS* clade, *AcWUS* showed high sequence similarity to Arabidopsis *AtWUS*. The *AcBBM* was identified as a member of the *APETALA2 (AP2)/ETHYLEN-RESPONSE-FACTOR (ERF)* gene family. The phylogenetic tree of *BBM* genes showed that pteridophyte *BBMs*, including *AcBBMs*, were grouped at the base of the seed plant euANT lineage (**Figure 4A**). Also, phylogenetic analysis of *AcLBD* and its counterparts of other plants indicated that they all possess the signature motif of Class IB. In addition, phylogenetic tree showed that *AcLBD16* gene, though scattering among seed plant clades, resided in the Class 1B clade with strong support (**Figure 4C**). Hence, *AcLBD16* may be a putative ortholog of Arabidopsis *LBD16*, *LBD17*, *LBD18*, *LBD29*. A maximum-likelihood tree constructed from the whole RKD protein sequences showed that all the plant RKDs were clustered in a single clade which was well separated from the outgroup RWP-RK proteins (**Figure 4B**). *AcRKD* had high sequence similarity with Arabidopsis *RKDs* at the RWP-RK and carboxy-terminal domains. In addition, the phylogenetic position of *AcAGL* remains uncertain based on our analysis on the MADS Type II sequences using RAxML (**Figure 4E**). Seventeen branches (MIKC*, AGL2/AGL6/FLC/SQUA, DEF/GLO/OsMADS32/GGM13, AGAMOUS, AGL12, AGL15, AGL17, GpMADS4, StMADS11, TM3, and TM8) can be defined in the tree, but *AcAGL* had a close relationship with *MpoMADS1* and *TM8* rather than with *AGL15* of Arabidopsis and *Amborella trichopoda* (**Figure 4E**).

DISCUSSION

Shoot Regeneration *via* Somatic Embryogenesis

An efficient *in vitro* regeneration system *via* SE was developed for *A. capillus-veneris*. Direct SE via adventitious shoots and green

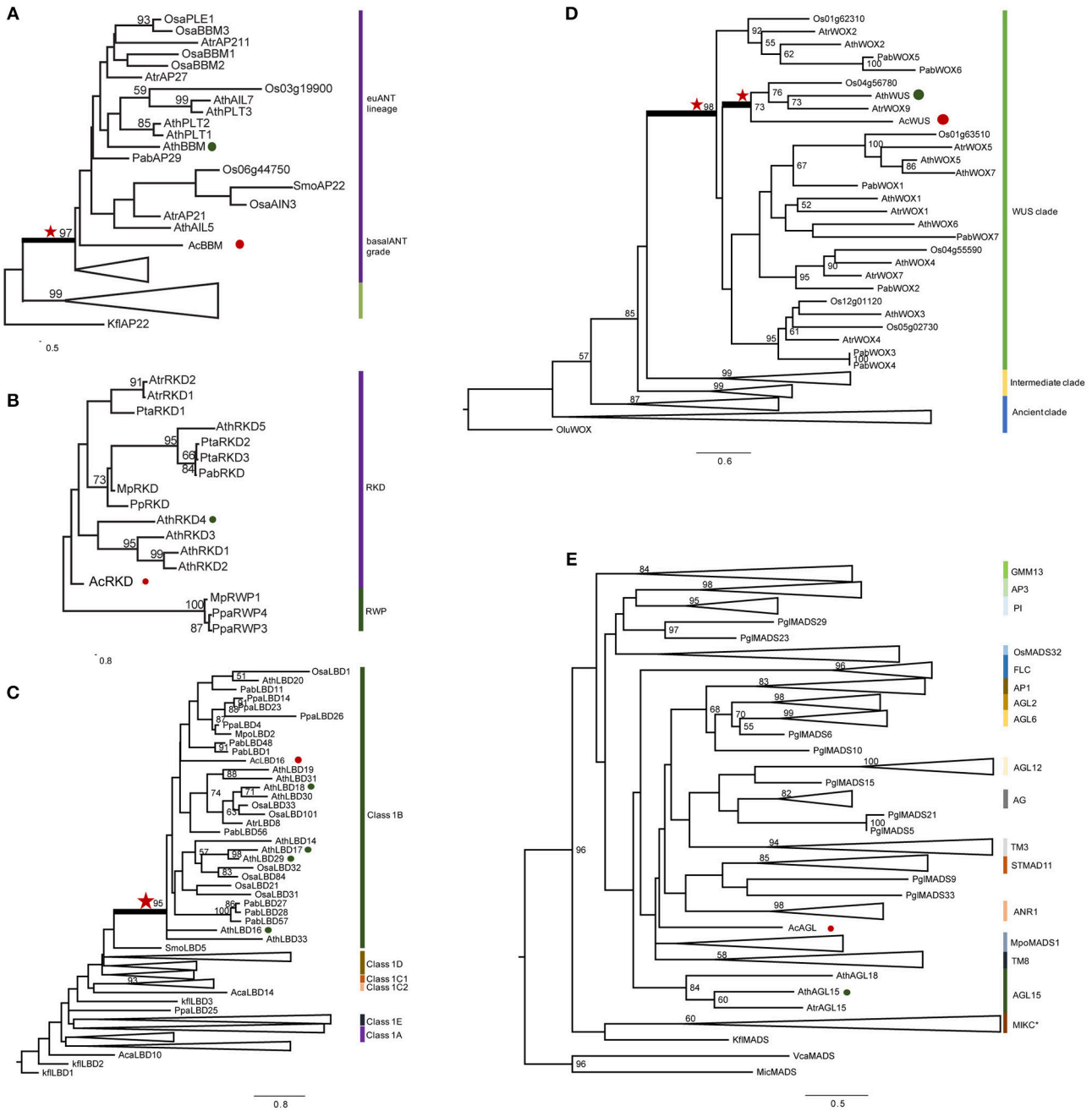

FIGURE 4 | Phylogenetic analysis of *AcWUS, AcBBM, AcLBD16, AcAGL, and AcRKD*. Maximum-likelihood tree of five gene family proteins constructed using sequences of *A. capillus-veneris* in this study and other sequences of representative plant species. See **Table S4** for sequences and accession numbers. Numbers at the branches indicate bootstrap values calculated from 1,000 replicates. Only values higher than 50 are shown. In each tree, the different clades are indicated by colored boxes and named. Red stars refer homologous genes with high confidence. Red circles refer the genes from *A. capillus-veneris*. Green circles refer the genes from *A. thaliana*. **(A)** AcBBM, **(B)** AcRKD, **(C)** AcLBD16, **(D)** AcWUS, and **(E)** AcAGL.

globular bodies (GGBs), and indirect SE *via* calli were obtained with the maximal rate on the MS media. Shoot regeneration *via* direct SE is usually initiated by plant growth regulators (PGRs) although their usage is rare (Fernández et al., 1997; Bertrand et al., 1999). *In vitro* adventitious shoot initiation was found on the medium with very low PGR concentration or without any PGRs (Beck and Caponetti, 1983; **Table S1**). GGBs became dominant with the increase of BA concentration. Amaki and Higuchi (1991) reported that the optimal medium for GGB proliferation of *Adiantum* was ½ MS with 1.0 mg/L BA, whereas our data showed that MS or ½ MS medium with a higher concentration of BA (2.0 mg/L) obtained the best proliferation.

Indirect SE, especially callus induction, has rarely been successful in ferns. In the present study, we found that the medium containing 0.5 mg/L 2,4-D and 0.5–1.0 mg/L BA is the most efficient one for the callus induction of *A. capillus-veneris* (**Table S1**). This result is in agreement with Byrne and Caponetti (1992), who reported that 2,4-D and sucrose were necessary to produce calli in the Boston fern, *Nephrolepis exaltata*. Calli are very sensitive to *in vitro* culture conditions and easily turn brown (Ahloowalia, 1982; Northmore et al., 2012). It has been reported to be difficult for generating intact sporophytes from a callus in ferns (Kwa et al., 1997; Byrne and Caponetti, 1992). This is in line with our results on the frequency of shoot organogenesis of *A. capillus-veneris* (**Table 1**). The morphogenetic pathway could be important for improving the regeneration rate (Fernández and Revilla, 2003). The meristemoid tissue found in the indirect SE of *A. capillus-veneris* is critical for organogenesis of a callus *in vitro*, which has not previously been described in ferns (Attfield and Evans, 1991; Bobák et al., 1993; Ovečka et al., 2000).

Phylogenetic Relationships of Embryogenesis-Associated Genes in Land Plants

Although only six embryogenesis-associated genes were studied in the present study, phylogenetic analyses of *AcBBM, AcWUS, AcAGL, AcLBD16,* and *AcRKD* of *A. capillus-veneris* showed that all those gene homologs can be found in other land plants, hardly in algae. The homologous genes were generally clustered as a clade in their respective phylogenetic trees (**Figure 4**), suggesting that the embryogenesis-associated genes could originate and evolve with colonization of plants to terrestrial environments. However, the mechanisms behind these evolutionary events remain unresolved. WUSCHEL-related homeobox (WOX) members contain a conserved homeodomain essential for plant development by regulating cell division and differentiation (Zuo et al., 2002; Li et al., 2013). So far, there has been no data concerning evolution and function of fern WUS homologs. Our phylogenetic analysis revealed that AcWUS is a putative ortholog of Arabidopsis WUS with high bootstrap value. In addition, the WUS clade was the latest derived lineage in the phylogenetic tree of WOX family genes (**Figure 4D**), which is consistent with previous findings in Arabidopsis as well as other plants (Lian et al., 2014). The RKD family of plant RWP-RK factors is expressed in reproductive cells of land plants, and has a single origin (Koi et al., 2016). In the gene trees (**Figures 4B,C**), AcRKD resided in the RKD clade corresponding to the RKD subfamily designated by Chardin et al. (2014); AcLBD is located in the Class IB LBD gene lineage, which was reported to be involved in root development (Coudert et al., 2012; Chanderbali et al., 2015). The BBM genes were described in *A. capillus-veneris* for first time. Our analysis showed that AcBBM shares high similarity with BBMs in other land plants, and is imbedded in the clade euANT (**Figure 4A**). All of these suggested that the embryogenesis-associated genes were highly conserved, and they originated early, at least earlier than occurrence of ferns.

Expression of Six Embryogenesis-Associated Genes during Shoot Regeneration

Embryogenesis-associated genes have been extensively characterized in carrot and Arabidopsis by using SE (Ikeuchi et al., 2013; Radoeva and Weijers, 2014), but less have been evaluated in ferns. In this study, the putative orthologs of Arabidopsis *BBM*, *LEC1*, *WUS*, *AGL15*, *LBD16,* and *RKD4* were identified and cloned from *A. capillus-veneris*. The developmental stage-specific expression patterns of all these six genes during GGBs and calli-derived SE are shown in **Figure 5**. We found the expression pattern of each gene is in agreement with that of its counterparts in angiosperms. For instance, expression of *AcLBD16* in callus development is consistent with the expression patterns of Arabidopsis *LBD16–18* and *LBD29*, and poplar *PtaLBD1*, which are sufficient to promote callus formation under auxin conditions (Yordanov et al., 2010; Fan et al., 2012). Our analyses showed that *AcBBM* was expressed during PGR-induced embryogenesis or callus formation (**Figure 5**), similar to the reports on orthologs of Arabidopsis, *Brassica napus* and *Glycine max* (Boutilier et al., 2002; El Ouakfaoui et al., 2010). It is well documented in many species that *WUS* and *WOX* genes regulate the shoot meristem cells, and their overexpression can induce callus formation (Mayer et al., 1998; Loyola-Vargas and Ochoa-Alejo, 2016). During the SE of *A. capillus-veneris*, *AcWUS* was detected with high expression levels in GGB and callus developments. This finding, together with the observation of somatic embryos in Arabidopsis as well as *WUS* expression in several callus lines suggests that the *WUS* genes may be involved in the regulation of both meristematic and embryogenic cells (Zuo et al., 2002; Iwase et al., 2011; Fehér, 2015). *AcRKD* was highly expressed in GGB induction and callus development (**Figure 5**), a phenomenon consistent with the result of ectopic overexpression of *RKD1* and *RKD2* that induced callus development without PGRs, and the expression of *RKD4* in early embryos (Waki et al., 2011).

Key Regulatory Genes Involved in Embryogenesis in Land Plants

SE, in response to exogenous and/or endogenous signals, has been studied and applied in plants for more than 50 years (Radoeva and Weijers, 2014; Fehér, 2015; Loyola-Vargas and Ochoa-Alejo, 2016), but the molecular mechanisms initiating and controlling this process remain unclear. As the ultimate product of the SE is similar, it can be expected that the basic regulatory mechanism involved in this process is very conserved during plant evolution. Numerous molecular studies have identified many regulatory genes and gain the entry into the regulatory networks underling the SE processes of various plant species. Based on previous and present studies (Radoeva and Weijers, 2014; Fehér, 2015; Ikeuchi et al., 2015; Guan et al., 2016; Loyola-Vargas and Ochoa-Alejo, 2016), we summarized a basic graphic illustration of the regulatory networks controlling SE (**Figure 5**). Although promising progress in characterizing the molecular mechanisms of SE has been made in seed plants, but little is known about the regulatory genes and mechanisms of

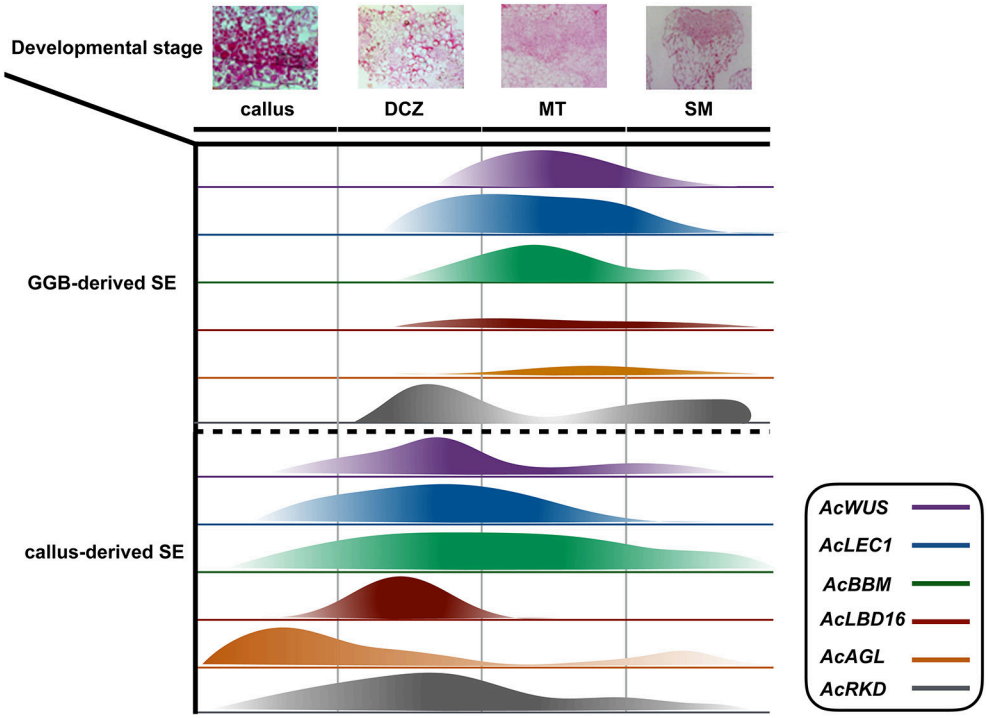

FIGURE 5 | Schematic diagram of the expression of *AcWUS, AcLEC1, AcBBM, AcLBD16, AcAGL,* and *AcRKD* during somatic embryogenesis in *Adiantum capillu-veneris*. Four important developmental stages callus, dividing cells zone (dcz), meristematic tissue (MT), shoot meritem (SM) were chosen and the width of the bars represents the results of those genes' expression.

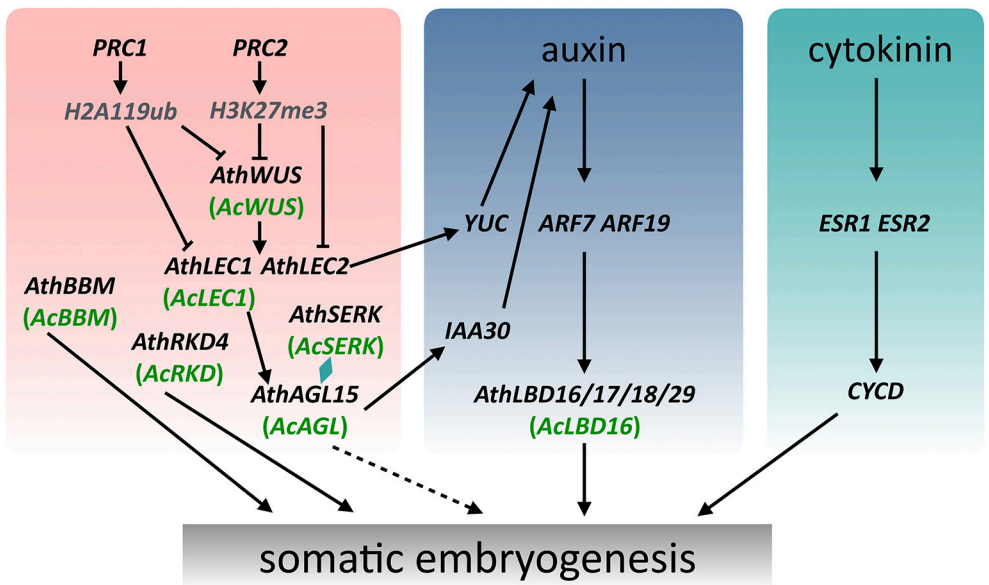

FIGURE 6 | A schematic model showing the regulation of somatic embryogenesis in Arabidopsis and *Adiantum capillus-veneris*. The WUS expression subsequently induces expression of LEC1 and LEC2, which together with AGL15 and SERK modulate the endogenous levels of auxin to promote somatic embryogenesis. Arrows with a solid line indicate direct transcriptional regulation by molecular evidence. Arrows with a dotted line indicate transcriptional regulation that mechanisms are not clear.

this process in ferns. Compared with some model plants such as Arabidopsis and carrot, it is more difficult to understand the molecular mechanism of the fern SE due to a lack of effective defective mutants, genome sequence data, and different phylogenetic positions in the evolution of land plants. Even so, the identification and expression analysis of key SE-associated

genes in *A. capillus-veneris* can provide a global view of transcriptional events important for GGB-/callus-derived SE in this species, and will help us to understand the regulatory networks of SE, even of ZE in ferns. These data, coupled with the phylogenetic analyses of six regulatory genes, offer new information for a better understanding of the fern SE and the evolution of key regulatory genes associated with embryogenesis in land plants (**Figure 6**).

Evolution of Reproductive Organs: Embryos to Seeds

Reproduction in land plants can be viewed as a complex, partly hierarchical, series of developmental processes, which together with their underlying genetic regulators produce morphological innovations, such as embryos, seeds and flowers. Adaptation of land plants to terrestrial environments occurs as the variation in genetic and developmental processes is winnowed by selection (Crane and Kenrick, 1997; Pires and Dolan, 2012). Embryo formation is the first innovation acquired by land plants during evolution, and followed by the development of seeds (Becker and Marin, 2009; Radoeva and Weijers, 2014). These two developmental processes are closely connected, and the former is a prerequisite for the latter. Although the two processes could be controlled by different developmental pathways, they probably share many regulatory genes. For example, in Arabidopsis, *LEC1* is not only involved in the embryogenesis, but also regulates seed maturation (Goldberg et al., 1994; Harada, 1997; Radoeva and Weijers, 2014); the up-regulated expression of *AcLEC1*, a *LEC1* homolog in *A. capillus-veneris*, can facilitate the formation of seed-like traits, such as the accumulation of nutrient reserves and delayed development of embryos in this fern species under some laboratory conditions (Fang et al., unpublished data), which are completely similar to the seed traits produced in Arabidopsis. All the those suggests that the embryogenesis-associated genes could be co-optioned to a new developmental program, which produces morphological innovations, like formation of seed-like traits in *A. capillus-veneris*. Thus, seed formation may have resulted from a newly built regulatory network, which is established by cooption and modification of existing genes or networks.

AUTHOR CONTRIBUTIONS

GR, XL, and SB designed the experiments. XL and JH performed the experiments. XL, JH, and YF analyzed the data. XL and GR wrote the manuscript. All authors read and approved the final manuscript.

ACKNOWLEDGMENTS

This work was supported by the National Natural Science Foundation of China (NSFC, Grant no. 91231105).

SUPPLEMENTARY MATERIAL

The Supplementary Material for this article can be found online at: http://journal.frontiersin.org/article/10.3389/fpls.2017.00658/full#supplementary-material

Table S1 | Effect of different media on induction rates of shoots, GGBs, and calli.

Table S2 | Primers used for the sequences verified.

Table S3 | Primers used for the qRT-PCR reaction.

Table S4 | MADS-box family sequences and accession numbers.

REFERENCES

Abascal, F., Zardoya, R., and Posada, D. (2005). ProtTest: selection of best-fit models of protein evolution. *Bioinformatics* 21, 2104–2105. doi: 10.1093/bioinformatics/bti263

Ahloowalia, B. (1982). Plant regeneration from callus culture in wheat. *Crop Sci.* 22, 405–410. doi: 10.2135/cropsci1982.0011183X002200020047x

Amaki, W., and Higuchi, H. (1991). A possible propagation system of nephrolepis, *Asplenium, Pteris, Adiantum* and *Rumohra* (*Arachniodes*) through tissue culture. *Sci. Hortic.* 300, 237–244. doi: 10.17660/ActaHortic.1992.300.33

Attfield, E., and Evans, P. (1991). Stages in the initiation of root and shoot organogenesis in cultured leaf explants of *Nicotiana tabacum* cv. *Xanthi nc. J. Exp. Bot.* 42, 59–63. doi: 10.1093/jxb/42.1.59

Beck, M. J., and Caponetti, J. D. (1983). The effects of kinetin and naphthaleneacetic acid on *in vitro* shoot multiplication and rooting in the fishtail fern. *Am. J. Bot.* 70, 1–7.

Becker, B., and Marin, B. (2009). Streptophyte algae and the origin of embryophytes. *Ann. Bot.* 103, 999–1004. doi: 10.1093/aob/mcp044

Bertrand, A., Albuerne, M., Fernández, H., González, A., and Sánchez-Tamés, R. (1999). *In vitro* organogenesis of *Polypodium cambricum*. *Plant Cell Tissue Organ Cult.* 57, 65–69. doi: 10.1023/A:1006348628114

Bobák, M., Blehová, A., Šamaj, J., Ovečka, M., and Krištín, J. (1993). Studies of organogenesis from the callus culture of the sundew (*Drosera spathulata Labill.*). *J. Plant Physiol.* 142, 251–253. doi: 10.1016/S0176-1617(11)80974-0

Boutilier, K., Offringa, R., Sharma, V. K., Kieft, H., Ouellet, T., Zhang, L., et al. (2002). Ectopic expression of BABY BOOM triggers a conversion from vegetative to embryonic growth. *Plant Cell* 14, 1737–1749. doi: 10.1105/tpc.001941

Byrne, T. E., and Caponetti, J. D. (1992). Morphogenesis in three cultivars of Boston fern. II. Callus production from stolon tips and plantlet differentiation from callus. *Am. Fern. J.* 82, 1–11. doi: 10.2307/1547755

Chanderbali, A. S., He, F., Soltis, P. S., and Soltis, D. E. (2015). Out of the water: origin and diversification of the LBD gene family. *Mol. Biol. Evol.* 32, 1996–2000. doi: 10.1093/molbev/msv080

Chardin, C., Girin, T., Roudier, F., Meyer, C., and Krapp, A. (2014). The plant RWP-RK transcription factors: key regulators of nitrogen responses and of gametophyte development. *J. Exp. Bot.* 65, 5577–5587. doi: 10.1093/jxb/eru261

Chugh, A., and Khurana, P. (2002). Gene expression during somatic embryogenesis-recent advances. *Curr. Sci.* 83, 715–730.

Coudert, Y., Dievart, A., Droc, G., and Gantet, P. (2012). ASL/LBD phylogeny suggests that genetic mechanisms of root initiation downstream of auxin are distinct in lycophytes and euphyllophytes. *Mol. Biol. Evol.* 30, 569–572. doi: 10.1093/molbev/mss250

Crane, P., and Kenrick, P. (1997). Diverted development of reproductive organs: a source of morphological innovation in land plants. *Plant Syst. Evol.* 206, 161–174. doi: 10.1007/BF00987946

El Ouakfaoui, S., Schnell, J., Abdeen, A., Colville, A., Labbé, H., Han, S., et al. (2010). Control of somatic embryogenesis and embryo development by AP2 transcription factors. *Plant Mol. Biol.* 74, 313–326. doi: 10.1007/s11103-010-9674-8

Fan, M., Xu, C., Xu, K., and Hu, Y. (2012). LATERAL ORGAN BOUNDARIES DOMAIN transcription factors direct callus formation in Arabidopsis regeneration. *Cell Res.* 22, 1169–1180. doi: 10.1038/cr.2012.63

Fehér, A. (2015). Somatic embryogenesis—stress-induced remodeling of plant cell fate. *Biochim. Biophys. Acta Gene Regul. Mech.* 1849, 385–402. doi: 10.1016/j.bbagrm.2014.07.005

Fernández, H., Bertrand, A., and Sánchez-Tamés, R. (1997). Plantlet regeneration in *Asplenium nidus* L. and *Pteris ensiformis* L. by homogenization of BA treated rhizomes. *Sci. Hortic.* 68, 243–247.

Fernández, H., and Revilla, M. (2003). *In vitro* culture of ornamental ferns. *Plant Cell Tissue Organ Cult.* 73, 1–13. doi: 10.1023/A:1022650701341

Goldberg, R. B., De Paiva, G., and Yadegari, R. (1994). Plant embryogenesis: zygote to seed. *Science* 266, 605–614. doi: 10.1126/science.266.5185.605

Guan, Y., Li, S. G., Fan, X. F., and Su, Z. H. (2016). Application of somatic embryogenesis in woody plants. *Front. Plant Sci.* 7:938. doi: 10.3389/fpls.2016.00938

Harada, J. J. (1997). "Seed maturation and control of dormancy," in *Cellular and Molecular Biology of Plant Seed Development*, ed. B. A. Larkins and I. K. Vasil (Gainesville, FL: University of Florida Press), 545–592.

Harding, H. P., Zhang, Y., Zeng, H., Novoa, I., Lu, P. D., Calfon, M., et al. (2003). An integrated stress response regulates amino acid metabolism and resistance to oxidative stress. *Mol. Cell* 11, 619–633. doi: 10.1016/S1097-2765(03)00105-9

Ikeuchi, M., Iwase, A., Rymen, B., Harashima, H., Shibata, M., Ohnuma, M., et al. (2015). PRC2 represses dedifferentiation of mature somatic cells in Arabidopsis. *Nat. Plants* 1, 1–7. doi: 10.1038/nplants.2015.89

Ikeuchi, M., Sugimoto, K., and Iwase, A. (2013). Plant callus: mechanisms of induction and repression. *Plant Cell* 25, 3159–3173. doi: 10.1105/tpc.113.116053

Iwase, A., Mitsuda, N., Koyama, T., Hiratsu, K., Kojima, M., Arai, T., et al. (2011). The AP2/ERF transcription factor WIND1 controls cell dedifferentiation in Arabidopsis. *Curr. Biol.* 21, 508–514. doi: 10.1016/j.cub.2011.02.020

Jenik, P. D., and Barton, M. K. (2005). Surge and destroy: the role of auxin in plant embryogenesis. *Development* 132, 3577–3585. doi: 10.1242/dev.01952

Johnson, G. P., and Renzaglia, K. S. (2009). Evaluating the diversity of pteridophyte embryology in the light of recent phylogenetic analyses leads to new inferences on character evolution. *Plant System. Evol.* 283, 149–164. doi: 10.1007/s00606-009-0222-4

Katoh, K., and Standley, D. M. (2013). MAFFT multiple sequence alignment software version 7: improvements in performance and usability. *Mol. Biol. Evol.* 30, 772–780. doi: 10.1093/molbev/mst010

Kenrick, P., and Crane, P. (1997). The origin and early evolution of plants on land. *Nature* 389, 33–39. doi: 10. 1038/37918

Koi, S., Hisanaga, T., Sato, K., Shimamura, M., Yamato, K. T., Ishizaki, K., et al. (2016). An evolutionarily conserved plant RKD factor controls germ cell differentiation. *Curr. Biol.* 26, 1775–1781. doi: 10.1016/j.cub.2016.05.013

Koszegi, D., Johnston, A. J., Rutten, T., Czihal, A., Altschmied, L., Kumlehn, J., et al. (2011). Members of the RKD transcription factor family induce an egg cell–like gene expression program. *Plant J.* 67, 280–291. doi: 10.1111/j.1365-313X.2011.04592.x

Kwa, S. H., Wee, Y. C., Lim, T. M., and Kumar, P. P. (1997). Morphogenetic plasticity of callus reinitiated from cell suspension cultures of the fern *Platycerium coronarium*. *Plant Cell Tissue Organ Cult.* 48, 37–44. doi: 10.1023/A:1005756822370

Leyser, O. (2005). Auxin distribution and plant pattern formation: how many angels can dance on the point of PIN? *Cell* 121, 819–822. doi: 10.1016/j.cell.2005.06.005

Li, X., Fang, Y. H., Yang, J., Bai, S. N., and Rao, G. Y. (2013). Overview of the morphology, anatomy and ontogeny of *Adiantum capillus-veneris*: an experimental system to study the development of ferns. *J. Syst. Evol.* 51, 499–510. doi: 10.1111/jse.12034

Lian, G., Ding, Z., Wang, Q., Zhang, D., and Xu, J. (2014). Origins and evolution of WUSCHEL-related homeobox protein family in plant kingdom. *Sci. World J.* 2014:534140. doi: 10.1155/2014/534140

Liao, Y. K., and Wu, Y. H. (2011). *In vitro* propagation of *Platycerium bifurcatum* (Cav.) C. Chr. via green globular body initiation. *Bot. Stud.* 52, 455–463.

Livak, K. J., and Schmittgen, T. D. (2001). Analysis of relative gene expression data using real-time quantitative PCR and the $2^{-\Delta\Delta C_T}$ method. *Methods* 25, 402–408. doi: 10.1006/meth.2001.1262

Loyola-Vargas, V. M., and Ochoa-Alejo, N. (eds.). (2016). "Somatic Embryogenesis. An Overview," in *Somatic Embryogenesis: Fundamental Aspects and Applications* (Springer Press), 1–8.

Mallón, R., Rodríguez-Oubiña, J., and González, M. L. (2011). Shoot regeneration from *in vitro*-derived leaf and root explants of *Centaurea ultreiae*. *Plant Cell Tissue Organ Cult.* 106, 523–530. doi: 10.1007/s11240-011-9934-6

Mayer, K. F., Schoof, H., Haecker, A., Lenhard, M., Jürgens, G., and Laux, T. (1998). Role of WUSCHEL in regulating stem cell fate in the Arabidopsis shoot meristem. *Cell* 95, 805–815. doi: 10.1016/S0092-8674(00)81703-1

Mikuła, A., Pożoga, M., Grzyb, M., and Rybczyński, J. J. (2015). An unique system of somatic embryogenesis in the tree fern *Cyathea delgadii* Sternb.: the importance of explant type, and physical and chemical factors. *Plant Cell Tissue Organ Cult.* 123, 467–478. doi: 10.1007/s11240-015-0850-z

Northmore, J. A., Zhou, V., and Chuong, S. D. (2012). Multiple shoot induction and plant regeneration of the single-cell C4 species *Bienertia sinuspersici*. *Plant Cell Tissue Organ Cult.* 108, 101–109. doi: 10.1007/s11240-011-0018-4

Ovečka, M., Bobák, M., and Šamaj, J. (2000). A comparative structural analysis of direct and indirect shoot regeneration of *Papaver somniferum* L. *in vitro*. *J. Plant Physiol.* 157, 281–289. doi: 10.1016/S0176-1617(00)80049-8

Pires, N. D., and Dolan, L. (2012). Morphological evolution in land plants: new designs with old genes. *Philos. Trans. R. Soc. B.* 367, 508–518. doi: 10.1098/rstb.2011.0252

Pryer, K. M., Schneider, H., Smith, A. R., Cranfill, R., Wolf, P. G., Hunt, J. S., et al. (2001). Horsetails and ferns are a monophyletic group and the closest living relatives to seed plants. *Nature* 409, 618–622. doi: 10.1038/35054555

Radoeva, T., and Weijers, D. (2014). A roadmap to embryo identity in plants. *Trends Plant Sci.* 19, 709–716. doi: 10.1016/j.tplants.2014.06.009

Salome, M., Pais, S., and Casal, M. (1985). Propagation of the fern *Adiantum capillus-veneris* through tissue culture of the circinate part of young leaves. *Acta Hortic.* 212, 651–654. doi: 10.17660/ActaHortic.1987.212.109

Somer, M., Arbesú, R., Menéndez, V., Revilla, M., and Fernández, H. (2010). Sporophyte induction studies in ferns *in vitro*. *Euphytica* 171, 203–210. doi: 10.1007/s10681-009-0018-1

Stamatakis, A., Hoover, P., and Rougemont, J. (2008). A rapid bootstrap algorithm for the RAxML web servers. *Systematic Boil.* 57, 758–771. doi: 10.1080/10635150802429642

Stasolla, C., Belmonte, M. F., van Zyl, L., Craig, D. L., Liu, W., Yeung, E. C., et al. (2004). The effect of reduced glutathione on morphology and gene expression of white spruce (*Picea glauca*) somatic embryos. *J. Experim. Bot.* 55, 695–709. doi: 10.1093/jxb/erh074

Tzafrir, I., Pena-Muralla, R., Dickerman, A., Berg, M., Rogers, R., Hutchens, S., et al. (2004). Identification of genes required for embryo development in Arabidopsis. *Plant Physiol.* 135, 1206–1220. doi: 10.1104/pp.104.045179

Vasco, A., Moran, R. C., and Ambrose, B. A. (2013). The evolution, morphology, and development of fern leaves. *Front. Plant Sci.* 4:345. doi: 10.3389/fpls.2013.00345

Wada, M. (2007). The fern as a model system to study photomorphogenesis. *J. Plant Res.* 120, 3–16. doi: 10.1007/s10265-006-0064-x

Waki, T., Hiki, T., Watanabe, R., Hashimoto, T., and Nakajima, K. (2011). The Arabidopsis RWP-RK protein RKD4 triggers gene expression and pattern formation in early embryogenesis. *Curr. Biol.* 21, 1277–1281. doi: 10.1016/j.cub.2011.07.001

Xie, Z., Li, X., Glover, B. J., Bai, S., Rao, G. Y., Luo, J., et al. (2008). Duplication and functional diversification of HAP3 genes leading to the origin of the seed-developmental regulatory gene, *LEAFY COTYLEDON1* (*LEC1*), in nonseed plant genomes. *Mol. Biol. Evol.* 25, 1581–1592. doi: 10.1093/molbev/msn105

Yordanov, Y. S., Regan, S., and Busov, V. (2010). Members of the LATERAL ORGAN BOUNDARIES DOMAIN transcription factor family are involved in the regulation of secondary growth in Populus. *Plant Cell* 22, 3662–3677. doi: 10.1105/tpc.110.078634

Zuo, J., Niu, Q. W., Frugis, G., and Chua, N. H. (2002). The WUSCHEL gene promotes vegetative-to-embryonic transition in Arabidopsis. *Plant J.* 30, 349–359. doi: 10.1046/j.1365-313X.2002.01289.x

Conflict of Interest Statement: The authors declare that the research was conducted in the absence of any commercial or financial relationships that could be construed as a potential conflict of interest.

frontiers in Plant Science

ORIGINAL RESEARCH
published: 17 February 2017
doi: 10.3389/fpls.2017.00153

Function Identification of the Nucleotides in Key *cis*-Element of *DYSFUNCTIONAL TAPETUM1* (*DYT1*) Promoter

*Shumin Zhou †, Hongli Zhang †, Ruisha Li, Qiang Hong, Yang Li, Qunfang Xia and Wei Zhang **

Lab of Plant Development Biology, School of Life Sciences, Shanghai University, Shanghai, China

OPEN ACCESS

Edited by:
Zhong-Jian Liu,
The National Orchid Conservation Center of China, The Orchid Conservation and Research Center of Shenzhen, China

Reviewed by:
Tatiana Arias,
The Corporation for Biological Research, Colombia
Miguel Angel Flores-Vergara,
North Carolina State University, USA
Yan Liang,
Institute of Genetics and Developmental Biology (CAS), China
Jiaqiang Dong,
Rutgers University, USA

***Correspondence:**
Wei Zhang
zhw62207@shu.edu.cn

† These authors have contributed equally to this work.

Specialty section:
This article was submitted to Plant Evolution and Development, a section of the journal Frontiers in Plant Science

Received: *07 November 2016*
Accepted: *25 January 2017*
Published: *17 February 2017*

Citation:
Zhou S, Zhang H, Li R, Hong Q, Li Y, Xia Q and Zhang W (2017) Function Identification of the Nucleotides in Key cis-Element of DYSFUNCTIONAL TAPETUM1 (DYT1) Promoter. Front. Plant Sci. 8:153. doi: 10.3389/fpls.2017.00153

As a core regulatory gene of the anther development, *DYSFUNCTIONAL TAPETUM1* (*DYT1*) was expressed in tapetum preferentially. Previous study had confirmed that a "CTCC" sequence within *DYT1* promoter was indispensable for correct *DYT1* expression. However, precise analysis on the function of each nucleotide of this sequence still lacks. Here we employed site mutation assay to identify the function roles of the nucleotides. As a result, the "T" and final "C" of "CTCC" were found essential for the temporal and spatial specificity of *DYT1* expression, whereas the other two "C" nucleotides exhibited substitutable somewhat. The substitutes of two flanking nucleotides of "CTCC," however, hardly affected the normal promoter function, suggesting that the "CTCC" sequence as a whole did meet the standard of a canonical *cis*-element by definition. In addition, it was found that as short as 497 bp *DYT1* promoter was sufficient for tissue-specific expression, while longer 505 bp *DYT1* promoter sequence was sufficient for species-specific expression.

Keywords: *Arabidopsis, DYT1, cis*-element, tissue specificity, tapetum

Key message: Through site mutation assay it was found that the "T" and final "C" nucleotides of key *cis*-element "CTCC" of *Arabidopsis* tapetum gene *DYT1* promoter were irreplaceable for tissue specific gene expression.

INTRODUCTION

Anther development is crucial for successful pollen production in flowering plants. The *Arabidopsis* anther during meiosis is a four-lobed structure comprised of concentric outer epidermis, endothecium, middle fibrous layer, tapetum and pollen mother cell (PMC; Goldberg et al., 1993; Yeung et al., 2011). The tapetum initially turns out as a single-cell layer surrounding PMC, and is the main nutrient tissue of PMC and pollen subsequently in the anther (Koltunow et al., 1990; Scott et al., 2004; Feng and Dickinson, 2007; Zhang et al., 2014; Li et al., 2015). A serial of regulatory genes have been identified to be essential for the tapetum function in *Arabidopsis* up to date, including *DYSFUNCTIONAL TAPETUM1* (*DYT1*), *DEFECTIVE IN TAPETAL DEVELOPMENT AND FUNCTION1* (*TDF1*), *MYB103/MYB80*, *ABORTED MICROSPORE* (*AMS*), *MALE STERILITY1* (*MS1*), etc. (Zhang et al., 2006, 2007; Yang et al., 2007; Zhu et al., 2008; Phan et al., 2011; Wang et al., 2012; Fernández-Gómez and Wilson, 2014; Xu et al., 2014, 2015; Shumin et al., 2015; Yi et al., 2016). Among them, *DYT1* as one of the earliest tapetum-preferential genes, initiates all aspects of tapetum function through regulating transcription of approximately 1,000 anther genes involved in callose synthesis and degradation, peptide and lipid transport,

exine formation, etc. (Schiefthaler et al., 1999; Higginson et al., 2003; Sorensen et al., 2003; Ito et al., 2007; Liu et al., 2009; Feng et al., 2012; Phan et al., 2012; Li et al., 2013; Cui et al., 2016).

The expression profile of *DYT1* is highly tissue-specific. Weak expression of *DYT1* can be detected in the secondary parietal cell and sporogenous cell, the precursors of tapetum and PMC respectively at as early as anther stage 4 (Zhang et al., 2006; Shumin et al., 2015). Then *DYT1* expression significantly enhances and culminates with maturation of tapetum at the anther stages 6, and exhibits as a tapetum-preferential pattern (Zhang et al., 2006; Shumin et al., 2015). With the end of meiosis of PMC, *DYT1* expression declines rapidly, and disappears at stage 8 (Zhang et al., 2006; Gu et al., 2014; Shumin et al., 2015). The underlying mechanism(s) controlling *DYT1* temporal and spatial expression pattern remains as a puzzle since *DYT1* was firstly characterized one decade ago (Zhang et al., 2006). It has been known that at least two signal pathways are involved in initiation of *DYT1* expression. The first one seems to be governed by transcription regulatory factors, including nuclear proteins NZZ/SPL and LFR, and SBP-domain transcription factor SPL8 (Yang et al., 1999; Xing et al., 2010; Wang et al., 2012). The second pathway is mediated by protein phosphorylation triggered by a series of receptor-like kinases, such as EXS/EMS1, SERK1 and SERK2, BAM1 and BAM2 (Zhao et al., 2002, 2008; Albrecht et al., 2005; Colcombet et al., 2005; Hord et al., 2006; Li et al., 2017). Both signal pathways are essential for normal *DYT1* expression, though few details are known about how they crosstalk and activate *DYT1* expression together (Zhang et al., 2006; Shumin et al., 2015).

In our previous study, it had been confirmed that as short as 513 bp sequence in front of the transcription start site (TSS) of *DYT1* was essential and sufficient for proper temporal and spatial specificity of *DYT1* expression. In addition, the deletion of a "CTCC" sequence at the position of −468 bp (i.e., 468 bp from the TSS) abolished *DYT1* expression completely at the anther stage 6, suggesting that the "CTCC" sequence was indispensable for normal *DYT1* expression (Shumin et al., 2015). Including our previous study, there have been only a couple of related reports about "CTCC" as a putative *cis*-element crucial for gene expression regulation in plants (Kano-Murakami et al., 1991; Ku et al., 2011). However, whether the "CTCC" sequence is a canonical *cis*-element in which the nucleotides are irreplaceable, remains to be addressed. In this study, we employed site mutation assay to characterize the function roles of the nucleotides, including the two flanking ones of the "CTCC" sequence to answer the question whether the "CTCC" sequence met the standard of a canonical *cis*-element or not. In addition, more truncation analysis was performed through using both transgenic *Arabidopsis* and tobacco bright yellow 2 (BY2) cell suspensions to identify which regions of *DYT1* promoter were essential for tissue, and further species specificity of *DYT1* expression.

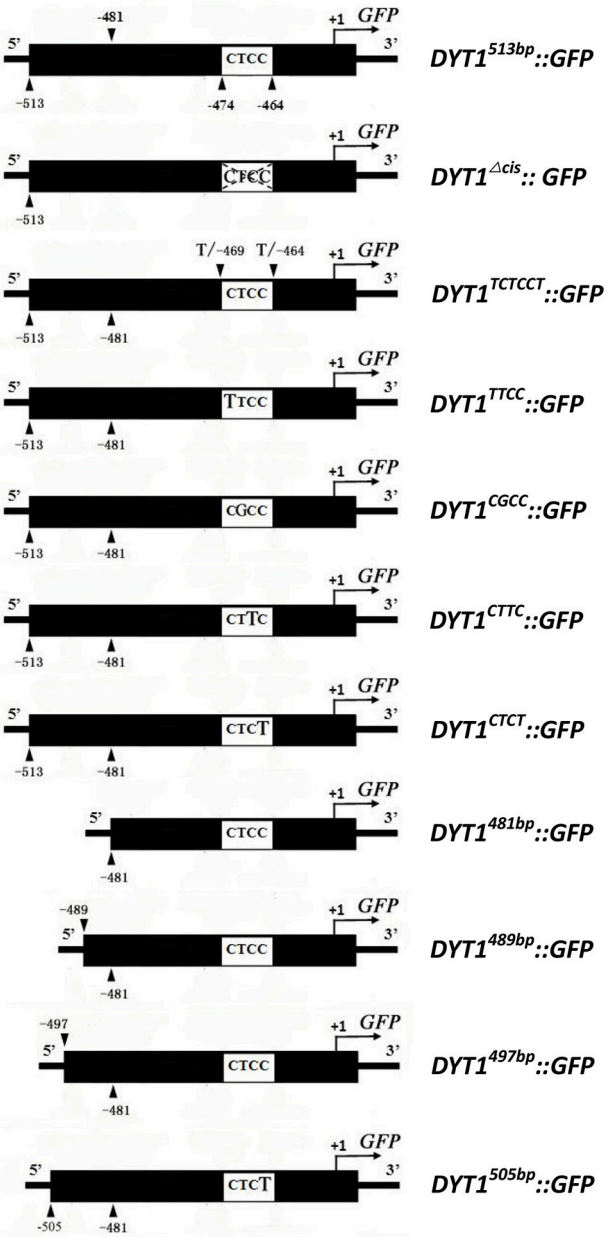

FIGURE 1 | Promoter constructs used to drive *GFP* expression in transgenic plant anthers and BY2 cells.

MATERIALS AND METHODS

Plant Materials and Growth Conditions

Arabidopsis thaliana ecotype Col-0 was used in all of the transformation and promoter analysis in this study. The plants were cultivated under 16 h light/8 h dark photoperiod with 300 $Es^{-1}m^{-2}$ illumination intensity, at 22 ± 1°C. The seeds were stratified at 4°C for 4 days prior to growth.

The tobacco (*Nicotiana tabacum* L. cv Bright Yellow 2, BY2) was cultivated in a modified liquid Murashige and Skoog (MS) medium (Zhou et al., 2014) at 28°C with 120 rpm shaking avoiding light and maintained by weekly dilution (V/V = 1/10) of cell.

Transformation Constructs

The pre-existing 513 bp *DYT1* promoter-driven GFP expression construct, designated as $DYT1^{513bp}$*::GFP* (Shumin et al., 2015), was used as PCR template in this study. The primers

TABLE 1 | PCR primers in this study.

Primer name	Sequence (5′–3′)
p*DYT1F*-513	CCCAAAGCTTCTAACGTTGGACCTGTGGACT
p*DYT1*F-505	CCCAAAGCTTGGACCTGTGGACTCAGTTTAC
p*DYT1*F-497	CCCAAAGCTTTTTACAGAGCCGTGGTCGAGCCTC
p*DYT1*F-489	CCCAAAGCTTGGACTCAGTTTACAGAGCCGTGG
p*DYT1F*-481	CCCAAAGCTTGCCGTGGTCGAGCCTCCGC
p*513F*$^{\Delta cis}$	CCCAAAGCTTTGGACCTGTGGACTCAGTTTACAGAGCCGTGGTCGAGCGCGAGGTG
p*513F*^{TCTCCT}	CTAACGTTGGACCTGTGGACTCAGTTTACAGAGCCGTGGTCGAGTCTCCTCGAGGTGTGGAG
p*513F*^{TTCC}	CTAACGTTGGACCTGTGGACTCAGTTTACAGAGCCGTGGTCGAGCTTCCGCGAGGTGTGGAG
p*513F*^{CGCC}	CTAACGTTGGACCTGTGGACTCAGTTTACAGAGCCGTGGTCGAGCCGCCGCGAGGTGTGGAG
p*513F*^{CTTC}	CTAACGTTGGACCTGTGGACTCAGTTTACAGAGCCGTGGTCGAGCCGCCGCGAGGTGTGGAG
p*513F*^{CTCT}	CTAACGTTGGACCTGTGGACTCAGTTTACAGAGCCGTGGTCGAGCCTCTGCGAGGTGTGGAG
p*DYT1R*-co	CGGAGCTCTTATTTCTTCTTCTTTGATAATT
p*GFP*-RT-F	ATGGTGAGCAAGGGCGAGGAG
p*GFP*-RT-R	TTACTTGTACAGCTCGTCC
p*513*^{d1}F	CCCAAAGCTTACAGAGCCGTGGTCGAGCGCGAG
p*513*^{c1}F	CCCAAAGCTTACAGAGCCGTGGTCGAGCCTCC
p*513*^{i1}F	TTACAGAGCCGTGGTCGAGTCTCCT
p*513*^{i2}F	CAGTTTACAGAGCCGTGGTCGAGCT
p*513*^{i3}F	AGTTTACAGAGCCGTGGTCGAGCCG
p*513*^{i4}F	GTTTACAGAGCCGTGGTCGAGCCTT
p*513*^{i5}F	TTTACAGAGCCGTGGTCGAGCCTCT
P*513R*-co	TTATTTCTTCTTCTTTGATAATT

to generate site mutations of the constructs*DYT1*^{TTCC}*::GFP*, *DYT1*^{CGCC}*::GFP*, *DYT1*^{CTTC}*::GFP* and *DYT1*^{CTCT}*::GFP*; CTCC flanking site mutation construct*DYT1*^{TCTCCT}*::GFP* were designed and synthesized respectively. Novel 5′ end primers of truncation constructs *DYT1*^{489bp}*::GFP*, *DYT1*^{497bp}*::GFP* and *DYT1*^{505bp}*::GFP* were designed and synthesized, respectively (**Figure 1**). The PCR products were obtained and cloned into pCAMBIA1300 to make reporting constructs according to the report of Zhou (Shumin et al., 2015).

Plant Transformation

Transgenic plants were generated via floral-dip transformation. The positive transgenic seedlings were screened on MS medium containing 25 mg/L hygromycin (Clough and Bent, 1998). At least 10 independent transgenic T1 generation lines for each construct were observed in this study.

BY2 Cell Suspension Transformation

The transformation of BY2 suspension was carried out according to the report of Zhou (Zhou et al., 2014). BY2 cell suspension was co-cultivated with the *Agrobacterium* GV3101 strain harboring transgenic construct in liquid medium without antibiotics avoiding light at 28°C for 48 h, so that the final concentration of cell suspension was approximately $OD_{600} = 0.6$. The resulted BY2 cell suspension was enriched by centrifuge and plated on MS solid medium containing 50 μg/ml hygromycin and 100 μg /ml vancomycin, and incubated at 28°C avoiding light. Two weeks later, grown-up antibiotics-resistant callus were subjected to amplified liquid cultivation, and the resulted BY2 cell suspension was used for genotyping and fluorescence observation. At least 10 independent original antibiotics-resistant callus were observed for each construct. The pre-existing transgenic callus of cauliflower mosaic leaf virus 35S promoter-driven GFP expression *35S::GFP* was used as a positive control (Zhou et al., 2014).

Semi-Quantification PCR

Total RNA was extracted from the transgenic BY2 cell suspension and performed reverse transcription according to Zhou et al. (2014). Then *GFP* cDNA fragment was PCR amplified with *GFP* specific (*GFP* RT-F&R) primers with the sequence listed in **Table 1**.

Observation of GFP Fluorescence

Anthers were stripped and collected from transgenic plants flower bud just around male meiosis (anther stage 4–9) on a microscopy slides. Added one drop of sterile water on the anthers and covered a slide carefully without squeezing. Then the sample was observed and photographed under Zeiss LSM-710 confocal microscope (Zeiss, Germany) and Leica DM2500 fluorescence microscope. As for semi-quantification of the fluorescence intensity, randomly 10 sites on fluorescence images were selected and the intensity was measured and normalized by the SMART software. Statistics of at least 15 anthers per line, 10 independent T1 generation transgenic lines were counted for each construct transformation. As for BY2 cell suspension, at least 100 cells per callus ancestor were observed, and 10 callus were counted for each construct transformation.

RESULTS

Two Nucleotides of "CTCC" *cis*-Element Were Essential for the Accurate Expression Pattern of *DYT1* Gene

Previous studies showed that the 513 bp length *DYT1* promoter could faithfully regenerate the temporal and spatial profile

of native *DYT1* expression (Shumin et al., 2015). The GFP signal of transgenic *DYT1*^{513bp}*::GFP* firstly appeared in the secondary parietal cell and microsporocyte of stage 4 *Arabidopsis* anther. Then the GFP expression increased significantly and reached its peak preferentially in the tapetum of stage 5 and 6 anthers. Subsequently, the GFP signal rapidly weakened at stage 7 and disappeared at stage 8 (**Figures 2A,G**). The "CTCC" *cis*-element locating at −468 bp from the TSS is particularly important for the correct expression of the *DYT1* gene. The deletion of "CTCC" completely knocked out GFP expression (Shumin et al., 2015). To investigate the function of each nucleotide in the "CTCC" *cis*-element, a series of modifying constructs based on *DYT1*^{513bp}*::GFP* with site mutations in or around the "CTCC" sequence were made, and transformed into *Arabidopsis*, respectively (**Figure 1**). The transgenic plants were identified by PCR using nucleotide specific primers (**Table 1**) and restriction endonuclease digestion assay (Supplementary Figure 1). The site mutations of the two flanking nucleotides

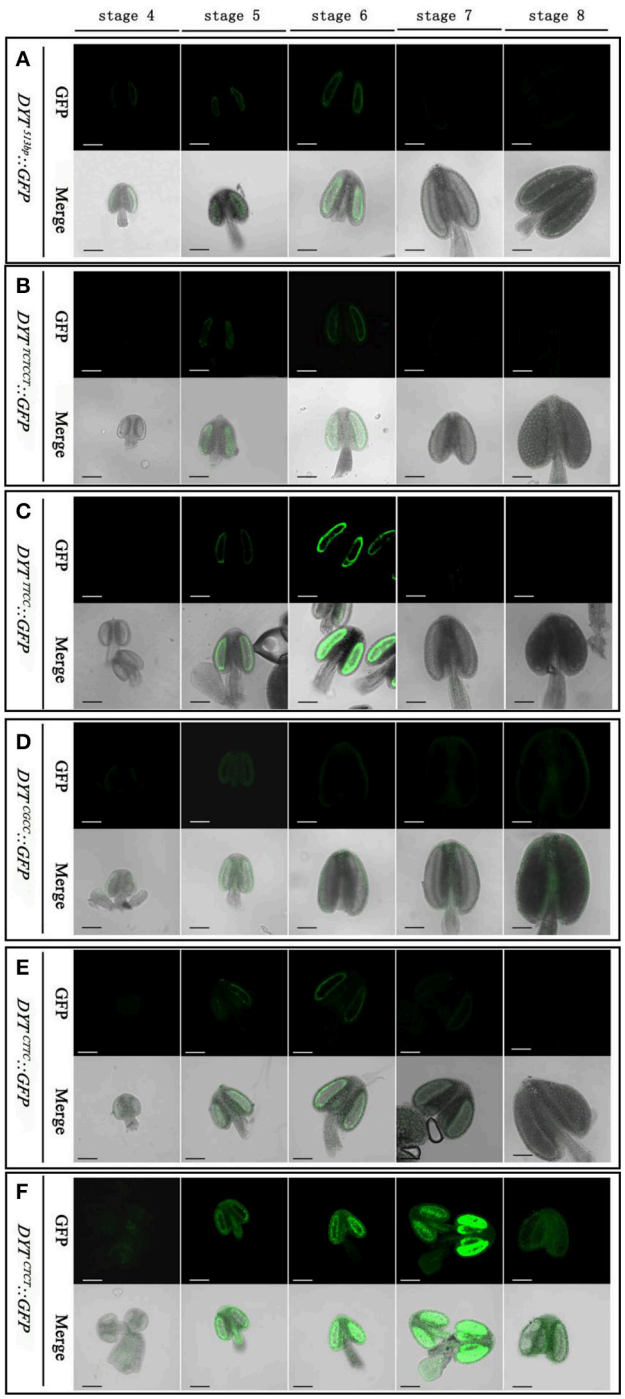

FIGURE 2 | Continued

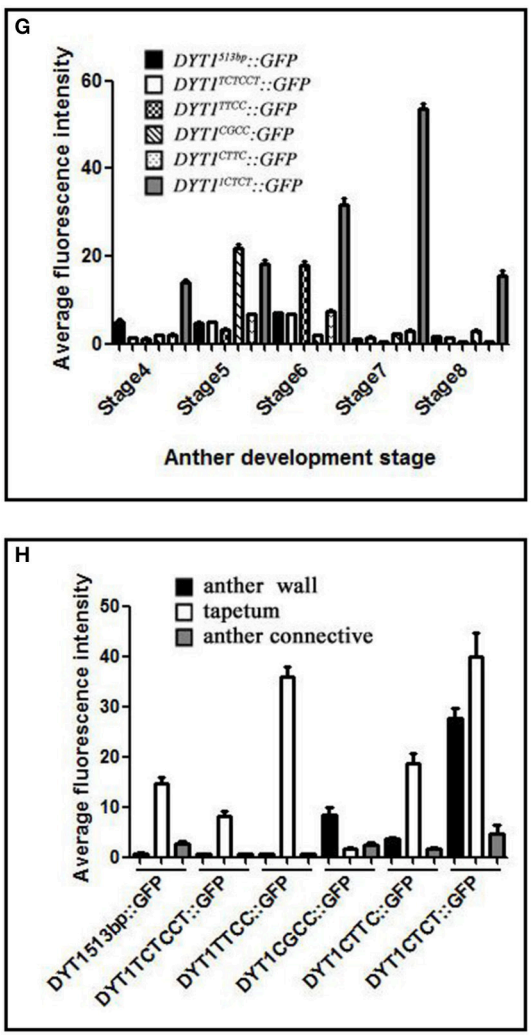

FIGURE 2 | *GFP* expression in "CTCC" site mutation transgenic plant anthers. (A–F) Green fluorescence images of anthers at stage 4–8 in *DYT1*^{513bp}*::GFP*, *DYT1*^{TCTCCT}*::GFP*, *DYT1*^{TTCC}*::GFP*, *DYT1*^{CGCC}*::GFP*, *DYT1*^{CTTC}*::GFP,* and *DYT1*^{CTCT}*::GFP* in transgenic plants. **(G,H)** Semi-quantification of the average fluorescence intensity in stage 4–8 anthers and in different parts of stage 6 anthers of *DYT1*^{513bp}*::GFP*, *DYT1*^{TCTCCT}*::GFP*, *DYT1*^{TTCC}*::GFP*, *DYT1*^{CGCC}*::GFP*, *DYT1*^{CTTC}*::GFP,* and *DYT1*^{CTCT}*::GFP* transgenic plantsthrough SMART software assay ($n \geq 30$, $\pm SD$; $p < 0.1$, Student's *t*-test), values were obtained from 3 independent lines of transgenic plants. Bar = 10 μm.

of the "CTCC" *cis*-element (5′ end from "C" to "T," and 3′ end from "C" to "T," respectively), and the first and third nucleotide substitutes from "C" to "T" in the "CTCC" imposed no effect on the expression pattern of GFP (**Figures 2B,C,E,G**). On the contrast, however, "G" replacing "T" in the "CTCC" resulted in weak expression of *GFP* in the connective and epidermis tissues in addition to the tapetum and PMC (before stage 6, then microspore at stage 7 and 8; **Figures 2D,H**). Furthermore, "T" replacing the final "C" resulted in strong *GFP* expression in all tissues of stage 4–8 anthers (**Figures 2F,H**). Thus, the "T" and final "C" of the "CTCC" *cis*-element were suggested to play predominant roles in controlling the tissue specificity and appropriate intensity of the gene expression.

As Short as 497 bp *DYT1* Promoter Was Sufficient for Tissue-Specific Expression

The previous study had elucidated that beside the core motif "CTCC," the −481 to −513 bp region of *DYT1* promoter was also indispensable for appropriate expression. To uncover finer structure within this region, in addition to original 481 and 513 bp truncated *DYT1* promoter-driven *GFP* reporter constructs, 489, 497, and 505 bp truncated *DYT1* promoter-driven *GFP* reporter constructs were made and transformed into *Arabidopsis*, respectively. As a result, both 505 and 497 bp *DYT1* promoter gave rise of the identical expression pattern as the 513 bp *DYT1* promoter (**Figures 3A,B,E**), suggesting as short as 497 bp *DYT1* promoter was sufficient to recapitulate appropriate *DYT1* expression in *Arabidopsis* anther. On the other side, in DYT^{489bp}*::GFP* transgenic plants, *GFP* exhibited an ectopic and weaker expression losing the tapetum-preferential pattern, similar to that of the 481 bp *DYT1* promoter. The detectable green fluorescence was distributed not only in the tapetum and PMC (before stage 6, then microspore at stage 7 and 8), but also in the connective and epidermis tissues (**Figures 3C,D,F**), suggesting that the sequence from −489 to −497 bp in *DYT1* promoter was essential for tapetum-preferential expressing pattern, and

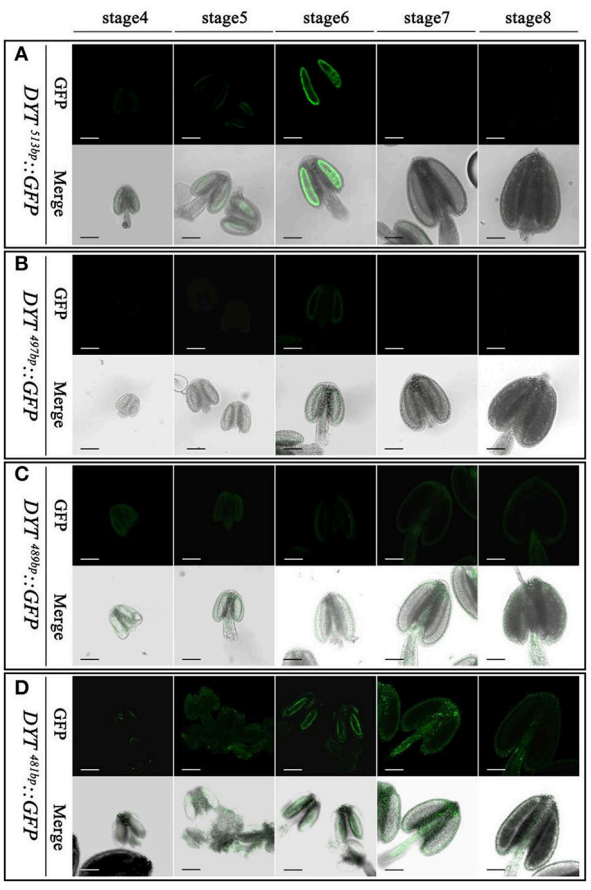

FIGURE 3 | Continued

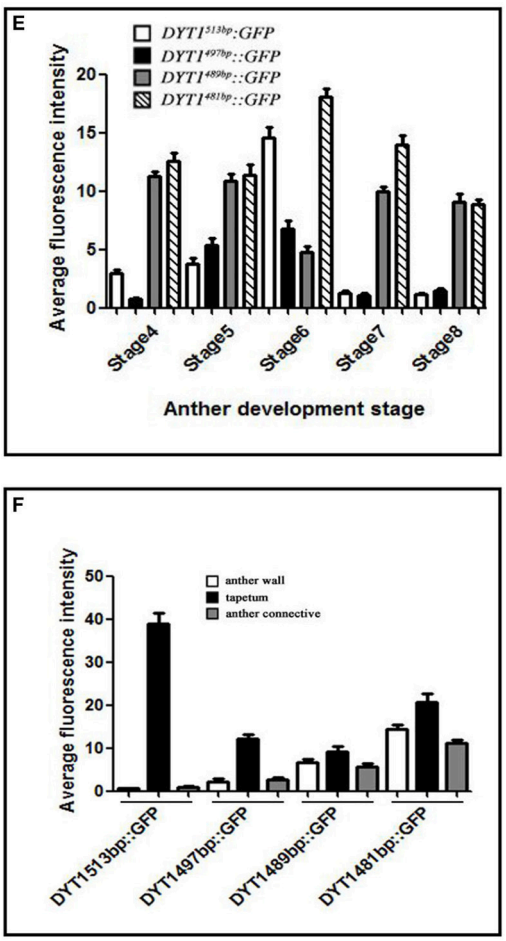

FIGURE 3 | GFP expressing in $DYT1^{513bp}$*::GFP*, $DYT1^{489bp}$*::GFP*, $DYT1^{497bp}$*::GFP and* $DYT1^{481bp}$*::GFP* transgenic Arabidopsis anthers. **(A)** The green-fluorescence concentrates in the tapetal cells of transgenic plant anthers; **(B–D)** Obvious green-fluorescence displays both in the anther locules, tapetum and epidermis. The upper row are images of fluorescence, and the under row are merged images of light and fluorescence. **(E,F)** Semi-quantification of the average fluorescence intensity in stage4-8 anthers and in different parts of stage 6 anthers of $DYT1^{513bp}$*::GFP*, $DYT1^{497bp}$*::GFP*, $DYT1^{489bp}$*::GFP*, and $DYT1^{481bp}$*::GFP* transgenic plants through SMART software assay ($n \geq 30$, $\pm SD$; $p < 0.1$, Student's *t*-test), values were obtained from 3 to 5 independent lines of transgenic plants. Bar = 10 μm.

as short as 497 bp *DYT1* promoter sequence was sufficient for tissue-specific expression.

505 bp *DYT1* Promoter Was Sufficient for Species-Specific Expression

As mentioned before, the flanking −489 to −497 bp region seemed to play as a restriction element to limit *DYT1* expression with certain spaces so that *DYT1* expression exhibited as a specific spatial profile. Then one more question was brought up whether there was other region in 513 bp *DYT1* promoter imparting the species specificity. In order to test such possibility, the series of truncated *DYT1* promoter-driven *GFP* reporting constructs were transformed into tobacco BY2 cell suspension. In $DYT1^{497bp}$::*GFP*, $DYT1^{489bp}$::*GFP* and $DYT1^{481bp}$::*GFP* transgenic BY2 cell suspension, weaker GFP expression comparing with that of *35S::GFP* transgenic cells was found (**Figures 4A,D–F,M**). However, in $DYT1^{513bp}$::*GFP* and $DYT1^{505bp}$::*GFP* transformed cell lines, no GFP signal could be detected (**Figures 4B,C,M**). Thus, 505 bp *DYT1* promoter sequence was sufficient for restricting the gene expression in *A. thaliana* rather than in other species such as tobacco BY2 cell suspension.

Furthermore, all site mutations within "CTCC" based on $DYT1^{513bp}$::*GFP* gave rise of ectopic GFP expression in BY2 cell

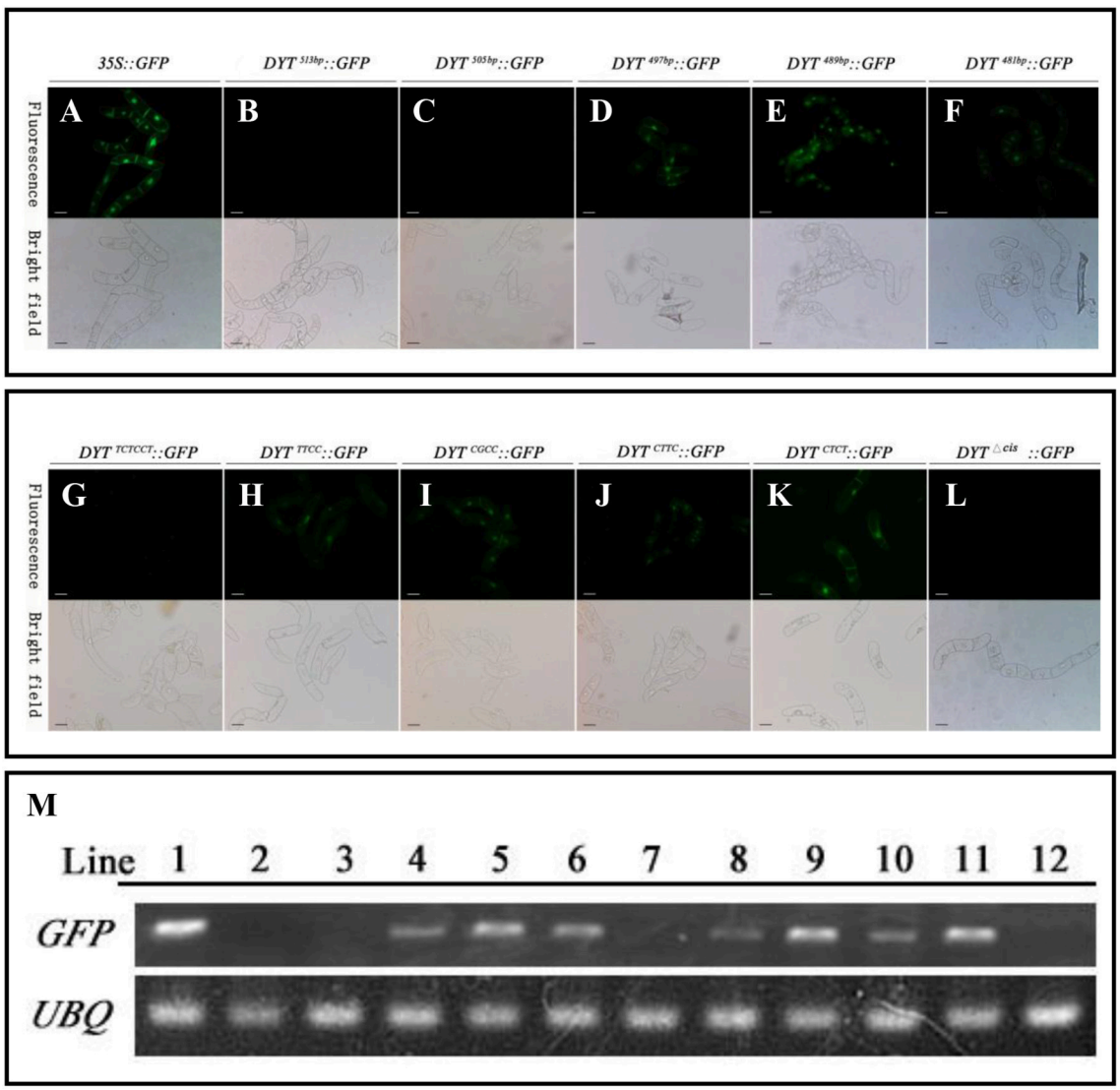

FIGURE 4 | Functional segments assay of *DYT1* promoterin transgenic BY2 cells. GFP fluorescence was detected under Confocal microscope. **(A–F)** The fluorescence and bright images of GFP driven by *35S* promoter and different truncated *DYT1* promoters. **(G–L)** The function assay of "CTCC" segment in *DYT1* promoter driving GFP expression in BY2 cells. **(M)** RT-PCR analysis of *GFP/ACTIN* expression in different transgenic BY2 cells. Lane 1–12 represented *35S::GFP*, $DYT1^{513bp}$::*GFP*,$DYT1^{505bp}$::*GFP*, $DYT1^{497bp}$::*GFP*, $DYT1^{489bp}$::*GFP*, $DYT1^{481bp}$::*GFP*, $DYT1^{TCTCCT}$::*GFP*, $DYT1^{TTCC}$::*GFP*, $DYT1^{CGCC}$::*GFP*, $DYT1^{CTTC}$::*GFP*, $DYT1^{CTCT}$::*GFP,* and $DYT1^{\Delta cis}$::*GFP* transgenic cells. Bar = 20 μm.

suspension, suggesting that the "CTCC" *cis*-element participated in determining species specificity. However, the substitutes of the "T" and final "C" generated stronger ectopic expression than the other two nucleotides (**Figures 4I,K**), suggesting the "T" and final "C" also contributed in determining species specificity more than the other two "C" nucleotides (**Figures 4H,J**), though not so exclusively as in determining tissue specificity in *Arabidopsis*. Consistent to the results obtained from *Arabidopsis* study (**Figure 2**), the mutations of "CTCC" flanking nucleotides had no effect on the driven gene expression (**Figure 4G**), further supporting "CTCC" itself was a four-nucleotides motif. Unlike site mutations, the "CTCC" deletion $DYT1^{513bp\Delta cis}$*:: GFP* generated little GFP fluorescence either in *Arabidopsis* anther (Shumin et al., 2015), or in BY2 cell suspension (**Figures 4L,M**), adding complexity to the function of intact "CTCC." One explanation is that in addition to controlling spatial expression pattern of the driven gene, "CTCC" as a whole is also important for gene expression activation.

DISCUSSION

The findings of this study that the substitutes of the "T" and final "C" nucleotides in the "CTCC" sequence dramatically changed the driven gene (*GFP* here) expression profile, whereas the nucleotide replaces just out of "CTCC" imposed little effect on either tissue or species specificity, confirmed that the "CTCC" sequence did satisfy the definition of a canonical *cis*-element, and play as the core role in determining *DYT1* expression profile. Furthermore, with more "CTCC" flanking sequences truncated from *DYT1* promoter, the extent of gene expression specificity became weaker, reflected in the facts that the species specificity was lost firstly, then the expression region extended from the central locule to the connective tissue and epidermis in the *Arabidopsis* anther, resulting in a constitutive pattern at last. Thus it was suggested that *DYT1* promoter was a functional unit comprised of multiple parts whose absence would lead to expression specificity attenuation, from both species and tissue-specific to only tissue-specific, and finally to constitutive. In other words, the core motif "CTCC" and its flanking sequences need work together to restrict the driven gene expressed precisely in specific tissues, and furthermore in specific species.

With the key *cis*-element identified, undoubtedly the main task of next stage work is to identify the *trans*-factor(s) which recognizes and binds to the "CTCC" *cis*-element, and finally activates *DYT1* expression. As mentioned before, among the known *DYT1* upstream regulatory factors which are involved in transcription regulation, SPL8 participates in the small RNA signaling in cell differentiation regulation in anther. As a SBP domain factor, the DNA-binding motif of SPL8 is zinc-binding motif rather than "CTCC" (Xing et al., 2010). Furthermore, both SPL/NZZ and LFR lack functional DNA-binding domain (Yang et al., 1999; Wang et al., 2012). Thus, it is proposed that the regulatory factor recognizing and binding to the "CTCC" *cis*-element of *DYT1* promoter still needs to be characterized in future work. This unknown factor might be unable to activate *DYT1* expression alone. Conversely it would associate with SPL/NZZ and/or LFR to form an active transcription complex to trigger *DYT1* expression.

AUTHOR CONTRIBUTIONS

WZ and SZ designed all experiments, analyzed data, and wrote the manuscript. HZ performed experiments on transgenic expression assays. RL worked on the transgenic lines. QH performed experiments on construction of transformation vector. YL performed analysis of promoter function element. QX performed statistical analysis of fluorescence intensity.

ACKNOWLEDGMENTS

This research was supported by grants from the Natural Science Foundation of Shanghai (Project Nos. 15ZR1416700), the National Natural Science Foundation of China (Project Nos. 30870225).

SUPPLEMENTARY MATERIAL

The Supplementary Material for this article can be found online at: http://journal.frontiersin.org/article/10.3389/fpls.2017.00153/full#supplementary-material

REFERENCES

Albrecht, C., Russinova, E., Hecht, V., Baaijens, E., and de Vries, S. (2005). The *Arabidopsis thaliana* SOMATIC EMBRYOGENESIS RECEPTOR-LIKE KINASES1 and 2 control male sporogenesis. *Plant Cell* 17, 3337–3349. doi: 10.1105/tpc.105.036814

Clough, S. J., and Bent, A. F. (1998). Floral dip: a simplified method for Agrobacterium -mediated transformation of *Arabidopsis thaliana*. *Plant J.* 16, 735–743. doi: 10.1046/j.1365-313x.1998.00343.x

Colcombet, J., Boisson-Dernier, A., Ros-Palau, R., Vera, C. E., and Schroeder, J. I. (2005). Arabidopsis SOMATIC EMBRYOGENESIS RECEPTOR KINASES1 and 2 are essential for tapetum development and microspore maturation. *Plant Cell* 17, 3350–3361. doi: 10.1105/tpc.105.036731

Cui, J., You, C., Zhu, E., Huang, Q., Ma, H., and Chang, F. (2016). Feedback regulation of DYT1 by interactions with downstream bHLH factors promotes DYT1 nuclear localization and anther development. *Plant Cell* 28, 1078–1093. doi: 10.1105/tpc.15.00986

Feng, B., Lu, D., Ma, X., Peng, Y., Sun, Y., Ning, G., et al. (2012). Regulation of the Arabidopsis anther transcriptome by DYT1 for pollen development. *Plant J.* 72, 612–624. doi: 10.1111/j.1365-313X.2012.05104.x

Feng, X., and Dickinson, H. G. (2007). Packaging the male germline in plants. *Trends Genet.* 23, 503–510. doi: 10.1016/j.tig.2007.08.005

Fernández-Gómez, J., and Wilson, Z. A. (2014). A barley PHD finger transcription factor that confers male sterility by affecting tapetal development. *Plant Biotechnol. J.* 12, 765–777. doi: 10.1111/pbi.12181

Goldberg, R. B., Beals, T. P., and Sanders, P. M. (1993). Anther development: basic principles and practical applications. *Plant Cell* 5, 1217–1229. doi: 10.1105/tpc.5.10.1217

Gu, J. N., Zhu, J., Yu, Y., Teng, X. D., Lou, Y., Xu, X. F., et al. (2014). DYT1 directly regulates the expression of TDF1 for tapetum development and

pollen wall formation in Arabidopsis. *Plant J.* 80, 1005–1013. doi: 10.1111/tpj.12694

Higginson, T., Li, S. F., and Parish, R. W. (2003). AtMYB103 regulates tapetum and trichome development in *Arabidopsis thaliana*. *Plant J.* 35, 177–192. doi: 10.1046/j.1365-313X.2003.01791.x

Hord, C. L., Chen, C., Deyoung, B. J., Clark, S. E., and Ma, H. (2006). The BAM1/BAM2 receptor-like kinases are important regulators of Arabidopsis early anther development. *Plant Cell* 18, 1667–1680. doi: 10.1105/tpc.105.036871

Ito, T., Nagata, N., Yoshiba, Y., Ohme-Takagi, M., Ma, H., and Shinozaki, K. (2007). Arabidopsis MALE STERILITY1 encodes a PHD-type transcription factor and regulates pollen and tapetum development. *Plant Cell* 19, 3549–3562. doi: 10.1105/tpc.107.054536

Kano-Murakami, Y, Suzuki, I., Sugiyama, T., and Matsuoka, M. (1991). Sequence-specific interactions of a maize factor with a GC-rich repeat in the phosphoenolpyruvate carboxylase gene. *Mol. Gen. Genet.* 225, 203–208. doi: 10.1007/BF00269849

Koltunow, A. M., Truettner, J., Cox, K. H., Wallroth, M., and Goldberg, R. B. (1990). Different temporal and spatial gene expression patterns occur during anther development. *Plant Cell* 2, 1201–1224. doi: 10.1105/tpc.2.12.1201

Ku, L., Wei, X., Zhang, S., Zhang, J., Guo, S., and Chen, Y. (2011). Cloning and characterization of a putative TAC1 ortholog associated with leaf angle in maize (*Zea mays* L.). *PLoS ONE* 6:e20621. doi: 10.1371/journal.pone.0020621

Li, J., Chen, X., Luo, L. Q., Yu, J., and Ming, F. (2013). Functions of ANAC092 involved in regulation of anther development in *Arabidopsis thaliana*. *Yi Chuan* 35, 913–922. doi: 10.3724/SP.J.1005.2013.00913

Li, L., Li, Y., Song, S., Deng, H., Li, N., Fu, X., et al. (2015). An anther development F-box (ADF) protein regulated by tapetum degeneration retardation (TDR) controls rice anther development. *Planta* 241, 157–166. doi: 10.1007/s00425-014-2160-9

Li, Z., Wang, Y., Huang, J., Ahsan, N., Biener, G., Paprocki, J., et al. (2017). Two SERK receptor-like kinases interact with EMS1 to control anther cell fate determination. *Plant Physiol.* 173, 326–337. doi: 10.1104/pp.16.01219

Liu, X., Huang, J., Parameswaran, S., Ito, T., Seubert, B., Auer, M., et al. (2009). The SPOROCYTELESS/NOZZLE gene is involved in controlling stamen identity in Arabidopsis. *Plant Physiol.* 151, 1401–1411. doi: 10.1104/pp.109.145896

Phan, H. A., Iacuone, S., Li, S. F., and Parish, R. W. (2011). The MYB80 transcription factor is required for pollen development and the regulation of tapetal programmed cell death in *Arabidopsis thaliana*. *Plant Cell* 23, 2209–2224. doi: 10.1105/tpc.110.082651

Phan, H. A., Li, S. F., and Parish, R. W. (2012). MYB80, a regulator of tapetal and pollen development, is functionally conserved in crops. *Plant Mol. Biol.* 78, 171–183. doi: 10.1007/s11103-011-9855-0

Schiefthaler, U., Balasubramanian, S., Sieber, P., Chevalier, D., Wisman, E., and Schneitz, K. (1999). Molecular analysis of NOZZLE, a gene involved in pattern formation and early sporogenesis during sex organ development in *Arabidopsis thaliana*. *Proc. Natl. Acad. Sci. U.S.A.* 96, 11664–11669. doi: 10.1073/pnas.96.20.11664

Scott, R. J., Spielman, M., and Dickinson, H. G. (2004). Stamen structure and function. *Plant Cell* 16(Suppl.), 46–60. doi: 10.1105/tpc.017012

Shumin, Z., Yan, C., Hulin, S., Bang, Z., Licheng, S., and Wei, Z. (2015). One novel cis-element is essential for correct DYSFUNCTIONAL TAPETUM (DYT1) expression in *Arabidopsis thaliana*. *Plant Cell Rep.* 34, 1773–1780. doi: 10.1007/s00299-015-1823-8

Sorensen, A. M., Kröber, S., Unte, U. S., Huijser, P., Dekker, K., and Saedler, H. (2003). The Arabidopsis ABORTED MICROSPORES (AMS) gene encodes a MYC class transcription factor. *Plant J.* 33, 413–423. doi: 10.1046/j.1365-313X.2003.01644.x

Wang, X. T., Yuan, C., Yuan, T. T., and Cui, S. J. (2012). The Arabidopsis LFR gene is required for the formation of anther cell layers and normal expression of key regulatory genes. *Mol. Plant* 5, 993–1000. doi: 10.1093/mp/sss024

Xing, S. P., Salinas, M., Höhmann, S., Berndtgen, R., and Huijser, P. (2010). miR156-targeted and nontargeted SBP-box transcription factors act in concert to secure male fertility in Arabidopsis. *Plant Cell* 22, 3935–3950. doi: 10.1105/tpc.110.079343

Xu, X. F., Wang, B., Lou, Y., Han, W. J., Lu, J. Y., Li, D. D., et al. (2015). Magnesium transporter 5 plays an important role in Mg transport for male gametophyte development in Arabidopsis. *Plant J.* 84, 925–936. doi: 10.1111/tpj.13054

Xu, Y., Iacuone, S., Li, S. F., and Parish, R. W. (2014). MYB80 homologues in Arabidopsis cotton and Brassica: regulation and functional conservation in tapetal and pollen development. *BMC Plant Biol.* 14:278. doi: 10.1186/s12870-014-0278-3

Yang, C., Vizcay-Barrena, G., Conner, K., and Wilson, Z. A. (2007). MALE STERILITY1 is required for tapetal development and pollen wall biosynthesis. *Plant Cell* 19, 3530–3548. doi: 10.1105/tpc.107.054981

Yang, W. C., Ye, D., Xu, J., and Sundaresan, V. (1999). The SPOROCYTELESS gene of Arabidopsis is required for initiation of sporogenesis and encodes a novel nuclear protein. *Genes Dev.* 13, 2108–2117. doi: 10.1101/gad.13.16.2108

Yeung, E. C., Oinam, G. S., Yeung, S. S., and Harry, I. (2011). Anther, pollen and tapetum development in safflower, *Carthamustinctorius* L. *Sex Plant Reprod.* 24, 307–317. doi: 10.1007/s00497-011-0168-x

Yi, J., Moon, S., Lee, Y.-S., Zhu, L., Liang, W., Zhang, D., et al. (2016). Defective tapetum cell death 1 (DTC1) regulates ROS levels by binding to metallothionein during tapetum degeneration. *Plant Physiol.* 170, 1611–1623. doi: 10.1104/pp.15.01561

Zhang, D., Liu, D., Lv, X., Wang, Y., Xun, Z., Liu, Z., et al. (2014). The cysteine protease CEP1, a key executor involved in tapetal programmed cell death, regulates pollen development in Arabidopsis. *Plant Cell* 26, 2939–2961. doi: 10.1105/tpc.114.127282

Zhang, W., Sun, Y., Timofejeva, L., Chen, C., Grossniklaus, U., and Ma, H. (2006). Regulation of Arabidopsis tapetum development and function by DYSFUNCTIONAL TAPETUM1 (DYT1) encoding a putative bHLH transcription factor. *Development* 133, 3085–3095. doi: 10.1242/dev.02463

Zhang, Z. B., Zhu, J., Gao, J.F., Wang, C., Li, H., Li, H., et al. (2007). Transcription factor AtMYB103 is required for anther development by regulating tapetum development, callose dissolution and exine formation in Arabidopsis. *Plant J.* 52, 528–538. doi: 10.1111/j.1365-313X.2007.03254.x

Zhao, D. Z., Wang, G. F., Speal, B., and Ma, H. (2002). Theexcess microsporocytes1 gene encodes a putative leucine-rich repeat receptor protein kinase that controls somatic and reproductive cell fates in the Arabidopsis anther. *Genes Dev.* 16, 2021–2031. doi: 10.1101/gad.997902

Zhao, X., de-Palma, J., Oane, R., Gamuyao, R., Luo, M., Chaudhury, A., et al. (2008). Os TDL1A binds to the LRR domain of rice receptor kinase MSP1, and is required to limit sporocyte numbers. *Plant J.* 54, 375–387. doi: 10.1111/j.1365-313X.2008.03426.x

Zhou, S. M., Chu, Y. X., Zheng, B., and Zhang, W. (2014). Optimization of BY2 cell suspension as a stable transformable system. *Not. Bot. HortiAgrobo.* 42, 472–477.

Zhu, J., Chen, H., Li, H., Gao, J. F., Jiang, H., Wang, C., et al. (2008). Defective in tapetal development and function1 is essential for anther development and tapetal function for microspore maturation in Arabidopsis. *Plant J.* 55, 266–277. doi: 10.1111/j.1365-313X.2008.03500.x

Conflict of Interest Statement: The authors declare that the research was conducted in the absence of any commercial or financial relationships that could be construed as a potential conflict of interest.

frontiers in Plant Science

ORIGINAL RESEARCH
published: 09 May 2017
doi: 10.3389/fpls.2017.00704

Molecular Evidence for Natural Hybridization between *Cotoneaster dielsianus* and *C. glaucophyllus*

Mingwan Li[1], Sufang Chen[1], Renchao Zhou[1], Qiang Fan[1], Feifei Li[2,3]* and Wenbo Liao[1]*

[1] Guangdong Key Laboratory of Plant Resources, Key Laboratory of Biodiversity Dynamics, Conservation of Guangdong Higher Education Institutes, Sun Yat-sen University, Guangzhou, China, [2] State Key Laboratory of Environmental Criteria and Risk Assessment, Chinese Research Academy of Environmental Sciences, Beijing, China, [3] College of Life and Environmental Sciences, Minzu University of China, Beijing, China

Hybridization accompanied by polyploidization and apomixis has been demonstrated as a driving force in the evolution and speciation of many plants. A good example to study the evolutionary process of hybridization associated with polyploidy and apomixis is the genus *Cotoneaster* (Rosaceae), which includes approximately 150 species, most of which are polyploid apomicts. In this study, we investigated all *Cotoneaster* taxa distributed in a small region of Malipo, Yunnan, China. Based on the morphological characteristics, four *Cotoneaster* taxa were identified and sampled: *C. dielsianus*, *C. glaucophyllus*, *C. franchetii*, and a putative hybrid. Flow cytometry analyses showed that *C. glaucophyllus* was diploid, while the other three taxa were tetraploid. A total of five low-copy nuclear genes and six chloroplast regions were sequenced to validate the status of the putative hybrid. Sequence analyses showed that *C. dielsianus* and *C. glaucophyllus* are distantly related and they could be well separated using totally 50 fixed nucleotide substitutions and four fixed indels at the 11 investigated genes. All individuals of the putative hybrid harbored identical sequences: they showed chromatogram additivity for all fixed differences between *C. dielsianus* and *C. glaucophyllus* at the five nuclear genes, and were identical with *C. glaucophyllus* at the six chloroplast regions. Haplotype analysis revealed that *C. dielsianus* possessed nine haplotypes for the 11 genes, while *C. glaucophyllus* had ten, and there were no shared haplotypes between the two species. The putative hybrid harbored two haplotypes for each nuclear gene: one shared with *C. dielsianus* and the other with *C. glaucophyllus*. They possessed the same chloroplast haplotype with *C. glaucophyllus*. Our study provided convincing evidence for natural hybridization between *C. dielsianus* and *C. glaucophyllus*, and revealed that all hybrid individuals were derivatives of one initial F1 via apomixes. *C. glaucophyllus* served as the maternal parent at the initial hybridization event. We proposed that anthropological disturbance provided an opportunity for hybridization between *C. dielsianus* and *C. glaucophyllus*, and a tetraploid F1 successfully bred many identical progenies via apomixis. Under this situation, species integrity could be maintained for these *Cotoneaster* species, but attentions should be kept for this new-born hybrid.

Keywords: *Cotoneaster*, natural hybridization, low-copy nuclear genes, chloroplast DNA, polyploidy, apomixes

OPEN ACCESS

Edited by:
Borja Cascales-Miñana, University of Liège, Belgium

Reviewed by:
Yongpeng Ma, Kunming Institute of Botany (CAS), China
Tatiana Arias, Corporation for Biological Research, Colombia

****Correspondence:***
Sufang Chen
chsuf@mail.sysu.edu.cn
Feifei Li
lifeifei30761@gmail.com

Specialty section:
This article was submitted to Plant Evolution and Development, a section of the journal Frontiers in Plant Science

Received: *12 January 2017*
Accepted: *18 April 2017*
Published: *09 May 2017*

Citation:
Li M, Chen S, Zhou R, Fan Q, Li F and Liao W (2017) Molecular Evidence for Natural Hybridization between Cotoneaster dielsianus and C. glaucophyllus. Front. Plant Sci. 8:704. doi: 10.3389/fpls.2017.00704

INTRODUCTION

Hybridization, previously viewed as a mere side branch or noise of evolution, is now recognized as a major evolutionary force and a significant portion of speciation (e.g., Arnold, 1997; Rieseberg and Willis, 2007; Soltis and Soltis, 2009; Soltis et al., 2014). The process of hybridization can help us understand the origin of adaptations, the maintenance of plant diversity, and the formation of new species. As early as 1917, Winge first introduced a theory linking the formation of hybridization and the development of polyploids, proposing that reproductive isolation could be rapidly established between new polyploids and their parental species, so that new polyploid hybrid species could arise in just a few generations (Winge, 1917). Several plant species have originated via hybridization and polyploidy within the past 150 years, such as *Spartina anglica* (Ainouche et al., 2003), *Senecio cambrensis* and *S. eboracensis* (Abbott and Lowe, 2004), *Cardamine schultzii* (Urbanska et al., 1997), and *Tragopogon mirus* and *T. miscellus* (Soltis et al., 2004). It was also proposed that "allopolyploidy, perhaps more than any other process, has played a major role in the origin of many species and thus has driven and shaped the evolution of vascular plants" (Feldman and Levy, 2005) and many angiosperms are ultimately of ancient polyploid origin (Wagner and Wagner, 1980).

The production of viable progenies is a key for the establishment of a hybrid lineage. Allopolyploids may frequently produce pollen with meiotic irregularities, leading to partial or complete sterility of the progenies (Comai et al., 2003; Comai, 2005). A potential evolutionary solution to this problem is asexual reproduction, i.e., apomixis or agamospermy (Asker and Jerling, 1992; Sochor et al., 2015). With usually uniparental reproduction, lowered cost of sex, maintenance of adapted genotypes and occasional seed reproduction (Hörandl, 2006), many apomictic plants can achieve great ecological and evolutionary success. Apomixis has been well documented in numerous genera of Rosaceae, particularly *Cotoneaster* (Nybom and Bartish, 2007), *Crataegus* (Lo et al., 2009), *Rubus* (Sochor et al., 2015), *Sorbus* (Robertson et al., 2010; Ludwig et al., 2013), and *Potentilla* sensu lato (Morgan et al., 1994).

Derived from hybridization and chromosome doubling, allopolyploids always display intermediate morphologies compared to their parents. Many allopolyploid apomicts are facultative, and their backcrossing with sexual relatives is hypothesized to lead to multiple evolutionary origins for apomictic lineages; the morphological differences between these species with apomixis can be very small (Van der Hulst et al., 2000; Paun et al., 2006; Sochor et al., 2015). The interplay of hybridization, polyploidy and apomixis generated a great number of described species in Rosaceae, whose taxonomic classification has been a challenging task for generations of researchers. These species are not easily distinguishable and have only relatively minor morphological differences.

As a typical example, the genus *Cotoneaster* Medik. (Rosaceae, subtribe Malinae) is fraught with hybridization accompanied by polyploidy and apomixis. The genus occurs throughout Europe, North Africa and temperate areas of Asia excluding Japan. The Himalayas and neighboring mountains in Yunnan and Sichuan of China are the most important species diversity center for this genus. Furthermore, the majority (70%) of *Cotoneaster* taxa have so far proven to be tetraploid ($2n = 68$), which are mostly inbreeding apomictic taxa; only 10% are diploid ($2n = 34$) (Fryer and Hylmö, 2009). Observations from seedling morphology and embryo sac development also revealed that apomictic breeding systems are very common in this genus (Bartish et al., 2001), as further confirmed by Nybom and Bartish (2007) based on RAPD analysis. The number of *Cotoneaster* species described is progressively increasing (80 species, Rehder, 1927; 176 species, Flinck and Hylmö, 1966; 261, Phipps et al., 1990), and the latest monograph by Fryer and Hylmö (2009) has added c. 70 "new species," bringing the total number known to approximately 400.

Previous studies have proposed that many hybridization events may have occurred in *Cotoneaster* (Fryer and Hylmö, 2009; Dickoré and Kasperek, 2010). Nonetheless, no sufficient genetic evidence has been provided for the natural hybridization occurring in this genus. Based on the phylogenetic tree constructed from three combined chloroplast regions (Li et al., 2014), 56 *Cotoneaster* species were divided into two main clades: one clade consisting of most species with erect red or pink petals, while the other clade comprised species with spreading white petals. However, it is apparent that many *Cotoneaster* species in that report exhibit intermediate morphological characters, and there is discordance between chloroplast and nrITS trees for 14 species. Nevertheless, it is difficult to identify parental species based on phylogenetic trees. First, it is difficult to collect all *Cotoneaster* species, which in many cases are morphologically undistinguished in the field. In the study by Li et al. (2014), only a small portion of the hundreds of described species in China were collected. Second, radical evolution, polyploidy and apomixis also create comb structures in the phylogenetic trees, making it even more difficult to identify their parental species.

In this study, we focused our objectives on a limited area (approximately 50 km^2) of Malipo county, Yunnan, China, where a species with erect red petals (identified as *C. dielsianus*), a species with erect pink petals (*C. franchetii*), a species with spreading white petals (*C. glaucophyllus*), and an unidentified taxon with intermediate characteristics between *C. dielsianus* and *C. glaucophyllus* (the putative hybrid) can be found (**Figure 1**; **Table 1**). To validate the hybridization between *C. dielsianus* and *C. glaucophyllus*, we collected population samples for the three *Cotoneaster* species and the putative hybrid. Flow cytometry was applied to estimate their ploidy level, and then five low-copy nuclear genes and six chloroplast DNA fragments were sequenced for all samples. Through these efforts, we endeavored to answer the following questions: (1) Are these *Cotoneaster* species diploid or polyploid? (2) Are the morphologically intermediate individuals really hybrids o *C. dielsianus* and *C. glaucophyllus*? (3) If so, is the hybridization unidirectional? What is the make-up of the hybrid zone with respect to classes (i.e., F1, backcross and complex hybrid derivatives)? (4) Did the species *C. franchetii* participate in the hybridization? Based on the results, we further discussed factors contributing to the hybridization events, consequences and possible mechanism of the formation of hybrids between the parent species.

FIGURE 1 | Morphological illustrations for three *Cotoneaster* taxa, *C. dielsianus* (a,b), putative hybrid **(c,d)**, and *C. glaucophyllus* **(e,f)** investigated in this study. Flowers and fruits of three taxa are shown in the six frames.

TABLE 1 | Comparison of morphological characteristics among putative hybrid, *C. dielsianus* and *C. glaucophyllus*.

Morphological characters	*C. dielsianus*	Putative hybrid	*C. glaucophyllus*
Habit	Deciduous shrub, 1–2 m	Semi-evergreen shrub, 1–2 m	Semi-evergreen shrub, 2–5 m
Lower surface of leaf	Tomentose	Pubescent	Pubescent when young, soon glabrescent
Number of pyrenes	3–5	2	2
Flowers per cyme	3–7	4–10	10–50
Petal characters	Erect	Semi-spreading	Spreading
Petal color	Red	Pinkish white	White
Ploidy level	4	4	2
2C DNA (pg, mean ± SD)	2.05 ± 0.126	2.02 ± 0.023	1.09 ± 0.034

METHODS

Sampling

Based on the principal morphological characteristics of leaf blade size, number of flowers per cyme, petal characters and petal color (**Figure 1**; **Table 1**; Fryer and Hylmö, 2009), at least 18 individuals were collected for each of the three *Cotoneaster* taxa and the putative hybrid from Malipo county, Yunnan, China (**Table 2**). In addition, one congeneric species, *C. frigidus*, was sampled in Tibet and used as a outgroup (**Table 1**). For each individual, fresh leaves were collected and deposited in silica gel in zip-lock plastic bags for DNA extraction. Voucher specimens were stored in the Herbarium of Sun Yat-sen University (SYS).

DNA Extraction, Primer Design, PCR, and Sequencing

Total genomic DNA was extracted from dried leaf tissue using a modified CTAB method (Doyle and Doyle, 1987). According to Duarte et al. (2010), a total of 959 single copy nuclear genes were identified based on comparison of the genomes of *Arabidopsis thaliana*, *Populus trichocarpa*, *Vitis vinifera* and *Oryza sativa*, and the sequences for these 959 genes in *Arabidopsis* were downloaded. Of these, 640 obtained BLASTN hits in the cDNA library of *Malus domestica* (not shown) with a cut-off *e*-value of $1e^{-10}$, and sequences for the top hits were extracted and identified as putative single-copy genes in *M. domestica*.

TABLE 2 | Sampling detail of putative hybrid groups, relative and outgroup species (*C.frigidus*) used in this study.

Taxon	Collecting number (DNA sample no.)	Geographical origin (China)	Coordinates (N, E)	Altitude (m)
Putative hybrid	13917 (01–30)	Malipo County, Yunnan	23.13°, 104.80°	1,900–2,159
C. dielsianus	13916 (31–48)	Malipo County, Yunnan	23.13°, 104.80°	2,159
C. franchetii	13915 (49–70)	Malipo County, Yunnan	23.13°, 104.80°	2,159
C. glaucophyllus	13949 (71–96)	Malipo County, Yunnan	23.18°, 104.82°	1,501–2,159
C. frigidus	14650	Jilong County, Tibet	28.43°, 85.26°	2,972

Of these, 33 paired PCR primers for exon-primed, intron-crossing (EPIC) amplifications were designed from randomly selected sequences using Primer Premier 6.0 (PREMIER Biosoft International, Palo Alto, CA, USA). Among these, five were widely amplified in *Cotoneaster* with a single clear band and obtained good sequencing results. Annotations using BLASTX against the NCBI non-redundant protein database showed that three (DUF, UPF, and WD) significant hits. Six chloroplast regions were selected: *ndh*F, *rpl*16, *rps*16, *trn*C-*ycf*6, *trn*G-*trn*S, and *trn*H-*rpl*2 (Campbell et al., 2007; Lo and Donoghue, 2012). Primers and annotation for all nuclear and chloroplast genes are shown in **Table 3**.

PCR reactions were conducted in 20 μL total volumes containing 25 ng of template DNA, 2 μL of 10 × Mg^{+2}FreeBuffer, 1.0 mM MgCl2, 0.2 mM each dNTP, 0.2 μM each primer, and 1 unit Taq DNA polymerase (Apex Bioresearch Products, Research Triangle Park, NC, USA). The amplifications were performed using the following conditions: initial denaturation at 94°C for 4 min, followed by 35 cycles of 94°C for 30 s, an annealing temperature of 55°C for 30 s, 72°C for 1 min, and a final extension of 72°C for 10 min. The PCR products were purified by electrophoresis on a 1.2% agarose gel, followed by extraction using a Pearl Gel Extraction Kit (Pearl Biotech, Guangzhou, China). The purified PCR products were then sequenced on an ABI 3730 DNA Analyzer with the BigDye Terminator Cycle Sequencing Ready Reaction Kit (Applied Biosystems, Foster City, CA). All sequences were deposited in GenBank with the accession numbers KY469293-KY470828.

Ploidy Determination

For the 96 individuals sampled, the ploidy of putative hybrid, *C. dielsianus* and *C. glaucophyllus*, were obtained using four randomly selected individuals in each taxon. The ploidy of silica-dried leaf material was determined by flow cytometry analysis (performed by the Flow Cytometry Lab in Benaroya Research Institute at Virginia Mason, USA) using a modified version of the hand-chopping method described by Roberts et al. (2009). For each sample, approximately 4 mg of dried leaf material and one drop of chicken erythrocyte nuclei (2.5 pg/2C) as the internal standard were finely chopped using a single-edged razor blade in 1000 μL of cold lysis buffer [0.1 M citric acid, 0.5% v/v Triton X-100, 1% w/v PVP-40 (polyvinylpyrrolidone, average molecular weight 40,000)] (Yokoya et al., 2000; Hanson et al., 2005) in a petri dish on a cold chopping surface. After 5 min of incubation on ice and intermittent gentle mixing by pipetting up and down, each sample was filtered using a 5-mL polystyrene round-bottomed tube with a cell-strainer cap (BD Falcon; Becton Dickinson and Co., Franklin Lakes, NJ, USA). A 140-μL aliquot of filtrate was placed in a new 1.5-mL Eppendorf tube with 1 μL of RNaseA (1 mg mL^{-1}) (Thermo Scientific Molecular Biology, Fisher Scientific, Pittsburgh, PA, USA) and incubated at room temperature for 30 min. Next, 350 μL of propidium iodide (PI) staining solution (0.4 M $NaPO_4$, 10 mM sodium citrate, 25 mM sodium sulfate, 50 μg mL^{-1} PI) was added to each tube of nuclei suspension. After 1 h at room temperature, the stained nuclei suspensions were analyzed at 14 μL min^{-1} on an Accuri C6 flow cytometer (BD Biosciences, San Jose, CA, USA) fitted with a 488-nm laser. Fluorescence measurements were made using the FL2 (585/40 nm) optical filter, capturing 10 000 events and utilizing the FL2-A values for the 2C peak.

Sequence Analysis

The obtained sequences were edited and analyzed by Geneious R8 software (Biomatters, Ltd., Auckland, New Zealand). To determine possible copy numbers in the genome, a BLASTN search against apple genome databases (http://www.rosaceae.org/species/malus/malus_x_domestica/genome_v1.0) was performed with a bit score threshold of >100 and a cut-off *E*-value of $1e^{-6}$. No more than two hits were detected in each of the five investigated genes (**Table 3**), indicating that they were single-copy or low-copy regions in the genome. Furthermore, an additional 2–3 pairs of primers were developed to anchor different sites for each nuclear genes (data not shown). We obtained identical sequences using fragments from PCR products traced by these primers, confirming that they are very likely orthologous in *Cotoneaster*.

Polymorphisms at variable sites were identified as superimposed nucleotides (additive patterns) from chromatograms of direct sequences (Whittall et al., 2000), and indel polymorphisms were determined by reading the sequence chromatogram in both directions. At the five nuclear genes, we phased the haplotypes using DnaSPv5 (Librado and Rozas, 2009), and used Network 5001 (www.fluxus-engineering.com) to resolve the relationships of the haplotypes with the median-joining method (Bandelt et al., 1999).

For each nuclear gene and combined chloroplast datasets, we reconstructed the phylogeny of the haplotypes using maximum parsimony (MP) and maximum likelihood (ML) methods, as estimated by PAUP4.0b (Swofford, 2001). For

TABLE 3 | Primers of five low-copy nuclear genes based on *Malus domestica* genome and six universal chloroplast fragments.

Locus	Primer sequences (5′–3′)	Length (bp)	ID for apple coding sequence/reference	Score (*E*-value)
DUF	f:ACAAGTCCAATGCCAATGA	840	MDP0000336096	152(7e-36)
	r:AATATGCCGTAGCCTCCTA			
NA1	f:GCTGGATCACGACTGAGATAAG	568	MDP0000144617 and MDP0000246780	285(3e-76) and 127(2e-28)
	r:TTGTTGAAGCCTCATTCTCTGG			
NA2	f:CCTTTCTCCACTGGGTTAA	461	MDP0000130385	258(8e-68)
	r:GCACTTGAGGTAGCATAATAG			
UPF	f:CAGACTGCTGCCATAATAGA	645	MDP0000174677 and MDP0000940113	127(1e-28) and 222(5e-57)
	r:TAGAAGTAATCGCCACAGAG			
WD	f:GTTCCTCTATCATCACCAGTT	811	MDP0000283138	222(6e-57)
	r:ACCAGTGCCAAGTCTATTC			
*ndh*F	2f:ACTCATGCTTATTCGAAAGC	1036	Campbell et al., 2007	
	1.6r:CCTACTCCATTGGTAATTCCAT			
*rpl*16	f71:GCTATGCTTAGTGTGTGACTCGTTG	891	Campbell et al., 2007	
	r1516:CCCTTCATTCTTCCTCTATGTTG			
*rps*16	f:GTGGTAGAAAGCAACGTGCGACTT	662	Campbell et al., 2007	
	r2:TCGGGATCGAACATCAATTGCAAC			
*trn*C-*ycf*6	f:GCTTGATTCTAAGTATCTGGG	648	Design base on NCBI data (Lo and Donoghue, 2012)	
	r:CAACACCGTTGATGAAACA			
*trn*G-*trn*S	f:CGTGTTGTATCAGAGAACC	415	Identical with *trn*C-*ycf*6	
	r:TTTCATCCGAGAGTGCTTT			
*trn*H-*rpl*2	f:TCTTCGTCGCCGTAGTAA	316	Identical with *trn*C-*ycf*6	
	r:AAGGCAGTGGATTGTGAAT			

parsimony analyses, a heuristic search with tree bisection-reconnection branch swapping, the MulTrees option, accelerated transformation optimization, and 100 random addition replicates was implemented. We defined indels as the fifth state and each indel with two or more nucleotides as a single mutational event. One thousand bootstrap replicates were computed with maxtrees being set to 500. For ML analysis, we selected an appropriate nucleotide substitution model for each gene based on the result of Modeltest 3.7 (Posada and Buckley, 2004). Best-fit models based on the Hierarchical Likelihood Ratio tests (hLRTs) in Modeltest were calculated (Table S1); four of the six models were F81 and the other was HKY+G. Similarly, ML analysis was performed using a heuristic search with tree bisection-reconnection branch swapping, holding one tree at each step. Node support was estimated with 1000 bootstrap replicates and the maxtrees was also set to 500.

RESULTS

The aligned sequences of the five nuclear genes and six chloroplast regions obtained from all individuals of *C. dielsianus*, *C. glaucophyllus*, *C. franchetii* and the putative hybrid are shown in **Table 3**. The shortest aligned length among the 11 makers is 316 bp (*trn*H-*rpl*2), while the longest is 1036 bp (*ndh*F). Considerable sequence variations and high divergence were detected in these four taxa among the 11 fragments (**Table 4**). Surprisingly, all individuals of the putative hybrid shared identical sequences.

Sequence Analyses of the Five Nuclear Genes

The aligned lengths and number of variable sites at the five nuclear genes in the four taxa are shown in **Tables 3**, **4**, respectively. There were a total of 36 fixed nucleotide substitutions and one fixed 6-bp indel (insertion/deletion) between *C. dielsianus* and *C. glaucophyllus* across the whole nuclear gene data set. All individuals of the putative hybrid showed chromatogram additivity at these fixed sites. *C. franchetii* also showed chromatogram additivity at 29 fixed variations and one fixed 6-bp indel between *C. dielsianus* and *C. glaucophyllus*.

In the haplotype analysis, each taxon exhibited a low level of haplotype diversity, and no more than three haplotypes were observed for each of the five genes (**Figure 2**, **Table 4**). *C. dielsianus* possessed 1–2 haplotypes at each gene: 1 haplotype observed at NA2 and WD and 2 haplotypes each at DUF, NA1 and UPF. *C. glaucophyllus* harbored 1–3 haplotypes at each gene: 3 haplotypes observed at NA1; 2 haplotypes at NA2; and 1 haplotype each at DUF, UPF and WD. Nevertheless, no haplotype was shared between the two species. Each individual of the putative hybrid had two haplotypes for each gene: one was shared with *C. dielsianus* and the other was shared with *C. glaucophyllys*. For the other species, *C. franchetii*, one haplotype at NA1 and NA2 was shared with *C. glaucophyllus*, the other haplotype at

TABLE 4 | Fixed nucleotide substitutions and gaps between putative hybrid, *C. dielsianus*, *C. glaucophyllus,* and *C. franchetii* in the five nuclear genes (DUF, NA1, NA2, UPF, and WD) and six chloroplast genes (*ndh*F, *rpl*16, *rps*16, *trn*C-*ycf*6, *trn*G-*trn*S, *trn*H-*rpl*2).

Gene	DUF										NA1							
Site (bp)	66	117	266	285	412	454	532	571	581	607	649	672	766	810	379	397	435	443
Putative hybrid	S	W	Y	W	Y	Y	R	Y	S	Y	R	W	Y	K	Y	K	W	K
C. dielsianus	G	A	T	A	C	T	A	C	G	C	A	A	C	G	C	T	A	G
C. glaucophyllus	C	T	C	T	T	C	G	T	C	T	G	T	T	T	T	G	T	T
C. franchetii	S	A	Y	W	Y	Y	R	Y	S	Y	R	T	C	K	Y	K	W	K
						NA2					UPF						WD	
517	520	521	525	526	527	149	215	268	340	408	187	195	257	278	623	625	40-45	364
R	R	R	W	W	R	R	Y	K	S	R	Y	Y	R	W	K	K	——/ TCACAT	M
G	A	A	T	A	G	G	C	T	C	G	C	C	A	T	G	G	——	A
A	G	G	A	T	A	A	T	G	G	A	T	T	G	A	T	T	TCACAT	C
R	R	R	W	W	R	R	Y	K	S	R	C	C	A	T	K	K	——/ TCACAT	M

Gene	*ndh*F			*rpl*16		*rps*16			*trn*C-*ycf*6				*trn*G-*trn*S			*trn*H-*rpl*2	
Site (bp)	379	716	582	589	635	67	90	651	259	373	44	109	188-190	191-219	19	59-92	254
Putative hybrid	A	C	G	T	G	T	T	G	A	C	T	G	TTC	TTTATTCCTTTTATTTTAGTTAAAGTAAA	A	ATAAATATTTAATATAAATATTAA ATATAAATGG	A
C. dielsianus	T	A	T	G	A	C	C	T	G	G	–	T	CCT	– –	C	TTAAA – – – – – – – – – – – – –	A
C. glaucophyllus	A	C	G	T	G	T	T	G	A	C	T	G	TTC	TTTATTCCTTTTATTTTAGTTAAAGTAAA	A	ATAAATATTTAATATAAATAT TAAATATAAATGG	A
C. franchetii	A	C	T	G	A	T	T	G	A	C	–	G	TTC	TTTATTCCTTTTATTTTAGTTAAAGTAAA	A	– – – – – – – – – – AATATA AATATTAAATATAAATGG	C

NA1 and UPF was shared with *C. dielsianus*, and the other six were unique.

MP and ML algorithms were used to construct phylogenetic trees (**Figure 3**) using the haplotypes at each nuclear gene. The number of parsimony-informative characteristics, steps and values of CI, RI, and RC with the MP algorithm were shown in Table S1 (see Supplementary Material). In the MP tree (bootstrap values above branches), the two haplotypes of the putative hybrid, identical to *C. dielsianus* and *C. glaucophyllus*, formed two well-separated clades. The two haplotypes of *C. franchetii* were also well-separated clades and tended to gather the two haplotypes of putative hybrid. The topologies of these trees were the same as those generated using the ML analysis (bootstrap values below branches).

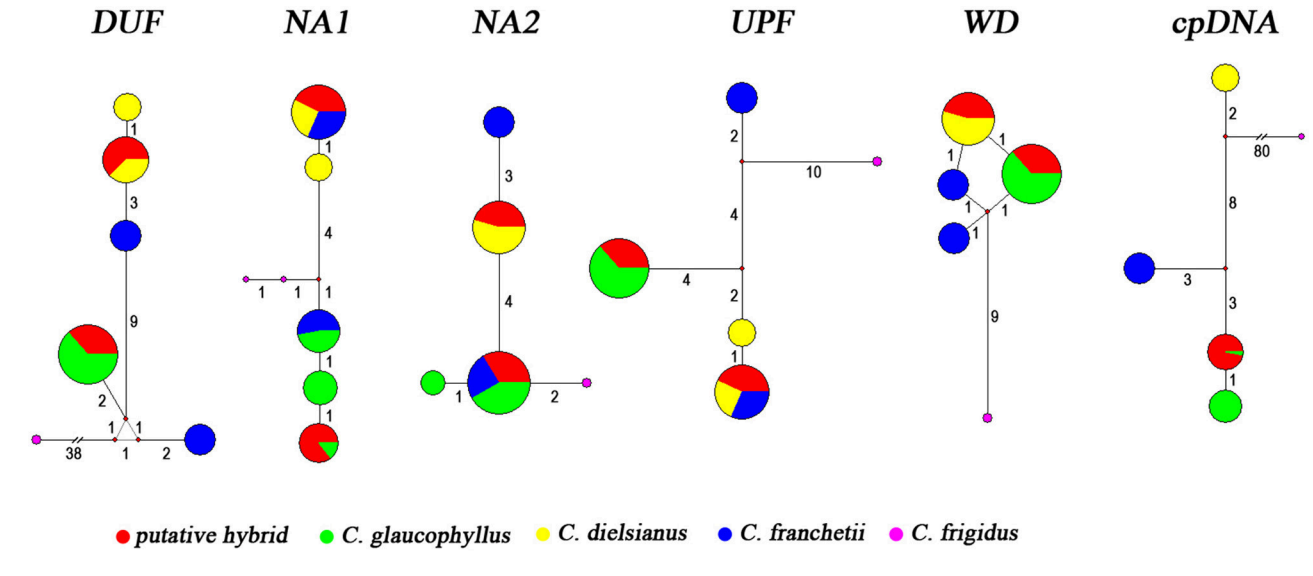

FIGURE 2 | Haplotype networks of five nuclear genes and six cpDNAs for putative hybrid, *C. dielsianus*, *C. glaucophyllus,* and *C. franchetii*. Mutation steps are shown by the length of the connecting lines.

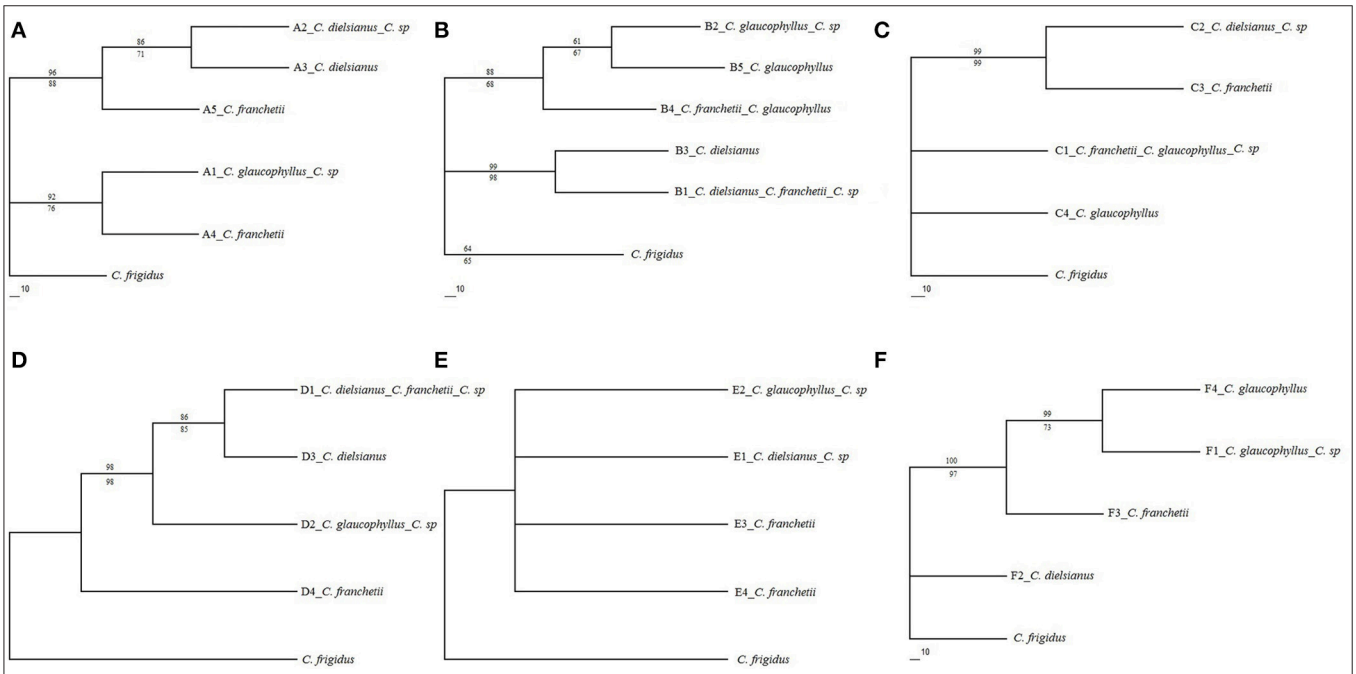

FIGURE 3 | Phylogenetic analyses of haplotype data for five nuclear genes (A–E) and six cpDNAs for the four taxa of *Cotoneaster* (**F**; *C.* sp represents putative hybrid), rooted with outgroup *C. frigidus*. Numbers above and below branches indicate maximum parsimony and maximum likelihood bootstrap values (>50%).

Sequence Analyses for the Combined Chloroplast Regions

The aligned length of the six concatenated chloroplast fragments in *C. dielsianus*, *C. glaucophyllus*, *C. franchetii* and the putative hybrid was 3,968 bp (**Table 3**). A total of 14 fixed nucleotide substitutions and three fixed indels were detected between *C. dielsianus* and *C. glaucophyllus*. No within-species polymorphism was detected in the putative hybrid, *C. dielsianus* or *C. franchetii* (**Figure 3**). *C. glaucophyllus* had two closely related haplotypes and in the tree, these two haplotypes were gathered together and well separated from *C. dielsianus* (**Figure 3**). All sequences of the putative hybrid were identical to those of *C. glaucophyllus*. For *C. franchetii*, the single haplotype was unique.

Ploidy of *C. dielsianus*, *C. glaucophyllus*, and Their Putative Hybrid

The ploidy of the putative hybrid, *C. dielsianus* and *C. glaucophyllus*, was obtained using four randomly selected individuals in each taxon. The average 2C-values/genome sizes are shown in **Table 1**. As Kroon (1975) reported, the examined seed stocks and chromosome numbers of 28 species in *Cotoneaster* were determined, including *C. dielsianus*, which has a chromosome count of $2n = 68$ (tetraploid). In addition, based on a previous study by Folta and Gardiner (2009), 2C-values and ploidies for *C. melanocarpa* were provided (2C-value = 2.24, tetraploid); these values are close to the 2C-values of *C. dielsianus* and the putative hybrid in our results (2.05 ± 0.126; 2.02 ± 0.023). The consistency of these data indicate that our results are credible and it was inferred that the putative hybrid and *C. dielsianus* were tetraploid. As the 2C-value of *C. glaucophyllus* was estimated to be 1.09 ± 0.034, it was inferred that *C. glaucophyllus* was diploid.

DISCUSSION

Molecular Identification of Natural Hybridization between *C. dielsianus* and *C. glaucophyllus*

The application of low-copy nuclear genes in combination with chloroplast regions has become an efficient way to validate hybridization events. Many hybrids have been proposed and validated, including *Melastoma* (Dai et al., 2012), *Acrostichum* (Zhang et al., 2013), *Eriobotrya* (Fan et al., 2014), and *Ilex* (Shi et al., 2016). In this study, we collected multiple individuals for each *Cotoneaster* species observed in the small confined area (southeastern Malipo, approximately 50 km^2). Five low-copy nuclear genes and six chloroplast regions were sequenced to validate the hybridization between *C. diesianus* and *C. glaucophyllus*.

Our molecular data support the hypothesis that *C. dielsianus* and *C. glaucophyllus* are two distantly related species, between which a total of 50 fixed nucleotide substitutions and four fixed indels were identified across 11 investigated genes. The putative hybrid was identified as chromatogram additivity between *C. dielsianus* and *C. glaucophyllus*, as observed for all the individuals of the putative hybrid. All hybrid individuals likely arose from an initial F1 individual and its derivatives via apomixis, since each individual harbored two haplotypes at each of the five nuclear genes that were matched with *C. dielsianus* and *C. glaucophyllus*. Further, based on the chloroplast sequence data, *C. glaucophyllus* obviously served as the maternal species for all investigated individuals of the hybrid.

C. franchetii did not participate in the formation of the hybrid, as most of its haplotypes at the nuclear level are unique (**Table 4**). Surprisingly, *C. franchetii* showed chromatogram additivity in many differentially fixed sites between *C. glaucophyllus* and *C. dielsianus*. Furthermore, it always possessed two haplotypes for each nuclear gene, and the genotypes of all five nuclear genes from all individuals were identical to each other. This evidence indicated that *C. franchetii* might also be a hybrid taxon and that all the individuals were F1s, yet neither *C. dielsianus* nor *C. glaucophyllus* could serve as its parent species, as *C. franchetii* harbored many unique haplotypes and one variable site that was not shared by *C. dielsianus* or *C. glaucophyllus*. However, its hybrid status and parentage are beyond the scope of this study. Further studies are needed to confirm its hybrid origin and parentage.

It is interesting that all the investigated individuals of the hybrid are F1s, with the same genotypes for all the nuclear genes, and that the hybrid samples detected are tetraploid. It is possible that natural hybridization between *C. glaucophyllus* and *C. dielsianus* could have produced many F1s, but that most disappeared quickly and only one tetraploid F1 individuals was successful and it produced many progeny through apomixis. This phenomenon would be in accord with previous studies showing that many apomictic taxa are of allopolyploid origin (Robertson et al., 2010; Sochor et al., 2015). *C. dielsianus* was mostly tetraploid, while *C. glaucophyllus* was mostly diploid, and thus the formation of the tetraploid hybrid may arise from the cross of a 2n gamete produced by through apomeiosis of *C. glaucophyllus* and the other 2n gamete produced from normal meiosis of *C. dielsianus*. This explains why the hybridization was unidirectional, as all of the hybrid individuals are apomictic progeny of a single individual, in which *C. glaucophyllus* serves as maternal species.

In addition, the combined chloroplast haplotype of the hybrid individuals was identical to the minor haplotype of *C. glaucophyllus* (H_A; only one individual has this haplotype). One explanation for this phenomenon is that hybridization between the two species is a very rare event. Another explanation is that F1 hybrids containing the H_A chloroplast haplotype may have some advantages for survival in the disturbed environment.

Factors Contributing to Natural Hybridization between *C. dielsianus* and *C. glaucophyllus*

C. dielsianus and *C. glaucophyllus* overlap significantly in geographic distribution (**Figure 4**) and share the same flowering periods from June to July, despite their distinct flower morphologies. The two species differ in petal color and shape, and may attract different pollinators: *C. dielsianus* displays red and erect petals which are more attractive to butterflies and moths,

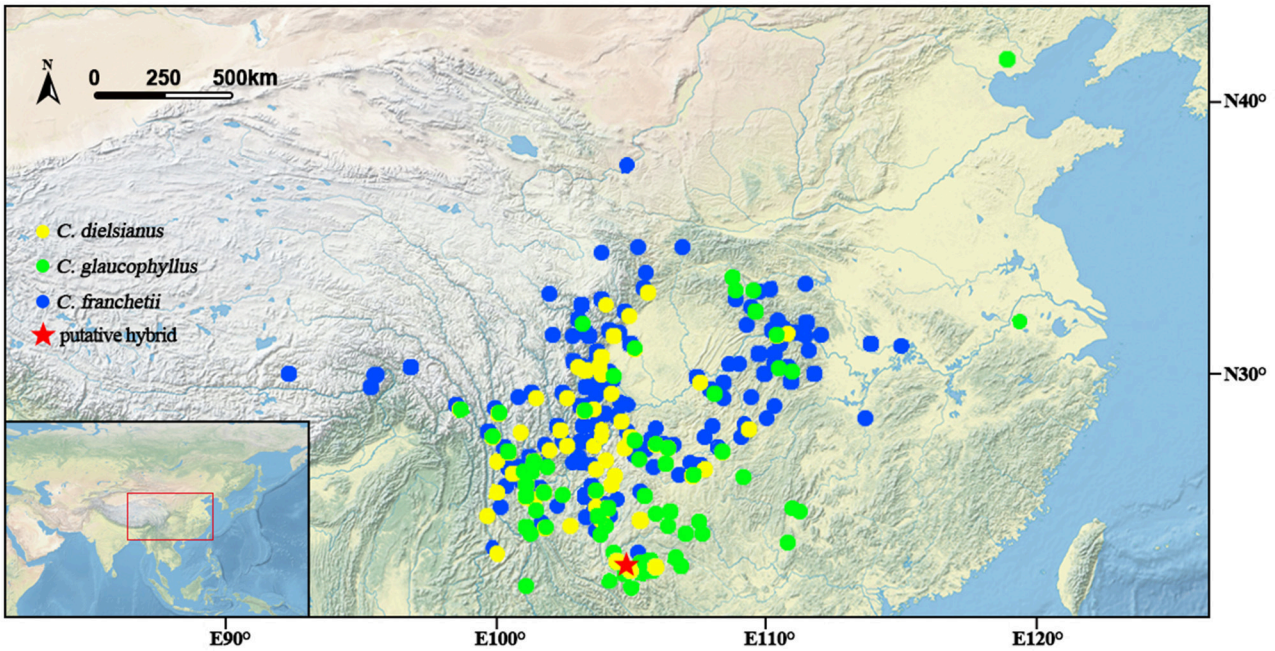

FIGURE 4 | Distribution of three taxa of *Cotoneaster* investigated around China according to the Chinese Virtual Herbarium database (CVH[1]) and location of the putative hybrid.

whereas *C. glaucophyllus* presents white, spreading petals that are preferable to bees and flies (Lovell, 1902). These phenomena were in agreement with our field observations. Furthermore, the two species prefer different habitats: *C. dielsianus* mainly occurs in sparse forests, while *C. glaucophyllus* is always found on cliffs and steep slope (personal observations; Lu and Brach, 2003).

In the study area of southeastern Malipo, which is close to the border with Vietnam, intensive agricultural development began in the 1950s and has resulted in widespread fragmentation of forests due to severe logging (Tang et al., 2011). The hybrid and three other *Cotoneaster* species were found in a deserted grass land where the primitive forest was destroyed approximately 50 years ago. However, in another location (Weixi county, Yunnan, China; 27.56° N, 99.03° E), both *C. dielsianus* and *C. glaucophyllus* were found on a rather steep slope with sparse forests. No hybrids were found. It appears that anthropogenic disturbances may be the major factor promoting hybridization between *C. dielsianus* and *C. glaucophyllus*, leading to mixing of previously distinct gene pools (Arnold, 1997). This provides an opportunity for the two species to contact each other. More importantly, it can create a new ecological niche in which the hybrid can establish its populations.

Consequences of Hybridization between *C. dielsianus* and *C. glaucophyllus*

In this study, all sampled hybrids could be produced through hybridization and subsequent apomixis, and no sign of backcross and introgression was detected between the hybrid and its parental species, based on the 11 investigated genes. It is very likely that this tetraploid hybrid may not be able to produce viable progeny through sexual reproduction in most cases. This also matched the common observation that genome doubling reduces or eliminates the possibility of new polyploid backcrossing with its parents (Soltis and Soltis, 2009). Therefore, genetic isolation can maintain the species integrity of *C. dielsianus* and *C. glaucophyllus* despite hybridization.

The distribution range of the new-born hybrid *C. dielsianus* × *C. glaucophyllus* is currently very limited. However, the distribution for allopolyploidy could also be very widespread. For example, for *C. franchetii*, we inferred another allopolyploidy whose individuals are widely distributed in China and other countries. Previous studies also showed that many invasive species exhibited allopolyploidy, such as *Spartina anglica*, *Viola riviniana* and *Rhododendron ponticum* (Ellstrand and Schierenbeck, 2000). Attentions should be focused on the future development of *C. dielsianus* × *C. glaucophyllus*, which may eventually threaten other *Cotonearster* species.

Conservation Implications

Hybridization, in combination with polyploidy and apomixes, has produced numerous novel phenotypes, leading to increasing numbers of species in Rosaceae. A key element for understanding these agamic complexes is the identification of diploid sexual taxa. These are the foundations of the complex (Bayer and Stebbins, 1987), and it is very important to pay attention to the diploid species whose current species status could be threatened by the increasing polyploidy number. However, the ploidy level

[1]CVH (2014). *Chinese Virtual Herbarium*. Available online: http://www.cvh.ac.cn/ (accessed on 10 May 2014).

of many species is still unknown in most genera of Rosaceae (Dickinson et al., 2007). In this study, dried leaves were used to estimate the ploidy level of these *Cotoneaster* species via flow cytometry, in which a large volume of cold lysis buffer was added to reduce the viscosity of the chopped tissue suspension before filtering (Talent and Dickinson, 2005). By comparison with the conventional method of chromoson counting, this technology appears to be more convenient and economical, especially when fresh tissue is not available, and will serve as a reference for the evaluation of the ploidy of other Roseaceae species.

SUMMARY

In this study, the sequence and haplotype analyses of five low-copy nuclear genes and six chloroplast regions, in combination with ploidy level analysis, provided convincing evidence for the hybridization of *C. dielsianus* (tetraploid) and *C. glaucophyllus* (diploid), in which all *C. dielsianus* × *C. glaucophyllus* individuals (allotetraploid) were identified as F1s and harbored identical sequences, indicating that they were produced via apomixis by a single F1 individual. We have shown that hybridization, polyploidy and apomixis lead to astonishing complexities in Roseaceae. Our study also provides a reliable way to screen and validate hybridization events occurring in this family. The five low-copy nuclear genes and the screening method may also be useful in these studies.

AUTHOR CONTRIBUTIONS

ML analyzed data and wrote the paper, QF and SC designed the research, and RZ, FL, and WL revised the paper. All authors approved this manuscript for publication.

ACKNOWLEDGMENTS

This study was supported by the National Natural Science Foundation of China (NSFC, No. 31570195, No. 31400192, No. 31670189), the Chang Hongda Scientific Research Fund of Sun Yat-sen University, and Basic Work Special Project of the National Ministry of Science and Technology of China (2013FY111500). ML was awarded a scholarship from 2015 to 2016 by the China Scholarship Council as a visiting scholar in the Soltis lab of the University of Florida.

SUPPLEMENTARY MATERIAL

The Supplementary Material for this article can be found online at: http://journal.frontiersin.org/article/10.3389/fpls.2017.00704/full#supplementary-material

REFERENCES

Abbott, R. J., and Lowe, A. J. (2004). Origins, establishment and evolution of new polyploid species: *Senecio cambrensis* and *S. eboracensis* in the British Isles. *Biol. J. Linn. Soc.* 82, 467–474. doi: 10.1111/j.1095-8312.2004.00333.x

Ainouche, M. L., Baumel, A., Salmon, A., and Yannic, G. (2003). Hybridization, polyploidy and speciation in *Spartina* (Poaceae). *New Phytol.* 161, 165–172. doi: 10.1046/j.1469-8137.2003.00926.x

Arnold, M. L. (1997). *Natural Hybridization and Evolution*. NewYork, NY: Oxford University Press.

Asker, S., and Jerling, L. (1992). *Apomixis in Plants*. Boca Raton, FL: CRC Press.

Bandelt, H. J., Forster, P., and Röhl, A. (1999). Median-joining networks for inferring intraspecific phylogenies. *Mol. Biol. Evol.* 16, 37–48. doi: 10.1093/oxfordjournals.molbev.a026036

Bartish, I. V., Hylmö, B., and Nybom, H. (2001). RAPD analysis of interspecific relationships in presumably apomictic *Cotoneaster* species. *Euphytica* 120, 273–280. doi: 10.1023/A:1017585600386

Bayer, R. J., and Stebbins, G. L. (1987). Chromosome numbers, patterns of distribution, and apomixis in *Antennaria* (Asteraceae: Inuleae). *Syst. Bot.* 12, 305–319. doi: 10.2307/2419326

Campbell, C. S., Evans, R. C., Morgan, D. R., Dickinson, T. A., and Arsenault, M. P. (2007). Phylogeny of subtribe Pyrinae (formerly the Maloideae, Rosaceae): limited resolution of a complex evolutionary history. *Plant Syst. Evol.* 266, 119–145. doi: 10.1007/s00606-007-0545-y

Comai, L. (2005). The advantages and disadvantages of being polyploid. *Nat. Rev. Genet.* 6, 836–846. doi: 10.1038/nrg1711

Comai, L., Madlung, A., Josefsson, C., and Tyagi, A. (2003). Do the different parental 'heteromes' cause genomic shock in newly formed allopolyploids? *Philos. Trans. R. Soc. B Biol. Sci.* 358, 1149–1155. doi: 10.1098/rstb.200 3.1305

Dai, S., Wu, W., Zhang, R., Liu, T., Chen, Y., Shi, S., et al. (2012). Molecular evidence for hybrid origin of *Melastoma intermedium*. *Biochem. Syst. Ecol.* 41, 136–141. doi: 10.1016/j.bse.2011.12.010

Dickinson, T. A., Lo, E., and Talent, N. (2007). Polyploidy, reproductive biology, and Rosaceae: understanding evolution and making classifications. *Plant Syst. Evol.* 266, 59–78. doi: 10.1007/s00606-007-0541-2

Dickoré, W. B., and Kasperek, G. (2010). Species of *Cotoneaster* (Rosaceae, Maloideae) indigenous to, naturalising or commonly cultivated in Central Europe. *Willdenowia* 40, 13–45. doi: 10.3372/wi.40.40102

Doyle, J. J., and Doyle, J. L. (1987). A rapid DNA isolation procedure for small quantities of fresh leaf tissue. *Phytochem. Bull.* 19, 11–15.

Duarte, J. M., Wall, P. K., Edger, P. P., Landherr, L. L., Ma, H., Pires, P. K., et al. (2010). Identification of shared single copy nuclear genes in *Arabidopsis*, *Populus*, *Vitis* and *Oryza* and their phylogenetic utility across various taxonomic levels. *BMC Evol. Biol.* 10:61. doi: 10.1186/1471-2148-10-61

Ellstrand, N. C., and Schierenbeck, K. A. (2000). Hybridization as a stimulus for the evolution of invasiveness in plants? *Proc. Natl. Acad. Sci. U.S.A.* 97, 7043–7050. doi: 10.1073/pnas.97.13.7043

Fan, Q., Chen, S., Li, M., Guo, W., Jing, H., Wu, W., et al. (2014). Molecular evidence for natural hybridization between wild loquat (*Eriobotrya japonica*) and its relative *E. prinoides*. *BMC Plant Biol.* 14:275. doi: 10.1186/s12870-014-0275-6

Feldman, M., and Levy, A. A. (2005). Allopolyploidy–a shaping force in the evolution of wheat genomes. *Cytogenet. Genome Res.* 109, 250–258. doi: 10.1159/000082407

Flinck, K. E., and Hylmö, B. (1966). A list of series and species in the genus *Cotoneaster*. *Bot. Notiser* 119, 445–463.

Folta, K. M., and Gardiner, S. E. (2009). *Genetics and Genomics of Rosaceae*. New York, NY: Springer.

Fryer, J., and Hylmö, B. (2009). *Cotoneasters: A Comprehensive Guide to Shrubs for Flowers, Fruit, and Foliage*. Portland; London: Timber Press.

Hanson, L., Boyd, A., Johnson, M. A., and Bennett, M. D. (2005). First nuclear DNA C-values for 18 eudicot families. *Ann. Bot.* 96, 1315–1320. doi: 10.1093/aob/mci283

Hörandl, E. (2006). The complex causality of geographical parthenogenesis. *New Phytol.* 171, 525–538. doi: 10.1111/j.1469-8137.2006.01769.x

Kroon, G. H. (1975). Polyploidy in cotoneaster II. *Acta Bot. Neerland.* 24, 417–420. doi: 10.1111/j.1438-8677.1975.tb01032.x

Li, F., Fan, Q., Li, Q., Chen, S., Guo, W., Cui, D., et al. (2014). Molecular phylogeny of *Cotoneaster* (Rosaceae) inferred from nuclear ITS and multiple chloroplast sequences. *Plant Syst. Evol.* 300, 1533–1546. doi: 10.1007/s00606-014-0980-5

Librado, P., and Rozas, J. (2009). DnaSP v5: a software for comprehensive analysis of DNA polymorphism data. *Bioinformatics* 25, 1451–1452. doi: 10.1093/bioinformatics/btp187

Lo, E. Y., and Donoghue, M. J. (2012). Expanded phylogenetic and dating analyses of the apples and their relatives (Pyreae, Rosaceae). *Mol. Phylogenet. Evol.* 63, 230–243. doi: 10.1016/j.ympev.2011.10.005

Lo, E. Y., Stefanovic, S., and Dickinson, T. A. (2009). Population genetic structure of diploid sexual and polyploid apomictic hawthorns (*Crataegus*; Rosaceae) in the Pacific Northwest. *Mol. Ecol.* 18, 1145–1160. doi: 10.1111/j.1365-294X.2009.04091.x

Lovell, J. H. (1902). The colors of Northern polypetalous flowers. *Am. Nat.* 36, 203–242. doi: 10.1086/278101

Lu, L., and Brach, A. R. (2003). "Cotoneaster," in *Flora of China* 9, eds Z. Y. Wu, P. H. Raven, and D. Y Hong (Beijing: Science Press and St. Louis; Missouri Botanical Garden Press), 85–108.

Ludwig, S., Robertson, A., Rich, T. C., Djordjević, M., Cerović, R., Houston, L., et al. (2013). Breeding systems, hybridization and continuing evolution in Avon Gorge *Sorbus*. *Ann. Bot.* 111, 563–575. doi: 10.1093/aob/mct013

Morgan, D. R., Soltis, D. E., and Robertson, K. R. (1994). Systematic and evolutionary implications of rbcL sequence variation in Rosaceae. *Am. J. Bot.* 81, 890–903. doi: 10.2307/2445770

Nybom, H., and Bartish, I. V. (2007). DNA markers and morphometry reveal multiclonal and poorly defined taxa in an apomictic *Cotoneaster* species complex. *Taxon* 56, 119–128. Available online at: http://www.jstor.org/stable/25065742

Paun, O., Stuessy, T. F., and Hörandl, E. (2006). The role of hybridization, polyploidization and glaciation in the origin and evolution of the apomictic *Ranunculus cassubicus* complex. *New Phytol.* 171, 223–236. doi: 10.1111/j.1469-8137.2006.01738.x

Phipps, J. B., Robertson, K. R., Smith, P. G., and Rohrer, J. R. (1990). A checklist of the subfamily Maloideae (Rosaceae). *Can. J. Bot.* 68, 2209–2269. doi: 10.1139/b90-288

Posada, D., and Buckley, T. (2004). Model selection and model averaging in phylogenetics: advantages of akaike information criterion and bayesian approaches over likelihood ratio tests. *Syst. Biol.* 53, 793–808. doi: 10.1080/10635150490522304

Rehder, A. (1927). *Manual of Cultivated Trees and Shrubs*. New York, NY: Macmillan Co.

Rieseberg, L. H., and Willis, J. H. (2007). Plant speciation. *Science* 317, 910–914. doi: 10.1126/science.1137729

Roberts, A. V., Gladis, T., and Brumme, H. (2009). DNA amounts of roses (*Rosa,* L.) and their use in attributing ploidy levels. *Plant Cell Rep.* 28, 61–71. doi: 10.1007/s00299-008-0615-9

Robertson, A., Rich, T. C., Allen, A. M., Houston, L., Roberts, C., Bridle, J. R., et al. (2010). Hybridization and polyploidy as drivers of continuing evolution and speciation in *Sorbus*. *Mol. Ecol.* 19, 1675–1690. doi: 10.1111/j.1365-294X.2010.04585.x

Shi, L., Li, N., Wang, S., Zhou, Y., Huang, W., Yang, Y., et al. (2016). Molecular evidence for the hybrid origin of *Ilex dabieshanensis* (Aquifoliaceae). *PLoS ONE* 11:e0147825. doi: 10.1371/journal.pone.0147825

Sochor, M., Vašut, R. J., Sharbel, T. F., and Trávnícek, B. (2015). How just a few makes a lot: speciation via reticulation and apomixis on example of European brambles (Rubus subgen. Rubus, Rosaceae). *Mol. Phylogenet Evol.* 89, 13–27. doi: 10.1016/j.ympev.2015.04.007

Soltis, P. S., and Soltis, D. E. (2009). The role of hybridization in plant speciation. *Annu. Rev. Plant Biol.* 60, 561–588. doi: 10.1146/annurev.arplant.043008.092039

Soltis, D. E., Soltis, P. S., Pires, J. C., Kovarik, A., Tate, J. A., and Mavrodiev, E. (2004). Recent and recurrent polyploidy in *Tragopogon* (Asteraceae): cytogenetic, genomic and genetic comparisons. *Biol. J. Linn. Soc.* 82, 485–501. doi: 10.1111/j.1095-8312.2004.00335.x

Soltis, P. S., Liu, X., Marchant, D. B., Visger, C. J., and Soltis, D. E. (2014). Polyploidy and novelty: gottlieb's legacy. *Phil. Trans. R. Soc. B* 369:20130351. doi: 10.1098/rstb.2013.0351

Swofford, D. L. (2001). *Paup*. Phylogenetic Analysis using Parsimony (*And other Methods)*. Version 4. Sunderland, MA: Sinauer Associates.

Talent, N., and Dickinson, T. A. (2005). Polyploidy in *Crataegus* and *Mespilus* (Rosaceae, Maloideae): evolutionary inferences from flow cytometry of nuclear DNA amounts. *Botany* 83, 1268–1304. doi: 10.1139/b05-088

Tang, C. Q., He, L.-Y., Gao, Z., Zhao, X.-F., Sun, W.-B., and Ohsawa, M. (2011). Habitat fragmentation, degradation, and population status of endangered *Michelia coriacea* in southeastern Yunnan, China. *Mt. Res. Dev.* 31, 343–350. doi: 10.1659/MRD-JOURNAL-D-11-00004.1

Urbanska, K. M., Hurka, H., Landolt, E., Neuffer, B., and Mummenhoff, K. (1997). Hybridization and evolution in *Cardamine* (Brassicaceae) at Urnerboden, Central Switzerland: biosystematic and molecular evidence. *Plant Syst. Evol.* 204, 233–256. doi: 10.1007/BF00989208

Van der Hulst, R. G. M., Mes, T. H. M., Den Nijs, J. C. M., and Bachmann, K. (2000). Amplified fragment length polymorphism (AFLP) markers reveal that population structure of triploid dandelions (*Taraxacum officinale*) exhibits both clonality and recombination. *Mol. Ecol.* 9, 1–8. doi: 10.1046/j.1365-294x.2000.00704.x

Wagner W. H. Jr., and Wagner, F. S. (1980). "Polyploidy in pteridophytes," in *Polyploidy: Biological Relevance*, ed W. H. Lewis (New York, NY: Plenum), 199–214.

Whittall, J., Liston, A., Gisler, S., and Meinke, A. R. (2000). Detecting nucleotide additivity from direct sequences is a SNAP: an example from *Sidalcea* (Malvaceae). *Plant Biol.* 2, 211–217. doi: 10.1055/s-2000-9106

Winge, O. (1917). The chromosomes. Their numbers and general importance. *Carlsberg. Lab. Copenhagen C.R. Trav.* 13, 131–175.

Yokoya, K., Roberts, A. V., Mottley, J., Lewis, R., and Brandham, P. E. (2000). Nuclear DNA amounts in roses. *Ann. Bot.* 85, 557–561. doi: 10.1006/anbo.1999.1102

Zhang, R., Liu, T., Wu, W., Li, Y., Chao, L., Huang, L., et al. (2013). Molecular evidence for natural hybridization in the mangrove fern genus *Acrostichum*. *BMC Plant Biol.* 13:74. doi: 10.1186/1471-2229-13-74

Conflict of Interest Statement: The authors declare that the research was conducted in the absence of any commercial or financial relationships that could be construed as a potential conflict of interest.

frontiers in Plant Science

ORIGINAL RESEARCH
published: 21 April 2017
doi: 10.3389/fpls.2017.00541

Sugar Treatments Can Induce *AcLEAFY COTYLEDON1* Expression and Trigger the Accumulation of Storage Products during Prothallus Development of *Adiantum capillus-veneris*

Yu-Han Fang[1], Xia Li[2], Shu-Nong Bai[1] and Guang-Yuan Rao[1]*

[1] College of Life Sciences, Peking University, Beijing, China, [2] RDFZ XiShan School, Beijing, China

OPEN ACCESS

Edited by:
Zhong-Jian Liu,
The National Orchid Conservation Center of China, The Orchid Conservation and Research Center of Shenzhen, China

Reviewed by:
Yin-Zheng Wang,
Institute of Botany (CAS), China
Ji Yang,
Fudan University, China

***Correspondence:**
Shu-Nong Bai
shunongb@pku.edu.cn

Specialty section:
This article was submitted to Plant Evolution and Development, a section of the journal Frontiers in Plant Science

Received: *26 January 2017*
Accepted: *27 March 2017*
Published: *21 April 2017*

Citation:
Fang Y-H, Li X, Bai S-N and Rao G-Y (2017) Sugar Treatments Can Induce AcLEAFY COTYLEDON1 Expression and Trigger the Accumulation of Storage Products during Prothallus Development of Adiantum capillus-veneris. Front. Plant Sci. 8:541. doi: 10.3389/fpls.2017.00541

A seed is an intricate structure. Of the two development processes involved in seed formation, seed maturation, or seed program includes accumulation of storage products, acquisition of desiccation tolerance, and induction of dormancy. Little is known about how these processes were originated and integrated into the life cycle of seed plants. While previous investigation on seed origin was almost exclusively through fossil comparison in paleobotany, a wealth of information about the key role of *LEAFY COTYLEDON1* (*LEC1*) in seed formation of spermatophyte inspired a new approach to investigating the seed origin mystery. Here, we examined the expression pattern of *AcLEC1* during the entire life cycle of *Adiantum capillus-veneris*, a non-seed plant, confirmed no *AcLEC1* gene expression detectable in prothalli, demonstrated inductive expressed by both sucrose and glucose in prothalli. As expected, we found that sugar treatments delayed prothallus development, promoted differentiation of reproductive organs, and triggered accumulation of storage products. These findings demonstrated links between the sugar treatments and the induction of *AcLEC1* expression, as well as the sugar treatments and the events such as accumulation of storage products, which is similar to those considered as seed maturation process in seed plants. These links support a modified hypothesis that inductive expression of *LEC1* homologs during embryogenesis might be a key innovation for the origin of the seed program.

Keywords: ***Adiantum capillus-veneris*, *LEAFY COTYLEDON1*, seed maturation process, sugar treatments, prothallus development**

INTRODUCTION

The seed habit represents the most successful innovation in land plant sexual reproduction (Linkies et al., 2010). It not only contributes to the remarkable prosperity of spermatophytes, but also serves as essential food for humans (Kenrick and Crane, 1997; Becker and Marin, 2009; Radoeva and Weijers, 2014). The seed is an intricate structure comprising of an early embryo derived from a zygote, the seed coat derived from integuments, and extraembryonic tissues.

Two developmental processes are involved in the seed formation: one is morphogenesis, through which, cells derived from zygote division are organized as a particular structure called embryo which will further elaborates into sporophyte (Goldberg et al., 1994; Harada, 1997; Gutierrez et al., 2007). Another is called seed maturation or seed program, of which, three physiological and biochemical processes are included, i.e., accumulation of storage products, acquisition of desiccation tolerance, and induction of dormancy (Harada, 1997; Sreenivasulu and Wobus, 2013). While all land plants are embryophyta, i.e., plants with embryos, the seed maturation is unique for spermatophytes (Goldberg et al., 1994; Harada, 1997; Vicente-Carbajosa and Carbonero, 2005). This process generally starts from heart stage embryo, superposing over the embryogenesis, and ends as a mature seed in which the morphogenesis of the embryo was repressed (Harada, 1997). When a favorable environment comes, the dormancy is broken, the reserves are consumed and morphogenesis of the embryo resumes. It is generally considered that the seed maturation enables embryos of spermatophytes to better endure harsh environments and get more chances of dispersal, and therefore benefits the prosperity of seed-bearing plants on land territory (Becker and Marin, 2009; Pires and Dolan, 2012). However, little is known about how such a process is originated and integrated into the life cycle of seed plants.

Previous studies on seed origin was almost exclusively through fossil comparison in paleobotany (Taylor and Taylor, 1993; Niklas, 1997; Doyle, 2006). However, identification of an *Arabidopsis* mutant *leafy cotyledon 1* (*lec1*) opened up a window to peer the secret of seed origin (Meinke, 1992). While the function of *LEAFY COTYLEDON1* (*LEC1*) gene was first considered as taking responsible for homeotic transition from cotyledons to true leaves (Meinke, 1992), later investigations indicated it serving as a master regulator that coordinates many facets of seed maturation (Meinke et al., 1994; West et al., 1994).

LEC1 gene encodes a LEC1-type *HAP3* subunit of the CCAAT-binding transcription factor. Overexpression of *LEC1* leads to suppression of shoot development regeneration and induction of somatic embryos (Lotan et al., 1998; Casson and Lindsey, 2006; Junker et al., 2012). Moreover, LEC1 protein is required for proper expression of genes involved in seed maturation (Kwong et al., 2003; Lee et al., 2003; Braybrook and Harada, 2008). According to Harada (1997), the seed maturation is an intrusive process into embryogenesis. If it was the case, the master regulator *LEC1* gene should be an ideal subject to test a hypothesis that seed maturation process should be emerged along with the origin of *LEC1*.

Yang et al. (2005) and Xie et al. (2008) have conducted systematic analysis of *LEC1* related *HAP3* genes among a wide range of species covering green algae, bryophytes, pteridophytes, and spermatophytes. They found that these genes could be classified into LEC1-type and non-LEC1-type. While LEC1-type *HAP3* gene exists in all spermatophytes but not in green algae and bryophytes as anticipated, it was unexpected that such genes were identified in pteridophytes, including lycophytes *Selaginella sinensis* and *Selaginella davidii*, as well as fern *Adiantum capillus-veneris* (Xie et al., 2008; Kirkbride et al., 2013). The LEC1-type *HAP3 SsLEC1, SdLEC1,* and *AcLEC1* can complement the *lec1* mutant phenotype of *Arabidopsis* and expressed upon drought and ABA stress (Xie et al., 2008). These findings suggest that pteridophytes LEC1-type *HAP3* genes are not pseudo- but functional genes. Although no LEC1-type *HAP3* gene found in green algae and bryophytes supports the hypothesis that seed maturation process is emerged along with the origin of *LEC1* gene, existence of functional LEC1-type *HAP3* genes in pteridophytes is contradict to the hypothesis.

Parallel to the above mentioned gene sequence and function analysis, Li et al. (2013) have developed *A. capillus-veneris* as an experimental system. They not only systematically described the morphological process of this plant (Li et al., 2013), but established a culture system for shoot regeneration (Li et al., 2017). In the assay of gene expression during shoot regeneration from sporophyte tissue, they found that expression of *AcLEC1* was not only induced by stresses such as drought and ABA (Xie et al., 2008), but also by cultural conditions (Li et al., 2017). These observations sparked a modified hypothesis about the relationship between the origin of the seed maturation process and the *LEC1* gene: LEC1-type *HAP3* genes may origin for other functions, as it was induced upon stresses. However, if this gene expression was induced during embryogenesis, it may be endowed a novel function to be a master regulator for a seed maturation process.

The best way to test the hypothesis is to ectopically express *LEC1* gene during embryogenesis or archegonia development in pteridophytes to examine if the *LEC1* gene can trigger the seed maturation process, i.e., accumulation of storage products, acquisition of desiccation tolerance, and induction of dormancy (Harada, 1997). Unfortunately, gene transformation system of *A. capillus-veneris* has not yet been established. However, the induction of *AcLEC1* expression during tissue culture of sporophyte (Li et al., 2017) suggests that other approach can be used to test the hypothesis. While the prothalli cannot tolerant drought or ABA treatment, sugar might be the best candidate as an inducer of *AcLEC1* expression. The rationale of using sugar to induce *AcLEC1* expression during archegonia development underlies not only that the sugar is an important component in tissue culture in the MS media, but also the reports that sugar exerts its effect through induction of *LEC1* gene expression during drought response (Gupta and Kaur, 2005; Eveland and Jackson, 2012; Poonam et al., 2016) and more specifically affects genes involved in seed maturation including *LEC1* (Tsukagoshi et al., 2007).

Here, we firstly examined the expression pattern of *AcLEC1* during the entire life cycle of *A. capillus-veneris* and confirmed that no *AcLEC1* gene expression was detectable in prothallus. Afterward, we demonstrated that *AcLEC1* expression can be induced by both sucrose and glucose. Finally, as expected, we found that sugar treatments delayed prothallus development, promoted differentiation of reproduction organs, triggered accumulation of storage products. These findings demonstrated links between the sugar treatments and the induction of *AcLEC1* expression, as well as the sugar treatments and the events such as accumulation of storage products, which is similar to those considered as seed maturation process in seed plants. These links are supportive to the above mentioned modified hypothesis

about the role of *LEC1* gene in origin of seed maturation process.

MATERIALS AND METHODS

Plant Growth and Cultivation Conditions

Adult *A. capillus-veneris* plants were cultivated in greenhouses at Peking University (Beijing, China). Spores were collected and cultivated into cordate prothalli in sugar-free Knop's agar medium as described (Li et al., 2013). For the sugar treatment, cordate prothalli were picked up with sterile hypodermic needles under anatomical lens and placed on Knop's agar medium containing various sugar concentrations. When both antheridia and archegonia appeared, prothalli were sprinkled with sterile water to create appropriate conditions for fertilization. All prothallus cultivation experiments were conducted in a clean bench.

Quantitative Reverse Transcription-PCR

Total RNA from all samples was extracted with the PureLink^{TM} Plant RNA Reagent (Invitrogen, Carlsbad, CA, USA) according to the manufacturer's protocol. The total RNA samples were then treated with RQ1 RNase-Free DNase (Promega, Madison, WI, USA) to remove DNA contaminants. Each sample was reverse-transcribed into cDNA using the SuperScript First-Strand System for RT-PCR (Invitrogen, Carlsbad, CA, USA) following the manufacturer's protocol. The quality of the RNA and cDNA was assessed by agarose gel electrophoresis. The RNA concentration was determined using a NanoDrop ND 1000 Spectrophotometer (Nano-Drop, Wilmington, DE, USA). qRT-PCR was performed with a 7500 Real-Time PCR System (Applied Biosystems, USA). The amplification reaction was carried out in a total volume of 20 μL, with 0.5 μL of each primer (10 μM), 1 μL of cDNA, 10 μL of Power SYBR Green I Master Mix kit (Bio-Rad, Hercules, CA, USA), and 8 μL RNase-free water. The PCR program was as follows: denaturing at 95°C for 10 min, followed by 40 two-step cycles (95°C for 15 s and 60°C for 64 s) and a final extension at 72°C for 5 min. Relative quantification of each gene was performed using the comparative threshold cycle method as described by Livak and Schmittgen (2001). It is reported that *AcCRYPTOCHROME GENE 2* (*AcCRY2*) stayed at the same level through the haploid and diploid phases (Imaizumi et al., 2000), thus we used *AcCRY2* as the internal control. Each sample was quantified at least in triplicate. The primer sets for each gene are listed in Supplementary Table 1.

In situ Hybridization

Prothalli and pinnae at various stages were fixed in 4% paraformaldehyde (PFA) overnight at 4°C. After fixation, tissue samples were washed, dehydrated, and embedded in wax for sectioning and *in situ* hybridization as described by Zhang et al. (2013). *AcLEC1*-specific regions were amplified with primer sets 5′-GAAGATAGCAGATGATGCCAAGG-3′ and 5′-ATGAATCCCCCCGATACTACTAA-3′ and transcribed *in vitro* as probes using the Digoxigenin RNA labeling kit (Roche, Mannhein, Germany).

Transient Sugar Treatment

Based on a report of sugar-dependent *LEC1* expression in *A. thaliana* (Tsukagoshi et al., 2007), *A. capillus-veneris* prothalli were treated transiently with sucrose or glucose. Cordate prothalli were immersed in buffer containing 30 g/L glucose for 30 min. Sugar-free buffer served as control. After rinsing in water, the treated cordate prothalli were transferred to a sugar-free medium. Prothalli were harvested 30 min, 1, 2 h, 1, 2, and 6 days after treatment followed by qRT-PCR to determine *AcLEC1* expression levels.

Persist Sugar Treatment

Under sterile conditions, cordate prothalli growing on sugar-free medium were picked and transferred to medium containing 30 g/L glucose or 30 g/L sucrose. Sugar-free medium served as the control treatment. Prothalli were harvested 5, 10, 15, 20, and 25 days after transfer (DAT) for examination of *AcLEC1* gene expression by qRT-PCR.

SEM Observation

The dissected samples were dehydrated, followed by submersion in a series of gradient alcohol-isoamyl acetate solutions as described previously (Li et al., 2013). Subsequently, the samples were dried by critical-point drying in CO_2 (Hitachi HCP-2) for 6 h, mounted, and sputter-coated with gold/palladium (Hitachi E-1010). All samples were viewed under a Hitachi S-4800 SEM at 10.0 kV.

Density and Size of Antheridia and Archegonia Analysis

Fertilized prothalli with apparently swollen archegonia were selected as samples. This method ensured that every prothallus sample was under similar developmental stage. For each treatment group, five fertilized prothalli were selected as samples and were observed under SEM. For each sample, three 25-mm^2 area were randomly picked, in which the number of antheridia and archegonia were counted and the density was calculated. The diameter of mature archegonia or antheridia on the prothallus was measured by taking plotting scale as reference.

Cytochemical Stain Assay

The control and sugar-treated prothalli were harvested 10, 20, and 30 DAT, dehydrated in a series of ethanol solutions, followed by exposure to a series of alcohol-acetone solutions as describe (Li et al., 2013). Next, the tissue samples were exposed to a series of acetone-Spurr's resin solutions (acetone:resin ratio: 2:1, 1:1, 1:2, 0:1, 0:1, and 0:1), which were replaced every 8 h. Finally, the samples were embedded in Spurr's resin. Sections (3 μm thick) were cut using a microtome (Leitz 1512, Germany) as described previously (Hu and Xu, 1990; Li et al., 2013). The periodic acid-Schiff (PAS) staining, Sudan black B staining, and Coomassie brilliant blue staining were chosen to label polysaccharides, lipids, and protein bodies, respectively, as described by Hu and Xu (1990). Images were captured with a light microscope (Zeiss Axioskop 2 Plus, Germany) using Axioplan software.

A. capillus-veneris Storage Products Accumulation Related Gene Identification

In *Arabidopsis*, 184 seed-specific genes, excluding 30 genes that encode transcription factors, are known to be involved in storage products accumulation (Le et al., 2010). We screened the datasets of seed-specific genes (Mu et al., 2008; Le et al., 2010) and selected the genes involved in storage products accumulation by gene annotation. After gaining the gene candidates, we screened the *A. capillus-veneris* expressed sequence tags (ESTs) database by BLAST to find out the high identities ESTs of *A. capillus-veneris*. The genes with identities higher than 50% were considered to be storage products accumulation related genes in *A. capillus-veneris*. The three high identities genes were listed in Supplementary Table 2.

RESULTS

Standardization of Developmental Stages of *A. capillus-veneris*

Previously, Li et al. (2013) have described the entire life cycle of *A. capillus-veneris* under cultivate conditions on the duration and morphogenetic characteristics. To clarify the expression pattern of *AcLEC1* during the life cycle of *A. capillus-veneris,* it is necessary to further divide the life cycle into development stages with distinguishable morphological characteristics for unambiguous sample collection. Based on the morphogenetic features, we divided the life cycle of *A. capillus-veneris* into 11 stages (**Figure 1**).

It needs to be mentioned that the above dividing system for developmental stages was mainly designed for the convenience of clarifying the expression pattern of *AcLEC1*. In general, it is more reasonable to set the zygote as a start point to describe a life cycle (Bai, 1999, 2015a,b, 2016, 2017). However, for the convenience of experimental operation, here we used spores as a start point. It should be better to adjust the start point into zygote if it becomes more accessible along with technology development. Another pragmatic consideration is that the above dividing system did not further divide prothallus into more stages although several morphologically distinguishable stages can be easily identified, such as club-shaped, early heart-shaped and so on (Li et al., 2013). Such a simplification mainly because of the growth condition for these stages are similar in terms of their effects on *AcLEC1* expression.

AcLEC1 Is Expressed in the Aerial Tissues of *A. capillus-veneris*

To test the hypothesis that the specific spatiotemporal pattern of LEC1-type *HAP3* gene expression is critical for proper execution of the seed maturation process, we examined the expression pattern of *AcLEC1* in *A. capillus-veneris*. Samples of 10 stages during the entire life cycle and stem were collected according to **Figure 1**. Quantitative reverse transcription-PCR (qRT-PCR) was employed to determine *AcLEC1* expression levels. **Figure 2A** shows that *AcLEC1* mRNA was rarely detectable in the prothallus samples and 1-leaf-sporophyte samples. In contrast, *AcLEC1* mRNA was detected at various levels in the stem and pinna at various stages. The highest expression level was detected in the sample of phase 3 pinna where sporangia forms (**Figures 1**, **2A**). Such expression pattern is consistent to previous finding that *LEC1* genes are expressed in aerial tissues and at high level in sporangia (Kirkbride et al., 2013).

To further examine the preference of *AcLEC1* expression in difference tissues, *in situ* hybridization was carried out. Signal of *AcLEC1* mRNA was detected from juvenile to phase 3 pinna (**Figures 2B–F**). Consistent to the highest expression level detected with qRT-PCR, the *in situ* hybridization confirmed the highest signals in phase 3 pinna (**Figures 2E,F**). It is interesting that no *AcLEC1* mRNA is detected after spore release in phase 4 pinna (**Figures 2A,G**).

AcLEC1 Expression Is Sugar-inducible during Prothallus Development

The above data demonstrated that under normal growth conditions, there is no *AcLEC1* expression in prothallus development (**Figure 2A**). Therefore, we can use prothalli to examine whether sugar can induce *AcLEC1* expression.

In our pilot experiments, we found 20 and 30 g/L sugar can induce *AcLEC1* expression but 50 g/L can inhibit prothalli growth. So we used concentration of 30 g/L as a treatment. Firstly, we examined whether the *AcLEC1* expression can be transiently induced. **Figure 3A** shows that *AcLEC1* expression can be induced upon 30 min treatment, higher than the control. Such expression is dependent on existence of the sugar (Glucose here), as the expression decrease upon withdraw of the sugar.

To observe the effects of sugar treatments on prothallus development, we further examined the *AcLEC1* expression in prothallus development under continuous sugar-medium culture. Considering the developmental process from spore germination to cordate prothallus taking 20 days and from cordate prothallus to fertilization taking about 25 days (Li et al., 2013), here we examined *AcLEC1* expression every 5 days starting from the cordate prothallus culture. **Figure 3B** shows that *AcLEC1* gene expression was significantly induced after 10-days culture on the sugar media, both sucrose and glucose. Interestingly the expression level on sucrose medium showed one peak at 15-days, but that on glucose medium showed two peaks, one at 10-days culture and another at 20-days culture.

To verify the *AcLEC1* expression during prothallus development, *in situ* hybridization was carried out. Strong signals of *AcLEC1* probe were detected in prothalli, especially in archegonia and antheridia (**Figures 3C–F**).

Sugar Treatments Inhibit Prothallus Development

To examine the effects of sugar treatments on prothallus development, we analyzed the differentiation status of prothallus development. As described in Li et al. (2013), prothallus development goes through filament, clavate, broadened and cordate stages after spore germination. Following cordate stage, differentiation of prothallus mainly exhibits as

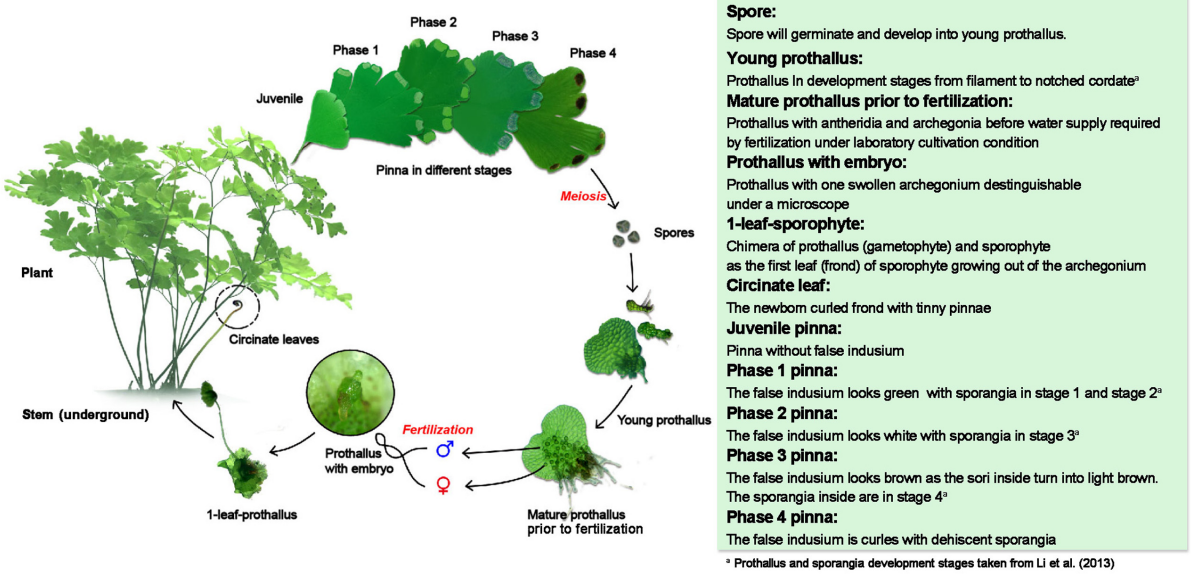

FIGURE 1 | Development stages of *Adiantum capillus-veneris*. Schematic diagram in left part represents the 11 development stages during life cycle of *A. capillus-veneris*. Major morphological features are described in the right green box.

initiation and differentiation of antheridia and archegonia (Li et al., 2013). As the prothalli were cultured from young cordate stage, we monitored the rate of initiation of antheridia and archegonia under sugar treatments. **Figures 4A–D** show typical differentiation status of prothalli, in which A shows the cordate prothallus without antheridium or archegonium initiation; B shows antheridium initiation (red arrowhead pointed); C shows both antheridium (pointed by red arrowhead) and archegonium initiation (pointed by black arrow); and D shows opened archegonia with embryogenesis (magnified in the inset). For convenience, each status from A to D framed with different colors.

Using the above morphological criteria, percentage of correspondent differentiation status in all the examined prothalli were counted (**Figure 4E**). On control medium, majority of cultured prothalli entered the stage B (antheridium initiation) in 5 DAT. In 15 DAT, all prothalli entered the stage C. In comparison, the differentiation process slowed down on 30 g/L sucrose medium, indicated by larger proportions of 5 DAT prothalli retaining at stage A and 10 DAT prothalli retaining at stage B. The differentiation of prothalli was more severely postponed on the 30 g/L glucose medium.

Sugar Treatments Promote Formation of Reproductive Organs

While the differentiation rate was decreased upon the sugar treatment, the densities of antheridia and archegonia were increased. Based on SEM observation, we can count the number of antheridia and archegonia for density calculation. **Figures 5A–C** (five panels in each lane represent the differentiation status of antheridia and archegonia at 10, 20, 30, 40, and 50 DAT) shows that comparing to the sugar-free Knop's culture, density of both antheridia and archegonia increases. The quantitation of the densities at the fertilization stage (40 DAT) were shown in **Figure 5D**.

In addition, although no distinguishable alteration in architecture of antheridium nor archegonium were found, the size of archegonia and antheridia were increased, significantly for antheridia (**Figures 5E,F** respectively).

Sugar Treatments Trigger Accumulation of Storage Products

Among the three physiological and biochemical processes consisting the seed maturation process, the accumulation of storage products is the most prominent characteristic. To examine whether the sugar treatments can trigger the accumulation of storage products, we analyzed the accumulation of representative storage macromolecules, e.g., polysaccharides, proteins, and lipids during prothalli development by histochemical stain.

Figures 6A–C show the accumulation of polysaccharides with PAS stain during prothalli development at three different stages (10, 20, and 30 DAT), and on three different mediums, i.e., the sugar-free Knop's (as control), 30 g/L sucrose and 30 g/L glucose. It is obvious that no PAS signals were detected at 10 DAT prothalli on all three mediums. However, after 20 DAT, obvious PAS signals were detected on the sugar-treated prothalli, not on the control prothalli. The strongest staining was detected on the prothalli at 30 DAT on the sucrose medium (**Figure 6B**, 30 DAT). This suggests the unambiguous accumulation of polysaccharides in the prothalli under sugar treatment.

Figures 6D–F show the accumulation of protein with Coomassie brilliant blue stain during prothalli cultured under sugar treatments. While not that obvious signals detected for

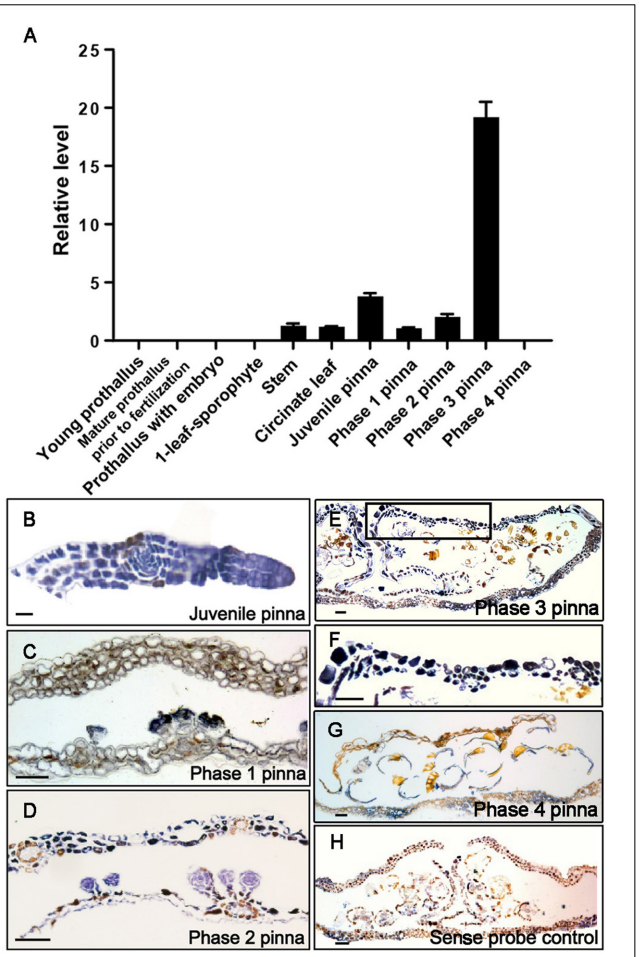

FIGURE 2 | The expression pattern of *AcLEC1*. (A) *AcLEC1* expression level in 10 development stages and stem. The samples are collected according to **Figure 1**. At least four independent *A. capillus-veneris* lines were analyzed by quantitative reverse transcription-PCR (qRT-PCR) and results of three representative lines are shown. *AcCRY2* was used as an internal control. Results represent the average from three independent isolations of RNA ± SD. **(B–H)** *In situ* localization of *AcLEC1* transcripts in pinnae. The development stages of pinna proceed from **(B–E)** and **(G)** are indicated and **(F)** is the magnified image of black frame in **(E)**. Sense probe was used as a negative control **(H)**. Bar = 50 μm.

storage protein as did for starch in prothalli under sugar treatments, the signals (stained to blue) were more intensive in sugar-treated prothalli than control.

Figures 6G–I show the accumulation of lipid with Sudan black B stain. The typical lipid signal by Sudan black B stain should be gray-blue and the background should be sky blue or blue (Supplementary Figure 1A). The signals in sugar-treated prothalli is much intensive than control (Supplementary Figures 1B,C).

Sugar Treatments Induce Expression of Homologs of *Arabidopsis* Seed Genes

To further explore whether the accumulation of storage products in prothalli grown on sugar mediums is similar to that in seed maturation process, we carried out a molecular analysis.

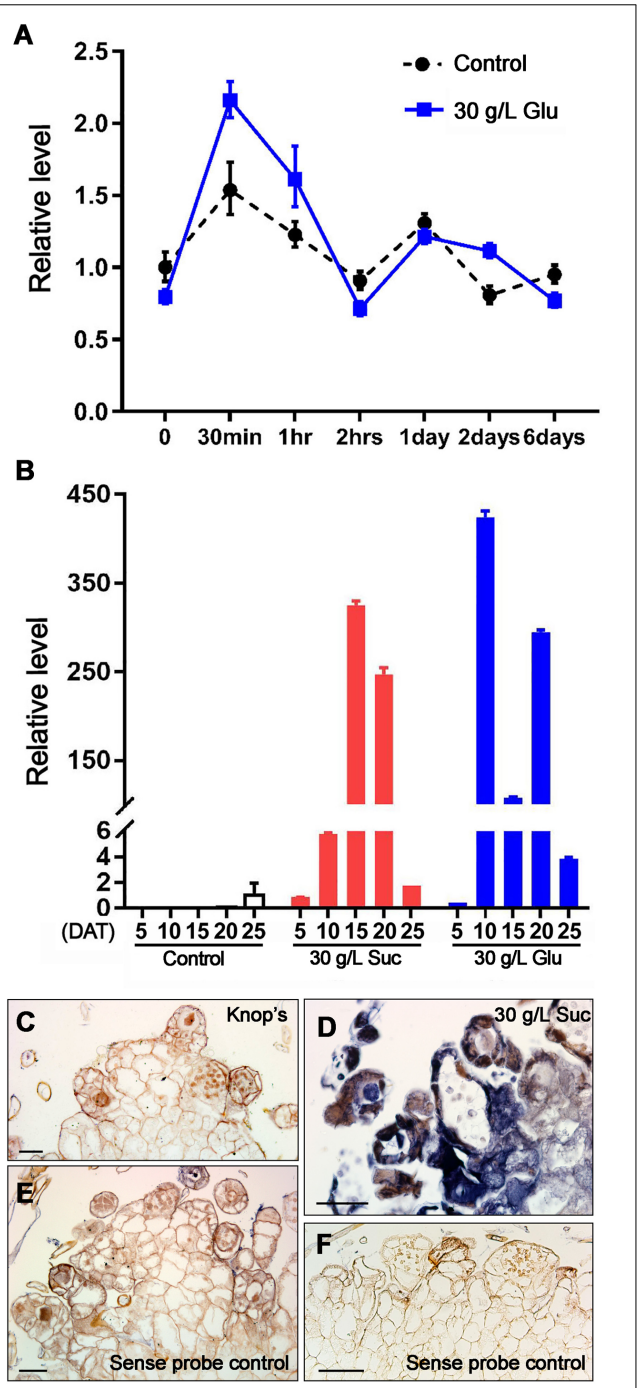

FIGURE 3 | *AcLEC1* is sugar-inducible. (A) qRT-PCR result of *AcLEC1* expression levels in prothalli which respectively grown for 0–6 days after transient (DAT) treatment with either 30 g/L glucose (blue line) or sugar-free buffer (black dotted line). **(B)** qRT-PCR result of *AcLEC1* expression levels in prothalli which grown for 5, 10, 15, 20, or 25 DAT to medium containing sucrose (red columns) or glucose (blue columns). Control stands for Knop's medium (blank columns). In **(A,B)**, *AcCRY2* was used as an internal reference. Results represents the average from three independent isolations of RNA ± SD. **(C–F)** *In situ* localization of *AcLEC1* transcripts in prothalli. Mature prothalli transferred to Knop's medium **(C)** or medium containing 30 g/L sucrose **(D)** were detected by anti-sense probe of *AcLEC1*. **(E,F)** Negative control using sense probe for samples in **(C,D)**, respectively. Bar = 50 μm.

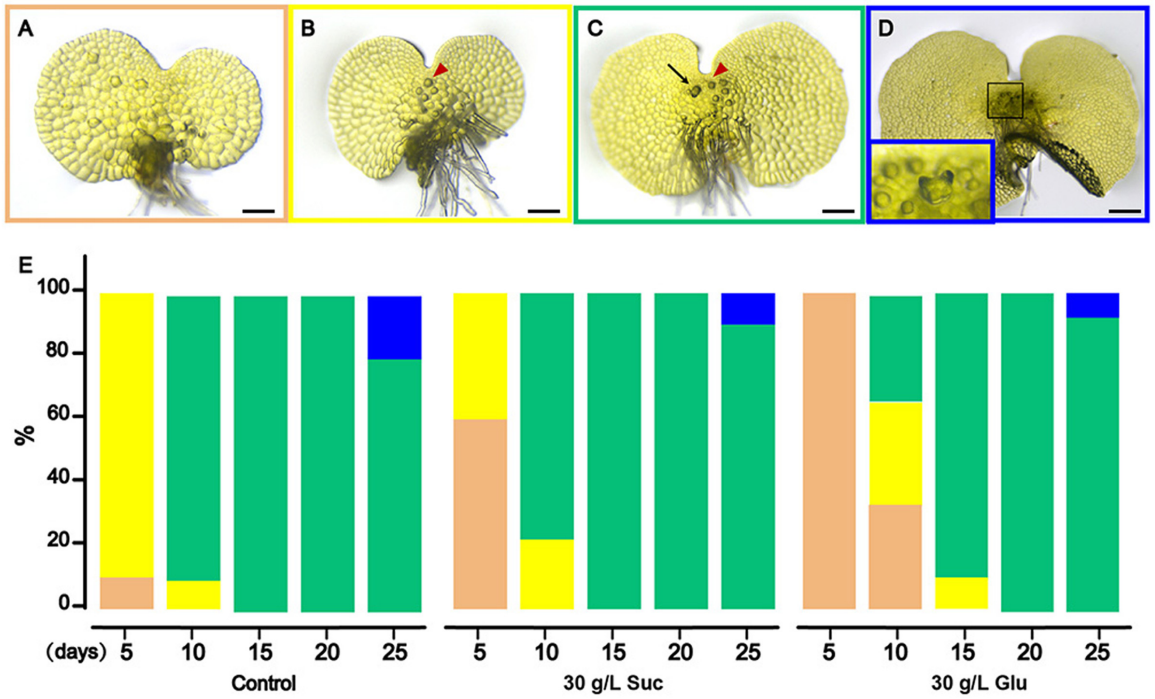

FIGURE 4 | Sugar treatment inhibits prothallus development. (A–D) The bright field images of prothalli in four development stages monitored in this research: the cordate prothallus **(A)**, antheridia initiation **(B)**, archegonia initiation **(C)**, and embryogenesis **(D)**. The embryogenesis is happened in the swollen archegonium indicated by a black frame and magnified in the embedded inset at the bottom left corner. Red arrowheads point to the antheridium. Black arrow points to the archegonium. **(E)** Percentage of correspondent differentiation status. The colors of columns in **(E)** are corresponding to the same colors in **(A–D)**, respectively. Bar = 200 μm.

Firstly, we used three *Arabidopsis* seed-specific genes, *SUCROSE-PHOSPHATE SYNTHASE* (*SPS*), *CRUCIFERIN2* (*CRU2*), and *FATTY ACID ELONGASE1* (*FAE1*), as queries to screen *A. capillus-veneris* homologs from NCBI EST database. These three genes are respectively involved in accumulation of starch (*SPS*), storage protein (*CRU2*) and lipid (*FAE1*). The ESTs homologous in *A. capillus-veneris* to these three genes were therefore designated as *AcSPS*, *AcCRU2,* and *AcFAE1,* respectively. Afterward, we analyzed the expression pattern during prothallus development.

Figure 7 shows that consistent to the accumulation of storage macromolecules in the sugar-treated prothalli, the *AcSPS* expression was significantly induced in the prothalli on the sucrose medium at 20 DAT (**Figure 7A**). The induction of *AcCRU2* is highest in the prothalli on the glucose medium at 20 DAT (**Figure 7B**). High induction of *AcFAE1* was also observed in the prothalli on the sucrose medium, but delayed to 25 DAT (**Figure 7C**).

DISCUSSION

Based on the current knowledge about the role of *LEC1* gene in seed maturation process, we proposed a modified hypothesis that the process called seed maturation identified in seed plants may be triggered by the induction of *LEC1* gene expression during embryogenesis in non-seed plants. To test the hypothesis, we firstly confirmed that there is no detectable expression of *AcLEC1*, a homolog to *Arabidopsis LEC1* in a non-seed plants *A. capillus-veneris*, during prothallus development, where the embryogenesis occurs in archegonia (**Figure 2**). Then, we demonstrated that *AcLEC1* expression can be induced by sugar treatments during prothallus development (**Figure 3**). In parallel, we found that the sugar treatment can trigger accumulation of storage products (**Figure 6**), one of the hallmark events in seed maturation process during prothallus development; promote differentiation of reproductive organs (**Figure 5**), i.e., antheridia and archegonia; and delay the differentiation of prothalli (**Figure 4**), the effect similar to another hallmark event, dormancy. Consistent to the accumulation of storage products, we found that the genes homologous to so called seed-specific genes were activated in sugar-treated prothalli (**Figure 7**). While these findings indicate the links between sugar treatments and *AcLEC1* expression, as well as sugar treatments and events such as accmulation of storage products, which is occurring in prothalli, mimicking to that called seed maturation process, what would these findings imply to the origin of the seed maturation process?

Firstly, the property of inductive expression *AcLEC1* imply its potential to be coopted into the origin of seed maturation process. Previous investigation already demonstrated that in *Arabidopsis*, *LEC1* expression can be induced in the *KK* mutant at seedling

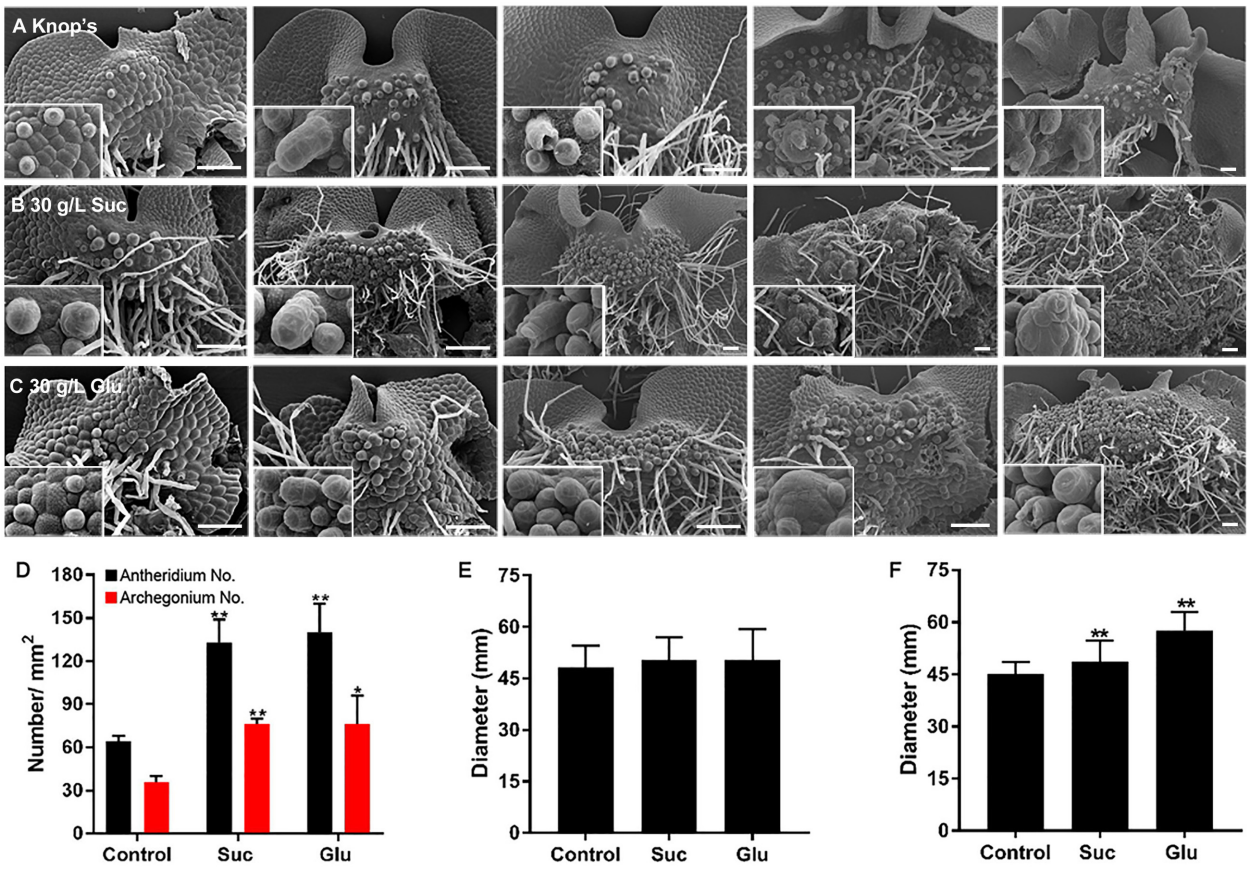

FIGURE 5 | Sugar treatments promote formation of reproductive organs. (A–C) SEM images of prothalli on Knop's medium **(A)**, 30 g/L sucrose medium **(B)** or 30 g/L glucose medium **(C)** at 10, 20, 30, 40, and 50 DAT. Higher magnification images of reproductive organs or distinguishable embryo were shown in embedded insets. **(D)** The density of antheridium (black columns) and archegonium (red columns) in fertilized prothalli. The diameter of archegonium **(E)** and antheridium **(F)** of fertilized prothalli with or without sugar treatment. Data represents means of five independent samples ± SE. Asterisks above the bars report the results of a significance test (Student's *t*-test) for differences between the control and the treated samples: $^{**}P < 0.01$, $^{*}P < 0.5$. Bar = 200 μm.

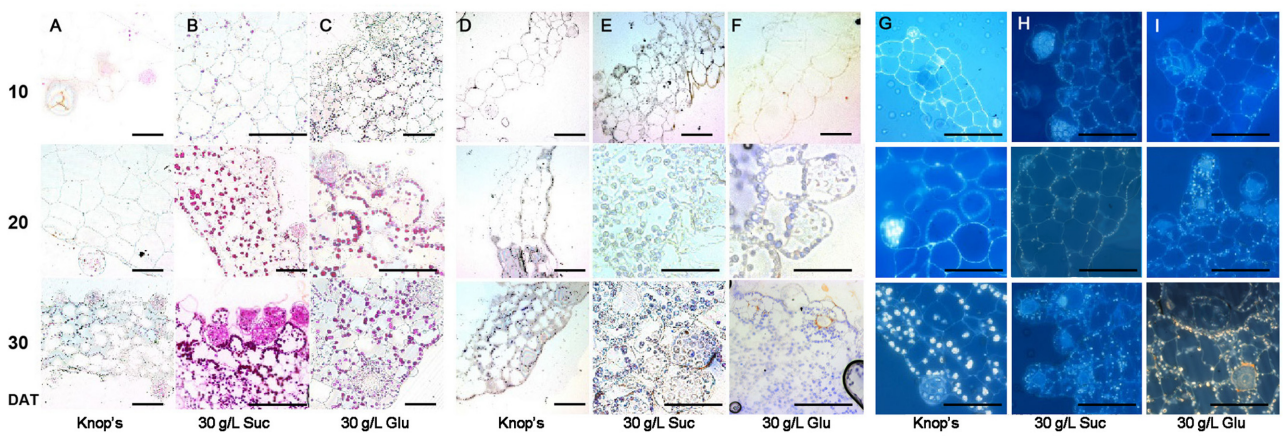

FIGURE 6 | Sugar treatment triggers accumulation of storage products. Prothalli were persistently treated by 30 g/L sucrose or glucose. 10, 20, and 30 DAT prothalli were labeled by cytochemical stain technique. The images of representative sections under the same treatment during 10–30 DAT were arranged in one column. **(A–C)** Cherry red indicates the polysaccharides which labeled by PAS reaction. **(D–F)** Blue display the protein body after Coomassie brilliant blue staining. **(G–I)** The lipid bodies were manifested by gray-blue using Sudan black B staining. Bar = 50 μm.

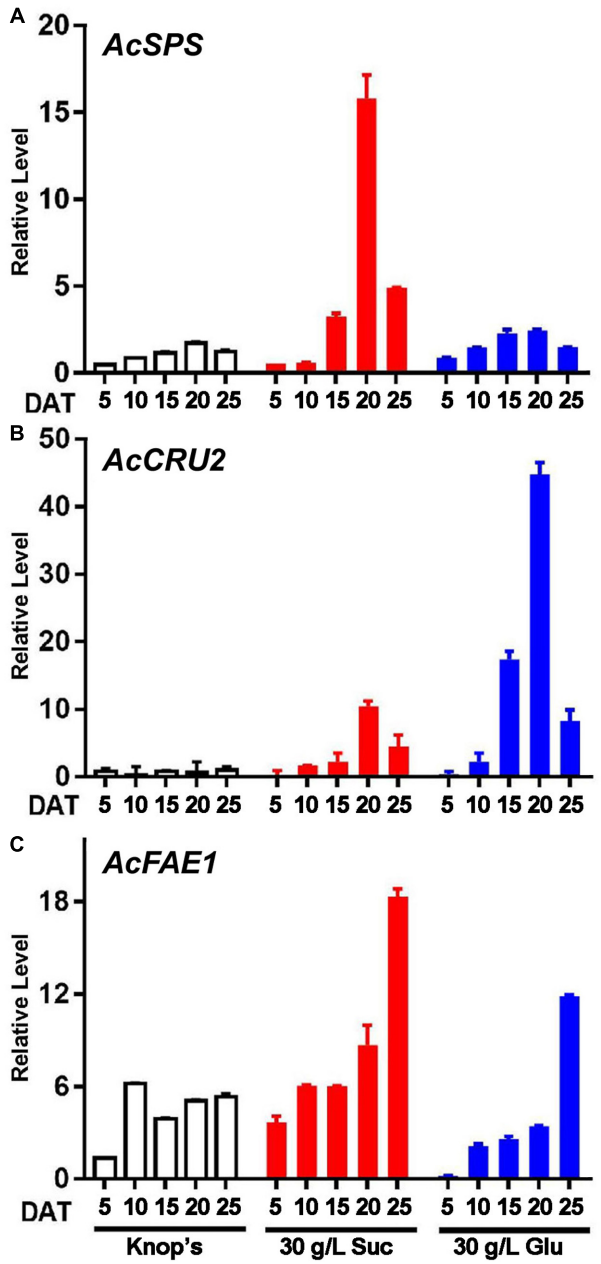

FIGURE 7 | Sugar treatment induces expression of *Arabidopsis* seed homologs. qRT-PCR examine results of **(A)** *AcSPS*, **(B)** *AcCRU2*, and **(C)** *AcFAE1*. *AcCRY* was used as an internal reference. Results represents the average from three independent isolations of RNA ± SD.

stage (Tsukagoshi et al., 2007). Xie et al. (2008) and Li et al. (2017) also demonstrated that *AcLEC1* can be induced under drought and ABA treatment of sporophyte and tissue culture respectively. It seems that the *LEC1*-like gene was not originated to be a key regulator of seed maturation process as it does not express during embryogenesis of non-seed plants, rather a stress response gene as it expressed in aerial tissue as we demonstrated in **Figure 2** and its expression can be induced by drought and ABA (Xie et al., 2008). Such an inducibility makes it possible that the expression of *LEC1*-like gene can be induced in nature by chance during embryogenesis as we found in this work in lab by intention. From this perspective, our findings in this work open up a new window to investigate origin of seed maturation process by further investigation of molecular mechanism of induction of *LEC1*-like gene expression in non-seed plants.

Secondly, if the accumulation of storage products is a hallmark event of seed maturation process, it would be interesting to ask, whether such a process is seed specific or not. According to Harada (1997), the seed maturation process is intrusive to the embryogenesis, implying that it is an independently originated process of embryogenesis. The accumulation of storage products can be found in other tissues such as tuberous roots in cassava and sweet potato and tubers in potato. From this perspective, the accumulation of storage products should not be specific to the structure called seed. While our findings revealed the sugar treatments can trigger the accumulation of storage products during prothallus development, it would be interesting ask a reverse question that why there is no obvious accumulation of storage products in prothallus development in nature?

If we consider the stress inductive property of *LEC1* expression and sugar induction of both *AcLEC1* expression and accumulation of storage products in prothalli, it will be interesting to hypothesize that the reasons for no accumulation of storage products come from lack of stress conditions, as the prothalli grown in wet habitation, and/or lack of additional assimilate supply for storage products to be synthesis. Such a hypothesis is mutually complementary to the current theory on origin of seeds. Current theory suggests that the seed is originated from the terminally located ovule where the embryogenesis occurs (Taylor and Taylor, 1993; Herr, 1995; Niklas, 1997; Doyle, 2006). According to the telome theory, the terminally grown ovules are obvious the aerial grown tissues. If our findings are generally applicable, the *LEC1*-like genes should be expressed in the aerial grown ovules. On the other hand, according to the "source-sink" theory of assimilation allocation (Rolland et al., 2006; Eveland and Jackson, 2012), the terminally located ovules should function as a sink in an assimilation flow. If it is the case, the imported assimilates, similar to the sugar treatments in our experiments, can trigger jointly by enhancing the expression of *LEC1*-like genes, the accumulation of storage products in the terminally localized ovules and superposed upon embryogenesis occurring in the ovules, and therefore a novel structure emerged, latterly called seed. Once it happened, no force can prevent such a trait been selected during evolution for the obvious adaptive advantages. With this hypothesis in mind, the mechanism of origin of seed maturation process, or briefly called seed program, can be empirically investigated, and the exploration of origin of seed would be no longer the privilege of paleobotanists.

Finally, although it is demonstrated that *LEC1* gene is a key regulator in seed maturation process or seed program, because of the lack of tools of gene transformation, it is not yet clear whether the effects on prothallus development of sugar treatments come directly from the sugar-induced *AcLEC1* expression or other mechanisms. Even though, the findings in this

work paved a road to the prosperous future to uncover the secret on origin of the seed.

AUTHOR CONTRIBUTIONS

Y-HF designed the experiments, conducted the experiments and drafted the manuscript. XL designed the experiments, conducted cytochemical stain assay and time course assay, and revised the manuscript. S-NB and G-YR conceived the study, reviewed and edited the manuscript. All authors read and approved the manuscript.

ACKNOWLEDGMENTS

This work was supported by the National Natural Science Foundation of China (NSFC, Grant no. 91231105). We thank two reviewers for valuable comments.

SUPPLEMENTARY MATERIAL

The Supplementary Material for this article can be found online at: http://journal.frontiersin.org/article/10.3389/fpls.2017.00541/full#supplementary-material

REFERENCES

Bai, S. N. (1999). "Phenomena, interpretation of the phenomena and the developmental unit in plants," in *Advances of Botany*, Vol. II, ed. C. S. Li (Beijing: Higher Education Publish House), 52–69.

Bai, S. N. (2015a). The concept of the sexual reproduction cycle and its evolutionary significance. *Front. Plant Sci.* 6:11. doi: 10.3389/fpls.2015.00011

Bai, S. N. (2015b). Plant developmental program: sexual reproduction cycle derived "double ring". *Sci. Sin. Vitae* 45, 811–819. doi: 10.1360/N052015-00208

Bai, S. N. (2016). Make a new cloth for a grown body: from plant developmental unit to plant developmental program. *Annu. Rev. New Biol.* 2015, 73–116.

Bai, S.-N. (2017). Reconsideration of plant morphological traits: from a structure-based perspective to a function-based evolutionary perspective. *Front. Plant Sci.* 8:345 doi: 10.3389/fpls.2017.00345

Becker, B., and Marin, B. (2009). Streptophyte algae and the origin of embryophytes. *Ann. Bot.* 103, 999–1004. doi: 10.1093/aob/mcp044

Braybrook, S. A., and Harada, J. J. (2008). LECs go crazy in embryo development. *Trends Plant Sci.* 13, 624–630. doi: 10.1016/j.tplants.2008.09.008

Casson, S. A., and Lindsey, K. (2006). The *turnip* mutant of *Arabidopsis* reveals that *LEAFY COTYLEDON1* expression mediates the effects of auxin and sugars to promote embryonic cell identity. *Plant Physiol.* 142, 526–541. doi: 10.1104/pp.106.080895

Doyle, J. A. (2006). Seed ferns and the origin of the angiosperms. *J. Torrey Bot. Soc.* 133, 169–209. doi: 10.3159/1095-5674(2006)133[169:SFATOO]2.0.CO;2

Eveland, A. L., and Jackson, D. P. (2012). Sugars, signalling, and plant development. *J. Exp. Bot.* 63, 3367–3377. doi: 10.1093/jxb/err379

Goldberg, R. B., Paiva, P., and Yadegari, R. (1994). Plant embryogenesis: zygote to seed. *Science* 266, 605–614. doi: 10.1126/science.266.5185.605

Gupta, A. K., and Kaur, N. (2005). Sugar signalling and gene expression in relation to carbohydrate metabolism under abiotic stresses in plants. *J. Biosci.* 30, 761–776. doi: 10.1007/BF02703574

Gutierrez, L., Wuytswinkel, O., Castelain, M., and Bellini, C. (2007). Combined networks regulating seed maturation. *Trends Plant Sci.* 12, 294–300. doi: 10.1016/j.tplants.2007.06.003

Harada, J. J. (1997). "Seed maturation and control of dormancy," in *Cellular and Molecular Biology of Plant Seed Development*, eds B. A. Larkins and I. K. Vasil (Gainesville, FL: University of Florida Press), 545–592. doi: 10.1007/978-94-015-8909-3_15

Herr, J. M. (1995). The origin of the ovule. *Am. J. Bot.* 82, 547–564. doi: 10.2307/2445703

Hu, S. Y., and Xu, L. Y. (1990). A cytochemical technique for demonstration of lipids, polysaccharides and protein bodies in thick resin sections. *Acta Bot. Sin.* 32, 841–846.

Imaizumi, T., Kanegae, T., and Wada, M. (2000). Cryptochrome nucleocytoplasmic distribution and gene expression are regulated by light quality in the fern *Adiantum capillus-veneris*. *Plant Cell* 12, 81–96. doi: 10.1105/tpc.12.1.81

Junker, A., Monke, G., Rutten, T., Keilwagen, J., Seifert, M., Thi, T. M., et al. (2012). Elongation-related functions of *LEAFY COTYLEDON1* during the development of *Arabidopsis thaliana*. *Plant J.* 71, 427–442. doi: 10.1111/j.1365-313X.2012.04999.x

Kenrick, P., and Crane, P. (1997). The origin and early evolution of plants on land. *Nature* 389, 33–39. doi: 10.1038/37918

Kirkbride, R. C., Fischer, R. L., and Harada, J. J. (2013). *LEAFY COTYLEDON1*, a key regulator of seed development, is expressed in vegetative and sexual propagules of *Selaginella moellendorffii*. *PLoS ONE* 8:e67971. doi: 10.1371/journal.pone.0067971

Kwong, R. W., Bui, A. Q., Lee, H., Kwong, L. W., Fischer, R. L., Goldberg, R. B., et al. (2003). *LEAFY COTYLEDON1-LIKE* defines a class of regulators essential for embryo development. *Plant Cell* 15, 5–18. doi: 10.1105/tpc.006973

Le, B. H., Cheng, C., Bui, A. Q., Wagmaister, J. A., Henry, K. F., Pelletier, J., et al. (2010). Global analysis of gene activity during *Arabidopsis* seed development and identification of seed-specific transcription factors. *Proc. Natl. Acad. Sci. U.S.A.* 107, 8063–8070. doi: 10.1073/pnas.1003530107

Lee, H., Fischer, R. L., Goldberg, R. B., and Harada, J. J. (2003). *Arabidopsis LEAFY COTYLEDON1* represents a functionally specialized subunit of the CCAAT binding transcription factor. *Proc. Natl. Acad. Sci. U.S.A.* 100, 2152–2156. doi: 10.1073/pnas.0437909100

Li, X., Fang, Y. H., Yang, J., Bai, S. N., and Rao, G. Y. (2013). Overview of the morphology, anatomy, and ontogeny of *Adiantum capillus-veneris*: an experimental system to study the development of ferns. *J. Syst. Evol.* 51, 499–510. doi: 10.1111/jse.12034

Li, X., Han, J.-D., Fang, Y.-H., Bai, S.-N., and Rao, G.-Y. (2017). Expression analyses of embryogenesis-associated genes during somatic embryogenesis of *Adiantum capillus-veneris* L. *in vitro*: new insights into the evolution of reproductive organs in land plants. *Front. Plant Sci.* 8:658. doi: 10.3389/fpls.2017.00658

Linkies, A., Graeber, K., Knight, C., and Leubner-Metzger, G. (2010). The evolution of seeds. *New Phytol.* 186, 817–831. doi: 10.1111/j.1469-8137.2010.03249.x

Livak, K. J., and Schmittgen, T. D. (2001). Analysis of relative gene expression data using real-time quantitative PCR and the 2(-Delta Delta C (T)) Method. *Methods* 25, 402–408. doi: 10.1006/meth.2001.1262

Lotan, T., Ohto, M., Yee, K. M., West, M. A. L., Lo, R., Kwong, R. W., et al. (1998). *Arabidopsis LEAFY COTYLEDON1* is sufficient to induce embryo development in vegetative cells. *Cell* 93, 1195–1205. doi: 10.1016/S0092-8674(00)81463-4

Meinke, D. W. (1992). A homoeotic mutant of *Arabidopsis thaliana* with leafy cotyledons. *Science* 258, 1647–1650. doi: 10.1126/science.258.5088.1647

Meinke, D. W., Franzmann, L. H., Nickle, T. C., and Yeung, E. C. (1994). *Leafy cotyledon* mutants of *Arabidopsis*. *Plant Cell* 6, 1049–1064. doi: 10.1105/tpc.6.8.1049

Mu, J., Tan, H., Zheng, Q., Fu, F., Liang, Y., Zhang, J., et al. (2008). *LEAFY COTYLEDON1* is a key regulator of fatty acid biosynthesis in *Arabidopsis*. *Plant Physiol.* 148, 1042–1054. doi: 10.1104/pp.108.126342

Niklas, K. J. (1997). *The Evolutionary Biology of Plants*. Chicago, IL: The University of Chicago Press.

Pires, N. D., and Dolan, L. (2012). Morphological evolution in land plants: new designs with old genes. *Philos. Trans. R. Soc. Lond. B Biol. Sci.* 367, 508–518. doi: 10.1098/rstb.2011.0252

Poonam, R. B., Handa, N., Kaur, H., Rattan, A., Bali, S., et al. (2016). "Sugar signalling in plants: a novel mechanism for drought stress management," in *Water Stress and Crop Plants*, ed. P. Ahmad (Chichester: John Wiley & Sons, Ltd), 287–302. doi: 10.1002/9781119054450.ch19

Radoeva, T., and Weijers, D. (2014). A roadmap to embryo identity in plants. *Trends Plant Sci.* 19, 709–716. doi: 10.1016/j.tplants.2014.06.009

Rolland, F., Baena-Gonzalez, E., and Sheen, J. (2006). Sugar sensing and signaling in plants: conserved and novel mechanisms. *Annu. Rev. Plant. Biol.* 57, 675–709. doi: 10.1146/annurev.arplant.57.032905.105441

Sreenivasulu, N., and Wobus, U. (2013). Seed-development programs: a systems biology-based comparison between dicots and monocots. *Annu. Rev. Plant. Biol.* 64, 189–217. doi: 10.1146/annurev-arplant-050312-120215

Taylor, T. N., and Taylor, E. L. (1993). *The Biology and Evolution of Fossil Plants*. New York, NY: Prentice Hall.

Tsukagoshi, H., Morikami, A., and Nakamura, K. (2007). Two B3 domain transcriptional repressors prevent sugar-inducible expression of seed maturation genes in *Arabidopsis* seedlings. *Proc. Natl. Acad. Sci. U.S.A.* 104, 2543–2547. doi: 10.1073/pnas.0607940104

Vicente-Carbajosa, J., and Carbonero, P. (2005). Seed maturation: developing an intrusive phase to accomplish a quiescent state. *Int. J. Dev. Biol.* 49, 645–651. doi: 10.1387/ijdb.052046jc

West, M., Yee, K. M., Danao, J., Zimmerman, J. L., Fischer, R. L., Goldberg, R. B., et al. (1994). *LEAFY COTYLEDON1* is an essential regulator of late embryogenesis and cotyledon identity in *Arabidopsis*. *Plant Cell* 6, 1731–1745. doi: 10.1105/tpc.6.12.1731

Xie, Z. Y., Li, X., Glover, B. J., Bai, S. N., Rao, G. Y., Luo, J., et al. (2008). Duplication and functional diversification of *HAP3* genes leading to the origin of the seed-developmental regulatory gene, *LEAFY COTYLEDON1* (*LEC1*), in nonseed plant genomes. *Mol. Biol. Evol.* 25, 1581–1592. doi: 10.1093/molbev/msn105

Yang, J., Xie, Z. Y., and Glover, B. J. (2005). Asymmetric evolution of duplicate genes encoding the CCAAT-binding factor NF-Y in plant genomes. *New Phytol.* 165, 623–631. doi: 10.1111/j.1469-8137.2004.01260.x

Zhang, X., Zhou, Y., Ding, L., Wu, Z., Liu, R., and Meyerowitz, E. M. (2013). Transcription repressor HANABA TARANU controls flower development by integrating the actions of multiple hormones, floral organ specification genes, and GATA3 family genes in *Arabidopsis*. *Plant Cell* 25, 83–101. doi: 10.1105/tpc.112.107854

Conflict of Interest Statement: The authors declare that the research was conducted in the absence of any commercial or financial relationships that could be construed as a potential conflict of interest.

frontiers in Plant Science

ORIGINAL RESEARCH
published: 03 May 2017
doi: 10.3389/fpls.2017.00682

Time-Course Transcriptome Analysis of Compatible and Incompatible Pollen-Stigma Interactions in *Brassica napus* L.

Tong Zhang[1†], Changbin Gao[2†], Yao Yue[1], Zhiquan Liu[1], Chaozhi Ma[1], Guilong Zhou[1], Yong Yang[1], Zhiqiang Duan[1], Bing Li[1], Jing Wen[1], Bin Yi[1], Jinxiong Shen[1], Jinxing Tu[1] and Tingdong Fu[1]*

[1] National Key Laboratory of Crop Genetic Improvement, National Center of Rapeseed Improvement in Wuhan, Huazhong Agricultural University, Wuhan, China, [2] Department of Leafy Vegetable, Wuan Institute of Vegetable Science, Wuhan, China

Brassica species exhibit both compatible and incompatible pollen-stigma interactions, however, the underlying molecular mechanisms remain largely unknown. Here, RNA-seq technology was applied in a comprehensive time-course experiment (2, 5, 10, 20, and 30 min) to explore gene expression during compatible/incompatible pollen-stigma interactions in stigma. Moderate changes of gene expression were observed both in compatible pollination (PC) and incompatible pollination (PI) within 10 min, whereas drastic changes showed up by 30 min, especially in PI. Stage specific DEGs [Differentially Expressed Gene(s)] were identified, and signaling pathways such as stress response, defense response, cell wall modification and others were found to be over-represented. In addition, enriched genes in all samples were analyzed as well, 293 most highly expressed genes were identified and annotated. Gene Ontology and metabolic pathway analysis revealed 10 most highly expressed genes and 37 activated metabolic pathways. According to the data, downstream components were activated in signaling pathways of both compatible and incompatible responses, and incompatible response had more complicated signal transduction networks. This study provides more detailed molecular information at different time points after compatible and incompatible pollination, deepening our knowledge about pollen-stigma interactions.

Keywords: time-course, self-(in) compatibility, stigma, transcriptome, *Brassica napus*

OPEN ACCESS

Edited by:
Zhong-Jian Liu, The National Orchid Conservation Center of China, The Orchid Conservation and Research Center of Shenzhen, China

Reviewed by:
John E. Fowler, Oregon State University, USA
Anna N. Stepanova, North Carolina State University, USA

***Correspondence:**
Chaozhi Ma
yuanbeauty@mail.hzau.edu.cn

† These authors have contributed equally to this work.

Specialty section:
This article was submitted to Plant Evolution and Development, a section of the journal Frontiers in Plant Science

Received: *02 December 2016*
Accepted: *13 April 2017*
Published: *03 May 2017*

Citation:
Zhang T, Gao C, Yue Y, Liu Z, Ma C, Zhou G, Yang Y, Duan Z, Li B, Wen J, Yi B, Shen J, Tu J and Fu T (2017) Time-Course Transcriptome Analysis of Compatible and Incompatible Pollen-Stigma Interactions in Brassica napus L. Front. Plant Sci. 8:682. doi: 10.3389/fpls.2017.00682

INTRODUCTION

The proper interactions between pollen and stigma play a vital role in successful pollination which is the key process in reproduction for angiosperms. The *Brassicaceae* plants have evolved complicated and elaborate mechanisms for successful fertilization to produce vigorous progenies. These mechanisms involve blocking the adherence and growth of inter-species pollen, rejecting "self" pollen (self-incompatibility, SI) and only allowing the fertilization of compatible pollen with different genetic background. The *Brassicaceae* plants have dry stigmas (with no exudate) whose epidermis is composed of large specialized papillae cells covered by a waxy cuticle and a superficial proteinaceous pellicle layer (Elleman et al., 1988, 1992). Once compatible pollen lands on the stigma, a series of signaling events are triggered. During this process, a pollen grain

experiences several steps, including adhesion, foot formation, pollen hydration, germination and penetration through the stigmatic cell walls. Following these steps, pollen tube grows down through the transmitting tissue of the style, and ultimately reaches an ovule where fertilization takes place (reviewed in Chapman and Goring, 2010). However, when "self" pollen lands on the stigma, the SI reaction occurs rapidly, blocking the self-compatible reaction from pollen adhesion to pollen tube penetration (reviewed in De Nettancourt, 2001; Franklin-Tong, 2008).

Several stigma specific genes have been shown to participate in compatible and incompatible pollen-stigma interactions in *Brassicaceae*. A stigma specific *S*-locus related-1 (*SLR1*) gene is involved in pollen adhesion, and knocking down of *SLR1* reduces pollen adhesion in *B. napus* (Luu et al., 1997). Another stigma specific protein, SLG (*S*-locus glycoprotein), could bind PCP-A1, a small pollen coat protein (Doughty et al., 1998). By treating *B. oleracea* stigmas with antibodies of SLG or SLR1 also reduced pollen adhesion (Luu et al., 1999). Samuel et al. (2009) reported that a non-stigma specific protein, EXO70A1, is required in the stigma for the acceptance of compatible pollen in both *Brassica* and *Arabidopsis* and is negatively regulated during SI in *Brassica*. In *Brassicaceae*, the SI reaction involves the interaction of SRK (*S*-locus receptor kinase) expressed in stigma and its pollen-coat localized ligand SCR/SP11 (*S*-locus cysteine-rich protein or *S*-locus protein 11) which is allele-specific, leading to autophosphorylation of SRK and triggering several signaling cascades within the stigma epidermal cells (Kachroo et al., 2001; Takayama et al., 2001). The phosphorylated SRK, together with the plasma membrane-tethered MLPK (M-locus Protein Kinase), can phosphorylate ARC1 (Armadillo Repeat-Containing protein 1), a U-box E3 ubiquitin ligase (Murase et al., 2004; Kakita et al., 2007a,b; Samuel et al., 2009). ARC1 is proposed to function in the proteasome-mediated degradation pathway, and it can target stigma proteins required for the compatible reaction (for example Exo70A1) (Samuel et al., 2011).

Knowledge about incompatible and compatible pollen-stigma interactions has increased considerably in recent years. In *B. rapa*, time-lapse imaging of pollen behavior during self- and cross-pollinations illustrates that pollen hydration is regulated by a balanced process of hydration, dehydration and nutrient supply to pollen grains from stigmatic papilla cells (Hiroi et al., 2013). Compatible pollination induces actin polymerization and leads to vacuolar rearrangements toward the pollen attachment site. During incompatible pollination, actin reorganizes (likely depolymerization) and disrupts vacuole networks toward the site of pollen attachment (Iwano et al., 2007). Safavian and Goring (2013) found that secretory activity was rapidly induced in stigmatic papillae by compatible pollen, with vesicle or multi-vesicular bodies (MVBs) observed at the stigmatic papillar plasma membrane under the pollen grain. In incompatible pollination the secretory activity was inhibited in *Brassicaceae*. Microarray technology and a cDNA library were used to build a profile of candidate stigma genes that facilitate early pollination events in *Arabidopsis* (Swanson et al., 2005). Through proteomic analysis of stigmatic proteins following incompatible pollination in *B. napus*, 19 down-regulated unique candidate proteins were identified specially in SI (Samuel et al., 2011). Matsuda et al. (2014) applied laser microdissection (LM) and RNA sequencing (RNA-seq) to detect the cell type-specific transcriptome in *Brassicaceae* papillae cells and characterized gene expression 1 h after compatible and incompatible pollination. Although these studies contributed to our understanding of the molecular mechanisms related to pollen-stigma interactions, the consecutive changes of gene expression and dynamic molecular activities during the early stages (within 30 min) of pollination remained to be revealed. In addition, compared with the intensive study of signal transduction pathways in hormones and disease resistance in *Brassicaceae*, the knowledge of downstream components in self-incompatibility is still quite limited.

Self- incompatibility of *B. napus* is regulated by the interaction between *BnSP11* and *BnSRK*, together with the activated downstream components following the interaction. *BnSRK* could recognize *BnSP11* specifically and get autophosphorylated, then phosphorylated SRK would phosphorylate ARC1 which could cause ubiquitination of its target proteins (e.g., Exo70A1). An insertion of a DNA fragment with a length of 3606 bp in the promoter region of *BnSP11-1* was responsible for the self-compatibility (SC) of *B. napus* line "Westar" (Okamoto et al., 2007; Tochigi et al., 2011). By complementing the function of *BnSP11-1* in "Westar," we obtained the transgenic line "W-3" which showed strong SI (Gao et al., 2016). When pollen of "Westar" lands on its own stigma, compatible interaction occurs and normal pods are set; when pollen of "W-3" lands on the stigma of "Westar," self-incompatible reaction occurs and pods seldom set seeds. These are ideal materials for us to shed further light on the complex responses of compatible/incompatible pollen-stigma interactions using next-generation RNA-seq coupled with a comprehensive time-course experiment.

MATERIALS AND METHODS

Plant Material and Growth Conditions

The wild type self-compatible *B. napus* line "Westar" and transgenic self-incompatible line "W-3" (Gao et al., 2016) were grown in the greenhouse with 16/8 h day/night photoperiod and temperatures of 22/15°C. Floral buds of wild type self-compatible *B. napus* line "Westar" were emasculated 1 day before anthesis to avoid pollen contamination. The next day, stigma samples were collected by cutting the pistil just below the base of the stigma and immediately frozen in liquid nitrogen. By this method, stigma samples of "Westar" with no pollen pollinated (UP) and pollinated stigmas (PC2, PC5, PC10, PC20, PC30: self-pollinated stigmas of "Westar" at 2, 5, 10, 20, and 30 min; PI2, PI5, PI10, PI20, PI30: stigmas of "Westar" pollinated with the incompatible pollen of "W-3" at 2, 5, 10, 20, and 30 min) were collected.

Transmission Electron Microscopy

The pollinated stigmas (PI30 and PC30) were vacuum-infiltrated and pre-fixed in a solution of 2.5% glutaraldehyde adjusted to pH 7.4 with 0.1 M phosphate buffer, fixed in 2% OsO_4 in the same buffer, and then dehydrated and embedded in epoxy

resin and SPI-812 (Structure Probe, Inc., http://www.2spi.com/), respectively. Ultra-thin sections were obtained using a Leica UC6 ultramicrotome (http://www.leica.com/) and were stained with uranyl acetate and subsequently with lead citrate. The observations and recording of images were performed using a Hitachi H-7650 transmission electron microscope (http://www.hitachi-hitec.com/) at 80 kV and a Gatan 832 CCD camera (http://www.gatan.com/).

cDNA Library Construction and Solexa/Illumina Sequencing

Total RNA was extracted using the DNA/RNA isolation kit (Qiagen). The quality and quantity of purified RNA were determined by measuring absorbance at 260 nm/280 nm (A260/A280) using a SmartSpec plus (BioRad). In total, 22 RNA samples (UP, PC2, PC5, PC10, PC20, PC30, PI2, PI5, PI10, PI20, and PI30, each with two biological replicates) were subjected to library construction using an Illumina® TruSeq™ RNA Sample Preparation Kit following the manufacturer's instructions. All samples were sequenced using an Illumina HiSeq 2500 sequencer at the National Key Laboratory of Crop Genetic Improvement, Huazhong Agricultural University.

Sequence Data Analysis

Raw sequences were processed by removal of the 3' adaptor sequence, low-quality reads, and reads that are too short (less than 20 nt), leaving clean reads for subsequent analysis. All high-quality reads were mapped to the *B. napus* genome (Chalhoub et al., 2014) by TopHat v2.0.11 using the default parameters (Trapnell et al., 2009). Only uniquely mapped reads were considered for gene expression analysis. The program Cufflinks v2.2.0 was used to calculate differential gene expression and transcript abundance (Trapnell et al., 2010). Transcript abundance of each gene was estimated by FPKM. DEGs (differentially expressed genes) between UP and PC/PI samples were identified according to the restrictive conditions of an absolute value of $\log_2$ fold changes ≥ 1 and a FDR ≤ 0.01.

Analysis and Annotation of DEGs

Gene function annotation was performed in accordance with the method described by Wu et al. (2016). All *B. napus* genes (Chalhoub et al., 2014) were searched against the NCBI non-redundant (Nr) protein database using BlastP with an *E*-value $\leq$ 1E-05. GO terms associated with each BLAST hit were annotated using Blast2GO (Conesa et al., 2005). Then, all *B. napus* genes were searched against the InterPro database (http://www.ebi.ac.uk/interpro/) using InterProScan5 (Jones et al., 2014). Finally, *B. napus* genes were annotated by merging the annotation results of Blast2GO and InterPro. Blast2GO was also applied for GO enrichment analysis with a false discovery rate (FDR) ≤ 0.01, which can provide all GO terms that were significantly enriched in DEGs compared with the genome background.

RT-PCR and qRT-PCR

Total RNA was extracted using the DNA/RNA isolation kit (Qiagen). Five micrograms of RNA was DNase-treated using a DNA-free kit (Ambion, http://www.ambion.com). First-strand cDNA synthesis was performed using a SuperScript kit (Gibco BRL, http://www.invitrogen.com). Real-time RT-PCR was also performed using a Bio-Rad IQ5 with SYBR Green detection (http://www.bio-rad.com/). *Actin* (Gene-Bank accession no.: AF111812) was used as an internal control to normalize transcript levels for all expression analyses. Supplemental Table S1 lists the specific primers used to test the genes.

Accession Numbers

Sequence data from this article can be found in the TAIR, NCBI (the NIH SRA) and *Brassica napus* Genome Resources (http://www.genoscope.cns.fr/brassicanapus/) data libraries.

RESULTS

Comparative Transcript Profiling of Compatible and Incompatible Reactions

Transmission electron micrography (TEM) was used to compare SI and SC pollen-stigma interactions 30 min after pollination. When pollen of "W-3" was applied to the stigma of "Westar," 23 pollen grains were observed being captured by the stigma papilla cell but there was no change in morphology of the pollen (**Figure 1A**, left panel). However, when "Westar" was self-pollinated, 39 pollen grains were captured and two kinds of pollen-stigma interaction patterns were observed. One pattern (**Figure 1A**, middle panel; 18 pollen grains) was similar to that observed in the "Westar" × "W-3" cross, with no change in morphology. The second pattern (**Figure 1A**, right panel; eight pollen grains) showed germination of the pollen tube and invasion of the cell wall of the stigma papilla cell. It could be deduced that it was possible for a compatible pollen grain to have experienced all initial steps of pollen-stigma interaction (adhesion, foot formation, hydration, germination and penetration) during the first 30 min following compatible pollination; incompatible pollen exhibited the first two steps in the same time period.

To explore the molecular mechanisms underlying compatible and incompatible pollen-stigma interactions, we employed Illumina (Solexa) sequencing technology to investigate the stigma transcriptome. Different kinds of stigma samples from wild type "Westar" were collected: un-pollinated stigmas (termed UP), stigmas pollinated with compatible pollen (PC) at multiple time points (2, 5, 10, 20, and 30 min, termed PC2, PC5, PC10, PC20, and PC30, respectively) and stigmas pollinated with incompatible pollen (PI) of "W-3" at the same time points as PC (termed PI2, PI5, PI10, PI20, and PI30, respectively). Compared with the genes expressed in UP, differential expression ($\log_2$ fold changes ≥ 1 and a FDR ≤ 0.01) analysis showed a moderate change of gene expression level in PC2, PC5, PC10, PI2, PI5, and PI10 (varying from 419 to 528 DEGs) and a drastic change in PC20, PC30, PI20, and PI30 (varying from 1080 to 4896 DEGs) (**Figure 1B**; Supplemental File S1). Based on the distribution of DEGs at each time point, we defined pollen-stigma interactions at 2, 5, 10 min as the "early stage pollination event," and pollen-stigma interactions at 20 and 30 min as the "late stage pollination event," relatively. At the early stage of

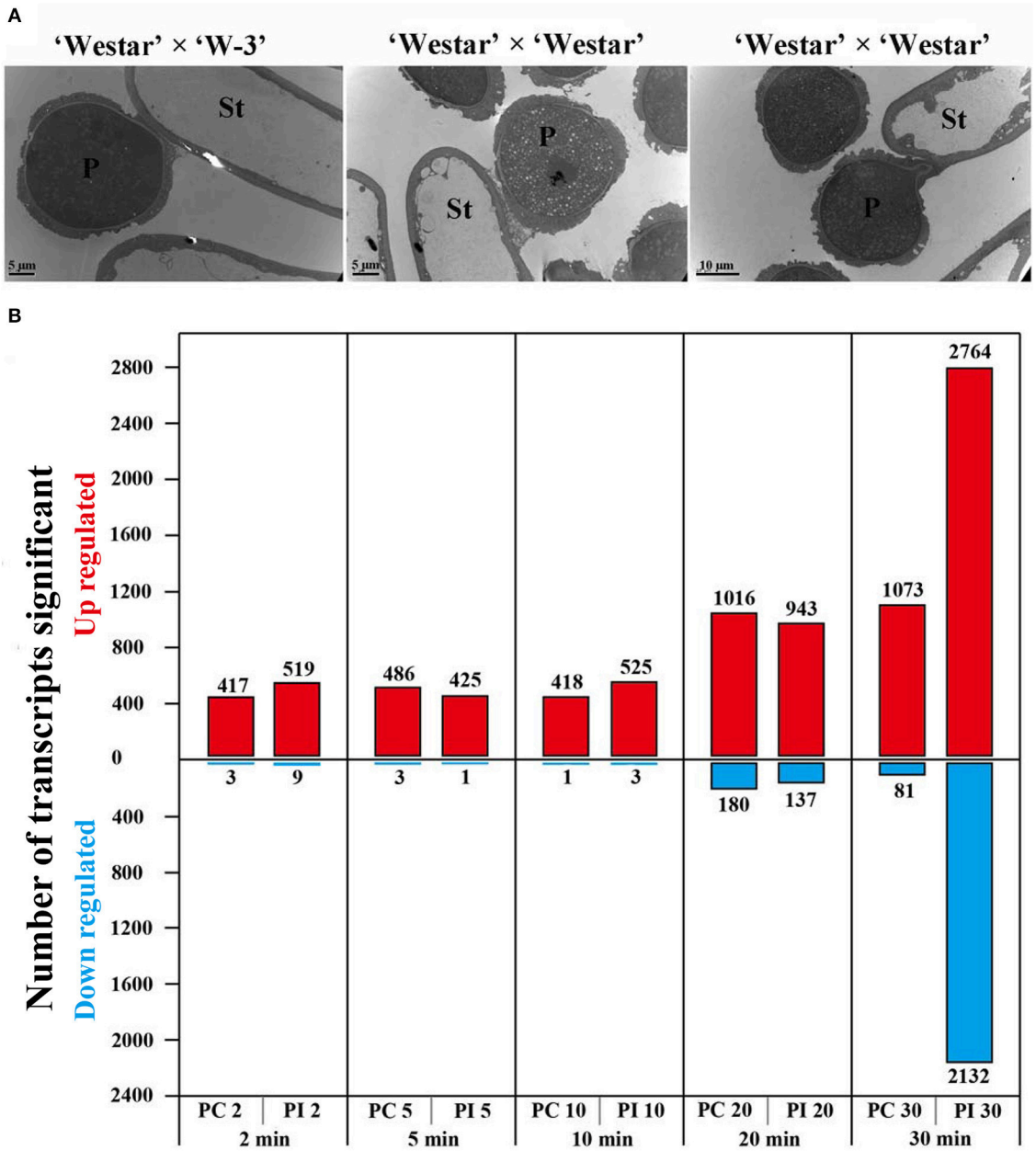

FIGURE 1 | Pollen-stigma interactions and DEGs (differentially expressed genes) identified in PC and PI samples. (A) Transmission electron micrographs (TEM) of compatible and incompatible pollen-stigma interactions 30 min after pollination. In "Westar" × "W-3" (left, incompatible), pollen was (i.e., showed no change in morphology) intact in 6/6 samples. In "Westar" × "Westar" (middle and right, compatible), two patterns were observed in all the analyzed 5 samples (39 pollen grains): pollen intact (18 pollen grains); pollen germinated and beginning to invade the cell wall of the stigma papilla cell (eight pollen grains). P, pollen grain; St, stigma papilla cell; Bars = 5 μm in the left and middle pictures; 10 μm in the right picture. **(B)** Number of DEGs up- or down-regulated at different time points in UP vs. PC and UP vs. PI ($\log_2$ fold changes $\geq$ 1 and a FDR $\leq$ 0.01).

pollination, 64 DEGs were up-regulated and only five were down-regulated (**Figure 1B**; Supplemental File S1). At the late stage of pollination, a drastic increase of DEGs was observed in UP vs. PI30 (2764 genes up-regulated and 2132 down regulated) (**Figure 1B**; Supplemental File S1), which further confirmed that pollen-stigma interaction already occurred by 30 min following pollination.

A total of 1453 DEGs and 5071 DEGs were detected in all samples of UP vs. PC and UP vs. PI, respectively (Supplemental File S2). They were grouped by cluster analysis into nine distinct time-course clusters respectively according to their expression patterns with minor manual revision (Supplemental File S3). This classification revealed that only a small number of DEGs (nine in UP vs. PC and 60 in UP vs. PI) were early stage pollination

specific (**Figures 2A,B**; Supplemental File S4). A moderate number of DEGs appeared during all stages of pollination and they were all up-regulated, with 529 DEGs in UP vs. PC and 542 DEGs in UP vs. PI (Supplemental File S5). The majority of DEGs were late stage specific, including 915 in UP vs. PC (704 up-regulated, 211 down-regulated) and 4469 in UP vs. PI (2337 up-regulated, 2132 down-regulated) (Supplemental File S6). The significant difference in the number of DEGs between UP vs. PC and UP vs. PI was mainly at the late stage of pollination with many more DEGs found in UP vs. PI, indicating that the signal transduction networks may be more complicated in UP vs. PI than UP vs. PC.

Early Stage Specific DEGs

A total of 69 early stage specific DEGs were identified. Of the nine early stage-specific DEGs in UP vs. PC, seven were up-regulated and involved in pectinesterase activity (*BnaCnng76410D*), xylanase activity (*BnaA04g00410D*), chlorophyll binding (*BnaA07g07570D*) and other biological processes; the other two were down-regulated and involved in vacuolar sorting signal binding (*BnaC08g24040D*) and glucosidase activity (*BnaC07g27160D*) (**Figures 2A,B**; Supplemental File S7).

Among the 60 early stage specific DEGs in UP vs. PI, 59 genes were up-regulated with 57 found in UP vs. PI2 and two in UP vs. PI10 (**Figure 2B**). The most over-represented

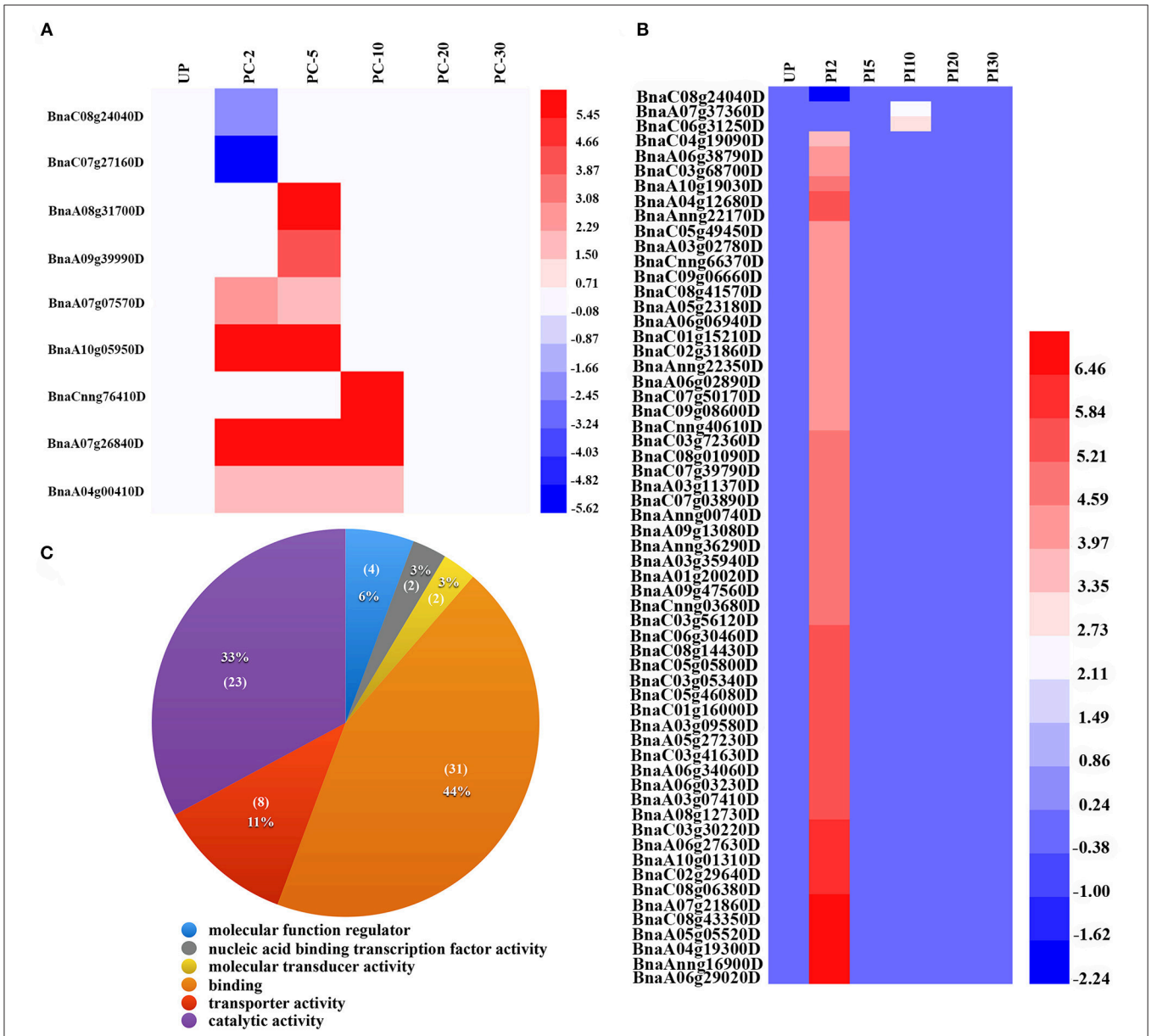

FIGURE 2 | Identification and annotation of early stage specific DEGs. (A) Expression patterns of early stage specific DEGs in UP vs. PC. **(B)** Expression patterns of early stage specific DEGs in UP vs. PI. **(C)** GO annotation results of early stage specific DEGs in UP vs. PI.

GO terms in molecular function were "binding" (GO:0005488) and "catalytic activity" (GO:0003824), accounting for 44% (31 genes) and 33% (23 genes) of the annotated terms, respectively (**Figure 2C**; Supplemental File S7). The term "binding" included genes related to phospholipid binding, metal ion binding, actin binding, DNA binding, ribonucleoside binding and tubulin binding. Of the 23 genes associated with catalytic activity, 11 were involved in protein serine/threonine kinase activity (GO:0004674). In addition, the terms "transporter activity" (GO:0005215), "molecular function regulator" (GO:0098772) and "transcription factor activity" (GO:0001071) were also identified (**Figure 2C**; Supplemental File S7). The only gene down-regulated was involved in vacuolar sorting signal binding (*BnaC08g24040D*). The majority of the DEGs at early stage in UP vs. PC and UP vs. PI were up-regulated, indicating that some biological processes might be activated by pollination; in the meanwhile, pollen expressed genes might contribute to the up-regulated DEGs.

Late Stage Specific DEGs

Among the up-regulated genes, 542 DEGs were shared by UP vs. PI and UP vs. PC, 1795 were UP vs. PI specific and only 162 were UP vs. PC specific. For down-regulated genes, 173 DEGs were shared in UP vs. PC and UP vs. PI, with 1959 specific in UP vs. PI and 38 in UP vs. PC (**Figure 3A**; Supplemental File S8). The biological functions of the DEGs were annotated and shown in Supplemental File S9. The 20 most highly represented GO terms

A

B

	PC-special	No. of genes	Common	No. of genes	PI-special	No. of genes
Up	response to carbohydrate stimulus	47	response to chitin	104	response to endoplasmic reticulum stress	147
	response to chitin	43	response to carbohydrate stimulus	116	multi-organism process	378
	response to fungus	29	response to wounding	67	ER-nucleus signaling pathway	84
	response to jasmonic acid stimulus	27	hyperosmotic salinity response	38	systemic acquired resistance	143
	response to organic substance	68	response to water	62	defense response, incompatible interaction	156
	intracellular signal transduction	25	ER-nucleus signaling pathway	38	immune system process	228
	response to wounding	27	endoplasmic reticulum unfolded protein response	37	cellular response to stress	290
	response to other organism	43	response to organic substance	189	innate immune response	207
	response to chemical stimulus	78	response to water deprivation	60	response to biotic stimulus	298
	respiratory burst involved in defense response	15	response to abscisic acid stimulus	73	response to other organism	294
	fatty acid metabolic process	21	fatty acid biosynthetic process	40	response to temperature stimulus	212
	response to hormone stimulus	43	response to fungus	62	response to water	126
	response to mechanical stimulus	11	response to mechanical stimulus	28	response to water deprivation	125
	response to bacterium	23	response to chemical stimulus	218	response to heat	93
	jasmonic acid biosynthetic process	14	response to cold	65	defense response	300
	jasmonic acid metabolic process	15	hyperosmotic response	39	response to chitin	125
	multi-organism process	44	intracellular signal transduction	58	endoplasmic reticulum unfolded protein response	71
	fatty acid biosynthetic process	18	negative regulation of cell death	30	programmed cell death	131
	response to stimulus	96	response to jasmonic acid stimulus	54	response to stress	584
	immune effector process	17	response to temperature stimulus	78	response to stimulus	838
Down	regulation of protein dephosphorylation	6	circadian rhythm	10	phenylpropanoid metabolic process	127
	photosynthesis, light reaction	7	plant-type cell wall loosening	5	cellular aromatic compound metabolic process	228
	photosynthetic electron transport in photosystem I	4	polysaccharide metabolic process	19	polysaccharide metabolic process	182
	generation of precursor metabolites and energy	9	gibberellic acid mediated signaling pathway	7	carbohydrate metabolic process	379
	rRNA processing	6	carbohydrate metabolic process	38	secondary metabolic process	199
	serine family amino acid metabolic process	6	cytidine to uridine editing	3	response to hormone stimulus	340
	glycosylceramide catabolic process	2	steroid biosynthetic process	10	response to endogenous stimulus	341
	sulfur amino acid metabolic process	6	response to gibberellin stimulus	9	RNA methylation	77
	cysteine biosynthetic process	5	response to hormone stimulus	33	flavonoid metabolic process	85
	response to sucrose stimulus	5	chemical homeostasis	12	metabolic process	1406
	amine biosynthetic process	7	cellular polysaccharide metabolic process	15	cellular ion homeostasis	72
	photosystem II assembly	4	cellular ion homeostasis	9	biological regulation	817
	response to copper ion	2	inositol catabolic process	2	transport	520
	sulfur compound biosynthetic process	6	response to auxin stimulus	14	phenylpropanoid biosynthetic process	97
	plastid organization	5	response to brassinosteroid stimulus	7	aromatic compound biosynthetic process	172
	cellular amino acid biosynthetic process	6	glucan metabolic process	13	cellular cation homeostasis	67
	cellular amine metabolic process	7	response to external stimulus	19	establishment of localization	525
	photosynthesis, light harvesting	2	cell wall modification	12	hormone-mediated signaling pathway	198
	cellular carbohydrate catabolic process	6	response to mechanical stimulus	5	regulation of biological quality	244
	glycoside catabolic process	2	sterol biosynthetic process	7	localization	546

FIGURE 3 | Identification and annotation of late stage specific DEGs. (A) Venn diagrams of late stage specific DEGs, comparing up- and down-regulated genes between UP vs. PC and UP vs. PI. **(B)** The 20 most highly represented GO terms for biological process in each DEG data set.

of each DEG data set were listed in **Figure 3B** and Supplemental File S9.

For 162 genes up-regulated only in UP vs. PC, more than half of the over-represented GO terms were involved in stress response, such as responses to carbohydrate stimulus, chitin, fungus, and wounding. Besides, jasmonic acid related GO terms including response to jasmonic acid stimulus, jasmonic acid biosynthetic process and jasmonic acid metabolic process were found. Fatty acid metabolic process and fatty acid biosynthetic process were also identified in the annotation results. GO terms related to stress response were over-represented in genes up-regulated in both UP vs. PC and UP vs. PI. In addition, the terms "ER-nucleus signaling pathway," "endoplasmic reticulum unfolded protein response," "response to abscisic acid stimulus," and "negative regulation of cell death" were also found. For genes up-regulated only in UP vs. PI, "response to endoplasmic reticulum stress" (147 genes), "multi-organism process" (378 genes) and "ER-nucleus signaling pathway" (84 genes) were the three most over-represented GO terms. In addition, defense response-related GO terms were also found, including "systemic acquired resistance," "incompatible interaction," "immune system process" and other processes. Stress response related GO terms were highly represented in all three DEG data sets for up-regulated genes, implying that pollen-stigma interactions might require elements involved in the processes of responding to stress.

For 38 genes down-regulated only in UP vs. PC, "regulation of protein dephosphorylation" was the most predominant GO term. GO terms involved in generation of precursor metabolites and energy, serine family amino acid metabolic process and cysteine biosynthesis were highly represented. GO terms related to photosynthesis, light reaction and photosynthetic electron transport in photosystem were also over-represented. GO terms of genes down-regulated both in UP vs. PC and UP vs. PI are mainly involved in polysaccharide metabolism (glucan metabolic process, plant-type cell wall loosening and cell wall modification) and response to hormone stimulus (by gibberellins, auxins and brassinosteroids). Besides, GO terms "circadian rhythm" and "carbohydrate metabolism" were also found in this category. GO terms of genes down-regulated only in UP vs. PI are mainly involved in metabolic processes, such as phenylpropanoid, cellular aromatic compound, polysaccharide, carbohydrate, secondary and flavonoid metabolism. A larger number of down-regulated genes were identified specifically in UP vs. PI and annotated to be related to metabolic processes, making the hypothesis possible that signaling transduction relying on some metabolic pathways might be cut off in incompatible response.

DEGs at All Stages of Pollination

529 DEGs in UP vs. PC and 542 DEGs in UP vs. PI DEGs were found and up-regulated at all stages of pollination, including 457 genes in both UP vs. PC and UP vs. PI, 72 in UP vs. PC only, and 85 in UP vs. PI only (Supplemental File S10). The predominant biological process GO terms of DEGs up-regulated both in UP vs. PC and in UP vs. PI involved "plant-type cell wall modification," "pollen tube growth," and "pollination." "Extracellular region," "pollen tube," and "plant-type cell wall" were the three most over-represented GO terms for cellular components. The most over-represented GO terms in molecular functions were "pectinesterase activity" and "hydrolase activity" (Supplemental File S11).

GO terms "pollen tube growth," "reproductive process," "extracellular region part," and "plant-type cell wall modification" were also highly represented in UP vs. PC specific DEGs. (Supplemental File S11). The enriched GO term "pollination" (GO:0009856) was further analyzed, containing 21 of 72 UP vs. PC specific genes (**Table 1**) and several homologs of *Arabidopsis* genes involved in the pollination process. *ACA9* (*BnaA01g25310D*) was identified as a member of the ACA family; another member in this family, *ACA13*, was reported to function as an auto-inhibited Ca^{2+} transporter and was required for compatible pollination (Iwano et al., 2014). *ANXUR2* (*ANX2*), the homolog of *BnaA02g31020D*, was reported to function together with *ANXUR1* (*ANX1*) to regulate timing of rupture in pollen—pollen tubes of *anx1/anx2* mutants ruptured before arriving at the egg apparatus (Miyazaki et al., 2009). *LIP2* (homolog of *BnaA03g28130D*) and *LIP1* were anchored to the membrane in the pollen tube tip region via palmitoylation, which was essential for controlling pollen tube guidance into the micropyle (Liu et al., 2013). Ca^{2+}-dependent protein kinase11 (*CPK11*) and *CPK24* (homolog of *BnaA04g19460D*) were involved in Ca^{2+}-dependent regulation of the inward K^+ (K^+ in) channels in pollen tubes—disruption of *CPK11* or *CPK24* completely impaired Ca^{2+}-dependent inhibition of K^+ in currents and enhanced pollen tube growth (Zhao et al., 2013).

UP vs. PI specific DEGs were mainly involved in stress response and defense response (Supplemental File S11) and had totally different enriched GO-terms from UP vs. PC specific DEGs. As the mechanisms of SI and pathogen resistance (PR) are remarkably similar: SI involves recognition and rejection of "self" pollen grains and pathogen resistance (PR) involves recognition and rejection of pathogens (Hodgkin et al., 1988; Sanabria et al., 2008; Rea et al., 2010), thus the GO term "immune system process" (GO:0002376) was further analyzed and 21 of 85 UP vs. PI specific genes were identified (**Table 2**). *WRKY33* (a homolog of *BnaA03g17820D* and *BnaC03g21360D*) is a key transcriptional regulator of response to necrotrophic fungal pathogen *Botrytis cinerea* and *Alternaria brassicicola* infection in *Arabidopsis*, which involves cross-talk between jasmonate- and salicylate-regulated disease response pathways (Zheng et al., 2006; Birkenbihl et al., 2012). The expression of *AtCAF1A* (homolog of *BnaC03g54940D*) can be induced by multiple stress-related hormones and stimuli. Mutation of *AtCAF1A* caused defective deadenylation of stress-related mRNAs and reduced expression of pathogenesis-related (PR) genes *PR1* and *PR2*, making plants more susceptible to *Pseudomonas syringae pv.* tomato DC3000 (Pst DC3000) infection (Liang et al., 2009). *ERF4* (homolog of *BnaA03g33790D* and *BnaC03g39000D*) negatively regulates the expression of gene related to JA-responsive defense and the resistance to the necrotrophic fungal pathogen *Fusarium oxysporum* (McGrath et al., 2005). *JAZ1* (homolog of *BnaC08g36840D*), a member of the JAZ family, was a repressor of JA signaling pathways. *WRKY40* (homolog of *BnaA07g35260D*

TABLE 1 | Enriched UP vs. PC specific DEGs in the GO term "pollination."

Brassica napus gene ID	*Arabidopsis* gene ID	Gene name	Gene description
BnaA01g25310D	*AT3G21180*	*ACA9*	Autoinhibited Ca^{2+}-ATPase
BnaA01g21610D	*AT1G58122*	*CPUORF45*	Conserved upstream opening reading frame relative to major ORF AT1G58120.1
BnaA02g07080D	*AT5G59370*	*ACT4*	Belongs to the reproductive actin subclass that expressed in developing and reproductive tissues
BnaA02g31020D	*AT5G28680*	*ANX2*	Receptor-like kinase required for maintenance of pollen tube growth
BnaA03g15420D	*AT2G33420*	None	Unknown function
BnaA03g28130D	*AT3G02810*	*LIP2*	Receptor-like cytoplasmic kinase that controls micropylar pollen tube guidance
BnaA03g37560D	*AT3G24715*	None	Protein kinase superfamily protein with octicosapeptide/Phox/Bem1p domain
BnaA04g18240D	*AT3G24715*	None	Protein kinase superfamily protein with octicosapeptide/Phox/Bem1p domain
BnaA04g19460D	*AT2G31500*	*CPK24*	Member of Calcium Dependent Protein Kinase
BnaA05g19830D	*AT2G33420*	None	Unknown function
BnaA07g08200D	*AT3G21180*	*ACA9*	Autoinhibited Ca^{2+}-ATPase
BnaA07g19700D	*AT1G29140*	None	Pollen Ole e 1 allergen and extensin family protein
BnaA07g26300D	*AT1G79860*	*ATROPGEF12*	Encodes a member of KPP-like gene family, homolog of KPP (kinase partner protein) gene in tomato
BnaA08g18440D	*AT1G67290*	*GLOX1*	Glyoxal oxidase-related protein
BnaA09g30960D	*AT1G28270*	*RALF4*	Member of a diversely expressed predicted peptide family showing sequence similarity to tobacco Rapid Alkalinization Factor (RALF)
BnaC05g14980D	*AT1G23540*	*PERK12*	Encodes a member of the PERK family of putative receptor kinases
BnaC05g30810D	*AT1G23540*	*PERK12*	Encodes a member of the PERK family of putative receptor kinases
BnaC06g28370D	*AT3G21180*	*ACA9*	Autoinhibited Ca^{2+}-ATPase
BnaC08g32350D	*AT1G67290*	*GLOX1*	Glyoxal oxidase-related protein
BnaC09g19870D	*AT5G47000*	None	Peroxidase superfamily protein
BnaCnng62360D	*AT1G29140*	None	Pollen Ole e 1 allergen and extensin family protein

and *BnaC06g40170D*) was reported to regulate plant defense response in *Arabidopsis* in a complex pattern (Xu et al., 2006; Shen et al., 2007).

Genes Enriched in All Stigma Samples

Three self-incompatibility related genes, the stigma determinant gene *BnSRK-1* (*BnaA07g25970D*) (Stein et al., 1991; Takasaki et al., 2000; Okamoto et al., 2007), pollen adhesion related genes *SLG* (*BnaA07g25960D*) and two copies of *SLR1* (*BnaC03g37350D* and *BnaA03g32070D*) (Luu et al., 1997, 1999) were found to be expressed highly in un-pollinated stigma, and the expression levels of these reported pollen-stigma interaction genes showed no obvious differences between compatible and incompatible pollinations. Thus, enriched genes in all stigma samples might also participate in pollen-stigma interactions. Genes with FPKM values above 250 in UP were selected, and 293 most highly expressed genes were identified and annotated (Supplemental File S12). Gene Ontology (GO) analysis and GO-term enrichment analysis were conducted to elucidate the biological functions of the stigma-enriched genes (Supplemental File S12). The GO term "recognition of pollen" (GO:0048544) was over-represented, with *BnSRK-1* (*BnaA07g25970D*), *SLG* (*BnaA07g25960D*) and *SLR1* (*BnaC03g37350D* and *BnaA03g32070D*) identified (Supplemental File S12).

The 10 most highly represented GO terms in each category of biological process, cellular components and molecular functions are shown in **Figure 4A**. Several over-represented GO terms related to stress response were found, such as "response to abiotic stimulus" (osmotic stress and temperature stimulus), and "response to inorganic substance" (such as cadmium and metal ions) (**Figure 4A**; Supplemental File S12). GO term "cell wall" was identified in the category of cellular components. Plant cell wall is a highly dynamic, responsive structure that extends to the plasma membrane and underlying cytoskeleton during signal transduction (reviewed by Baluska et al., 2003). The cell wall of stigma is regarded as an obstacle for pollen tube growth and it also plays an important role in relaying information from external stimuli (reviewed by Humphrey et al., 2008). In addition, the terms "water transport" in molecular function and "water channel activity" in biological process were over-represented, confirming the role of stigma in providing resources for the hydration and germination of pollen grains in compatible pollination. Chloroplast related terms "thylakoid," "chloroplast part," and "chloroplast envelope" in cellular components, "chlorophyll binding" and "ribulose-bisphosphate carboxylase activity" in molecular functions were also found.

To characterize metabolic pathways activated in the stigma, stigma-enriched genes were mapped to metabolic pathways using the GO-EnzymeCode Mapping tool with the software Blast2Go. A total of 37 metabolic pathways were identified and ranked according to the number of mapped enzymes (Supplemental File S13). Starch and sucrose metabolism (eight enzymes including nine genes), biosynthesis of antibiotics (six enzymes, 16 genes) and cysteine and methionine metabolism (five enzymes, seven genes) were the three most over-represented

TABLE 2 | UP vs. PI specific DEGs involving the enriched GO term "immune system process."

Brassica napus gene ID	*Arabidopsis* gene ID	Gene name	Gene description
BnaA01g05060D	None	None	Unknown
BnaA02g28700D	*AT3G27210*	None	Unknown
BnaA03g17820D	*AT2G38470*	*WRKY33*	Member of the plant WRKY transcription factor family
BnaA03g33790D	*AT3G15210*	*ERF-4*	Encodes a member of the ERF (ethylene response factor) subfamily B-1 of ERF/AP2 transcription factor family (ATERF-4)
BnaA03g55320D	*AT5G06320*	*NHL3*	Encodes a protein whose sequence is similar to tobacco hairpin-induced gene (HIN1) and Arabidopsis non-race specific disease resistance gene (NDR1)
BnaA05g19210D	*AT3G19970*	None	Alpha/beta-Hydrolases superfamily protein
BnaA06g12890D	*AT1G18740*	None	Unknown
BnaA06g21090D	none	None	Unknown
BnaA06g24410D	*AT5G65530*	*RLCK VI_A3*	Encodes a protein kinase involved in mediating resistance to fungi and also trichome branch number
BnaA07g15770D	*AT3G52800*	Unknown	Unknown
BnaA07g35260D	*AT1G80840*	*WRKY40*	Pathogen-induced transcription factor
BnaA08g30600D	*AT4G32150*	*VAMP711*	Member of Synaptobrevin-like AtVAMP7C, v-SNARE (soluble N-ethyl-maleimide sensitive factor attachment protein receptors) protein family
BnaC03g21360D	*AT2G38470*	*WRKY33*	Member of the plant WRKY transcription factor family
BnaC03g22390D	*AT2G40000*	*HSPRO2*	Ortholog of sugar beet HS1 PRO-1 2 (HSPRO2)
BnaC03g39000D	*AT3G15210*	*ERF-4*	Encodes a member of the ERF (ethylene response factor) subfamily B-1 of ERF/AP2 transcription factor family (ATERF-4)
BnaC03g54940D	*AT3G44260*	*CAF1A*	Encodes one of the homologs of the yeast CCR4-associated factor 1
BnaC05g09910D	*AT1G13530*	None	Unknown
BnaC05g50160D	none	None	Unknown
BnaC06g40170D	*AT1G80840*	*WRKY40*	Pathogen-induced transcription factor
BnaC08g24010D	*AT2G36320*	none	Unknown
BnaC08g36840D	*AT1G19180*	*JAZ1*	Nuclear-localized protein involved in jasmonate signaling

metabolic pathways (Supplemental File S13). In addition to the results of metabolic pathway analysis, we also found that "adenosylhomocysteinase activity" (GO:0004013), "histone methyltransferase activity" (H3-K36 specific) (GO:0046975), "S-methyltransferase activity" (GO:0008172) and "methionine synthase activity" (GO:0008705) were over-represented in the GO-term enrichment analysis (Supplemental File S12). The identified five enzymes in the pathway of cysteine and methionine metabolism included all the four S-adenosyl-L-methionine (SAM) cycle related enzymes (Plant Metabolic Network, PMN, http://www.plantcyc.org/) (**Figure 4B**), implying that the active SAM cycle pathway may participate in the pollen-stigma interaction. Alongside the results of metabolic pathways analysis, the adenosylhomocysteinase activity (GO:0004013), histone methyltransferase activity (H3-K36 specific) (GO:0046975), S-methyltransferase activity (GO:0008172) and methionine synthase activity (GO:0008705) were also found to be over-represented (Supplemental File S12).

Validation of RNA-Seq Data by Quantitative Real-Time RT-PCR

To verify the DEGs and stigma-enriched genes identified by RNA-seq data, quantitative real-time RT-PCR was conducted with stigma samples harvested independently at the same time point as those collected for RNA-seq analysis. Five genes were selected randomly from DEGs at different stages, *BnSRK-1* and two genes enriched in all stigma samples involved in SAM cycle were chosen as well (**Figure 5**). The expression patterns of the DEGs analyzed by qRT-PCR were mostly consistent with the original RNA-seq data (a mean correlation coefficient of 0.81), few differences were found in the time points when gene expression level significantly changed (for example *Bna03g30180D*, **Figure 5E**), which was possibly caused by diverse sensitivities and algorithms between these two measuring means. The other three genes were expressed at high levels in all the samples and showed no significant difference in gene expression levels in each sample (**Figures 5F–H**). Their expression characteristics tested by qRT-PCR agreed well with those analyzed by RNA-seq, although low correlation coefficients were shown. These results indicated that the RNA-seq data were reliable.

DISCUSSION

Transcriptional Characteristics of Pollen-Stigma Interactions

We have created one transgenic self-incompatible *B. napus* line "W-3" by complementing the function of *BnSP11-1* in self-compatible *B. napus* line "Westar" (Gao et al., 2016). There is a 3606-bp DNA fragment inserting into the promoter region of *BnSP11-1*, which is supposed to be responsible for the

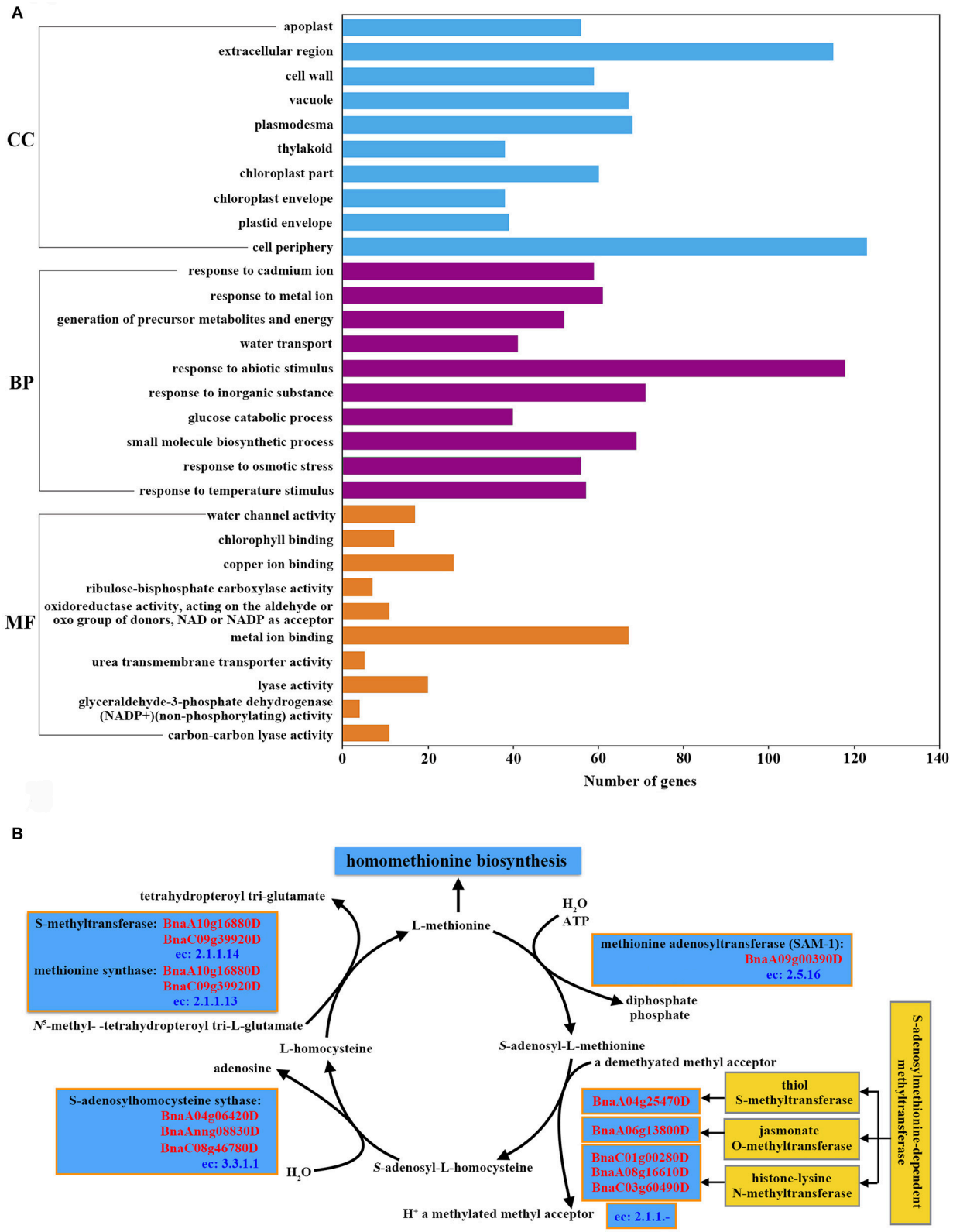

FIGURE 4 | Annotation of stigma-enriched genes. (A) The 10 most highly represented GO terms in each category (biological process, cellular components and molecular functions). **(B)** Identification of the genes in the S-adenosyl-L-methionine (SAM) cycle and S-adenosylmethionine-dependent methyltransferases.

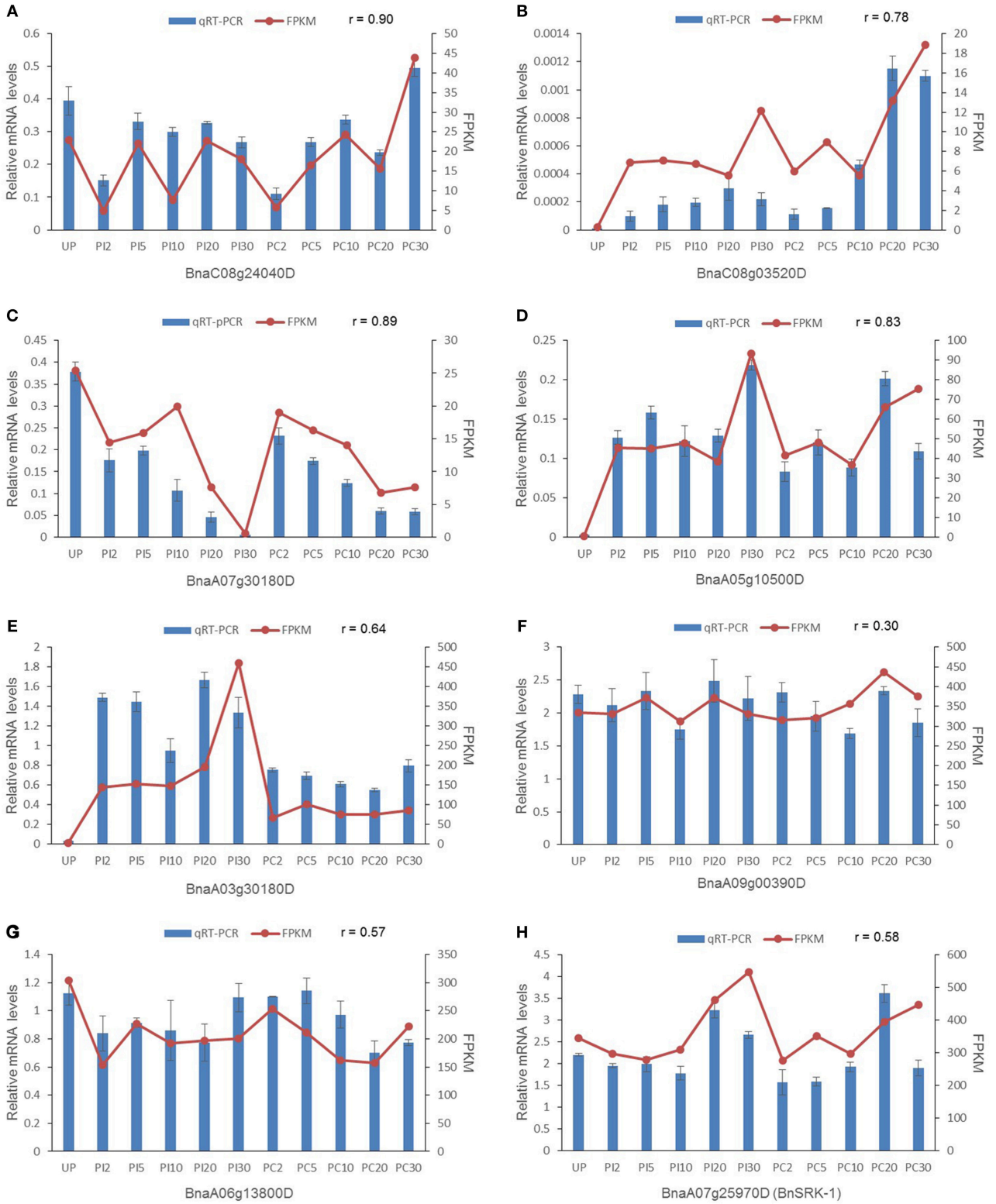

FIGURE 5 | Validation of eight randomly selected genes by qRT-PCR. (A) One of the early stage DEGs. **(B,C)** Two DEGs at late stage. **(D,E)** Two DEGs at all stages. **(F–H)** Stigma-enriched genes. *BnaA09g00390D* and *BnaA06g13800D* are genes involved in SAM cycle. mRNA expression levels were normalized to the expression of *ACTIN*, and means from three biological replicates are shown. Error bars indicate ± SE. r represents the correlation coefficient.

self-compatibility of "Westar" (Okamoto et al., 2007; Tochigi et al., 2011). "W-3" shows strong self-incompatibility and has the identical genetic background with "Westar" except for the induced functional *BnSP11-1*. Therefore, the transgenic *B. napus* line "W-3" was ideal to study compatible and incompatible pollen-stigma interactions. By observation of "Westar" stigmas 30 min after pollination using TEM, all "W-3" pollen grains were found to be intact (i.e., showed no change in morphology), while some "Westar" pollen grains germinated and began to invade the cell wall of the stigma papilla cell (**Figure 1A**). A time-course transcriptome analysis was employed to investigate compatible and incompatible pollen-stigma interactions, a moderate change in gene expression level was observed at 2, 5, and 10 min after pollination (varying from 419 to 528 DEGs), and a drastic change was found at 20 and 30 min after pollination (varying from 1080 to 4896 DEGs) (**Figure 1B**; Supplemental File S1). A moderate number of DEGs (529 in compatible interaction and 542 in incompatible interaction) appeared during all stages of pollination and they were all up-regulated; the majority of DEGs were detected at time points of 20 and 30 min, including 915 in compatible interaction (704 up-regulated, 211 down-regulated) and 4469 in incompatible interaction (2337 up-regulated, 2132 down-regulated). From the above results, it could be deduced that pollen-stigma interaction would complete 30 min after pollination, and downstream components were activated in signaling pathways of both compatible and incompatible responses, while the signal transduction networks in incompatible response might be more complicated than that in compatible response.

Enriched genes in all stigma samples including un-pollinated stigmas were firstly analyzed in our present study. We found the reported pollen-stigma interaction genes, the stigma determinant gene *BnSRK-1* (Stein et al., 1991; Takasaki et al., 2000; Okamoto et al., 2007), pollen adhesion related genes *SLG* and *SLR1* (Luu et al., 1997, 1999), were expressed highly in un-pollinated stigma and all pollinated stigmas, which is in accordance with the demonstration by Nasrallah (1974) that the SI response is regulated during stigma maturation: stigmas are initially compatible with self-pollen and acquire the ability to reject self-pollen in conjunction with anther dehiscence 1–2 days before flower opening or anthesis. Based on this feature, bud-pollination was developed by Shivanna et al. (1978), and has been used widely to amplify self-incompatible lines in *Brassica*. A total of 37 metabolic pathways were identified. Starch and sucrose metabolism is one of the three most over-represented metabolic pathways, which has been reported by Matsuda et al. (2014). Biosynthesis of antibiotics, and cysteine and methionine metabolism pathways are first annotated in this study. Genes involved in cysteine and methionine metabolismwere tested by qRT-PCR and shown to be expressed at high levels in each sample. Further researches on other enriched genes might reveal genes necessary for pollen-stigma reaction signaling pathways.

Genes expressed differentially in compatible or incompatible reactions at all-time points compared to un-pollinated stigmas were also firstly identified in this study. A moderate change of gene expression was observed at 2, 5, and 10 min after pollination, but only nine in compatible and 60 in incompatible reactions were early stage specific DEGs. Quite limited genes expressed in pollen might be included because there was only one gene shared by UP vs. PC and UP vs. PI at early stage, and genes abundant in pollen would not lead to such a limited number of early stage DEGs in compatible reaction. For the 60 DEGs incompatible reaction, the most over-represented GO terms in molecular function were "binding" and "catalytic activity," accounting for 44% (31 genes) and 33% (23 genes) of the annotated terms, respectively. The term "binding" included genes related to phospholipid binding, metal ion binding, actin binding, DNA binding, ribonucleoside binding and tubulin binding. A subunit of the microtubule (MT) network, alpha 2–4 tubulin, was identified in the proteomic analysis for self-incompatibility response in *Brassica napus* (Samuel et al., 2011). It was proposed that the depolymerization of MT is necessary for accepting compatible pollen. Thus, genes related to tubulin binding might regulate self-pollen rejection by affecting the stability of MT network. In addition, compared to previous studies, a quantity of DEGs were also represented here, such as genes related to jasmonic acid production and plant-type cell wall metabolism were up-regulated at late stage in UP vs. PC samples, which is consistent with results reported by Swanson et al. (2005) and Matsuda et al. (2014). Most genes involved in stress response or defense response were up-regulated in both incompatible and compatible reactions at late-time points (20 and 30 min after pollination), while the unique proteins in the same GO terms were found to be down-regulated in incompatible pollination previously (Samuel et al., 2011). There is no discrepancy between this study and the previous one, since the previous study focused more on degraded proteins that were possibly ubiquitinated (Samuel et al., 2011).

Pollen-Stigma Interactions and Pathogen-Plant Interactions

Compatible pollen can penetrate the cell wall of papillae cells while incompatible pollen-stigma interactions can cause blocks in pollen hydration, germination and pollen tube growth at the stigma. However, the downstream molecular events were largely unknown. In pathogen-plant interactions, a classic "zigzag" model was proposed to illustrate this process, which involves two branches of the plant immune system: PTI (PAMP-triggered immunity, inducing responses activated upon recognition of conserved PAMPs, such as peptidoglycan, flagellin, chitin and others) and ETI [effector-triggered immunity, inducing R (resistance) gene-mediated resistance reactions activated upon recognition of an avirulence factor] (Chisholm et al., 2006; Jones and Dangl, 2006). First, PAMPs (pathogen-associated molecular patterns) can be perceived by plants, inducing PTI which can stop the colonization of pathogens. Then the pathogens can adapt the effectors that contribute to pathogen virulence to interfere with PTI and induce effector-triggered susceptibility (ETS), permitting successful invasion of the plant cells. However, if the plant contains an R protein which can specifically recognize the effector, then ETI is induced, preventing the pathogen from invading the plant cells. In partial summary, two contrary

interaction patterns (compatible and incompatible) occur both in pollen-stigma interactions and pathogen-plant interactions.

Close parallels between SI and plant–pathogen interactions have been suggested (Hogenboom, 1983; Hodgkin et al., 1988; Nasrallah, 2005; Sanabria et al., 2008), both involving recognition and rejection, albeit of genetically similar ("self") pollen grains vs. "non-self" pathogens. It is hypothesized that both SI and plant–pathogen interaction processes may share the same basal genetic defense network, and genes involved in SI and defense might have common ancestors (Rea et al., 2010; reviewed by Sanabria et al., 2008). In addition, both SI and disease resistance signaling pathways were triggered by interactions between small peptide ligands (located in pollen or pathogen) and plasma membrane-spanning receptor kinases. We speculate that close parallels between SC and plant–pathogen interactions (mainly effector-triggered susceptibility, ETS) may also exist. Both processes comprise the recognition of extracellular materials (pollen/pathogen) and penetration into the "host" by a tubular cell emanating from a spore-like structure. Defense-related genes might function not only in defense against pathogens, but also in response to pollination (Tung et al., 2005). In rice, many stigma-specific genes encode stress and defense related proteins and stigma-specific genes shared some common cis-regulatory elements (GCC box for example) with stress-responsive genes (Li et al., 2007). In our annotation results of late stage specific DEGs, of the 20 most over-represented GO terms, stress response related ones appeared in all three DEG data sets: genes up-regulated only in UP vs. PC, genes up-regulated only in UP vs. PI and genes up-regulated both in UP vs. PC and UP vs. PI (**Figure 3B**; Supplemental File S9). Especially in the genes up-regulated only in UP vs. PC, more than half of the most over-represented GO terms were involved in stress response, such as responses to carbohydrate stimulus, chitin, fungus, wounding and others (**Figure 3B**; Supplemental File S9). However, in the genes up-regulated only in UP vs. PI, defense response related GO terms were over-represented, such as systemic acquired resistance, incompatible interaction, immune system process and others (**Figure 3B**; Supplemental File S9), which supports the hypothesis that SI and pathogen-plant interactions showed some common signaling pathways. Also in the DEGs found in all stages of pollination, stress and defense response related GO terms were over-represented in UP vs. PI specific genes but not in UP vs. PC specific genes (Supplemental File S11). We speculated that in pollen-stigma interactions, the stigma can recognize components located on the compatible pollen coat (just like PAMPs in the pathogen) and induce the stress response, a process similar to PTI and ETS. But when incompatible pollen is applied, the stigma can recognize components located on the pollen coat and the SP11/SCR protein (just like effectors in the pathogen), inducing both the stress and defense responses, a process similar to PTI and ETI.

S-adenosyl-L-methionine (SAM) Cycle in Stigma

Genes most highly expressed in stigmas consistently showed no obvious differences in the expression levels between compatible and incompatible pollinations, but they may also play important roles in pollen-stigma interactions, possibly through a means of post-translational modification such as phosphorylation, glycosylation, or methylation. In our expression data, several genes implicated in pollen-stigma interactions were found, including self-incompatibility gene *BnSRK-1* (*BnaA07g25970D*) (Stein et al., 1991; Takasaki et al., 2000; Okamoto et al., 2007), pollen adhesion related gene *SLG* (*BnaA07g25960D*) and two copies of *SLR1* (*BnaC03g37350D* and *BnaA03g32070D*) (Luu et al., 1997, 1999) (Supplemental File S12). We inferred that more unknown genes abundant in stigma may be required for pollen-stigma interactions. By analyzing the involved metabolic pathways of the stigma enriched genes, we found that the pathway of cysteine and methionine metabolism was over-represented, and all the four S-adenosyl-L-methionine (SAM) cycle related enzymes were found in this pathway (**Figure 4B**; Supplemental File S13). In the SAM cycle, S-methyltransferase and methionine synthase (*BnaA10g16880D* and *BnaC09g39920D*) were responsible for the generation of methionine. Then methionine adenosyltransferase (*SAM-1*, *BnaA09g00390D*) can convert methionine to SAM which is a methyl donor used for many cellular transmethylation reactions. In the transmethylation reactions SAM is converted to S-adenosyl-homocysteine (SAH) under the catalysis of S-adenosylmethionine-dependent methyltransferases, and three of them were identified in our data (*BnaA04g25470D*, *BnaA06g13800D*, *BnaC01g00280D*, *BnaA08g16610D,* and *BnaC03g60490D*). Finally S-adenosylhomocysteine synthase (*BnaA04g06420D*, *BnaAnng08830D,* and *BnaC08g46780D*) can convert SAH to homocysteine which was the precursor of methionine. SAM is then regenerated from methionine to finish the cycle (**Figure 4B**) (Giovanelli et al., 1985). Methionine synthase 1 (*MS1*, *BnaA10g16880D,* and *BnaC09g39920D*) plays a key role for the continual reactions of SAM cycle, which catalyzes the last reaction in *de novo* Met synthesis and helps to regenerate the methyl group of AdoMet following methylation reactions (Ravanel et al., 2004). Interestingly, *BnMS1* (also named *ATCIMS*, ortholog of *At5g17920*) was identified among the 19 down-regulated proteins following the SI reaction in *B. napus* as well (Samuel et al., 2011), indicating that *BnMS1* might play a role in regulating compatible and incompatible reactions.

AUTHOR CONTRIBUTIONS

TZ and CG designed and performed the research, analyzed data, and wrote the article with contributions of all the authors; YAY and ZL performed research and analyzed data; GZ, YOY, ZD, and BL provided technical assistance to TZ and CG; CM, JW, BY, JS, JT, and TF supervised the experiments; CM supervised and complemented the writing.

FUNDING

This work was funded by grants from the National Key Research and Development Program of China (No. 2016YFD0101301),

China Postdoctoral Science Foundation (2014M552055; 2015T80816), National Natural Science Foundation of China (3157101052).

ACKNOWLEDGMENTS

We thank Professor Daohong Jiang (State Key Laboratory of Agricultural Microbiology, Huazhong Agricultural University; Provincial Key Laboratory of Plant Pathology of Hubei Province, Huazhong Agricultural University) for advices on this work, and two reviewers for kind and constructive comments. Illumina HiSeq 2500 sequencer was provided by the National Key Laboratory of Crop Genetic Improvement, Huazhong Agricultural University.

SUPPLEMENTARY MATERIAL

The Supplementary Material for this article can be found online at: http://journal.frontiersin.org/article/10.3389/fpls.2017.00682/full#supplementary-material

REFERENCES

Baluska, F., Samaj, J., Wojtaszek, P., Volkmann, D., and Menzel, D. (2003). Cytoskeleton-plasma membrane-cell wall continuum in plants. *Plant Physiol.* 133, 482–491. doi: 10.1104/pp.103.027250

Birkenbihl, R. P., Diezel, C., and Somssich, I. E. (2012). Arabidopsis WRKY33 is a key transcriptional regulator of hormonal and metabolic responses toward botrytis cinerea infection. *Plant Physiol.* 159, 266–285. doi: 10.1104/pp.111.192641

Chalhoub, B., Denoeud, F., Liu, S., Parkin, I. A., Tang, H., Wang, X., et al. (2014). Early allopolyploid evolution in the post-Neolithic *Brassica napus* oilseed genome. *Science* 345, 950–953. doi: 10.1126/science.1253435

Chapman, L. A., and Goring, D. R. (2010). Pollen-pistil interactions regulating successful fertilization in the Brassicaceae. *J. Exp. Bot.* 61, 1987–1999. doi: 10.1093/jxb/erq021

Chisholm, S. T., Coaker, G., Day, B., and Staskawicz, B. J. (2006). Host-microbe interactions, shaping the evolution of the plant immune response. *Cell* 124, 803–814. doi: 10.1016/j.cell.2006.02.008

Conesa, A. I., Götz, S., García-Gómez, J. M., Terol, J., Talón, M., and Robles, M. (2005). Blast2GO, a universal tool for annotation, visualization and analysis in functional genomics research. *Bioinformatics* 21, 3674–3676. doi: 10.1093/bioinformatics/bti610

De Nettancourt, D. (2001). *Incompatibility and Incongruity in Wild and Cultivated Plants, 2nd Edn*. Berlin: Springer.

Doughty, J., Dixon, S., Hiscock, S. J., Willis, A. C., Parkin, I. A., and Dickinson, H. G. (1998). PCP-A1, a defensin-like Brassica pollen coat protein that binds the S locus glycoprotein, is the product of gametophytic gene expression. *Plant Cell* 10, 1333–1347. doi: 10.1105/tpc.10.8.1333

Elleman, C. J., Franklin-Tong, V., and Dickinson, H. G. (1992). Pollination in species with dry stigmas, the nature of the early stigmatic response and the pathway taken by pollen tubes. *New Phytol.* 121, 413–424. doi: 10.1111/j.1469-8137.1992.tb02941.x

Elleman, C. J., Willson, C. E., Sarker, R. H., and Dickinson, H. G. (1988). Interaction between the pollen tube and stigmatic cell wall following pollination in Brassica oleracea. *New Phytol.* 109, 111–117. doi: 10.1111/j.1469-8137.1988.tb00225.x

Franklin-Tong, V. E. (2008). *Self-Incompatibility in Flowering Plants, Evolution, Diversity, and Mechanisms*. Berlin: Springer-Verlag.

Gao, C., Zhou, G., Ma, C., Zhai, W., Zhang, T., Liu, Z., et al. (2016). Helitron-like transposons contributed to the mating system transition from out-crossing to self-fertilizing in polyploid *Brassica napus* L. *Sci. Rep.* 6:33785. doi: 10.1038/srep33785

Giovanelli, J., Mudd, S. H., and Datko, A. H. (1985). Quantitative analysis of pathways of methionine metabolism and their regulation in Lemna, *Plant Physiol.* 78, 555–560. doi: 10.1104/pp.78.3.555

Hiroi, K. I., Sone, M., Sakazono, S., Osaka, M., Masuko-Suzuki, H., Matsuda, T., et al. (2013). Time-lapse imaging of self- and cross-pollinations in *Brassica rapa*. *Ann. Bot.* 112, 115–122. doi: 10.1093/aob/mct102

Hodgkin, T., Lyon, G. D., and Dickinson, H. G. (1988). Recognition in flowering plants, a comparison of the Brassica self-incompatibility system and plant pathogen interactions. *New Phytol.* 110, 557–569. doi: 10.1111/j.1469-8137.1988.tb00296.x

Hogenboom, N. G. (1983). Bridging the gap between related fields of research, pistil-pollen relationships and the distinction between incompatibility and incongruity in nonfunctioning host-parasite relationships. *Phytopathology* 73, 381–383. doi: 10.1094/Phyto-73-381

Humphrey, T. V., Bonetta, D. T., and Goring, D. R. (2008). Sentinels at the wall, cell wall receptors and sensors. *New Phytol.* 176, 7–21. doi: 10.1111/j.1469-8137.2007.02192.x

Iwano, M., Igarashi, M., Tarutani, Y., Kaothien-Nakayama, P., Nakayama, H., Moriyama, H., et al. (2014). A pollen coat–inducible autoinhibited Ca^{2+}-ATPase expressed in stigmatic papilla cells is required for compatible pollination in the brassicaceae. *Plant Cell* 26, 639–649. doi: 10.1105/tpc.113.121350

Iwano, M., Shiba, H., Matoba, K., Miwa, T., Funato, M., Entani, T., et al. (2007). Actin dynamics in papilla cells of *Brassica rapa* during self- and cross-pollination. *Plant Physiol.* 144 , 72–81. doi: 10.1104/pp.106.095273

Jones, J. D., and Dangl, J. L. (2006). The plant immune system. *Nature* 444, 323–329. doi: 10.1038/nature05286

Jones, P., Binns, D., Chang, H. Y., Fraser, M., Li, W., McAnulla, C., et al. (2014). InterProScan 5, genome-scale protein function classification. *Bioinformatics* 30, 1236–1240. doi: 10.1093/bioinformatics/btu031

Kachroo, A., Schopfer, C. R., Nasrallah, M. E., and Nasrallah, J. B. (2001). Allele-specific receptor-ligand interactions in Brassica self-incompatibility. *Science* 293, 1824–1826. doi: 10.1126/science.1062509

Kakita, M., Murase, K., Iwano, M., Matsumoto, T., Watanabe, M., Shiba, H., et al. (2007a). Two distinct forms of M-locus protein kinase localize to the plasma membrane and interact directly with S-locus receptor kinase to transduce self-incompatibility signaling in *Brassica rapa*. *Plant Cell* 19, 3961–3973. doi: 10.1105/tpc.106.049999

Kakita, M., Shimosato, H., Murase, K., Isogai, A., and Takayama, S. (2007b). Direct interaction between S-locus receptor kinase and M-locus protein kinase involved in Brassica self-incompatibility signaling. *Plant Biotechnol.* 24, 185–190. doi: 10.5511/plantbiotechnology.24.185

Li, M., Xu, W., Yang, W., Kong, Z., and Xue, Y. (2007). Genome-wide gene expression profiling reveals conserved and novel molecular functions of the stigma in rice. *Plant Physiol.* 144, 1797–1812. doi: 10.1104/pp.107.101600

Liang, W., Li, C., Liu, F., Jiang, H., Li, S., Sun, J., et al. (2009). The Arabidopsis homologs of CCR4-associated factor 1 show mRNA deadenylation activity and play a role in plant defence responses. *Cell Res.* 19, 307–316. doi: 10.1038/cr.2008.317

Liu, J., Zhong, S., Guo, X., Hao, L., Wei, X., Huang, Q., et al. (2013). Membrane-bound RLCKs LIP1 and LIP2 are essential male factors controlling male-female attraction in Arabidopsis. *Curr. Biol.* 23, 993–998. doi: 10.1016/j.cub.2013.04.043

Luu, D. T., Heizmann, P., Dumas, C., Trick, M., and Cappadocia, M. (1997). Involvement of SLR1 genes in pollen adhesion to the stigmatic surface in Brassicaceae. *Sex. Plant Reprod.* 10, 227–235. doi: 10.1007/s00497005091

Luu, D. T., Marty-Mazars, D., Trick, M., Dumas, C., and Heizmann, P. (1999). Pollen-stigma adhesion in Brassica spp involves SLG and SLR1 glycoproteins. *Plant Cell* 11, 251–262. doi: 10.2307/3870854

Matsuda, T., Matsushima, M., Nabemoto, M., Osaka, M., Sakazono, S., Masuko-Suzuki, H., et al. (2014). Transcriptional characteristics and differences in

Arabidopsis stigmatic papilla cells pre- and post-Pollination. *Plant Cell Physiol.* 56, 663–673. doi: 10.1093/pcp/pcu209

McGrath, K. C., Dombrecht, B., Manners, J. M., Schenk, P. M., Edgar, C. I., Maclean, D. J., et al. (2005). Repressor- and activator-type ethylene response factors functioning in jasmonate signaling and disease resistance identified via a genome-wide screen of Arabidopsis transcription factor gene expression. *Plant Physiol.* 139, 949–959. doi: 10.1104/pp.105.068544

Miyazaki, S., Murata, T., Sakurai-Ozato, N., Kubo, M., Demura, T., Fukuda, H., et al. (2009). MANXUR1 and 2, sister genes to FERONIA/SIRENE, are male factors for coordinated fertilization. *Curr. Biol.* 19, 1327–1331. doi: 10.1016/j.cub.2009.06.064

Murase, K., Shiba, H., Iwano, M., Che, F. S., Watanabe, M., Isogai, A., et al. (2004). A membrane-anchored protein kinase involved in Brassica self-incompatibility signaling. *Science* 303, 1516–1519. doi: 10.1126/science.1093586

Nasrallah, J. (2005). Recognition and rejection of self in plant self-incompatibility, comparisons to animal histocompatibility. *Trends Immunol.* 26, 412–418. doi: 10.1016/j.it.2005.06.005

Nasrallah, M. E. (1974). Genetic control of quantitative variation of self-incompatibility proteins detected by immunodiffusion. *Genetics* 76, 45–50.

Okamoto, S., Odashima, M., Fujimoto, R., Sato, Y., Kitashiba, H., and Nishio, T. (2007). Self-compatibility in *Brassica napus* is caused by independent mutations in S-locus genes. *Plant J.* 50, 391–400. doi: 10.1111/j.1365-313X.2007.03058.x

Ravanel, S., Block, M. A., Rippert, P., Jabrin, S., Curien, G., Rebeille, F., et al. (2004). Methionine metabolism in plants, chloroplasts are autonomous for de novo methionine synthesis and can import S-adenosylmethionine from the cytosol. *J. Biol. Chem.* 279, 22548–22557. doi: 10.1074/jbc.M313250200

Rea, A. C., Liu, P., and Nasrallah, J. B. (2010). A transgenic self-incompatible Arabidopsis thaliana model for evolutionary and mechanistic studies of crucifer self-incompatibility. *J. Exp. Bot.* 61, 1897–1906. doi: 10.1093/jxb/erp393

Safavian, D., and Goring, D. R. (2013). Secretory activity is rapidly induced in stigmatic papillae by compatible pollen, but inhibited for self-incompatible pollen in the brassicaceae. *PLoS ONE* 8:e84286. doi: 10.1371/journal.pone.0084286

Samuel, M. A., Chong, Y. T., Haasen, K. E., Aldea-Brydges, M. G., Stone, S. L., and Goring, D. R. (2009). Cellular pathways regulating responses to compatible and self-incompatible pollen in Brassica and Arabidopsis stigmas intersect at Exo70A1, a putative component of the exocyst complex. *Plant Cell* 21, 2655–2671. doi: 10.1105/tpc.109.069740

Samuel, M. A., Tang, W., Jamshed, M., Northey, J., Patel, D., Smith, D., et al. (2011). Proteomic analysis of Brassica stigmatic proteins following the self-incompatibility reaction reveals a role for microtubule dynamics during pollen responses. *Mol. Cell Proteomics* 10, M111–M11338. doi: 10.1074/mcp.m111.011338

Sanabria, N., Goring, D., Nürnberger, T., and Dubery, I. (2008). Self/nonself perception and recognition mechanisms in plants, a comparison of self-incompatibility and innate immunity. *New Phytol.* 178, 503–514. doi: 10.1111/j.1469-8137.2008.02403.x

Shen, Q. H., Saijo, Y., Mauch, S., Biskup, C., Bieri, S., Keller, B., et al. (2007). Nuclear activity of MLA immune receptors links isolate-specific and basal disease-resistance responses. *Science* 315, 1098–1103. doi: 10.1126/science.1136372

Shivanna, K. R., Heslop-Harrison, Y., and Heslop-Harrison, J. (1978). The pollen-stigma interaction: bud pollination in the cruciferae. *Acat. Bot. Neerl.* 27, 107–119. doi: 10.1111/j.1438-8677.1978.tb00265.x

Stein, J. C., Howlett, B., Boyes, D. C., Nasrallah, M. E., and Nasrallah, J. B. (1991). Molecular cloning of a putative receptor protein kinase gene encoded at the self-incompatibility locus of Brassica oleracea. *Proc. Natl. Acad. Sci. U.S.A.* 88, 8816–8820. doi: 10.1073/pnas.88.19.8816

Swanson, R., Clark, T., and Preuss, D. (2005). Expression profiling of Arabidopsis stigma tissue identifies stigma-specific genes. *Sex. Plant Reprod.* 18, 163–171. doi: 10.1007/s00497-005-0009-x

Takasaki, T., Hatakeyama, K., Suzuki, G., Watanabe, M., Isogai, A., and Hinata, K. (2000). The S receptor kinase determines self-incompatibility in Brassica stigma. *Nature* 403, 913–916. doi: 10.1038/35002628

Takayama, S., Shimosato, H., Shiba, H., Funato, M., Che, F. S., Watanabe, M., et al. (2001). Direct ligand-receptor complex interaction controls Brassica self-incompatibility. *Nature* 413, 534–538. doi: 10.1038/35097104

Tochigi, T., Udagawa, H., Li, F., Kitashiba, H., and Nishio, T. (2011). The self-compatibility mechanism in *Brassica napus* L. is applicable to F1 hybrid breeding. *Theor. Appl. Genet.* 123, 475–482. doi: 10.1007/s00122-011-1600-1

Trapnell, C., Pachter, L., and Salzberg, S. L. (2009). TopHat, discovering splice junctions with RNA-Seq. *Bioinformatics* 25, 1105–1111. doi: 10.1093/bioinformatics/btp120

Trapnell, C., Williams, B. A., Pertea, G., Mortazavi, A., Kwan, G., Van Baren, M. J., et al. (2010). Transcript assembly and quantification by RNA-Seq reveals unannotated transcripts and isoform switching during cell differentiation. *Nat. Biotechnol.* 28, 511–515. doi: 10.1038/nbt.1621

Tung, C. W., Dwyer, K. G., Nasrallah, M. E., and Nasrallah, J. B. (2005). Genome-wide identification of genes expressed in Arabidopsis pistils specifically along the path of pollen tube growth. *Plant Physiol.* 138, 977–989. doi: 10.1104/pp.105.060558

Wu, J., Zhao, Q., Yang, Q., Liu, H., Li, Q., Yi, X., et al. (2016). Comparative transcriptomic analysis uncovers the complex genetic network for resistance to Sclerotinia sclerotiorum in *Brassica napus*. *Sci. Rep.* 6:19007. doi: 10.1038/srep19007

Xu, X., Chen, C., Fan, B., and Chen, Z. (2006). Physical and functional interactions between pathogen-induced Arabidopsis WRKY18, WRKY40, and WRKY60 transcription factors. *Plant Cell* 18, 1310–1326. doi: 10.1105/tpc.105.037523

Zhao, L. N., Shen, L. K., Zhang, W. Z., Zhang, W., Wang, Y., and Wu, W. H. (2013). Ca^{2+}-dependent Protein Kinase11 and 24 modulate the activity of the inward rectifying K^+ channels in Arabidopsis pollen tubes. *Plant Cell* 25, 649–661. doi: 10.1105/tpc.112.103184

Zheng, Z., Qamar, S. A., Chen, Z., and Mengiste, T. (2006). Arabidopsis WRKY33 transcription factor is required for resistance to necrotrophic fungal pathogens. *Plant J.* 48, 592–605. doi: 10.1111/j.1365-313X.2006.02901.x

Conflict of Interest Statement: The authors declare that the research was conducted in the absence of any commercial or financial relationships that could be construed as a potential conflict of interest.

frontiers in Plant Science

ORIGINAL RESEARCH
published: 10 May 2017
doi: 10.3389/fpls.2017.00783

Stigma Sensitivity and the Duration of Temporary Closure Are Affected by Pollinator Identity in *Mazus miquelii* (Phrymaceae), a Species with Bilobed Stigma

Xiao-Fang Jin[1,2], Zhong-Ming Ye[3], Grace M. Amboka[2,4], Qing-Feng Wang[2] and Chun-Feng Yang[2]**

[1] Institute of Ecology and Environmental Science, Nanchang Institute of Technology, Nanchang, China, [2] Key Laboratory of Aquatic Botany and Watershed Ecology, Wuhan Botanical Garden, Chinese Academy of Sciences, Wuhan, China, [3] Jiangxi Provincial Key Laboratory of Soil Erosion and Prevention, Jiangxi Institute of Soil and Water Conservation, Nanchang, China, [4] College of Life Sciences, University of Chinese Academy of Sciences, Beijing, China

OPEN ACCESS

Edited by:
Zhong-Jian Liu, The Orchid Conservation and Research Center of Shenzhen, China

Reviewed by:
Yanwen Zhang, Eastern Liaoning University, China
Youhao Guo, Wuhan University, China

***Correspondence:**
Qing-Feng Wang
qfwang@wbgcas.cn
Chun-Feng Yang
cfyang@wbgcas.cn

Specialty section:
This article was submitted to Plant Evolution and Development, a section of the journal Frontiers in Plant Science

Received: *23 January 2017*
Accepted: *25 April 2017*
Published: *10 May 2017*

Citation:
Jin X-F, Ye Z-M, Amboka GM, Wang Q-F and Yang C-F (2017) Stigma Sensitivity and the Duration of Temporary Closure Are Affected by Pollinator Identity in Mazus miquelii (Phrymaceae), a Species with Bilobed Stigma. Front. Plant Sci. 8:783. doi: 10.3389/fpls.2017.00783

A sensitive bilobed stigma is thought to assure reproduction, avoid selfing and promote outcrossing. In addition, it may also play a role in pollinator selection since only pollinators with the appropriate body size can trigger this mechanism. However, no experimental study has investigated how the sensitive stigma responds to different pollinators and its potential effects on pollination. *Mazus miquelii* (Phrymaceae), a plant with a bilobed stigma was studied to investigate the relationship between stigma behaviors and its multiple insect pollinators. The reaction time of stigma closure after touched, duration of temporary closure, and factors determining permanent closure of the stigma were studied when flowers were exposed to different visitors and conducted with hand pollination. Manual stimulation was also used to detect the potential differences in stigmas when touched with different degrees of external forces. Results indicated that, compared to pollinators with a small body size, larger pollinators transferred more pollen grains to the stigma, causing a rapid stigma response and resulting in a higher percentage of permanent closures. Duration of temporary closure was negatively correlated with the speed of stigma closure; a stigma that closed more rapidly reopened more slowly. Manual stimulation showed that reaction time of stigma closure was likely a response to external mechanical forces. Hand pollination treatments revealed that the permanent closure of a stigma was determined by the size of stigmatic pollen load. For large pollinators, the speedy reaction of the stigma might help to reduce pollen loss, enhance pollen germination and avoid obstructing pollen export. Stigmas showed low sensitivity when touched by inferior pollinators, which may have increased the possibility of pollen deposition by subsequent visits. Therefore, the stigma behavior in *M. miquelii* is likely a mechanism of pollinator selection to maximize pollination success.

Keywords: *Mazus miquelii*, mechanical stimulation, pollen load, pollination efficiency, pollinator body size, pollinator selection, stigma behavior, touch-sensitive stigma

INTRODUCTION

A sensitive stigma will close when touched by pollinator and may reopen after a visit. Behavior of a sensitive stigma reflects a special relationship between plants and animals by way of pollination (Darwin, 1876; Fetscher and Kohn, 1999; Fetscher et al., 2002; Sharma et al., 2008, and references therein). Plants with sensitive stigma are widely spread in the high core Lamiales (Newcombe, 1922, 1924; Angiosperm Phylogeny Group, 2009; Schaferhoff et al., 2010). Generally, behaviors of a sensitive stigma consist of three consecutive events, temporary closure, reopening and permanent closure (Newcombe, 1922, 1924). The stigma closes temporarily after being touched and reopens quickly or slowly after touching, and may close permanently when enough pollen has been deposited on the stigma (Newcombe, 1922, 1924; Bertin, 1982; Yang et al., 2004; Sritongchuay et al., 2010; Ai et al., 2013). The temporary closure of stigma may prevent self-pollination. The stigma receives pollen grains from a pollinator visiting from another flower and the visit may cause stigma closure until the pollinator flies away. Thus the pollen grains transferred by pollinators have a limited probability of being deposited on its own stigma (Newcombe, 1922; Sharma et al., 2008). In addition, a closed stigma may also enhance the efficiency of pollen removal (Fetscher et al., 2002). This purports a rapid reaction time of stigma temporary closure may enhance pollen export and effectively avoid self pollen deposition. Reopening appears to be a response to insufficient pollen deposited on a stigma for production of a full seed set (Fetscher, 1999). However, the correlation between the duration of temporary closure and pollen load size is still unclear. In addition, the closure status of a stigma has been considered effective for creation of the appropriate microenvironment for pollen to germinate and/or prevent the pollen from removal by subsequent pollinators or wind (Newcombe, 1922, 1924).

Behavior of sensitive stigma has been found to differ greatly between different plant taxa (Newcombe, 1922, 1924; Bertin, 1982; James and Knox, 1993; Gibbs and Bianchi, 1999; Yang et al., 2004; Hobbhahn et al., 2006; Qu et al., 2007; Guimaraes et al., 2008; Milet-Pinheiro et al., 2009; Rana, 2009; Sritongchuay et al., 2010; Jin et al., 2015) and within the same plants (Anderson, 1922; Sweety et al., 2009; Ren and Tang, 2010; Bittencourt et al., 2011; Ai et al., 2013). Since stigma sensitivity (reaction time of temporary closure after touched) and duration of temporary closure may be adaptive significance in pollination, studies on the effects of different pollinators on behaviors of a sensitive stigma would be of importance in understanding the evolution of sensitive stigmas. However, whether stigma sensitivity, the duration of temporary closure, and permanent closure are mediated by similar or different factors still remain unclear. In addition, the behavior of a bilobed sensitive stigma should be regarded as a mechanism of pollinator selection because only pollinators with the appropriate body size can trigger stigma closure. However, to our knowledge, no experimental studies have been conducted to investigate the effects of different pollinators on behavior of a sensitive stigma, especially for plant species with a variety of pollinators.

We hypothesized that behavior of a bilobed sensitive stigma may vary in response to a variety of pollinators with different body sizes, which could be mediated by variations in pollination efficiencies. In this study, *Mazus miquelii* Makino, a plant with a bilobed stigma (**Figure 1**) was used to test this hypothesis. *M. miquelii* is visited by several pollinators with different body sizes including Anthophorine bees, *Osmia* spp., *Lasioglossum* spp., and *Halictus* spp. (Jin et al., 2015). We addressed the following questions: (a) Do pollinators with different body sizes cause differences in stigma behavior? Reaction time of temporary closure after touched, duration of temporary closure, and the probability of permanent closure were studied when enclosed flowers were exposed to different pollinators. (b) Are there any differences in factors determining reaction time of temporary closure after touched, duration of temporary closure, and permanent closure of the stigma?

MATERIALS AND METHODS

Study Species and Site

Mazus miquelii Makino (Phrymaceae) is a perennial herb that grows in wet places by trails and sparse forests. It is widespread in central and eastern China and is also found in Japan and North eastern America as an introduced species. *M. miquelii* can reproduce both sexually with seeds and asexually with a short stolon. Usually, each plant produces one to 16 inflorescences each with 13–20 whitish to blue flowers. One to 10 inflorescences are available at the same time in a given individual. The flowers often open at about 9 AM and each flower stays open for 2–5 days (Jin, 2015). A flower consists of upper and lower lips with four anthers and style incorporated in the upper lip. In addition, the flower produces nectar at the bottom of corolla tube. The bilobed stigma is located adjacent to the corolla-opening and sheltered by the upper lip, which is the route for pollinators foraging for pollen or nectar (Jin et al., 2015). Furthermore, an inflorescence yields one flower in a day, each flower producing about 400 ovules (Jin et al., 2015). *M. miquelii* is partially self-compatible, nonetheless it is incapable of setting seeds without pollination (Kimata, 1978; Jin et al., 2015).

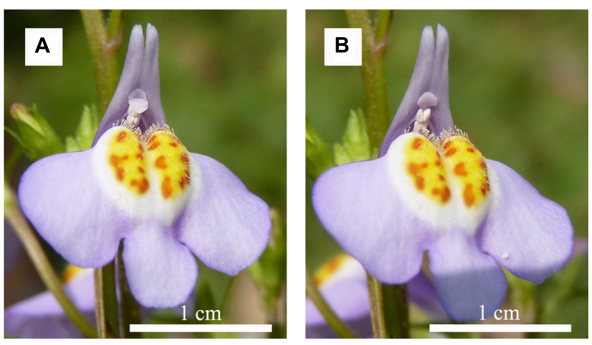

FIGURE 1 | Flower morphology and size of *Mazus miquelii*; (A) indicating a flower with an open stigma and **(B)** indicating a flower with a closed stigma.

Field investigation was conducted in 2014 on a naturally occurring population with at least 500 individual plants at the Wuhan Botanical Garden (WBG), Hubei Province, China. Leaf-cutter bees (Megachilidae: *Osmia rufina* and *Osima jacoti*), Anthophorine bees (Anthophoridae: *Habropoda tainanicola*, *Tetralonia chinensis*, and *Tetralonia jacoti*), and sweat bees [Halictidae: *Halictus (Seladonia) aerarius*, *Halictus (Seladonia) varentzowi*, and *Lasioglossum* sp.] were the primary pollinators of *M. miquelii* at the study site during the study period (Jin et al., 2015). In this study, pollinators were divided into four groups according to body size, namely *Halictus* spp., *Lasioglossum* spp., Anthophorine bees, and *Osmia* spp. Body sizes and foraging behaviors of individuals among species within the same group were similar (Jin et al., 2015). About 100 plants were randomly selected and enclosed with fine mesh netting for pollinator exclusion before the flowers opened. The plants were either exposed to pollinators or artificial manipulation when the flowers opened.

Pollination Observations and Stigma Behavior in Response to Different Pollinators

Field investigations were conducted from 11 am to 5 pm on April 1–9, 2014. Foraging behaviors of each group of the pollinators were carefully observed in sunny days. The floral resource sought by each pollinator group was recorded when the pollinator came into contact with the stigma and/or anther. Pollinator found grooming pollen from anthers was described as pollen foragers whilst those that licked the nectar at the flower bottom were termed as nectar foragers. The body size of each pollinator group was measured by a vernier caliper. Ten individuals from each of the pollinator groups were used for measurement of body size. The *Halictus* spp. and *Lasioglossum* spp. entered into the floral tube while the latter stayed at the flower opening to seek for nectar (Jin, 2015). We then measured the body diameter of *Halictus* spp. and *Lasioglossum* spp., and the head diameter of Anthophorine bees and *Osmia* spp. to estimate the body size of the pollinators.

Different pollinators may have different abilities of depositing pollen on a stigma. The enclosed flowers were used to evaluate this variance. Flowers that received a single visit by a pollinator were enclosed immediately and picked on the day after being visited and fixed in FAA solution (formalin: acetic acid: 70% ethanol at a ratio of 5:5:90 by volume) for further analysis in the laboratory. Stigmatic pollen load was counted under a fluorescence microscope (Nikon E-600) after treatment with 8 mol/L NaOH for 10 h followed by 0.1% aniline blue dye. The sampled flowers were 27, 18, 27, and 36 for *Halictus* spp., *Lasioglossum* spp., Anthophorine bees, and *Osmia* spp., respectively. The duration of a single visit for each group of the pollinators was recorded, from landing on the flower to taking off. In this survey, we recorded 21, 22, 18, and 23 visits for *Halictus* spp., *Lasioglossum* spp., Anthophorine bees, and *Osmia* spp., respectively.

To study stigma behavior in response to the pollinators with different body sizes, enclosed plants were exposed to pollinators of each group separately when the flowers were fully open. A flower that received a single visit from a pollinator that had previously visited another *M. miquelii* flower was marked with a string with different color for marking pollinators from different groups. The plant was again enclosed after the flower received a visit for observation of the stigma behavior. The stigma behavior was recorded in three aspects: percentage of temporary closure, duration of temporary closure (min) and percentage of permanent closure. The reaction time of stigma temporary closure during pollination observations was not measured due to difficulties in estimating the exact time of contact between the pollinator and the stigma. However, this was manipulated by artificial stimulation. To detect the differences in the percentage of temporary closure after a single visit among pollinator groups, it was observed that 27, 20, 10, and 30 flowers received a single visit by *Halictus* spp., *Lasioglossum* spp., Anthophorine bees, and *Osmia* spp., respectively. The stigmas closed after visitation but reopened later were recorded as a temporary closure. The duration of temporary closure (min) when flowers received a single visit by different pollinators was recorded as 8, 20, 10, and 30 flowers were visited by *Halictus* spp., *Lasioglossum* spp., Anthophorine bees, and *Osmia* spp., respectively. The duration of temporary closure indicated the period from the moment of stigma temporary closure to that of reopening. The percentage of permanent closure when flowers received a single visit by different pollinators was recorded as 27, 20, 10, and 30 flowers visited by *Halictus* spp., *Lasioglossum* spp., Anthophorine bees and *Osmia* spp., respectively. Permanent closure was observed for the stigma of enclosed flower (after a single visit) as it closed automatically and did not reopen until flower wilt. The interval between flower visited by a pollinator and stigma permanent closure was recorded.

One-way ANOVA was used to detect the differences of different pollinators on duration of stigma temporary closure. The foraging duration and body size of pollinators from different pollinators were also analyzed by a one-way ANOVA test. A *post hoc* test was used for multiple comparisons when a significant difference was observed. Chi-squared test was used to examine the differences in the influences of different pollinators on percentage of temporary and permanent closure. Fisher's exact test was used and the frequency was weighted before the Chi-squared test. Partitions of the χ^2 method were used in pairwise comparison.

Stigma Behavior in Response to Manual Stimulation and Hand Pollination

To disentangle the behavior of the stigma in response to mechanical touch, manual stimulation was applied to the flower. We used three sizes of cotton balls, namely 2, 3.5, and 4.5 mm in diameter, to create different external forces when touching the stigma. Former studies (Jin, 2015) revealed that the height of corolla-opening (the distance from lower stigma lobe to the lower corolla lip) was about 2.5 mm for *M. miquelii* flowers with an open stigma. This distance was similar to the smaller cotton ball but shorter than the two bigger cotton balls. When the cotton balls with different sizes were pushed through the corolla-opening, they should create different levels of external force on

stigma. We then named the forces evoked by the cotton balls as small, medium and large forces, respectively.

Stimulations of each level of forces on stigma were replicated on at least 30 newly opened flowers from previously enclosed plants. The reaction time of stigma temporary closure was recorded (in seconds, from the moment of interaction to the moment of complete closure of the two lobes) and duration of stigma temporary closure (in minutes, from stigma temporary closure to reopening of the two lobes). The relationship between reaction time of temporary closure and duration of stigma temporary closure was tested. Likewise, we included flowers ($N = 10$) in their 2nd day of opening in the manual stimulation experiment to detect whether stigma sensitivity was influenced by flowering stage. Furthermore, to determine whether the stigma repeatedly closed and reopened during anthesis of a flower, mechanical touch with a large force was applied to the stigma as soon as it opened or reopened. One-way ANOVA was used to detect the effects of different external forces on reaction time of stigma temporary closure and duration of stigma temporary closure and followed by a *post hoc* test for multiple comparisons when a significant difference was found. Unary Linear Regression Model was used to analyze the relationship between stigma reaction time of temporary closure and duration of temporary closure.

The influence of different pollen sources on stigma behavior was detected in *M. miquelii*. Pollen from the same plant, pollen from another individual (1 m in distance), pollen from another *Mazus* species (*M. pumilus*), and pollen from a co-flowering plant in the habitat (*Glechoma longituba*) were used as the sources of pollen. For each pollen source, hand pollination with large cotton ball was conducted on 10 flowers each from different individuals. Moreover, stigma of each of the flowers was deposited on more than 1,000 pollen grains (more than twice of the ovule number per flower). Before hand pollination, pollen grains were deposited on a glass slide and counted under a portable microscope. For each of the treatments, we recorded the reaction time of stigma temporary closure and duration of stigma temporary closure. The results were also compared with those of the manual touch with a large force. One-way ANOVA was used in analysis of different pollen sources on reaction time of stigma temporary and duration of stigma temporary closure. A *post hoc* test was used for multiple comparisons when a significant difference was detected by one-way ANOVA.

To detect whether stigma permanent closure was determined by pollen load size, various amounts of pollen grains from other individuals were deposited on stigma of different flowers ($N = 70$). All flowers used for hand pollination were from enclosed plants. On the 2nd day, flowers with open and closed stigma were fixed in FAA solution for subsequent counting of pollen load size. Load size was later counted under a fluorescence microscope (Nikon E-600) after treatment with 8 mol/L NaOH for 10 h followed by dyeing with 0.1% aniline blue. We recorded the pollen load size of each stigma with open or closed status and moreover, we calculated the percentage of stigmas with permanent closure out of total stigmas checked under different pollen load sizes. All the data was analyzed with SPSS 18.0.

RESULTS

Stigma Behavior in Response to Different Pollinators

Among the flower visitors, Anthophorine bees and *Osmia* spp. foraged for nectar while *Lasioglossum* spp. and *Halictus* spp. collected both pollen and nectar. In addition, they differed significantly in body sizes. Individuals of *Halictus* spp. were the smallest while those of Anthophorine bees had the largest body sizes ($F_{3,36} = 240.002$, $P < 0.001$, **Table 1**). When newly opened flowers visited, respectively, by pollinators from the four groups, the percentages of flowers with a closed stigma out of total flowers differed significantly ($\chi^2 = 49.815$, $P < 0.001$). All stigmas from flowers visited by Anthophorine bees, *Lasioglossum* spp., and *Osmia* spp. closed, whereas only 29.6% of the stigmas from flowers visited by *Halictus* spp. closed (**Table 1**). However, all closed stigmas reopened while the duration of stigma temporary closure among flowers visited by different pollinators was significantly different ($F_{3,64} = 13.966$, $P < 0.001$). Stigmas of flowers visited by *Halictus* spp. had a shorter duration of temporary closure than those visited by pollinators from the other three groups (**Table 1**).

For flowers with permanently closed stigmas, the time from flower visited by a pollinator to stigma permanent closure was about 8 h with no observable differences between open and enclosed flowers. That is, before permanent closure, the stigma repeatedly closed and reopened in response to touch by pollinators with large body size, e.g., Anthophorine bees, *Lasioglossum* spp., and *Osmia* spp. For the enclosed flowers which received a single visit by different pollinators, stigmas of some flowers closed automatically and stayed a status of closure after 8 h from the time of flower visited by a pollinator. The percentage of stigma permanent closure was significantly different among flowers visited by pollinators from the four groups ($\chi^2 = 44.713$, $P < 0.001$); as it was lower in *Halictus* spp. than in the pollinators from other three groups (**Table 1**).

Results indicated that pollen load on a stigma after a single visit differed significantly among flowers visited by different pollinators ($F_{3,101} = 14.086$, $P < 0.001$). *Halictus* spp. deposited significantly less pollen on the stigma than pollinators from the other three groups, and there was no significant difference among them (**Table 1**). Duration of flower foraging time also differed significantly among pollinators from the four groups ($F_{3,80} = 84.435$, $P < 0.001$); Anthophorine bees had the shortest foraging duration while *Halictus* spp. had the longest duration (**Table 1**).

Stigma Behavior in Response to Manual Stimulation and Hand Pollination

Flowers did not display a significant difference between the 1st and 2nd day on reaction time of stigma temporary closure ($F_{1,18} = 0.053$, $P = 0.820$) and duration of stigma temporary closure in flowers ($F_{1,18} = 0.640$, $P = 0.434$). The stigma closed and reopened repeatedly in response to manual stimulation within the whole flowering period. However, reaction time of

TABLE 1 | Stigma behavior when flowers were exposed to different insects, and foraging behavior and efficiency for each pollinator.

Flower visitors	*Halictus* spp.	*Lasioglossum* spp.	Anthophorine bees	*Osmia* spp.
Stigma behavior in response to different pollinators				
Percentage of temporary closure after a single visit	29.6% ($n = 27$)^a	100% ($n = 20$)^b	100% ($n = 10$)^b	100% ($n = 30$)^b
Duration of temporary closure (min)	5.11 ± 0.58 ($n = 8$)^a	7.19 ± 1.00 ($n = 20$)^b	8.46 ± 2.13 ($n = 10$)^{bc}	8.49 ± 1.49 ($n = 30$)^c
Percentage of permanent closure after a single visit	7.4% ($n = 27$)^a	85.00% ($n = 20$)^b	60.00% ($n = 10$)^b	83.33% ($n = 30$)^b
Behavior and efficiency of different pollinators				
Foraged resource	Pollen, nectar	Pollen, nectar	Nectar	Nectar
Contact with sexual organs (s)	Anther, sometimes with stigma	Anther, often with stigma	Anther and stigma	Anther and stigma
Pollen deposition after single visit	42.11 ± 11.71 ($n = 27$)^a	662.00 ± 87.33 ($n = 18$)^b	572.37 ± 84.16 ($n = 27$)^b	398.14 ± 68.68 ($n = 36$)^b
Visit duration per flower (s)	30.37 ± 2.36 ($n = 21$)^a	18.37 ± 1.59 ($n = 22$)^b	1.85 ± 0.06 ($n = 18$)^d	3.65 ± 0.17 ($n = 23$)^c
Body/head diameter (mm)	1.64 ± 0.03 ($n = 10$)^a	2.79 ± 0.10 ($n = 10$)^b	4.34 ± 0.20 ($n = 10$)^d	3.56 ± 0.25 ($n = 10$)^c

Data are mean ± SE with sample size in parentheses. Values with the same super scripted letters are not significantly different ($P < 0.05$).

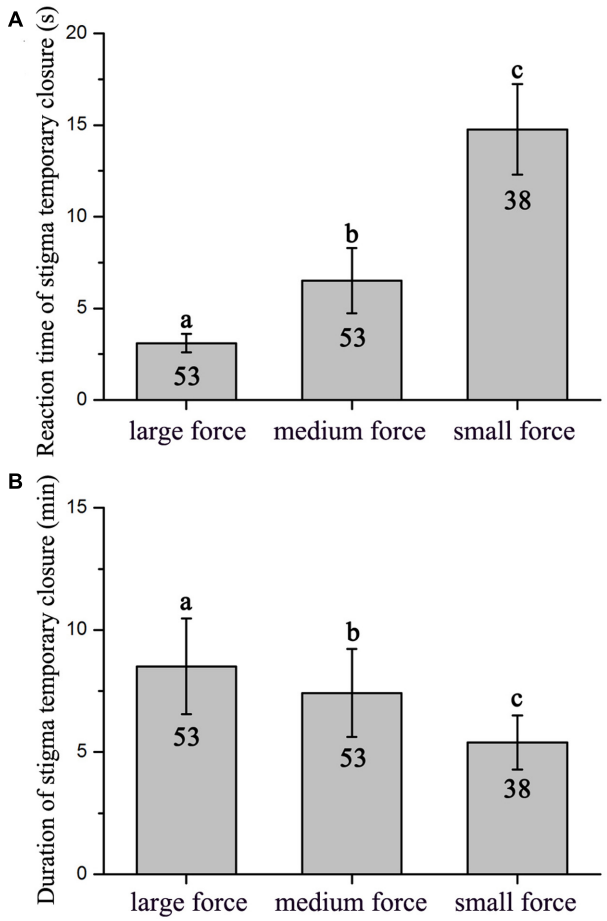

FIGURE 2 | Reaction time of stigma temporary closure (A) and duration of stigma temporary closure **(B)** under different levels of mechanical forces (Mean ± 1 SD). Values with the same super scripted letters are not significantly different ($P < 0.05$).

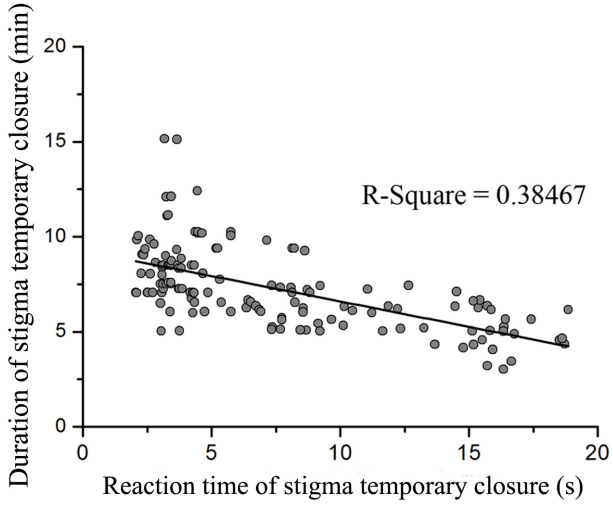

FIGURE 3 | The relationship between reaction time of stigma temporary closure and duration of stigma temporary closure when mechanically stimulated with different forces ($P < 0.001$).

stigma temporary closure and duration of temporary closure was significantly different in response to touch with small, medium, and large forces (reaction time of stigma temporary closure: $F_{2,141} = 155.094$, $P < 0.001$, **Figure 2A**; duration of temporary closure: $F_{2,141} = 29.704$, $P < 0.001$, **Figure 2B**). Moreover, a significant negative relationship between the reaction time of stigma temporary closure and duration of temporary closure was identified [$Y = 9.267$ (±0.248)–0.267 (±0.028) X, $R^2 = 0.38$, $df = 143$, $P < 0.001$, **Figure 3**]. The stigma of the flowers under manual stimulation did not close permanently despite the touch from small, medium, and large forces.

Different pollen sources and mechanical touch with a large force showed no significant differences in reaction time of stigma temporary closure ($F_{4,45} = 0.855$, $P = 0.498$) and duration of temporary closure ($F_{4,45} = 0.447$, $P = 0.774$). Hand pollination disclosed that stigma permanent closure was highly dependent on the size of stigmatic pollen load. After 8 h of hand pollination, it was observed that stigmas remained open when pollen load was lower than 400 pollen grains; 44% of stigmas remained open when pollen load was between 400 and 600 pollen grains and all the stigmas closed permanently when pollen load was higher than 600 pollen grains.

DISCUSSION

Stigma behavior of *M. miquelii* differed significantly when foraged by pollinators with different body sizes. Pollinators with a smaller body size, for example, *Halictus* spp., triggered a slower response in stigma closure but a shorter duration of stigma temporary closure. It could be attributed to the fact that small pollinators made limited contact with stigmas and thus imposing a small mechanical force on the stigma. This argument was supported by results of manual stimulation that small external forces caused a slower reaction time of stigma closure and a shorter duration of stigma temporary closure. Hand pollination revealed that stigma permanent closure was determined by load size of legitimate pollen grains (see also Yang et al., 2004; Sritongchuay et al., 2010; Jin et al., 2015; but see Milet-Pinheiro et al., 2009). The results indicated that it may be different in factors influencing reaction time of stigma closure, duration of stigma temporary closure, and stigma permanent closure.

Manual stimulations suggested that in *M. miquelii*, reaction time of stigma temporary closure was likely a response to the mechanical forces imposed upon the stigma. A bigger force resulted in a more rapid reaction of stigma temporary closure. Although the duration of stigma temporary closure was correlating to pollen source in a self-incompatible plant, *Anemopaegma chamberlaynii*, the closed stigma did not reopen after treatment of outcross-pollination but did reopen under self-pollination treatment (Correia et al., 2006), our results of hand pollination treatments indicated that in *M. miquelii*, neither reaction time of stigma temporary closure nor duration of stigma temporary closure was affected by different pollen sources. This was also observed in *Oroxylum indicum* (Bignoniaceae) (Sritongchuay et al., 2010). The duration of stigma temporary closure was negatively related to the reaction time of stigma temporary closure. Stigma temporary closure was likely an instant reaction to mechanical stimulation by external forces. Larger forces stimulated a wider stigma surface than smaller forces thus triggering a rapid response and complete closure of the stigma; therefore, the stigma would need a longer time to recover.

In *M. miquelii*, the novel finding that reaction time of stigma temporary closure was negatively correlated with duration of stigma temporary closure might contribute to facilitate pollination. Compared to larger pollinators, those with a smaller body size had lower pollen transfer efficiency resulting to a longer reaction time of stigma temporary closure but a shorter duration of stigma temporary closure. The slow closure and rapid reopening of a stigma increased the possibility of pollen deposition for the flower in subsequent visits. For the ongoing visit, the reopening stigma may be weak in obstructing pollen removal for a small pollinator. On the other hand, pollinators with a large body size deposited a large amount of pollen grains on a stigma and resulted in rapid stigma temporary closure; and the stigma maintained the status of temporary closure for a long time. A closed stigma might not only reduce pollen loss (Newcombe, 1922) and provide a comfortable microenvironment for pollen germination (Newcombe, 1922; Edlund et al., 2004), but also enhance the efficiency of pollen removal (Fetscher et al., 2002). In addition, a higher probability of stigma permanent closure caused by larger pollinators could facilitate pollination since larger pollinators may deposit more pollen grains on the stigma compared to pollinators with a smaller body size (Richardson, 2004; Yang et al., 2004; Milet-Pinheiro et al., 2009). Besides, larger pollinators normally have a greater flight capability; thus capable in transporting pollen from very distant plants of different populations and in turn benefiting plants by increasing rate of outcrossing and assuring a constant gene flow (Schlindwein et al., 2014). The sensitive stigma in *M. miquelii* might be a mechanism of pollinator selection that maximize plant reproductive success.

Stigma permanent closure was deemed to be an indication of enough pollen grains deposited on a stigma to fulfill full seed set (Yang et al., 2004; Sritongchuay et al., 2010; Jin et al., 2015). This study supported the argument because permanent closure of *M. miquelii* stigmas required a minimum pollen load on stigma. Otherwise, the stigma remained opened for receiving pollen. Sufficient pollen grain deposition is essential to maximize female reproductive output (Fetscher, 1999). Consequently, when pollen load meet the demand of seed yield, stigma temporary closure could benefit male fitness by avoiding obstruction for pollen removal (Fetscher et al., 2002). Permanent stigma closure in response to pollen load size was therefore suggested to be a mechanism facilitating pollination (Yang et al., 2004). The previous study suggested that stigma permanent closure in *Mazus* might be facilitated by adequate growth pollen tubes in the style (Jin et al., 2015). However, direct experimental evidence is needed to support this hypothesis.

CONCLUSION

This study revealed the relationship between stigma behavior and pollinators with different body sizes for a plant species with a sensitive bilobed stigma, *M. miquelii*. A larger pollinator deposited more pollen grains on stigmas resulting in higher possibility of stigma permanent closure than a small pollinator. Compared to larger pollinators, stigmas touched by pollinators with a smaller body size had a longer reaction time of stigma temporary closure, maintained the status of temporary closure for a shorter time and thus, had a relatively longer time to receive pollen grains. The stigma behavior in *M. miquelii* might be regarded as a mechanism of pollinator selection to maximize pollination success. However, further studies should focus on the physiological basis of stigma behavior to uncover the internal factors controlling reversible stigma opening (closure and reopening) and the completion of this process (permanent closure); other studies on touch-sensitive plant might be essential for referencing (Cameron et al., 2002; Braam, 2005; Forterre, 2013; Kruse et al., 2014).

AUTHOR CONTRIBUTIONS

X-FJ, Q-FW, and C-FY designed the study. X-FJ and Z-MY carried out the fieldwork. X-FJ, Z-MY, GA, and C-FY analyzed the results and wrote the manuscript.

ACKNOWLEDGMENTS

This work was supported by the National Natural Science Foundation of China (Grant Nos. 31070206 and 31370263 to C-FY). We thank Wen-Kui Dai and Jian Yang for assistance in field investigations, Chao-Dong Zhu for insect identification. X-FJ would like to thank Xishuangbanna Tropical Botanical Garden (XTBG), Chinese Academy of Science for organizing the "Scientific Paper Writing: XTBG Advanced Workshop" that taught by Professor Richard Corlett.

REFERENCES

Ai, H., Zhou, W., Xu, K., Wang, H., and Li, D. (2013). The reproductive strategy of a pollinator-limited Himalayan plant, *Incarvillea mairei* (Bignoniaceae). *BMC Plant Biol.* 13:195–204. doi: 10.1186/1471-2229-13-195

Anderson, F. (1922). The development of the flower and embryogeny of *Martynia louisiana*. *Bull. Torrey Bot. Club* 49, 141–157. doi: 10.2307/2480094

Angiosperm Phylogeny Group (2009). An update of the Angiosperm Phylogeny Group classification for the orders and families of flowering plants: APG III. *Bot. J. Linn. Soc.* 161, 105–121. doi: 10.1111/j.1095-8339.2009.00996.x

Bertin, R. I. (1982). Floral biology, hummingbird pollination and fruit production of Trumpet Creeper (*Campsis radicans*, Bignoniaceae). *Am. J. Bot.* 69, 122–134. doi: 10.2307/2442837

Bittencourt, N. S., Pereira, E. J., Sao-Thiago, P. D., and Semir, J. (2011). The reproductive biology of *Cybistax antisyphilitica* (Bignoniaceae), a characteristic tree of the south American savannah-like "Cerrado" vegetation. *Flora* 206, 872–886. doi: 10.1016/j.flora.2011.05.004

Braam, J. (2005). In touch: plant responses to mechanical stimuli. *New Phytol.* 165, 373–389. doi: 10.1111/j.1469-8137.2004.01263.x

Cameron, K. M., Wurdack, K. J., and Jobson, R. W. (2002). Molecular evidence for the common origin of snap-traps among carnivorous plants. *Am. J. Bot.* 89, 1503–1509. doi: 10.3732/ajb.89.9.1503

Correia, M. C. R., Pinheiro, M. C. B., and Lima, H. A. D. (2006). Floral biology and pollination of *Anemopaegma chamberlaynii* Bur. and K. Schum. (Bignoniaceae). *Lundiana* 7, 39–46.

Darwin, C. R. (1876). *The Effects of Cross and Self Fertilization in the Vegetable Kingdom*. London: John Murray.

Edlund, A. F., Swanson, R., and Preuss, D. (2004). Pollen and stigma structure and function: the role of diversity in pollination. *Plant Cell* 16, S84–S97. doi: 10.1105/Tpc.015800

Fetscher, A. (1999). *Evolutionary Significance of Stigma Closure in Bush Monkeyflower*. Ph.D. dissertation, University of California, San Diego, CA.

Fetscher, A. E., and Kohn, J. R. (1999). Stigma behavior in *Mimulus aurantiacus* (Scrophulariaceae). *Am. J. Bot.* 86, 1130–1135. doi: 10.2307/2656976

Fetscher, A. E., Rupert, S. M., and Kohn, J. R. (2002). Hummingbird foraging position is altered by the touch-sensitive stigma of bush monkeyflower. *Oecologia* 133, 551–558. doi: 10.1007/s00442-002-1079-1

Forterre, Y. (2013). Slow, fast and furious: understanding the physics of plant movements. *J. Exp. Bot.* 64, 4745–4760. doi: 10.1093/Jxb/Ert230

Gibbs, P. E., and Bianchi, M. B. (1999). Does late-acting self-incompatibility (LSI) show family clustering? Two more species of Bignoniaceae with LSI: *Dolichandra cynanchoides* and *Tabebuia nodosa*. *Ann. Bot.* 84, 449–457. doi: 10.1006/anbo.1999.0933

Guimaraes, E., Di Stasi, L. C., and Maimoni-Rodella, R. D. S. (2008). Pollination biology of *Jacaranda oxyphylla* with an emphasis on staminode function. *Ann. Bot.* 102, 699–711. doi: 10.1093/aob/mcn152

Hobbhahn, N., Kuchmeister, H., and Porembski, S. (2006). Pollination biology of mass flowering terrestrial *Utricularia* species (Lentibulariaceae) in the Indian Western Ghats. *Plant Biol.* 8, 791–804. doi: 10.1055/s-2006-924566

James, E. A., and Knox, R. B. (1993). Reproductive-biology of the Australian species of the genus *Pandorea* (Bignoniaceae). *Aust. J. Bot.* 41, 611–626. doi: 10.1071/BT9930611

Jin, X. F. (2015). *Diversity of Behaviours of Touch-Sensitive Stigmas in Flowering Plants and its Adaptive Significance*. Ph.D. dissertation, University of the Chinese Academy of Sciences, Beijing.

Jin, X. F., Ye, Z. M., Wang, Q. F., and Yang, C. F. (2015). Relationship of stigma behaviors and breeding system in three *Mazus* (Phrymaceae) species with bilobed stigma. *J. Syst. Evol.* 53, 259–265. doi: 10.1111/jse.12137

Kimata, M. (1978). Comparative studies on reproductive systems of *Mazus japonicus* and *M. miquelii* (Scrophulariaceae). *Plant Syst. Evol.* 129, 243–253. doi: 10.1007/Bf00982750

Kruse, J., Gao, P., Honsel, A., Kreuzwieser, J., Burzlaff, T., Alfarraj, S., et al. (2014). Strategy of nitrogen acquisition and utilization by carnivorous *Dionaea muscipula*. *Oecologia* 174, 839–851. doi: 10.1007/s00442-013-2802-9

Milet-Pinheiro, P., Carvalhoa, A. T., Kevan, P. G., and Schlindwein, C. (2009). Permanent stigma closure in Bignoniaceae: mechanism and implications for fruit set in self-incompatible species. *Flora* 204, 82–88. doi: 10.1016/j.flora.2007.11.006

Newcombe, F. C. (1922). Significance of the behavior of sensitive stigmas. *Am. J. Bot.* 9, 99–120. doi: 10.2307/2435484

Newcombe, F. C. (1924). Significance of the behavior of sensitive stigmas II. *Am. J. Bot.* 11, 85–93. doi: 10.2307/2435490

Qu, R., Li, X., Luo, Y., Dong, M., Xu, H., Chen, X., et al. (2007). Wind-dragged corolla enhances self-pollination: a new mechanism of delayed self-pollination. *Ann. Bot.* 100, 1155–1164. doi: 10.1093/Aob/Mcm209

Rana, A. (2009). Morphological differences in the stigma of fruitbearing and fruitless plants of *Kigelia pinnata* DC. (Bignoniaceae). *J. Plant Repro. Biol.* 1, 43–48.

Ren, M. X., and Tang, J. Y. (2010). Anther fusion enhances pollen removal in *Campsis grandiflora*, a hermaphroditic flower with didynamous stamens. *Int. J. Plant Sci.* 171, 275–282. doi: 10.1086/650157

Richardson, S. C. (2004). Benefits and costs of floral visitors to *Chilopsis linearis*: pollen deposition and stigma closure. *Oikos* 107, 363–375. doi: 10.1111/j.0030-1299.2004.12504.x

Schaferhoff, B., Fleischmann, A., Fischer, E., Albach, D. C., Borsch, T., Heubl, G., et al. (2010). Towards resolving Lamiales relationships: insights from rapidly evolving chloroplast sequences. *BMC Evol. Biol.* 10:352. doi: 10.1186/1471-2148-10-352

Schlindwein, C., Westerkamp, C., Carvalho, A. T., and Milet-Pinheiro, P. (2014). Visual signalling of nectar-offering flowers and specific morphological traits favour robust bee pollinators in the mass-flowering tree *Handroanthus impetiginosus* (Bignoniaceae). *Bot. J. Linn. Soc.* 176, 396–407. doi: 10.1111/boj.12212

Sharma, M. V., Kuriakose, G., and Shivanna, K. R. (2008). Reproductive strategies of *Strobilanthes kunthianus*, an endemic, semelparous species in southern Western Ghats. India. *Bot. J. Linn. Soc.* 157, 155–163. doi: 10.1111/j.1095-8339.2008.00786.x

Sritongchuay, T., Bumrungsri, S., Meesawat, U., and Mazer, S. J. (2010). Stigma closure and re-opening in *Oroxylum indicum* (Bignoniaceae): causes and consequences. *Am. J. Bot.* 97, 136–143. doi: 10.3732/Ajb.0900100

Sweety, S., Seema, C., and Leonardo, G. (2009). Reproductive biology of *Pyrostegia venusta* (Ker-Gawl.) Miers (Bignoniaceae) with special reference to seedlessness. *J. Plant Reprod. Biol.* 1, 87–92.

Yang, S. X., Yang, C. F., Zhang, T., and Wang, Q. F. (2004). A mechanism facilitates pollination due to stigma behavior in *Campsis radicans* (Bignoniaceae). *Acta Bot. Sin.* 46, 1071–1074.

Conflict of Interest Statement: The authors declare that the research was conducted in the absence of any commercial or financial relationships that could be construed as a potential conflict of interest.

frontiers in Plant Science

ORIGINAL RESEARCH
published: 22 June 2017
doi: 10.3389/fpls.2017.01106

Lack of S-RNase-Based Gametophytic Self-Incompatibility in Orchids Suggests That This System Evolved after the Monocot-Eudicot Split

Shan-Ce Niu[1,2,3], Jie Huang[3], Yong-Qiang Zhang[3], Pei-Xing Li[3], Guo-Qiang Zhang[3], Qing Xu[3], Li-Jun Chen[3], Jie-Yu Wang[3], Yi-Bo Luo[1] and Zhong-Jian Liu[3,4,5,6]**

[1] State Key Laboratory of Systematic and Evolutionary Botany, Institute of Botany, Chinese Academy of Sciences, Beijing, China, [2] Graduate University of the Chinese Academy of Sciences, Beijing, China, [3] Shenzhen Key Laboratory for Orchid Conservation and Utilization, The National Orchid Conservation Centre of China and The Orchid Conservation and Research Centre of Shenzhen, Shenzhen, China, [4] The Centre for Biotechnology and BioMedicine, Graduate School at Shenzhen, Tsinghua University, Shenzhen, China, [5] College of Forestry and Landscape Architecture, South China Agricultural University, Guangzhou, China, [6] College of Arts, College of Landscape Architecture, Fujian Agriculture and Forestry University, Fuzhou, China

OPEN ACCESS

Edited by:
Verónica S. Di Stilio,
University of Washington,
United States

Reviewed by:
Jinling Huang,
East Carolina University, United States
Wei-Ning Bai,
Beijing Normal University, China
Takashi Tsuchimatsu,
Chiba University, Japan

***Correspondence:**
Zhong-Jian Liu
liuzj@sinicaorchid.org
Yi-Bo Luo
luoyb@ibcas.ac.cn

Specialty section:
This article was submitted to Plant Evolution and Development, a section of the journal Frontiers in Plant Science

Received: 16 January 2017
Accepted: 07 June 2017
Published: 22 June 2017

Citation:
Niu S-C, Huang J, Zhang Y-Q, Li P-X, Zhang G-Q, Xu Q, Chen L-J, Wang J-Y, Luo Y-B and Liu Z-J (2017) Lack of S-RNase-Based Gametophytic Self-Incompatibility in Orchids Suggests That This System Evolved after the Monocot-Eudicot Split. Front. Plant Sci. 8:1106. doi: 10.3389/fpls.2017.01106

Self-incompatibility (SI) is found in approximately 40% of flowering plant species and at least 100 families. Although orchids belong to the largest angiosperm family, only 10% of orchid species present SI and have gametophytic SI (GSI). Furthermore, a majority (72%) of *Dendrobium* species, which constitute one of the largest Orchidaceae genera, show SI and have GSI. However, nothing is known about the molecular mechanism of GSI. The S-determinants of GSI have been well characterized at the molecular level in Solanaceae, Rosaceae, and Plantaginaceae, which use an S-ribonuclease (S-RNase)-based system. Here, we investigate the hypothesis that Orchidaceae uses a similar S-RNase to those described in Rosaceae, Solanaceae, and Plantaginaceae SI species. In this study, two SI species (*Dendrobium longicornu* and *D. chrysanthum*) were identified using fluorescence microscopy. Then, the S-RNase- and SLF-interacting SKP1-like1 (SSK1)-like genes present in their transcriptomes and the genomes of *Phalaenopsis equestris*, *D. catenatum*, *Vanilla shenzhenica*, and *Apostasia shenzhenica* were investigated. Sequence, phylogenetic, and tissue-specific expression analyses revealed that none of the genes identified was an S-determinant, suggesting that Orchidaceae might have a novel SI mechanism. The results also suggested that RNase-based GSI might have evolved after the split of monocotyledons (monocots) and dicotyledons (dicots) but before the split of Asteridae and Rosidae. This is also the first study to investigate S-RNase-based GSI in monocots. However, studies on gene identification, differential expression, and segregation analyses in controlled crosses are needed to further evaluate the genes with high expression levels in GSI tissues.

Keywords: Orchidaceae, self-incompatibility, evolution, transcriptomics and genomics, S-RNase-based GSI

INTRODUCTION

Orchidaceae, which represents approximately 8% of all vascular plant species and contains five subfamilies (Apostasioideae, Vanilloideae, Cypripedioideae, Orchidoideae, and Epidendroideae), is one of the largest plant families and includes more than 25,000 species that are known for their diverse specialized reproductive and ecological strategies (Givnish et al., 2015). The large morphological variation exhibited by this family is mostly attributable to the striking adaptations these plants have made to attract pollinators, including insects and birds (Barbosa et al., 2009; Holzinger and Pichrtova, 2016). Although the reproductive systems of the members of a given population are important factors in determining their genetic variability, most Orchidaceae are self-compatible (SC), "avoiding" self-pollination by other means (Gontijo et al., 2010). Self-incompatibility (SI) is estimated to occur in 10% of orchid species; however, a majority (72%) of the 61 *Dendrobium* species that are self-pollinated show self-sterility (Johansen, 1990). Interestingly, nearly one-half of orchid SI species are from *Dendrobium*. As one of the largest Orchidaceae genera, the high SI rate in *Dendrobium* species might contribute to their high levels of species diversity.

SI influences seed and fruit setting, the growth of pollen tubes, seed filling, seed germination, and seedling development in Orchidaceae. Therefore, the capsule set, seed filling, and growth of pollen tubes following self- and cross-pollination are the main SI indicators (Millner et al., 2015). Studies performed on Pleurothallidinae and *Dendrobium* (Johansen, 1990; Barbosa et al., 2009; Millner et al., 2015; Pinheiro et al., 2015) suggest that the sites of incompatibility reactions vary among groups, implying that various SI molecular mechanisms exist in Orchidaceae. The pollen tubes of certain *Dendrobium* SI species (e.g., *D. farmeri*) exhibited similar reactions in self- and cross-pollination (Johansen, 1990), while the pollen grains of most self-pollinated flowers, such as *Masdevallia infracta* and *Octomeria*, *Stelis*, *Specklinia*, and *Anathallis* species (except *A. microphyta*), did not germinate (Gontijo et al., 2010). In addition, self-pollinations performed across 26 species of *Restrepia* (Orchidaceae) revealed that pollen tubes grew only into the top third of the ovary (Millner et al., 2015). *Pleurothallis adamantinensis* and *P. fabiobarrosii* are strictly self-incompatible because pollen tube growth ceases near the base of the column (Borba et al., 2001).

In gametophytic SI (GSI) systems, the SI phenotype of the pollen is determined by its own (haploid) S genotype, and the pollen tube growth is typically arrested at some point on its path through the transmitting tract towards the ovary (Borba et al., 2001). Although previous studies reported pollen tube reactions of some SI orchid species that were similar to those observed in species with GSI (Borba et al., 2001; Millner et al., 2015), little is known about the physiology and genetic control of SI in Orchidaceae due to their very long lifecycles, which effectively preclude genetic analysis (Johansen, 1990). One type of GSI has been well studied: S-ribonuclease (S-RNase)-based GSI in Rosaceae, Solanaceae, and Plantaginaceae. The female S-determinant is an S-RNase glycoprotein belonging to the RNase-T2 family and with style-specific expression, and the male S-determinant encodes an F-box protein (Yamashita et al., 2004), which has been designated the S-locus F-box (SLF) protein and has pollen-specific expression. According to plant RNase-T2 family phylogenetic analysis, this family can be divided into two different subfamilies: S-RNases involved in the rejection of self-pollen during the establishment of SI in the Rosaceae, Solanaceae, and Plantaginaceae plant families and S-RNase-like RNases-T2. Furthermore, S-RNase-based GSI evolved only once—before the split of Asteridae and Rosidae approximately 120 million years ago (MYA)—which may suggest that other plant families featured this GSI molecular mechanism (Igic and Kohn, 2001; Steinbachs and Holsinger, 2002; Vieira et al., 2008a; MacIntosh et al., 2010). However, the phylogenetic origin of the S-RNase-based SI system remains undated, and thus, whether the same GSI molecular mechanism exists in monocots is unknown.

Amino acid pattern analysis of RNase-T2 genes revealed four patterns: amino acid patterns 1, 2, 3 and 4 (Vieira et al., 2008a). The amino acid motifs encoded by S-RNases differ from those of other RNase-T2 genes (Vieira et al., 2008a; Nowak et al., 2011). Although amino acid patterns 1 and 2 are exclusively found in the proteins encoded by S-RNase lineage genes, amino acid pattern 4 is not found in any protein encoded by these genes (Vieira et al., 2008a; Nowak et al., 2011). This difference can be used to identify putative S-RNase lineage genes. In addition, all S-RNases have an isoelectric point (IP) between 8 and 10 (Roalson, 2003), which may be further refined in the different homologs. The number of introns can also be used to select S-RNase lineage genes because S-RNases have only one or two introns, and these genes are expected to be specifically and highly expressed in pistils, although they can show lower expression levels in stigma and styles. Moreover, S-RNase lineage genes must be demonstrated to have high polymorphism levels, be positively selected, and, in controlled crosses, co-segregate with S-locus alleles. Finally, the phylogenetic position of S-lineage gene homologs and a set of reference genes should be used to determine whether the genes belong to the S-RNase lineage. One male S-determinant gene has been identified in *Prunus* spp. (Rosaceae; the S haplotype-specific F-box (SFB) gene (Ushijima, 2003; Ikeda et al., 2004; Sonneveld et al., 2005; Nunes et al., 2006; Vieira et al., 2008b)), whereas multiple genes have been identified in Pyrinae (Rosaceae; S-locus F-box brothers [SFBB] genes [Cheng et al., 2006; Kakui et al., 2007; Sassa et al., 2007; Minamikawa et al., 2010; De Franceschi et al., 2011; Kakui et al., 2011; Okada et al., 2011; Aguiar et al., 2013]) and Solanaceae [S-locus F-box (SLF) genes (Wheeler and Newbigin, 2007; Kubo et al., 2010; Williams et al., 2014)]. These genes belong to a large gene family, but no typical protein features have been reported to date. The only known feature is pollen-specific expression, which makes identifying pollen S-gene(s) using sequence data alone difficult.

In addition, as the diagnostic marker for the presence or absence of RNase-based GSI, the SLF-interacting S-phase kinase-associated protein 1-like (SKP1-like)1 (SSK1) proteins, have been described only in the SI reactions of Rosaceae, Solanaceae, and Plantaginaceae (Hua and Kao, 2006; Huang et al., 2006; Zhao et al., 2010; Xu et al., 2013). SKP1-like proteins are also adapters that connect several F-box proteins to the SCF complex and

are necessary in a wide range of cellular processes involving proteasome degradation (Huang et al., 2006). They are also highly conserved and have a unique C-terminus that comprises 5–9 amino acid residues following the conventional "WAFE" motif that is found in most plant SKP1 proteins (Zhao et al., 2010) and can be easily identified. The sequence "GVDED" is conserved in Rosaceae, and although it is not as well conserved in Solanaceae and Plantaginaceae, the D residue is always found at the last position of the motif. These genes are expressed only in the pollen of Solanaceae, Plantaginaceae, and Pyrinae and the styles of *Prunus* spp. (Hua and Kao, 2006; Huang et al., 2006; Zhao et al., 2010; Xu et al., 2013).

The present study aimed to verify whether the SI molecular mechanism of Orchidaceae is similar to that of S-RNase-based GSI and to further explore the phylogenetic origin of S-RNase-based GSI. Based on the genomic data associated with the representative phylogenetic positions and self-compatibility of four species belonging to three different Orchidaceae subfamilies—*Phalaenopsis equestris* (SC) (Cai et al., 2015), *D. catenatum* (partial SI) (Zhang et al., 2016), *Vanilla shenzhenica* (SC) (Liu et al., unpublished), and *Apostasia shenzhenica* (SC) (Liu et al., unpublished)—and the transcriptome data obtained here for two SI species (*D. longicornu* and *D. chrysanthum*), S-RNase lineage genes and SKP1-like genes were characterized. The two SI species were identified by observing the growth of their pollen tubes after self- and cross-pollination using fluorescence microscopy. Combining amino acid pattern, tissue-specific expression, and phylogenetic analyses, homologous S-RNases and SKP1-like genes were investigated in the four genomes and the transcriptomes of two orchid species. No evidence of RNase-based GSI was found in *D. longicorn* or *D. chrysanthum,* and no S-determinant orthologous sequences were found in the potential S-locus region in four orchid genomes. The results revealed that Orchidaceae GSI might not be determined by S-RNase-lineage genes, as it is in Rosaceae, Solanaceae, and Plantaginaceae. Therefore, we propose that RNase-based GSI might have originated after the split of monocots and eudicots but before the split of Asteridae and Rosidae.

MATERIALS AND METHODS

Identification of SI

Two days after flowering, the plants were self- and cross-pollinated. *D. chrysanthum* pistils were collected 12, 24, 48, 72, and 96 h after self- and cross-pollination (HASP and HACP, respectively), and *D. longicornu* pistils were collected 2, 3, 4, 5, 7, and 9 days after self- and cross-pollination (DASP and DACP, respectively). The pistils were immersed in a fixing solution (formalin-acetic acid-80% alcohol [1:1:8]) for at least 24 h, rinsed in 70% alcohol, softened in a strong (8 N) sodium hydroxide solution for 3 h, and cleared in distilled water. The pistils were stained with 0.1% water-soluble aniline blue dye dissolved in 0.1 N K_3PO_4 for 12 h and then observed under a fluorescence microscope (Axioskop 40, Zeiss, Germany). The ultraviolet light used (wavelength: approximately 356 μm) facilitated the examination of the growth of pollen tubes on the style because the pollen tubes were lined with callose, which fluoresced bright yellow-green and contrasted strongly with the bluish or grayish fluorescence of the style and ovary tissues. The lengths of the majority of the pollen tubes in compatible and incompatible styles at specific times after pollination were measured using fluorescence microscopy software. Statistical analyses were performed using the software package GraphPad Prism 6 for Mac OS X (version 6.0c; GraphPad Software, Inc., La Jolla, CA, United States). All values were reported as the mean and SEM. The data were presented as the average of three independent measurements with error bars (SEM) indicated. The data were analysed by two-way repeated measures analysis of variance (ANOVA) using Sidak's *post hoc* test ($^{***}P < 0.001$, $^{****}P < 0.0001$).

Plant Materials, RNA Extraction, Library Construction, and Sequencing

Mature pollen, styles (containing stigma) and leaves of *D. chrysanthum* and the 3 DACP styles (containing pollen), 3 DASP styles (containing pollen) and leaves of *D. longicornu* were simultaneously collected during the pollination of the same plants, placed in 2-ml tubes in liquid nitrogen, and stored at −80°C until RNA extraction. Three biological replicates of each *D. chrysanthum* tissue were collected.

Total RNA was extracted from *Dendrobium* spp. tissues using an RNA prep Pure Plant Kit, and genomic DNA contamination was removed using RNase-free DNase I (both from Tiangen, Beijing, China). The integrity of the RNA was evaluated on a 1.0% agarose gel stained with ethidium bromide (EB), and its quality and quantity were assessed using a NanoPhotometer® spectrophotometer (IMPLEN, Westlake, CA, United States) and an Agilent 2100 Bioanalyzer (Agilent Technologies, Santa Clara, CA, United States). Because the RNA integrity number (RIN) was greater than 7.0 for all samples, the samples were used for cDNA library construction and Illumina® sequencing, which was completed by Beijing Novogene Bioinformatics Technology Co., Ltd. (China). The cDNA library was constructed using the NEBNext® Ultra™ RNA Library Prep Kit for Illumina® (NEB, United States) with 3 μg of RNA per sample, following the manufacturer's recommendations. The polymerase chain reaction (PCR) products obtained were purified (AMPure XP system), and the library quality was assessed on the Agilent Bioanalyzer 2100 system. Library preparations were sequenced on an Illumina® HiSeq 2000 platform, generating 100-bp paired-end reads. Raw sequence reads were deposited in the National Center for Biotechnology Information (NCBI) Sequence Read Archive[1] (SRA) under accession number SRP097204.

Before assembly, adaptor sequences were removed from the raw reads, and FASTQC[2] reports were generated. Based on this information, the reads were trimmed at both ends. Nucleotide positions with a QC score lower than 20 were masked (replaced by an N), and the resulting high-quality reads were *de novo* assembled and annotated with TRINITY (Haas et al., 2013).

[1] http://www.ncbi.nlm.nih.gov/Traces/sra

[2] http://www.bioinformatics.babraham.ac.uk/projects/fastqc/

The commands and parameters used for running TRINITY were as follows: Trinity –seqType fq –JM 200G –left sample_1.fq –right sample_2.fq –normalize_by_read_set –CPU 32 –output –min_kmer_cov 2 –full_cleanup. The transcript abundance level was normalized using the fragments per kilobase per million reads (FPKM) method, and FPKM values were computed as proposed by Mortazavi et al. (2008). In genes with more than one transcript, the longest was used to calculate the transcript abundance and coverage.

Homolog Identification and Comparative Analysis

We first collected S-RNase-related RNase-T2 protein sequences from previous studies (Aguiar et al., 2015; Kubo et al., 2015). Then, we combined the genomic data of *P. equestris* (SC) (Cai et al., 2015), *D. catenatum* (partial SI) (Zhang et al., 2016), *V. shenzhenica* (SC) (Liu et al., unpublished), and *A. shenzhenica* (SC) (Liu et al., unpublished) with six transcriptome sequences in the proteome datasets.

These S-RNase-related RNase-T2 protein sequences were used as seeds to search against proteome datasets using basic local alignment search tools (tBLASTn and BLASTp) with default parameters. To confirm the identities of orchid S-RNase-related RNase-T2 candidate genes, the hidden Markov model (HMM)-based HMMER program 3.1b2 (Eddy, 2011) was used to identify all proteins containing a Ribonuclease_T2 domain. This domain (PF00445.16 in the Pfam database) (Finn et al., 2016) was then used to perform local searches in the proteome datasets. Sequences obtained from both methods were then aligned and manually adjusted in Multiple Alignment using Fast Fourier Transform (MAFFT) (Katoh and Standley, 2013) using the E-INS-I alignment strategy for sequence integrity analysis. Sequences with obvious errors were excluded from subsequent analyses. Each predicted sequence was subsequently verified using BLAST searches against public databases, including NCBI, Pfam (Finn et al., 2016) and Simple Modular Architecture Research Tool (SMART) (Letunic et al., 2012), to confirm its reliability. The HMM profiles of the Skp1 gene family (PF01466.17 in the Pfam database) obtained in the analysis were used in local searches. To maximize confidence, putative Skp1 sequences were also aligned and manually adjusted in MAFFT using the E-INS-I strategy for sequence integrity analysis. The IPs of all peptides were calculated in ExPASy (Gasteiger, 2003).

As monocots, most orchids are SC species; therefore, the SSK1 genes may be non-functional or not involved in the SI pathway. Thus, we chose orchid species of several SI degrees and phylogenetic positions and allowed for some variability regarding the "WAFE" and "GVDED" motifs when retrieving sequences. Angiosperms have two types (I and II) of SKP1-like genes, with type II being much longer than type I and encoding chimeric proteins (Kong et al., 2007). Multiple Skp1 homologs from the same species were shown to have evolved at highly heterogeneous rates, indicating that they have different evolutionary histories (Kong et al., 2004, 2007). Due to the effect of long-branch attraction, when both gene types are included, the analysis typically gives unstable results; in addition, SSK1-like genes belong to type I SKP1-like genes (Kong et al., 2004, 2007; Huang et al., 2006; Zhao et al., 2010; Matsumoto et al., 2012; Xu et al., 2013). For these two reasons, type II genes were excluded from the analysis.

Multiple Sequence Alignment and Phylogenetic Tree Construction

The amino acid sequences of SSK1 genes, SSK1-like genes from selected land plant species (Kong et al., 2004, 2007; Huang et al., 2006; Zhao et al., 2010; Matsumoto et al., 2012; Xu et al., 2013), and Orchidaceae SSK1-like genes were used for phylogenetic analysis. Multiple sequence alignment was carried out using MAFFT with the E-INS-I strategy and adjusted manually as necessary, and the phylogenetic tree was generated by the maximum likelihood method using PhyML 3.0 (Guindon et al., 2010). The approximate likelihood-ratio test (aLRT) branch support, which was based on a Shimodaira-Hasegawa-like procedure, was estimated with a Whelan and Goldman (WAG) model.

The amino acid sequences of Orchidaceae S-RNase like genes and S-RNase-related RNase-T2s from species with S-RNase-based SI, maize and barley (Igic and Kohn, 2001; Hillwig et al., 2010; Kubo et al., 2015), were used for phylogenetic analysis the same method as that described for SSK1-related genes.

The data sets (the alignments file and the tree file of SKP1 and S-RNase protein sequences) are available through TreeBASE[3], and also in the **Supplementary Files S3, S4**.

RESULTS

Pollen tube development

The development of pollen tubes that were stained with water-soluble aniline blue in the pistils of *D. longicornu* and *D. chrysanthum* was observed 12 h after pollination (HAP) using fluorescence microscopy. In *D. longicornu*, pollen tubes started to develop in the stigma 2 DASP or DACP (**Figures 1**, **7**). At 3 DAP, when the pollen tubes started to grow into the style, the cross-pollination pollen tubes were longer than the self-pollination pollen tubes; however, approximately 4 DAP, the self-pollination pollen tubes stopped growing at the top of the style. There was a highly significant difference between the self- and cross-pollination pollen tubes beginning at 5 DASP or DACP (**Figure 7**). Approximately 7 DACP, the pollen tubes developed rapidly and reached the ovary. In *D. chrysanthum*, the pollen tubes started to develop in the stigma 24 h after self-pollination or cross-pollination (**Figures 2**, **8**). Although the self-pollination pollen tubes grew slowly into the style during the 72 h after pollination and stopped growing before flower (containing ovary) senescence (120 h after pollination), the cross-pollination pollen tubes developed rapidly and reached the ovary 72 h after pollination. There was a highly significant difference between the self- and cross-pollination pollen tubes beginning at 48 HASP or HACP (**Figure 8**).

[3]http://purl.org/phylo/treebase/phylows/study/TB2:S21138

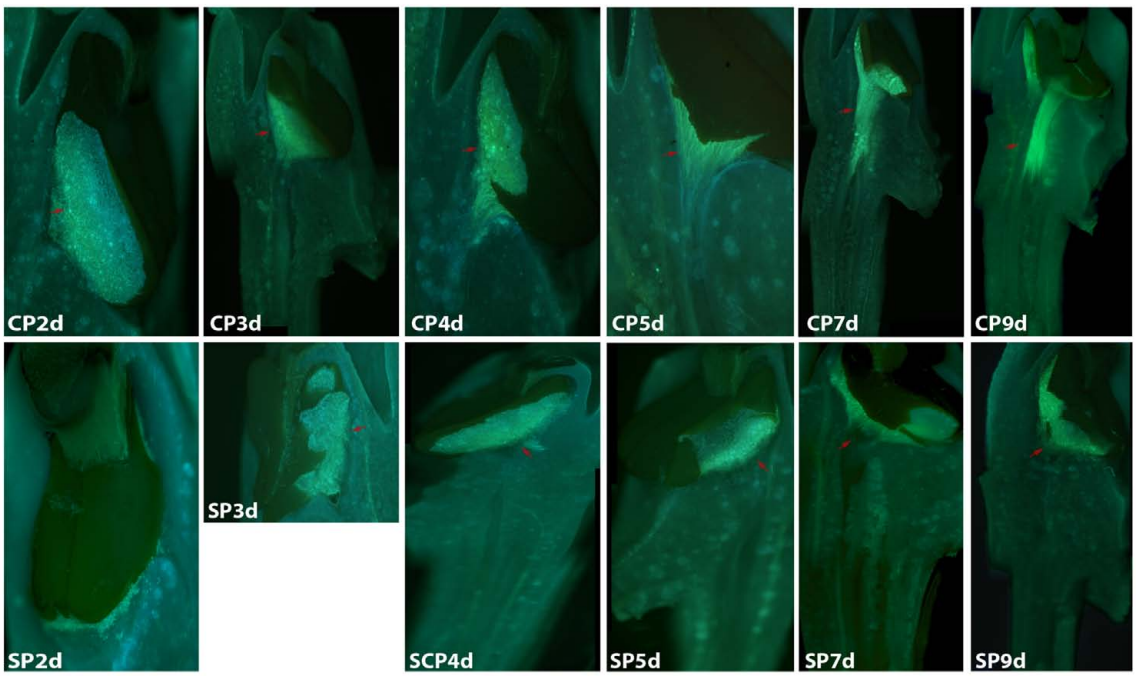

FIGURE 1 | Growth of pollen tubes after the self- and cross-pollination of *Dendrobium longicornu.* CP2d/SP2d: the pollen tubes started to develop in the stigma; CP3d: the pollen tubes started to grow into the style and longer than in SP3d; SP4d, SP5d, SP7d, and SP9d: the self-pollination pollen tubes stopped growing at the top of the style; CP7d: the pollen tubes developed rapidly and reached the ovary. Bar = 100 μm; red arrows indicate the pollen tubes. CP and SP stand for cross-pollination and self-pollination, respectively, d means day.

Overall, the germination of pollen tubes inside the stigma of *D. longicornu* occurred later than that in *D. chrysanthum*, and their growth took longer in *D. longicornu* styles than in *D. chrysanthum* styles. The self-pollination pollen tubes of *D. longicornu* grew to the top of the style before flower senescence, while in *D. chrysanthum*, they stopped growing before flower senescence. Thus, SI was identified in two orchid species by observing the development of pollen tubes using fluorescence microscopy.

SKP1-Like Genes in Orchidaceae

We retrieved 42 sequences from orchids, including five *A. shenzhenica* (SC), two *V. shenzhenica* (SC), six *D. catenatum* (partial SI), and five *P. equestris* (SC) genome sequences; four sequences from the leaves and self- and cross-pollinated styles (containing pollen) of *D. longicornu* (SI); and four sequences from the leaves, five sequences from the pollen, and three sequences from the styles (containing stigma) of *D. chrysanthum* (SI). Two genes had a "WAFGE" motif rather than the conventional "WAFE" motif in the 3' region; that is, a glycine was inserted between phenylalanine and glutamic acid. One of these genes was found in the leaves, pollen, and styles of *D. chrysanthum* (*Dch1_L, Dch1_P*, and *Dch1_S*, respectively) (**Supplementary File S1**), and the other was expressed in the styles (containing stigma and pollen) of *D. longicornu* (*Dlo1_O* and *Dlo1_S*) (**Supplementary File S1**). Similarly, the conserved C-terminus with the "WAFE" motif was replaced by "WAFAE" in one *D. catenatum* sequence (*Dca004172*) (**Supplementary File S1**), and a 16-amino acid deletion was found near the C-terminus of this sequence. Another *D. catenatum* sequence (*Dca007256*) presented a "WAFDLICL" motif, and one *A. shenzhenica* sequence (*Ash003413*) presented a "WAFEPQQ" motif at the C-terminus (**Supplementary File S1**). The *Dca007256* gene was expressed in stigma, and the *Ash003413* gene was also expressed in leaves, stems and tubers (data not shown). The FPKM analysis of the combined transcriptome data of the three *D. chrysanthum* tissues revealed that all of the abovementioned genes were expressed in *D. chrysanthum* leaves and, therefore, were not pollen-specific, except *Dch3_P* (**Figure 3**, **Supplementary File S2**, and Table S1).

In the phylogenetic analysis, SSK1 genes, SSK1-like genes from selected land plant species, and Orchidaceae SSK1-like genes were combined. The SSK1-like genes from Orchidaceae were divided into group I (35 genes) and group II (6 genes), and one gene was clustered with one *A. thaliana* gene (*ASK2*) (**Figure 5**) shown in blue. Within group I, all genes expressed in the style and/or pollen were also expressed in the leaf and thus were not pollen-specific genes (**Supplementary File S2** and Table S1); this was the case for *Dlo2_L*, *Dlo2_O,* and *Dlo2_S* or *Dch2_L, Dch2_P*, and *Dch2_S*. In group II, which was a sister to that formed by the SSK1 genes, no genes were expressed in leaf tissues, and with a few exceptions, all genes in this group were expressed in the pollen of self- and cross-pollinated orchids, suggesting that these might be pollen-specific genes; the exceptions were *PEQU_01554* and *Ash012058,* which were expressed in the leaf, stem, root, and pollen, and *Dca025410*, which was also found in the root tissue (data not shown).

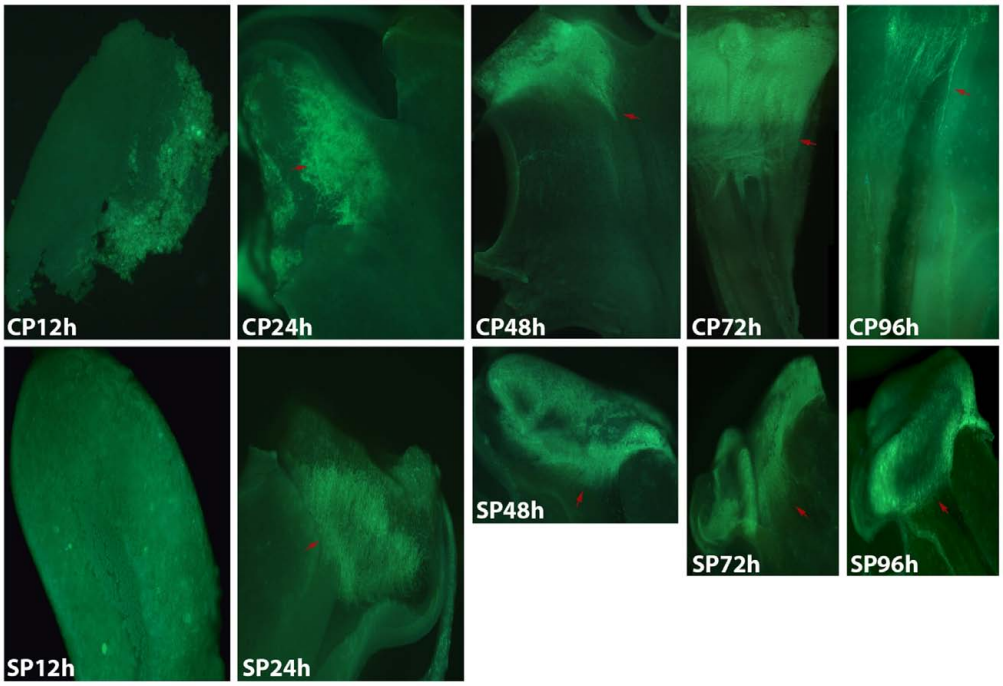

FIGURE 2 | Growth of pollen tubes after the self- and cross-pollination of *D. chrysanthum.* CP12h and SP12h: the pollen grains did not germinate; CP24h/SP24h: the pollen tubes started to develop in the stigma; SP48h, SP72h, and SP96h: the pollen tubes developed slowly or even stopped growing; CP72h and CP96h: the cross-pollination pollen tubes developed rapidly and reached the ovary 72 h after pollination. Bar = 100 μm; red arrows indicate the pollen tubes. CP and SP stand for cross-pollination and self-pollination, respectively, h means hour.

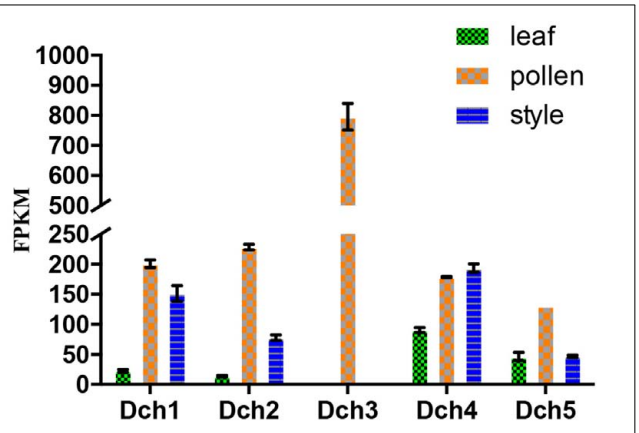

FIGURE 3 | Expression analysis based on the fragments per kilobase per million reads (FPKM) performed for the putative SKP1-like genes in the various tissues (i.e., leaf, pollen, and style) of *Dendrobium chrysanthum* (see also Supplementary Table S1).

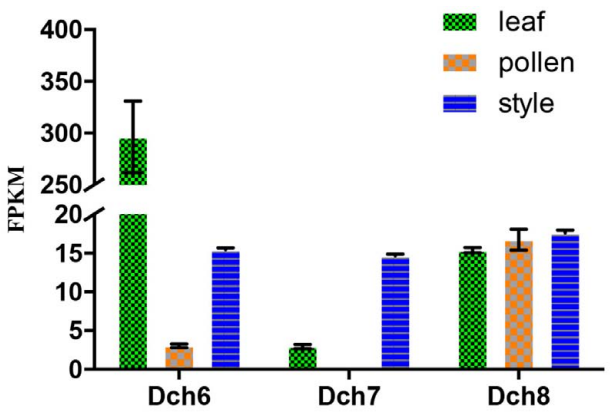

FIGURE 4 | Expression analysis based on the fragments per kilobase per million reads (FPKM) performed for the putative S-RNase-like genes in the various tissues (i.e., leaf, pollen, and style) of *Dendrobium chrysanthum* (see also Supplementary Table S2).

The phylogenetic tree positions and tissue-specific expression analyses revealed that the genes *Dch3_P* in *D. chrysanthum* and *Dlo3_S* and *Dlo3_O* in *D. longicornu* may be Orchidaceae SSK1-like genes, despite their lack of a "GVDED" motif. Indeed, in SI Orchidaceae, the conserved "WAFE/D" motif might have evolved into a sequence different from that generally observed in S-RNase-based GSI.

RNase-T2 S-Lineage Genes in Orchidaceae

As RNase-based GSI might be present in Orchidaceae, we attempted to identify an S-RNase gene in this family. Based on four criteria, S-RNase-like genes were identified in *A. shenzhenica, V. shenzhenica, D. catenatum,* and *P. equestris*

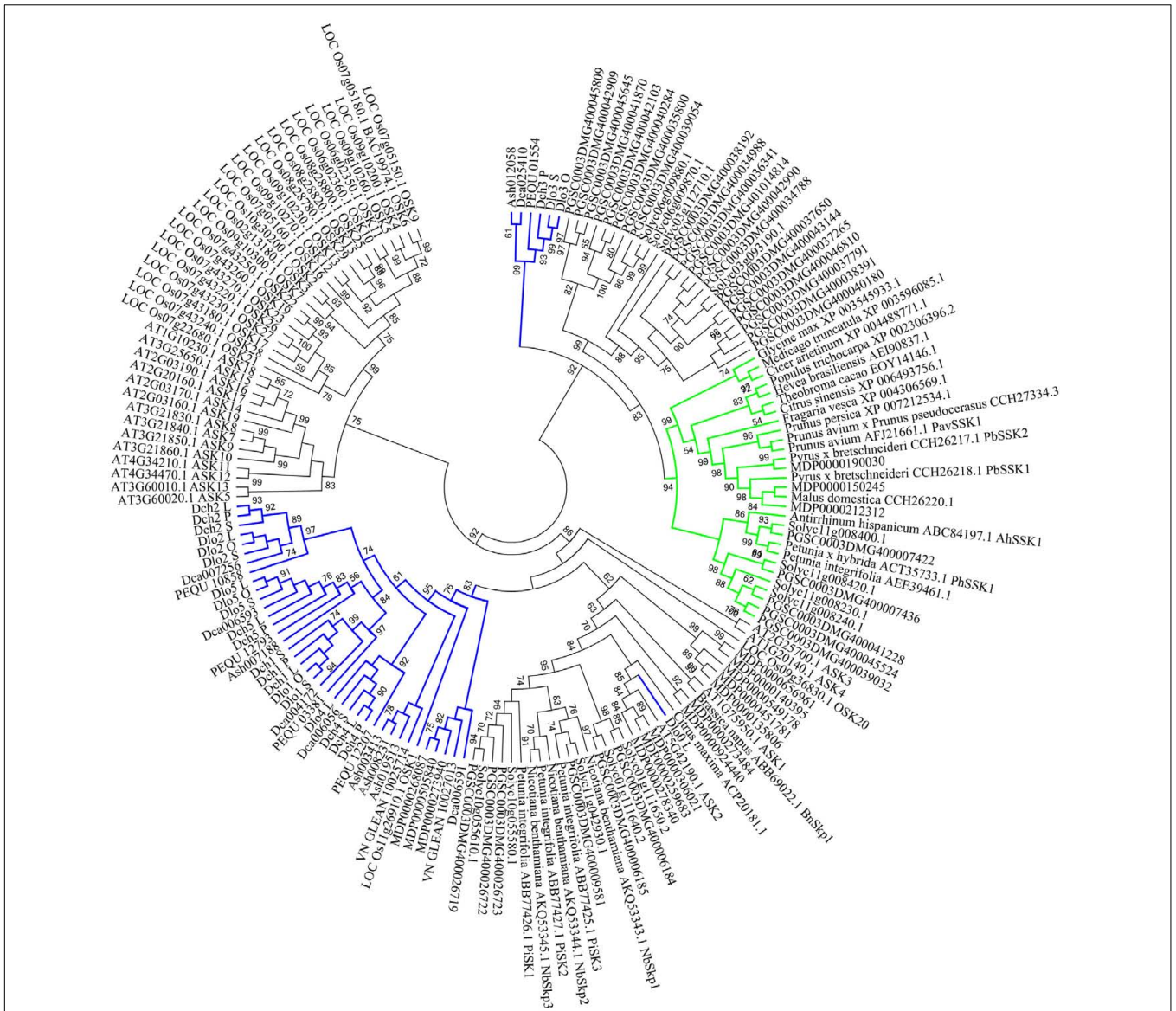

FIGURE 5 | Unrooted maximum likelihood phylogenetic tree based on the aligned amino acid sequences of 42 Skp1-like orchid proteins and 129 Skp1-like proteins from other plants. The 129 deduced amino acid sequences are from *Antirrhinum hispanicum* (AhSSK1), *Arabidopsis thaliana* (ASK1-ASK19, except ASK6), *Brassica napus* (BnSkp1), *Cicer arietinum* (XP_004488771.1), *Citrus maxima* (ACP20181.1), *Citrus sinensis* (XP_006493756.1), *Fragaria vesca* (XP_004306569.1), *Glycine max* (XP_003545933.1), *Hevea brasiliensis* (AEI90837.1), *Oryza sativa* (25 Skp1-like proteins), *Malus domestica* (CCH26220.1 and 16 Skp1-like proteins), *Medicago truncatula* (XP_003596085.1), *Nicotiana benthamiana* (NbSkp1- NbSkp3), *Petunia* spp. (AEE39461.1, PiSK1-PiSK3 and PhSSK1), *Solanum tuberosum* (32 Skp1-like proteins), *Prunus* spp. (PavSSK1, CCH27334.3, XP_007212534.1), *Pyrus* sp. (PbSSK1 and PbSSK2), *Theobroma cacao* (EOY14146.1), *Solanum lycopersicum* (13 Skp1-like proteins), and *Populus trichocarpa* (XP_002306396.2). The SSK1 family is highlighted in green, and SKP1-like genes are highlighted in blue. Values on branches are bootstrap values from SH-like amino acid analysis.

genomes and the transcriptomes from the leaves, pollen, and styles of *D. chrysanthum* and the leaves and self- and cross-pollination styles of *D. longicornu*. The criteria were as follows: (1) The genes were similar, at the amino acid level, to those involved in S-RNase-based GSI in Rosaceae, Solanaceae, and Plantaginaceae. (2) The genes encoded a protein in which amino acid pattern 4 was absent; this pattern is found in proteins encoded by non-S-RNase lineage genes only (Vieira et al., 2008a; Nowak et al., 2011). (3) The genes encoded a protein with an IP higher than 7.5 because S-RNases are always basic proteins (Igic and Kohn, 2001; Roalson, 2003). Finally, (4) the genes should be mainly expressed in the style. Given that little is known about the physiology and genetic control of SI in Orchidaceae, we chose SC species (*A. shenzhenica, V. shenzhenica,* and *P. equestris*), a partial SI species (*D. catenatum*), and SI species (*D. chrysanthum* and *D. longicornu*) to identify putative S-genes, although mutations that disrupt the coding region might exist in the putative S-locus region (Tao et al., 2007).

We identified 34 RNase-T2-like genes in Orchidaceae: five in *A. shenzhenica* (SC); four in *V. shenzhenica* (SC); three in *D. catenatum* (partial SI); five in *P. equestris* (SC); two in the leaves, three in the self-pollination styles, and three in the cross-pollination styles (containing pollen) of *D. longicornu* (SI); and three in the leaves, three in the pollen, and three in the styles (containing stigma) of *D. chrysanthum* (SI). The features of all 34 gene sequences, including the IP, sequence motifs, intron numbers, and gene location, are summarized in **Table 1**. The gene intron numbers in *D. longicornu* and *D. chrysanthum* were determined by an alignment with *D. catenatum* and *P. equestris* genes. Six genes had IPs higher than 7.5: *Ash010024*, *Ash010025*, *Dlo9_L, Dlo9_S, Dch6_S,* and *VN_GLEAN_10017549*. Twenty-five genes presented amino acid pattern 4 ([R]) and, thus, had S-like amino acid patterns rather than S-RNase amino acid patterns. The patterns "CGS" and "CSS" were found in eight and one gene sequence, respectively. Among the eight "CGS" genes, *Dlo9_L, Dlo9_O,* and *Dlo9_S* were the same gene expressed in different *D. longicornu* tissues, suggesting that this gene was not involved in RNase-based GSI because no style-specific expression was observed. The genes *Dch8_L, Dch8_P*, and *Dch8_S* in *D. chrysanthum* were also the same gene, demonstrating that

TABLE 1 | The RNases-T2 found in *Apostasia shenzhenica, Vanilla shenzhenica, Phalaenopsis equestris*, and *Dendrobium catenatum* genomes, and in *D. chrysanthum* and *D. longicornu* transcriptomes according to Vieira et al. (2008a).

Name	Locus	IP	Intron number	Motif 1	Motif 2	Motif 4	Location
Ash005005	Ash005005	7.01	1	–	WPTLACP	CPRSD	scaffold55; 447338 451513
Ash010024	Ash010024	8.41	2	MTFN	WANIRCP	CPSNN	scaffold68; 488619 489372
Ash010025	Ash010025	8.58	3	FLIRDLVTFN	WANIKCP	CPSND	scaffold68; 494201 495995
Ash013339	Ash013339	6.56	5	FTIHGLWPDY	WPSLSCS	CSSPS	scaffold196; 352867 369358
Ash014350	Ash014350	4.82	3	FGIHGLWPNY	WPTLACP	CPSSD	scaffold222; 581014 582068
Dlo9_L	changju_leaf_c28921_g1_i1_30083	8.15	6	FTIHGLWPDY	WPSLSCG	CGSPS	NO
Dlo10_L	changju_leaf_c29478_g1_i1_29530	5.31	3	FLIKDLITYN	WANIKCP	CPSNN	NO
Dca000983	Dca000983	4.76	3	FGIHGLWPNY	WPTLSCP	CPSSD	scaffold367; 1365130 1368120
Dca006359	Dca006359	4.85	1	–	MACP	CPSSN	scaffold1649; 452598 453612
Dca023087	Dca023087	5.95	3	FFIKDLIPYN	WANIKCP	CPSNN	scaffold10610; 57466 59114
Dch8_L	leaf_c55532_g1_i1_37221	6.23	6	FTIHGLWPDY	WPSLSCG	CGSPS	NO
Dch6_L	leaf_c59996_g1_i1_9691	7.05	3	FLIKDLITYN	WANIKCP	CPSNN	NO
Dch7_L	leaf_c63740_g1_i3_734	4.83	3	FGIHGLWPNY	WPTLSCP	CPSSD	NO
Dlo10_O	outcross_c46017_g1_i3_8375	5.18	3	FLIKDLITYN	WANIKCP	CPSNN	NO
Dlo11_O	outcross_c47428_g2_i1_5144	4.71	3	FGIHGLWPNY	WPTLSCP	CPSSD	NO
Dlo9_O	outcross_c50036_g1_i4_12591	7.03	6	FTIHGLWPDY	WPSLSCG	CGSPS	NO
PEQU_19416	PEQU_19416	4.98	1	–	WPTLACP	CPSSD	Scaffold000058; 533575 534082
PEQU_19713	PEQU_19713	5.62	1	FLIRDLITYS	WANIKCP	CPSNN	Scaffold000118; 1096315 1097761
PEQU_20427	PEQU_20427	6.32	6	FTIHGLWPDY	WPSLGCG	CGSPS	Scaffold000745; 594430 630710
PEQU_34178	PEQU_34178	4.38	3	FLIHGLWPNN	WPSLACP	CPSNN	Scaffold000980; 33489 35116
PEQU_39075	PEQU_39075	5.1	1	–	WPTLACP	CPSSD	Scaffold197838; 3150 3660
Dch8_P	pollen_c51787_g2_i1_26873	6.39	6	FTIHGLWPDY	WPSLSCG	CGSPS	NO
Dch6_P	pollen_c62345_g1_i8_8230	6.68	3	FLIKDLITYN	WANIKCP	CPSNN	NO
Dch7_P	pollen_c96382_g1_i1_24172	4.38	3	FLIHGLWPNN	WPSMACP	CPSSN	NO
Dlo11_S	self_c28091_g1_i1_8847	4.71	3	FGIHGLWPNY	WPTLSCP	CPSSD	NO
Dlo10_S	self_c32500_g1_i1_25199	5.45	3	FLIKDLITYN	WANIKCP	CPSNN	NO
Dlo9_S	self_c34090_g1_i1_23588	7.92	6	FTIHGLWPDY	WPSLSCG	CGSPS	NO
Dch7_S	style_c55158_g1_i1_13594	5.17	3	FGIHGLWPNY	WPTLSCP	CPSND	NO
Dch8_S	style_c55684_g1_i1_24618	6.23	6	FTIHGLWPDY	WPSLSCG	CGSPS	NO
Dch6_S	style_c64099_g1_i2_18556	7.9	3	FLIKDLITYN	WANIKCP	CPSNN	NO
VN_GLEAN_10005747	VN_GLEAN_10005747	5.54	6	FTIHGLWPDY	WPSLSCG	CGSSS	scaffold240; 471068 483351
VN_GLEAN_10007222	VN_GLEAN_10007222	4.49	3	FGIHGLWPNY	WPSLSCP	CPSSN	scaffold197; 10918 11825
VN_GLEAN_10007555	VN_GLEAN_10007555	4.77	3	FGIHGLWPNY	WPTLACP	CPSSD	scaffold189; 990282 991684
VN_GLEAN_10017549	VN_GLEAN_10017549	7.95	3	FLVKDLLTYT	WANIACP	CPSNN	scaffold56; 2937062 2938131

Ash: A. shenzhenica; changju_leaf: D. longicornu leaf; Dca: D. catenatum; leaf: D. chrysanthum leaf; outcross: cross-pollination style (containing pollen) of D. longicornu; PEQU: P. equestris; pollen: D. chrysanthum pollen; self: self-pollination style (containing pollen) of D. longicornu; VN_GLEAN: V. shenzhenica.
The intron number and location of genes in D. catenatum and D. chrysanthum transcriptomes were based on their homologs in D. catenatum and P. equestris.
The four different colors (light and dark blue, orange, and green) indicate the same gene (same color) or homologs (different colors).
IP: isoelectric point.
–: amino acids that were not present in the motifs reported by Vieira et al. (2008a).
NO: without data.

this gene is also not involved in RNase-based GSI processing. The other two genes (*PEQU_20427* and *VN_GLEAN_10005747*) were found in the SC species *P. equestris* and *V. shenzhenica*; we investigated the functions of the genes located at the two gene scaffolds and analyzed the expression levels of the genes with SLF function (data not shown). The results indicated that these genes were not at the putative S-locus region and not primarily expressed in the style, which also suggested that they are not involved in RNase-based GSI processing. The gene *Ash013339*, which contained the sequence "CSS" in the SC species *A. shenzhenica*, was also determined to not be involved in RNase-based GSI based on the results of adjacent gene function and expression analyses (data not shown).

Phylogenetic analyses of these 34 genes and S-RNase-related RNase-T2s from species with S-RNase-based SI, maize and barley, were performed (**Figure 6**). The classification of RNase-T2s into Class-I RNase-T2s, Class-II RNase-T2s, and the S-RNase clade followed that of previous studies (Igic and Kohn, 2001; Hillwig et al., 2010; Kubo et al., 2015). The 34 genes were clustered into Class-I RNase-T2s or Class-II RNase-T2s and were therefore not involved in RNase-based GSI. Three orchid clusters were found in Class-I RNase-T2s: Class-I orchid RNase-T2s I; Class-I orchid RNase-T2s II; and Class-I orchid RNase-T2s III. The genes in Class-I orchid RNase-T2s I clustered with *Zea mays kin1* (AAB37265.1), which is an S-RNase-like gene, and with *Hordeum vulgare* subsp. *vulgare rsh1* (AAF45043.1), which is exclusively expressed in young leaf tissues. The genes within Class-I orchid RNase-T2s II and Class-I orchid RNase-T2s III grouped with *Nicotiana alata* RNase *NE* (AAA21135.1), which is not linked to the SI locus and not specifically expressed in styles, and *Prunus dulcis* RNase *PD2* (AAG31930.1), which is predominantly expressed in petals, the pistils of open flowers, and leaves. Class-II orchid RNase-T2s were a sister group to *Solanum lycopersicum* RNase *LER*, which is not specifically expressed in styles (Kothke and Kock, 2011); *Antirrhinum majus* × *Antirrhinum hispanicum AhSL28* (an S-RNase-like gene), which is not only expressed in pistils; and *Nicotiana glutinosa* RNase *NGR2*, which is constitutively expressed in leaves. Overall, the orchid S-RNase-like genes clustered with S-RNase-like genes that were not specifically expressed in styles (**Figure 4**, **Supplementary File S2**, and Table S2), suggesting that these genes might not be involved in orchid SI.

DISCUSSION

Phylogenetic analysis based on the RNase-T2 genes from four Orchidaceae genomes; the pollen, style, and leaf transcriptomes of *D. chrysanthum*; and the pollen, self-pollination style, and cross-pollination style (containing pollen) transcriptomes of *D. longicornu*, which represent SC, partial SI, and SI species, respectively, suggested that these genes were not phylogenetically related to S-RNases and were clustered with Class-I and Class-II RNase-T2s from other species. It could be argued that S-RNases were not expressed in the selected tissue transcriptomes of the two SI species and that the S-locus region might not be present in the four available genomes. If the SI molecular mechanisms were similar to S-RNase-based GSI, the S-locus region should be present in SC orchids, although male and female S-determinant genes might be truncated and/or non-functional. In Rosaceae, SC species are present in the S-locus region, but the S-RNase and SFB genes are non-functional (Tao et al., 2007); a similar pattern has been described in Brassicaceae SI systems. For instance, although the S-locus is present in the genome of SC *Arabidopsis thaliana*, the genes determining S-specificity are non-functional (Bechsgaard et al., 2006; Boggs et al., 2009). Moreover, the open reading frames (ORFs) of all S-locus cysteine-rich (SCR) alleles and some S-receptor kinase (SRK) alleles are truncated in *Capsella rubella* (Guo et al., 2009), and one *A. lyrata* haplotype, Aly-S38, which is very similar to *C. rubella*, contains a closely related SCR with a truncated ORF and an SRK with a complete ORF (Guo et al., 2011). Thus, the genomes of SC species can also aid in the identification of putative S-locus genes.

Analyses of *D. chrysanthum* and *D. longicornu* S-RNase-like genes revealed no specific gene expression in the style, and amino acid pattern 4 was present in all identified orchid S-RNase-like genes, suggesting that GSI in *D. chrysanthum* and *D. longicornu* is not S-RNase based. We analyzed the expression of the S-RNase-like adjacent genes that were annotated as having SLF function (data not shown), which were also did not exhibit pollen-specific expression patterns, suggesting a non-S-RNase-based GSI mechanism. As S-RNase-based GSI markers, SSK1 genes are typically found in Rosaceae, Solanaceae and Plantaginaceae species. One of the SKP1-like genes identified was specifically expressed in the pollen; this might suggest that the GSI of Orchidaceae is not S-RNase based but does involve SSK1. Nevertheless, to clarify the molecular mechanism of SI in this family, analyses of gene expression, diversity level and segregation in controlled crosses as well as S-locus region identification should be performed to determine which gene(s) are involved in S-pistil specificity.

The growth of pollen tubes following self- and cross-pollination was observed using fluorescence microscopy and revealed that *D. chrysanthum* and *D. longicornu* are SI species (**Figures 7**, **8**). The pollen from both pollination types germinated one and two DAP in *D. chrysanthum* and *D. longicornu*, respectively, but the self-pollination pollen tubes grew much more slowly than the cross-pollination pollen tubes (**Figures 7**, **8**). The delay in pollen tube growth may be critical for the SI reaction because by the time the self-pollination pollen tubes penetrate the ovary, the pistil may have already been primed for abscission, as self-pollination flowers fade earlier than normal flowers. After self-pollination, the development of the pollen tube in SI orchids slowed on the stigmatic surface and became arrested at different positions on the pistil that varied among species, similar to the pollen tubes of self- and cross-pollinated *D. farmeri* (Johansen, 1990). The site of the incompatibility reaction in species of representative genera of the main clades of Pleurothallidinae, the largest myophilous group in Orchidaceae, has been investigated (Barbosa et al., 2009); however, most pollen grains of self-pollinated *M. infracta* and *Octomeria*, *Stelis*, *Specklinia*, and *Anathallis* (except *A. microphyta*) species failed to germinate. By contrast, in *Acianthera* spp. and *A. microphyta*, pollen tube growth after self-pollination was similar to that

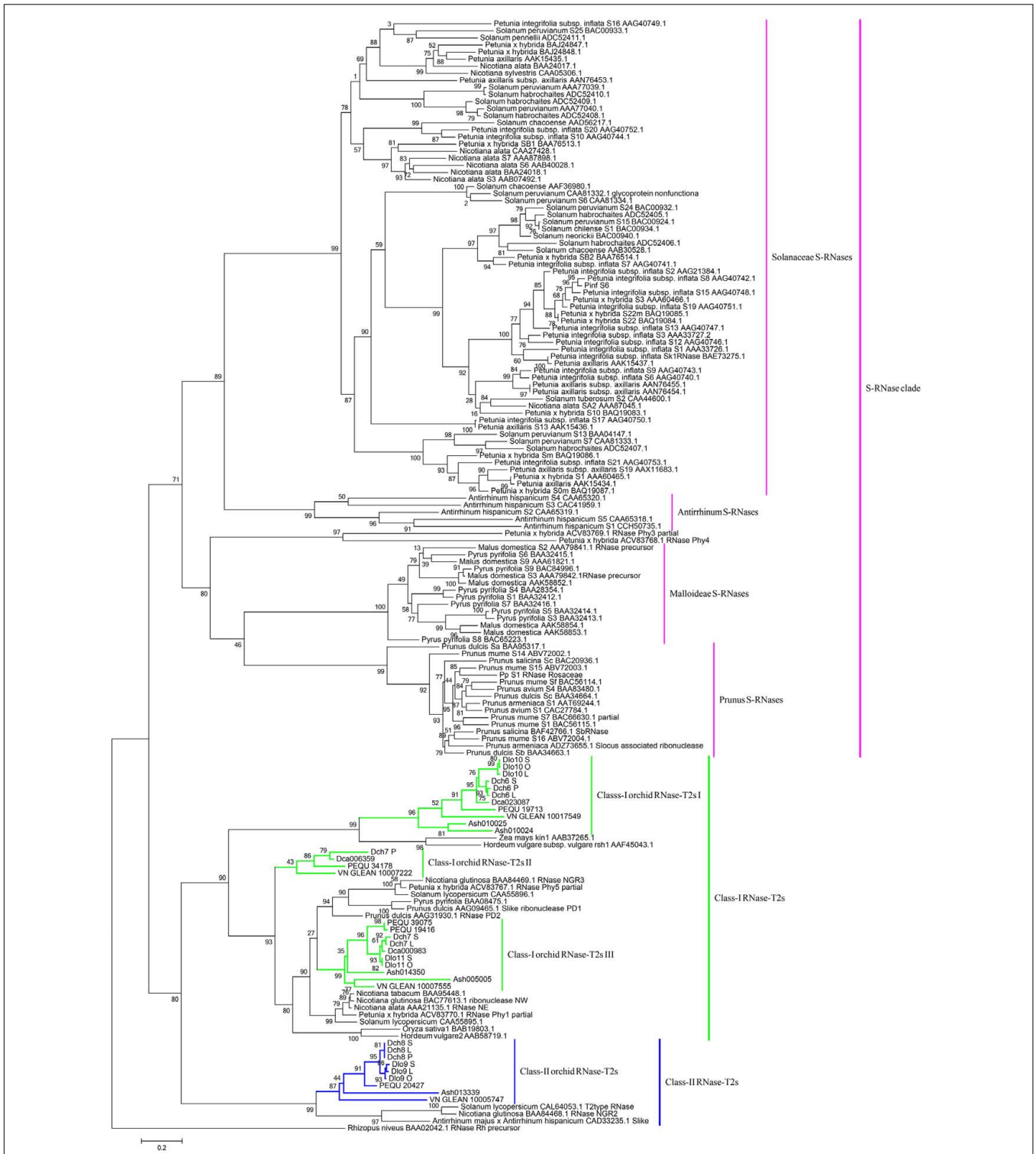

FIGURE 6 | Maximum likelihood phylogenetic tree of the RNase-T2-like genes obtained from orchid species and S-RNase-related RNase-T2s obtained from species possessing S-RNase-based SI, maize, and barley. The tree was constructed in PhyML 3.0 and is based on S-RNase-related RNase-T2s from Solanaceae, Plantaginaceae, and Rosaceae and their homologs in four orchid genomes, two SI *Dendrobium* species transcriptomes, maize, and barley. The classification of RNase-T2s was based on previous studies. RNase-T2s from the filamentous fungus *Rhizopus niveus* were used as the outgroup. Gene subgroups are indicated with different colors. Taxon labels are depicted in pink for the S-RNase clade, which contains Solanaceae S-RNases, *Antirrhinum* S-RNases, Maloideae S-RNases, and *Prunus* S-RNases; in green for Class-I RNase-T2s, which include Class-I orchid RNase-T2s I, Class-I orchid RNase-T2s II, and Class-I orchid RNase-T2s III; and in blue for Class-II RNase-T2s, which contain Class-II orchid RNase-T2s. Values on branches are bootstrap values from SH-like amino acid analysis.

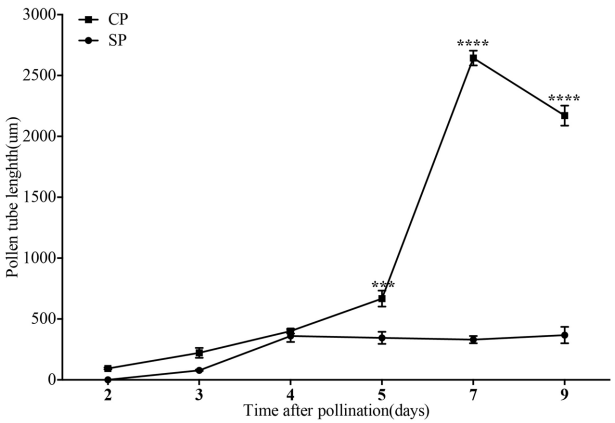

FIGURE 7 | The lengths of the majority of *D. longicornu* pollen tubes present in compatible and incompatible styles at different times after pollination. Pollen tubes were measured at 2 D, 3 D, 4 D, 5 D, 7 D, and 9 D after pollination. Each point is a mean value based on measurements of tubes in three styles, and the error bars represent ± the standard error of the mean. *P*-values were calculated by two-way repeated measures analysis of variance (ANOVA) using Sidak's *post hoc*-test in GraphPad Prism 6 (***$P < 0.001$, ****$P < 0.0001$). CP and SP stand for cross-pollination and self-pollination, respectively, D means day.

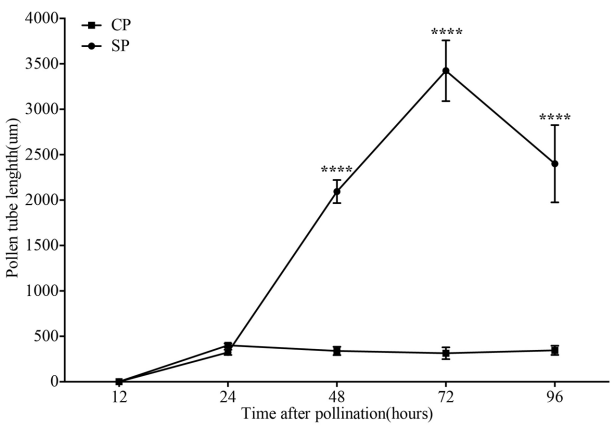

FIGURE 8 | The lengths of the majority of *D. chrysanthum* pollen tubes present in compatible and incompatible styles at different times after pollination. Pollen tubes were measured at 12, 24, 48, 72, and 96 h after pollination. Each point is a mean value based on measurements of tubes in three styles, and the error bars represent ± the standard error of the mean. *P*-values were calculated by two-way repeated measures analysis of variance (ANOVA) using Sidak's *post hoc* test in GraphPad Prism 6 (***$P < 0.001$, ****$P < 0.0001$). CP and SP stand for cross-pollination and self-pollination, respectively, h means hour.

observed after cross-pollination until approximately seven days after pollination. However, from that point onward, the self-pollination pollen tubes began to appear abnormal, with irregular trajectories, variations in their diameters, and excessive callose deposition. Approximately 15 DAP in these flowers, pollen tubes with abnormal characteristics had reached the base of the column, although they never penetrated the ovary. In addition, the pollen tubes of *Acianthera saurocephala* never reached the base of the column. Recently, self-pollinations of 26 *Restrepia* species were performed, but pollen tubes grew only into the top third of the ovary (Millner et al., 2015). The variety of incompatibility reaction sites reported suggests that more than one molecular mechanism for SI may exist.

According to the S-RNase-based GSI and SSK1 homologous genes identified and the sites of the incompatibility reaction, the SI molecular mechanism of Orchidaceae might differ from that determined for S-RNase-based GSI, and diverse SI molecular mechanisms may exist. According to the phylogenetic analyses of the RNases-T2, S-RNase-based GSI evolved only once, before the split of Asteridae and Rosidae approximately 120 MYA (Igic and Kohn, 2001; Steinbachs and Holsinger, 2002; Vieira et al., 2008a). However, the phylogenetic origin of the S-RNase-based GSI system remained unresolved. In the present study, homologs of the male and female SI determinants of S-RNase-based GSI were first investigated in Orchidaceae (monocotyledons) using genome and transcriptome data, which suggested that this RNase-based GSI system might have originated after the split of monocots and eudicots but before the split of Asteridae and Rosidae. Further research on other monocotyledons and Orchidaceae species is needed to confirm this hypothesis.

AUTHOR CONTRIBUTIONS

S-CN, Z-JL, and Y-BL conceived and designed the study. S-CN and G-QZ prepared the final datasets. S-CN, Y-QZ, J-YW, and QX analyzed and acquired the data. S-CN, JH, and P-XL collected the plant materials. S-CN, Y-BL, and Z-JL wrote the manuscript. All authors read and approved the final manuscript.

ACKNOWLEDGMENTS

This work was funded by the Development Funds for Emerging Industries of Strategic Importance of Shenzhen (NYSW20140331010039), the Development Funds for Emerging Industries of Strategic Importance of Shenzhen (JCYJ20140402093332029) and Fundamental Research Project of Shenzhen Municipality (JCYJ20150403150235943). We also thank Xi-Bing Guo, Xu-Hui Chen and Ying-Qiu Tian for their assistance in collecting the plant materials.

SUPPLEMENTARY MATERIAL

The Supplementary Material for this article can be found online at: http://journal.frontiersin.org/article/10.3389/fpls.2017.01106/full#supplementary-material

FILE S1 | Multiple alignment of orchid SKP1-like protein sequences.

FILE S2 | The FPKM values of SKP1-like genes (Supplementary Table 1) and S-RNase like genes (Supplementary Table 2) in different tissues of *D. chrysanthum*.

FILE S3 | The alignment file and the tree file of SKP1 protein sequences.

FILE S4 | The alignment file and the tree file of S-RNase protein sequences.

REFERENCES

Aguiar, B., Vieira, J., Cunha, A. E., Fonseca, N. A., Reboiro-Jato, D., Reboiro-Jato, M., et al. (2013). Patterns of evolution at the gametophytic self-incompatibility *Sorbus aucuparia* (Pyrinae) S pollen genes support the non-self recognition by multiple factors model. *J. Exp. Bot.* 64, 2423–2434. doi: 10.1093/jxb/ert098

Aguiar, B., Vieira, J., Cunha, A. E., and Vieira, C. P. (2015). No evidence for Fabaceae Gametophytic self-incompatibility being determined by Rosaceae, Solanaceae, and Plantaginaceae S-RNase lineage genes. *BMC Plant Biol.* 15:129. doi: 10.1186/s12870-015-0497-492

Barbosa, A. R., de Melo, M. C., and Borba, E. L. (2009). Self-incompatibility and myophily in Octomeria (Orchidaceae, Pleurothallidinae) species. *Plant Syst. Evol.* 283, 1–8. doi: 10.1007/s00606-009-0212-6

Bechsgaard, J. S., Castric, V., Charlesworth, D., Vekemans, X., and Schierup, M. H. (2006). The transition to self-compatibility in *Arabidopsis thaliana* and evolution within S-haplotypes over 10 Myr. *Mol. Biol. Evol.* 23, 1741–1750. doi: 10.1093/molbev/msl042

Boggs, N. A., Nasrallah, J. B., and Nasrallah, M. E. (2009). Independent S-locus mutations caused self-fertility in *Arabidopsis thaliana*. *PLoS Genet.* 5:e1000426. doi: 10.1371/journal.pgen.1000426

Borba, E. L., Semir, J., and Shepherd, G. J. (2001). Self-incompatibility, inbreeding depression and crossing potential in five brazilian Pleurothallis (Orchidaceae) Species. *Ann. Bot.* 88, 89–99. doi: 10.1006/anbo.2001.1435

Cai, J., Liu, X., Vanneste, K., Proost, S., Tsai, W. C., Liu, K. W., et al. (2015). The genome sequence of the orchid *Phalaenopsis equestris*. *Nat. Genet.* 47, 65–72. doi: 10.1038/ng.3149

Cheng, J., Han, Z., Xu, X., and Li, T. (2006). Isolation and identification of the pollen-expressed polymorphic F-box genes linked to the S-locus in apple (*Malus* × *domestica*). *Sex. Plant Reprod.* 19, 175–183. doi: 10.1007/s00497-006-0034-4

De Franceschi, P., Pierantoni, L., Dondini, L., Grandi, M., Sansavini, S., and Sanzol, J. (2011). Evaluation of candidate F-box genes for the pollen S of gametophytic self-incompatibility in the Pyrinae (Rosaceae) on the basis of their phylogenomic context. *Tree Genet. Genomes* 7, 663–683. doi: 10.1007/s11295-011-0365-7

Eddy, S. R. (2011). Accelerated profile HMM searches. *PLoS Comput. Biol.* 7:e1002195. doi: 10.1371/journal.pcbi.1002195

Finn, R. D., Coggill, P., Eberhardt, R. Y., Eddy, S. R., Mistry, J., Mitchell, A. L., et al. (2016). The Pfam protein families database: towards a more sustainable future. *Nucleic Acids Res.* 44, D279–D285. doi: 10.1093/nar/gkv1344

Gasteiger, E. (2003). ExPASy: the proteomics server for in-depth protein knowledge and analysis. *Nucleic Acids Res.* 31, 3784–3788. doi: 10.1093/nar/gkg563

Givnish, T. J., Spalink, D., Ames, M., Lyon, S. P., Hunter, S. J., Zuluaga, A., et al. (2015). Orchid phylogenomics and multiple drivers of their extraordinary diversification. *Proc. Biol. Sci.* 282, 2108–2111. doi: 10.1098/rspb.2015.1553

Gontijo, S. L., Barbosa, A. R., de Melo, M. C., and Borba, E. L. (2010). Occurrence of different sites of self-incompatibility reaction in four *Anathallis* (Orchidaceae, Pleurothallidinae) species. *Plant Species Biol.* 25, 129–135. doi: 10.1111/j.1442-1984.2010.00277.x

Guindon, S., Dufayard, J. F., Lefort, V., Anisimova, M., Hordijk, W., and Gascuel, O. (2010). New algorithms and methods to estimate maximum-likelihood phylogenies: assessing the performance of PhyML 3.0. *Syst. Biol.* 59, 307–321. doi: 10.1093/sysbio/syq010

Guo, Y. L., Bechsgaard, J. S., Slotte, T., Neuffer, B., Lascoux, M., Weigel, D., et al. (2009). Recent speciation of *Capsella rubella* from *Capsella grandiflora*, associated with loss of self-incompatibility and an extreme bottleneck. *Proc. Natl. Acad. Sci. U.S.A.* 106, 5246–5251. doi: 10.1073/pnas.0808012106

Guo, Y. L., Zhao, X., Lanz, C., and Weigel, D. (2011). Evolution of the S-locus region in Arabidopsis relatives. *Plant Physiol.* 157, 937–946. doi: 10.1104/pp.111.174912

Haas, B. J., Papanicolaou, A., Yassour, M., Grabherr, M., Blood, P. D., Bowden, J., et al. (2013). De novo transcript sequence reconstruction from RNA-seq using the Trinity platform for reference generation and analysis. *Nat. Protoc.* 8, 1494–1512. doi: 10.1038/nprot.2013.084

Hillwig, M. S., Liu, X., Liu, G., Thornburg, R. W., and Macintosh, G. C. (2010). Petunia nectar proteins have ribonuclease activity. *J. Exp. Bot.* 61, 2951–2965. doi: 10.1093/jxb/erq119

Holzinger, A., and Pichrtova, M. (2016). Abiotic stress tolerance of charophyte green algae: new challenges for omics techniques. *Front. Plant Sci.* 7:678. doi: 10.3389/fpls.2016.00678

Hua, Z., and Kao, T. H. (2006). Identification and characterization of components of a putative petunia S-locus F-box-containing E3 ligase complex involved in S-RNase-based self-incompatibility. *Plant Cell* 18, 2531–2553. doi: 10.1105/tpc.106.041061

Huang, J., Zhao, L., Yang, Q., and Xue, Y. (2006). AhSSK1, a novel SKP1-like protein that interacts with the S-locus F-box protein SLF. *Plant J.* 46, 780–793. doi: 10.1111/j.1365-313X.2006.02735.x

Igic, B., and Kohn, J. R. (2001). Evolutionary relationships among self-incompatibility RNases. *Proc. Natl. Acad. Sci. U.S.A.* 98, 13167–13171. doi: 10.1073/pnas.231386798

Ikeda, K., Igic, B., Ushijima, K., Yamane, H., Hauck, N. R., Nakano, R., et al. (2004). Primary structural features of the S haplotype-specific F-box protein, SFB, in *Prunus*. *Sex. Plant Reprod.* 16, 235–243. doi: 10.1007/s00497-003-0200-x

Johansen, B. (1990). Incompatibility in *Dendrobium* (Orchidaceae). *Bot. J. Linn. Soc.* 103, 165–196. doi: 10.1111/j.1095-8339.1990.tb00183.x

Kakui, H., Kato, M., Ushijima, K., Kitaguchi, M., Kato, S., and Sassa, H. (2011). Sequence divergence and loss-of-function phenotypes of S locus F-box brothers genes are consistent with non-self recognition by multiple pollen determinants in self-incompatibility of Japanese pear (*Pyrus pyrifolia*). *Plant J.* 68, 1028–1038. doi: 10.1111/j.1365-313X.2011.04752.x

Kakui, H., Tsuzuki, T., Koba, T., and Sassa, H. (2007). Polymorphism of SFBB-gamma and its use for S genotyping in Japanese pear (*Pyrus pyrifolia*). *Plant Cell Rep.* 26, 1619–1625. doi: 10.1007/s00299-007-0386-8

Katoh, K., and Standley, D. M. (2013). MAFFT multiple sequence alignment software version 7: improvements in performance and usability. *Mol. Biol. Evol.* 30, 772–780. doi: 10.1093/molbev/mst010

Kong, H., Landherr, L. L., Frohlich, M. W., Leebens-Mack, J., Ma, H., and dePamphilis, C. W. (2007). Patterns of gene duplication in the plant SKP1 gene family in angiosperms: evidence for multiple mechanisms of rapid gene birth. *Plant J.* 50, 873–885. doi: 10.1111/j.1365-313X.2007.03097.x

Kong, H., Leebens-Mack, J., Ni, W., dePamphilis, C. W., and Ma, H. (2004). Highly heterogeneous rates of evolution in the SKP1 gene family in plants and animals: functional and evolutionary implications. *Mol. Biol. Evol.* 21, 117–128. doi: 10.1093/molbev/msh001

Kothke, S., and Kock, M. (2011). The *Solanum lycopersicum* RNaseLER is a class II enzyme of the RNase T2 family and shows preferential expression in guard cells. *J. Plant Physiol.* 168, 840–847. doi: 10.1016/j.jplph.2010.11.012

Kubo, K., Entani, T., Takara, A., Wang, N., Fields, A. M., Hua, Z., et al. (2010). Collaborative non-self recognition system in S-RNase-based self-incompatibility. *Science* 330, 796–799. doi: 10.1126/science.1195243

Kubo, K., Paape, T., Hatakeyama, M., Entani, T., Takara, A., Kajihara, K., et al. (2015). Gene duplication and genetic exchange drive the evolution of S-RNase-based self-incompatibility in *Petunia*. *Nat. Plants* 1, 14005. doi: 10.1038/nplants.2014.5

Letunic, I., Doerks, T., and Bork, P. (2012). SMART 7: recent updates to the protein domain annotation resource. *Nucleic Acids Res.* 40, D302–D305. doi: 10.1093/nar/gkr931

MacIntosh, G. C., Hillwig, M. S., Meyer, A., and Flagel, L. (2010). RNase T2 genes from rice and the evolution of secretory ribonucleases in plants. *Mol. Genet. Genomics* 283, 381–396. doi: 10.1007/s00438-010-0524-9

Matsumoto, D., Yamane, H., Abe, K., and Tao, R. (2012). Identification of a Skp1-like protein interacting with SFB, the pollen S determinant of the gametophytic self-incompatibility in *Prunus*. *Plant Physiol.* 159, 1252–1262. doi: 10.1104/pp.112.197343

Millner, H. J., McCrea, A. R., and Baldwin, T. C. (2015). An investigation of self-incompatibility within the genus *Restrepia*. *Am. J. Bot.* 102, 487–494. doi: 10.3732/ajb.1400555

Minamikawa, M., Kakui, H., Wang, S., Kotoda, N., Kikuchi, S., Koba, T., et al. (2010). Apple S locus region represents a large cluster of related, polymorphic and pollen-specific F-box genes. *Plant Mol. Biol.* 74, 143–154. doi: 10.1007/s11103-010-9662-z

Mortazavi, A., Williams, B. A., McCue, K., Schaeffer, L., and Wold, B. (2008). Mapping and quantifying mammalian transcriptomes by RNA-Seq. *Nat. Methods* 5, 621–628. doi: 10.1038/nmeth.1226

Nowak, M. D., Davis, A. P., Anthony, F., and Yoder, A. D. (2011). Expression and trans-specific polymorphism of self-incompatibility RNases in coffea (Rubiaceae). *PLoS ONE* 6:e21019. doi: 10.1371/journal.pone.0021019

Nunes, M. D., Santos, R. A., Ferreira, S. M., Vieira, J., and Vieira, C. P. (2006). Variability patterns and positively selected sites at the gametophytic self-incompatibility pollen SFB gene in a wild self-incompatible *Prunus spinosa* (Rosaceae) population. *New Phytol.* 172, 577–587. doi: 10.1111/j.1469-8137.2006.01838.x

Okada, K., Tonaka, N., Taguchi, T., Ichikawa, T., Sawamura, Y., Nakanishi, T., et al. (2011). Related polymorphic F-box protein genes between haplotypes clustering in the BAC contig sequences around the S-RNase of Japanese pear. *J. Exp. Bot.* 62, 1887–1902. doi: 10.1093/jxb/erq381

Pinheiro, F., Cafasso, D., Cozzolino, S., and Scopece, G. (2015). Transitions between self-compatibility and self-incompatibility and the evolution of reproductive isolation in the large and diverse tropical genus *Dendrobium* (Orchidaceae). *Ann. Bot.* 116, 457–467. doi: 10.1093/aob/mcv057

Roalson, E. (2003). S-RNases and sexual incompatibility: structure, functions, and evolutionary perspectives. *Mol. Phylogenet. Evol.* 29, 490–506. doi: 10.1016/s1055-7903(03)00195-7

Sassa, H., Kakui, H., Miyamoto, M., Suzuki, Y., Hanada, T., Ushijima, K., et al. (2007). S locus F-box brothers: multiple and pollen-specific F-box genes with S haplotype-specific polymorphisms in apple and Japanese pear. *Genetics* 175, 1869–1881. doi: 10.1534/genetics.106.068858

Sonneveld, T., Tobutt, K. R., Vaughan, S. P., and Robbins, T. P. (2005). Loss of pollen-S function in two self-compatible selections of *Prunus avium* is associated with deletion/mutation of an S haplotype-specific F-box gene. *Plant Cell* 17, 37–51. doi: 10.1105/tpc.104.026963

Steinbachs, J. E., and Holsinger, K. E. (2002). S-RNase-mediated gametophytic self-incompatibility is ancestral in eudicots. *Mol. Biol. Evol.* 19, 825–829. doi: 10.1093/oxfordjournals.molbev.a004139

Tao, R., Watari, A., Hanada, T., Habu, T., Yaegaki, H., Yamaguchi, M., et al. (2007). Self-compatible peach (*Prunus persica*) has mutant versions of the S haplotypes found in self-incompatible *Prunus* species. *Plant Mol. Biol.* 63, 109–123. doi: 10.1007/s11103-006-9076-0

Ushijima, K. (2003). Structural and transcriptional analysis of the self-incompatibility locus of almond: identification of a pollen-expressed F-box gene with haplotype-specific polymorphism. *Plant Cell* 15, 771–781. doi: 10.1105/tpc.009290

Vieira, J., Fonseca, N. A., and Vieira, C. P. (2008a). An S-RNase-based gametophytic self-incompatibility system evolved only once in eudicots. *J. Mol. Evol.* 67, 179–190. doi: 10.1007/s00239-008-9137-x

Vieira, J., Santos, R. A., Ferreira, S. M., and Vieira, C. P. (2008b). Inferences on the number and frequency of S-pollen gene (SFB) specificities in the polyploid *Prunus spinosa*. *Heredity (Edinb)* 101, 351–358. doi: 10.1038/hdy.2008.60

Wheeler, D., and Newbigin, E. (2007). Expression of 10 S-class SLF-like genes in *Nicotiana alata* pollen and its implications for understanding the pollen factor of the S locus. *Genetics* 177, 2171–2180. doi: 10.1534/genetics.107.076885

Williams, J. S., Der, J. P., dePamphilis, C. W., and Kao, T. H. (2014). Transcriptome analysis reveals the same 17 S-locus F-box genes in two haplotypes of the self-incompatibility locus of *Petunia inflata*. *Plant Cell* 26, 2873–2888. doi: 10.1105/tpc.114.126920

Xu, C., Li, M., Wu, J., Guo, H., Li, Q., Zhang, Y., et al. (2013). Identification of a canonical SCF(SLF) complex involved in S-RNase-based self-incompatibility of *Pyrus* (Rosaceae). *Plant Mol. Biol.* 81, 245–257. doi: 10.1007/s11103-012-9995-x

Yamashita, S., Miyagi, C., Fukada, T., Kagara, N., Che, Y. S., and Hirano, T. (2004). Zinc transporter LIVI controls epithelial-mesenchymal transition in zebrafish gastrula organizer. *Nature* 429, 298–302. doi: 10.1038/nature02545

Zhang, G. Q., Xu, Q., Bian, C., Tsai, W. C., Yeh, C. M., Liu, K. W., et al. (2016). The *Dendrobium catenatum* Lindl. genome sequence provides insights into polysaccharide synthase, floral development and adaptive evolution. *Sci. Rep.* 6:19029. doi: 10.1038/srep19029

Zhao, L., Huang, J., Zhao, Z., Li, Q., Sims, T. L., and Xue, Y. (2010). The Skp1-like protein SSK1 is required for cross-pollen compatibility in S-RNase-based self-incompatibility. *Plant J.* 62, 52–63. doi: 10.1111/j.1365-313X.2010.04123.x

Conflict of Interest Statement: The authors declare that the research was conducted in the absence of any commercial or financial relationships that could be construed as a potential conflict of interest.

frontiers in Plant Science

ORIGINAL RESEARCH
published: 30 March 2017
doi: 10.3389/fpls.2017.00430

Temporal Petal Closure Benefits Reproductive Development of *Magnolia denudata* (Magnoliaceae) in Early Spring

Liya Liu[1†], Chulan Zhang[1,2†], Xiangyu Ji[1,2], Zhixiang Zhang[2] and Ruohan Wang[1]*

[1] National Engineering Laboratory for Tree Breeding, Key Laboratory for Genetics and Breeding of Forest Trees and Ornamental Plants, Ministry of Education, College of Biological Sciences and Biotechnology, Beijing Forestry University, Beijing, China, [2] Lab of Systematic Evolution and Biogeography of Woody Plants, College of Nature Conservation, Beijing Forestry University, Beijing, China

The Magnoliaceae shows strong phylogenetic niche conservatism, in which temporal petal closure has been extensively reported. However, it is yet elusive whether temporal petal closure is an idle floral character inherited from their ancestors or an adaptive trait to their habitats. Here, we monitored the process of temporal floral closure and re-opening in a thermogenic plant, *Magnolia denudata* (Magnoliaceae). Furthermore, we artificially interrupted temporal petal closure and investigated its effects on development of female and male gametophytes. Intriguingly, we found considerable anatomical changes in the anthers shortly after temporal closure of petals: disintegration of tapeta, crack of anther walls, and release of matured pollens. In comparison with normal flowers, artificially interrupted flowers (no petal closure) showed delayed anther development and slower pollen germination on stigmas, while little difference in embryo morphology was observed during the early stage of embryo development. Moreover, seed set and quality were significantly decreased when petal closure was prevented. In addition, we found pollination accelerated floral closure in *M. denudata*. Taken together, temporal floral closure benefits reproduction of *M. denudata* in early spring by promoting anther development and pollen function, which suggests that it is an adaptive floral trait to its specific habitat.

Keywords: adaptation, anther development, floral closure, petal movement, pollination

OPEN ACCESS

Edited by:
Xin Wang,
Nanjing Institute of Geology and Paleontology (CAS), China

Reviewed by:
Xinqiang He,
Peking University, China
Wen-Zhe Liu,
Northwest University, China

***Correspondence:**
Ruohan Wang
wangrh@bjfu.edu.cn

[†] These authors have contributed equally to this work.

Specialty section:
This article was submitted to Plant Evolution and Development, a section of the journal Frontiers in Plant Science

Received: *05 January 2017*
Accepted: *13 March 2017*
Published: *30 March 2017*

Citation:
Liu L, Zhang C, Ji X, Zhang Z and Wang R (2017) Temporal Petal Closure Benefits Reproductive Development of Magnolia denudata (Magnoliaceae) in Early Spring. Front. Plant Sci. 8:430. doi: 10.3389/fpls.2017.00430

INTRODUCTION

The flowering stage is of crucial importance to plants since it marks the onset of double fertilization and subsequent seed set, which leads to regeneration of the population. In order to adapt to diverse environments, flowers have evolved wonderful variation in morphology, such as color, shape, and size, which is beneficial for pollinator visiting and protection of internal structures (Clark and Husband, 2007). Except for morphological variations, there are non-morphological changes in flowers, namely floral movement. Many plant species are capable of moving some portions of their anatomy, such as petal and pistil in response to internal and/or external factors (Hase et al., 2006; Ren and Tang, 2012), which could affect reproduction of flowering plants deeply.

As one of the most extensively observed non-morphological changes of flowers, the opening and closure of petals is an important trait of the productive syndrome (van Doorn and Kamdee, 2014). During the anthesis, some flowers maintain open until petal withering, such as rose, while others

show temporal closure and repeated opening of petals, such as lotus. From a physiological point of view, flower opening involves a high rate of cell expansion (Singh et al., 2011; Pei et al., 2013). It has attracted extensive attention of scientists by the complex regulation and also has inspired artists and common people by the impressive and emotional petal movements. Although several suspected regulatory mechanisms, such as internal circadian rhythm (Trivellini et al., 2016; Yon et al., 2016), light control (Trivellini et al., 2016), temperature control (Calinger et al., 2013), and moisture control (Magalhaes and Angelocci, 1976), have been raised, ecological roles of the various types of flower opening remain elusive.

Magnolia denudata belongs to the Magnoliaceae and usually flowers in cold early spring. In former studies, we found that thermogenic flowers of *M. denudata* were hermaphroditic and protogynous, usually with temporal petal closure occurring during the anthesis (Wang et al., 2013). However, little is known regarding the ecological roles of this temporary petal closure. In this study, we investigated the process of floral opening and closure during the anthesis of *M. denudata*, with emphasis on the effects of temporal floral closure on stamen development, pollen function, embryo development, as well as seed production.

MATERIALS AND METHODS

Study Species and Area

Magnolia denudata trees used in this study were located in the campus of Beijing Forestry University (40°00′03″ N, 116°20′25″ E; 68 m a.s.l.), with 10–15 m in height and 20–25 cm in diameter at breast height. The study site had a temperate climate, with mean annual rainfall of 400 mm and mean air temperature of 4–13°C. Trees flower from mid-March to mid-May, with a peak in mid-April.

Timing of Flower Opening and Closure

Twenty swollen flower buds (nearly open) of *M. denudata* were arbitrarily selected in a sunny morning for observation of flower opening and closure. The outer petals maintained open throughout the anthesis and the inner petals showed repeated opening and closure, thus opening angles of the inner petals were measured to monitor the process of flower opening and closure. Measurements were performed at 2-h intervals from 8:00 to 20:00 each day during the anthesis of each individual flower.

Effects of Temporal Floral Closure on Stamen Development

Based on observation of the timing of flower opening and closure, there were four stages of inner petal movements before floral withered, including pre-pistillate, pistillate, post-pistillate, and staminate stages (see Results, **Figure 1**). Androecia of three flowers were fixed in FAA for each of the four stages. To estimate the effects of temporal floral closure on stamen development, six flowers were prevented from closure by stacking inner petals at the pistillate stage. During the subsequent post-pistillate and staminate stages, androecia were collected and fixed in FAA for these six flowers, with three for each stage. The fixed androecia were dehydrated in an ethylalcohol series, embedded in paraffin wax, sectioned (8–10 μm thickness), and then stained with toluidine blue. All sections were observed under an Olympus BH-2 microscope and photographed using an Olympus DP 70 photo micrography system.

Effects of Floral Closure on Pollen Function

Six flowers were manually pollinated at the pistillate stage and divided into two groups: three flowers were stuck with gummed tape to prevent floral closure as described above, the rest three were kept at natural conditions and used as a control. Apocarpous pistils were sampled from these flowers to examine pollen germination and pollen tube growth in 6 h after pollination. Apocarpous pistils collection was conducted at a 2-h interval and one flower from each of the stuck and control group was used for each time. The collected apocarpous pistils were fixed in ethanol: acetic acid (3:1) for 30 min and then stored in 70% ethanol until use. After being softened in 1 mol/L NaOH overnight and washed in distilled water for three times, the samples were stained with decolorized aniline blue, squashed, examined, and photographed using a fluorescence microscope (Olympus BX51).

Effects of Floral Closure on Ovule Development

Twelve flowers were manually pollinated at the pistillate stage and divided into two groups: six flowers were stuck by gummed tape to prevent floral closure as described above, the rest six were kept under natural conditions and used as a control. On the 4th and 8th days, ovules were sampled form three flowers for each of the stuck and control group. The ovule samples were fixed in 2.5% glutaraldehyde and 4% paraformaldehyde for 24 h and sectioned (6 μm thick), stained with toluidine blue, and observed under an Olympus BH-2 microscope. Photographing was performed using an Olympus DP 70 system.

Effects of Temporal Closure on Seed Production

To estimate the effects of temporary closure on seed production, 20 flowers were manual pollinated in April. Ten of the 20 flowers were prevented from temporary closure as described above, the rest 10 flowers were kept under natural conditions, until seeds produced by these flowers got mature. Fruits from these flowers were collected in September and seed size and seed mass analyzed.

Effects of Pollination on Floral Closure

Twenty pistilate-stage flowers were chosen in a sunny morning to estimate the effects of pollination on floral closure. Artificial pollination was performed at 10:00 for 10 of the 20 flowers. The rest 10 flowers were covered using plastic meshes to prevent pollination by insects. Movements of the inner petals were examined for the 20 flowers every 2-h before 20:00.

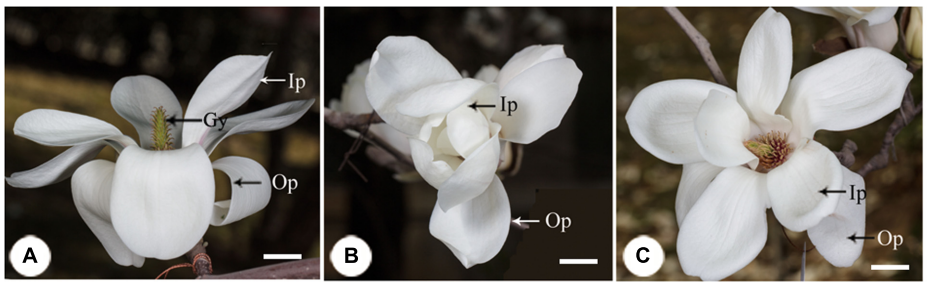

FIGURE 1 | The process of floral closure and re-opening in *Magnolia denudata*. (A) Flower was first opening at the pistillate stage. The stigmas were receptive and stamens appressed tightly to the style with no anthers dehiscence. **(B)** Temporal closure of the flower at the post-pistillate stage. The inner petals were closed and formed a chamber in the evening. **(C)** Flowers re-opened at the staminate stage. The gynoeciums withered and the stamens matured with anthers dehisced. Ip, inner petal; Op, outer petal; Gy, gynoecium. Bars: 2 cm.

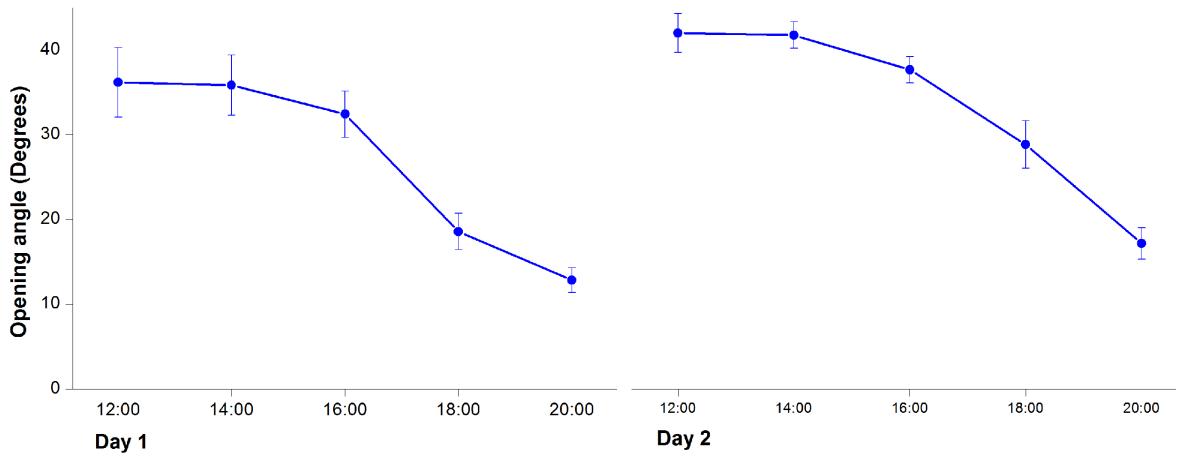

FIGURE 2 | Changes of opening angles during floral closure and re-opening. Values are means ± SE.

RESULTS

Timing of Floral Closure and Re-opening

In the first morning, *M. denudata* flowers were tightly closed at 8:00. The outer petals started to loosen at 10:00, which indicated the onset of flower opening. Then inner petals also opened gradually. The flowers fully opened at 12:00 when the opening angle reached 36.18 ± 0.14° (**Figures 1A**, **2**). During this period, stigmas were receptive with some crystalline secretion on the surface and stamens appressed tightly to the style with no anthesis dehiscence, indicative of the pistillate stage of the flowers. The flowers maintained fully-open by 16:00, after which the opening angles decreased sharply. The angles decreased to 12.83 ± 0.08° and the inner petals formed a chamber at 20:00, which marks the temporal closure of the flowers at the post-pistillate stage (**Figures 1B**, **2**).

In the second day, inner petals started to open again at 10:00 and fully opened at 12:00 when the opening angles reached 42 ± 0.13° (**Figures 1C**, **2**). At this stage, the gynoeciums withered and the stamens matured with anthers dehisced, suggesting that the flowers entered the staminate stage. Inner petals of the fully opened flowers started to close again after 16:00 and formed chambers with the inner petals at 20:00 as they did in the first day. In the third morning, the inner petals re-opened again at 10:00 and maintained open until the flowers withered.

Effects of Temporal Floral Closure on Male and Female Gametophytes

At the pre-pistillate stage, anthers stayed intact and no pollen was released. The tetrasporangiate anther wall consisted of epidermis, endothecium, 2–3 middle layers, and glandular tapetum of 1–2 cells (**Figure 3A**). When the inner petals were opened for the first time and flowers entered the pistillate stage, tapetum began to disintegrate gradually (**Figure 3B**). The tapetum totally disappeared and stomium formed at the junction of two pollen sacs at the post-pistillate stage (**Figures 3C,D**). In the second morning, inner petals re-opened and flowers were at the staminate stage. The stomium ruptured, the fiber layers expanded, and the connective cells broke down, which led to release of pollen grains (**Figure 3E**). When the inner petals were stuck to disrupt floral closure at the pistillate stage, anther dehiscence and pollen release were observed 18 h later than the non-stuck control flowers (**Figure 3F**).

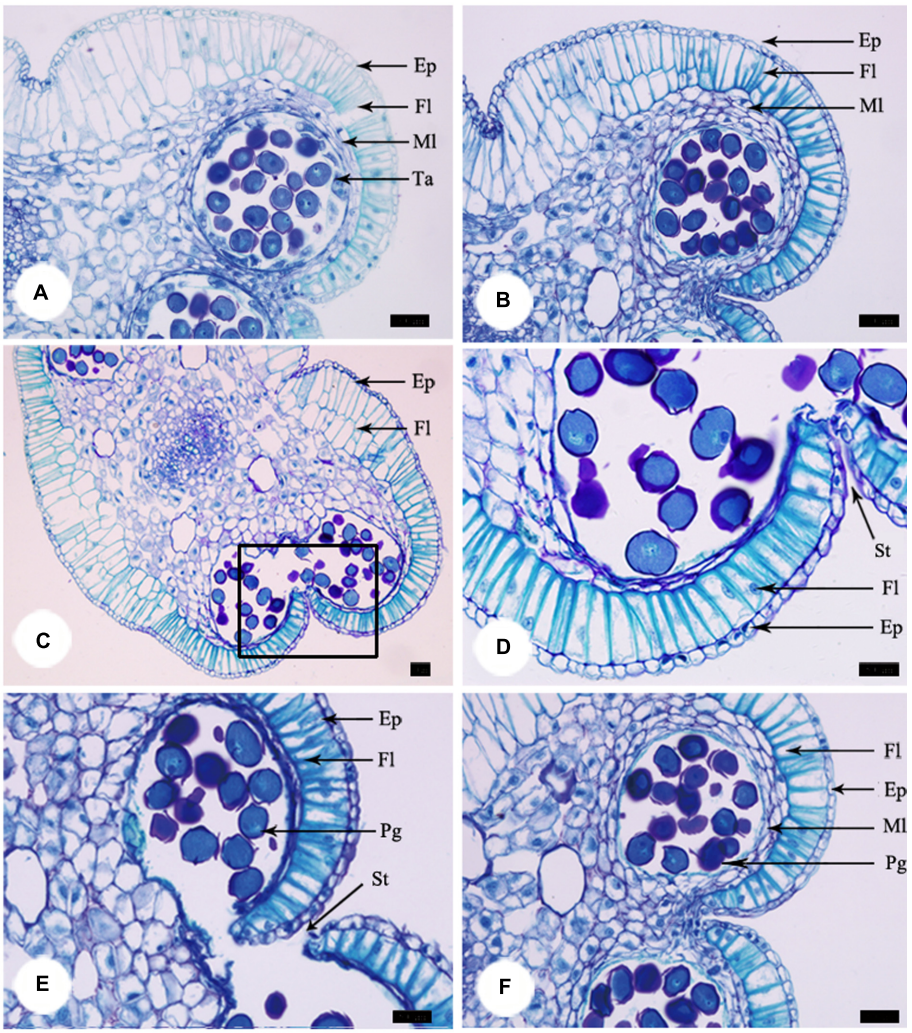

FIGURE 3 | Anther development during the process of floral closure and re-opening. (A) Anther was intact and no pollen was released at the pre-pistillate stage. **(B)** Tapetum began to disintegrate gradually at the pistillate stage. **(C)** The tapetum disappeared and stomium formed at the post-pistillate stage. **(D)** A higher magnification of the region of interest in **(C)**. **(E)** Stomium ruptured, fiber layers expanded, connective cells broke down, and pollen grains released at the staminate stage. **(F)** Anther of stuck flowers at the staminate stage. Ep, epidermis; Fl, fiber layer; Ml, middle layer; Ta, tapetum; St, stomium. Bars: 50 μm.

Furthermore, we examined pollen germination and pollen tube growth after artificial pollination. In non-stuck flowers, pollen germination was observed 4 h after pollination (**Figures 4A,B**). In stuck flowers, pollens did not start to germinate until 6 h after pollination, by which time some pollen tubes entered the transmitting tissue in the styles of non-stuck flowers (**Figures 4C,D**). The embryo sacs of *M. denudata* were immature at the pistillate stage. When the petals were stuck at the pistillate stage after artificial pollination, the embryo development showed little difference from that of non-stuck flowers in 8 days (**Figure 5**).

Effects of Temporal Floral Closure on Seed Set

The carpals began to expand 10 days after artificial pollination. The follicles produced by non-stuck flowers were erect and grew to as long as 18 cm. For the stuck flowers, follicles were wound in shape (**Figure 6**). Follicles contained an average of 81.55 ± 9.82 seeds for the non-stuck flowers ($n = 9$, for one fruit was lost before ripening). The stuck flowers produced 39.60 ± 7.03 seeds per follicle, which was significantly ($p < 0.05$) fewer than that of non-stuck flowers (**Figure 6**). Seed mass was 0.17 ± 0.03 g per seed ($n = 30$) for the non-stuck flowers, which was significantly higher than that of stuck flowers (0.11 ± 0.02 g per seed, **Figure 6**). Seeds size was also significantly smaller for stuck flowers than non-stuck flowers (**Figure 6**).

Effects of Pollination on Floral Closure

When the pistillate-stage flowers were artificially pollinated, inner petals began to close at16: 00. After 2 h, 9 out of the 10 flowers were fully closed, and the rest one was nearly closed. For the

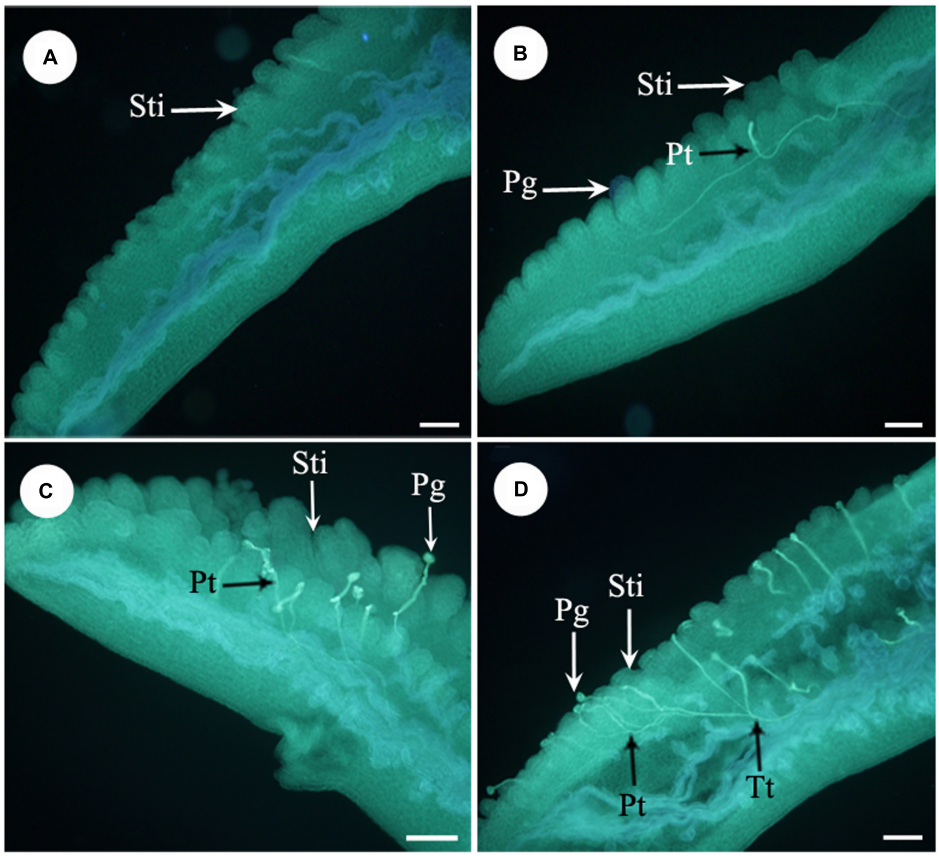

FIGURE 4 | Fluorescence micrographs of pollens in the apocarpous gynaecium. (A) No pollen germinated on stigmas of stuck flowers 4 h after artificial pollination. **(B)** Pollens started to germinate 4 h after artificial pollination of non-stuck flower. **(C)** Pollens start to germinate 6 h after pollination in stuck flowers. **(D)** Pollen tubes entered the transmitting tissue in non-stuck flowers 6 h after pollination. Sti, stigma; Pg, pollen grain; Pt, pollen tube; Tt, transmitting tissue. Bars: 100 μm.

non-pollinated flowers, closure of inner petals was also observed whilst the closure was much slower. When the inner petals of pollinated flowers fully closed, only 2 out of 10 were nearly closed for the non-pollinated flowers and the rest eight flowers were in the process of closure, with an average opening angle of $33.8 \pm 2.6°$.

DISCUSSION

The flowering stage, in which pollination and fertilization occur, leading to seed set in female and bisexual flowers, is a crucial period for plant life history. There is great variation of floral period among different plants; it can range from a few minutes to days or even months (Ashman and Schoen, 1994; Clark and Husband, 2007). Some flowers remain open and functional during the anthesis, while others could show repeated opening and closure (Abdusalam and Tan, 2014). In the present study, *M. denudata* flowers showed a repeated and diurnal opening in response to the day/night cycle during its anthesis. It is intriguing to note that there is vast variation of flower opening types within the *Magnolia* genus. *Magnolia sprengeri*, like *M. denudata* in the current study, flowers in daytime (Wang et al., 2014), while *M. ovata* and *M. virginiana* in night (Gottsberger et al., 2012; Losada et al., 2014). Some *Magnolia* species, such as *M. praecocissima*, *M. schiedeana*, and *M. tamaulipana* have a single flower opening (Dieringer and Espinosa, 1994; Ishida, 1996; Dieringer et al., 1999), while others show repetitive opening, such as *M. denudata*, *M. sprengeri*, *M. ovata*, and *M. virginiana* (Wang et al., 2010, 2014; Gottsberger et al., 2012; Losada et al., 2014). Considering that these *Magnolia* species are living in different habitats and pollination was mediated by different insects (Dieringer et al., 1999; Gottsberger et al., 2012; Wang et al., 2014), the vast variance in flowering types might be an adaptation to their pollinators with distinct activity rhythms.

A "chamber" was formed when the flowers of *M. denudata* temporally closed, which has also been frequently reported in some other thermogenic plants (Seymour et al., 2009a, 2010; Dieringer et al., 2014). There are different ways to form a floral chamber for thermogenic plants. For *Arum* species, the spathes directly develop into a chamber shape (Seymour et al., 2009a). Floral chambers are formed as a result of partial open of the petals at the female stage in *M. ovata*

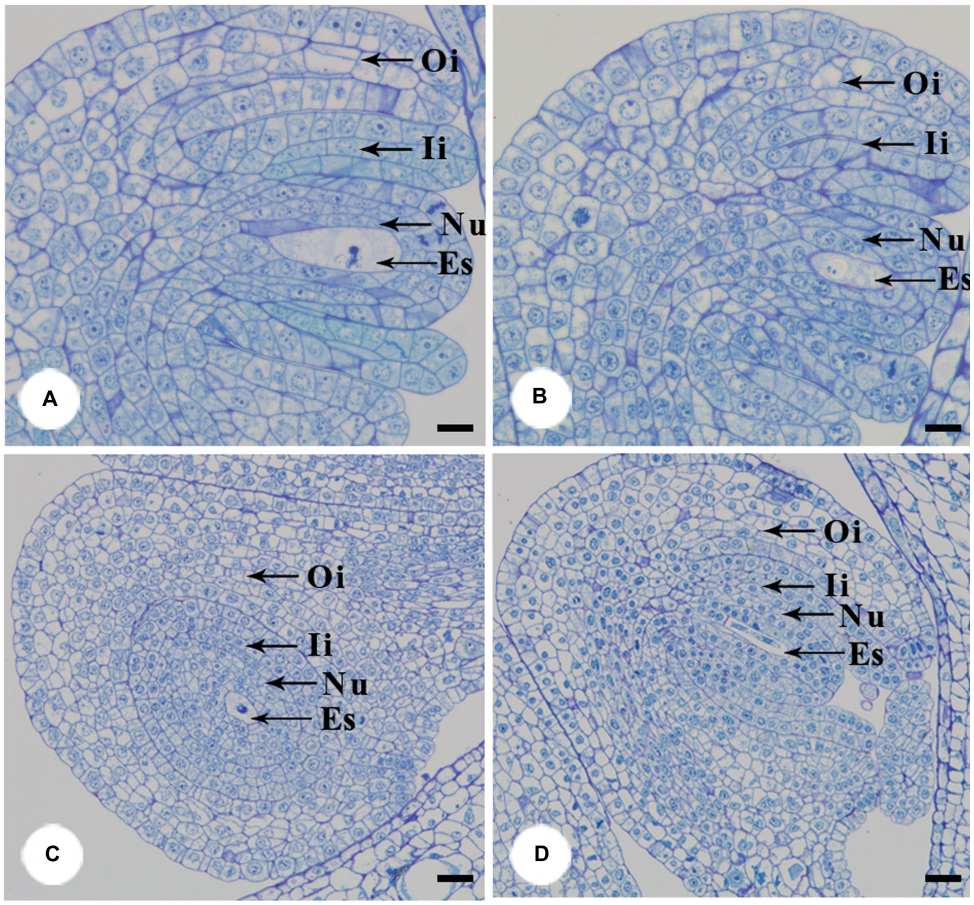

FIGURE 5 | Anatomical structures of ovule after artificial pollination. The functional megasporeis, inner and outer integuments developed of stuck **(A)** and non-stuck flowers **(B)** on the 4th day after pollination. Growth of inner and outer integument of stuck **(C)** and non-stuck **(D)** flowers on the 8th day after pollination. Ii, inner integuments; Oi, outer integuments; Nu, nucellus; Es, embryo sac. Bars: 20 μm.

(Seymour et al., 2010). Being different from *Arum* species and *M. ovata*, *Nelumbo lutea* flowers form chambers by temporal closure of the petals (Dieringer et al., 2014). In *M. denudata*, we found similar situation to *N. lutea*, with a slight difference that the temporal closure of the flowers was restricted to inner petals.

Despite of different ways to form floral chambers, it has been putatively assumed that floral chambers can attract pollinators to stay in the flowers for longer time by providing a favorable micro-environment for foraging and mating (Seymour et al., 2010; Gottsberger et al., 2012; Dieringer et al., 2014). In this study, pollen dehiscence was delayed, pollen germination was low, and pollen tube growth was slow, when the floral chamber was disturbed in *M. denudata*. It has been demonstrated in plants with both thermogenic and non-thermogenic flowers that pollen function was considerably affected by temperature (Seymour et al., 2009b; Coast et al., 2016), which might involve regulation mediated by the GA pathway and Ca^{2+} signals (Mähs et al., 2013; Sakata et al., 2014). Thus, retardance of heat loss by the floral chamber may also play a role in facilitating pollen function. Although little anatomical difference was observed in the embryo at the early stage between stuck and non-stuck flowers, seed set and seed mass were significantly decreased when petal closure was disturbed for *M. denudata*, suggesting the importance of floral chamber in seed development at the post-embryonic stage. Our findings suggested new ecological roles of floral chambers other than attracting pollinators by heat reward.

Floral open and closure involve complex regulatory mechanisms. Since the concept of "floral clock" was proposed by Linné (1783), the circadian pattern of floral opening and closure has been more and more widely appreciated (Burghardt et al., 2016; Mora-García et al., 2017). Besides the endogenous circadian rhythm of flowers, daily changes of light/dark and temperature were also regarded to take roles in regulation of the circadian rhythm (Johansson and Staiger, 2015; Burghardt et al., 2016). Here, we found that pollinated flowers closed considerably earlier than non-pollinated flowers in *M. denudata*. For single opening flowers, an earlier closure may save some energy for the plants. The ecological advantages of early closure after pollinator remain unclear for repeated opening flowers. Some Asteraceae flowers were also reported to show earlier closure after pollination

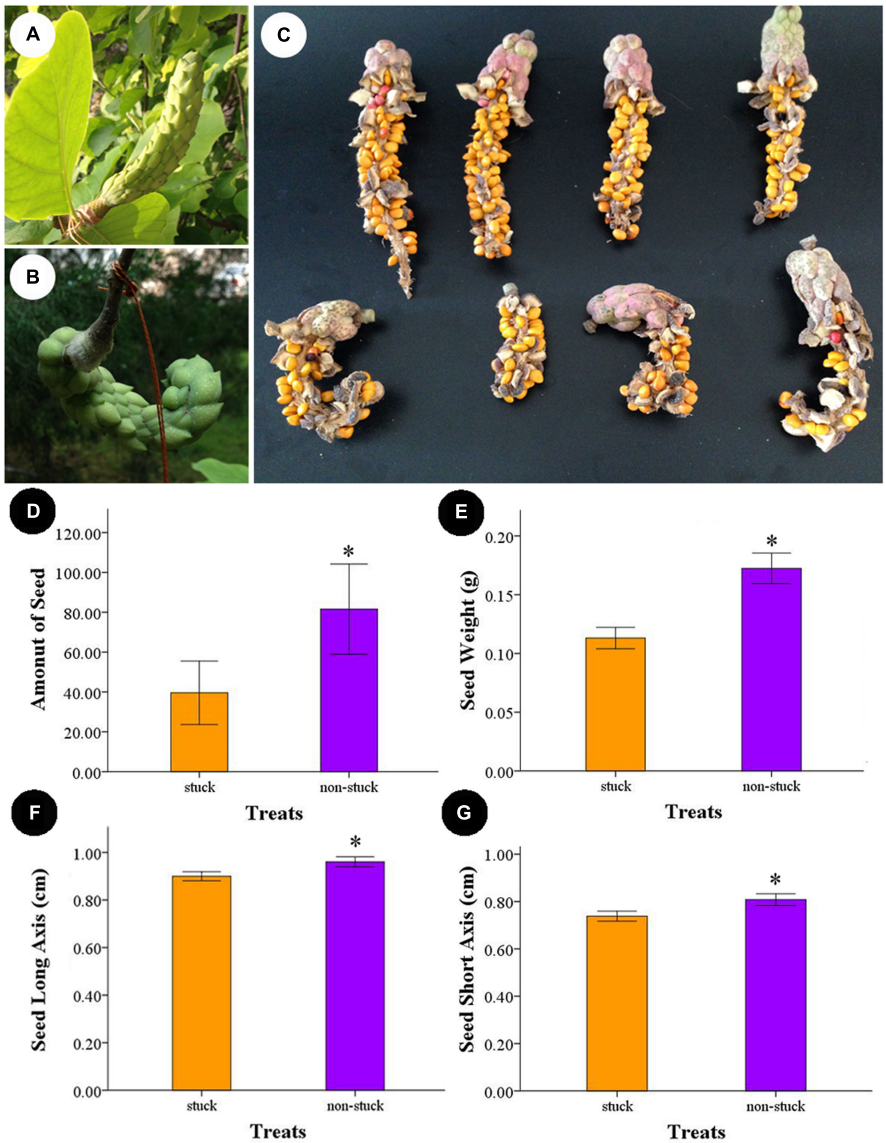

FIGURE 6 | Follicle and seeds produced by non-stuck and stuck flowers. (A) Young fruits produced by non-stuck flowers were plump and erect. **(B)** Young fruits produced by stuck flowers were curled. **(C)** Seeds in the follicle produced by non-stuck and stuck flowers. Comparison of seed production between non-stuck and stuck flowers: seed set **(D)**, seed weight **(E)**, and long **(F)** and short **(G)** axis of seeds. Asterisks indicate significant difference ($p < 0.05$) between non-stuck and stuck flowers.

(Fründ et al., 2011). These results provided new clues for investigating the regulatory framework of floral opening and closure.

In summary, *M. denudata* showed repeated closure of inner petals in night to form floral chambers. We demonstrated new ecological roles of floral chambers in facilitating pollen function and seed development, besides the commonly suspected role of favorable micro-environment for pollinators. In addition, the vast variance in types of floral opening and closure within the *Magnolia* genus may provide diverse genetic resources for studying phylogeny and ecological roles of temporal floral closure.

AUTHOR CONTRIBUTIONS

Conceived and designed the experiments: RW, LL, CZ. Performed the experiments: LL, CZ, XJ. Analyzed the data: LL, CZ, RW. Wrote the paper: RW. Provided crucial suggestion on the experiment: ZZ.

ACKNOWLEDGMENT

This work was supported by the National Science Fund of China (No. 31100450) and Fundamental Research Funds for Central Universities (No. 2015PY-09).

REFERENCES

Abdusalam, A., and Tan, D. Y. (2014). Contribution of temporal floral closure to reproductive success of the spring-flowering *Tulipa iliensis*. *J. Syst. Evol.* 52, 186–194. doi: 10.1111/jse.12036

Ashman, T. L., and Schoen, D. J. (1994). How long should flowers live. *Nature* 371, 788–791. doi: 10.1038/371788a0

Burghardt, L. T., Runcie, D. E., Wilczek, A. M., Cooper, M. D., Roe, J. L., Welch, S. M., et al. (2016). Fluctuating warm temperatures decrease the effect of a key floral repressor on flowering time in *Arabidopsis thaliana*. *New Phytol.* 210, 564–576. doi: 10.1111/nph.13799

Calinger, K. M., Queenborough, S., and Curtis, P. S. (2013). Herbarium specimens reveal the footprint of climate change on flowering trends across north-central North America. *Ecol. Lett.* 16, 1037–1044. doi: 10.1111/ele.12135

Clark, M. J., and Husband, B. C. (2007). Plasticity and timing of flower closure in response to pollination in *Chamerion angustifolium* (Onagraceae). *Int. J. Plant Sci.* 168, 619–625. doi: 10.1086/513486

Coast, O., Murdoch, A. J., Ellis, R. H., Hay, F. R., and Jagadish, K. S. V. (2016). Resilience of rice (*Oryza* spp.) pollen germination and tube growth to temperature stress. *Plant Cell Environ.* 39, 26–37. doi: 10.1111/pce.12475

Dieringer, G., Cabrera, L. R., Lara, M., Loya, L., and Reyes-Castillo, P. (1999). Beetle pollination and floral thermogenicity in *Magnolia tamaulipana* (Magnoliaceae). *Int. J. Plant Sci.* 160, 64–71. doi: 10.1086/314099

Dieringer, G., and Espinosa, S. J. E. (1994). Reproductive ecology of *Magnolia schiedeana* (Magnoliaceae): a threatened cloud forest tree species in Veracruz Mexico. *Bull. Torrey Bot. Club* 121, 154–159. doi: 10.2307/2997167

Dieringer, G., Leticia Cabrera, R., and Mottaleb, M. (2014). Ecological relationship between floral thermogenesis and pollination in *Nelumbo lutea* (Nelumbonaceae). *Am. J. Bot.* 101, 357–364. doi: 10.3732/ajb.1300370

Fründ, J., Dormann, C. F., and Tscharntke, T. (2011). Linné's floral clock is slow without pollinators-flower closure and plant-pollinator interaction webs. *Ecol. Lett.* 14, 896–904. doi: 10.1111/j.1461-0248.2011.01654.x

Gottsberger, G., Silberbauer-Gottsberger, I., Seymour, R. S., and Dötterl, S. (2012). Pollination ecology of *Magnolia ovata* may explain the overall large flower size of the genus. *Flora* 207, 107–118. doi: 10.1016/j.flora.2011.11.003

Hase, A. V., Cowling, R. M., and Ellis, A. G. (2006). Petal movement in cape wildflowers protects pollen from exposure to moisture. *Plant Ecol.* 184, 75–87. doi: 10.1007/s11258-005-9053-8

Ishida, K. (1996). Beetle pollination of *Magnolia praecocissima* var, borealis. *Plant Species Biol.* 11, 199–206. doi: 10.1111/j.1442-1984.1996.tb00146.x

Johansson, M., and Staiger, D. (2015). Time to flower: interplay between photoperiod and the circadian clock. *J. Exp. Bot.* 66, 719–730. doi: 10.1093/jxb/eru441

Linné, C. (1783). *Philosophia Botanica*, 2nd Edn. Vienna: Typis Joannis Thomae Trattner.

Losada, J. M., Herrero, M., Hormaza, J. I., and Friedman, W. E. (2014). Arabinogalactan proteins mark stigmatic receptivity in the protogynous flowers of *Magnolia virginiana* (Magnoliaceae). *Am. J. Bot.* 101, 1963–1975. doi: 10.3732/ajb.1400280

Magalhaes, A. C., and Angelocci, L. R. (1976). Sudden alterations in water balance associated with flower bud opening in coffee plants. *J. Hortic. Sci.* 51, 419–423. doi: 10.1080/00221589.1976.11514707

Mähs, A., Steinhorst, L., Han, J.-P., Shen, L.-K., Wang, Y., and Kudla, J. (2013). The calcineurin B-Like Ca2+ sensors CBL1 and CBL9 function in pollen germination and pollen tube growth in *Arabidopsis*. *Mol. Plant* 6, 1149–1162. doi: 10.1093/mp/sst095

Mora-García, S., de Leone, M. J., and Yanovsky, M. (2017). Time to grow: circadian regulation of growth and metabolism in photosynthetic organisms. *Curr. Opin. Plant Biol.* 35, 84–90. doi: 10.1016/j.pbi.2016.11.009

Pei, H., Ma, N., Tian, J., Luo, J., Chen, J., Li, J., et al. (2013). An NAC transcription factor controls ethylene-regulated cell expansion in flower petals. *Plant Physiol.* 163, 775–791. doi: 10.1104/pp.113.223388

Ren, M. X., and Tang, J. Y. (2012). Up and down: stamen movements in *Ruta graveolens* (Rutaceae) enhance both outcrossing and delayed selfing. *Ann. Bot.* 110, 1017–1025. doi: 10.1093/aob/mcs181

Sakata, T., Oda, S., Tsunaga, Y., Shomura, H., Kawagishi-Kobayashi, M., Aya, K., et al. (2014). Reduction of gibberellin by low temperature disrupts pollen development in rice. *Plant Physiol.* 164, 2011–2019. doi: 10.1104/pp.113.234401

Seymour, R. S., Gibernau, M., and Pirintsos, S. A. (2009a). Thermogenesis of three species of Arum from Crete. *Plant Cell Environ.* 32, 1467–1476. doi: 10.1111/j.1365-3040.2009.02015.x

Seymour, R. S., Ito, Y., Onda, Y., and Ito, K. (2009b). Effects of floral thermogenesis on pollen function in Asian skunk cabbage *Symplocarpus renifolius*. *Biol. Lett.* 5, 568–570. doi: 10.1098/rsbl.2009.0064

Seymour, R. S., Silberbauer-Gottsberger, I., and Gottsberger, G. (2010). Respiration and temperature patterns in thermogenic flowers of *Magnolia ovata* under natural conditions in Brazil. *Funct. Plant Biol.* 37, 870–878. doi: 10.1071/FP10039

Singh, A. P., Tripathi, S. K., Nath, P., and Sane, A. P. (2011). Petal abscission in rose is associated with the differential expression of two ethylene-responsive xyloglucan endotransglucosylase/hydrolase genes, *RbXTH1* and *RbXTH2*. *J. Exp. Bot.* 62, 5091–5103. doi: 10.1093/jxb/err209

Trivellini, A., Cocetta, G., Hunter, D. A., Vernieri, P., and Ferrante, A. (2016). Spatial and temporal transcriptome changes occurring during flower opening and senescence of the ephemeral hibiscus flower, *Hibiscus rosa-sinensis*. *J. Exp. Bot.* 67, 5919–5931. doi: 10.1093/jxb/erw295

van Doorn, W. G., and Kamdee, C. (2014). Flower opening and closure: an update. *J. Exp. Bot.* 65, 5749–5757. doi: 10.1093/jxb/eru327

Wang, R. H., Jia, H., Wang, J. Z., and Zhang, Z. X. (2010). Flowering and pollination patterns of *Magnolia denudata* with emphasis on anatomical changes in ovule and seed development. *Flora* 205, 259–265. doi: 10.1016/j.flora.2009.04.003

Wang, R. H., Liu, X. Y., Mou, S. L., Xu, S., and Zhang, Z. X. (2013). Temperature regulation of floral buds and floral thermogenicity in *Magnolia denudata* (Magnoliaceae). *Trees* 27, 1755–1762. doi: 10.1007/s00468-013-0921-x

Wang, R. H., Xu, S., Liu, X. Y., Zhang, Y. Y., Wang, J. Z., and Zhang, Z. X. (2014). Thermogenesis, flowering and the association with variation in floral odour attractants in *Magnolia sprengeri* (Magnoliaceae). *PLoS ONE* 9:e99356. doi: 10.1371/journal.pone.0099356

Yon, F., Joo, Y., Cortés Llorca, L., Rothe, E., Baldwin, I. T., and Kim, S. G. (2016). Silencing *Nicotiana attenuata LHY* and *ZTL* alters circadian rhythms in flowers. *New Phytologist* 209, 1058–1066. doi: 10.1111/nph.13681

Conflict of Interest Statement: The authors declare that the research was conducted in the absence of any commercial or financial relationships that could be construed as a potential conflict of interest.

frontiers in Plant Science

ORIGINAL RESEARCH
published: 01 March 2017
doi: 10.3389/fpls.2017.00261

Transcriptomic Analysis Reveals Mechanisms of Sterile and Fertile Flower Differentiation and Development in *Viburnum macrocephalum* f. *keteleeri*

*Zhaogeng Lu, Jing Xu, Weixing Li, Li Zhang, Jiawen Cui, Qingsong He, Li Wang and Biao Jin **

College of Horticulture and Plant Protection, Yangzhou University, Yangzhou, China

OPEN ACCESS

Edited by:
Zhong-Jian Liu,
The National Orchid Conservation Center of China, The Orchid Conservation & Research Center of Shenzhen, China

Reviewed by:
Marie Monniaux,
Max Planck Society, Germany
Jinling Huang,
East Carolina University, USA

****Correspondence:***
Biao Jin
bjin@yzu.edu.cn

Specialty section:
This article was submitted to Plant Evolution and Development, a section of the journal Frontiers in Plant Science

Received: *23 November 2016*
Accepted: *13 February 2017*
Published: *01 March 2017*

Citation:
Lu Z, Xu J, Li W, Zhang L, Cui J, He Q, Wang L and Jin B (2017) Transcriptomic Analysis Reveals Mechanisms of Sterile and Fertile Flower Differentiation and Development in Viburnum macrocephalum f. keteleeri. Front. Plant Sci. 8:261. doi: 10.3389/fpls.2017.00261

Sterile and fertile flowers are an important evolutionary developmental (evo-devo) phenotype in angiosperm flowers, playing important roles in pollinator attraction and sexual reproductive success. However, the gene regulatory mechanisms underlying fertile and sterile flower differentiation and development remain largely unknown. *Viburnum macrocephalum* f. *keteleeri*, which possesses fertile and sterile flowers in a single inflorescence, is a useful candidate species for investigating the regulatory networks in differentiation and development. We developed a *de novo*-assembled flower reference transcriptome. Using RNA sequencing (RNA-seq), we compared the expression patterns of fertile and sterile flowers isolated from the same inflorescence over its rapid developmental stages. The flower reference transcriptome consisted of 105,683 non-redundant transcripts, of which 5,675 transcripts showed significant differential expression between fertile and sterile flowers. Combined with morphological and cytological changes between fertile and sterile flowers, we identified expression changes of many genes potentially involved in reproductive processes, phytohormone signaling, and cell proliferation and expansion using RNA-seq and qRT-PCR. In particular, many transcription factors (TFs), including MADS-box family members and ABCDE-class genes, were identified, and expression changes in TFs involved in multiple functions were analyzed and highlighted to determine their roles in regulating fertile and sterile flower differentiation and development. Our large-scale transcriptional analysis of fertile and sterile flowers revealed the dynamics of transcriptional networks and potentially key components in regulating differentiation and development of fertile and sterile flowers in *Viburnum macrocephalum* f. *keteleeri*. Our data provide a useful resource for *Viburnum* transcriptional research and offer insights into gene regulation of differentiation of diverse evo-devo processes in flowers.

Keywords: sterile flower, fertile flower, transcriptome, gene expression, differentiation and development, *Viburnum macrocephalum* f. *keteleeri*

INTRODUCTION

Flower development is attracting great attention as a fascinating topic for studying plant development and evolution. Angiosperm flowers and inflorescences display great diversity in morphology, with various shapes, sizes, and other traits (Cooley et al., 2008), underlying the diverse consequences of the evolutionary development ("evo-devo") of flowering plants. According to the capacity for sexual reproduction and gamete formation, flowers can be divided into fertile and sterile flowers. Fertile flowers are capable of producing fertile gametes for further generations, due to their normal sexual organs. In contrast, sterile flowers have abnormal stamens, defective anthers, or no viable pollen, and thus fail to produce seeds (Donoghue et al., 2003; Jin et al., 2010). Many sterile flowers are far larger and more conspicuous than fertile flowers within the same inflorescence (Nielsen et al., 2002; Donoghue et al., 2003; Jin et al., 2010). Such sterile flowers exist in many genera, including *Viburnum* (Adoxaceae) and *Hydrangea* (Hydrangeaceae), and in the Asteraceae family, and are considered to be an evolutionary consequence of long-term ecological selection by pollinator attraction, which plays an important role in enhancing reproductive success (Donoghue et al., 2003; Jin et al., 2010). However, the developmental regulation of sterile flowers, which makes them conspicuously different from fertile flowers in appearance and structure, remains unclear.

RNA-seq approaches have been used extensively to characterize gene expression and determine genetic networks in flower development (Ó'Maoiléidigh et al., 2014; Zhang et al., 2014). In recent years, many of the key floral regulators in *Arabidopsis thaliana* and other species have been identified through large-scale analyses of floral transcriptomes (Ó'Maoiléidigh et al., 2014; Zhang et al., 2014; Vining et al., 2015). For example, the MADS-box family genes encode a family of transcription factors that control diverse developmental processes such as flowering time, meristem identity, and floral organ identity (Becker and Theißen, 2003; Ó'Maoiléidigh et al., 2014). The ABCDE-class genes act in a combinatorial way to specify sepal, petal, stamen, carpel, and ovule formation (Pelaz et al., 2000; Theissen and Melzer, 2007). Many other genes, including genes encoding transcription factors (TFs), have also been shown to be required for the development of anthers, pollen, and the tapetum. For instance, the altered function of *ABORTED MICROSPORES* (*AMS*; Xu et al., 2010), callose synthase 5 (*CALS5*; Dong et al., 2005), SBP-Like 8 (*SPL8*; Xing et al., 2010), or *EXCESS MICROSPOROCYTES1/EXTRA SPOROGENOUS* (*EMS1/EXS*; Canales et al., 2002) can result in reduced fertility or male sterility in flowering plants. Phytohormone signaling molecules, including auxin (Cecchetti et al., 2008), gibberellin (Cheng et al., 2004), jasmonate (Yuan and Zhang, 2015), cytokinin (Bartrina et al., 2011; Han et al., 2014), and brassinosteroid (Ye et al., 2010), are involved in regulating the development and fertility of flowers. For example, gibberellins promote flower growth via cell expansion and/or proliferation (Achard et al., 2009). Overexpression of jasmonate signaling pathway proteins (JAZs) usually results in low fertility or male sterility (Yuan and Zhang, 2015). These investigations have indicated the presence of a complex gene regulatory network underlying floral organ development and fertility; however, our current knowledge and understanding of the gene regulatory networks involved in the differentiation and development of sterile and fertile flowers remain limited.

Viburnum macrocephalum f. *keteleeri*, a Chinese wild shrub, is a useful candidate species for investigating sterile and fertile flowers (Jin et al., 2010). Its inflorescence consists of an outer ring of eight large sterile flowers surrounding a center of small bisexual fertile flowers (**Figure 1M**). Previous morphological and anatomical studies in this species have shown that sterile and fertile flowers are similar during the early developmental stages and diverge in subsequent developmental stages (Jin et al., 2010). The divergence between sterile and fertile flowers is prominent in the blooming stage. Relative to normal fertile flowers, sterile flowers have big, showy petals, ruptured stigmas, defective anthers, and abnormal microsporogenesis, apparently with a role in pollinator attraction (Jin et al., 2010). These findings

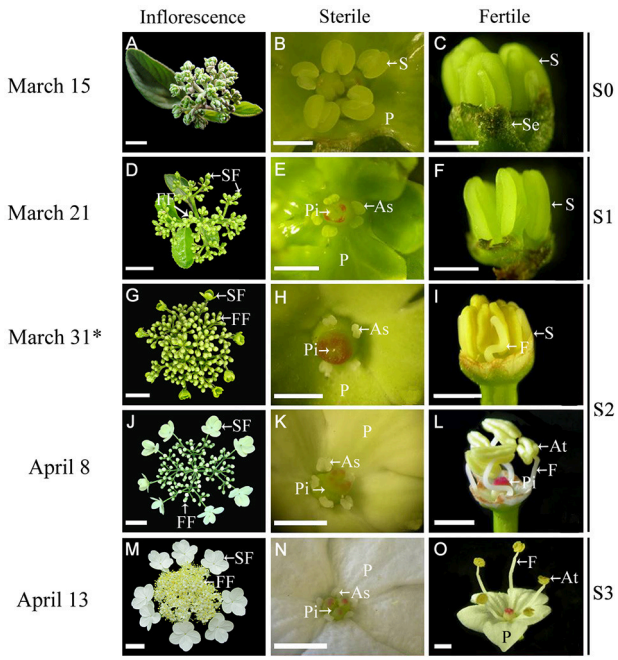

FIGURE 1 | Morphological comparison of fertile and sterile flowers during development stages in *V. macrocephalum* f. *keteleeri*. (A–C) Inflorescence at early developmental stages (March 15, S0). Normal stamens, pistils, and petals were seen in fertile and sterile flowers. **(D–F)** Inflorescence ~1 week before anthesis (March 21, S1). Stamens (or anthers) and pistils (or stigmas) of sterile flowers appeared abnormal, but were normal in fertile flowers. **(G–L)** Inflorescence at the rapid developmental stage (March 31 to April 8, at anthesis, S2). Sterile flowers generally bloomed, with enlarged petals and degraded stamens and pistils, whereas fertile flowers showed elongated filaments, plump anthers, and pistils. **(M–O)** Inflorescence at the peak flowering stage (April 13, S3). Fully degraded stamens and pistils were seen in sterile flowers, whereas dehiscent anthers produced pollen grains in fully developed fertile flowers. SF, sterile flower; FF, fertile flower; S, stamen; P, petal; Pi, pistil; As, abnormal stamen; At, anther; Se, sepal; and F, filament. Asterisks indicate RNA-seq samples for Illumina sequencing. Bars = 2 cm **(A)**, 3 cm **(D,G,J,M)**, 1 mm **(B,C,E,F,H,K,N)**, 2 mm **(I,L,O)**.

showed that the sterile flowers developed and differentiated from early fertile flowers in the same inflorescence, and thus could be model materials to compare the formation mechanism with that of fertile flowers in the same genetic background.

To investigate the gene and molecular regulation mechanism underlying the development of fertile and sterile flowers, we used Illumina RNA-seq technology to generate a comprehensive floral transcriptome from *V. macrocephalum* f. *keteleeri*. Combined with morphological and cytological comparisons between fertile and sterile flowers, we screened and identified candidate differentially expressed genes (DEGs). A global analysis of TFs was performed to identify differentially expressed TFs. We also performed quantitative reverse transcription PCR (qRT-PCR) experiments to determine expression changes in several key regulators involved in multiple functions at different developmental stages. These results provide a first comprehensive overview of the genes and related functions that are required for the differentiation and development of sterile and fertile flowers.

MATERIALS AND METHODS

Plant Materials and RNA Extraction

Fertile and sterile flowers were collected from 15-year-old *V. macrocephalum* f. *keteleeri* plants grown on the campus of Yangzhou University (32°39′ N, 119°43′ E, Yangzhou, China) under natural conditions. To collect samples for RNA, fertile and sterile flowers from inflorescences at various developmental stages [early developmental stage S0 (**Figures 1A–C**), initial flowering stage S1 (**Figures 1D–F**), rapid flowering stage S2 (**Figures 1G–L**), and peak flowering stage S3 (**Figures 1M–O**)] were sampled separately, snap-frozen in liquid nitrogen, and stored at −80°C until used for total RNA isolation. The fertile and sterile flowers from earlier developmental stages (S0, S1) are difficult to distinguish by morphological observation, although their anatomical structural differences can be visualized under a stereomicroscope in S1. Thus, fertile and sterile flowers derived from one inflorescence at S2 (March 31) were selected for RNA-seq. Three biological replicates for each sample were selected randomly from three individuals, and each biological replicate contained 4–6 sterile or fertile flowers. Samples from fertile and sterile flowers at S1, S2, and S3 were used for qRT-PCR experiments. Additionally, 10 inflorescences with fertile and sterile flowers were collected and prepared for morphological and anatomical observations.

All total RNA samples were extracted from fertile and sterile flowers using the Mini BEST Plant RNA Extraction Kit (TaKaRa, Dalian, China) and treated with genomic DNA (gDNA) Eraser (TaKaRa, Dalian, China) to reduce or eliminate any DNA contamination. RNA quality and quantity were determined using a Nanophotometer spectrophotometer (IMPLEN, CA, USA) and the Qubit RNA Assay Kit with a Qubit 2.0 Fluorometer (Life Technologies, CA, USA). RNA integrity was assessed using the RNA Nano 6000 Assay Kit for the Agilent Bioanalyzer 2100 system (Agilent Technologies, CA, USA), and RNA samples with RNA integrity numbers (RINs) > 7.1 were used for RNA-seq.

Morphological and Anatomical Observations

For inflorescences containing fertile and sterile flowers at different developmental stages, we first took photographs against a black background using a digital camera. Similarly, the developmental processes of stamens and pistils within fertile and sterile flowers were captured using a stereomicroscope (Olympus SZX7, Tokyo, Japan). In addition, petal lengths and widths of fertile and sterile flowers were determined using AutoCAD software, based on photographs from 30 samples at the S1, S2, and S3 stages.

From morphological observations, about 20 petal specimens were cut separately from fertile and sterile flowers at S2, using a razor blade, and ∼3 mm^3 of each sample was prefixed in 2.5% (v/v) glutaraldehyde (in 0.1 mol/L phosphate buffer, pH 7.2) at 4°C overnight. After postfixing in 1% (w/v) osmium tetroxide for 6 h at room temperature, the samples were washed three times in 0.2 M phosphate buffer (pH 7.2), dehydrated through an ethanol series, treated twice for 30 min with propylene oxide, and then infiltrated with 1:1 propylene oxide/resin in embedding capsules overnight, before finally embedding in Spurr's resin (Wang et al., 2016). For ultrastructural observations, 70 nm-thick sections were cut with a Leica EM UC6 ultramicrotome (Leica Microsystems GmbH, Wetzlar, Germany), and stained with 1% (w/v) uranyl acetate and 1% (w/v) lead citrate. Petals cells were observed and photographed under a Philips Tecnai 12 transmission electron microscope (JEOL Ltd., Tokyo, Japan).

Illumina Sequencing and *De novo* Assembly

RNA (∼3 μg per sample) was used as the input material for constructing libraries. RNA-seq libraries were prepared using the TruSeq Paired-End (PE) Cluster Kit v3-cBot-HS (Illumina, PE125) according to the manufacturer's protocol. Libraries from fertile and sterile flowers, with three biological replicates, were sequenced in a single Illumina Hiseq 2500 flowcell, generating >139 million paired-end reads per sample. A Perl script was written to remove low-quality sequences (reads with a base quality < 20). For *de novo* reference transcriptome assembly, all high-quality RNA-Seq reads were pooled from the Illumina sequencing of each of the six samples (three biological replicates) and were then used as input for assembly using Trinity software (Grabherr et al., 2011). All raw sequence data have been deposited in the NCBI Sequence Read Archive (SRA, accession number SRP076665).

Functional Annotation and Classification

All Illumina-assembled unigenes (the longest transcript for each gene) were aligned against the NCBI non-redundant protein (Nr) (http://www.ncbi.nlm.nih.gov/), NCBI non-redundant nucleotide sequence (Nt), Pfam (http://pfam.xfam.org/), KOG (http://www.ncbi.nlm.nih.gov/COG/), Swiss-Prot (http://www.uniprot.org/), and KEGG (http://www.genome.jp/kegg) databases using BLASTX alignments with an *E*-value cut-off of 10^{-5}. With Nr annotation, Gene ontology (GO) annotations of unigenes were obtained using the Blast2GO software (http://

www.geneontology.org; Götz et al., 2008). GO has three ontologies describing molecular function, cellular components, and biological processes (Ashburner et al., 2000). We then used the WEGO software to perform GO functional classifications of all unigenes to understand the distribution of gene functions at the macro level (Ye et al., 2006). Based on KEGG mapping, unigenes were assigned to multiple pathways, using BLASTx, thereby retrieving KEGG Orthology (KO) information.

Differential Gene Expression Analysis

Before performing differential expression analysis of unigenes, we estimated gene expression levels for each sample using the RSEM software package (Li and Dewey, 2011). The FPKM (expected number of fragments per kilobase of transcript sequence per million base pairs sequenced) value was used to quantify gene expression levels (Trapnell et al., 2010), which takes the influence of both the sequencing depth and gene length on read count into account. These expressed data sets are available at the NCBI GEO, under accession number GSE83429. Next, we conducted a differential expression analysis of two conditions using the DESeq R package (ver. 1.10.1; Anders and Huber, 2010). DESeq provides statistical routines for determining differential expression in digital gene expression data using a model based on a negative binomial distribution. The *P*-value was adjusted using the Benjamini and Hochberg approach (Benjamini and Hochberg, 1995). Genes with an adjusted *P*-value < 0.05, as found by DESeq, were deemed to be differentially expressed. GO functional enrichment analysis of the differentially expressed genes (DEGs) was carried out with the GOseq R package, based on a Wallenius non-central hyper-geometric distribution (Young et al., 2010), which can find significantly enriched GO terms in DEGs vs. the genome background. To understand high-level functions and utilities of the biological system, all DEGs were assigned to the diverse pathways of the KEGG database. Then, we used the KOBAS software to test the statistical enrichment of differentially expressed genes within the KEGG pathways (Mao et al., 2005).

qRT-PCR Validation and Expression Analysis

We conducted qRT-PCR experiments to confirm and analyze basic expression levels of a subset of candidate functional genes. Treated RNA solutions (10 μL) (without DNA contamination) from fertile and sterile flowers at S1, S2, and S3 were subjected to reverse transcriptase reactions with the PrimeScript RT Reagent Kit (TaKaRa, Dalian, China) according to the manufacturer's protocol. Gene-specific primers were designed using Primer 5.0 software (Table S1). The *SAND* (NC_003071.7) gene was used as a housekeeping gene to normalize the expression of the investigated genes. qRT-PCR was performed using a CFX Connect Real-Time thermal cycler (Bio-Rad, USA) using a SYBR Premix Ex Taq Kit (TaKaRa) following the manufacturer's protocol. PCR reactions were performed as follows: 95°C for 30 s, followed by 40 cycles of 95°C for 5 s, 60°C for 30 s, and 72°C for 10 s. Each reaction had three biological replicates, and comparative threshold (Ct) values were determined with the Bio-Rad CFX Manager software (ver. 3.1.1517.0823). Relative expression levels of target genes were calculated using the $2^{-\Delta\Delta Ct}$ method (Livak and Schmittgen, 2001). Standard errors of the mean among the replicates were calculated. Non-overlapping letters (a–c) indicate significant differences between fertile or sterile flowers at different stages, based on ANOVA analysis and Multiple Range Tests with a confidence level of 95%. Similar significance analyses were conducted comparing fertile and sterile flowers in each stage.

Phylogenetic Analyses

The MADS-box gene sequences used were from the *V. macrocephalum* f. *keteleeri* transcriptome and from *A. thaliana*. The *A. thaliana* MADS-box gene sequences were downloaded from the Arabidopsis Information Resource (TAIR10) (http://www.arabidopsis.org). All multiple sequence alignments and phylogenetic trees for MADS-box genes were constructed using MEGA6.06 software and the neighbor-joining (NJ) algorithm, according to the manual (Tamura et al., 2013). Bootstrap analyses with 1,000 replicates were used to assess the robustness of the tree.

RESULTS

De novo Assembly of the *V. macrocephalum* f. *keteleeri* Flower Transcriptome

We observed inflorescence development at four stages, from March 15 to April 13 (**Figure 1**). At the early stage (March 15, S0) sterile flowers developed five petals and one pistil surrounded by five stamens, similar to fertile flowers (**Figures 1A–C**). One week later (March 21, before anthesis, S1), the fertile flowers had normal stamens (or anthers) and pistils (**Figures 1D,F**), while the sterile flowers exhibited degenerated stamens (or anthers) and ruptured stigmas (**Figures 1D,E**). During the rapid developmental process (March 31 to April 8, at anthesis, S2), sterile flowers bloomed gradually, petals enlarged (**Figures 1G,J**), and stamens and pistils continued to deform or collapse (**Figures 1H,K**), whereas the fertile flowers developed elongated filaments, plump anthers, and pistils (**Figures 1I,L**). At the peak flowering stage (April 13, S3), fertile flowers produced pollen grains, and pistils were developed fully (**Figures 1M,O**), whereas in the sterile flowers, the stamens and pistils had degenerated completely (**Figure 1N**).

To investigate differences in the transcriptomes of sterile and fertile flowers, we sequenced RNA samples extracted from sterile and fertile flowers at S2 (March 31), using the Illumina Hiseq2500 platform. Three biological replicates were prepared for sterile and fertile flowers, resulting in 139.05 and 139.86 million raw reads in the two samples, respectively (Table S2). After removal of filtering adapters, low-quality sequences, and ambiguous reads, we obtained approximately 133.40 million and 134.32 million paired-end clean reads in sterile and fertile flowers, respectively (Table S2). In total, 267.72 million pooled clean reads were used for the assembly of sequences with the *de novo* Trinity software. This assembly resulted in 132,788 transcripts with a mean length of 740 bp (N50 = 1323 bp; **Figure 2A**), and included 105,683

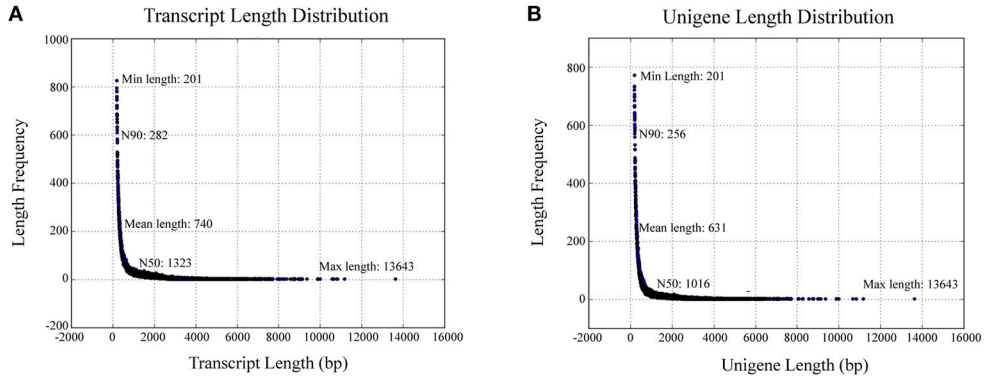

C

Length (bp)	Total number (trancripts/unigenes)	Percentage (trancripts/unigenes)
200-500	79,595 / 70,565	59.94% / 66.77%
500-1000	24,040 / 177,32	18.10% / 16.77%
1000-2000	18,440 / 11,366	13.89% / 10.76%
≥ 2000	10,713 / 6,020	8.07% / 5.70%
Total	132,788 / 105,683	100% / 100%

FIGURE 2 | Length distribution of assembled transcripts and unigenes. N50/N90 represents 50 or 90% length of all unigenes sequences. (A) Distribution of assembled transcripts. **(B)** Distribution of assembled unigenes. **(C)** Percentage of assembled transcripts and unigenes within different length intervals.

unigene sequences with a mean length of 631 bp (N50 = 1016 bp; **Figure 2B**). Sequences ranging from 200 to 2,000 bp in length accounted for nearly 91.9% of the total transcripts and 94.3% of the total unigenes. In total, 10,713 (8.1%) transcripts and 6020 (5.7%) unigenes were >2,000 bp in length (**Figure 2C**). For the validation and annotation of the assembled unigenes, all unigene sequences (105,683 unigenes) were searched against public protein databases using the BlastX program ($E < 1e^{-5}$). The results indicated that 20,724 (19.6%) unigenes had significant matches in the Nt database, while 38,224 (36.16%), 26,744 (25.3%), 26,629 (25.19%), 13,637 (12.9%), 30,381 (28.74%), and 12201 (11.54%) unigenes showed significant similarities to known proteins in the Nr, Swiss-Prot, Pfam, KOG, GO, and KO databases, respectively (Figure S1A). Of the 105,683 unigenes, 43,870 (41.51%) were successfully annotated from at least one database. Additionally, the species distribution in the Nr database showed that 18,615 (48.70%) unigenes had highest similarities to sequences from *Vitis vinifera* (48.7%), *Populus trichocarpa* (10.60%), or *Ricinus communis* (9.20%; Figure S1B).

To further characterize the functional classifications of the annotated unigenes, we searched the annotated sequences for genes involved in GO classifications. Using Nr annotations, 30,381 (28.74%) unigenes could be categorized into 58 functional groups and summarized into the three main GO categories (biological processes, cellular components, and molecular functions; Figure S1C). In each of the three main GO classifications, "binding," "cell," and "cellular process" were the most highly represented groups. We also noticed some identified genes involved in other important biological processes, such as reproductive processes and growth. KEGG analysis revealed the biological pathways in which the unigenes were likely involved. Assembled unigenes were compared with the KEGG database using BLASTx and the corresponding pathways were identified. In total, 12,201 unigenes showed significant matches and were assigned to 274 KEGG pathways (Figure S1D). A large proportion of these unigenes belonged to translation (1,530 unigenes), followed by signal transduction (1,254 unigenes), and carbohydrate metabolism (1,169 unigenes). We also noticed that many genes were involved in cell growth and death (428 unigenes) and developmental (75 unigenes) pathways.

Global Analyses of Gene Expression Profiles and Distinct Enrichment Analysis of DEGs between Sterile and Fertile Flowers

The numbers of clean reads that mapped preferentially to the assembled unigenes were 110,816,400 in fertile flowers and 113,073,500 in sterile flowers (Table S3). Based on the mapping results, we further estimated the expression levels of these

unigenes in terms of FPKM values. We filtered the unigenes with low expression by applying a cut-off of RPKM < 0.3, and the remaining 72,908 and 69,372 unigenes for sterile and fertile flowers, respectively, were deemed to be expressed genes (data not shown). DEGs were determined using DEseq with an adjusted $P \leq 0.05$. Based on the DEG analysis, 1,908 unigenes were upregulated in sterile flowers, whereas 3,767 unigenes were downregulated in sterile flowers (Table S4; **Figures 3A,B**). Among those DEGs, 742 DEGs were only expressed in fertile flowers, and only 34 DEGs were specifically expressed in sterile flowers (Table S4; **Figure 3C**).

We further performed GO and KEGG enrichment analyses to investigate the biological functions of the DEGs we identified. We found that, in sterile flowers, 1,340 (36.68%) upregulated DEGs were successfully assigned to 45 significantly enriched GO terms, and 2,313 (63.32%) downregulated unigenes were significantly enriched in 42 GO terms (corrected $P \leq 0.05$; Table S5). Among these significantly enriched GO terms, we focused on some important factors that may be involved in differentiation and development of fertile and sterile flowers. We found that many upregulated DEGs were enriched significantly in photosynthesis (GO: 0015979) and light harvesting (GO: 0009765), and many downregulated genes were enriched significantly in the starch metabolic process (GO: 0005982) and sucrose metabolic process (GO: 0005985) terms (**Table 1**). Moreover, we found that genes related to pollen development (GO: 0009555) and gametophyte development (GO: 0048229), such as gene homologs of dynamin-related protein 1C (c101321_g1, *DRP1C*), copper transporter 1 (c49933_g1, *COPT1*), spermidine hydroxycinnamoyl transferase (c57651_g1, *SHT*), and transcription factor GAMYB (c57595_g3, *GAM1*) (Table S5), were downregulated significantly in sterile flowers (**Table 1**). The KEGG enrichment results were similar to the GO-enriched terms and the gene expression profiles. KEGG pathway annotations showed that upregulated and downregulated unigenes were enriched in 131 and 149 KEGG pathways, respectively. We listed the top 20 enriched pathways with the highest representation in a scatter plot (**Figure 4A**). Of these, photosynthesis was the most significantly enriched pathway among the upregulated DEGs in sterile flowers (corrected $P \leq 0.05$), and 31 DEGs encoding proteins associated with photosynthesis were identified: for example, ferredoxin-NADP reductase (c48707_g1, *PETH*), photosystem II oxygen-evolving enhancer protein 2 (c428_g1, *PSBP*), and photosystem I subunit XI (c40849_g1, *PSAL*; **Figure 4B**). The most significantly enriched pathway among downregulated DEGs in sterile flowers was starch and sucrose metabolism. In total, 49 DEGs encoding proteins related to starch and sucrose metabolism, including pectinesterase (c57992_g8, *PME*), beta-glucosidase (c679_g1, *BGLU*), sucrose-phosphate synthase (c45976_g1, *SPS*), and UDP-glucose 6-dehydrogenase (c34950_g1, *UGD*) were identified (**Figure 4B**). Through ultrastructural observations, we found that chloroplasts were clearly visible in petal cells of sterile flowers, but were only rarely present in fertile flowers. Furthermore, fewer starch grains were contained in the petal cells of sterile flowers than in fertile flowers (**Figure 4C**). These significant differences in chloroplast and starch grain distributions in petal cells from sterile and

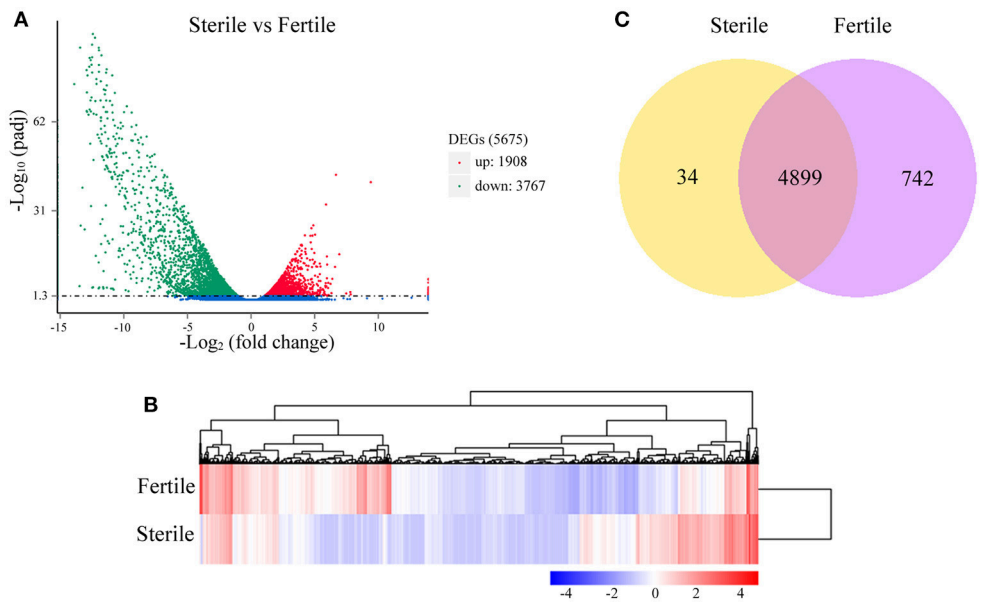

FIGURE 3 | Distribution of DEGs between fertile and sterile flowers. (A) Red spots represent upregulated DEGs and green spots indicate downregulated DEGs. Those shown in blue are unigenes that did not show obvious changes. **(B)** Clustering analysis of all DEGs between fertile and sterile flowers. Each row corresponds to a gene, while the samples are represented by the columns. The expression levels for each gene [($\log^{10}$ FPKM (number of fragments per kilobase of transcript sequence per million base pairs sequenced) + 1] in a given sample is represented on a blue (low expression) to red (high expression) scale. **(C)** Specifically- and commonly-expressed genes in fertile and sterile flowers.

TABLE 1 | GO terms significantly enriched among up- and downregulated DEGs.

GO term[a]	Description	Number in input list	Number in BG/Ref[b]	Corrected *P*
UPREGULATION				
GO:0006464	Cellular protein modification process	196	2,602	3.41E-07
GO:0006118	Electron transport	52	715	0.020327
GO:0015979	Photosynthesis	47	440	0.0001254
GO:0009416	Response to light stimulus	24	145	4.43E-05
GO:0019684	Photosynthesis, light reaction	14	93	0.0086153
GO:0007267	Cell–cell signaling	13	64	0.0016466
GO:0009765	Photosynthesis, light harvesting	8	22	0.00021899
GO:0009638	Phototropism	3	3	0.025256
DOWNREGULATION				
GO:0044042	Glucan metabolic process	111	502	2.17E-19
GO:0005984	Disaccharide metabolic process	110	478	2.60E-20
GO:0005985	Sucrose metabolic process	100	442	5.01E-18
GO:0005982	Starch metabolic process	98	441	3.40E-17
GO:0046351	Disaccharide biosynthetic process	14	53	0.0042711
GO:0005992	Trehalose biosynthetic process	14	49	0.0019354
GO:0009555	Pollen development	14	40	0.00066549
GO:0048229	Gametophyte development	14	58	0.030959

[a] *These significantly enriched GO terms were selected from Table S5 for their important functions in flower development.* [b] *BG/Ref, Background/Reference.*

fertile flowers confirmed a close correlation between petal organs and the KEGG enrichment analysis and GO-enriched results.

Identification of Candidate DEGs Involved in Reproductive Processes and Expression Dynamics Analysis

Sterile flowers exhibited degenerated stamens (or anthers) and pistils, which were distinct from fertile flowers with normal stamens and pistils (**Figure 1**). Thus, we concentrated on genes involved in reproductive processes, including anther and pollen development, tapetum development, callose synthase, female gametophyte development, meiosis, and programmed cell death (PCD), and found that many candidate genes were differentially expressed between sterile and fertile flowers (Table S6; **Figure 5A**). For example, the homologs of genes involved in another development, such as *LAT52*, which encodes the anther-specific LAT52 protein, showed significantly lower expression in sterile flowers. Most of the homologous regulators related to pollen development, including the bidirectional sugar transporter NEC1 (*NEC1*), myb-like DNA-binding domain transcription factor GAMYB (*GAM1*), pollen-specific protein SF3 (*SF3*), and 4-coumarate-CoA ligase-like 1 (*ACOS5*) were downregulated in sterile flowers. Additionally, gene homologs related to callose synthase, tapetum development, and female gametophyte development, such as callose synthase 2 (*CALS2*), transcription factor ABORTED MICROSPORES (*AMS*), and protein RADIALIS-like 1 (*RL1*), and homologs of meiosis-related PAIR1-like protein (*PAIR1*-like), also showed lower expression in sterile flowers than in fertile flowers. In contrast, the expression levels of all these genes were upregulated significantly in fertile flowers, indicating that these genes are important for the normal development of reproductive organs.

Programmed cell death (PCD) occurs commonly in flowering and reproduction processes, and is required for tapetum and pollen development (Thomas and Franklin-Tong, 2004; Zhang et al., 2014). Thus, we next analyzed the homologs of PCD negative regulators, such as aspartic proteinase PCS1 (*PCS1*); calcium-transporting ATPase 4, plasma membrane-type (*ACA4*); Bax inhibitor 1 (*BI-1*); and tapetal PCD-associated KDEL-tailed cysteine endopeptidase CEP1 (*CEP1*) and found that their expression levels were all low in sterile flowers and higher in fertile flowers. Additionally, BAG family molecular chaperone regulator 1 (*BAG1*) and *BAG2*, which may act as positive regulatory factors in PCD, were upregulated in sterile flowers and downregulated in fertile flowers. These results indicate that these PCD regulators may be associated with the degenerescence of reproductive organs contributing to differentiation and development of sterile and fertile flowers.

To validate the differential expression results, eight DEGs involved in reproductive processes, *LAT52*, *SF3*, *GAM1*, *AMS*, *CALS5*, *RL1*, *PAIR1*-like, and *BAG2*, were selected for qRT-PCR analysis (**Figure 5B**). The results showed that the relative expression levels of seven key regulators were lower in sterile flowers than in fertile flowers at S2, confirming, in all cases, the differential expression observed with RNA-Seq. Moreover, we compared the changes in these expression levels during the various development stages of sterile and fertile flowers and found that *LAT52*, *SF3*, *GAM1*, *AMS*, *CALS5*, *RL1*, and *PAIR1*-like genes showed higher levels of expression from S1 to S3 in fertile than sterile flowers. In contrast, *BAG1* showed a lower level of expression from S1 to S3 in fertile flowers. We further found that the levels of the *LAT52*, *SF3*, and *CALS5* remained

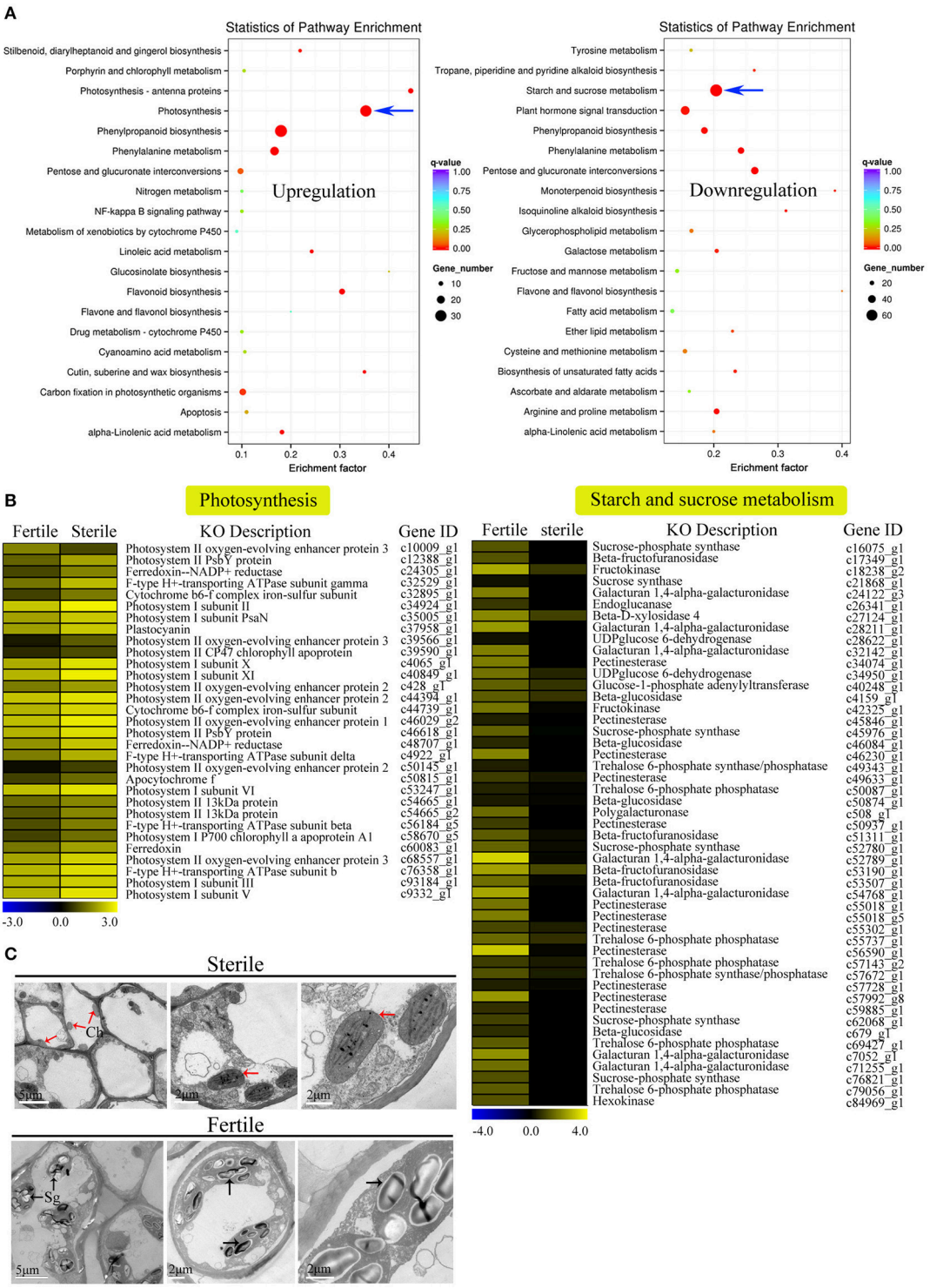

FIGURE 4 | KEGG enrichment analysis of DEGs (upregulated and downregulated) revealed significantly enriched photosynthesis pathway, starch and sucrose metabolism pathway, and related genes. (A) Statistics for the top 20 enriched pathways among upregulated and downregulated genes. The degree of KEGG enrichment was determined by the enrichment factor, *q*-value, and gene number. The sizes and colors of spots represent the number of DEGs and the *q*-value. Blue arrow points to the most significantly enriched pathways. **(B)** Expression profile of DEGs involved in photosynthesis (31 DEGs) and starch and sucrose metabolism pathways (49 DEGs) between fertile and sterile flowers. Heatmap shows expression profiles of DEGs. The rows and columns represent genes and samples (fertile and sterile flowers), respectively. Expression differences are shown in different colors. Yellow indicates a high expression level and blue indicates a low expression level. **(C)** Ultrastructural observations of petals of fertile and sterile flowers. Ch, chloroplast; Sg, starch grain. Red and black arrows indicate chloroplasts (sterile flowers) and starch grains (fertile flowers), respectively.

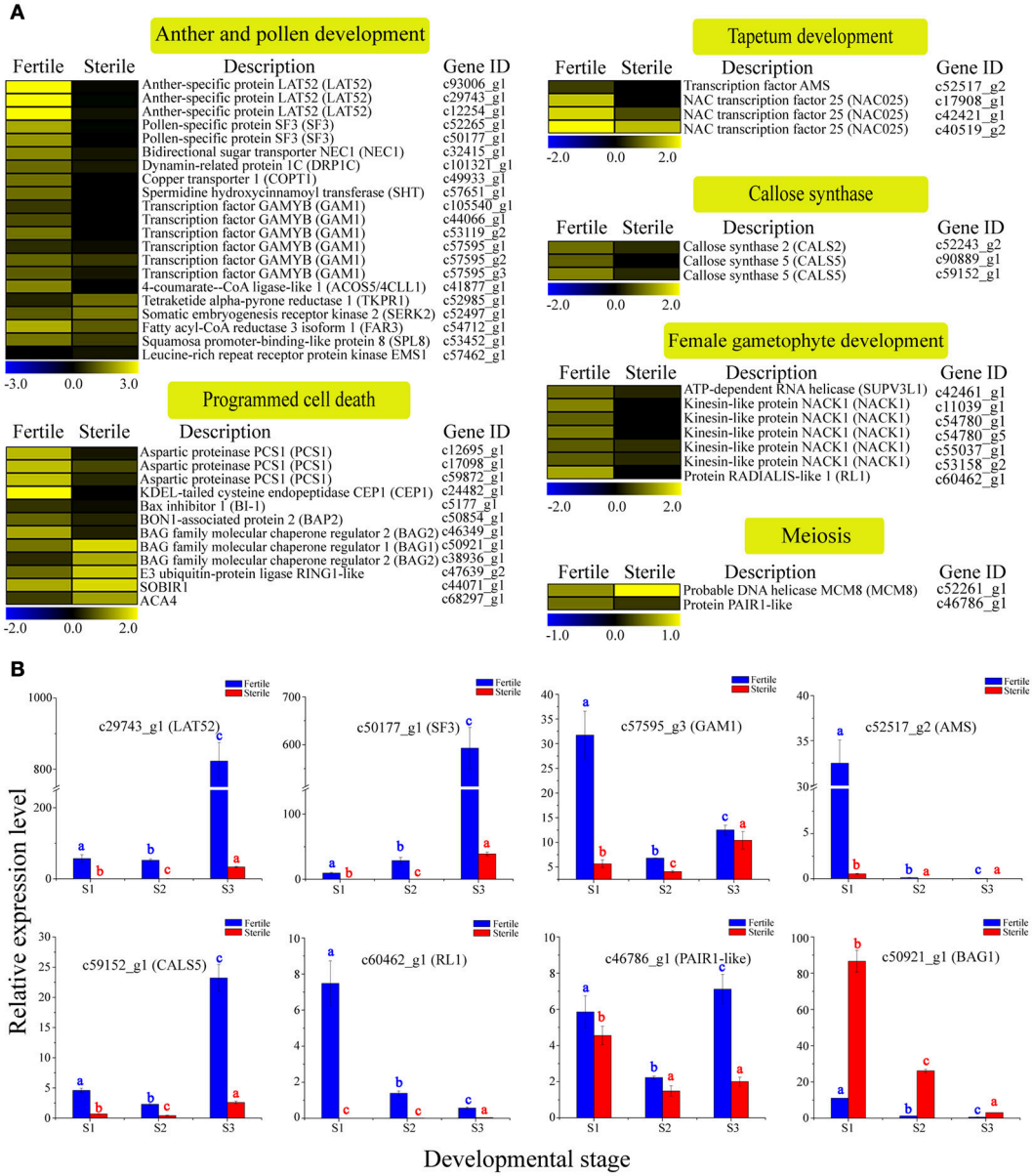

FIGURE 5 | Expression profile of 49 DEGs involved in reproductive processes between fertile and sterile flowers of *V. macrocephalum* f. *keteleeri* and qRT-PCR analysis. (A) Heatmap shows expression of genes associated with anther and pollen development, tapetum development, callose synthase, female gametophyte development, meiosis, and programmed cell death (PCD) in RNA-seq samples (fertile and sterile flowers at March 31). The bar represents the scale of the expression levels for each gene in fertile and sterile flowers, as indicated by blue (low expression) and yellow rectangles (high expression). **(B)** qRT-PCR analysis of the expression profiles of eight transcripts during fertile (blue) and sterile flower (red) development. The points (S1–S3) from left to right on the *x*-axis represent different developmental stages. The *y*-axes show relative expression levels analyzed by qRT-PCR. Columns and error bars indicate means and standard deviations of relative expression levels ($n = 3$), respectively. Non-overlapping letters (a–c) indicate significant differences ($P < 0.05$) between fertile (blue letters) or sterile flowers (red letters) from different stages. Significant differences ($P < 0.05$) between fertile and sterile flowers in each stage were also evaluated.

low in S1 and S2 and then increased significantly from S2 to S3 in fertile flowers, whereas *AMS* showed highest expression in S1 and was almost undetectable in S2 and S3, indicating that *LAT52*, *SF3*, and *CALS5* are involved in maintaining pollen and tapetum development, and *AMS* made a greater contribution to regulating early tapetum development of fertile flowers than of sterile flowers.

Identification of Candidate DEGs Associated with Cell Proliferation and Expansion and Expression Dynamics Analyses

Through morphological analyses of petal development at the S1, S2, and S3 stages of fertile and sterile flowers, we found that

the lengths and widths of petals in sterile flowers (2.31 ± 0.11 in length; 1.91 ± 0.12 in width at S3) were markedly larger than in fertile flowers (0.53 ± 0.04 in length; 0.37 ± 0.02 in width at S3; **Figure 6A**). Given the rapid expansion in sterile flower petals, compared with fertile flowers, we investigated genes associated with cell proliferation and expansion. In total, 41 candidate DEGs were identified and most of them were upregulated in sterile flowers, such as genes encoding expansin-like A2 (*EXPA2*), *EXPA13*, protein COBRA (*COB*), receptor protein kinase TMK1 (*TMK1*), receptor-like protein kinase FERONIA (*FER*), THESEUS 1 (*THE1*), kinesin-like protein NACK1 (*NACK1*), and MIXTA-like 8 protein (Table S7; **Figure 6B**). Additionally, a negative regulator of cell proliferation and expansion, BIG PETAL (*BPE*, Varaud et al., 2011), was identified and showed lower expression levels in sterile flowers. In particular, we detected many genes of the TCP family, which plays significant roles in the morphological characteristics of the floral organ (Yang et al., 2015), and found their expression levels were also higher in sterile flowers than in fertile flowers. These included *TCP2*, *TCP5*, *TCP7*, *TCP8*, *TCP13*, *TCP14*,

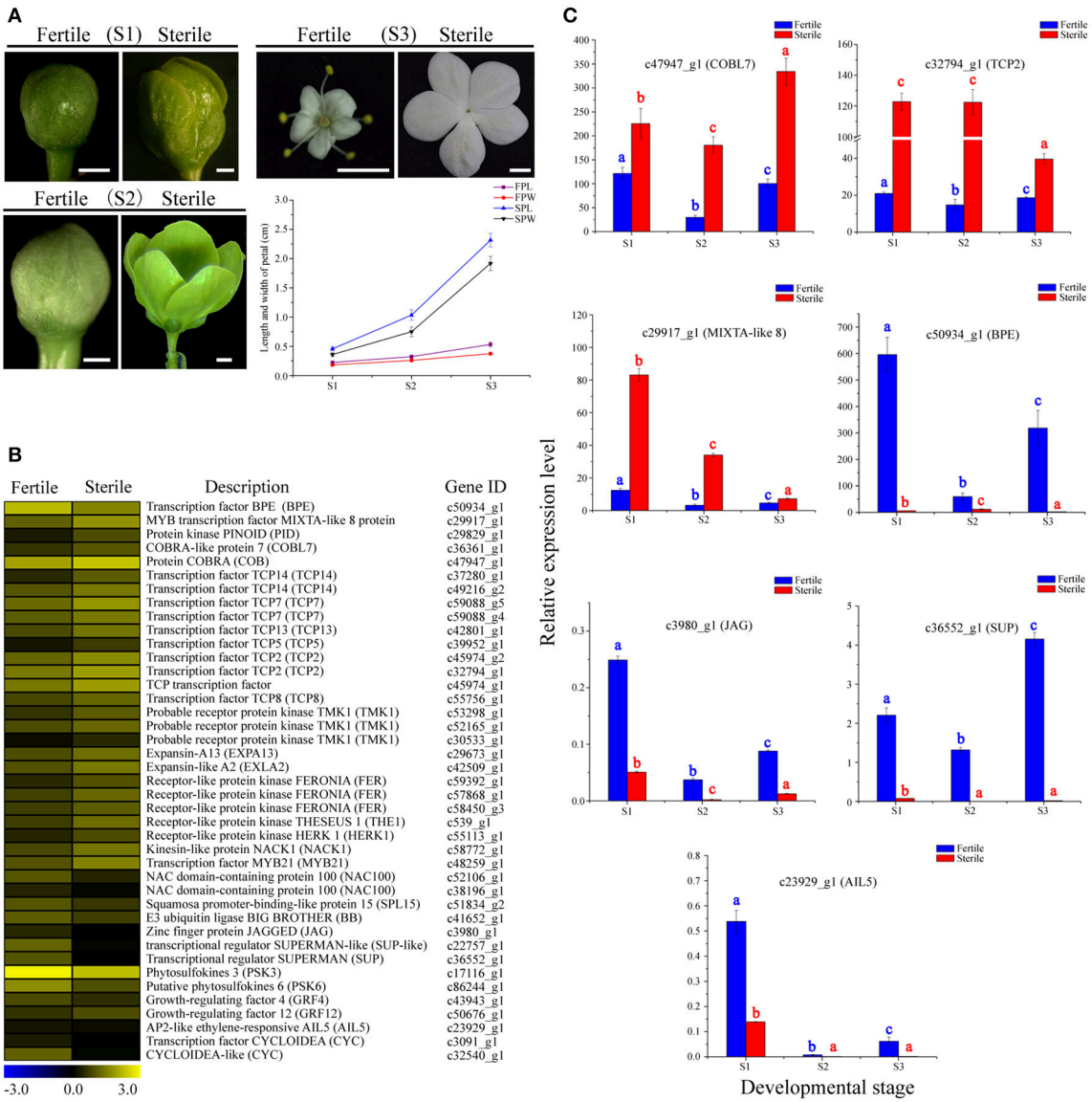

FIGURE 6 | Expression profiles of 41 DEGs involved in cell proliferation and expansion between fertile and sterile flowers of *V. macrocephalum* f. *keteleeri* and qRT-PCR analysis. (A) Morphological analysis of petal development of fertile and sterile flowers. The lengths and widths of petals were measured from stereoscope images of 30 petals at each developmental stage using AutoCAD software. The *x*-axis shows different developmental stages (S1–S3), while the *y*-axes show corresponding measured data from AutoCAD. FPL, length of fertile petal; FPW, width of fertile petal; SPL, length of sterile petal; and SPW, width of sterile petal. Bars = 0.1 cm (S1, S2), 1 cm (S3). **(B)** Heatmap shows expression of genes in RNA-seq samples. The representation of bars is the same as in **Figure 5A**. **(C)** qRT-PCR analysis of the expression profiles of seven DEGs during fertile (blue) and sterile flower (red) development. The representation of the *x*-axis, *y*-axis, significance tests and error bars are as described in **Figure 5B**.

and *TCP15*. These results suggested that these TCP family members may contribute to controlling floral morphology in *V. macrocephalum* f. *keteleeri*. However, we also detected other candidate genes associated with proliferation and expansion, including the transcriptional regulators SUPERMAN (*SUP*), AINTEGUMENTA-like 5 (*AIL5*), zinc finger protein JAGGED (*JAG*), and squamosa promoter-binding-like protein 15 (*SPL15*), and found that they were upregulated in fertile flowers. We propose that these upregulated genes play important roles in controlling reproductive organ development.

We examined the expression level changes of seven key cell proliferation- and expansion-related DEGs, *BPE*, *COBL7*, *TCP2*, *MIXTA*-like 8, *JAG*, *AIL5*, and *SUP*, by qRT-PCR during the development stages of sterile and fertile flowers (**Figure 6C**). Our results showed that the expression levels of *COBL7*, *TCP2*, and *MIXTA*-like 8 genes were higher during the development stages of sterile flowers vs. fertile flowers. In contrast, significantly lower expression levels of *BPE*, *AIL5*, *JAG*, and *SUP* were observed in sterile flowers. We found that the expression levels for the regulatory factor *TCP2* and *MIXTA*-like 8 were highest in sterile flowers at S1 and S2, and then decreased markedly in S3, consistent with the rapid development of sterile flowers from S1 to S2. In contrast, the level of *BPE*, acting as a negative regulatory factor, showed highest expression levels at S1 in fertile flowers, and then declined significantly in S2 and S3, indicating its important role in regulating floral organ development. Our qRT-PCR results were also generally consistent with the RNA-Seq data, despite some differences in expression levels.

Identification of Candidate DEGs Related to Phytohormone Signaling and Expression Dynamics Analyses

Phytohormone signaling plays a vital role in regulating floral organ growth and reproductive processes (Song et al., 2013). We identified many homologous genes involved in phytohormone signaling, including genes related to auxin, cytokinin, brassinosteroid, gibberellin, and jasmonate that showed differential expression between sterile and fertile flowers (Table S8; **Figures 7A,B**). For example, in the auxin signaling pathway, most of the genes encoding auxin-response factors (ARFs), the indole-3-acetic acid-amido synthetase GH3 family, and SAUR family proteins were upregulated in fertile flowers. In contrast, the auxin-responsive proteins (AUX/IAA), involved in auxin signaling function as repressors of early auxin response genes, were downregulated in fertile flowers. In the gibberellin and jasmonate signaling pathways, genes encoding the protein TIFY (*JAZ1/6/10*) and the gibberellin receptor GID1 (*GID1*) were upregulated in fertile flowers, whereas the DELLA proteins (*GAI*, *RGL1*), which act as repressors of the gibberellin signaling pathway (Cheng et al., 2004), were downregulated. Additionally, the type-A response regulator genes (*ARR9*, *ARR17*), as negative regulators in the cytokinin signaling pathway, had higher expression levels in fertile flowers. These results indicate that auxin, gibberellin, jasmonate, and cytokinin signaling-related genes are involved in maintaining fertility/infertility or promoting the developmental divergence between fertile and sterile flowers.

We further selected two key DEGs (*IAA7* and *GAI1*) involved in auxin and jasmonate signaling to assess their expression level changes during different development stages (**Figure 7C**). qRT-PCR analysis showed that the expression of *IAA7* decreased slightly from S1 to S2 in sterile flowers (not significant), and was highest in S3. In contrast with *IAA7*, in sterile flowers, *GAI* expression was highest in S1 and declined from S1 to S3, indicating the genes' involvement in auxin and gibberellin signaling in sterile flower development.

Analysis of Putative TFs and Other Regulators Involved in Flower Development and Expression Dynamics Analyses

TFs are key regulatory proteins that play important roles in regulating gene expression in various plant biological processes, such as flower development, secondary metabolism, and responses to abiotic and biotic stresses (Riechmann and Ratcliffe, 2000; Singh et al., 2002; Yang et al., 2012). We found that 2,072 genes were putatively identified as TFs and associated with 79 TF families in the integrative plant transcription factor database (PlnTFDB; Pérez-Rodríguez et al., 2009). Of them, the most abundant TF family was the MYB superfamily (159, 7.68%), followed by AP2-EREBP (127, 6.13%), C2H2 (102, 4.93%), and bHLH (99, 4.78%; **Figure 8A**). In total, 50 TFs were associated with the MADS-box family, which are regarded as flower development regulators (Table S9). For example, gene homologs encoding DEFICIENS (*DEF*) and GLOBOSA (*GLO*) proteins were identified as B class genes, and *AGAMOUS* (*AG*) homologs have been identified as C class genes in *V. macrocephalum* f. *keteleeri*. To obtain a more comprehensive class of ABCDE gene homologs in this species, we selected 21 MADS-box genes and the 60 MADS-box genes of *A. thaliana* to perform a phylogenetic analysis (**Figure 8B**). This analysis showed that two orthologs (c48898_g1, c10961_g1) of *SEPALLATA 1* (*SEP1*) and *SEP2* formed a well-supported clade as class E gene homologs. The c35415_g2 and c51031_g1 transcripts were identified as *AGAMOUS* (*AG*) family genes, defined as class C gene homologs. Other MADS-box TFs of *V. macrocephalum* f. *keteleeri* also appeared to cluster with strong support with particular genes from *A. thaliana*, such as *SOC1*, *MADS6*, and *AGL18*-like genes. On the basis of this orthology analysis, we constructed putative orthologs of ABCDE-class genes, to characterize floral organ development in *V. macrocephalum* f. *keteleeri* (**Table 2**).

We next performed a differential expression analysis of the identified TFs, and found that 377 TFs could be classified into 54 TF families displaying differential expression between fertile and sterile flowers. The largest numbers of differentially expressed TFs were in the MYB family (36), followed by bHLH (28), C2H2 (28), and AP2-EREBP (25). We performed a screen on differentially expressed TFs ($|\log2(\text{ratio})| \geq 4$) to identify those that were significantly upregulated or downregulated in sterile flowers (**Figure 9A**). We found that among the differentially expressed TFs, the majority were significantly downregulated

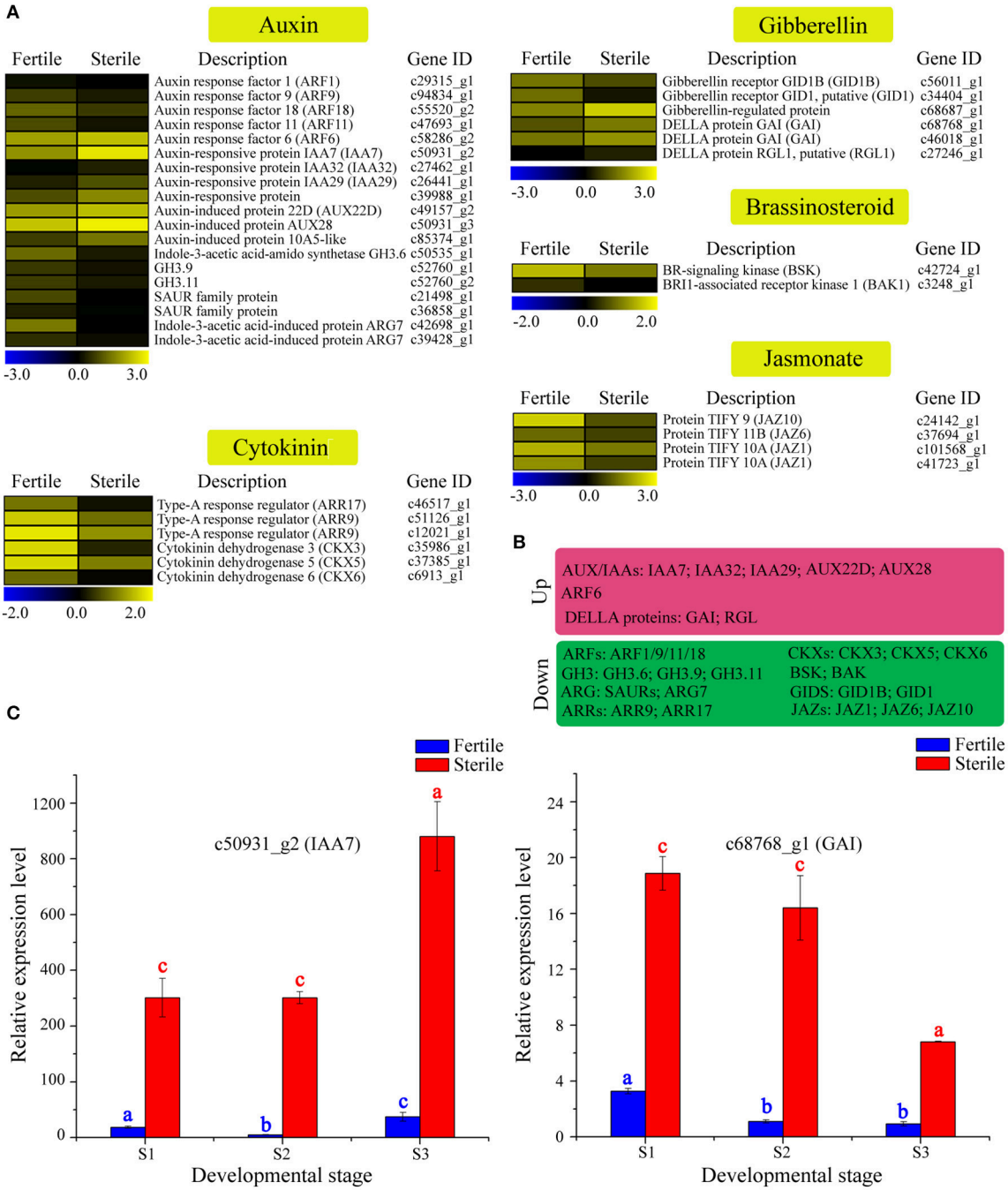

FIGURE 7 | Expression profile of 37 DEGs involved in phytohormone signaling between fertile and sterile flowers of *V. macrocephalum* f. *keteleeri* and qRT-PCR analysis. (A) Heatmap shows expression of genes associated with auxin, cytokinin, brassinosteroid, gibberellin, and jasmonate signaling in RNA-seq samples. The representation of the bars is as described in **Figure 5A**. **(B)** Overview of DEGs, summarized by upregulation and downregulation in sterile flowers. **(C)** qRT-PCR analysis of two transcripts during fertile (blue) and sterile flower (red) development. The representation of the *x*-axis, *y*-axis, significance tests and error bars are as described in **Figure 5B**.

in sterile flowers, while the majority, including MYB and MADS family members, were upregulated in fertile flowers (**Figure 9A**). All the differentially expressed MADS family TFs showed significantly lower expression in sterile flowers and high expression in fertile flowers (**Figure 9B**). We summarized all differentially expressed MADS-box genes that may be involved in controlling flowering time, floral organ identify, and other functions in **Figure 9B**. We also identified many other

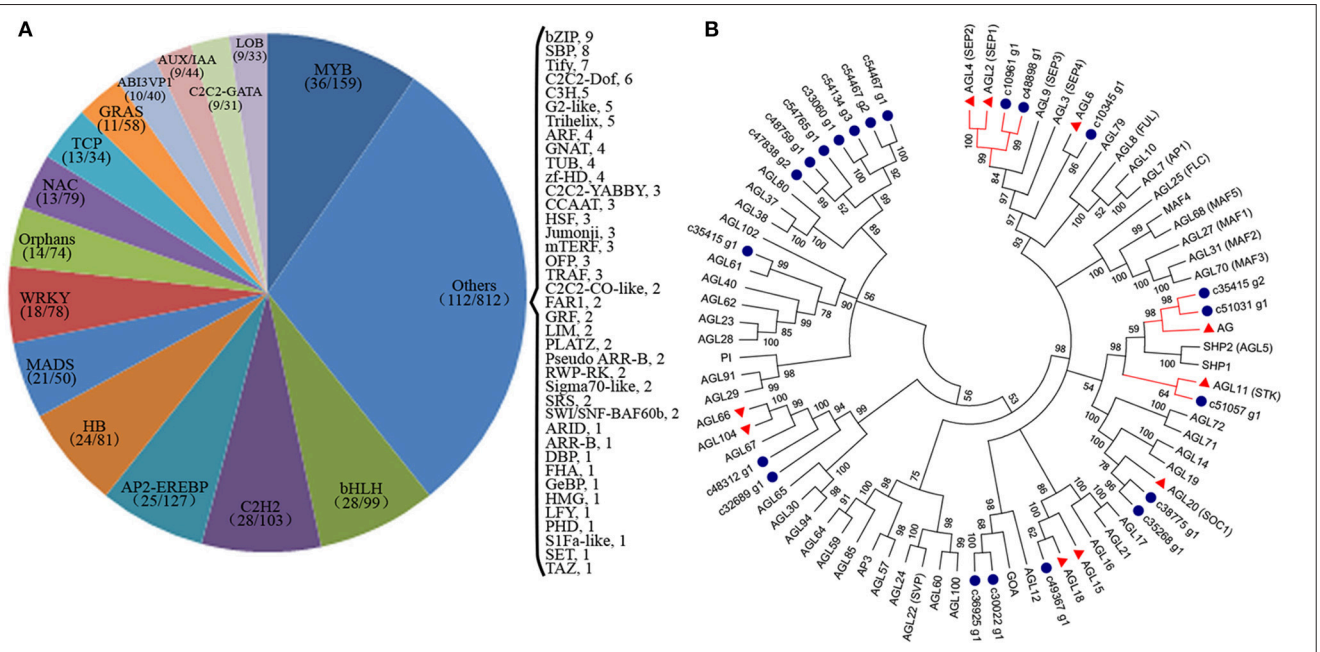

FIGURE 8 | Analysis of transcription factors (TFs) during flower development in *V. macrocephalum* f. *keteleeri*. (A) Distribution of TF families. TFs were identified in fertile and sterile flowers of *V. macrocephalum* f. *keteleeri*. Numbers in the parentheses after each TF family indicate the number of differentially expressed TFs (first number) and all members of this TF family identified by RNA-Seq (second number). **(B)** Phylogenetic analyses of MADS-box genes. A phylogenetic tree of 21 MADS-box genes from *V. macrocephalum* f. *keteleeri* and 60 MADS-box genes from *A. thaliana*. Blue circles indicate genes from *V. macrocephalum* f. *keteleeri*. The red clades show C, D, and E class MADS-box genes associated with floral organ identify. Red triangles correspond to floral regulators in *A. thaliana*.

regulators involved in floral meristem, floral patterning, floral organ polarity, floral patterning, flowering pathway, and others showing differential expression profiles between fertile and sterile flowers (Table S10; **Figure 9C**). Most of these TFs and genes also had lower expression levels in sterile flowers and higher levels in fertile flowers.

Furthermore, we performed qRT-PCR experiments to determine the expression patterns of key regulators, including *AG1*, *SEP1/2*, *SVP*, and *AGL15*, which are involved in regulating flowering time, floral organ development, and floral meristem during the different developmental stages (**Figure 9D**). We found that the expression levels of *AG1* and *SEP1/2* of classes B and E, respectively, declined from S1 to S3 in sterile flowers. Additionally, the levels of the negative regulatory factor genes *SVP* and *AGL15*, which are associated with flowering time, declined from S1 to S2 in fertile flowers and then increased in S3. However, all these key genes showed lower expression levels in sterile flowers than in fertile flowers, indicating their involvement in floral organ identify and flowering time.

DISCUSSION

De novo Assembly and Transcriptome Annotation

De novo transcriptome analyses have been used widely for flowering plants without a reference genome to discover genes and their expression patterns involved in flower and reproductive developmental processes. Previous studies with floral transcriptomes from different stages and tissues have contributed to identifying new floral-expressed genes (Zhang et al., 2014), floral biomarker genes, stage-specific genes, tissues-specific genes (Vining et al., 2015), transcription factors, lineage-specific genes (Bhide et al., 2014; Zhang et al., 2014), and flowering time regulators (Fan et al., 2015). Sterile and fertile flower differentiation and formation are driven by adaptive and selective stress, and as an important evo-devo phenotype associated with flower shape, size, and fertility. For example, from transcriptome profile analyses of fertile and sterile floral buds from plants with cytoplasmic male sterility (CMS) or genic male sterility (GMS) such as *Brassica napus* (An et al., 2014), cotton (Yang et al., 2014), and *Capsicum annuum* (Chen et al., 2015), changes in expression patterns of some genes involved in anther and pollen development have been identified between fertile and sterile floral buds. However, a comparative global expression analysis of fertile vs. sterile flowers has been lacking.

Because the inflorescence of *V. macrocephalum* f. *keteleeri* contains distinct sterile and fertile flowers, comparisons of sterile and fertile flower materials within one inflorescence enable analyses in a consistent genetic background. With no available genomic information for this species, we used RNA-seq to obtain large numbers of paired-end clean reads (34.4 G) from sterile and fertile flowers, and constructed more comprehensive transcripts (105,683 unigenes). This large number of reads produced more unigenes than those generated from some perennial shrubs (Gao et al., 2015; Zheng et al., 2015) and increased the coverage depth of the transcriptome, improving the *de novo* assembly and sequencing accuracy.

TABLE 2 | *V. macrocephalum* f. *keteleeri* unigenes that show homology with ABCDE-class genes.

Category	Transcript ID	Orthologous gene
A class	c15401_g1	Floral homeotic protein APETALA 1 (*AP1*)
	c79121_g1	
	c56198_g1	
	c31141_g1	Floral homeotic protein APETALA 2 (*AP2*)
	c44268_g1	
	c48961_g2	
	c50326_g1	
	c56440_g2	
B class	c44362_g2	Floral homeotic protein PISTILLATA (*PI*)
	c101101_g1	Floral homeotic protein GLOBOSA (*GLO*)
	c76268_g1	Floral homeotic protein DEFICIENS (*DEFA*)
	c47136_g1	
C class	c35415_g2	Floral homeotic protein AGAMOUS (*AG2/AG*)
	c51031_g1	
	c35415_g1	
D class	c51057_g1	Agamous-like MADS-box protein AGL11 (*STK*)
E class	c10961_g1	Developmental protein SEPALLATA 1/2 (*SEP1/2*)
	c48898_g1	

Further annotation of the unigenes revealed that reproductive processes, cell growth and death, and development-associated genes participated in the differentiation and development of fertile and sterile flowers. However, over 55% of unigenes still had no hits in public databases, which may be attributable to many short sequences; moreover, these unmatched unigenes might represent genes specific to *V. macrocephalum* f. *keteleeri*.

Global Changes in Gene Expression Reveal Significantly Enriched Pathways in Fertile and Sterile Flowers

Floral organ differentiation and development are highly regulated through temporal and spatial gene expression, with each organ having distinct transcriptomes (Zhang et al., 2014). Because the fertile flowers of *V. macrocephalum* f. *keteleeri* possess normal pistils and stamens, vs. the sterile flowers with abnormal reproductive components, thus we considered that some DEGs between fertile and sterile flowers would be associated with reproductive processes and/or plant fertility. Although over 5,000 DEGs between fertile and sterile flower development were found in this study, the key or upstream regulators triggering divergence may not be included in S2, as such regulators are likely expressed in an earlier stage. Therefore, the DEGs identified may refer to the downstream genes or regulators that maintain reproductive units underlying differentiation and development of fertile and sterile flowers during the rapid development stage.

Previous studies have confirmed that some genes, such as *COPT1*, sucrose-phosphate synthase (*SPS*), *SHT*, *GAM1*, and sucrose synthase (*SUS*), are required for pollen development and starch and sucrose metabolism (Sancenón et al., 2004; Park et al., 2008; Lin et al., 2014). In the present study, these genes were significantly downregulated in sterile flowers compared to fertile flowers, suggesting that they may participate in the degeneration and stagnation of stamens in sterile flowers during their differentiation and development.

Regarding upregulated DEGs in sterile flowers, many photosynthesis-related genes, such as *PSBP* and *PETH*, function in electron transfer in photosynthesis activity (Ishihara et al., 2007; Lintala et al., 2007). This result was consistent with the ultrastructural observations that more chloroplasts were distributed in the petal cells of sterile flowers, indicating that the sterile flowers had relatively high photosynthesis capabilities. Considering that sterile flowers have much greater size and higher biomass than do fertile flowers, we speculate that the process of flower formation and petal expansion in sterile flowers may be partially attributed to their higher photosynthetic capabilities. After all, having more photosynthetic products is beneficial to supplying the energy and materials needed to construct larger floral organs in sterile flowers.

Expression Level Changes in Genes Involved in Reproductive Processes in Fertile and Sterile Flowers

Sexual reproduction requires a developmental phase transition, and results in the formation of flowers with highly specialized organs, including anther-bearing stamens and ovule-bearing carpels (Xing et al., 2010). Within these organs, cells are recruited to undergo meiotic divisions to form male and female gametophytes. Many of the genes and regulatory pathways controlling anther and pollen development, meiosis, and female gametophyte development have been characterized (Irish, 2010). Molecular and genetic studies have found that the altered function of some genes can result in severe reductions in fertility. For example, knocking out the *CALS5* gene, encoding a callose synthase that is essential for exine formation in the pollen wall, can reduce *Arabidopsis* fertility (Dong et al., 2005). Similarly, mutations in *Arabidopsis EXTRA SPOROGENOUS CELLS/EXCESS MICROSPOROCYTES1* (*EMS1*/*EXS*) can cause abnormal tapetum development and result in male sterility (Canales et al., 2002). Ectopic expression or altered function of some other genes, including *PCS1*, *PAIR1*, *PAIR2*, *PAIR3*, and *MCM8*, also can lead to a failure in anther dehiscence and fertility, as well as meiosis (Ge et al., 2005; Nonomura et al., 2006; Yuan et al., 2009; Crismani et al., 2013), suggesting their important roles in reproductive organ development. Recently, many genes responsible for anther and pollen development in the CMS and GMS systems of *B. napus* and *Citrullus lanatus* have been identified and they showed differential expression levels between fertile and sterile flower buds (An et al., 2014; Rhee et al., 2015).

Here, our RNA-seq and qRT-PCR results revealed that many homologs of genes involved in anther and pollen development

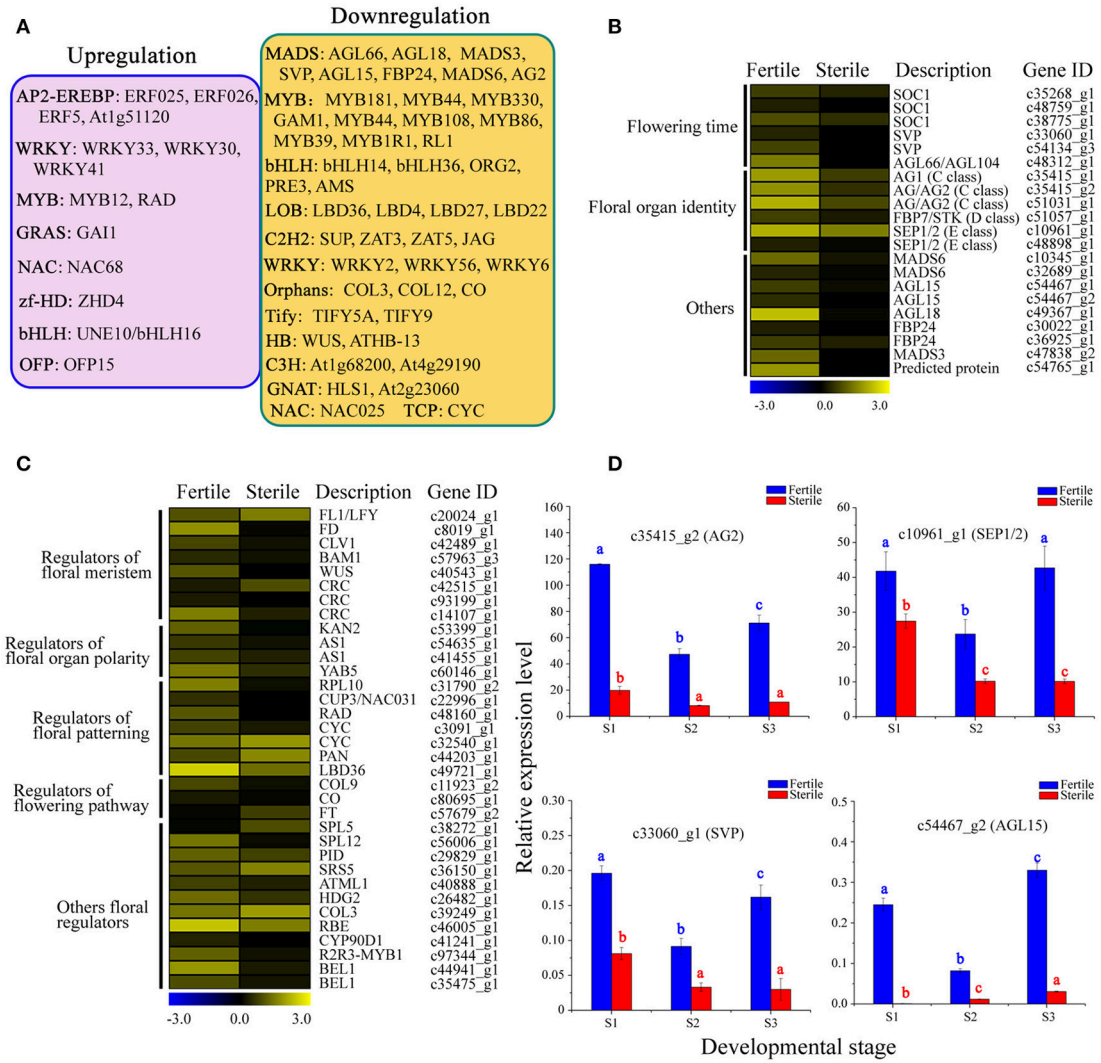

FIGURE 9 | Analysis of differentially expressed TFs and other floral regulators between fertile and sterile flowers. (A) Representative functions and genes showing different transcription factor families for fertile and sterile flowers. Significantly upregulated (pink) and downregulated (orange) TFs in sterile flowers were screened using a cut-off of $|\log2(\text{ratio})| \geq 4$. **(B)** Expression profile of MADS-box TFs involved in flowering time, floral organ identity, and other roles. The representation of the bar is as described in **Figure 5A**. **(C)** Expression profile of other differentially expressed TFs and other genes involved in floral meristem, floral patterning, floral organ polarity, floral patterning, flowering pathway, and other processes. The representation of the bar is as described in **Figure 5A**. **(D)** qRT-PCR analysis of four transcripts during fertile (blue) and sterile flower (red) development. The representation of the *x*-axis, *y*-axis, significance tests and error bars are as described in **Figure 5B**.

were significantly downregulated in sterile flowers, including *CALS5*, *AMS*, *GAM1*, *LAT52 SF3*, *NEC1*, *ASCO5*, *SHT*, and *DRP1C*, suggesting that they are potential factors causing stamen degradation in sterile flowers. Similar expression changes were also observed in female gametophyte development-associated genes, such as *NACK1*, ATP-dependent RNA helicase (*SUV3*), and *RL1*, which likely give rise to abnormal female gametophytes, subsequently resulting in the collapse of pistils in sterile flowers.

In particular, qRT-PCR results indicated that PCD-related *BAG1* was significantly expressed at higher levels from S1 to S3 in sterile flowers, suggesting that the gene may cause rapid PCD in degenerated stamens and pistils of sterile flowers. These results also suggest that some genes have conserved roles in regulating floral organ formation, and these reproduction-associated genes are involved in regulating fertility and sterility differentiation through temporal and spatial gene expression patterns.

Expression Level Changes in Genes Involved in Cell Proliferation and Cell Expansion in Fertile and Sterile Flowers

Flowers exhibit various colors, shapes, and sizes, in which petal or flower size is an important attractive characteristic for pollinators. The final size of a flower or an organ depends largely on cell proliferation and cell expansion (Powell and

Lenhard, 2012; Czesnick and Lenhard, 2015). Some genes related to cell proliferation and expansion have been identified (Powell and Lenhard, 2012; Czesnick and Lenhard, 2015). For example, a petal-specific transcription factor, *BIGPETAL* (*BPEp*), can interfere with petal cell expansion by interaction with *AUXIN RESPONSE FACTOR8* (*ARF8*) (Varaud et al., 2011). Similarly, the *MIXTA*-like genes have been demonstrated to regulate petal epidermal conical cell differentiation in multiple plant species (Perez-Rodriguez et al., 2005; Weng et al., 2011). In particular, a cascade of transcription factor Class II TCPs and GRFs (growth-response factors) is involved in promoting cell proliferation, and class I TCPs, including *TCP14*, *TCP15*, and *TCP20*, also modulate cell proliferation and expansion in an organ, suggesting essential roles in controlling organ growth and size (Czesnick and Lenhard, 2015).

In this study, homologs of genes associated with cell proliferation and expansion, such as *COBL*, *MIXTA*-like 8, *TMK1*, *EXPA2*, *EXPA13*, and TCP family members, were upregulated in sterile flowers, indicating that these genes may be associated with the petal size of sterile flowers. Further qRT-PCR analyses revealed that *TCP2* and *MIXTA*-like 8 were significantly highly expressed in S1 and S2 in sterile flowers, suggesting that they may be responsible for regulating cell proliferation or differentiation in rapid petal expansion. In contrast, a homolog of the negative regulator *BPE* showed significantly lower expression from S1 to S3 in sterile flowers, and much lower expression in S2 in sterile flowers, which is consistent with rapid petal expansion and suggests its key role in forming larger petals in sterile than in fertile flowers.

Expression Level Changes in Genes Involved in Phytohormone Signaling in Fertile and Sterile Flowers

Phytohormones including auxins, gibberellins (GA), cytokinins, brassinosteroids, abscisic acid, and jasmonates all play important roles in the regulation of flower or reproductive development (Yuan and Zhang, 2015). For example, most of the mutants in jasmonate biosynthesis are male sterile and can be rescued by the application of JA (Song et al., 2013; Yuan and Zhang, 2015). Similarly, brassinosteroid can regulate key genes in anther and pollen development (Ye et al., 2010). Increasing evidence indicates that the coordinated actions of jasmonate, auxin, gibberellin, cytokinin, and brassinosteroid play essential roles in the regulation of stamen development in *Arabidopsis* (Song et al., 2013).

In this study, our RNA-seq data revealed that many homologs of genes or proteins involved in auxin (e.g., ARFs, *GH3*, and SAUR family proteins), jasmonate (e.g., JAZs) and gibberellin (e.g., *GID1* and *GIDB*) signaling were downregulated in sterile flowers, in coordination with the downregulation of several genes related to fertility, implying that they may be involved in regulating fertility and sterility differentiation of *V. macrocephalum* f. *keteleeri* flowers. Similar expression patterns for cytokinin signaling-related negative regulators were also seen in sterile flowers, which is consistent with the upregulation of several genes related to cell proliferation and expansion. We propose that cytokinin-associated genes may be a factor in petal expansion through cell proliferation and expansion, contributing to flower size.

Transcriptional Regulation in Fertile and Sterile Flower Development

TFs are a group of proteins that act by activating or repressing the expression of downstream target genes; they play important roles in regulating flower development (Qu and Zhu, 2006). Previous studies in the model species *A. thaliana* and *Antirrhinum majus* have identified many TFs from various TF families involved in flower development, such as MADS, bHLH, and MYB family members (Egea-Cortines et al., 1999; Riechmann and Ratcliffe, 2000; Jin et al., 2015). Most *Arabidopsis* MADS family TFs were detected predominantly in flowers (Egea-Cortines et al., 1999; Ó'Maoiléidigh et al., 2014). They are also major components in the classical ABCDE model, and specific combinations of ABCDE genes correspond to the identity of each concentric whorl of sepals (A+E), petals (A+B+E), stamens (B+C+E), carpels (C+E), and ovules (D+E) (Pelaz et al., 2000; Theissen and Melzer, 2007). BHLH family proteins are one of the largest families of TFs, and many of them have been characterized functionally in plants (Carretero-Paulet et al., 2010). The gene *SPATULA*, encoding a bHLH TF, has been shown to be involved in controlling floral-organ formation as well as the morphogenesis of sepals, petals, and stamens in *Arabidopsis* and rice (Li et al., 2006; Groszmann et al., 2010).

In sterile and fertile flowers, most MYB, bHLH, AP2-EREBP, C2H2, and MADS family TFs were highly expressed, suggesting essential roles in regulating *V. macrocephalum* f. *keteleeri* flower development. Further phylogenetic analyses of MADS-box family genes revealed some important floral regulators including ABCDE-class homologous genes, which may contribute to floral organ identification and further functional research in the floral differentiation and development of the genus *Viburnum*. Moreover, RNA-seq and qRT-PCR results indicated many differentially expressed TFs, including MADS-box family members, and showed uniform lower expression in sterile flowers, suggesting probable functions in fertility degeneration in sterile flowers.

CONCLUSION

We constructed a transcriptome library from *V. macrocephalum* f. *keteleeri* and obtained large sets of transcript data from its flowers. We found that genes that were differentially expressed between fertile and sterile flowers were involved primarily in photosynthesis, starch and sucrose metabolism, pollen development, female gametophyte development, phytohormone signaling, and cell proliferation and expansion. Additionally, many transcription factors, including MADS-box genes, were involved in fertile vs. sterile flower differentiation. Our results showed involvement of comprehensive transcriptional regulation networks related to flower fertility and size in regulating differentiation and development of fertile and sterile flowers in *V. macrocephalum* f. *keteleeri*.

AUTHOR CONTRIBUTIONS

ZL and BJ carried out the design of the study and drafted the manuscript. ZL and JX performed the experimental work and data analysis. JX, LZ, JC, and QH participated in sample collection, RNA extraction, quantitative RT-PCR, and data analysis. ZL, LW, BJ, and WL revised the manuscript. All authors read and approved the final manuscript.

FUNDING

This work was financially supported by the Three New Forestry Engineering Foundation of Jiangsu Province (No. LYSX(2011)41, LYSX[2016]55), Natural Science Foundation of Jiangsu Province (No. BK20131228).

ACKNOWLEDGMENTS

We thank Novogene Company (Beijing) for helping with transcriptome sequencing and technical assistance.

SUPPLEMENTARY MATERIAL

The Supplementary Material for this article can be found online at: http://journal.frontiersin.org/article/10.3389/fpls.2017.00261/full#supplementary-material

REFERENCES

Achard, P., Gusti, A., Cheminant, S., Alioua, M., Dhondt, S., Coppens, F., et al. (2009). Gibberellin signaling controls cell proliferation rate in *Arabidopsis*. *Curr. Biol.* 19, 1188–1193. doi: 10.1016/j.cub.2009.05.059

An, H., Yang, Z. H., Yi, B., Wen, J., Shen, J. X., Tu, J. X., et al. (2014). Comparative transcript profiling of the fertile and sterile flower buds of *pol* CMS in *B. napus*. *BMC Genomics* 15:258. doi: 10.1186/1471-2164-15-258

Anders, S., and Huber, W. (2010). Differential expression analysis for sequence count data. *Genome Biol.* 11:R106. doi: 10.1186/gb-2010-11-10-r106

Ashburner, M., Ball, C. A., Blake, J. A., Botstein, D., Buter, H., Cherry, J. M., et al. (2000). Gene ontology: tool for the unification of biology. *Nat. Genet.* 25, 25–29. doi: 10.1038/75556

Bartrina, I., Otto, E., Strnad, M., Werner, T., and Schmülling, T. (2011). Cytokinin regulates the activity of reproductive meristems, flower organ size, ovule formation, and thus seed yield in *Arabidopsis thaliana*. *Plant Cell* 23, 69–80. doi: 10.1105/tpc.110.079079

Becker, A., and Theißen, G. (2003). The major clades of MADS-box genes and their role in the development and evolution of flowering plants. *Mol. Phylogenet. Evol.* 29, 464–489. doi: 10.1016/S1055-7903(03)00207-0

Benjamini, Y., and Hochberg, Y. (1995). Controlling the false discovery rate: a practical and powerful approach to multiple testing. *J. R. Stat. Soc.* 57, 289–300.

Bhide, A., Schliesky, S., Reich, M., Weber, A. P. M., and Becker, A. (2014). Analysis of the floral transcriptome of *Tarenaya hassleriana* (Cleomaceae), a member of the sister group to the Brassicaceae: towards understanding the base of morphological diversity in Brassicales. *BMC Genomics* 15:140. doi: 10.1186/1471-2164-15-140

Canales, C., Bhatt, A. M., Scott, R., and Dickinson, H. (2002). *EXS*, a putative LRR receptor kinase, regulates male germline cell number and tapetal identity and promotes seed development in *Arabidopsis*. *Curr. Biol.* 12, 1718–1727. doi: 10.1016/S0960-9822(02)01151-X

Carretero-Paulet, L., Galstyan, A., Roig-Villanova, I., Martínez-García, J. F., Bilibao-Castro, J. R., and Robertson, D. L. (2010). Genome-wide classification and evolutionary analysis of the bHLH family of transcription factors in *Arabidopsis*, poplar, rice, moss, and algae. *Plant Physiol.* 153, 1398–1412. doi: 10.1104/pp.110.153593

Cecchetti, V., Altamura, M. M., Falasca, G., Costantino, P., and Cardarelli, M. (2008). Auxin regulates *Arabidopsis* anther dehiscence, pollen maturation, and filament elongation. *Plant Cell* 20, 1760–1774. doi: 10.1105/tpc.107.057570

Chen, C. M., Chen, G. J., Cao, B. H., and Lei, J. J. (2015). Transcriptional profiling analysis of genic male sterile–fertile *Capsicum annuum* reveal candidate genes for pollen development and maturation by RNA-Seq technology. *Plant Cell Tiss. Org. Cult.* 122, 465–476. doi: 10.1007/s11240-015-0784-5

Cheng, H., Qin, L. J., Lee, S., Fu, X. D., Richard, D. E., Cao, D. N., et al. (2004). Gibberellin regulates *Arabidopsis* floral development via suppression of DELLA protein function. *Development* 131, 1055–1064. doi: 10.1242/dev.00992

Cooley, A. M., Carvallo, G., and Willis, J. H. (2008). Is floral diversification associated with pollinator divergence? Flower shape, flower colour and pollinator preference in Chilean *Mimulus*. *Ann. Bot.* 101, 641–650. doi: 10.1093/aob/mcn014

Crismani, W., Portemer, V., Froger, N., Chelysheva, L., Horlow, C., Vrielynck, N., et al. (2013). *MCM8* is required for a pathway of meiotic double-strand break repair independent of *DMC1* in *Arabidopsis thaliana*. *PLoS Genet.* 9:e1003165. doi: 10.1371/journal.pgen.1003165

Czesnick, H., and Lenhard, M. (2015). Size control in plants—lessons from leaves and flowers. *Cold Spring Harb. Perspect. Biol.* 7:a019190. doi: 10.1101/cshperspect.a019190

Dong, X. Y., Hong, Z. L., Sivaramakrishnan, M., Mahfouz, M., and Verma, D. P. S. (2005). Callose synthase (*CalS5*) is required for exine formation during microgametogenesis and for pollen viability in *Arabidopsis*. *Plant J.* 42, 315–328. doi: 10.1111/j.1365-313X.2005.02379.x

Donoghue, M. J., Bell, C. D., and Winkworth, R. C. (2003). The evolution of reproductive characters in Dipsacales. *Int. J. Plant Sci.* 164, S453–S464. doi: 10.1086/376874

Egea-Cortines, M., Saedler, H., and Sommer, H. (1999). Ternary complex formation between the MADS-box proteins SQUAMOSA, DEFICIENS and GLOBOSA is involved in the control of floral architecture in *Antirrhinum majus*. *EMBO J.* 18, 5370–5379. doi: 10.1093/emboj/18.19.5370

Fan, Z. Q., Li, J. Y., Li, X. L., Wu, B., Wang, J. Y., Liu, Z. C., et al. (2015). Genome-wide transcriptome profiling provides insights into floral bud development of summer-flowering *Camellia azalea*. *Sci. Rep.* 5:9729. doi: 10.1038/srep09729

Gao, L. X., Yang, H. X., Liu, H. F., Yang, J., and Hu, Y. H. (2015). Extensive transcriptome changes underlying the flower color intensity variation in *Paeonia ostii*. *Front. Plant Sci.* 6:1205. doi: 10.3389/fpls.2015.01205

Ge, X. C., Dietrich, C., Matsuno, M., Li, G. J., Beng, H., and Xia, Y. J. (2005). An *Arabidopsis* aspartic protease functions as an anti-cell-death component in reproduction and embryogenesis. *EMBO Rep.* 6, 282–288. doi: 10.1038/sj.embor.7400357

Götz, S., García-Gómez, J. M., Terol, J., Williams, T. D., Nagaraj, S. H., Nueda, M. J., et al. (2008). High-throughput functional annotation and data mining with the Blast2GO suite. *Nucleic Acids Res.* 36, 3420–3435. doi: 10.1093/nar/gkn176

Grabherr, M. G., Haas, B. J., Yassour, M., Levin, J. Z., Thompson, D. A., Amit, I., et al. (2011). Full-length transcriptome assembly from RNA-Seq data without a reference genome. *Nat. biotechnol.* 29, 644–652. doi: 10.1038/nbt.1883

Groszmann, M., Bylstra, Y., Lampugnani, E. R., and Smyth, D. R. (2010). Regulation of tissue-specific expression of *SPATULA*, a bHLH gene involved in carpel development, seedling germination, and lateral organ growth in *Arabidopsis*. *J. Exp. Bot.* 61, 1495–1508. doi: 10.1093/jxb/erq015

Han, Y. Y., Zhang, C., Yang, H. B., and Jiao, Y. L. (2014). Cytokinin pathway mediates *APETALA1* function in the establishment of determinate floral meristems in *Arabidopsis*. *Proc. Natl. Acad. Sci. U.S.A.* 111, 6840–6845. doi: 10.1073/pnas.1318532111

Irish, V. F. (2010). The flowering of *Arabidopsis* flower development. *Plant J.* 61, 1014–1028. doi: 10.1111/j.1365-313X.2009.04065.x

Ishihara, S., Takabayashi, A., Ido, K., Endo, T., Ifuku, K., and Sato, F. (2007). Distinct functions for the two PsbP-like proteins PPL1 and PPL2 in the

chloroplast thylakoid lumen of *Arabidopsis*. *Plant Physiol.* 145, 668–679. doi: 10.1104/pp.107.105866

Jin, B., Wang, L., Wang, J., Teng, N. J., He, X. D., Mu, X. J., et al. (2010). The structure and roles of sterile flowers in *Viburnum macrocephalum* f. *keteleeri* (Adoxaceae). *Plant Biol.* 12, 853–862. doi: 10.1111/j.1438-8677.2009.00298.x

Jin, J. P., He, K., Tang, X., Li, Z., Lv, L., Zhao, Y., et al. (2015). An *Arabidopsis* transcriptional regulatory map reveals distinct functional and evolutionary features of novel transcription factors. *Mol. Biol. Evol.* 32, 1767–1773. doi: 10.1093/molbev/msv058

Li, B., and Dewey, C. (2011). RSEM: accurate transcript quantification from RNA-Seq data with or without a reference genome. *BMC Bioinformatics* 12:323. doi: 10.1186/1471-2105-12-323

Li, N., Zhang, D. S., Liu, H. S., Yin, C. S., Li, X. X., Liang, W. Q., et al. (2006). The rice tapetum degeneration retardation gene is required for tapetum degradation and anther development. *Plant Cell* 18, 2999–3014. doi: 10.1105/tpc.106.044107

Lin, I. W., Sosso, D., Chen, L. Q., Gase, K., Kim, S. G., Kessler, D., et al. (2014). Nectar secretion requires sucrose phosphate synthases and the sugar transporter SWEET9. *Nature* 508, 546–549. doi: 10.1038/nature13082

Lintala, M., Allahverdiyeva, Y., Kidron, H., Piippo, M., Battchikova, N., Suorsa, M. J., et al. (2007). Structural and functional characterization of ferredoxin-$NADP^+$-oxidoreductase using knock-out mutants of *Arabidopsis*. *Plant J.* 49, 1041–1052. doi: 10.1111/j.1365-313X.2006.03014.x

Livak, K. J., and Schmittgen, T. D. (2001). Analysis of relative gene expression data using real-time quantitative PCR and the $2^{-\Delta\Delta CT}$ method. *Methods* 25, 402–408. doi: 10.1006/meth.2001.1262

Mao, X., Cai, T., Olyarchuk, J. G., and Wei, L. (2005). Automated genome annotation and pathway identification using the KEGG Orthology (KO) as a controlled vocabulary. *Bioinformatics* 21, 3787–3793. doi: 10.1093/bioinformatics/bti430

Nielsen, L. R., Philipp, M., and Siegismund, H. R. (2002). Selective advantage of ray florets in *Scalesia affinis* and *S. pedunculata* (Asteraceae), two endemic species from the Galápagos. *Evol. Ecol.* 16, 139–153. doi: 10.1023/A:1016301027929

Nonomura, K. I., Nakano, M., Eiguchi, M., Suzuki, T., and Kurata, N. (2006). *PAIR2* is essential for homologous chromosome synapsis in rice meiosis I. *J. Cell Sci.* 119, 217–225. doi: 10.1242/jcs.02736

Ó'Maoiléidigh, D. S., Graciet, E., and Wellmer, F. (2014). Gene networks controlling *Arabidopsis thaliana* flower development. *New Phytol.* 201, 16–30. doi: 10.1111/nph.12444

Park, J. Y., Canam, T., Kang, K. Y., Ellis, D. D., and Mansfield, S. D. (2008). Over-expression of an *Arabidopsis* family A sucrose phosphate synthase (SPS) gene alters plant growth and fibre development. *Transgenic Res.* 17, 181–192. doi: 10.1007/s11248-007-9090-2

Pelaz, S., Ditta, G. S., Baumann, E., Wisman, E., and Yanofsky, M. F. (2000). B and C floral organ identity functions require *SEPALLATA* MADS-box genes. *Nature* 405, 200–203. doi: 10.1038/35012103

Perez-Rodriguez, M., Jaffe, F. W., Butelli, E., Glover, B. J., and Martin, C. (2005). Development of three different cell types is associated with the activity of a specific MYB transcription factor in the ventral petal of *Antirrhinum majus* flowers. *Development* 132, 359–370. doi: 10.1242/dev.01584

Pérez-Rodríguez, P., Riaño-Pachón, D. M., Corrêa, L. G. G., Rensing, S. A., Kersten, B., and Mueller-Roeber, B. (2009). PlnTFDB: updated content and new features of the plant transcription factor database. *Nucleic Acids Res.* 38, D822–D827. doi: 10.1093/nar/gkp805

Powell, A. E., and Lenhard, M. (2012). Control of organ size in plants. *Curr. Biol.* 22, R360–R367. doi: 10.1016/j.cub.2012.02.010

Qu, L. J., and Zhu, Y. X. (2006). Transcription factor families in *Arabidopsis*: major progress and outstanding issues for future research. *Curr. Opin. Plant Biol.* 9, 544–549. doi: 10.1016/j.pbi.2006.07.005

Rhee, S. J., Seo, M., Jang, Y. J., Cho, S., and Lee, G. P. (2015). Transcriptome profiling of differentially expressed genes in floral buds and flowers of male sterile and fertile lines in watermelon. *BMC Genomics* 16:914. doi: 10.1186/s12864-015-2186-9

Riechmann, J. L., and Ratcliffe, O. J. (2000). A genomic perspective on plant transcription factors. *Curr. Opin. Plant Biol.* 3, 423–434. doi: 10.1016/S1369-5266(00)00107-2

Sancenón, V., Puig, S., Mateu-Andrés, I., Dorcey, E., Thiele, D. J., and Peñarrubia, L. (2004). The *Arabidopsis* copper transporter COPT1 functions in root elongation and pollen development. *J. Biol. Chem.* 279, 15348–15355. doi: 10.1074/jbc.M313321200

Singh, K. B., Foley, R. C., and Oñate-Sánchez, L. (2002). Transcription factors in plant defense and stress responses. *Curr. Opin. Plant Biol.* 5, 430–436. doi: 10.1016/S1369-5266(02)00289-3

Song, S. S., Qi, T. C., Huang, H., and Xie, D. X. (2013). Regulation of stamen development by coordinated actions of jasmonate, auxin, and gibberellin in *Arabidopsis*. *Mol. Plant* 6, 1065–1073. doi: 10.1093/mp/sst054

Tamura, K., Stecher, G., Peterson, D., Filipski, A., and Kumar, S. (2013). MEGA6: molecular evolutionary genetics analysis version 6.0. *Mol. Biol. Evol.* 30, 2725–2729. doi: 10.1093/molbev/mst197

Theissen, G., and Melzer, R. (2007). Molecular mechanisms underlying origin and diversification of the angiosperm flower. *Ann. Bot.* 100, 603–619. doi: 10.1093/aob/mcm143

Thomas, S. G., and Franklin-Tong, V. E. (2004). Self-incompatibility triggers programmed cell death in *Papaver* pollen. *Nature* 429, 305–309. doi: 10.1038/nature02540

Trapnell, C., Williams, B. A., Pertea, G., Mortazavi, A., Kwan, G., Baren, M. J., et al. (2010). Transcript assembly and quantification by RNA-Seq reveals unannotated transcripts and isoform switching during cell differentiation. *Nat. Biotechnol.* 28, 511–515. doi: 10.1038/nbt.1621

Varaud, E., Brioudes, F., Szécsi, J., Leroux, J., Brown, S., Perrot-Rechenmann, C., et al. (2011). AUXIN RESPONSE FACTOR 8 regulates *Arabidopsis* petal growth by interacting with the bHLH transcription factor BIGPETALp. *Plant Cell* 23, 973–983. doi: 10.1105/tpc.110.081653

Vining, K. J., Romanel, E., and Jones, R. C. (2015). The floral transcriptome of *Eucalyptus grandis*. *New Phytol.* 206, 1406–1422. doi: 10.1111/nph.13077

Wang, L., Lu, Z. G., Li, W. X., Xu, J., Luo, K. G., Lu, W. C., et al. (2016). Global comparative analysis of expressed genes in ovules and leaves of *Ginkgo biloba* L. *Tree Genet. Genom.* 12, 1–18. doi: 10.1007/s11295-016-0989-8

Weng, L., Tian, Z. X., Feng, X. Z., Li, X., Xu, S. L., Hu, X. H., et al. (2011). Petal development in *Lotus japonicus*. *J Integr Plant Biol.* 53, 770–782. doi: 10.1111/j.1744-7909.2011.01072.x

Xing, S., Salinas, M., Höhmann, S., Berndtgen, R., and Huijser, P. (2010). miR156-targeted and nontargeted SBP-box transcription factors act in concert to secure male fertility in *Arabidopsis*. *Plant Cell* 22, 3935–3950. doi: 10.1105/tpc.110.079343

Xu, J., Yang, C., Yuan, Z., Zhang, D. S., Gondwe, M. Y., Ding, Z. W., et al. (2010). The *ABORTED MICROSPORES* regulatory network is required for postmeiotic male reproductive development in *Arabidopsis thaliana*. *Plant Cell* 22, 91–107. doi: 10.1105/tpc.109.071803

Yang, C. Q., Fang, X., Wu, X. M., Mao, Y. B., Wang, L. J., and Chen, X. Y. (2012). Transcriptional regulation of plant secondary metabolism. *J. Integr. Plant Biol.* 54, 703–712. doi: 10.1111/j.1744-7909.2012.01161.x

Yang, P., Han, J., and Huang, J. (2014). Transcriptome sequencing and *de novo* analysis of cytoplasmic male sterility and maintenance in JA-CMS cotton. *PLoS ONE* 9:e112320. doi: 10.1371/journal.pone.0112320

Yang, X., Zhao, X. G., Li, C. H., Liu, J., Qiu, Z. J., Dong, Y., et al. (2015). Distinct regulatory changes underlying differential expression of TEOSINTE $BRANCHED_1$-CYCLOIDEA-PROLIFERATING CELL FACTOR genes associated with petal variations in zygomorphic flowers of *Petrocosmea* spp. of the family gesneriaceae. *Plant Physiol.* 169, 2138–2151. doi: 10.1104/pp.15.01181

Ye, J., Fang, L., Zheng, H., Zhang, Y., Chen, J., Zhang, Z., et al. (2006). WEGO: a web tool for plotting GO annotations. *Nucleic Acids Res.* 34, W293–W297. doi: 10.1093/nar/gkl031

Ye, Q., Zhu, W., Li, L., Zhang, S., Yin, Y., Ma, H., et al. (2010). Brassinosteroids control male fertility by regulating the expression of key genes involved in *Arabidopsis* anther and pollen development. *Proc. Natl. Acad. Sci. U.S.A.* 107, 6100–6105. doi: 10.1073/pnas.0912333107

Young, M. D., Wakefield, M. J., Smyth, G. K., and Oshlack, A. (2010). Gene ontology analysis for RNA-seq: accounting for selection bias. *Genome Biol.* 11:R14. doi: 10.1186/gb-2010-11-2-r14

Yuan, W. Y., Li, X. W., Chang, Y. X., Wen, R. Y., Chen, G. X., Zhang, Q. F., et al. (2009). Mutation of the rice gene *PAIR3* results in lack of bivalent formation in meiosis. *Plant J.* 59, 303–315. doi: 10.1111/j.1365-313X.2009.03870.x

Yuan, Z., and Zhang, D. B. (2015). Roles of jasmonate signalling in plant inflorescence and flower development. *Curr. Opin. Plant Biol.* 27, 44–51. doi: 10.1016/j.pbi.2015.05.024

Zhang, L. S., Wang, L., Yang, Y. L., Cui, J., Chang, F., Wang, Y. X., et al. (2014). Analysis of *Arabidopsis* floral transcriptome: detection of new florally expressed genes and expansion of Brassicaceae-specific gene families. *Front. Plant Sci.* 5:802. doi: 10.3389/fpls.2014.00802

Zheng, J., Hu, Z. H., Guan, X. L., Dou, D. Q., Bai, G., Wang, Y., et al. (2015). Transcriptome analysis of *Syringa oblata* Lindl. inflorescence identifies genes associated with pigment biosynthesis and scent metabolism. *PLoS ONE* 10:e0142542. doi: 10.1371/journal.pone.0142542

Conflict of Interest Statement: The authors declare that the research was conducted in the absence of any commercial or financial relationships that could be construed as a potential conflict of interest.

frontiers in Plant Science

ORIGINAL RESEARCH
published: 30 November 2017
doi: 10.3389/fpls.2017.01986

Dianthus chinensis L.: The Structural Difference between Vascular Bundles in the Placenta and Ovary Wall Suggests Their Different Origin

Xue-Min Guo[1], Ying-Ying Yu[2], Lan Bai[1] and Rong-Fu Gao[3]*

[1] College of Life Science and Technology, Hebei Normal University of Science and Technology, Qinhuangdao, China, [2] College of Biological Sciences, China Agricultural University, Beijing, China, [3] College of Life Science and Technology, Beijing Forestry University, Beijing, China

Dianthus chinensis is a perennial herbaceous plant with great ornamental, botanical, ecological, and medicinal value. The pistil of *D. chinensis* is composed of two fused carpels with free central placenta and two separate styles. The placenta is a columnar structure extending about two-thirds the length of the maturing fruit, which is typical of the Caryophyllaceous. Traditionally, free central placenta is thought to have evolved from axial placenta by septal disappearance, and axial placenta to have occurred through fusion of conduplicate carpels with marginal placenta. However, the traditional opinion is becoming more and more inconsistent with the new data gained in recent research of angiosperm systematics. To clarify the origin of *D. chinensis* pistil, the present anatomical study was carried out. The results show that the vascular system of placenta is independent to that of the ovary wall in *D. chinensis*. Moreover, in the central part of placenta there are one or two amphicribral bundles, and correspondingly numerous ones in the pistil which supply the ovules/seeds. It is obvious that the central amphicribral bundles in placenta are comparable to the counterparts in branches but not to those in leaves or their derivatives. Therefore, it is reasonable to deduce that the placenta of *D. chinensis* was not derived from conduplicate carpels through fusion of collateral vascular bundles, and actually a floral axis with ovules/seeds laterally adhering. On the contrary, the ovary wall was the lateral appendages of the floral axis. The result of the present study is completely in agreement with Unifying Theory, in which the placenta is taken as an ovule-bearing branch. Except for *D. chinensis*, the similar vascular organization has been observed in placenta of numerous isolated taxa. But till now, it is uncertain that whether this vascular organization pattern is popular in the whole angiosperms or not. More intensive and extensive investigations are needed.

Keywords: angiosperm, placenta, carpel, origin, comparative anatomy, *Dianthus chinensis*

OPEN ACCESS

Edited by:
José Bienvenido Diez, University of Vigo, Spain

Reviewed by:
Zhong Liu, Shanghai Jiao Tong University, China
Qingwen Ma, Beijing Museum of Natural History, China

****Correspondence:***
Xue-Min Guo
xueminguo@126.com

Specialty section:
This article was submitted to Plant Evolution and Development, a section of the journal Frontiers in Plant Science

Received: *13 January 2017*
Accepted: *03 November 2017*
Published: *30 November 2017*

Citation:
Guo X-M, Yu Y-Y, Bai L and Gao R-F (2017) Dianthus chinensis L.: The Structural Difference between Vascular Bundles in the Placenta and Ovary Wall Suggests Their Different Origin. Front. Plant Sci. 8:1986. doi: 10.3389/fpls.2017.01986

INTRODUCTION

The angiosperms, or flowering plants, one of the major clades of extant seed plants, are the largest group of embryophytes, with at least 260,000 living species classified in 453 families (Angiosperm Phylogeny Group, 2003). Angiosperms are amazingly diverse in their habitats, size, longevity, overall form, chemistry, reproductive morphology, and genome size and organization (Soltis and Soltis, 2004). Given this diversity, angiosperm phylogeny, branded "an abominable mystery" by

Darwin (Darwin and Seward, 1903), remains a topic of intense research to date. The structures of plant flowers are usually less affected by their environment than their vegetative parts over the long-term processes of evolution; therefore, the understanding of floral structure makes an important contribution to the discussion of angiosperm phylogeny, and has been studied by systematists in this context (Endress, 1994).

The carpel is an essential feature of angiosperms and understanding its origin is vitally important to improve of our knowledge of angiosperm phylogeny (Tang, 2008). Although the traditional theory of the origin of the carpel, in which the carpel is the basic unit of the angiosperm pistil and evolved by megasporophyll with ovule bearing on its edge (Eames, 1961; Cronquist, 1988), is widely accepted in angiosperm systematics, and is still taught in the classroom, recent progress in the field, based on molecular biology, has refuted the previously accepted hypothesis.

Arabidopsis thaliana flower has four-whorl floral organs, whose growth and development are controlled by different gene combinations (Skinner et al., 2004; Mathews and Kramer, 2012). After the gene that controls the development of the ovary wall is knocked out, the ovule can still develop in the branched placenta (Roe et al., 1997), suggesting that the loss of the ovary wall does not affect the development of the placenta and ovule and is independent of the latter two. When the gene of the control placenta is artificially altered, the ovary wall develops normally, but the placenta changes greatly (Wynn et al., 2014). The co-expression of *REV* and *STM* in the placenta primordium is the characteristic of the top of the branch, suggesting that the placenta is essentially a branch. The placenta may have evolved from an originally separate fertile structure that was recruited later onto so-called carpel (Skinner et al., 2004). In *Petunia* and *Oryza*, the ovary walls and the placenta are also controlled by two different sets of genes (Angenent et al., 1995; Li et al., 2011). Functional gene studies of these model plants indicate that the placenta and ovary wall of angiosperms are controlled by different genes, being equivalent to an ovule-bearing shoot and a foliar organ, respectively, which is obviously contrary to the traditional theory, because according to this theory, each part of the conduplicate carpel, including the ovary wall and placenta, has the same genome. Hence, it is necessary to re-examine the traditional doctrine.

The vascular bundle is a strand of conductive tissue extending lengthwise through the stems and roots of higher plants, including the ferns, fern allies, gymnosperms, and angiosperms. The vascular bundle consists of xylem, which conducts water and dissolved mineral substances from the soil to the leaves, and phloem, which conducts dissolved foods, especially sugars, from the leaves to the storage tissues of the stem and root. The structure of vascular bundles varies among different plant groups (Columbia Electronic Encyclopedia, 2016); however, compared with the softer tissues, which may or may not exhibit fusions, reductions, or elaborations, the vascular skeleton of plants is considered to be more resistant to change (Thomson, 1942). Accordingly, vascular anatomy is considered as an indicator of the ancestral condition (Douglas, 1936). The carpellary bundle, as a relatively conservative structure, has extreme significance phylogenetically. The vascular bundle has different origin and structure in the placenta and ovary wall of angiosperm, corresponding to a shoot and a leafy organ. In kiwi fruit with axile placenta, the axile placenta is independent of the surrounding ovary wall, and the vascular bundles in the placenta are amphicribral, collateral at least in the upper part of the ovary wall (Guo et al., 2013). In the flowers of *Magnolia*, the carpel with marginal placenta is composed of two mutually independent primordia (corresponding to the ovary wall and axilla placenta). The ovary wall and placenta respectively have their own independent

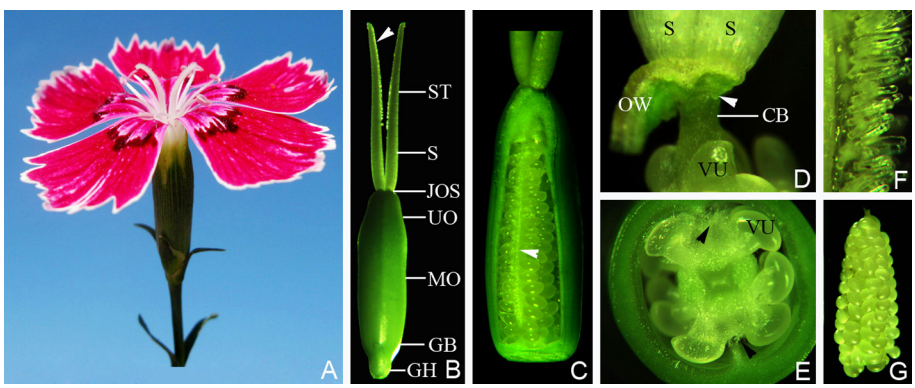

FIGURE 1 | The flower and pistil of *Dianthus chinensis* L. CB, connecting bands between placenta and styles; GB, gynobase; GH, gynophore; JOS, juncture of ovary and styles; MO, middle of ovary; VU, ovule; OW, ovary wall; UO, upper part of ovary; S, style; ST, stigma. **(A)** A flower, showing the upper parts of two separate stigmata. **(B)** The appearance of a pistil 2 days after flowering, showing the shapes of the gynophore, ovary, style, and stigma, and the location of the papillae (arrow). **(C)** A pistil (with part of the ovary wall removed), gynophore, and stigma, showing the central placenta bearing ovules in the ovary and the distribution of papillae covering the transmission tissue (arrow). **(D)** The pistil with the ovary wall removed, showing the lower end of the style (arrow) and connecting bands between the placenta and the styles. **(E)** Transection through the middle of an ovary, showing the papillae distributed at a position corresponding to the septum. **(F)** Part of the stigma, showing the form of the papillae on the abaxial side of the stigma. **(G)** A free central placenta bearing ovules, showing ovule arrangement on the placenta.

vascular bundles, and vascular bundles in them are totally different as showed by the amphicribral vascular bundle in the placenta and the collateral ones in the ovary wall (Liu et al., 2014).

Dianthus chinensis L. is an important ornamental, botanical, ecological, and medicinal perennial herbaceous plant which is widely cultivated in Europe and Asia. The investigation of propagation (Fu et al., 2008; Wang et al., 2014), cultivation (Yang et al., 2013), physiology (Ding et al., 2013; Dar et al., 2014), biochemistry (Croxdale and Outlaw, 1983; Han et al., 2015), genetic breeding (Wu et al., 2003; Zhu and Sun, 2015), and other features of *D. chinensis* has been extensive. Regarding pistil anatomy, the vascular supply to the ovary and styles was traced and described by Thomson (1942), and the pistil composition, ovule arrangement, and development of placenta, septum, and seeds were investigated by Buell (1952); however, these accounts barely discussed the evolutionary implications of the vascular bundles.

One of the typical characteristics of the *D. chinensis* pistil is its free central placenta. Over the past 130 years, the nature and origin of the free central placenta and carpel has been controversial, and discussed among investigators of the Caryophyllaceae. For example, Lister (1884) put forward that the placenta was carpellary according to detailed developmental studies of floral organs in Alsineae; but Gibbs (1907) considered the placenta axile for it was an upward extension of the axis arising between carpel primordia, with which it secondarily associated. Rocén endorsed that the placenta was carpellary since free central placenta was derived from central placenta through the fusion of carpels and vanish of the septum according to Buell (1952). In the light of vascular anatomy study in Primulaceae, Douglas (1936) also thought the placenta to be carpellary in this family. However, in Eames' opinion (1951), there were not only normally oriented bundles but also inverted ones in the placenta of Portulacaceae and Primulaceae, the two genera of the Caryophyllaceae, so that the placenta was composed of both axile and carpellary tissues, whereas in cases of only inverted bundles were present the placenta was entirely carpellary. In another study it was described that the placenta of Dianthus was presumed to be fused carpel tissue because the central placental vascular strand in Dianthus represented fused ventral carpellary traces (Thomson, 1942).

In the present study, we dissected *D. chinensis* pistils, and conducted a systematic observation of the shapes, types, and structures of the vascular bundles within it, to explore the difference of vascular structure between the plancenta and the ovary wall and the implications of the vascular anatomy of the forming carpel.

MATERIALS AND METHODS

Flowers in anthesis were collected from a nursery garden (119.17°E, 39.71°N) attached to the College of Horticulture Science and Technology, Hebei Normal University of Science & Technology. Two days after flowering, one flower was photographed and the pistil was isolated from the other parts of the flower, its morphology and structure examined, and the size of each part of 15 pistils was measured using Vernier calipers and expressed as mean ± standard deviation.

The ovary wall was partially or totally removed and the middle ovary transected. Then the pistil shape, the ovary with or without a large part of the ovary wall, the ovary transection, and the papillae of the stigma were observed and photographed using an Olympus ZX16 stereomicroscope with an Olympus Infinity1 digital camera.

Pistils were preserved in a formalin–acetic acid–alcohol mixture, embedded in paraffin, sectioned serially into sections of 8–10 μm thickness, and stained in safranin and fast green. Complete transverse and longitudinal series were examined and photographed under an Olympus BX51 microscope with an Olympus DP72 digital camera.

Pistils were also softened in 2 M NaOH solution in a 65°C water bath for 30–40 min, squashed, stained in safranin, and mounted with glycerol. The prepared slides were photographed under the microscope.

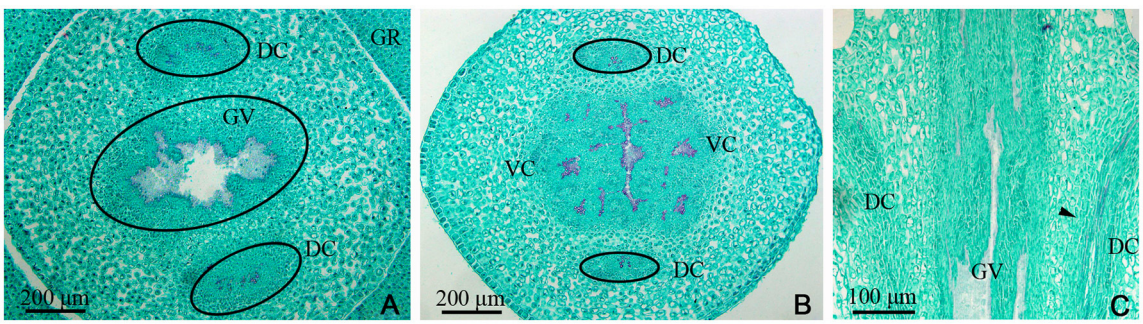

FIGURE 2 | *Dianthus chinensis* L. gynophore sections. DC, dorsal carpellary trace; GR, glandular ring; GV, gynophore vascular bundle; VC, ventral carpellary trace. **(A)** Transection of a gynobase surrounded by a nectary, showing an amphicribral gynophore vascular bundle and the xylem temporarily present in the center of the collateral dorsal carpellary traces branching out of the gynophore vascular bundle. **(B)** Transection a short distance above the level in **(A)**, showing the differentiating ventral and lateral carpellary traces from the gynophore vascular bundle and differentiated collateral dorsal carpellary traces (circle). **(C)** Longitudinal section of a gynophore, showing two differentiating dorsal carpellary traces from the gynophore vascular bundle and the transformation from an amphicribral to a collateral bundle observed ascending the gynophore (arrow).

RESULTS

The *D. chinensis* pistil consisted of four regions: gynophore, ovary, style, and stigma, that merged with one another. The gynophore was (3.08 ± 0.38) mm long, with the lower part surrounded by the nectary, and connected by the receptacle with the ovary. The ovary was shaped like a tiny vase, with a length of (6.8 ± 0.55) mm and a central diameter of (2.73 ± 0.44) mm. The placenta was a columnar structure extending to the bottom of the style. The ovules were arranged quite regularly along its surface in four vertical rows each containing about ∼10–15 ovules. Papillae covering transmission tissue (TT) were located on opposite sides of the placenta. The stigma (4.32 ± 0.18), mm long, with developed papillae on the abaxial side, was connected with the ovary through the style, which was (2.88 ± 0.18) mm long and with a base diameter of (0.53 ± 0.08) mm (**Figures 1A–G, 2A**).

Examination of a cross-section of the base of the gynophore indicated the presence of both one gynophore vascular bundle (GV), with only one bundle of xylem in its center, and two dorsal

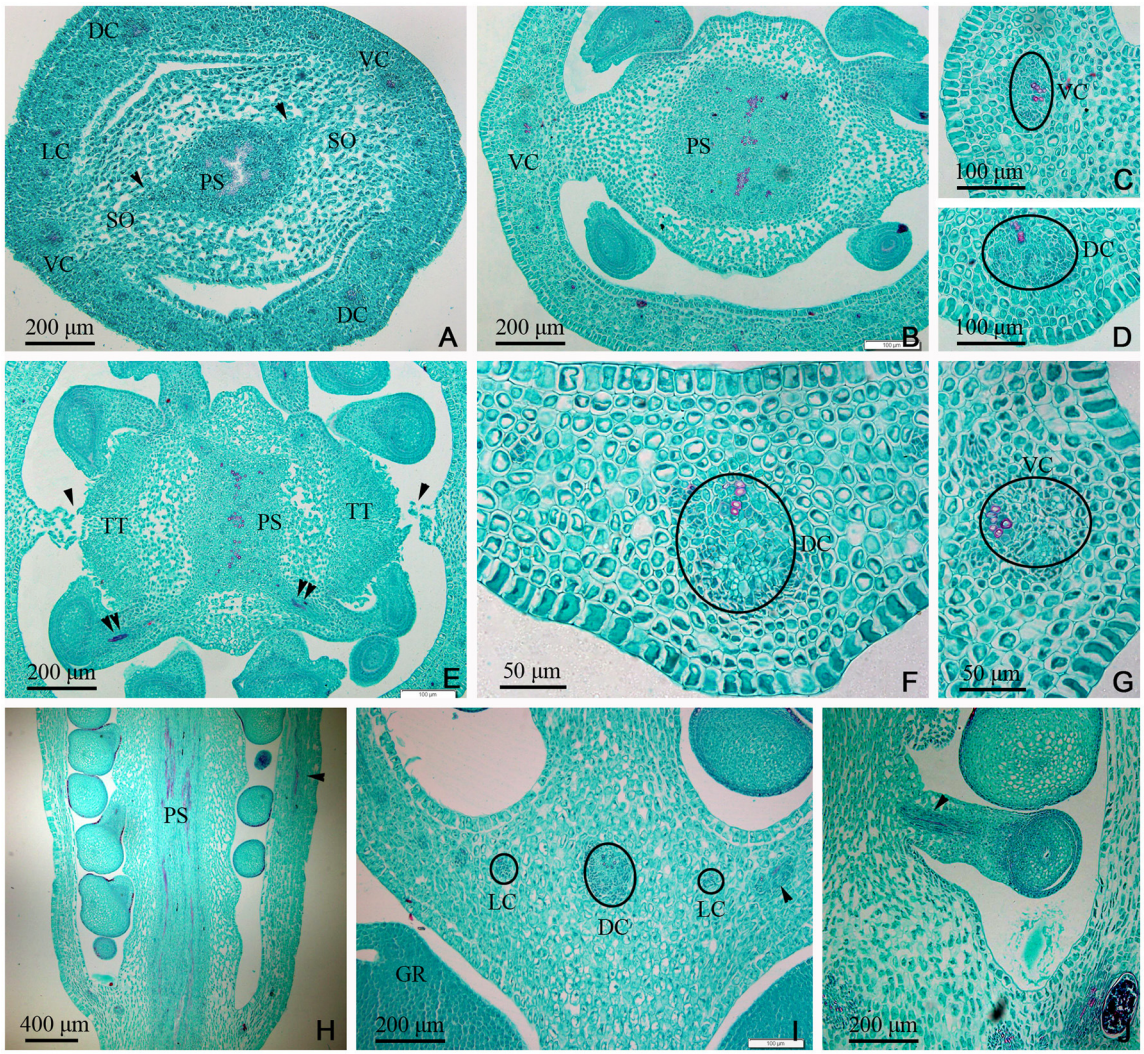

FIGURE 3 | *Dianthus chinensis* L. gynobase sections. LC, lateral carpellary trace; PS, placental strand; SO, septum of the ovary; TT, transmission tissue; DC, dorsal carpellary trace; GR, glandular ring; VC, ventral carpellary trace. **(A)** A gynobase transection, showing an amphicribral placental strand extending outward along the wide ovary septum (arrow), and a collateral vascular bundle, including two ventral carpellary traces, two dorsal carpellary traces, and some lateral carpellary traces. **(B)** Transection a short distance above the level in **(A)**, showing the differentiating ovule provascular tissue and the narrow ovary septum. **(C,D)** Detailed views of local regions of ovary wall in **(B)**, showing a collateral ventral carpellary trace and a collateral lateral carpellary trace, respectively. **(E)** Transection a short distance above the level in **(B)**, showing amphicribral ovule traces (double arrows), the disappearing ovary septum (arrow), and the differentiated TT. **(F,G)** Detailed view of local regions of the ovary wall in **(E)**, showing collateral lateral carpellary trace and ventral carpellary trace, respectively. **(H)** Longitudinal section of a gynobase through the middle of the placenta, showing amphicribral ovule traces continually branching out of a placental strand and a collateral vascular bundle in the ovary wall (arrow). **(I)** Longitudinal section of a gynobase, not through the middle of the placenta, showing at least three collateral lateral, and one dorsal carpellary, traces visible in transverse and longitudinal sections (circle and arrow), respectively. **(J)** Longitudinal section of a local region of the gynobase, showing an amphicribral ovule trace in the funicle (arrow).

carpellary traces (DC) on the outside of gynophore, which were amphicribral bundles (**Figure 2A**). The GV then differentiated into ventral and lateral carpellary traces (VC and LC), evidenced by the formation of many outer xylem bundles (**Figures 2B, 7B**), and the dorsal carpellary trace transformed into the collateral vascular bundle by gradual inward movement of the xylem (**Figures 2A–C**).

In the gynobase, the vascular bundles were mainly distributed in the placenta and ovary wall (carpel; **Figures 3, 7C**). The placental strand (PS) and GV were continuous with one another, and then differentiated into numerous branches into the ovules (ovule trace, OT). Although, the PS form became irregular in the cross-section view, both the PS and the OT formed by its branches remained amphicribral (**Figures 3A,B,H,J**). The vascular bundles in the ovary wall, including the DC, VC, and LC, were all collateral (**Figures 3C,D,F,G,I**). In addition, no vascular bundle was found in the septum of the ovary (SO) in its gradual narrowing from the ovary wall and the TT appeared on the opposite side from the placenta (**Figures 1C,E, 3A,B,E**).

In the middle of the ovary, the PS cross-sectional area became smaller compared to that at the gynobase, and assumed a curved quadrilateral morphology (**Figure 4A**). Papillae covering transmission tissue (PT) developed (**Figures 4A,B,I,J**) and appeared to connect with the ovary wall, which is adjacent to the pollen tube extending down into the embryo sac. In the ovary wall, the DC, VC, and LC constantly branched to form an intertwined vascular network (**Figures 4C, 7A**). However, the distribution, type, and structure of the vascular bundles in the middle of the ovary remained similar to that at its base (**Figures 4A–J**).

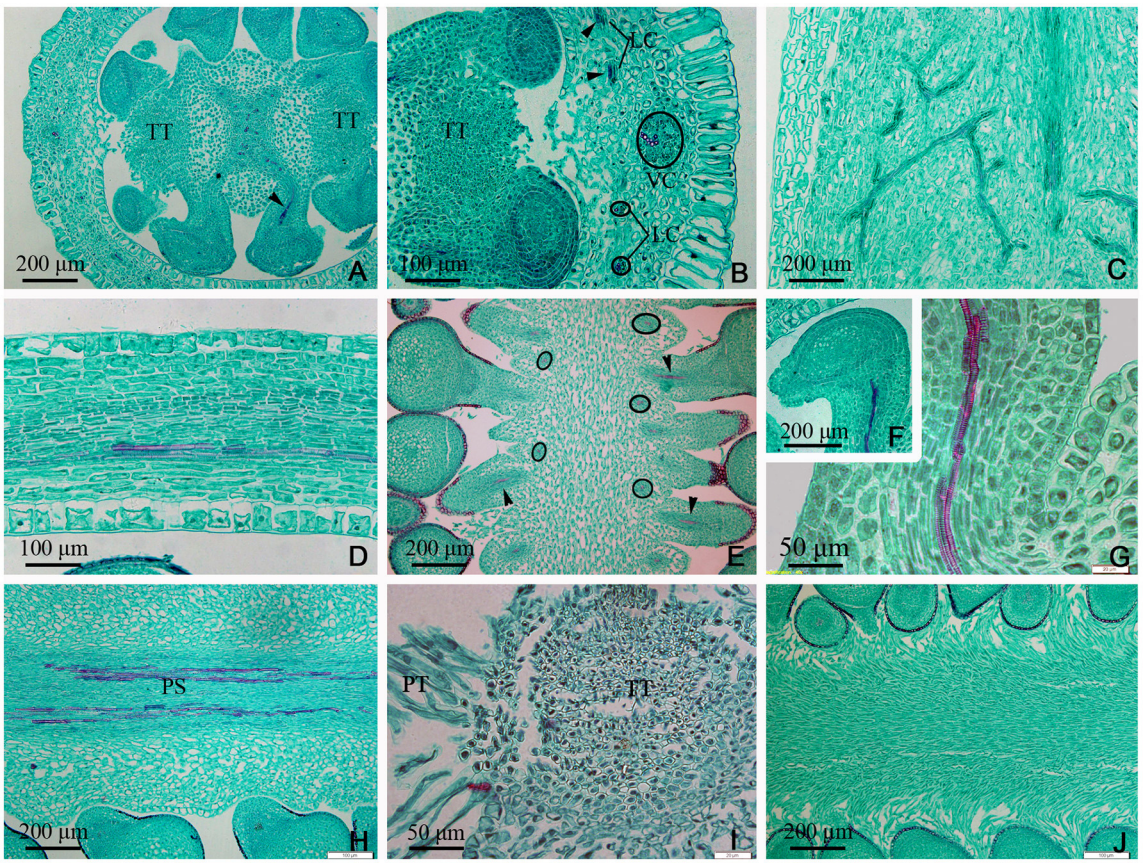

FIGURE 4 | Sections through the middle of the ovary of *Dianthus chinensis* L. PT, papillae covering transmission tissue; TT, transmission tissue; LC, lateral carpellary trace; VC, ventral carpellary trace; PS, placental strand. **(A)** A transection through the middle of an ovary, showing the curved quadrilateral amphicribral placental strand, amphicribral ovule trace (arrow) deriving from a placental strand, and central placenta, separating from the ovary wall. **(B)** A local transection a short distance above the level in **(A)**, showing four collateral lateral carpellary traces in the ovary wall, visible in two longitudinal sections in the upper part (arrows) and in two transections in the lower part (small circles), 1–2 vessels within them, and a collateral ventral carpellary trace (large circle). **(C)** Longitudinal section of an ovary wall, showing the branching pattern of the vascular bundles. **(D)** Transection of an ovary wall, showing annular vessels in the xylem of a collateral vascular bundle. **(E)** Longitudinal section of the central placenta, showing transverse (circles) and longitudinal (arrows) amphicribral ovule traces. **(F)** Transection of an ovule, showing an amphicribral ovule trace in the funicle. **(G)** Detailed view of the ovule trace in **(F)**, showing annular vessels in the xylem of the amphicribral ovule trace. **(H)** Longitudinal section of the central placenta, showing the pattern of annular vessels in an amphicribral placental strand. **(I)** Detailed view of TT, showing small cells with dense cytoplasm and PT. **(J)** Longitudinal section, not through the middle of the central placenta, showing the distribution pattern of the papillae.

In the upper part of the ovary, the placenta split into two (**Figures 5A,C–E, 7A,E**) and eventually appeared to be connected by papillae (**Figure 5F**). The PS split into three small bundles (**Figures 5D,E, 7E**), from eyebrow-like (**Figures 5A, 7D**) and oval tissues in succession (**Figure 5C**). There was no vascular bundle in the re-emerging SO at the apex of the ovary (**Figures 5D,F, 6I, 7A**). The vascular pattern in the upper part of the ovary was also similar to that in the middle and base of the ovary (**Figures 5A–J**).

The TT from the placenta extended upward to the style and stigma, forming their adaxial surface. The carpel also extended to the style and stigma, forming their abaxial tissue surface. Hence, the style and stigma comprised a composite structure, consisting of placenta and ovary wall; however, only the carpellary bundles entered the style and stigma (**Figures 5F**, **6C**), and the PS terminated at the apex of the placenta (**Figures 5E,F**, **6A,I**, **7A**). Therefore, there were three vascular bundles in the style base, including two VC and one DC (**Figures 6E**, **7F**). Subsequently, the VC branched once (**Figures 6I**, **7A**), forming five vascular bundles in the upper style and stigma (**Figure 6F**), which were all collateral (**Figures 6A–I**).

DISCUSSION

In this investigation, we examined the structure of the different component tissues of the pistil of *D. chinensis* L. flowers at anthesis, and in particular the configuration of its vascular bundles. This study constitutes an essential first step to understand either the origin of pistil. Vascular bundles are amphicribral in the placenta (PS and OT) and collateral in the carpel (ovary wall in the strict sense; DC, CV, and LC).

The transformations of the vascular bundles in the transition zone between the root and the stem have been of interest for

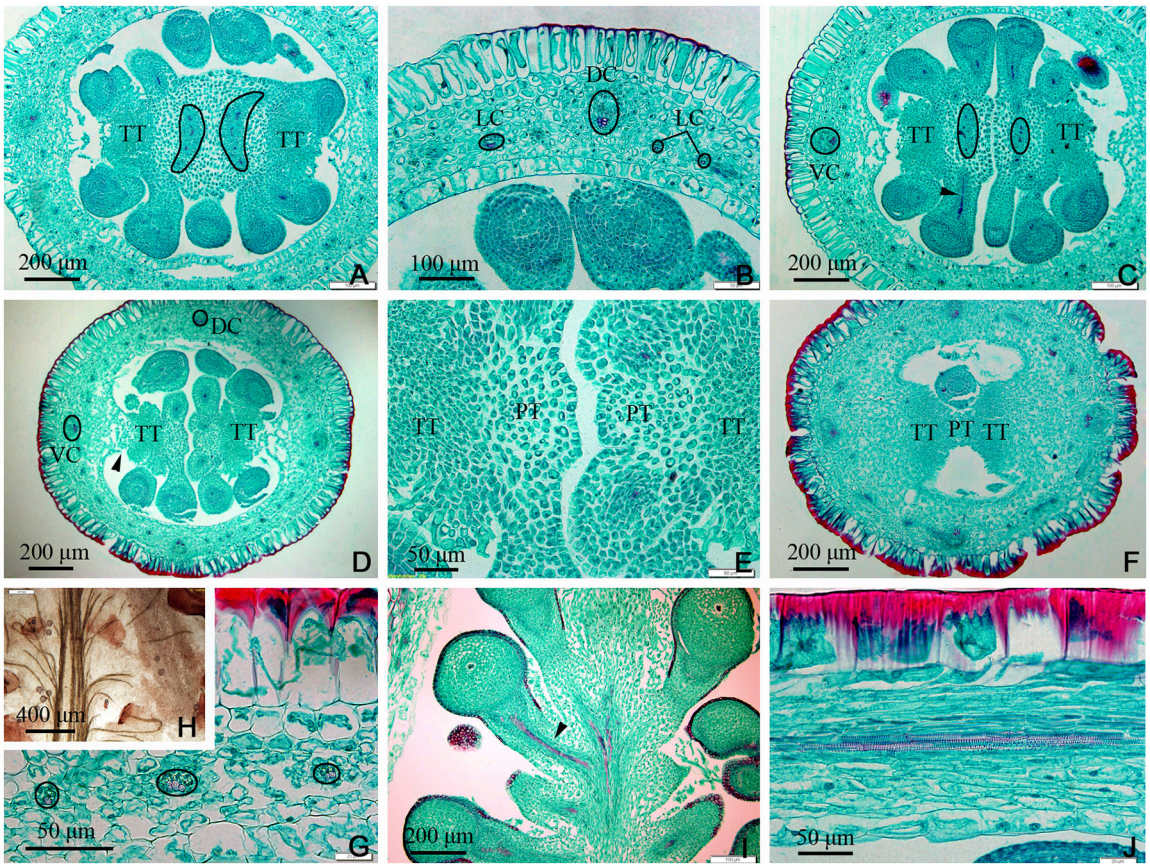

FIGURE 5 | Sections of the upper part of an ovary of *Dianthus chinensis* L. PT, papillae covering transmission tissue; TT, transmission tissue; LC, lateral carpellary trace; DC, dorsal carpellary trace; VC, ventral carpellary trace. **(A)** Transection of an ovary shoulder, showing two excurved amphicribral placental strands. **(B)** Detailed view of a local area in **(A)**, showing one collateral dorsal carpellary trace and at least three collateral lateral carpellary traces. **(C)** Transection a short distance above the level shown in **(A)**, showing preliminary separation of the central placenta and an amphicribral placental strand. **(D)** Transection a short distance above the level shown in **(C)**, showing clear separation of the central placenta, disappearance of the placental strand, and reappearance of the septum (arrow). **(E)** Detailed view of a local area in **(D)**, showing the disappearance of vascular bundles in the left branch of the placenta and a small ovule trace in its right branch. **(F)** Transection of the upper part of an ovary below the junction between the ovary and styles, showing two locules separated by a septum mainly composed of TT and papillae, and complete disappearance of the placental strand. **(G)** Transection of an ovary wall, showing three collateral lateral ovary wall traces. **(H)** Detailed view of the upper central placenta, showing the branching pattern of the placental strand. **(I)** Longitudinal section of the upper part of an ovary, showing the branching pattern of the amphicribral ovule traces in the apical placenta. **(J)** Longitudinal section of an ovary wall, showing annular vessels in the xylem of a collateral bundle.

some years (Basconsuelo et al., 2002); however, little attention has been paid to those between the gynophore and the ovary wall. According to the results of this study, there is a transformation of the vascular system of the gynophore, resulting in an amphicribral bundle visible in cross-sections of the vascular system of the collateral bundle in the ovary wall (**Figures 2A,B, 3C,D,F,G**), and in longitudinal section the transition region is characterized by inward displacement of xylem, in which the xylem in the central part of the amphicribral bundles in the gynophore moves inward to the inner side of the vascular bundles in the ovary wall (**Figure 2C**). This transformation may be an important indication of the transition from an axial to a foliar (carpel, in the pistil) vascular system.

In *D. chinensis* flowers, the gynophore is located between the receptacle and the ovary, and the ovary is superior. Both amphicribral PS and collateral ovary wall vascular bundles are differentiated from GV (gynophore vascular bundle), while bundles in sepals, petals and stamens all branch from the receptacle. In other words, whether in structure or in position the PS is distinct from the vascular bundles in other parts of the flower. The connecting bands (CB) between the placental tissue and style are ruptured after fertilization, and the placenta free (Buell, 1952). Therefore, structurally, the placenta may be an independent unique organ without any connection with other parts of the ovary wall. This conclusion is consistent with the findings of Guo et al. (2013) and Wang et al. (2015).

In accordance with traditional opinion, the pistil of *D. chinensis* is composed of two fused carpels with a free central placenta and two separate styles. If this were correct, both structures and types of vascular bundles in PS should be the same as those in ovary wall; but our observations are inconsistent with this conjecture. In our observations, the PS and ovule trace are amphicribral while those in the ovary wall are collateral, implying the axial derivation for the placental bundles and contrarily a leafy precursor characteristics for the ovary (**Figures 3–6**) respectively. This inconformity between

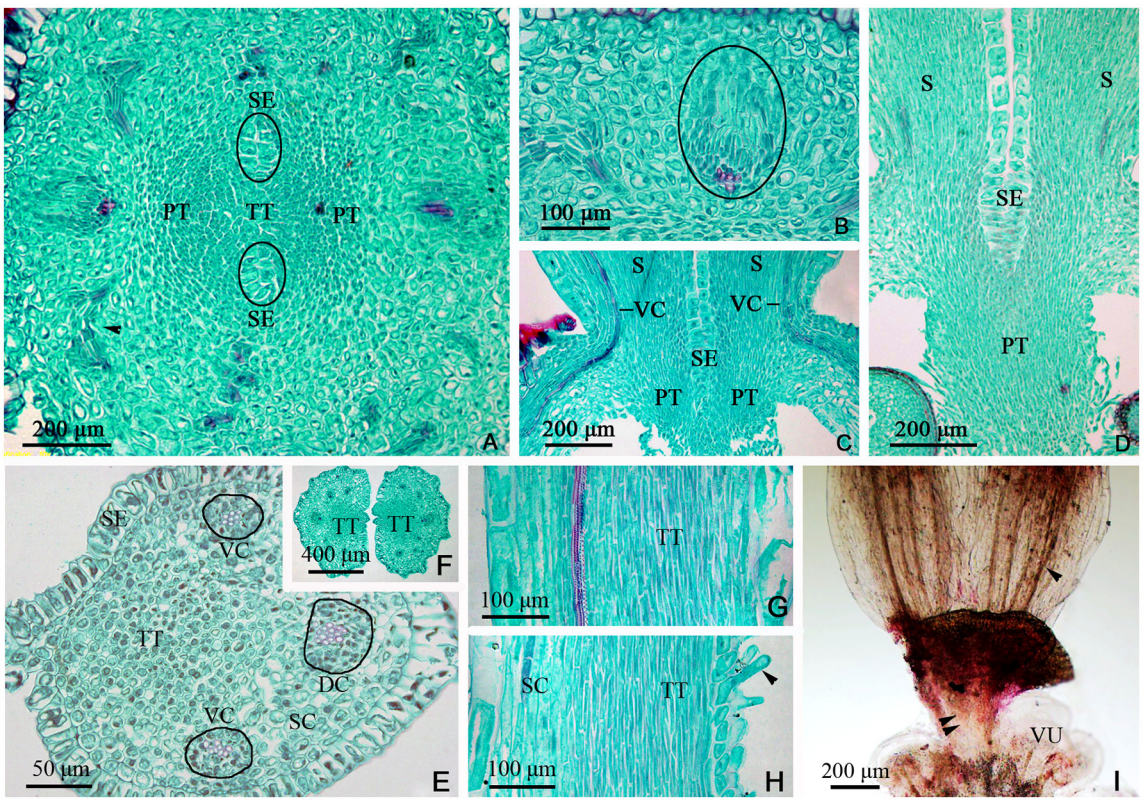

FIGURE 6 | Sections and segregation images of the style and stigma of *Dianthus chinensis* L. SC, style/stigma cortex. SE, style epidermal cells; S, style; PT, papillae covering transmission tissue; TT, transmission tissue; DC, dorsal carpellary trace; VC, ventral carpellary trace; VU, ovule. **(A–D)** Style base. **(E–I)** Styles and stigma. **(A)** Transection of the juncture of an ovary and styles, showing the branching pattern of vascular bundles in the carpel (arrow), the lower end of the style, and placental tissue without vascular bundles. **(B)** Detailed view of a local area in **(A)**, showing a collateral ventral carpellary trace. **(C)** Longitudinal section through opposite ventral carpellary traces in two styles, showing the traces entering the styles from the ovary wall. **(D)** Longitudinal section, not through the middle of the styles, showing placental tissue participating in the styles. **(E)** Transections of the base of a style, showing two collateral ventral carpellary traces, one collateral dorsal carpellary trace, and the structure of the style. **(F)** Transection a short distance above the level shown in **(E)**, showing five vascular bundles in each style, suggesting that the ventral carpellary traces branch. **(G)** Longitudinal section of a stigma, showing annular vessels in the xylem of a collateral vascular bundle and TT. **(H)** Longitudinal section of a stigma between two adjacent vascular bundles, showing PT (arrow) and the structure of the style. **(I)** Segregation view of the juncture of an ovary and styles, showing the branching of the ventral carpellary trace (arrow) and the connection bands without vascular bundles.

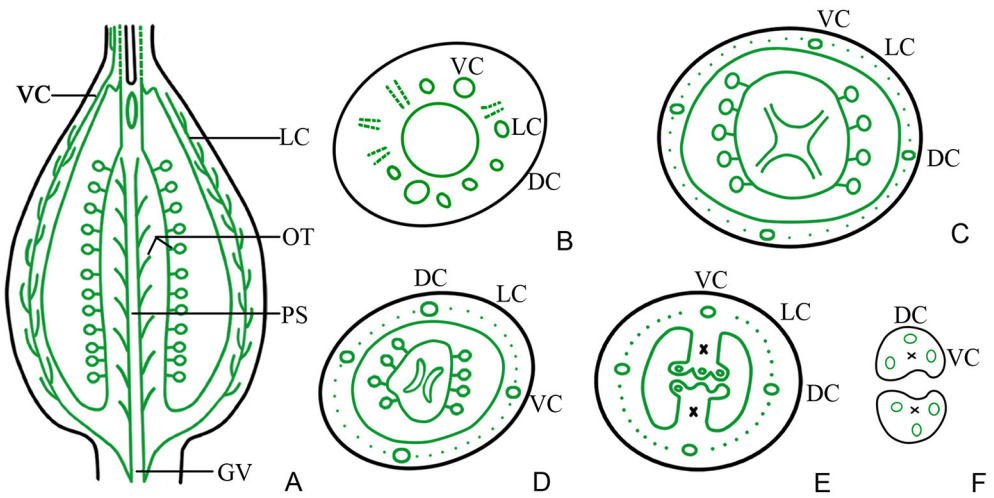

FIGURE 7 | Diagram showing the distribution of vascular bundles in a *D. chinensis* L. pistil. DC, dorsal carpellary trace; VC, ventral carpellary trace; LC, lateral carpellary trace; PS, placental strand; GV, gynophore vascular bundle; OT, ovule trace. **(A)** Longitudinal section of a pistil, showing the arrangement of the primary vascular bundles. **(B)** Transverse section of a gynophore, showing the differentiation of DC, VC, and LC from GV. **(C)** Transverse section of a gynobase, showing OT from PS. **(D)** Vascular bundles in the upper part of the ovary, showing eyebrow-like bundles separated from the PS. **(E)** Vascular bundles in the upper part of an ovary, a short distance above the level shown in **(D)**, showing the division of the placenta and separation of the vascular bundle. **(F)** Transverse section of a style base, showing two VC and one DC in each style. The region of the TT in the style and placenta is indicated by an ×.

traditional opinions and the present result is not confined to *D. chinensis*. Numerous taxa of angiosperms have been reported to support amphicribral vascular bundles in placenta, including Papaveraceae (Kapoor, 1973, 1995), Leguminosae (Lersten and Don, 1966), Winteraceae (Tucker, 1975), Solanaceae (Dave et al., 1981; Wang et al., 2015), Gesneriaceae (Wang and Pan, 1998), Buxaceae (Von Balthazar and Endress, 2002), Annonaceae (Endress and Armstrong, 2011), Actinidiaceae (Guo et al., 2013), and Magnoliaceae (Liu et al., 2014; Wang et al., 2015), etc. These taxa cover the whole scope of angiosperms from the basal clade magnoliids to the terminal eudicot lineage in the phylogenetic tree (Angiosperm Phylogeny Group, 2009). Nevertheless, it is unfortunate that little attention has been thrown on this common disagreement although it has caused a lot of doubts to the traditional opinion.

The Unifying Theory interprets that the carpel (in classic sense) is a compound organ because it comprises not only an ovule-bearing shoot (placenta) but also a foliar part enclosing the shoot (Wang, 2010). According to the theory, the vascular bundles in the placenta should appear as radial symmetry (namely, amphicribral bundles), as is exactly observed in the placenta of *D. chinensis* in the present study, which provides strong evidence for it, and the gene expression of the placenta and ovary wall may be different. Actually, studies on gene expression patterns in flowers of model plants such as *Arabidopsis*, *Petunia*, and *Oryza*, indicate that (1) the expression of *STK* is required for normal development of the funiculus in *Arabidopsis*; (2) *FBP7* and *FBP11* are involved in proper ovule development in *Petunia*; (3) *AGL11* plays important roles in flower development; (4) *OsMADS13* functioning in flower organ differentiation and meristem determinacy in rice is restrictedly expressed in the placenta/ovules; (5) *DL* regulates carpel specification and midrib development in *Oryza sativa*; (6) *CRC* participates in carpel identity differentiation and carpel polarity establishment in *Arabidopsis* and also acts as a regulator in carpel development; and (7) *YABBY* is only expressed in the ovary wall (Angenent et al., 1995; Rounsley et al., 1995; Pinyopich et al., 2003; Yamaguchi et al., 2004; Dreni et al., 2007; Yoo et al., 2010; Li et al., 2011; Finet et al., 2016). All of the above genetic data indicate that there are differences in gene expression between the placenta and the ovary wall. From this we can see the origins of the two are different. The evidence of molecular biology and vascular structure imply that the placenta is a distinct floral organ which is equivalent to a secondary shoot and independent to the carpel, and that the placenta was recruited onto the ovary wall later in the evolution of angiosperms (Angenent et al., 1995; Roe et al., 1997; Skinner et al., 2004). In addition, the theory has also been supported by the evidences as follows: (1) In gymnosperms ovules are borne on fertile shoots so that are not able to give rise to carpels (Bierhorst, 1971; Biswas and Johri, 1997); (2) The ovule formation is completely independent to carpel in angiosperms mutants (Lersten and Don, 1966; Dave et al., 1981; Skinner et al., 2004); and (3) The seed is borne directly on an axis (shoot) in *Umkomasia mongolica* sp. nov. (Shi et al., 2016). So, overall, the current conclusion is reasonable that the angiosperm placenta is essentially an ovule-bearing branch with the carpel wall actually to be its subtending bract.

AUTHOR CONTRIBUTIONS

X-MG planted and managed the experimental materials, designed the experiments, collected images, analyzed the data

and wrote the article; Y-YY. carried out the preparation of paraffin-sections; LB performed the segregation experiment; R-FG supervised the experiments and complemented the writing.

FUNDING

Doctoral research foundation of Hebei Normal University of Science and Technology (2013YB021).

ACKNOWLEDGMENTS

We thank Dr. Xin Wang (Nanjing Institute of Geology and Palaeontology, CAS) for inviting us to join this research topic and Shao-Hua Li (College of Horticulture Science and Technology, Hebei Normal University of Science and Technology, Qinhuangdao, Hebei, China) for drawing the distribution diagram of vascular bundle of *D. chinensis* L. pistil with a computer.

REFERENCES

Angenent, G. C., Franken, J., Busscher, M., van Dijken, A., van Went, J. L., Dons, H. J., et al. (1995). A novel class of MADS box genes is involved in ovule development in Petunia. *Plant Cell* 7, 1569–1582. doi: 10.1105/tpc.7.10.1569

Angiosperm Phylogeny Group (2003). An update of the Angiosperm Phylogeny Group classification for the orders and families of flowering plants: APG II. *Bot. J. Linn. Soc.* 141, 399–436. doi: 10.1046/j.1095-8339.2003.t01-1-00158.x

Angiosperm Phylogeny Group (2009). An update of the Angiosperm Phylogeny Group classification for the orders and families of flowering plants: APG III. *Bot. J. Linn. Soc.* 161, 105–121. doi: 10.1111/j.1095-8339.2009.00996.x

Basconsuelo, S., Weberling, F., and Kraus, T. (2002). Transition zone between root and stem vascular system in seedlings of members of the tribe Phaseoleae (Fabaceae). *Feddes Repert.* 113, 224–230. doi: 10.1002/1522-239X(200208)113:3/4<224::AID-FEDR224>3.0.CO;2-V

Bierhorst, D. W. (1971). "Morphology of vascular plants," in *The MacMillan Biology Series*, eds N. H. Giles and J. G. Torrey (New York, NY: Macmillan Company), 448–560.

Biswas, C., and Johri, B. M. (1997). *The Gymnosperms*. Berlin: Springer-Verlag.

Buell, K. M. (1952). Developmental morphology in Dianthus. I. Structure of the pistil and seed development. *Am. J. Bot.* 39, 194–210. doi: 10.2307/2438359

Columbia Electronic Encyclopedia (2016). *Columbia Electronic Encyclopedia, 6th Edn*. New York, NY: Columbia University Press.

Cronquist, A. (1988). *The Evolution and Classification of Flowering Plants*. Bronx: New York Botanical Garden.

Croxdale, J.-G. Jr., and Outlaw, W. H. (1983). Glucose-6-phosphate-dehydrogenase activity in the shoot apical meristem, leaf primordia, and leaf tissues of *Dianthus chinensis* L. *Planta* 157, 289–297. doi: 10.1007/BF00397399

Dar, R. A., Tahir, I., and Ahmad, S. S. (2014). Physiological and biochemical changes associated with flower development and senescence in *Dianthus chinensis* L. *Ind. J. Plant Physiol.* 19, 215–221. doi: 10.1007/s40502-014-0104-9

Darwin, F., and Seward, A. C. (1903). *More Letters of Charles Darwin*. London: Cambridge University Press.

Dave, Y. S., Patel, N. D., and Rao, K. S. (1981). Structural design of the developing fruit of *Nicotiana tabacum*. *Phyton* 21, 63–71.

Ding, J.-J., Pan, Y.-Z., Liu, S.-L., He, Y., Wang, L., and Li, L. (2013). Effect and mechanism of soil cadmium stress on *Dianthus chinensis* seedling growth. *Acta Pratacult. Sin.* 22, 77–85. doi: 10.11686/cyxb20130610

Douglas, G. E. (1936). Studies in the vascular anatomy of the Primulaceae. *Am. J. Bot.* 23, 199–212. doi: 10.2307/2436018

Dreni, L., Jacchia, S., Fornara, F., Fornari, M., Ouwerkerk, P. B., An, G., et al. (2007). The D-lineage MADS-box gene OsMADS13 controls ovule identity in rice. *Plant J.* 52, 690–699. doi: 10.1111/j.1365-313X.2007.03272.x

Eames, A. J. (1951). Again: "The new morphology." *New Phytol.* 50, 17–35. doi: 10.1111/j.1469-8137.1951.tb05167.x

Eames, A. J. (1961). *Morphology of the Angiosperms*. New York, NY: McGraw-Hill Book Company, Inc.

Endress, P. K. (1994). *Diversity and Evolutionary Biology of Tropical Flowers*. Cambridge: Cambridge University Press.

Endress, P. K., and Armstrong, J. E. (2011). Floral development and floral phyllotaxis in Anaxagorea (Annonaceae). *Ann. Bot.* 108, 835–845. doi: 10.1093/aob/mcr201

Finet, C., Floyd, S. K., Conway, S. J., Zhong, B., Scutt, C. P., and Bowman, J. L. (2016). Evolution of the YABBY gene family in seed plants. *Evol. Dev.* 18, 116–126. doi: 10.1111/ede.12173

Fu, X.-P., Yang, S.-H., and Bao, M.-Z. (2008). Factors affecting somatic embryogenesis in anther cultures of Chinese Pink (*Dianthus chinensis* L.) *in vitro*. *Cell. Dev. Biol. Plant* 44, 194–202. doi: 10.1007/s11627-008-9107-4

Gibbs, L. S. (1907). Notes on the development and structure of the seed in the Alsinoideae. *Ann. Bot.* 21, 25–55. doi: 10.1093/oxfordjournals.aob.a089122

Guo, X.-M., Xiao, X., Wang, G.-X., and Gao, R.-F. (2013). Vascular anatomy of kiwi fruit and its implications for the origin of carpels. *Front. Plant Sci.* 4:391. doi: 10.3389/fpls.2013.00391

Han, J., Huang, M., Wang, Z., Zheng, Y., Zeng, G., He, W., et al. (2015). Cyclopentapeptides from *Dianthus chinensis*. *J. Peptide Sci.* 21, 550–553. doi: 10.1002/psc.2746

Kapoor, L. D. (1973). Constitution of amphicribral vascular bundles in capsule of *Papaver somniferum*. *Linn. Bot. Gaz.* 134, 161–165. doi: 10.1086/336698

Kapoor, L. D. (1995). *Opium Poppy: Botany, Chemistry, and Pharmacology*. New York, NY: Haworth Press Inc.

Lersten, N. R., and Don, K. W. (1966). The discontinuity plate, a definitive floral characteristic of the Psoraleae (Leguminosae). *Am. J. Bot.* 53, 548–555. doi: 10.2307/2440004

Li, H., Liang, W., Yin, C., Zhu, L., and Zhang, D. (2011). Genetic interaction of OsMADS3, DROOPING LEAF, and OsMADS13 in specifying rice floral organ identities and meristem determinacy. *Plant Physiol.* 156, 263–274. doi: 10.1104/pp.111.172080

Lister, G. (1884). On the origin of the placentas in the tribe Alsineae of the order Caryophylleae. *J. Linn. Soc. Bot. Lond.* 20, 423–429. doi: 10.1111/j.1095-8339.1884.tb00643.x

Liu, W.-Z., Hilu, K., and Wang, Y.-L. (2014). From leaf and branch into a flower: Magnolia tells the story. *Bot. Stud.* 55:28. doi: 10.1186/1999-3110-55-28

Mathews, S., and Kramer, E. M. (2012). The evolution of reproductive structures in seed plants: a re-examination based on insights from developmental genetics. *New Phytol.* 194, 910–923. doi: 10.1111/j.1469-8137.2012.04091.x

Pinyopich, A., Ditta, G., Savidge, B., Liljegren, S., Baumann, E., Wisman, E., et al. (2003). Assessing the redundancy of MADS-box genes during carpel and ovule development. *Nature* 34, 85–88. doi: 10.1038/nature01741

Roe, J. L., Nemhauser, J. L., and Zambryski, P. C. (1997). TOUSLED participates in apical tissue formation during gynoecium development in Arabidopsis. *Plant Cell* 9, 335–353. doi: 10.1105/tpc.9.3.335

Rounsley, S. D., Ditta, G. S., and Yanofsky, M. F. (1995). Diverse roles for MADS box genes in Arabidopsis development. *Plant Cell* 7, 1259–1269. doi: 10.1105/tpc.7.8.1259

Shi, G., Leslie, A. B., Herendeen, P. S., Herrera, F., Ichinnorov, N., Takahashi, M., et al. (2016). Early Cretaceous Umkomasia from Mongolia: implications for homology of corystosperm cupules. *New Phytol.* 210, 1–12. doi: 10.1111/nph.13871

Skinner, D. J., Hill, T. A., and Gasser, C. S. (2004). Regulation of ovule development. *Plant Cell* 16, S32–S45. doi: 10.1105/tpc.015933

Soltis, P. S., and Soltis, D. E. (2004). The origin and diversification of angiosperms. *Am. J. Bot.* 91, 1614–1626. doi: 10.3732/ajb.91.10.1614

Tang, X.-H. (2008). *A Study on Carpel Diversity and Systematics in Ranunculaceae*. Master's thesis, Shaanxi Normal University, Xi'an.

Thomson, B. F. (1942). The floral morphology of the Caryophyllaceae. *Am. J. Bot.* 29, 333–349. doi: 10.2307/2437569

Tucker, S. C. (1975). Carpellary vasculature and the ovular vascular supply in Drimys. *Am. J. Bot.* 62, 191–197. doi: 10.2307/2441595

Von Balthazar, M., and Endress, P. K. (2002). Reproductive structures and systematics of Buxaceae. *Bot. J. Linn. Soc.* 140, 193–228. doi: 10.1046/j.1095-8339.2002.00107.x

Wang, J., Wang, Y.-Z., Wang, H.-X., Li, J., Shi, G.-S., Ji, Z.-R., et al. (2014). A study on collection and breeding utilization of the germplasm resources of wild Dianthus in Shanxi province. *Bull. Agric. Sci. Technol.* 11, 216–218.

Wang, X. (2010). *The Dawn Angiosperms*. Heidelberg: Springer.

Wang, X., Liu, Z.-J., Liu, W.-Z., Zhang, X., Guo, X.-M., Hu, G., et al. (2015). Breaking the stasis of current plant systematics. *Sci. Technol. Rev.* 33, 97–105. doi: 10.3981/j.issn.1000-7857.2015.22.017

Wang, Y. -Z., and Pan, K. -Y. (1998). "Comparative floral anatomy of Whytockia (Gesneriaceae) endemic to China," in *Floristic Characteristics and Diversity of East Asian Plants*, eds A. L. Zhang, and S. G. Wu (Beijing: China Higher Education Press), 352–366.

Wu, W., Cai, Y.-M., Zou, H.-Y., and Huang, M.-R. (2003). Genetic Diversity of *Dianthus chinensis* L. and *D. caryophyllus* L. with RAPD. *J. Nanjing Forest. Univ.* 27, 72–74.

Wynn, A. N., Seaman, A. A., Jones, A. L., and Franks, R. G. (2014). Novel functional roles for PERIANTHIA and SEUSS during floral organ identity specification, floral meristem termination, and gynoecial development. *Front. Plant Sci.* 5:130. doi: 10.3389/fpls.2014.00130

Yamaguchi, T., Nagasawa, N., Kawasaki, S., Matsuoka, M., Nagato, Y., and Hirano, H. Y. (2004). The YABBY gene DROOPING LEAF regulates carpel specification and midrib development in *Oryza sativa*. *Plant Cell* 16, 500–509. doi: 10.1105/tpc.018044

Yang, G.-F., Zhao, C.-L., and Yang, S.-F. (2013). Artificial cultivation technology of ornamental *Dianthus chinensis*. *Forest By Product Special. China* 1, 52–53.

Yoo, M. -J., Soltis, P. S., and Soltis, D. E. (2010). Expression of floral MADS-box genes in two divergent water lilies: Nymphaeales and Nelumbo. *Int. J. Plant Sci.* 171, 121–146. doi: 10.1086/648986

Zhu, Z.-S., and Sun, B.-M. (2015). Cross breeding of *Dianthus chinensis*. *China Flower Hortic.* 16, 19–20.

Conflict of Interest Statement: The authors declare that the research was conducted in the absence of any commercial or financial relationships that could be construed as a potential conflict of interest.

frontiers in Plant Science

MINI REVIEW
published: 24 April 2017
doi: 10.3389/fpls.2017.00631

Evolution of Lower Brachyceran Flies (Diptera) and Their Adaptive Radiation with Angiosperms

Qingqing Zhang[1,2] *and Bo Wang*[1,3]*

[1] State Key Laboratory of Palaeobiology and Stratigraphy, Nanjing Institute of Geology and Palaeontology, Chinese Academy of Sciences, Nanjing, China, [2] University of Science and Technology of China, Hefei, China, [3] Key Laboratory of Zoological Systematics and Evolution, Institute of Zoology, Chinese Academy of Science, Beijing, China

The Diptera (true flies) is one of the most species-abundant orders of Insecta, and it is also among the most important flower-visiting insects. Dipteran fossils are abundant in the Mesozoic, especially in the Late Jurassic and Early Cretaceous. Here, we review the fossil record and early evolution of some Mesozoic lower brachyceran flies together with new records in Burmese amber, including Tabanidae, Nemestrinidae, Bombyliidae, Eremochaetidae, and Zhangsolvidae. The fossil records reveal that some flower-visiting groups had diversified during the mid-Cretaceous, consistent with the rise of angiosperms to widespread floristic dominance. These brachyceran groups played an important role in the origin of co-evolutionary relationships with basal angiosperms. Moreover, the rise of angiosperms not only improved the diversity of flower-visiting flies, but also advanced the turnover and evolution of other specialized flies.

Keywords: brachyceran flies, angiosperm, mid-Cretaceous, pollinator, co-evolution

OPEN ACCESS

Edited by:
José Bienvenido Diez, University of Vigo, Spain

Reviewed by:
William Oki Wong, Institute of Botany (CAS), China
Andre Nel, National Museum of Natural History, France

***Correspondence:**
Bo Wang
bowang@nigpas.ac.cn

Specialty section:
This article was submitted to Plant Evolution and Development, a section of the journal Frontiers in Plant Science

Received: *27 January 2017*
Accepted: *07 April 2017*
Published: *24 April 2017*

Citation:
Zhang Q and Wang B (2017) Evolution of Lower Brachyceran Flies (Diptera) and Their Adaptive Radiation with Angiosperms. Front. Plant Sci. 8:631. doi: 10.3389/fpls.2017.00631

INTRODUCTION

The Diptera (true flies) is one of the most species-abundant orders of Insecta, and they are certainly one of the most ecologically ubiquitous and significant orders of insects (Grimaldi and Cumming, 1999). They are among the most ancient pollinators of flowering plants (Bernhardt and Thien, 1987; Labandeira, 1998), and played an important role in the origin of co-evolutionary relationships with flowering plants and insects (Thien et al., 2000; Ssymank et al., 2008).

The Cretaceous is a time of important developments in angiosperms that angiosperms rose to dominance during the Albian-Cenomanian, and become forest dominants during the Campanian-Maastrichtian (Friis et al., 2010; Peralta-Medina and Falcon-Lang, 2012). Although the rise of Angiosperms did not generate an immediate increase in insect diversification within major insect groups based on Bayesian fossil-based analyses, but the influence of the radiation of Angiosperms on insect diversification is not excludable (Condamine et al., 2016). The angiosperm radiations provided new food resources and habitats, and had a profound effect on flies, beetles, and other insects (Wang et al., 2013). The interval since the middle Early Cretaceous to early Late Cretaceous witnessed the significant transformation to the modern terrestrial world, between this time (from 125 million years ago to 90 million years ago), and there were significant shifts in the major ecological associations among plants, insects, and other organismic groups dominant on land (Labandeira, 2010).

Brachyceran flies are quite abundant during Mesozoic, especially from the Middle-Late Jurassic to mid-Cretaceous. The middle Early Cretaceous to the early Late Cretaceous is a significant period for brachyceran flies, including the ecological success of some flower-visiting flies and extinction of several important groups, such as Eremochaetidae and Zhangsolvidae (Arillo et al., 2015; Zhang et al., 2016a). The extant family Tabanidae, Nemestrinidae, Bombyliidae are among the commonest pollinators of most extant basal angiosperms, and their early evolution are important for understanding the co-evolution between flies and angiosperms. The probable impact of floristic changes on brachyceran flies during the Early Cretaceous has been widely accepted, but supporting fossils are still relatively few (Grimaldi, 1999; Labandeira and Currano, 2013). Recently abundant Cretaceous fossils have been described and our knowledge about the evolution of brachyceran flies has improved greatly (e.g., Grimaldi, 2016; Zhang et al., 2016a,b). In this paper, we review the fossil record and early evolution of five groups, and briefly discuss their probable ecological associations with early angiosperms.

FOSSIL RECORD

Tabanidae

Tabanidae, normally called horse flies or deer flies, is an ubiquity family, and the most diverse family-level clade that has more than 4000 species distributed in 156 genera worldwide (**Figure 1A**; Pape et al., 2011). They are stout-bodied flies, with larger first flagellomere and 4-8 apical flagellomeres; legs with two apical spurs on midtibia, tarsi with pulvilliform empodium; wing venation with R4 and R5 enclose wing apex, form a large 'Y' across the wing tip; cell br, bm and d large, cell cup closed near wing margin; calypters almost always well developed (Colless and McAlpine, 1991; Burger, 2009). Tabanidae is type family of Tabanidae which characteristiced by the presence of a venom canal of the larval mandible (Kerr, 2010; Morita et al., 2016).

Tabanids are relatively scarce in the fossil record, but in Cenozoic, they are quite abundant as fossil recorded from Miocene of Florissant, from North American, Germany, French, and Switzerland Oligocene, from England and Baltic amber Eocene/Oligocene, Pliocene from Europe and Africa (Martins-Neto, 2003). The oldest record of a true tabanid was reported from the Lower Cretaceous Durlston Formation of England. Till now, five species of tabanids was recorded in the Early Cretaceous and one species primitively in Therevidae was moved to the tabanid genus *Cratotabanus* Martins-Neto and Santos (1994; Ren, 1998; Martins-Neto, 2003; Mostovski et al., 2003; Zhang, 2012). Fossils from the Late Cretaceous are quite rare, with only one species and genus from Late Cretaceous of New Jersey amber, together with two newly described species in Burmese amber (Grimaldi et al., 2011; Grimaldi, 2016). Flower-feeding tabanids (Pangoniinae) appear at least in the Early Cretaceous (Martins-Neto and Santos, 1994; Ren, 1998; Zhang, 2012). A recent molecular analysis calibrated using several key fossils support that the divergence of Tabanidae and their sister clade Athericidae, in the Early Cretaceous, approximately 135 Ma (Morita et al., 2016).

Nemestrinidae

Nemestrinidae commonly called tangle-veined flies, is cosmopolitan but quite a small group of brachycerous flies, with about 300 extant species in over 20 genera (**Figure 1B**; Bernardi, 1973; Mostovski and Martínez-Delclòs, 2000). They are usually medium-sized flies with body stout and dense pilosity, wings are usually longer than body (Wedmann, 2007; Woodley, 2009). They can be easily recognized by a so-called diagonal vein, the compound diagonal vein obliquely aligned through the wing; they also have some characteristics including tibiae without apical spurs, empodium pulvilliform, and one segmented cercus and flagellum often formed into a slender stylus (Yeates, 1994; Wedmann, 2007). Fossil tangle-veined flies are quite abundant since Mesozoic, many nemestrinids were found in Late Jurassic and Early Cretaceous, and some Cenozoic nemestrinids were described, mainly from the Oligocene of Florissant, USA. Ansorge and Mostovski (2000) listed an updated list of all taxa of Nemestrinidae, and additional taxa have been described from the Eocene of Germany (Wedmann, 2007), mid-Cretaceous Burmese amber (Grimaldi, 2016; Zhang et al., 2017), and a doubtable genus without diagonal vein from the Late Jurassic of China (Zhang et al., 2008). The oldest fossil nemestrinids are from the Late Jurassic of Karabastau, Kazakhstan (Rohdendorf, 1968; Mostovski, 1998). Ansorge and Mostovski (2000) hypothesized that the family Nemestrinidae probably originated in the Late Triassic or Early Jurassic, as the oldest fossil Nemestrinidae appeared in Early Jurassic and fossil nemestrinids demonstrate a high taxonomic diversity since the Middle-Late Jurassic. Nemestrinidae is thought to be a sister group of Apioceridae in Nemestrinoidea supported by their parasitic larval lifestyle (Woodley, 1989; Yeates, 2002).

Bombyliidae

Bombyliidae (bee flies) is a quite diverse and widely distributed family of Asiloidea. It is a cosmopolitan group and a quite large family that comprising over 4500 described extant species around the world (**Figure 1C**; Evenhuis, 1994; Evenhuis and Greathead, 2003; Wedmann and Yeates, 2008). They are commonly robust flies, often with long projecting proboscis and usually densely hairs (Colless and McAlpine, 1991; Greathead et al., 2009). They feed on nectar as well as pollen, many of them using a long proboscis to probe flowers (Grimaldi, 2016). The fossil of adult bee flies can be distinguished by the following features: antenna usually with flagellomere coniform, usually with one or two flagellomeres and a terminal bristlelike stylus; wing R2+3 and R4 usually strongly curved distally, meeting costa at about a right angle; R4+5 branched, R4 and R5 usually encompass wing tip; three (rarely two) posterior cells (Greathead et al., 2009). Fossil bee flies are quite abundant in Cenozoic, especially in the Oligocene and Eocene. Till now, about 70 species in about 40 genera have been described from Florissant of USA, France, Germany, and Dominican and Baltic ambers. The fossil record of Bombyliidae has been reviewed by Hull (1973) and Evenhuis

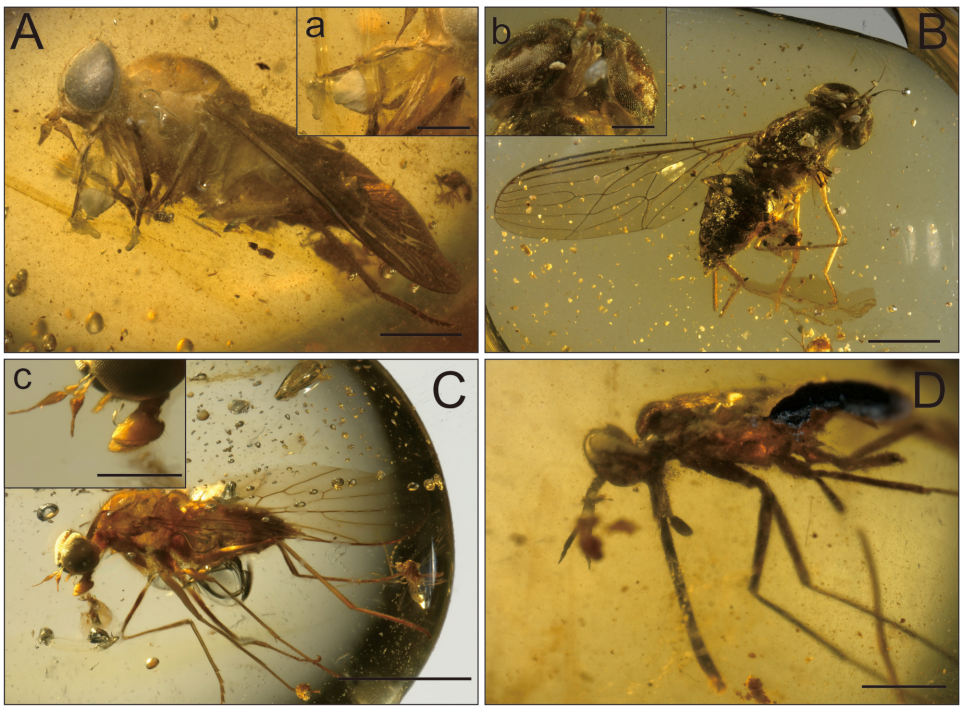

FIGURE 1 | Four types of mouthparts in mid-Cretaceous Burmese amber. (A) Tabanidae, scale bar = 2 mm; **(a)** Mouthparts, scale bar = 1 mm. **(B)** Nemestrinidae, scale bar = 2 mm; **(b)** Mouthparts, scale bar = 0.5 mm. **(C)** Bombyliidae, scale bar = 2 mm; **(c)** mouthparts, scale bar = 0.5 mm. **(D)** Zhangsolvidae with a long proboscid, scale bar = 1 mm.

(1994), and new taxa was recently described by Nel and De Ploëg (2004), Nel (2006), and Wedmann and Yeates (2008).

Grimaldi (2016) suggested that the radiation age of Bombyliidae is the Late Cretaceous, but Lamas and Nihei (2007) suggested a Middle Jurassic age based on the molecular phylogenetic analysis. Molecular models and biogeography support a Late Mesozoic diversification of asiloids, with Bombyliidae at the base of the Asiloidea (Winterton et al., 2015; Grimaldi, 2016). Unambiguous Mesozoic bombyliids are extremely rare. Recently, some definitive new records of Bombyliidae in mid-Cretaceous Burmese amber show that bombyliids have already diversified, and these fossils provide new insights into the early evolution of Cretaceous bee flies (Shi et al., 2012; Grimaldi, 2016; Zhang et al., 2016b).

Eremochaetidae

Eremochaetidae is a Mesozoic extinct family that was established by Ussatchov based on two species in two different genera (Ussatchov, 1968). Eremochaetidae is a quite rare family that was found only in Late Mesozoic, mainly in Early Cretaceous. Till now, only 15 species in nine genera have been described in China, Kazakhstan, Mongolia, Russia and Burmese amber (Ussatchov, 1968; Kovalev, 1989; Ren and Guo, 1995; Mostovski, 1996; Ren, 1998; Zhang, 2014; Zhang et al., 2014, 2016b). All eremochaetids have the characters: eyes very large, occupying the greater part of the head; thorax short and convex; Sc is stout, R1 is very long; cross-vein is absent, causing the vein R4+5 (sometimes R2+3 and R4+5) to arise from cell d; the ovipositor is needle-shaped in all female eremochaetids (Ussatchov, 1968; Zhang et al., 2014). Zhang (2014) described and illustrated the structures of the male genitalia for the first time, and reasoned that these characteristics probably represent the base type of the primitive lower Orthorrhapha of Brachycera. The latest occurrence of eremochaetids is from the mid-Cretaceous Burmese amber (Zhang et al., 2016a). The highly developed, hypodermic-like ovipositor and enlarged tridactylous characteristic in pretarsus supported their endoparasitoid life, and their primitive mouthparts were probably used to feed on nectar (Grimaldi and Barden, 2016; Zhang et al., 2016a). Eremochaetidae is probably related to the superfamily Archisargoidae based on the morphological characteristics (Grimaldi and Barden, 2016). The fossil record of eremochaetids reveals that the extinction of these ancient parasitoids probably occurred by the end of the Late Cretaceous and coincided with the rise of angiosperms, perhaps owing to competition from newly evolved parasitoid wasps and flies which extant ones are mostly flower-visiting insects (Eggleton and Belshaw, 1993; Feener and Brown, 1997; Gilbert and Jervis, 1998; Zhang et al., 2016a).

Zhangsolvidae

The Zhangsolvidae is an extinct family of brachyceran flies that erected by Nagatomi and Yang (1998) for the genus *Zhangsolva cupressa* found in the Early Cretaceous Laiyang Formation

(**Figure 1D**; Zhang et al., 1993; Nagatomi and Yang, 1998; Arillo et al., 2015). Zhangsolvidae is a quite rare family that till now six species in four genera that found only in Cretaceous: five species and three genera in Early Cretaceous of China, Spain, Brazil and one species and genus in Late Cretaceous Burmese amber (Zhang et al., 1993; Nagatomi and Yang, 1998; Mazzarolo and Amorim, 2000; Wilkommen and Grimaldi, 2007; Arillo et al., 2015). Zhangsolvidae has a stout body, with very long and quite slender proboscis, vein M1 strongly arched, M3 fused to M4 and CuA fused to CuP (Nagatomi and Yang, 1998; Arillo et al., 2015). The placement of Zhangsolvidae is within Stratiomyomorpha supported by the presentation of phylogenetic analysis of 52 morphological characters for 35 taxa (Arillo et al., 2015). New zhangsolvids specimens from Early Cretaceous Spanish amber and mid-Cretaceous Burmese amber provided a detailed structure of their unique proboscis. Surprisingly, a specimen in Spanish amber is carrying clumped pollen that is attributed to a Mesozoic gymnosperm (Peñalver et al., 2015). The co-occurrence of pollen with its insect vector conforms that these long-proboscid insects were gymnosperm pollinators. Zhangsolvids became extinct during the late Cretaceous probably due to the extinction of their gymnosperm food.

PROBABLE FLIES-ANGIOSPERM ASSOCIATIONS

Mutualisms between fossil insects and plants are among the most interesting biological associations (Ren et al., 2009; Labandeira and Currano, 2013). Direct evidence of early interactions between insects and their productive organs of plants is that pollen preserved in the guts of fossil insects (Bronstein et al., 2006; Labandeira et al., 2007). Some evidences that specimens with masses of pollen in their guts have been found from the Cretaceous (Krassilov and Rasnitsyn, 1982; Caldas et al., 1989; Huang et al., 2016). Although some pollen grains were found in the guts of several groups, but no record is reported from Mesozoic brachyceran flies till now. Further investigation of brachyceran flies from Cretaceous may provide more evidence.

Very rare definitive evidences of insects carrying pollen grains have been found, such as thrips and dipteran flies found in Early Cretaceous amber of Spain (Peñalver et al., 2012, 2015). The most important indirect evidence for co-evolution of flies and angiosperms may be the mouthparts (Labandeira, 2010). Long mouthparts flies were quite diverse during the Upper Jurassic and Lower Cretaceous, such as Nemestrinidae, Zhangsolvidae, and newly reported the first record of Hilarimorphidae from Lower Cretaceous Lebanese amber (Myskowiak et al., 2016). Mouthparts of fly in mid-Cretaceous Burmese amber also show a high morphological disparity, from thin long to short expanded ones (**Figure 1**). The diversity of proboscis strongly suggests diverse plant hosts (Larson et al., 2001). Modern flower-visiting brachyceran flies usually have long proboscis, such as bee flies and tangle-veined flies. Based on our mid-Cretaceous amber sources, however, tangle-veined flies and bee flies with long proboscis are quite rare, and nearly all specimens have relatively short and expand labellum. Most of these flies in Burmese amber have the labellum consisting of a broad, fleshy expansion that is probably used to feed on nectars, obviously distinct with extant ones that with quite long mouthparts (Grimaldi, 1999). These flies probably obtain nectar from open flowers of various families of plants, and species with longer mouthparts probably feed on deep tubular flowers.

CONCLUSION

Tabanidae, Nemestrinidae, Bombyliidae, Eremochaetidae, and Zhangsolvidae had already diversified during or before mid-Cretaceous based on the fossil record and supplementary molecular analyses. Tabanidae, Nemestrinidae, and Bombyliidae currently are among the most common pollinators of angiosperms, and their diversifications are consistent with the rise of angiosperms to widespread floristic dominance. These brachyceran groups probably played an important role in the origin of co-evolutionary relationships with basal angiosperms. Zhangsolvidae and Eremochaetidae became extinction perhaps owing to the Late Cretaceous floral turnover and competition from newly evolved groups. In this regard, the rise of angiosperms not only improved the diversity of flower-visiting flies, but also advanced the turnover and evolution of other specialized flies. Moreover, early reproductive organ-visiting flies (including on those gymnosperms) are responsible for the origin of flowers and the diversity of angiosperms. In this review, we have only scratched the surface of the co-evolution of Cretaceous brachyceran flies with angiosperm, our knowledge of Mesozoic flies-angiosperm mutualisms should greatly expand with more and better preserved fossils and improvements in phylogenetic analysis.

AUTHOR CONTRIBUTIONS

BW designed the project; QZ performed the comparative and analytical work, and wrote the manuscript.

ACKNOWLEDGMENTS

We thank Xin Wang for inviting us to contribute this review, and two reviewers for reviewing the manuscript and constructive criticisms. This research was supported by the National Natural Science Foundation of China (41572010, 41622201, 41688103), and Youth Innovation Promotion Association of CAS (No. 2011224).

REFERENCES

Ansorge, J., and Mostovski, M. B. (2000). Redescription of *Prohirmoneura jurassica* Handlirsch, 1906 (Diptera: Nemestrinidae) from the lower Tithonian lithographic limestone of Eiehstätt (Bavaria). *N. Jb. Geol. Paläont. Mh.* 4, 235–243.

Arillo, A., Peñalver, E., Pérez-de la Fuente, R., Delclòs, X., Criscione, J., Barden, P. M., et al. (2015). Long-proboscid brachyceran flies in Cretaceous amber (Diptera: Stratiomyomorpha: Zhangsolvidae). *Syst. Entomol.* 40, 242–267. doi: 10.1016/j.cub.2015.05.062

Bernardi, N. (1973). The genera of the family Nemestrinidae (Diptera: Brachycera). *Arq. Zool.* 24, 211–318. doi: 10.11606/issn.2176-7793.v24i4p211-318

Bernhardt, P., and Thien, L. B. (1987). Self-isolation and insect pollination in the primitive angiosperms: new evaluations of older hypotheses. *Plant Syst. Evol.* 156, 159–176. doi: 10.1007/BF00936071

Bronstein, J. L., Alarcón, R., and Geber, M. (2006). The evolution of plant–insect mutualisms. *New Phytol.* 172, 412–428. doi: 10.1111/j.1469-8137.2006.01864.x

Burger, J. F. (2009). "Tabanidae (horse flies, deer flies, tabanos)," in *Manual of Central American Diptera*, Vol. 1, eds B. V. Brown, A. Borkent, J. M. Cumming, D. M. Wood, N. E. Woodley, and M. A. Zumbado (Ottawa, ON: NRC Research Press), 495–507.

Caldas, E. B., Martins-Neto, R. G., and Lima Filho, F. P. (1989). *Afropollis* sp. (polém) no trato intestinal de vespa (Hymenoptera: Apocrita: Xyelidae) no Cretáceo da Bacia do Araripe. *Simpósio Geologia Nordeste* 13, 195–196.

Colless, D. H., and McAlpine, D. K. (1991). "Diptera (flies)," in *The Insects of Australia*, 2nd Edn, Vol. II, ed. CSIRO (Melbourne, VIC: Melbourne University Press), 717–786.

Condamine, F. L., Clapham, M. E., and Kergoat, G. J. (2016). Global patterns of insect diversification: towards a reconciliation of fossil and molecular evidence? *Sci. Rep.* 6:19208. doi: 10.1038/srep19208

Eggleton, P., and Belshaw, R. (1993). Comparison of dipteran, hymenopteran, and coleopteran parasitoids: provisional phylogenetic explanations. *Biol. J. Linn. Soc.* 48, 213–226. doi: 10.1111/j.1095-8312.1993.tb00888.x

Evenhuis, N. L. (1994). *Catalogue of the Fossil Flies of the World (Insecta: Diptera)*. Leiden: Backhuys Publishers.

Evenhuis, N. L., and Greathead, D. J. (2003). World catalogue of bee flies (Diptera: Bombyliidae): corrigenda and addenda. *Zootaxa* 300, 1–64. doi: 10.11646/zootaxa.300.1.1

Feener, D. H., and Brown, B. V. (1997). Diptera as parasitoids. *Annu. Rev. Entomol.* 42, 73–97. doi: 10.1146/annurev.ento.42.1.73

Friis, E. M., Pedersen, K. R., and Crane, P. R. (2010). Diversity in obscurity: fossil flowers and the early history of angiosperms. *Philos. Trans. R. Soc. Lond. B Biol. Sci.* 365, 369–382. doi: 10.1098/rstb.2009.0227

Gilbert, F. S., and Jervis, M. A. (1998). Functional, evolutionary and ecological aspects of feeding-related mouthpart specializations in parasitoid flies. *Biol. J. Linn. Soc.* 63, 495–535. doi: 10.1111/j.1095-8312.1998.tb00327.x

Greathead, D. J., Evenhuis, N. L., and Lamas, C. J. E. (2009). "Bombyliidae (bee flies)," in *Manual of Central American Diptera*, Vol. 1, ed. B. V. Brown (Ottawa, ON: Library and Archives Canada Cataloguing), 565–576.

Grimaldi, D., and Cumming, J. (1999). Brachyceran Diptera in Cretaceous ambers and Mesozoic diversification of the Eremoneura. *Bull. Am. Mus. Nat. Hist.* 239, 1–124.

Grimaldi, D. A. (1999). The co-radiations of pollinating insects and angiosperms in the Cretaceous. *Ann. Mo. Bot. Gard.* 86, 373–406. doi: 10.2307/2666181

Grimaldi, D. A. (2016). Diverse orthorrhaphan flies (Insecta: Diptera: Brachycera) in amber from the Cretaceous of Myanmar: Brachycera in Cretaceous Amber, Part VII. *Bull. Am. Mus. Nat. Hist.* 408, 1–131. doi: 10.1206/0003-0090-408.1.1

Grimaldi, D. A., Arillo, A., Cumming, J. M., and Hauser, M. (2011). Brachyceran Diptera (Insecta) in Cretaceous ambers, part IV, Significant new Orthorrhaphous taxa. *Zookeys* 148, 293–332. doi: 10.3897/zookeys.148.1809

Grimaldi, D. A., and Barden, P. (2016). The Mesozoic Family Eremochaetidae (Diptera: Brachycera) in Burmese amber and relationships of Archisargoidea: Brachycera in Cretaceous Amber, Part VIII. *Am. Mus. Novitates* 3865, 1–29. doi: 10.1206/3865.1

Huang, D. Y., Bechly, G., Nel, P., Engel, M. S., Prokop, J., Azar, D., et al. (2016). New fossil insect order Permopsocida elucidates major radiation and evolution of suction feeding in hemimetabolous insects (Hexapoda: Acercaria). *Sci. Rep.* 6:23004. doi: 10.1038/srep23004

Hull, F. M. (1973). *Bee Flies of the World: The Genera of the Family Bombyliidae*. Washington, DC: Smithsonian Institution Press.

Kerr, P. H. (2010). Phylogeny and classification of Rhagionidae, with implications for Tabanomorpha (Diptera: Brachycera). *Zootaxa* 2592, 1–133.

Kovalev, V. G. (1989). Bremochaetidae, the Mesozoic family of brachycerous dipterans. *Paleontol. J.* 1989, 100–105.

Krassilov, V. A., and Rasnitsyn, A. P. (1982). A unique finding: pollen in the intestine of early Cretaceous sawflies. *Paleontol. J.* 16, 80–95.

Labandeira, C. C. (1998). How old is the flower and the fly? *Science* 280, 57–59. doi: 10.1126/science.280.5360.57

Labandeira, C. C. (2010). The pollination of mid Mesozoic seed plants and the early history of long-proboscid insects. *Ann. Mo. Bot. Gard.* 97, 469–513. doi: 10.3417/2010037

Labandeira, C. C., and Currano, E. D. (2013). The fossil record of plant-insect dynamics. *Annu. Rev. Earth Planet. Sci.* 41, 287–311. doi: 10.1146/annurev-earth-050212-124139

Labandeira, C. C., Kvaèek, J., and Mostovski, M. B. (2007). Pollination fluids, pollen, and insect pollination of Mesozoic gymnosperms. *Taxon* 56, 663–695. doi: 10.1073/pnas.1120499109

Lamas, C. J. E., and Nihei, S. S. (2007). Biogeographic analysis of Crocidiinae (Diptera, Bombyliidae): finding congruence among morphological, molecular, fossil and paleogeographical data. *Rev. Bras. Entomol.* 51, 267–274. doi: 10.1590/S0085-56262007000300003

Larson, B. M. H., Kevan, P. G., and Inouye, D. W. (2001). Flies and flowers: taxonomic diversity of anthophiles and pollinators. *Can. Entomol.* 133, 439–465. doi: 10.4039/Ent133439-4

Martins-Neto, R., and Santos, J. (1994). Um novo gênero e uma nova espécie de Mutuca (Insecta, Diptera, Tabanidae) da Formação Santana (Cretáceo Inferior), Bacia do Araripe, Nordeste do Brasil. *Acta Geol. Leopoldensia* 39, 289–297.

Martins-Neto, R. G. (2003). The fossil tabanids (Diptera Tabanidae): when they began to appreciate warm blood and when they began transmit diseases? *Mem. Inst. Oswaldo Cruz* 98, 29–34. doi: 10.1590/S0074-02762003000900006

Mazzarolo, L. A., and Amorim, D. S. (2000). Cratomyia macrorrhyncha, a lower Cretaceous brachyceran fossil from the Santana Formation, Brazil, representing a new species, genus and family of the Stratiomyomorpha (Diptera). *Insect Syst. Evol.* 31, 91–102. doi: 10.1163/187631200X00336

Morita, S. I., Bayless, K. M., Yeates, D. K., and Wiegmann, B. M. (2016). Molecular phylogeny of the horse flies: a framework for renewing tabanid taxonomy. *Syst. Entomol.* 41, 56–72. doi: 10.1111/syen.12145

Mostovski, M. B. (1996). To the knowledge of Archisargoidea (Diptera, Brachycera). Families Eremochaetidae and Archisargidae. *Russ. Entomol. J.* 5, 117–124.

Mostovski, M. B. (1998). A revision of the nemestrinid flies (Diptera, Nemestrinidae) described by Rohdendorf, and a description of new taxa of the Nemestrinidae from the Upper Jurassic of Kazakhstan. *Paleontol. J.* 32, 369–375.

Mostovski, M. B., Jarzembowski, E. A., and Coram, R. A. (2003). Horseflies and athericids (Diptera: Tabanidae, Athericidae) from the lower Cretaceous of England and Transbaikalia. *Paleontol. J.* 37, 162–169.

Mostovski, M. B., and Martínez-Delclòs, X. (2000). New Nemestrinoidea (Diptera: Brachycera) from the Upper Jurassic-Lower Cretaceous of Eurasia, taxonomy and palaeobiology. *Entomol. Probl.* 31, 137–148.

Myskowiak, J., Azar, D., and Nel, A. (2016). The first fossil hilarimorphid fly (Diptera: Brachycera). *Gondwana Res.* 35, 192–197. doi: 10.1016/j.gr.2015.05.003

Nagatomi, A., and Yang, D. (1998). A review of extinct Mesozoic genera and families of Brachycera (Insecta, Diptera, Orthorrhapha). *Entomol. Monthly Mag.* 134, 95–192.

Nel, A. (2006). Oldest records of Bombyliidae: Phthiriinae and Mythicomyiidae: Glabellulinae from the Lowermost Eocene amber of France (Diptera: Bombylioidea). *Eur. J. Entomol.* 103, 109–114. doi: 10.14411/eje.2006.016

Nel, A., and De Ploëg, G. (2004). New fossil bee flies (Diptera: Bombylioidea) in the Lowermost Eocene amber of the Paris Basin. *Geol. Acta* 2, 57–65.

Pape, T., Blagoderov, V., and Mostovski, M. B. (2011). "Order Diptera Linnaeus, 1758," in *Animal Biodiversity: An Outline of Higher-level Classification and Survey of Taxonomic Richness*, ed. Z.-Q. Zhang (Auckland: Magnolia Press), 222–229.

Peñalver, E., Arillo, A., Pérez-de la Fuente, R., Riccio, M. L., Delclòs, X., Barrón, E., et al. (2015). Long-proboscid flies as pollinators of Cretaceous gymnosperms. *Curr. Biol.* 25, 1917–1923. doi: 10.1016/j.cub.2015.05.062

Peñalver, E., Labandeira, C. C., Barrón, E., Delclòs, X., Nel, P., Nel, A., et al. (2012). Thrips pollination of Mesozoic gymnosperms. *Proc. Natl. Acad. Sci. U.S.A.* 109, 8623–8628. doi: 10.1073/pnas.1120499109

Peralta-Medina, E., and Falcon-Lang, H. J. (2012). Cretaceous forest composition and productivity inferred from a global fossil wood database. *Geology* 40, 219–222. doi: 10.1130/G32733.1

Ren, D. (1998). Flower-associated brachycera flies as fossil evidence for Jurassic angiosperm origins. *Science* 280, 85–88. doi: 10.1126/science.280.5360.85

Ren, D., and Guo, Z. (1995). A new genus and two new species of short-horned flies of Upper Jurassic from northeast China (Diptera: Eremochaetidae). *Entomol. Sin.* 2, 300–307. doi: 10.1111/j.1744-7917.1995.tb00051.x

Ren, D., Labandeira, C. C., Santiago-Blay, J. A., Rasnitsyn, A. P., Shih, C. K., Bashkuev, A., et al. (2009). A probable pollination mode before angiosperms: Eurasian, long-proboscid scorpionflies. *Science* 326, 840–847. doi: 10.1126/science.1178338

Rohdendorf, B. B. (1968). "New Mesozoic nemestrinids (Diptera, Nemestrinidae)," in *(Jurassic Insects of Karatau)*, ed. B. B. Rohdendorf (Moscow: Nauka Press), 180–189.

Shi, G. H., Grimaldi, D. A., Harlow, G. E., Wang, J., Yang, M., Lei, W., et al. (2012). Age constraint on Burmese amber based on U-Pb dating of zircons. *Cretaceous Res.* 37, 155–163. doi: 10.1016/j.cretres.2012.03.014

Ssymank, A., Kearns, C. A., Pape, T., and Thompson, F. C. (2008). Pollinating flies (Diptera): a major contribution to plant diversity and agricultural production. *Biodiversity* 9, 86–89. doi: 10.1080/14888386.2008.9712892

Thien, L. B., Azuma, H., and Kawano, S. (2000). New perspectives on the pollination biology of basal angiosperms. *Int. J. Plant Sci.* 161, S225–S235. doi: 10.1086/317575

Ussatchov, D. A. (1968). New Jurassic Asilomorpha (Diptera) of the Karatau. *Entomol. Rev.* 47, 378–384.

Wang, B., Zhang, H., and Jarzembowski, E. (2013). Early Cretaceous angiosperms and beetle evolution. *Front. Plant Sci.* 4:360. doi: 10.3389/fpls.2013.00360

Wedmann, S. (2007). A nemestrinid fly (Insecta: Diptera: Nemestrinidae: cf. Hirmoneura) from the Eocene Messel pit (Germany). *J. Paleontol.* 81, 1114–1117. doi: 10.1666/pleo06-007.1

Wedmann, S., and Yeates, D. K. (2008). Eocene records of bee flies (Insecta, Diptera, Bombyliidae, Comptosia): their paleobiogeographic implications and remarks on the evolutionary history of bombyliids. *Palaeontology* 51, 231–240. doi: 10.1111/j.1475-4983.2007.00745.x

Wilkommen, J., and Grimaldi, D. A. (2007). "Diptera: true flies, gnats, and crane flies," in *The Crato Fossil Beds of Brazil: Window into an Ancient World*, eds D. M. Martill, G. Bechly, and R. F. Loveridge (Cambridge: Cambridge University Press), 369–387.

Winterton, S. L., Hardy, N. B., Gaimari, S. D., Hauser, M., Hill, H. N., Holston, K. C., et al. (2015). The phylogeny of stiletto flies (Diptera: Therevidae). *Syst. Entomol.* 41, 144–161. doi: 10.1111/syen.12147

Woodley, N. E. (1989). "Phylogeny and classification of the "orthorrhaphous" Brachycera," in *Manual of Nearctic Diptera*, Vol. 3, ed. J. F. McAlpine (Ottawa, ON: Research Branch, Agriculture Canada), 1371–1395.

Woodley, N. E. (2009). "Nemestrinidae (tangle-veined flies)," in *Manual of Central American Diptera*, Vol. 1, ed. B. V. Brown (Ottawa, ON: Library and Archives Canada Cataloguing), 557–560.

Yeates, D. K. (1994). The cladistics and classification of the Bombyliidae (Diptera: Asiloidea). *Bull. Am. Mus. Nat. Hist.* 219, 1–191.

Yeates, D. K. (2002). Relationships of extant lower Brachycera (Diptera): a quantitative synthesis of morphological characters. *Zool. Scr.* 31, 105–121. doi: 10.1046/j.0300-3256.2001.00077.x

Zhang, J. F. (2012). New horseflies and water snipe-flies (Diptera: Tabanidae and Athericidae) from the Lower Cretaceous of China. *Cretaceous Res.* 36, 1–5. doi: 10.1016/j.cretres.2012.01.004

Zhang, J. F. (2014). New male eremochaetid flies (Diptera, Brachycera, Eremochaetidae) from the Lower Cretaceous of China. *Cretaceous Res.* 49, 205–213. doi: 10.1016/j.cretres.2014.02.012

Zhang, J. F., Zhang, S., and Li, L. Y. (1993). Mesozoic gadflies (Insecta: Diptera). *Acta Palaeontol. Sin.* 26, 595–603.

Zhang, K. Y., Yang, D., and Ren, D. (2014). New short-horned flies (Diptera: Eremochaetidae) from the Early Cretaceous of China. *Zootaxa* 3760, 479–486. doi: 10.11646/zootaxa.3760.3.15

Zhang, K. Y., Yang, D., Ren, D., and Ge, F. (2008). New Middle Jurassic tangle-veined flies from Inner Mongolia, China. *Acta Palaeontol. Pol.* 53, 161–164. doi: 10.4202/app.2008.0112

Zhang, Q. Q., Zhang, J. F., Feng, Y. T., Zhang, H. C., and Wang, B. (2016a). An endoparasitoid Cretaceous fly and the evolution of parasitoidism. *Sci. Nat.* 103:2. doi: 10.1007/s00114-015-1327-y

Zhang, Q. Q., Zhang, J. F., and Wang, B. (2016b). A remarkable brachyceran fly (Diptera: Tabanomorpha) from Late Cretaceous Burmese amber. *Cretaceous Res.* 67, 1–7. doi: 10.1016/j.cretaes.2016.06.012

Zhang, Q. Q., Zhang, J. F., and Wang, B. (2017). First record of the subfamily Archinemestriinae in the family Nemestrinidae (Diptera: Brachycera) from Upper Cretaceous Burmese amber. *Cretaceous Res.* 75, 141–145. doi: 10.1016/j.cretres.2017.03.005

Conflict of Interest Statement: The authors declare that the research was conducted in the absence of any commercial or financial relationships that could be construed as a potential conflict of interest.

Advantages of publishing in Frontiers

OPEN ACCESS
Articles are free to read, for greatest visibility

COLLABORATIVE PEER-REVIEW
Designed to be rigorous – yet also collaborative, fair and constructive

FAST PUBLICATION
Average 85 days from submission to publication (across all journals)

COPYRIGHT TO AUTHORS
No limit to article distribution and re-use

TRANSPARENT
Editors and reviewers acknowledged by name on published articles

SUPPORT
By our Swiss-based editorial team

IMPACT METRICS
Advanced metrics track your article's impact

GLOBAL SPREAD
5'100'000+ monthly article views and downloads

LOOP RESEARCH NETWORK
Our network increases readership for your article

Frontiers
EPFL Innovation Park, Building I • 1015 Lausanne • Switzerland
Tel +41 21 510 17 00 • Fax +41 21 510 17 01 • info@frontiersin.org
www.frontiersin.org

Find us on